

# The Geologic Investigation of the Taurus-Littrow Valley: Apollo 17 Landing Site

---

GEOLOGICAL SURVEY PROFESSIONAL PAPER 1080

*Prepared on behalf of the National Aeronautics  
and Space Administration*



# The Geologic Investigation of the Taurus-Littrow Valley: Apollo 17 Landing Site

By EDWARD W. WOLFE, NORMAN G. BAILEY, BAERBEL K. LUCCHITTA,  
WILLIAM R. MUEHLBERGER, DAVID H. SCOTT, ROBERT L. SUTTON, *and*  
HOWARD G. WILSHIRE

*With a section on* APOLLO 17 LUNAR SURFACE PHOTOGRAPHY

By RAYMOND M. BATSON, KATHLEEN B. LARSON, *and* RICHARD L. TYNER

---

G E O L O G I C A L   S U R V E Y   P R O F E S S I O N A L   P A P E R   1 0 8 0

*Prepared on behalf of the National Aeronautics  
and Space Administration*

*A synthesis of Apollo 17 lunar  
surface data and sample results*



**UNITED STATES DEPARTMENT OF THE INTERIOR**

**JAMES G. WATT, *Secretary***

**GEOLOGICAL SURVEY**

**Dallas L. Peck, *Director***

Library of Congress Cataloging in Publication Data

The Geological investigation of the Taurus-Littrow  
valley, Apollo 17 landing site.

(Geological Survey Professional Paper 1080)

"A synthesis of Apollo 17 lunar surface data and  
sample results."

"Prepared on behalf of the National Aeronautics  
and Space Administration."

Supt. of Docs. no.: I 19.16:1080

1. Lunar Geology. 2. Project Apollo. I. Wolfe,  
Edward W. II. United States. National Aeronautics  
and Space Administration. III. Series: United  
States. Geological Survey. Professional Paper. 1080.

QB592.G45

559.9'1

80-607848

---

For sale by the Superintendent of Documents, U.S. Government Printing Office  
Washington, D.C. 20402

# CONTENTS

	Page		Page
Abstract.....	1	Traverse geology and samples — Continued	
Introduction .....	1	Station LRV-3 .....	47
Prepermission geologic interpretations .....	4	Location .....	47
Exploration objectives and plan .....	7	Objectives .....	48
Traverse geology and samples .....	7	General observations.....	48
Classification of samples .....	15	Summary of sampling.....	48
LM /ALSEP/SEP area.....	17	Sample 72150, 55.....	48
Location .....	17	Sample 72160-64 .....	50
Objectives .....	19	Station 2.....	51
General observations.....	19	Location .....	51
Geologic discussion.....	20	Objectives .....	51
Summary of sampling.....	20	General observations.....	51
Sample 70001-70009.....	20	Geologic discussion.....	53
Sample 70011 (fuel products contamination sample) .....	23	Summary of sampling.....	59
Sample 70012 .....	24	Sample 72215 .....	59
Sample 70017 .....	24	Sample 72220-24 .....	61
Sample 70018 .....	25	Sample 72235 .....	61
Sample 70019 .....	25	Sample 72240-44 .....	62
Sample 70035 .....	25	Sample 72255 .....	62
Sample 70075 .....	27	Sample 72260-64 .....	63
Sample 70135-39, 45-49, 55-57 .....	27	Sample 72275 .....	64
Sample 70160-64, 65 .....	27	Sample 72315 .....	65
Sample 70175 .....	29	Sample 72320-24 .....	68
Sample 70180-84, 85 .....	29	Sample 72335 .....	69
Sample 70215 .....	32	Sample 72355 .....	69
Sample 70255 .....	32	Sample 72375 .....	70
Sample 70270-74, 75 .....	33	Sample 72395 .....	70
Sample 70295 .....	34	Sample 72410 .....	71
Station 1 .....	34	Sample 72415-18 .....	71
Location .....	34	Sample 72430-34 .....	73
Objectives .....	34	Sample 72435 .....	73
General observations.....	35	Sample 72440-44 .....	73
Geologic discussion.....	35	Sample 72460-64 .....	74
Summary of sampling.....	36	Sample 72500-05 .....	75
Sample 71035-37 .....	36	Sample 72535-39, 45-49, 55-59 .....	76
Sample 71040-44, 45-49, 75 .....	36	Sample 72700-05 .....	77
Sample 71055 .....	38	Sample 72735-38 .....	77
Sample 71060-64, 65-69, 85-89, 95-97 .....	39	Station 2a (LVR-4) .....	78
Sample 71130-34, 35, 36 .....	40	Location .....	78
Sample 71150-54, 55-57 .....	42	Objectives .....	78
Sample 71175 .....	42	General observations.....	78
Sample 71500-04, 05-09, 15 .....	42	Geologic discussion.....	78
Sample 71525-29, 35-39, 45-49, 55-59, 65-69, 75-79, 85-89, 95-97 .....	43	Summary of sampling.....	78
Station LRV-1 .....	44	Sample 73120-24 .....	78
Location .....	44	Sample 73130-34 .....	79
Objectives .....	44	Sample 73140-46 .....	79
General observations.....	44	Sample 73150-56 .....	79
Summary of sampling.....	45	Station 3.....	80
Sample 72130-34, 35 .....	45	Location .....	80
Station LRV-2 .....	45	Objectives .....	80
Location .....	45	General observations.....	81
Objectives .....	45	Geologic discussion.....	81
General observations.....	45	Summary of sampling.....	82
Summary of sampling.....	46	Sample 73002/73001 (upper/lower) .....	82
Sample 72140-44, 45 .....	46	Sample 73210-14 .....	83
		Sample 73215 .....	83
		Sample 73216 .....	88
		Sample 73217 .....	88

	Page		Page
Traverse geology and samples — Continued		Traverse geology and samples — Continued	
Station 3 — Continued		Station LRV-10	117
Summary of sampling — Continued		Location	117
Sample 73218	88	Objectives	117
Sample 73219	88	General observations	117
Sample 73220-25	88	Summary of sampling	117
Sample 73235	89	Sample 76130-37	117
Sample 73240-45	91	Station 6	119
Sample 73255	92	Location	119
Sample 73260-64	92	Objectives	119
Sample 73275	93	General observations	119
Sample 73280-85	93	Geologic discussion	119
Station LRV-5	94	Summary of sampling	121
Location	94	Sample 76001	121
Objectives	94	Sample 76015	122
General observations	94	Sample 76030-37	125
Summary of sampling	94	Sample 76055	126
Sample 74110-19	94	Sample 76215	127
Station LRV-6	94	Sample 76220-24	128
Location	94	Sample 76235-39, 76305-07	128
Objectives	94	Sample 76240-46	130
General observations	94	Sample 76255	131
Summary of sampling	94	Sample 76260-65	131
Sample 74120-24	94	Sample 76275	133
Station 4	95	Sample 76280-86	134
Location	95	Sample 76295	135
Objectives	95	Sample 76315	139
General observations	95	Sample 76320-24	141
Geologic discussion	96	Sample 76335	142
Summary of sampling	98	Sample 76500-06	142
Sample 74002/74001 (upper/lower)	98	Sample 76535-39, 45-49, 55-59, 65-69,	
Sample 74220	100	75-77	143
Sample 74235	101	Station 7	145
Sample 74240-49, 85-87	102	Location	145
Sample 74255	103	Objectives	145
Sample 74260	104	General observations	145
Sample 74275	106	Geologic discussion	146
Station LRV-7	106	Summary of sampling	149
Location	106	Sample 77017	149
Objectives	106	Sample 77035	151
General observations	107	Sample 77075-77	152
Summary of sampling	107	Sample 77115	154
Sample 75110-15	107	Sample 77135	156
Station LRV-8	108	Sample 77215	157
Location	108	Sample 77510-19, 25-26	159
Objectives	108	Sample 77530-39, 45	159
General observations	108	Station LRV-11	162
Summary of sampling	109	Location	162
Sample 75120-24	109	Objectives	162
Station 5	109	General observations	162
Location	109	Summary of sampling	162
Objectives	109	Sample 78120-24	162
General observations	109	Station 8	162
Geologic discussion	109	Location	162
Summary of sampling	110	Objectives	162
Sample 75015	110	General observations	162
Sample 75035	110	Geologic discussion	163
Sample 75055	111	Summary of sampling	163
Sample 75060-66	112	Sample 78135	163
Sample 75075	112	Sample 78155	165
Sample 75080-89	114	Sample 78220-24	165
Station LRV-9	117	Sample 78230-36, 38	167
Location	117	Sample 78250, 55	168
Objectives	117	Sample 78420-24	169
General observations	117	Sample 78440-44	170
Summary of sampling	117	Sample 78460-65	170
Sample 76120-24	117	Sample 78480-84	172
		Sample 78500-09, 15-18	173

# CONTENTS

V

	Page		Page
Traverse geology and samples — Continued		Geologic synthesis .....	187
Station 8 — Continued		General setting and historical framework .....	187
Summary of sampling — Continued		Southern Serenitatis basin structure .....	187
Sample 78525-28, 30, 35-39, 45-49,		Significance of the third ring .....	189
55-59, 65-69, 75-79, 85-89, 95-99 .....	175	Stratigraphy of the Taurus-Littrow valley .....	192
Station 9 .....	175	Massifs .....	192
Location .....	175	Sculptured Hills .....	194
Objectives .....	175	Highlands materials younger than the southern	
General observations .....	176	Serenitatis basin .....	194
Geologic discussion .....	176	Subfloor basalt .....	202
Summary of sampling .....	178	Volcanic ash .....	205
Sample 79002/79001 (upper/lower) .....	178	Regolith .....	208
Sample 79035 .....	178	Highlands regolith .....	208
Sample 79115 .....	178	Older regolith of the valley floor .....	209
Sample 79120-25 .....	178	Cluster ejecta .....	209
Sample 79135 .....	178	Light mantle .....	212
Sample 79155 .....	179	Structural geology .....	213
Sample 79175 .....	180	Block faulting of the highlands .....	213
Sample 79195 .....	180	Deformation of the mare surfaces .....	213
Sample 79215 .....	181	Development of the ridge-scarp system .....	217
Sample 79220-28 .....	182	References cited .....	217
Sample 79240-45 .....	184	Apollo 17 lunar surface photography, by Raymond M. Batson,	
Sample 79260-65 .....	185	Kathleen B. Larson, and Richard L. Tyner .....	225
Sample 79510-19, 25-29, 35-37 .....	186	Introduction .....	225
Station LRV-12 .....	187	Photographic procedures .....	225
Location .....	187	The photographic data set .....	225
Objectives .....	187	Cartographic procedures .....	227
General observations .....	187	References cited .....	279
Summary of sampling .....	187	Glossary .....	280
Sample 70311-15 .....	187		
Sample 70320-24 .....	187		

# ILLUSTRATIONS

[Plates are in separate case]

- PLATE
1. Geologic map of the Taurus-Littrow area.
  2. Detailed geologic map of the Apollo 17 landing site.
  - 3-9. Apollo 17 panoramas showing sample localities and features identified:
    3. Panoramas 1-4.
    4. Panoramas 5-9.
    5. Panoramas 10-14.
    6. Panoramas 15-18.
    7. Panoramas 19-22.
    8. Panoramas 23-26.
    9. Panoramas 27-29.

	Page
FIGURE	
1. Photograph showing locations of Apollo landing sites and major features of lunar nearside .....	2
2. Photograph showing Taurus-Littrow valley as viewed from orbiting LM .....	3
3. Map showing ring structure of Serenitatis basin as interpreted by Wilhelms and McCauley (1971) .....	4
4. Photograph showing dark-haloed crater .....	6
5. Map showing preplanned traverses .....	8
6. Map showing Apollo 17 traverse path and stations .....	9
7. Detailed maps showing traverse path and stations .....	10
8. Planimetric map of LM/ALSEP/SEP area .....	19
9. Partial panorama of LM and ALSEP area .....	20
10. Triangular diagram showing relative amounts of TiO <sub>2</sub> , Al <sub>2</sub> O <sub>3</sub> , and FeO+MgO in sediment samples from LM/ALSEP/SEP area .....	21
11-20. Photographs showing:	
11. Deep core site .....	22
12. Sample 70011 area .....	23
13. Sample 70017 .....	24
14. Sample 70018 .....	25

FIGURES		Page
11-20.	Photographs showing — Continued	
15.	Breccia fragment 70019 on floor of shallow 3-m crater .....	26
16.	Sample 70019 .....	26
17.	Boulder from which sample 70035 was collected and locality of 70215 .....	27
18.	Sample 70035 .....	28
19.	Sample 70075 .....	28
20.	Geophone rock and probable area from which basalt fragments 70135-57 were collected .....	29
21.	Photomicrograph of sample 70135 .....	29
22-26.	Photographs showing:	
22.	70160-65 sample site .....	30
23.	Sample 70175 .....	30
24.	Presampling view of sample 70180-85 and 70185 with reconstructed lunar surface orientation .....	30
25.	Sample 70185 .....	31
26.	View of LM area and 70035 and 70215 sample sites .....	32
27.	Photomicrograph of sample 70215 .....	32
28-30.	Photographs showing:	
28.	Sample 70255 before collection and with reconstructed lunar surface orientation .....	33
29.	Sample 70255 .....	33
30.	Sample 70275 before collection and with reconstructed lunar surface orientation .....	34
31.	Photomicrograph of sample 70275 .....	34
32.	Photograph of sample 70295 .....	35
33.	Planimetric map of station 1 .....	36
34.	Triangular diagram showing relative amounts of $\text{TiO}_2$ , $\text{Al}_2\text{O}_3$ , and $\text{FeO} + \text{MgO}$ in sediment samples from station 1 .....	37
35-38.	Photographs showing:	
35.	Samples 71055 and 71035 before collection and with reconstructed lunar surface orientation .....	38
36.	Sample 71035 .....	39
37.	Sample 71036 .....	39
38.	Sample 71037 .....	40
39.	Photomicrograph of sample 71055 .....	40
40-54.	Photographs showing:	
40.	Sample 71065 .....	40
41.	Samples 71135, 71136, and 71155 before collection and sample 71175 with reconstructed lunar surface orientation .....	41
42.	Sample 71135 .....	41
43.	Sample 71136 .....	42
44.	Sample 71155 .....	42
45.	Sample 71175 .....	42
46.	Approximate locations of rake sample (71525-97) and associated sediment sample (71500-15) .....	43
47.	Sample 71546 .....	44
48.	Sample 71548 .....	44
49.	Sample 71556 .....	44
50.	Sample 71557 .....	45
51.	Sample 71559 .....	45
52.	Sample 71565 .....	45
53.	Sample 71566 .....	46
54.	Sample 71567 .....	46
55.	Photomicrograph of sample 71569 .....	46
56-67.	Photographs showing:	
56.	Sample 71576 .....	47
57.	Sample 71577 .....	47
58.	Sample 71578 .....	47
59.	Sample 71586 .....	48
60.	Sample 71587 .....	48
61.	Sample 71588 .....	48
62.	Sample 71595 .....	48
63.	Sample 71596 .....	48
64.	LRV-1 area .....	49
65.	72130-35 sample area .....	49
66.	Sample 72135 .....	49
67.	Approximate location of sample 72140-45 .....	50
68.	Triangular diagram showing relative amounts of $\text{TiO}_2$ , $\text{Al}_2\text{O}_3$ , and $\text{FeO} + \text{MgO}$ in sediment sample 72141 .....	51
69.	Photographs showing LRV-3 sampling area and probable location of sample 72155, and 72155 in tentatively reconstructed lunar surface orientation .....	52
70.	Photograph of sample 72155 .....	53

FIGURE		Page
71.	Triangular diagram showing relative amounts of $\text{TiO}_2$ , $\text{Al}_2\text{O}_3$ , and $\text{FeO} + \text{MgO}$ in sediment sample 72161 .....	54
72.	Planimetric map of station 2 .....	55
73.	Photograph showing station 2 area .....	56
74.	Photographs showing boulder 1 at station 2; locations of samples 72215, 72235, 72255, 72275, and 72220-24; reconstructed lunar surface orientations of 72215, 72235, 72255, and 72275 .....	57
75.	Graph showing plots of $\text{FeO}$ , $\text{MgO}$ , and $\text{CaO}$ contents in relation to $\text{Al}_2\text{O}_3$ content for analyzed rocks from station 2 ...	58
76.	Triangular diagram showing relative amounts of $\text{TiO}_2$ , $\text{Al}_2\text{O}_3$ , and $\text{FeO} + \text{MgO}$ in sediment samples from station 2 .....	60
77-92.	Photographs showing:	
77.	Sample 72215 .....	61
78.	Boulder 1 at station 2, showing 72275 after collection and 72220-24, 72240-44, and 72260-64 before collection .....	63
79.	Sample 72235 .....	64
80.	Sample 72255 .....	65
81.	Sample 72275 .....	66
82.	Boulder 2 at station 2, locations of samples 72315, 72335, 72355, 72375, and 72395; reconstructed lunar surface orientations of 72315, 72335, 72355, and 72395 .....	67
83.	Sample 72315 .....	68
84.	Sample 72335 .....	69
85.	Sample 72355 .....	69
86.	Sample 72375 .....	70
87.	Sample 72395 .....	71
88.	Boulder 3 at station 2; locations of samples 72410, 72415-18, 72435, 72440-44, and 72460-64; 72435 with reconstructed lunar surface orientation .....	72
89.	Sample 72415 .....	73
90.	Sample 72435 .....	74
91.	Areas from which 72500-05 and 72535-59 were collected .....	76
92.	Areas from which 72700-05 and 72735-38 were collected .....	78
93.	Triangular diagram showing relative amounts of $\text{TiO}_2$ , $\text{Al}_2\text{O}_3$ , and $\text{FeO} + \text{MgO}$ in sediment samples 73121 and 73141 ..	80
94.	Photograph of station 2a area showing locations of samples 73120-24, 73130-34, and 73140-46 .....	81
95.	Photograph showing 2-m crater from which sample 73130-34 was collected .....	81
96.	Photographs showing location and reconstructed lunar surface orientation of sample 73155 .....	82
97.	Photograph of sample 73155 .....	83
98.	Planimetric map of station 3 .....	83
99.	Graph showing plots of $\text{FeO}$ , $\text{MgO}$ , and $\text{CaO}$ against $\text{Al}_2\text{O}_3$ for analyzed station 3 rocks .....	84
100.	Triangular diagram showing relative amounts of $\text{TiO}_2$ , $\text{Al}_2\text{O}_3$ , and $\text{FeO} + \text{MgO}$ in sediment samples from station 3 .....	85
101-104.	Photographs showing:	
101.	Drive-tube sample 73002/73001 during sampling .....	86
102.	Locations of samples 73210-14, 15-19, and 73275 .....	86
103.	Area of samples 73210-14, 15-19, and eastern part of 10-m crater at station 3 .....	86
104.	Sample 73215 .....	87
105.	Photomicrograph of sample 73215 .....	88
106-112.	Photographs showing:	
106.	Sample 73216 .....	88
107.	Sample 73217 .....	88
108.	Sample 73218 .....	89
109.	Trench at station 3; areas from which samples 73220-25, 73240-45, 73260-64, and 73280-85 were collected ..	90
110.	Presampling view and reconstructed lunar surface orientations of samples 73235, 73255, and 73275 .....	91
111.	Trench at station 3; locations of samples 73235 and 73255; reconstructed lunar surface orientation of 73255 ..	92
112.	Sample 73235 .....	96
113.	Photomicrograph of sample 73235 .....	97
114-117.	Photographs showing:	
114.	Sample 73255 .....	97
115.	Sample 73275 .....	97
116.	LRV-5 area .....	98
117.	LRV-6 area .....	98
118.	Triangular diagram showing relative amounts of $\text{TiO}_2$ , $\text{Al}_2\text{O}_3$ , and $\text{FeO} + \text{MgO}$ in sediment sample 74121 .....	99
119.	Planimetric map of station 4 .....	100
120.	Photographs showing station 4 area; locations of drive tube (74002/74001), trench samples (74220, 74240-49, 85-87, 74260), and basalt samples 74255 and 74275; 74255 with reconstructed lunar orientation .....	103
121.	Triangular diagram showing relative amounts of $\text{TiO}_2$ , $\text{Al}_2\text{O}_3$ , and $\text{FeO} + \text{MgO}$ in sediment samples from station 4 .....	104
122.	Schematic cross section of trench and double drive tube on rim crest of Shorty crater .....	105
122.1	Scanning electron micrograph of a sphere from sample 74001, 2 .....	105
123.	Photomicrograph of sample 74220 .....	105
124.	Photomicrograph of sample 74235 .....	106
125.	Photograph of sample 74255 .....	106

FIGURE	126. Photographs of sample 74275 before collection and with reconstructed lunar surface orientation.....	107
	127. Photomicrograph of sample 74275.....	107
	128. Photograph showing LRV-7 area and probable location of sample 75110-15 collection site.....	108
	129. Photograph showing LRV-8 area and probable location of sample 75120-24 collection site.....	109
	130. Planimetric map of station 5.....	110
	131. Triangular diagram showing relative amounts of $\text{TiO}_2$ , $\text{Al}_2\text{O}_3$ , and $\text{FeO}+\text{MgO}$ in sediment samples from station 5.....	111
132-135.	Photographs showing:	
	132. Locations of samples 75015 and 75035, 75035 with reconstructed lunar surface orientation.....	113
	133. Sample 75015.....	114
	134. Sample 75035.....	115
	135. Location and reconstructed lunar surface orientation of sample 75055.....	116
136.	Photomicrograph of sample 75055.....	117
137.	Photographs showing locations of samples 75060-66 and 75075 and reconstructed lunar surface orientation of 75075.....	118
138.	Photomicrograph of sample 75075.....	119
139-142.	Photographs showing:	
	139. Locations of samples 75075 and 75080-89.....	120
	140. LRV-9 area.....	121
	141. LRV-10 area.....	121
	142. Sample 76135.....	122
143.	Photomicrograph of sample 76136.....	123
144.	Photograph of North Massif showing Turning Point rock (LRV-10) and stations 6 and 7.....	123
145.	Telephoto view of North Massif.....	124
146.	Planimetric map of station 6.....	125
147.	Photograph of blocks 1 and 2 of station 6 boulder.....	126
148.	Photograph of blocks 2 and 3 at station 6.....	127
149.	Map showing lithologic subdivisions inferred by Heiken and others (1973) for station 6 boulder.....	127
150.	Graph showing plots of $\text{FeO}$ , $\text{MgO}$ , and $\text{CaO}$ contents in relation to $\text{Al}_2\text{O}_3$ content for analyzed highlands rocks from station 6.....	128
151.	Triangular diagram showing relative amounts of $\text{TiO}_2$ , $\text{Al}_2\text{O}_3$ , and $\text{FeO}+\text{MgO}$ in sediment samples from station 6.....	129
152-155.	Photographs showing:	
	152. Drive-tube sample 76001 during sampling.....	130
	153. Location of sample 76015, and sample 76015 with reconstructed lunar surface orientation.....	130
	154. Sample 76015.....	132
	155. Sample 76030-37 area before collection and sample 76320-24 site after collection.....	133
156.	Photomicrograph of sample 76035.....	133
157-160.	Photographs showing:	
	157. Sample 76055.....	133
	158. Block 4; area from which sample 76215 rock was spalled.....	134
	159. Location of sample 76215, before sampling; sample 76215 with reconstructed lunar surface orientation.....	134
	160. Sample 76215.....	135
161.	Photomicrograph of sample 76215.....	135
162-168.	Photographs showing:	
	162. Boulder-track depression from which 76220-24 was collected.....	135
	163. Locations of samples 76235-39, 76305-07, 76255, 76275, and 76295; reconstructed lunar surface orientations of 76255, 76275, and 76295.....	136
	164. Sample 76235.....	137
	165. Locations of samples 76240-46, 76260-65, and 76280-86.....	137
	166. View of block 4, LRV area at station 6.....	137
	167. Clasts and locations of samples 76235-39, 76305-07, 76255, and 76295 in block 1.....	138
	168. Sample 76255.....	139
169.	Map of slab cut parallel to $N_1$ face of sample 76255.....	140
170-174.	Photographs showing:	
	170. Sample 76275.....	140
	171. Sample 76295.....	140
	172. Blocks 2 and 3 at station 6 and contact zone from which 76315 was collected.....	141
	173. Sample 76315.....	141
	174. Sample 76320-24 site.....	142
175.	Photomicrograph of sample 76335.....	142
176.	Photograph showing rake area at station 6.....	144
177.	Photograph of sample 76535.....	144
178.	Planimetric map of station 7.....	146
179.	Graph showing plots of $\text{FeO}$ , $\text{MgO}$ , and $\text{CaO}$ contents in relation to $\text{Al}_2\text{O}_3$ content for analyzed highlands rocks from station 7.....	147
180.	Map of station 7 boulder.....	148
181.	Summary of radiometric ages for the station 7 boulder.....	149

FIGURE	182. Triangular diagram showing relative amounts of $\text{TiO}_2$ , $\text{Al}_2\text{O}_3$ , and $\text{FeO} + \text{MgO}$ in sediment sample 77531 from station 7	150
183-188.	Photographs showing:	
	183. Sample 77017	151
	184. Sample 77035	152
	185. Locations of samples 77075-77 and 77215 in 3-m boulder at station 7	153
	186. Sample 77075	154
	187. Locations of samples 77115 and 77135, and sample 77115 with reconstructed lunar surface orientation	154
	188. Sample 77115	155
189.	Photomicrograph of sample 77115	155
190-204.	Photographs showing:	
	190. Sample 77135 before collection and with reconstructed lunar surface orientation	156
	191. Sample 77135	156
	192. Sample 77215	158
	193. Sample 77515	159
	194. Sample 77516	159
	195. Sample 77517	160
	196. Sample 77519	160
	197. Sample 77535	160
	198. Sample 77536	161
	199. Sample 77537	161
	200. Sample 77538	161
	201. Sample 77539	162
	202. Sample 77545	162
	203. Station LRV-11	163
	204. Station 8 area at Sculptured Hills and telephoto view of slope above station 8	164
205.	Planimetric map of station 8	165
206.	Graph showing plots of $\text{FeO}$ , $\text{MgO}$ , and $\text{CaO}$ contents in relation to $\text{Al}_2\text{O}_3$ content for analyzed highlands rocks from stations 8 and 9	166
207.	Triangular diagram showing relative amounts of $\text{TiO}_2$ , $\text{Al}_2\text{O}_3$ , and $\text{FeO} + \text{MgO}$ in sediment and regolith breccia from station 8	167
208.	Photographs showing sample 78135 before collection and with reconstructed lunar surface orientation	168
209.	Photograph of sample 78135	169
210.	Photograph showing sample 78155 in meter-size "pit crater"	169
211.	Photomicrograph of sample 78155	170
212.	Photograph of sample 78220-24 site	170
213.	Photographs showing samples 78235, 78236, and 78238 before collection, and reconstructed lunar surface orientations of samples 78235 and 78236	171
214.	Photograph of sample 78236	172
215.	Graph showing plots of $\text{MgO}$ , $\text{FeO}$ , and $\text{CaO}$ contents in relation to $\text{Al}_2\text{O}_3$ content for sample 78235	173
216.	Photograph showing trench and locations of samples 78420-24, 78440-44, 78460-65, and 78480-84	173
217.	Photograph of 78500-09, 15-18 sample area	174
218.	Photomicrograph of sample 78505	174
219.	Photograph of sample 78506	174
220.	Photograph of sample 78507	175
221.	Photograph showing area of rake sample 78525-99	176
222.	Planimetric map of station 9	176
223.	Triangular diagram showing relative amounts of $\text{TiO}_2$ , $\text{Al}_2\text{O}_3$ , and $\text{FeO} + \text{MgO}$ in sediment samples and regolith breccia from station 9	177
224-227.	Photographs showing:	
	224. Locations of drive-tube sample (79002/79001), trench samples 79220-28, 79240-45, 79260-65, rock sample 79215, closeup view of trench, and reconstructed lunar surface orientation of 79215	179
	225. Sample 79035,1	180
	226. Locations of samples 79115, 79120-25, 79135, and 79510-37	181
	227. Sample 79115	181
228.	Photomicrograph of sample 79115	182
229-234.	Photographs showing:	
	229. Sample 79135	182
	230. Sample 79155	183
	231. Reconstructed lunar surface orientation of sample 79175, and 79175 before collection	183
	232. Sample 79175	184
	233. Samples 79175 and 79195 before collection	185
	234. Sample 79195	186
235.	Photomicrograph of sample 79215	187
236.	Photograph showing probable location of samples 70311-15 and 70320-24 at station LRV-12	187
237.	Photograph of sample 70315	187

	Page
FIGURE 238. Map showing revised ring structure of Mare Serenitatis area .....	188
239. Lunar Orbiter image showing Rook Mountains in the southeastern quadrant of the Orientale basin.....	190
240. Photograph showing mountainous terrain southeast of Mare Serenitatis in the Apollo 17 region .....	190
241. Lunar Orbiter images showing eastern part of the Orientale basin.....	191
242. Cross section showing relations inferred among the major subregolith units.....	193
243. Telephoto panorama showing light-colored and bouldery patches on South Massif.....	195
244. Graphs showing plots of FeO, MgO, and CaO contents in relation to Al <sub>2</sub> O <sub>3</sub> content for all analyzed rocks from Apollo 17 highlands.....	196
245. Triangular diagram showing relative amounts of TiO <sub>2</sub> , Al <sub>2</sub> O <sub>3</sub> , and FeO + MgO in sediment samples grouped by station and stratigraphic unit .....	197
246. Triangular diagram showing relative amounts of FeO, CaO, and MgO in sediment samples grouped by station and stratigraphic unit .....	198
247. Graphic summary of published radiometric ages for rock samples from Apollo 17 highlands.....	200
248. Cross sections showing relations inferred among subfloor basalt and overlying units.....	203
249. Silica variation diagrams for Apollo 17 basalt.....	204
250. Graphic summary of published radiometric ages for subfloor basalt and volcanic ash .....	205
251. Histogram of elevation differences between precrater surfaces and floors of flat-floored or central-mound craters ....	207
252. Map showing areal distribution of clustered craters in Taurus-Littrow area.....	210
253. Map showing theoretical distribution of ejecta from larger craters in Apollo 17 landing area .....	211
254. Photograph showing major linear topographic breaks in Taurus-Littrow highlands .....	214
255. Diagram showing cumulative lengths of lineaments of figure 254 .....	215
256. Map showing topographic contours on mare basalt units .....	216
257. Sketch showing how morphology of Lee-Lincoln scarp might result from high-angle faulting .....	217
258. Sketched profiles showing lunar surface areas photographed with Apollo 17 500-mm camera .....	226
259. Perspective grid used for estimating size and distance.....	278

## TABLES

	Page
TABLE 1. General classification scheme for lunar samples .....	15
2. Summary classification of Apollo 17 samples larger than 5 g .....	18
3. Components of 90-150- $\mu$ m fractions of samples from approximately 27 to 59 cm depth in the deep core .....	22
4. Chemical analyses of deep core samples.....	23
5. Comparison of southern Serenitatis and Orientale basin structures.....	189
6. Usage of film on the lunar surface during the Apollo 17 mission .....	227
7. Chronological listing of 70-mm Apollo 17 lunar surface pictures .....	228
8. Sequential listing within each 70-mm magazine—Apollo 17 lunar surface pictures .....	250
9. Apollo 17 lunar surface film usage by camera number.....	278

# THE GEOLOGIC INVESTIGATION OF THE TAURUS-LITTROW VALLEY: APOLLO 17 LANDING SITE

By EDWARD W. WOLFE, NORMAN G. BAILEY, BAERBEL K. LUCCHITTA, WILLIAM R. MUEHLBERGER, DAVID H. SCOTT, ROBERT L. SUTTON, and HOWARD G. WILSHIRE

## ABSTRACT

Astronauts Cernan and Schmitt, of Apollo 17, landed in the Taurus-Littrow valley of the Moon on December 11, 1972. Their major objectives were (1) to sample very ancient lunar material such as might be found in pre-Imbrian highlands as distant as possible from the Imbrium basin and (2) to sample pyroclastic materials that had been interpreted as significantly younger than the mare basalts returned from previous Apollo landing sites. The crew worked approximately 22 hours on the lunar surface; they traversed about 30 km, collected nearly 120 kg of samples, took more than 2,200 photographs, and recorded many direct geologic observations. The lunar surface data, sample results, and geologic interpretation from orbital photographs are the bases for this geologic synthesis.

The Taurus-Littrow massifs are interpreted as the upper part of the thick, faulted ejecta deposited on the rim of the transient cavity of the large southern Serenitatis basin, which was formed about 3.9 to 4.0 b.y. ago by the impact of a planetesimal. The target rocks, predominantly of the dunite-anorthosite-norite-troctolite suite or its metamorphosed equivalents, were fractured, sheared, crushed, and melted by the impact. The resulting mixture of crushed rock and melt was transported up and out of the transient cavity and deposited on and beyond its rim. Hot fragmental to partly molten ejecta and relatively cool cataclasite and relict target rocks were intermixed in a melange of lenses, pods, and veins. Crystallization of melts and thermal metamorphism of fine-grained fragmental debris produced breccia composed of rock and mineral fragments in a fine-grained, coherent, crystalline matrix. Such breccia dominates the massif samples.

High-angle faults that bound the massifs were activated during formation of the basin, so that structural relief of several kilometers was imposed on the ejecta almost as soon as it was deposited. Massive slumping that produced thick wedges of colluvium on the lower massif slopes probably occurred nearly contemporaneously with the faulting. Material of the Sculptured Hills, perhaps largely cataclasite excavated from the southern Serenitatis basin by the same impact, was then deposited on and around the massifs.

Basalt, estimated to be about 1,400 m thick in the landing site, flooded the Taurus-Littrow graben before approximately 3.7 b.y. ago. The basalt (subfloor basalt) is part of a more extensive unit that was broadly warped and cut by extensional faults before the accumulation in Mare Serenitatis of younger, less deformed basalts that overlap it. A thin volcanic ash unit, probably about 3.5 b.y. old, mantled the subfloor basalt and the nearby highlands. It, too, was subsequently overlapped by the younger basalt of Mare Serenitatis.

In the time since deposition of the volcanic ash, continued bombardment by primary and secondary projectiles has produced regolith, which is a mechanical mixture of debris derived mainly from the subfloor basalt, the volcanic ash, and the rocks of the nearby massifs and Sculptured Hills. The regolith and the underlying vol-

canic ash form an unconsolidated surficial deposit with an average thickness of about 14 m, sufficiently thick to permit abnormally rapid degradation of the smaller craters, especially those less than 200 m in diameter, so as to create a surface that appears less cratered than other mare surfaces. Admixed volcanic ash gives the surface a distinctive dark color, which, in combination with the less cratered appearance, led to its interpretation before the mission as a young dark mantling unit.

The uppermost part of the regolith over much of the landing area is basalt-rich ejecta from the clustered craters of the valley floor. Most of the valley-floor craters are interpreted as part of a secondary cluster formed by projectiles of ejecta from Tycho. When they struck the face of the South Massif, the projectiles mobilized fine-grained regolith material that was deposited on the valley floor as the light mantle. Exposure ages suggest that the swarm of secondary projectiles struck the Taurus-Littrow area about 100 m.y. ago.

The Lee-Lincoln fault scarp is part of an extensive system of wrinkle ridges and scarps that transect both mare and highlands rocks. The scarp cuts the crater Lara, but the major part of the displacement occurred before deposition of the light mantle. Small extensional faults cut the surface of the light mantle west of the Lee-Lincoln scarp.

## INTRODUCTION

Apollo 17, the sixth and last manned lunar landing of the Apollo program, touched down in a mountain valley near the edge of Mare Serenitatis (fig. 1) on December 11, 1972. The landing site, south of the Taurus Mountains and the crater Littrow, was named Taurus-Littrow to distinguish it from an earlier proposed landing site nearby. During their 72-hour stay at Taurus-Littrow, astronauts Eugene A. Cernan and Harrison H. Schmitt spent more than 22 hours on the lunar surface, traversed about 30 km, collected nearly 120 kg of rocks and soil, and took more than 2,200 photographs. Their traverses, sampling, direct observations, and photographs spanned the full width of the spectacular Taurus-Littrow valley (fig. 2) to become the superlative finale to the first chapter of manned planetary exploration.

A chronological approach seems the most direct way to recount the geologic investigation of the Taurus-Littrow area. Hence this report consists of three major parts: (1) premission geologic interpretation based mainly on photogeology; (2) field and sample data

(including results published through 1976), and (3) postmission geologic synthesis.

Examination of the high-resolution photographs taken from lunar orbit by Apollo 15 indicated that a landing between Mare Serenitatis and Mare Crisium would be attractive. In February 1972, the National Aeronautics and Space Administration (NASA) selected the Taurus-Littrow site for exploration by

Apollo 17 (Hinnert, 1973). Before that time, published geologic maps of the Taurus-Littrow area consisted of a map of the Mare Serenitatis region (Carr, 1966), which was prepared from telescopic photographs and observations that included part of the Taurus-Littrow highlands west of the landing site, and the 1:5,000,000-scale map of the near side of the Moon (Wilhelms and McCauley, 1971). In addition, geologic sketch maps



FIGURE 1.—Full-moon photograph showing locations of Apollo landing sites and major features of lunar nearside. (Telescopic photograph L 18, taken January 17, 1946, from Lick Observatory, Mount Hamilton, Calif.)

prepared from Apollo 15 orbital photographs (Carr, 1972; El-Baz, 1972) were included in the Apollo 15 Preliminary Science Report.

Early in 1972, geologic study of the Taurus-Littrow area was greatly accelerated as preparations for Apollo 17 began. Utilizing Apollo 15 photographs, Scott and Carr (1972) prepared a 1:250,000-scale geologic map of the Taurus-Littrow region, Lucchitta (1972) prepared a 1:50,000-scale map of the Taurus-Littrow valley and its bordering highlands, and Wolfe and Freeman (1972)

prepared a 1:25,000-scale geologic map as the basis for detailed traverse planning. During this period, Scott and Pohn (1972) completed the 1:1,000,000-scale map of the Macrobis quadrangle, which includes the Apollo 17 landing site and spans almost the entire highland region between Mare Serenitatis and Mare Crisium. Related investigations also underway before the mission included a theoretical study of lunar cinder cones and the mechanics of their eruption (McGetchin and Head, 1973), a model for distribution of basin ejecta



FIGURE 2.—View to west of Taurus-Littrow valley from orbiting Lunar Module. South Massif, seen beyond orbiting Command Module (CM), is more than 2 km high; the light mantle projects northeast across valley floor from its base. Crossing the 7-km-wide valley floor and intersecting North Massif near right edge of photograph is east-facing Lee-Lincoln scarp. Circled cross shows landing point. (NASA photograph AS17-147-22466.)

and the resulting stratigraphy of the massifs (McGetchin and others, 1973), a structural analysis of the Taurus-Littrow region (Head, 1974a), an evaluation of the light mantle and its depositional mechanism (Howard, 1973), and an analysis of the composition and physical properties of the dark mantle (Pieters and others, 1973). The results of these studies were used by the Apollo 17 planners in the effort to maximize the scientific return from the mission.

Detailed plans for geologic exploration of the Apollo 17 site were prepared largely by a consortium that included V. L. Freeman, J. W. Head, W. R. Muehlberger, H. H. Schmitt, and E. W. Wolfe. The plans were subject to critical review and modification by NASA scientific and engineering panels. Special credit for the scientific success of the Apollo 17 mission is due J. R. Sevier, Chairman of the Traverse Planning Subcommittee of the Science Working Panel, and R. A. Parker, Apollo 17 Mission Scientist, both of the Manned Spacecraft Center (now the Lyndon B. Johnson Space Center). With patience and diplomacy, they integrated the lunar surface experiments and investigations and acted as liaison between the lunar surface science and operations communities.

Overall responsibility for planning the geologic exploration, preparing the crew for the scientific task, providing geologic guidance during the mission on the lunar surface, and interpreting the results of the field observations rested with the Apollo Field Geology Investigation Team. The team members, acting under the leadership of W. R. Muehlberger, principal investigator, were N. G. Bailey, R. M. Batson, V. L. Freeman, M. H. Hait, J. W. Head, H. E. Holt, K. A. Howard, E. D. Jackson, K. B. Larson, B. K. Lucchitta, T. R. McGetchin, Harold Masursky, L. R. Page, D. L. Peck, V. S. Reed, J. J. Rennilson, D. H. Scott, L. T. Silver, R. L. Sutton, D. E. Stuart-Alexander, G. A. Swann, S. R. Titley, N. J. Trask, R. L. Tyner, G. E. Ulrich, H. G. Wilshire, and E. W. Wolfe. Published post-mission reports of this group (Apollo Field Geology Investigation Team, 1973; Muehlberger and others, 1973) and unpublished reports (in particular, Apollo Field Geology Investigation Team, 1975) have been used extensively in this report in the sections dealing with traverse geology and postmission geologic interpretations.

The premission geologic maps are not reproduced here. The Apollo 17 orbital photographs of the Taurus-Littrow area are superior to the Apollo 15 photographs used for premission mapping, and a new 1:250,000-scale map (pl. 1) has been prepared. This map is similar to the premission map of Scott and Carr (1972), but it portrays more structural detail and embodies stratigraphic concepts developed as a consequence of

the mission results. A new 1:25,000-scale geologic map (pl. 2) was also prepared. It incorporates the premission mapping of Wolfe and Freeman (1972) with additional geologic details from Apollo 17 panoramic camera photographs. No revised version of the 1:50,000-scale map was prepared, because the premission map (Lucchitta, 1972) adequately portrays the distribution of units.

Planimetric station maps (for example, fig. 8), traverse maps (figs. 6 and 7), and panoramas (pls. 3-9) were prepared largely by R. M. Batson, K. B. Larson, and R. L. Tyner. Their methods are described in the section entitled, "Apollo 17 Lunar Surface Photography."

We thank G. H. Heiken (Los Alamos Scientific Laboratory) and H. J. Moore for their helpful critical reviews of the manuscript.

### PREMISSION GEOLOGIC INTERPRETATIONS

The Taurus-Littrow area is predominantly a highlands region near the intersection of Mare Serenitatis and Mare Tranquillitatis (fig. 3). Stuart-Alexander and Howard (1970) and Hartmann and Wood (1971) interpreted the Serenitatis basin as one of the Moon's old circular impact basins but considered it younger than basin structures associated with Mare Tranquillitatis.

Wilhelms and McCauley (1971) mapped the Serenitatis basin as a structure of four rings concentric to a single basin center (fig. 3). The diameter of their outermost ring is about 1,400 km. The outer two rings of their inferred basin structure are difficult to recog-

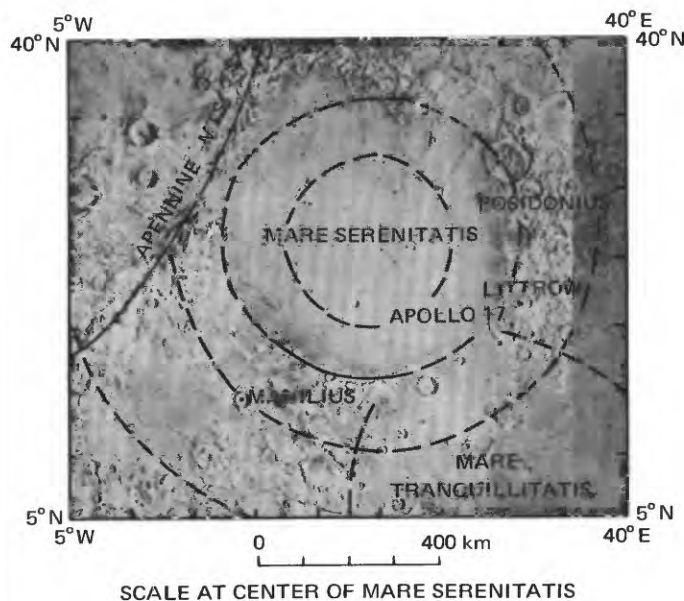


FIGURE 3.—Ring structure of Serenitatis basin as shown by Wilhelms and McCauley (1971).

nize; only the first ring, defined by wrinkle ridges within Mare Serenitatis, and segments of the second ring, defined by the discontinuous mountainous border of Mare Serenitatis, are distinct. Hence, Stuart-Alexander and Howard (1970) and Hartmann and Wood (1971) suggested that the second ring, less than 700 km in diameter, is the basin rim. As shown by Wilhelms and McCauley (1971), the crest of the second ring is slightly west of the Apollo 17 landing site.

The dominance of feldspathic impact breccia collected from other highlands localities by Apollos 14, 15, and 16 led Lucchitta (1972), Scott and Carr (1972), and Wolfe and others (1972a,b) to suggest that the Taurus-Littrow massifs would be largely impact breccia. However, a cautious alternate hypothesis—that the massifs might be of volcanic origin—was based on their domelike shapes.

There were various opinions about the origin of the massif breccias to be sampled. Wilhelms and McCauley (1971) interpreted the massifs to be primarily prebasin rocks uplifted during basin formation. This interpretation was adopted by Carr, Howard, and El-Baz (1971) for the massifs of the Apennine Mountains, which bound the Imbrium basin. In contrast, Scott and Carr (1972) wrote that the highlands in the Taurus-Littrow area are probably mostly breccia formed by the Serenitatis impact and preexisting breccia excavated by the impact. Lucchitta (1972) and McGetchin, Settle, and Head (1973) suggested that, while Serenitatis ejecta would be dominant in the massifs, it might be thin enough so that layers of ejecta from older basins would be exposed beneath it in the lower parts of the massifs. The general consensus was that post-Serenitatis crater and basin ejecta, particularly from the Imbrium and Crisium basins, might mantle or cap the massifs.

Detailed mapping (Lucchitta, 1972; Wolfe and Freeman, 1972) showed that rock ledges are exposed high on the massifs and that boulders had rolled from ledges to the valley floor. It was expected that the lower slopes of the massifs as well as the bounding faults were covered by talus from the upper parts of the massifs (Wolfe and others, 1972b).

The Sculptured Hills unit (hilly terra material of Scott and Carr, 1972; hilly material of Lucchitta, 1972) is characterized by closely spaced domical hills and is widespread in the highlands between the Serenitatis and Crisium basins. In comparison with the massifs, boulders and rocky ledges are relatively scarce in the Sculptured Hills, which suggested that they might be underlain by less coherent material that is lithologically distinct from the massif material (Wolfe and others, 1972b). However, the premission geologic mappers (Lucchitta, 1972; Scott and Carr, 1972; Wolfe and

Freeman, 1972) agreed that the unit most probably consists mainly of basin ejecta. Lucchitta (1972) and Head (1974a) noted the similarity in distribution and morphology of the Sculptured Hills unit of the Serenitatis basin and the Alpes Formation of the Imbrium basin, a relation from which Head interpreted the Sculptured Hills materials to be related to the Serenitatis impact.

A unit of low hills material was mapped locally within the Taurus-Littrow valley along the margins of the more prominent highland masses (Lucchitta, 1972; Wolfe and Freeman, 1972). It was interpreted as down-faulted highlands material or deposits formed by mass wasting of material from the massifs or the Sculptured Hills.

The premission geologic mappers interpreted the smooth surface of the Taurus-Littrow valley floor as indicating partial filling of the valley by material that behaved as a fluid during emplacement. Prior to Apollo 16, there probably would have been little reluctance to interpret the filling as basaltic lava flows, but caution was inspired by the discovery at the Apollo 16 site that the plains-forming Cayley Formation in that area consists of feldspathic impact breccia (Muehlberger and others, 1972). Hence, the valley filling was variously called mare or plains material (Scott and Carr, 1972), plains material (Lucchitta, 1972), and subfloor material (Wolfe and Freeman, 1972), and it was interpreted as either lava or impact products of Imbrian age. Abundant blocks up to several meters across were mapped on the walls and rims of many of the larger craters of the Taurus-Littrow valley floor (Wolfe and Freeman, 1972). These were interpreted as fragments of subfloor material excavated by crater impacts.

The valley floor, its westward extension between the Taurus-Littrow highlands and Mare Serenitatis, and discontinuous patches in the nearby highlands are covered by smooth dark material that looks less intensely cratered than the basalt filling of Mare Serenitatis. No blocks could be seen in orbital photographs with approximately 2-m resolution. This dark mantle was believed to overlie craters of early Copernican age and to be pocked by later Copernican craters. Although Scott and Carr (1972) noted that dark mantle material appeared to be overlapped by mare basalt of Imbrian age in the northwestern part of their map area, and that similar-looking material seemed to predate mare basalt along the southwestern edge of Mare Serenitatis, the unit was interpreted in the landing area as a young pyroclastic deposit up to tens of meters thick. Numerous dark craters, pits, and fissures in the Taurus-Littrow region were considered to be possible vents. Shorty crater, near the northeastern margin of the light mantle (called bright mantle in some premission

reports), has a dark rim and halo; El-Baz (1972) and Scott and Carr (1972) suggested that it, specifically, might have been either a vent for dark volcanic ash or an impact crater that excavated dark material from beneath the light mantle.

Particular interest in finding volcanic vents of Copernican age at the Apollo 17 site was generated by visual observations of the Apollo 15 Command Module pilot (El-Baz and Worden, 1972). In subsequent interpretation of those observations and of Apollo 15 orbital photographs, El-Baz (1972) interpreted dark-haloed craters (fig. 4) as probable cinder cones from which the dark mantling pyroclastic material was extruded. In a related model study, McGetchin and Head (1973) applied well-documented parameters from the eruption of Northeast Crater at Mount Etna to theoretical lunar conditions of vacuum and reduced gravity. They found that the lunar equivalent of the small cinder cone on Mount Etna would be less than a tenth as high and about four times as broad as its terrestrial counterpart. Maximum slope angles would be less than  $2^\circ$  instead of the  $30^\circ$  typical of terrestrial cinder cones, and ballistic ejecta would have been thrown more than six times as far. The Mount Etna cone, in the lunar environment, would be 3 m high and 1,200 m across, with

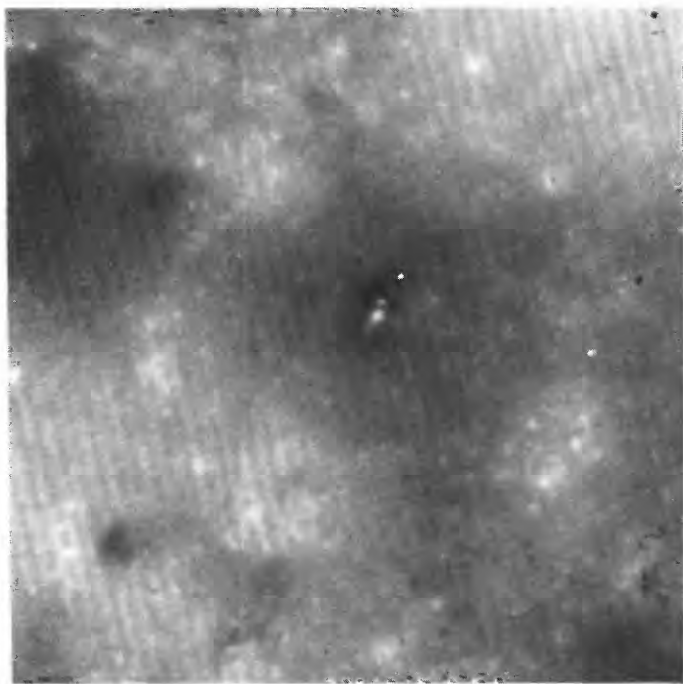


FIGURE 4.—Dark-haloed crater about 15 km west of Apollo 17 landing site. Crater was interpreted and illustrated as a probable volcanic cone (El-Baz and Worden, 1972; El-Baz, 1972) and mapped as a possible volcanic vent by Scott and Carr (1972) and Lucchitta (1972). Crater diameter is approximately 100 m. North at top. (Portion of Apollo 15 panoramic camera photograph AS15-9554.)

a ballistic range of nearly 2 km. The obvious implication was that vents so low and broad as to be unrecognizable in the orbital photographs could easily have produced overlapping pyroclastic deposits that cover the entire valley floor.

The raylike light mantle extends 6.5 km northeast across the Taurus-Littrow valley from the base of the South Massif. The premission mappers unanimously regarded it as the deposit of a relatively recent avalanche of debris from the face of the South Massif. No blocks could be detected in orbital photographs with 2-m resolution. The light mantle was estimated to thin from about 20 m near the South Massif to a feather edge at its distal end (Wolfe and others, 1972a). Underlying older craters and the fresh Lee-Lincoln fault scarp, both interpreted as older than the light mantle (Lucchitta, 1972; Wolfe and others, 1972b; Howard, 1973), are distinct even though mantled.

The avalanche was thought to have been initiated perhaps by a violent seismic event (Lucchitta, 1972) or by the impact of ejecta from a large, distant impact crater, possibly Tycho (Scott and Carr, 1972; Lucchitta, 1972). At the crest of the South Massif, Lucchitta as well as Scott and Carr mapped a cluster of secondary craters of Copernican age and indicated that they could have been formed by ejecta from Tycho. Scott and Carr suggested the additional hypothesis that the light mantle might consist of secondary crater ejecta intermixed with South Massif material. Howard (1973) described similar but less extensive lunar avalanches that were apparently triggered when secondary projectiles impinged on steep slopes that face away from the primary craters.

The light mantle was considered young because only late Copernican craters are superimposed on its surface. Generally, it appeared to overlie the dark mantle. However, Lucchitta (1972) and Scott and Carr (1972) recognized ambiguous age relations in places where the boundary was diffuse. Hence, Scott and Carr (1972) suggested that the slide and the dark mantle inter-finger and that, at least in part, they were deposited concurrently.

Chains and clusters of craters of Copernican age are abundant on the valley floor and in nearby highlands. The large central cluster in the landing area contains distinct 500- to 700-m craters (for example, craters Sherlock, Steno, and Emory, pl. 2) and abundant closely spaced or overlapping 100- to 300-m craters. Blocky light-colored patches in the walls and rims of the larger craters in particular were interpreted as crater materials exposed in windows through the overlying dark mantle. Scott and Carr (1972) and Lucchitta (1972) suggested that the Copernican clusters were formed by secondary projectiles from Tycho. More

subdued large craters near 700 m in diameter (craters Camelot, Henry, Shakespeare, and Cochise, pl. 2) were interpreted as possible secondary craters produced by ejecta from Römer (Lucchitta, 1972).

The deformational history of the Taurus-Littrow region was outlined by Scott and Carr (1972) and discussed in detail by Head (1974a). They concluded that systems of northwest- and northeast-trending fractures, the lunar grid (Strom, 1964), predated the Serenitatis impact and acted as loci along which faulting was more pronounced during later deformation. Major grabens, including the Taurus-Littrow valley, were formed radial and concentric to the Serenitatis basin by the Serenitatis impact. The steep-sided massif blocks now stand where these trends parallel the older lunar grid. Head (1974a) summarized evidence that, in other large impact basins, massifs also occur in regions where basin radials parallel the lunar grid. Imbrium-basin radials are parallel to the northwest-trending faults that bound the massifs. Possibly these faults were rejuvenated by the Imbrium impact. At a later time smaller grabens such as the Rimae Littrow, largely concentric to Serenitatis, were formed on the plains adjacent to the mare. These grabens, which are truncated or flooded by younger mare basalts, may have resulted from stresses due to isostatic readjustment of the Serenitatis basin or adjustments related to the accumulation of the mare fill. Scott and Carr (1972) mapped a few still younger grabens that are superimposed on the younger basalts of Mare Serenitatis.

The youngest deformational feature recognized prior to the mission was the east-facing Lee-Lincoln scarp. Locally as high as 80 m, it crosses the valley floor and continues onto the North Massif. The scarp consists of north- and northwest-striking segments, each on the order of 5 km long. Some segments are single, continuous, approximately straight scarps; others are zones of discontinuous en echelon scarps (Wolfe and others, 1972b). Head (1974a) suggested that it was either a high-angle reverse fault with frequent changes of strike where pre-existing structures were reactivated or a normal fault dipping gently but variably eastward. The scarp was generally interpreted as older than the dark and light mantles; but segments of it in the light mantle are so sharp as to suggest that some movement is younger than the light mantle (Lucchitta, 1972; Wolfe and others, 1972b).

#### EXPLORATION OBJECTIVES AND PLAN

Two major geologic objectives of the Apollo 17 mission were identified by the NASA Ad Hoc Site Evaluation Committee before selection of the Taurus-Littrow site (Hinnert, 1973). They were (1) sampling of very old lunar material such as might be found in pre-

Imbrian highlands as distant as possible from the Imbrium basin and (2) sampling of volcanic materials significantly younger than the mare basalts returned from the Apollos 11, 12, and 15 sites (that is, younger than about 3 b.y. old). Photogeologic interpretation had suggested that such young volcanic materials on the moon were pyroclastic, which would make them attractive not only for extending our knowledge of the Moon's thermal history, but also because they might provide a record of volatile materials from the Moon's interior; furthermore, they might contain xenoliths of deep-seated lunar rocks.

The Taurus-Littrow valley seemed ideally suited for these mission objectives. Accordingly, the major objectives for observation and sampling during the mission, ranked in order of decreasing priority, were (1) highlands (massifs and Sculptured Hills), (2) dark mantle, and (3) subfloor material.

Lunar Roving Vehicle (LRV) traverses were designed to achieve these objectives during the three extravehicular activity (EVA) periods (fig. 5). Extensive sampling and observations of both the South Massif and the North Massif as well as of the Sculptured Hills were planned to provide data on areal variation in the highlands materials. It was hoped that vertical variation in the South Massif might be reflected by lateral variation in the light mantle. Therefore, three sample stations on the light mantle were planned, with intermediate stops in which surficial materials would be sampled by scoop from the LRV.

Dark mantle material was to be examined and collected at several stations and LRV stops on the valley floor. Planned stops included the rims of the large craters Emory, Sherlock, and Camelot, where it was hoped that contact relations could be examined between the young dark mantle and the older crater rim, wall, and floor materials. Blocks larger than 2 m on the rims of these craters had been interpreted as ejecta from the subfloor unit; they were the prime targets for observation and sampling of subfloor material. Stops at Shorty and Van Serg craters were planned for study and collection of dark mantle material supposedly excavated by impacts or erupted from volcanic vents. The area around the lunar module (LM) and several LRV sample stops would provide opportunities for observation and sampling of the typical smooth dark mantle surface of the valley floor. Sampling of the dark mantle at different locations would provide information about lateral variation.

#### TRAVERSE GEOLOGY AND SAMPLES

The actual traverse (fig. 6) closely approximated the planned one. Unfortunately, shortage of time prevented visits to Emory and Sherlock craters. The major

part of EVA-1 was devoted to deployment of the Apollo Lunar Surface Experiments Package (ALSEP) near the landing point. Numerous samples and a deep drill core were collected in the LM/ALSEP/SEP area (SEP denotes the transmitter for the Surface Electrical Properties experiment). EVA's 2 and 3 were devoted primarily to exploration and sampling of the South and North Massifs, light mantle, Sculptured Hills, subfloor basalt, and the dark surficial materials of the valley floor. Gravity-meter readings were recorded during

these EVA's as part of the Traverse Gravimeter experiment.

Detailed maps of the traverses are shown in figure 7. In addition to showing stations and LRV stops, the maps show the location of the transmitter for the Surface Electrical Properties (SEP) experiment and the localities where explosive packages (EP's) for the Lunar Seismic Profiling experiment (LSPE) were deployed. Also shown are the positions from which the astronauts took 360° photographic panoramas, which

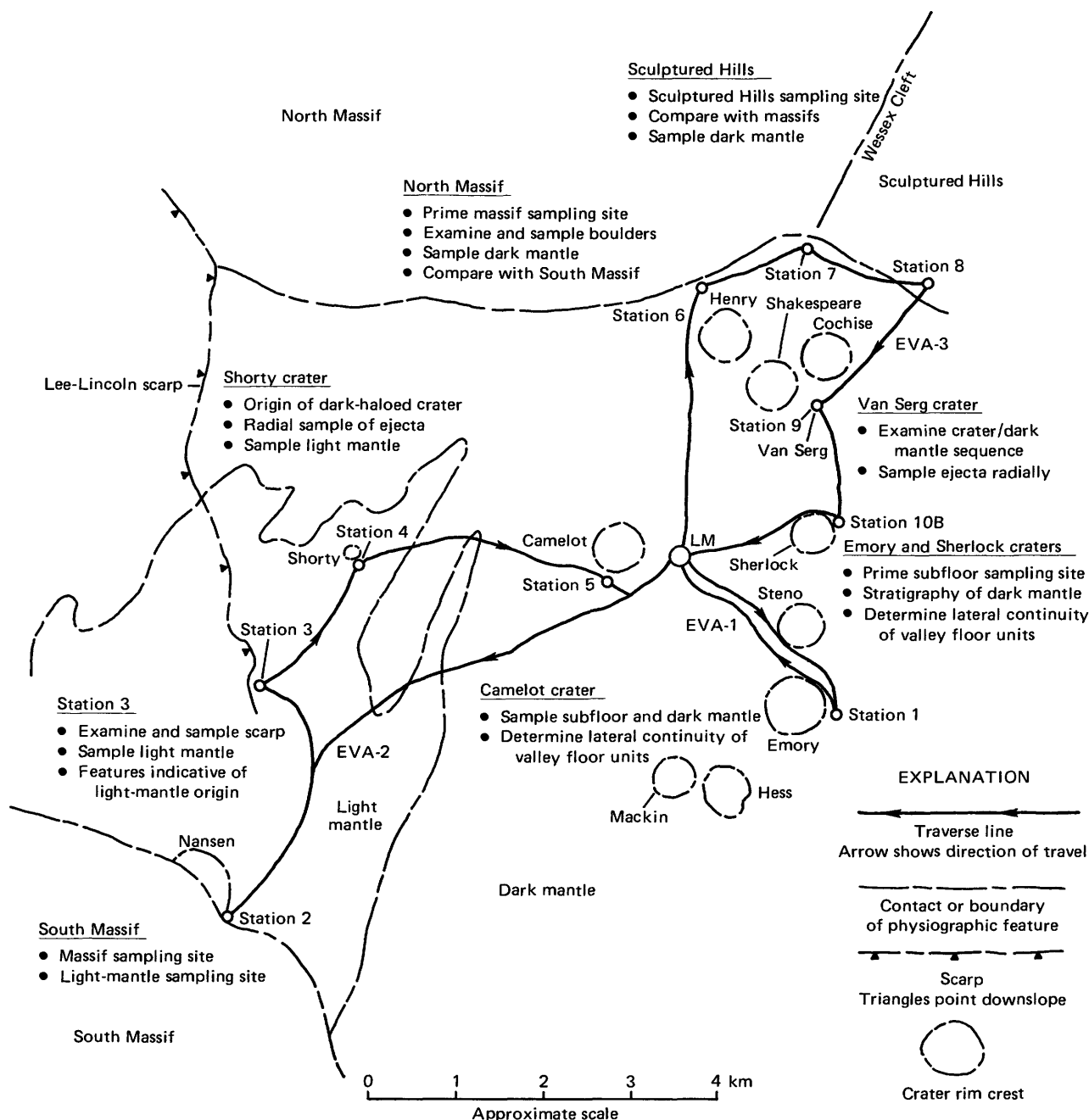


FIGURE 5.—Preplanned traverses and geologic objectives (after Muehlberger and others, 1973).

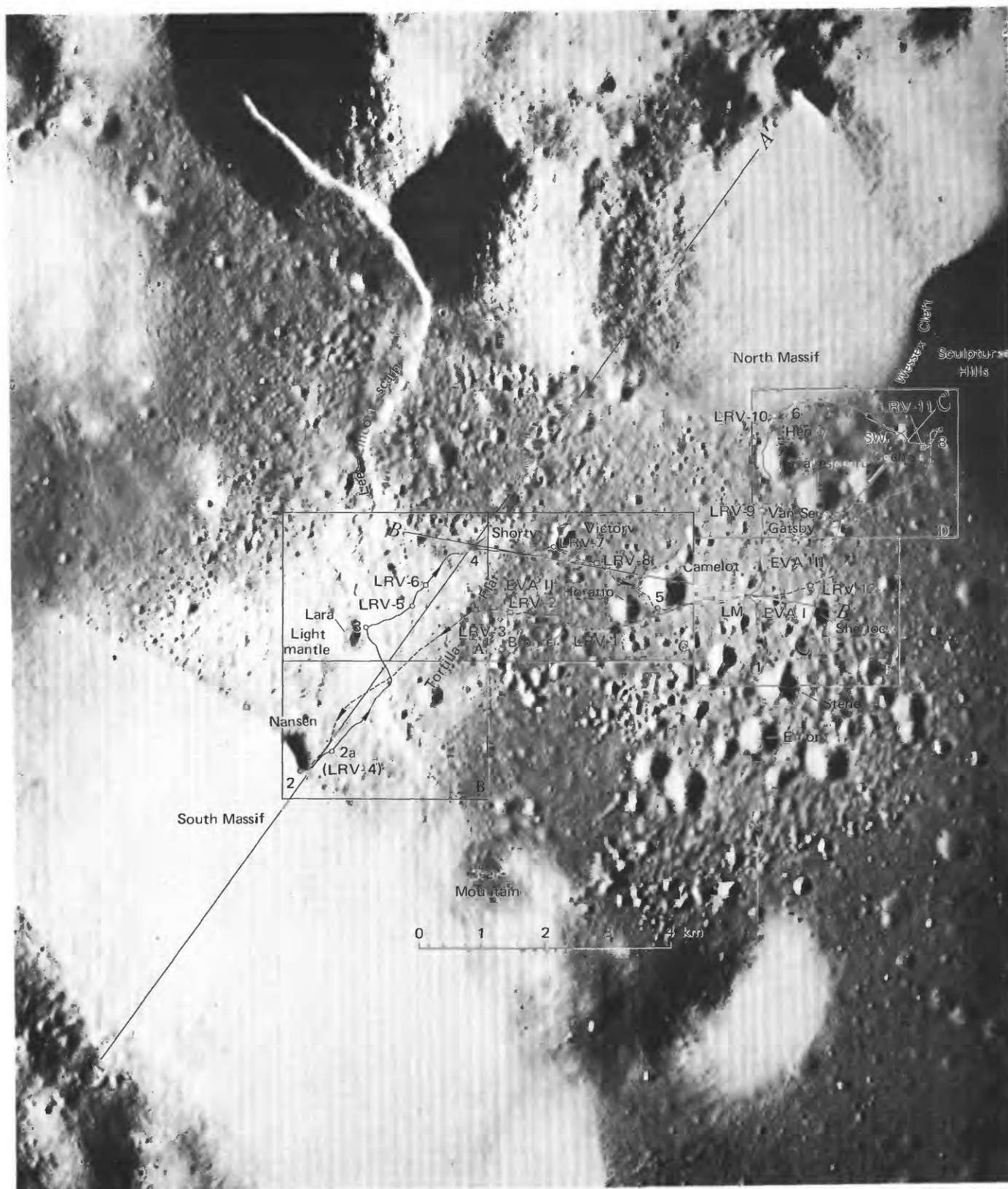


FIGURE 6.—Apollo 17 traverse path, stations (LM and 1 through 9), and Lunar Rover sample stops (LRV-1 through LRV-12). Circles, locations whose positions are known within 10 m; squares, approximate locations; solid line, traverse path, derived in part from very long base interferometry by I. M. Salzberg, Goddard Space Flight Center; dashed line, approximate traverse path; arrows, direction of travel. Lettered boxes (A through E), outlines of detailed traverse maps (fig. 7). Cross section of figure 242 is along line A-A'; cross sections of figure 248 are along lines B-B' and C-C'. (NASA panoramic camera photograph AS17-2309.) (Modified from Muehlberger and others, 1973; Apollo Field Geology Investigation Team, 1973.)



FIGURE 7.—Detailed maps showing traverse path and stations. Locations of detailed maps are shown on figure 6. Triangle, site of panorama, location accurate within 10 m, not shown in LM area; EP-1 through EP-8, lunar seismic profiling experiment (LSPE) explosive packages; SEP, transmitter for Surface Electrical Properties experiment; ALSEP, location of the central station for the Apollo Lunar Surface Experiments Package; other symbols as in figure 6. (NASA panoramic camera photograph AS 17-2309.) (Modified from Muehlberger and others, 1973.)

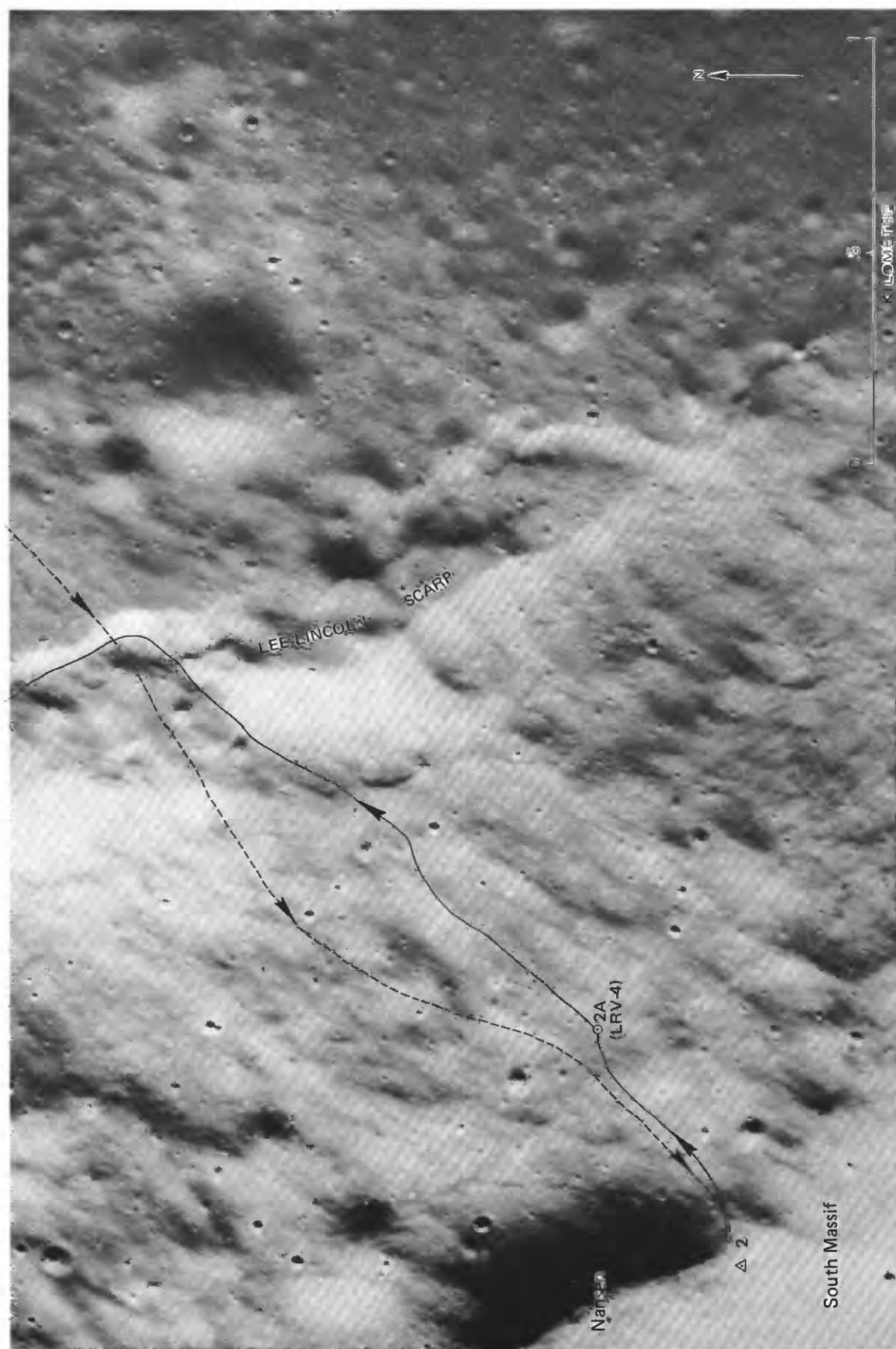


FIGURE 7.—Continued.



FIGURE 7.—Continued.



FIGURE 7.—Continued.

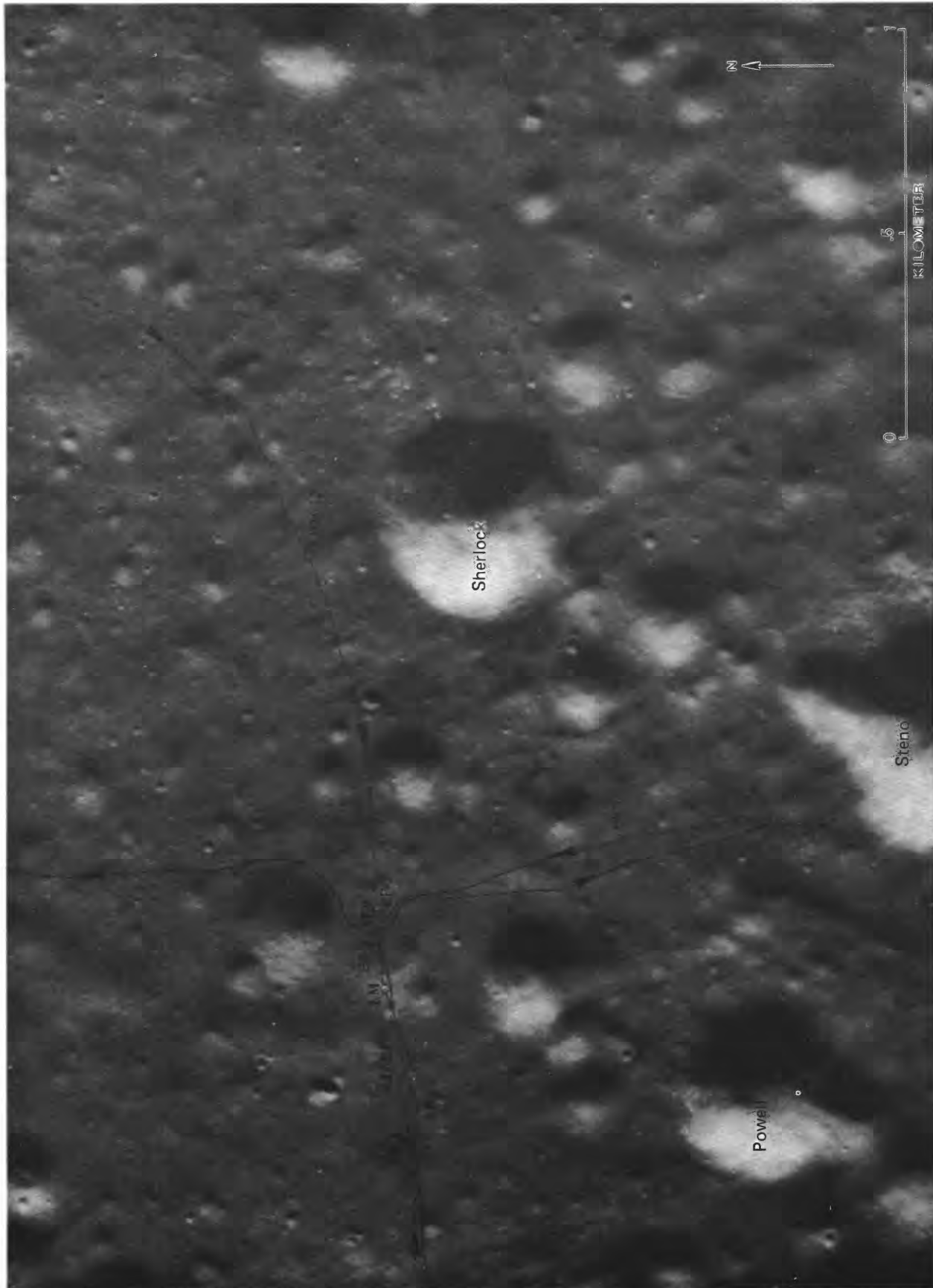


FIGURE 7.—Continued.

provide the primary data for determining precise station locations and for constructing maps showing sample locations at each station. Photographic and cartographic procedures as well as an annotated catalog of the Apollo 17 lunar surface photographs are described at the end of this report.

Samples were numbered in the Lunar Receiving Laboratory (LRL) according to a systematic scheme. The first digit (7) refers to an Apollo 17 sample, the second to the station number (0 represents the LM/ALSEP/SEP area). During EVA-2 and EVA-3, samples were collected from the surface between traverse station stops by the use of a long-handled sample bag holder without the need for the crew to dismount from the LRV. These LRV-stops are labeled LRV-1 through LRV-12 in figures 6 and 7. The second digit of samples from LRV-stops, and also from station 2a, is the number of the next station; hence, samples from LRV-7 and LRV-8, between stations 4 and 5, are, respectively, 75110-15 and 75120-24. LRL numbers for sediment samples end with digits 0 through 4; numbers for rock fragments larger than 1 cm end with digits 5 through 9.

#### CLASSIFICATION OF SAMPLES

Description and classification of the Apollo 17 samples larger than 5 g is based on direct observation of hand specimens in the Lunar Receiving Laboratory, on examination of one or more thin sections of some rocks, and on published descriptions.

Table 1 shows a general classification scheme for lunar samples. The classification represents an attempt to group the samples under the orthodox terrestrial headings of igneous, sedimentary, and metamorphic subdivisions to reflect the dominant process in their formation. Unlike the varied terrestrial processes of rock formation and modification, impact has been the principal process for modifying and redistributing the lunar igneous rocks. The products of this single process of rock modification are thus dominated by a spectrum of fragmented rocks showing varying degrees of thermal effects, and, while the names given them may be familiar, the relative abundances of the different rock types are unlike the relative abundances of similar rocks on the earth. As might be expected from a process that provides so little time for thermal and compositional equilibration, many of its products are mixtures of incompletely fragmented and melted materials. The temperature distribution in the ejecta deposits must, therefore, have been complex, with steep local gradients and variable development of post-depositional thermal effects. The returned samples fully illustrate these complexities.

The igneous rocks that originally formed the major part of the Moon's crust have been so disrupted and

TABLE 1.—General classification scheme for lunar samples

- I. Igneous.
  - A. Plutonic.
  - B. Volcanic.
- II. Sedimentary.
  - A. Unconsolidated (surface ejecta).
  - B. Impact consolidated.
  - C. Weakly lithified (welded or sintered).
- III. Metamorphic.
  - A. With recognizable igneous or metamorphic source rocks.
    - 1. Dynamically metamorphosed (cataclastic).
    - 2. Thermally metamorphosed (matrix recrystallized).
    - 3. Impact-fused (matrix substantially fused).
    - 4. Thermally metamorphosed or impact-fused, undifferentiated (aphanitic, poikilitic).
  - B. With indistinguishable or mixed source rocks.
    - 1. Dynamically metamorphosed (cataclastic): Aphanitic and coarser grained crystalline rock fragments and mineral debris mixed by cataclastic flow.
    - 2. Thermally metamorphosed: Recrystallized (granoblastic).
    - 3. Impact fused: Melt texture (glassy, feathery, intersertal, ophitic).
    - 4. Thermally metamorphosed or impact fused, undifferentiated (aphanitic, poikilitic).

modified by large basin-forming impacts that very few remnants of the original rock have survived intact. The classification has been applied as strictly as the sampling allows to show the dominant petrographic character of the rock rather than what we or others may infer its parent to have been. Thus, names of lunar plutonic igneous rocks must satisfy the characteristics of terrestrial plutonic igneous rocks (see for example Holmes, 1928). Where plutonic or volcanic igneous rocks have been significantly modified by mechanical and thermal effects, their classifications are changed to reflect those modifications. When the source rock is identifiable, its plutonic or volcanic rock name is used as a modifier to convey the maximum amount of information in the name (for example, norite cataclastite). The vast majority of impact-modified igneous rocks, however, have been so severely altered and mixed that the source rocks cannot be directly specified.

Products of impact cratering (Shoemaker, 1960; Moore, 1969, 1971; Shoemaker and others, 1973; Wilshire and Moore, 1974), whether ejected or remaining beneath the cavity, range from broken rock and mineral debris insufficiently heated to become consolidated after deposition (the sedimentary division) to impact melts that solidify to rocks with igneous textures (impact-fused rocks). Between these extremes are crushed but incompletely disaggregated rocks (cataclasites), heated rock debris that recrystallized after deposition (thermally metamorphosed rocks),

and complex mixtures of impact melt and solid debris that have small-scale transitions from melt to thermal metamorphic textures. Materials classified as sedimentary have been transported and mixed by the impact process. Unconsolidated clastic material may be reworked by later impact events to yield regolith breccia, which is poorly consolidated, weakly welded or sintered rock (Phinney and others, 1976) or sheared impact-indurated rock.

Rocks that have been severely modified by mechanical or thermal effects of impact are classified as metamorphic. They are subdivided first on the basis of whether their source rocks are identifiable and second on the basis of degree of thermal effect. Mechanically disrupted but weakly metamorphosed rocks are classed as cataclasites (dynamically metamorphosed). Such rocks are intensely shattered, but their sources are still identifiable. There is no sharp separation of these rocks from the sedimentary rocks because mobilization of disrupted rock (that is, cataclastic flow) during crater formation ultimately yields disaggregated ejecta (Wilshire and Moore, 1974).

Rocks that were sufficiently heated to have recrystallized are classed as thermally metamorphosed rocks. The majority of these are breccia, which is subdivided on the basis of dominant matrix texture. Where recognizable igneous or metamorphic relics indicative of the parent igneous rock are scarce or absent, the rocks are simply labeled "metaclastic" rocks. The thermally metamorphosed matrices have fine-grained granoblastic texture. Gradations between textures and inhomogeneous distribution of them in the same rock are commonplace.

Impact-fused rocks have textures ranging from glassy to intersertal to ophitic. There is evidence that some such rocks form by direct impact melting of plutonic igneous rocks (for example, Dowty and others, 1974), but many are complex mixtures of more than one parent rock type (Dymek and others, 1976b; James and Blanchard, 1976). There are rapid transitions among different textural types in the same sample, leading to difficulties in classification and contradictions among different workers, each of whom studied only a small part of the sample.

There is no sharp boundary between impact-metamorphosed rocks whose matrices have recrystallized in the solid state and those whose matrices were largely melted (impact-fused rocks); indeed, some rocks have both textures in the matrix. Moreover, rapid transitions within single breccia samples from cataclastic to melt to thermal-metamorphic texture in the matrix are a result of multiple impacts and of complex mixing of heated and unheated rock debris during excavation and transportation of ejecta. Classification thus becomes a matter of judgment, often swayed by

individual thin sections that may not be truly representative. To avoid too rigid a classification scheme, the uncertainties are accommodated by a class of undifferentiated thermally metamorphosed or impact-fused rocks.

Similarities between the coarser grained poikilitic and ophitic rocks have led to some controversy over the origin of the poikilitic rocks. Some authors consider all poikilitic rocks to be impact melts with various amounts of solid debris (Simonds, 1975; Simonds and others, 1973; Irving, 1975); others (Wilshire and others, 1981; Bence and others, 1973) consider them to be largely metamorphic in origin with various but subordinate degrees of impact melt in addition to the relict rock and mineral debris. Still others (for example, Chao, 1973; Chao and others, 1975b) consider some poikilitic rocks to be metamorphic and some to be dominantly igneous. It is our view that these rocks probably represent a spectrum of degrees of fusion: those containing abundant newly crystallized plagioclase laths and interstitial material with intersertal texture were largely fused, whereas those without such textures may have formed by recrystallization of largely solid rock and mineral debris. Both of these types contain evidence of having been fluidized, but the presence of gas cavities does not necessarily indicate fusion, as is commonly assumed. For example, Reynolds (1954) emphasized the presence of drusy cavities in a conglomerate dike as evidence of emplacement of the dike as a solid-gas mixture. Because of their transitional or uncertain genesis, rocks with poikilitic texture have been classed here as undifferentiated thermal metamorphic or impact fused.

Similar problems occur with the large group of polymict breccias with aphanitic matrices. Some authors (for example, Phinney and others, 1976) consider all of these to represent mixtures of melt and solid debris, while others (for example, Wilshire and Jackson, 1972) consider identical rocks from the Apollo 14 site to be thermally metamorphosed. Still others (for example, James, 1977) consider that some aphanites with granoblastic texture recrystallized from glass, a sequence also suggested by Chao (1973) for certain poikilitic rocks with metamorphic textures. In view of the enormous quantities of unmelted pulverized rock and mineral debris excavated from impact craters, it seems unreasonable to suppose that all aphanitic rocks must represent quenched impact melt. It is our view that these rocks, like the poikilitic rocks, represent a spectrum of degrees of fusion and cataclasis, and those with granoblastic texture may have formed by essentially solid-state recrystallization of powdered rock debris. These rocks are identified as breccia with aphanitic matrix without specifying the dominance of thermal metamorphism or impact fusion.

The Apollo 17 samples are classified in table 2. The rare surviving plutonic igneous rocks, clasts of such rocks in the impact breccia, and other impact-modified materials with known source rocks indicate that the dominant nonmare source rocks of the Apollo 17 suite are troctolite, olivine norite, norite, and noritic anorthosite with some dunite.

Mare rocks are classified according to their modal compositions as olivine basalt or basalt to allow classification of the many as yet unanalyzed rocks. This scheme will, of course, be supplanted in time by chemical classification. The orange glass, sample 74220, is considered to be pyroclastic (Heiken and others, 1974) and is classed as ash because of the particle size range.

The "soil" samples are classified as sedimentary materials. Their dominant components, usually mare basalt, highlands material, or glass that may have been derived from either mare or highlands, are indicated. In general, the dominant component of the samples reflects the nature of the local bedrock, but core samples are stratified and have various proportions of highlands and mare fragments; the variations are reflected in the bulk composition of the samples. "Soil" and core sample descriptions were obtained largely from Butler (1973) and Heiken (1974).

Reworking of surficial materials has led to weak consolidation of some of the heterogeneous sediments by welding of glass shards and sintering (Simonds, 1973; Phinney and others, 1976) to form weakly lithified polymict breccia (commonly called "regolith" or "soil" breccia). In practice, such breccia is distinguished from severely disrupted but relatively unrecrystallized cataclasite on the basis of abundance of glass shards and extreme diversity of lithic clasts in the regolith breccia, but there is a point beyond which the two types cannot be distinguished. Surficial material thought to have been merely compacted by impact (impact-indurated polymict breccia) has the same diverse components as the welded or sintered breccia but is generally more compact and has distinctive fracture patterns (for example, 79135).

Dynamically metamorphosed rocks with recognizable source rocks are mostly shattered plutonic rocks such as norite, troctolite, and dunite, but there are two cataclasites derived from mare basalt. Many of the plutonic rocks had undergone deep-seated partial thermal metamorphism before impact excavation (Wilshire, 1974; Stewart, 1975), yielding coarse granoblastic-polygonal textures that tend to survive cataclasis better than their unrecrystallized counterparts. Where such recrystallization is thought to have been substantial, the plutonic rock name is modified by "meta-". The majority, probably all, of the members of this group derived from plutonic source rocks are

clasts from more complex breccia.

The samples listed as cataclastic rocks with mixed source rocks are thought to be the products either of mixing of aphanite and crushed debris formed contemporaneously in a single impact or of cataclastic flow of breccia whose original components were plutonic rock clasts in a fine-grained thermally metamorphosed matrix. Slight para- and post-consolidation deformation of such rocks commonly inverts the original clast-matrix relations (Wilshire and others, 1973; Wilshire and Moore, 1974) so that broken pieces of the original matrix become isolated in material derived by disaggregation and cataclastic flow of the original clasts. Where this material has not been subsequently metamorphosed, it may be classed, as we have done, as cataclastic.

Breccias whose matrices have been unequivocally and substantially fused include gabbro, basalt, and polymict breccias, all with glassy matrices.

Thermally metamorphosed or undifferentiated thermally metamorphosed or impact-fused rocks with recognizable source rocks were largely derived from impact crushing and perhaps partial melting of single rock types (all plutonic sources) or from partly recrystallized plutonic rock (76535) that was thermally metamorphosed before excavation.

Thermally metamorphosed rocks or undifferentiated thermally metamorphosed or impact-fused rocks with indistinguishable or mixed sources are mainly polymict breccia, but some (metaclastic rocks) have few or no lithic clasts. It is likely that the great lithologic diversity of clasts in the polymict breccia actually represents only a small variety of plutonic source rocks, with the lithologic diversity representing various degrees of mechanical breakdown and mixing and various thermal effects resulting directly from the impact process. The matrix of this breccia shows a similar range of impact-related mechanical and thermal effects ranging from aphanitic to fine-grained granoblastic to coarse-grained poikilitic texture.

The dominant rock type returned from the Taurus-Littrow highlands is polymict breccia with an aphanitic matrix; polymict breccia with a poikilitic matrix is also common. Both are classified as undifferentiated thermally metamorphosed or impact-fused rocks with the understanding that either type of thermal effect could be dominant in any particular sample.

#### LM/ALSEP/SEP AREA LOCATION

The Lunar Module (LM) landed in a relatively smooth area about 800 m east of Camelot crater and near the northwest boundary of a large cluster of craters on the valley floor (fig. 6; pl. 2). Sampling was concentrated

TABLE 2.—Summary classification of Apollo 17 samples larger than 5 g

<i>Igneous, plutonic</i>		<i>Igneous, volcanic—Continued</i>		<i>Sedimentary, unconsolidated—Continued</i>	
78235.6.8.	Norite.	78509.	Basalt.	78500-04.	Dominantly agglutinate, breccia, glass, and feldspathic cataclastite.
78255.	Norite.	78528.	Basalt.	78530.	No description.
78527.	Norite(?).	78569.	Basalt.	79001-02.	Unopened double drive tube.
<i>Igneous, volcanic</i>		78575.	Olivine basalt.	79120-24.	Dominantly breccia.
70017.	Olivine basalt.	78576.	Basalt.	79220-24.	Dominantly breccia.
70035.	Olivine basalt.	78577.	Basalt.	79240-44.	Dominantly breccia and basalt.
70075.	Olivine basalt.	78578.	Basalt.	79260-64.	Dominantly breccia and basalt.
70135.	Basalt.	78579.	Olivine basalt.	79510-14.	Dominantly breccia.
70136.	Basalt.	78585.	Basalt.	<i>Sedimentary, impact consolidated</i>	
70137.	Basalt.	78586.	Basalt.	70018.	Impact-consolidated polymict breccia.
70185.	Basalt.	78587.	Basalt.	70175.	Impact-consolidated polymict breccia.
70215.	Olivine basalt.	78596.	Basalt.	79115.	Impact-consolidated polymict breccia.
70255.	Olivine basalt.	78597.	Olivine basalt.	79135.	Impact-consolidated polymict breccia.
70275.	Olivine basalt.	78598.	Basalt.	<i>Sedimentary, weakly lithified by welding or sintering</i>	
70315.	Basalt.	78599.	Basalt.	70295.	Weakly lithified polymict breccia.
71035.	Olivine basalt.	79515.	Olivine basalt.	74115.	Weakly lithified polymict breccia.
71036.	Olivine(?) basalt.	79516.	Olivine basalt.	74116.	Weakly lithified polymict breccia.
71037.	Olivine(?) basalt.	<i>Sedimentary, unconsolidated</i>		74246.	Weakly lithified polymict breccia.
71045.	Olivine basalt.	70001-09.	Dominantly basalt, breccia, and feldspathic clastic and metaclastic rocks.	76565.	Weakly lithified polymict breccia.
71055.	Olivine(?) basalt.	70011.	Unopened sample container.	76567.	Weakly lithified polymict breccia.
71065.	Olivine basalt.	70012.	Dominantly basalt.	78508.	Weakly lithified polymict breccia.
71066.	Olivine basalt.	70160-64.	Dominantly basalt.	78525.	Weakly lithified polymict breccia.
71135.	Olivine basalt.	70180-84.	Dominantly basalt.	78526.	Weakly lithified polymict breccia.
71136.	Olivine basalt.	70270-74.	Dominantly basalt.	78535.	Weakly lithified polymict breccia.
71155.	Olivine(?) basalt.	70311-14.	Dominantly basalt.	78536.	Weakly lithified polymict breccia.
71156.	Olivine(?) basalt.	70320-24.	Dominantly basalt.	78537.	Weakly lithified polymict breccia.
71175.	Olivine basalt.	71040-44.	Dominantly basalt.	78538.	Weakly lithified polymict breccia.
71505.	Olivine basalt.	71060-64.	Dominantly basalt.	78545.	Weakly lithified polymict breccia.
71506.	Olivine basalt.	71130-34.	Dominantly basalt.	78546.	Weakly lithified polymict breccia.
71526.	Basalt.	71150-54.	Dominantly basalt and breccia.	78547.	Weakly lithified polymict breccia.
71528.	Basalt.	71500-04.	Dominantly basalt and breccia.	78548.	Weakly lithified polymict breccia.
71529.	Basalt.	72130-34.	Dominantly basalt, in part balsaltic breccia.	78549.	Weakly lithified polymict breccia.
71535.	Basalt.	72140-44.	Dominantly basalt and glass.	78555.	Weakly lithified polymict breccia.
71536.	Basalt.	72150.	No description.	78556.	Weakly lithified polymict breccia.
71537.	Basalt.	72160-64.	Dominantly breccia and agglutinate.	78557.	Weakly lithified polymict breccia.
71538.	Basalt.	72220-24.	Dominantly breccia.	78567.	Weakly lithified polymict breccia.
71539.	Basalt.	72240-44.	Dominantly breccia and agglutinate.	79035.	Weakly lithified polymict breccia.
71545.	Basalt.	72260-64.	No description.	79195.	Weakly lithified polymict breccia.
71546.	Basalt.	72320-24.	Dominantly agglutinate and breccia.	79225.	Weakly lithified polymict breccia.
71547.	Basalt.	72410.	No description.	79226.	Weakly lithified polymict breccia.
71548.	Basalt.	72430-34.	Dominantly breccia.	79227.	Weakly lithified polymict breccia.
71549.	Basalt.	72440-44.	Dominantly breccia.	79517.	Weakly lithified polymict breccia.
71556.	Basalt.	72460-64.	Dominantly breccia.	79518.	Weakly lithified polymict breccia.
71557.	Basalt.	72500-04.	Dominantly breccia.	<i>Metamorphic, recognizable source rock, cataclastite</i>	
71558.	Olivine basalt.	72700-04.	Dominantly breccia.	72135.	Basalt cataclastite.
71559.	Basalt.	73001-02.	Unopened double drive tube.	72415-18.	Metadunite cataclastite.
71565.	Olivine basalt.	73120-24.	Dominantly breccia.	76235-39.	Olivine metanorite cataclastite.
71566.	Basalt.	73130-34.	Dominantly breccia.	76335.	Troctolite cataclastite.
71567.	Olivine basalt.	73140-44.	Dominantly breccia.	76536.	Olivine(?) norite cataclastite.
71568.	Olivine basalt.	73150-54.	Dominantly breccia.	76568.	Basalt cataclastite.
71569.	Olivine basalt.	73210-14.	Dominantly breccia.	77215.	Norite cataclastite.
71576.	Olivine basalt.	73220-24.	Dominantly breccia.	78155.	Metagabbro cataclastite.
71577.	Olivine basalt.	73240-44.	Dominantly breccia.	<i>Metamorphic, recognizable source rock, thermally metamorphosed</i>	
71578.	Olivine basalt.	73260-64.	Dominantly breccia.	76535.	Metatroctolite.
71579.	Basalt.	73280-84.	Dominantly breccia.	79215.	Metatroctolite(?) breccia with a granoblastic matrix.
71585.	Olivine basalt.	74110-14.	Dominantly basalt breccia, feldspathic cataclastite, agglutinate, and glass.	<i>Metamorphic, recognizable source rock, impact fused</i>	
71586.	Olivine basalt.	74120-24.	Dominantly breccia and agglutinate.	77017.	Olivine gabbro breccia with a glassy matrix.
71587.	Olivine basalt.	74240-44.	Dominantly basalt.	79155.	Olivine gabbro breccia with a glassy matrix.
71588.	Olivine basalt.	74260.	Dominantly breccia, glass, and agglutinate.	<i>Metamorphic, recognizable source rock, thermally metamorphosed or impact fused, undifferentiated</i>	
71589.	Olivine basalt.	75060-64.	Dominantly basalt.	72736.	Metanorite(?) breccia with a poikilitic(?) matrix.
71595.	Olivine basalt.	75080-84.	Dominantly basalt.	73145.	Metagabbroid(?) breccia with an aphanitic matrix.
71596.	Olivine basalt.	75110-14.	Dominantly basalt.	79245.	Troctolite(?) breccia with an aphanitic matrix.
71597.	Olivine basalt.	75120-24.	Dominantly basalt.	<i>Metamorphic, source rocks indistinguishable or mixed, cataclastic</i>	
72155.	Volcanic ash.	76001.	Unopened drive tube.	72235.	Polymict breccia with a cataclastic matrix.
74001-02.	Volcanic ash.	76030-34.	Dominantly basalt.	72275.	Polymict breccia with a cataclastic matrix.
74220.	Volcanic ash.	76120-24.	Dominantly breccia.	73155.	Polymict breccia with a cataclastic matrix.
74235.	Olivine basalt.	76130-34.	No description.	73215.	Polymict breccia with a cataclastic matrix.
74245.	Olivine basalt.	76220-24.	No description.	73235.	Polymict breccia with a cataclastic matrix.
74247.	Olivine(?) basalt.	76240-44.	Dominantly basalt.	76255.	Polymict breccia with a cataclastic matrix.
74248.	Basalt.	76260-64.	Dominantly breccia.	<i>Metamorphic, source rocks indistinguishable or mixed, thermally metamorphosed</i>	
74255.	Olivine basalt.	76280-84.	Dominantly breccia.	72315.	Polymict breccia with a granoblastic matrix.
74275.	Olivine basalt.	76320-24.	Dominantly breccia.	72355.	Polymict breccia with a granoblastic matrix.
75015.	Basalt.	76500-04.	Dominantly breccia.	73216.	Polymict breccia with a granoblastic matrix.
75035.	Basalt.	77510-14.	Dominantly breccia.	73275.	Metaclastic, with a granoblastic matrix.
75055.	Olivine basalt.	77530-34.	Dominantly breccia.	76055.	Polymict breccia with a granoblastic matrix.
75075.	Olivine basalt.	78120-24.	Incomplete description.	<i>Metamorphic, source rocks indistinguishable or mixed, impact fused</i>	
76136.	Olivine basalt.	78220-24.	Dominantly breccia.	70019.	Polymict breccia with a glassy matrix.
76537.	Olivine basalt.	78230-34.	No description.	76545.	Polymict breccia with a glassy matrix.
76538.	Basalt.	78250.	No description.	76546.	Polymict breccia with a glassy matrix.
76539.	Basalt.	78420-24.	Dominantly breccia.	76547.	Polymict breccia with a glassy matrix.
77516.	Olivine basalt.	78440-44.	Dominantly breccia and agglutinate.	76549.	Polymict breccia with a glassy matrix.
77535.	Basalt.	78460-64.	Dominantly breccia and agglutinate.	79175.	Polymict breccia with a glassy matrix.
77536.	Olivine basalt.	78480-84.	Dominantly agglutinate, breccia, glass, and feldspathic cataclastite.		
78135.	Olivine basalt.				
78505.	Olivine basalt.				
78506.	Olivine basalt.				
78507.	Olivine basalt.				

TABLE 2.—Summary classification of Apollo 17 samples larger than 5 g—Continued

Metamorphic, source rock indistinguishable or mixed, thermally metamorphosed or impact fused, undifferentiated	Metamorphic, source rock indistinguishable or mixed, thermally metamorphosed or impact fused, undifferentiated—Continued	Metamorphic, source rock indistinguishable or mixed, thermally metamorphosed or impact fused, undifferentiated—Continued
72215. Polymict breccia with an aphanitic matrix.	72735. Metaclastic, with an aphanitic matrix.	76576. Breccia with an aphanitic matrix.
72255. Polymict breccia with an aphanitic matrix.	72738. Polymict(?) breccia with an aphanitic matrix.	76577. Metaclastic, with an aphanitic matrix.
72335. Polymict breccia with a poikilitic(?) matrix.	73217. Polymict breccia with an aphanitic matrix.	77035. Polymict breccia with an aphanitic matrix.
72375. Polymict breccia with a poikilitic(?) matrix.	73218. Polymict breccia with an aphanitic matrix.	77075. Monomict(?) breccia with an aphanitic matrix.
72395. Polymict breccia with an aphanitic matrix.	73255. Polymict breccia with an aphanitic matrix.	77076. Monomict(?) breccia with an aphanitic matrix.
72435. Polymict breccia with a poorly developed poikilitic matrix.	76015. Metaclastic, with a poikilitic matrix.	77077. Monomict(?) breccia with an aphanitic matrix.
72535. Polymict breccia with an aphanitic matrix.	76035. Polymict breccia with an aphanitic matrix.	77115. Polymict breccia with an aphanitic matrix.
72536. Polymict breccia with an aphanitic matrix.	76135. Metaclastic, with a poikilitic matrix.	77135. Polymict breccia with a poikilitic matrix.
72537. Polymict breccia with an aphanitic matrix.	76215. Metaclastic, with a dominantly poikilitic matrix.	77515. Polymict breccia with a poikilitic(?) matrix.
72538. Polymict breccia with an aphanitic matrix.	76245. Metaclastic, with a poikilitic(?) matrix.	77517. Polymict breccia with an aphanitic matrix.
72539. Polymict breccia with an aphanitic matrix.	76246. Metaclastic, with a poikilitic(?) matrix.	77518. Breccia with a poikilitic(?) matrix.
72547. Polymict breccia with an aphanitic matrix.	76275. Polymict breccia with an aphanitic matrix.	77519. Polymict breccia with a poikilitic(?) matrix.
72548. Polymict(?) breccia with an aphanitic matrix.	76295. Polymict breccia with an aphanitic matrix.	77537. Breccia with a poikilitic(?) matrix.
72549. Metaclastic, with a poikilitic(?) matrix.	76315. Polymict breccia with an aphanitic matrix.	77538. Polymict breccia with an aphanitic matrix.
72555. Metaclastic, with a poikilitic(?) matrix.	76555. Polymict breccia with an aphanitic matrix.	77539. Polymict breccia with a poikilitic(?) matrix.
72558. Metaclastic, with a poikilitic(?) matrix.	76556. Polymict breccia with an aphanitic matrix.	77545. Polymict breccia with a poikilitic(?) matrix.
72559. Metaclastic, with an aphanitic matrix.	76557. Polymict breccia with an aphanitic matrix.	
	76575. Polymict breccia with an aphanitic matrix.	

in three general areas (fig. 8): (1) the ALSEP area about 200 m west of the LM, (2) the LM area, and (3) the area near the transmitter for the Surface Electrical Properties experiment (SEP) about 150 m east of the LM.

#### OBJECTIVES

As far as could be determined from premission photographs, the immediate landing area was free of blocks and was one of the less cratered parts of the valley floor. It was considered likely to be less informative about the geology of the region than were the planned traverse stations. Therefore, except for the acquisition of a 3-m-long core in the ALSEP area, no rigorously structured plans for sampling or observation were made for the LM/ALSEP/SEP area. It was anticipated, however, that observations would be made and samples collected as opportunities arose during deployment of the ALSEP and SEP hardware as well as during the near-LM activities at the beginnings and ends of the three EVA's.

#### GENERAL OBSERVATIONS

The valley floor in the LM/ALSEP/SEP area is gently rolling to locally flat (fig. 9). Boulders and cobbles are more abundant in this area than over the valley floor in general; the larger ones, near the ALSEP, reach about 4 m in size. In contrast, no such concentration of large boulders was seen on the valley floor west of Camelot crater.

Rocks of the LM/ALSEP/SEP area are predominantly vesicular coarse-grained subfloor basalt, but fine-grained basalt occurs also. All of the larger rocks are partly buried by loose sediment. Clods of regolith breccia presumably formed by impact are also present.

Unconsolidated sediment of the regolith is commonly medium dark gray. Throughout the LM/ALSEP/SEP area the bulk of the regolith is less than about 3 or 4 cm in grain size; larger fragments are scattered. The regolith becomes increasingly cohesive with depth, to about 25-35 cm. Alternating zones offering more or

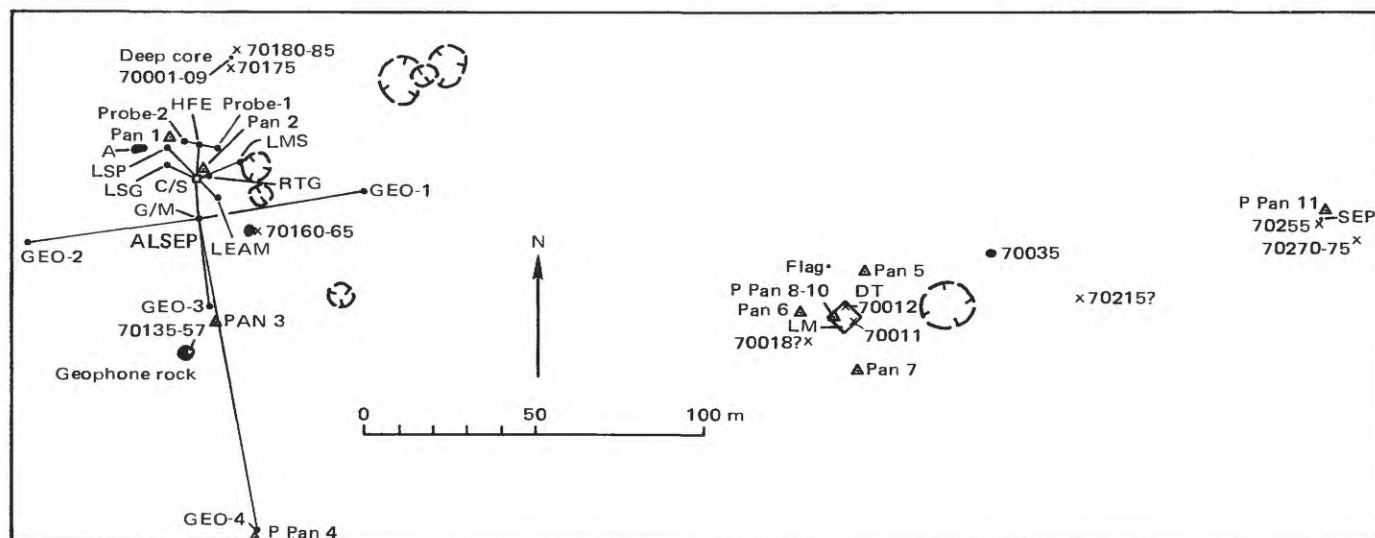


FIGURE 8.—Planimetric map of LM/ALSEP/SEP area. See glossary for explanation of symbols.

less resistance to drilling were encountered in the holes drilled for the Heat Flow experiment and the deep core. The most resistant layer is at a depth of about 2 m.

There are no conspicuous surface lineaments in the station area. Pitted "raindrop" texture is common but is most pronounced at the SEP site.

The surface in the LM/ALSEP/SEP area contains many 20-cm to 2-m craters, some of which have glassy material on their floors. The nearest large craters to the station are Rudolph (80 m in diameter), 70 m north of ALSEP, and highly subdued Poppy (100 m in diameter), 70 m south of the LM.

#### GEOLOGIC DISCUSSION

Basalt in the LM/ALSEP/SEP area consists of fragments excavated by impacts from the upper part of the subfloor basalt, which partially filled the Taurus-Littrow valley about 3.75 b.y. ago. The basalt is now overlain by unconsolidated material estimated to average 14 m in thickness (Wolfe and others, 1975). The source craters for the larger blocks have not been identified, but most of them probably came from the craters clustered south and east of the LM (pl. 2); the large crater Camelot, to the west, is a less likely source because (1) scarcity of large blocks elsewhere outside Camelot suggests that the large blocks in the LM area are not Camelot ejecta (Muehlberger and others, 1973) and (2) analyzed LM-area basalt is chemically unlike

the sampled boulders on the rim of Camelot, but is similar to some basalt from station 1 on the ejecta blanket of Steno crater. Exposure ages determined on LM-area boulders range from 95 to 106 m.y.; they are approximately equivalent to exposure ages measured for the two boulders sampled at station 1 (102 and 110 m.y.).

The sedimentary materials and the pebble- and cobble-size basalt fragments collected from the surface in the LM/ALSEP/SEP area are regolith materials that are largely derived from the subfloor basalt and are representative of the basalt-rich cluster ejecta. This unit, ejecta of the abundant clustered craters of the valley floor, may comprise approximately the upper 80 cm of the deep drill core. The lower 2 m or more of the drill core are from the more heterogeneous older regolith of the valley floor (fig. 10).

#### SUMMARY OF SAMPLING

##### Sample 70001-70009

	Weight (g)	Returned sample length (cm)
70009 Drill core stem (top) .....	143.3	24.9
70008 Drill core stem .....	261.0	38
70007 Drill core stem .....	179.4	30
70006 Drill core stem .....	234.2	39.9
70005 Drill core stem .....	240.7	39.9
70004 Drill core stem .....	238.8	39.9
70003 Drill core stem .....	237.8	39.9
70002 Drill core stem .....	207.8	42.0
70001 Drill core bit .....	29.78	
	1772.8	294.5

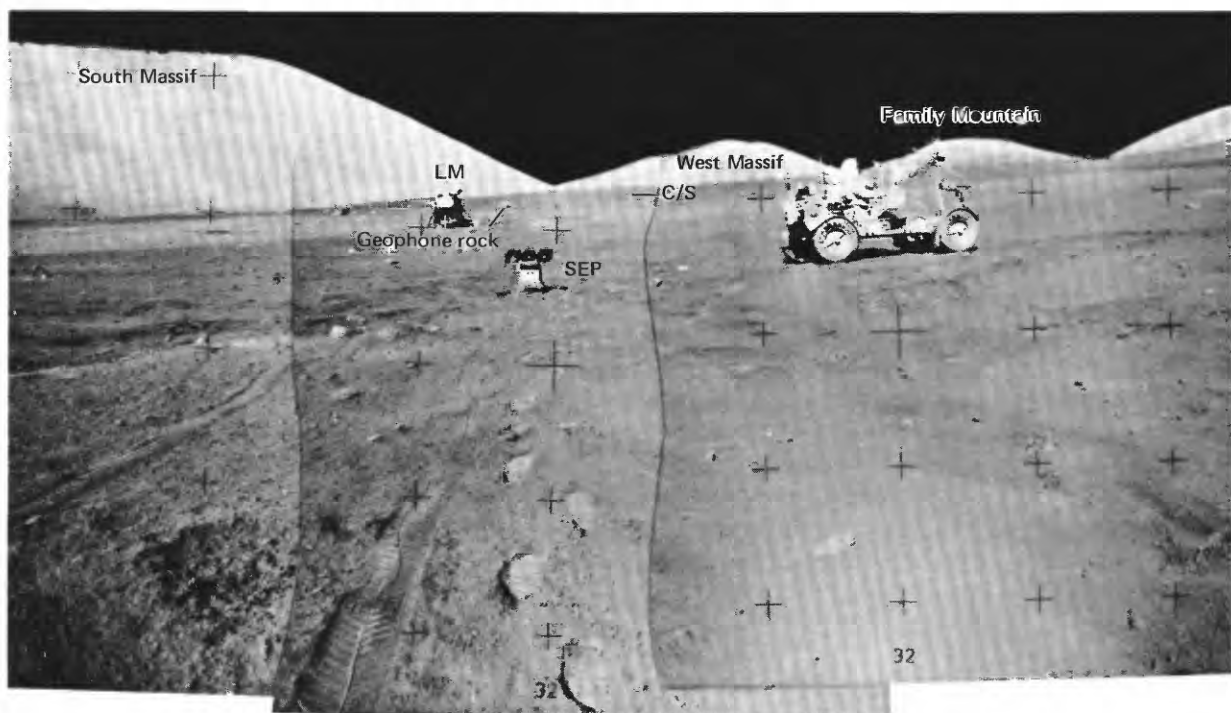


FIGURE 9.—Partial panorama looking west from SEP site toward LM and ALSEP areas. (NASA photographs AS17-141-21515, 21516, and 21517.)

*Depth:* Approximately 0 to 3.2 m.

*Location:* Approximately 35 m north-northeast of ALSEP central station (fig. 8).

*Illustrations:* Pan 1; figures 11, 24.

*Comments:* The deep core was drilled within a slight depression, perhaps a greatly subdued crater, that the crew estimated to be about 4 m across. The regolith surface at the deep drill site was extensively disturbed by the astronauts. The sediment at the surface is loose; it is more coherent below 3 to 4 cm depth. The drill penetrated to about 3 m, alternating between easy and difficult in penetration. Regolith sample 70180-84 was later collected 3 m to the east for comparison with the materials of the core.

*Stratigraphy:* Direct observation of the upper 93 cm (core stems 70007, 08, 09) shows that the upper

part of the deep core is dominated by a very coarse grained basalt-rich unit that extends from approximately 18 to 83 cm depth (Waltz and Nagle, 1976).

The uppermost unit, approximately 18 cm thick, is fine-grained sediment composed largely of fragments of glass, regolith breccia, and agglutinate (Waltz and Nagle, 1976). It overlies a coarse basalt-rich unit about 65 cm thick (table 3). Many fragments in the upper part of the basalt-rich unit are coated with frothy or vesicular glass. Reworked material (presumably agglutinate, glass, and regolith breccia) increases downward in the lower part of the basalt-rich unit. Waltz and Nagle concluded that the basalt-rich unit might have been deposited as ejecta of a single cratering event in which both regolith, represented by the reworked material in

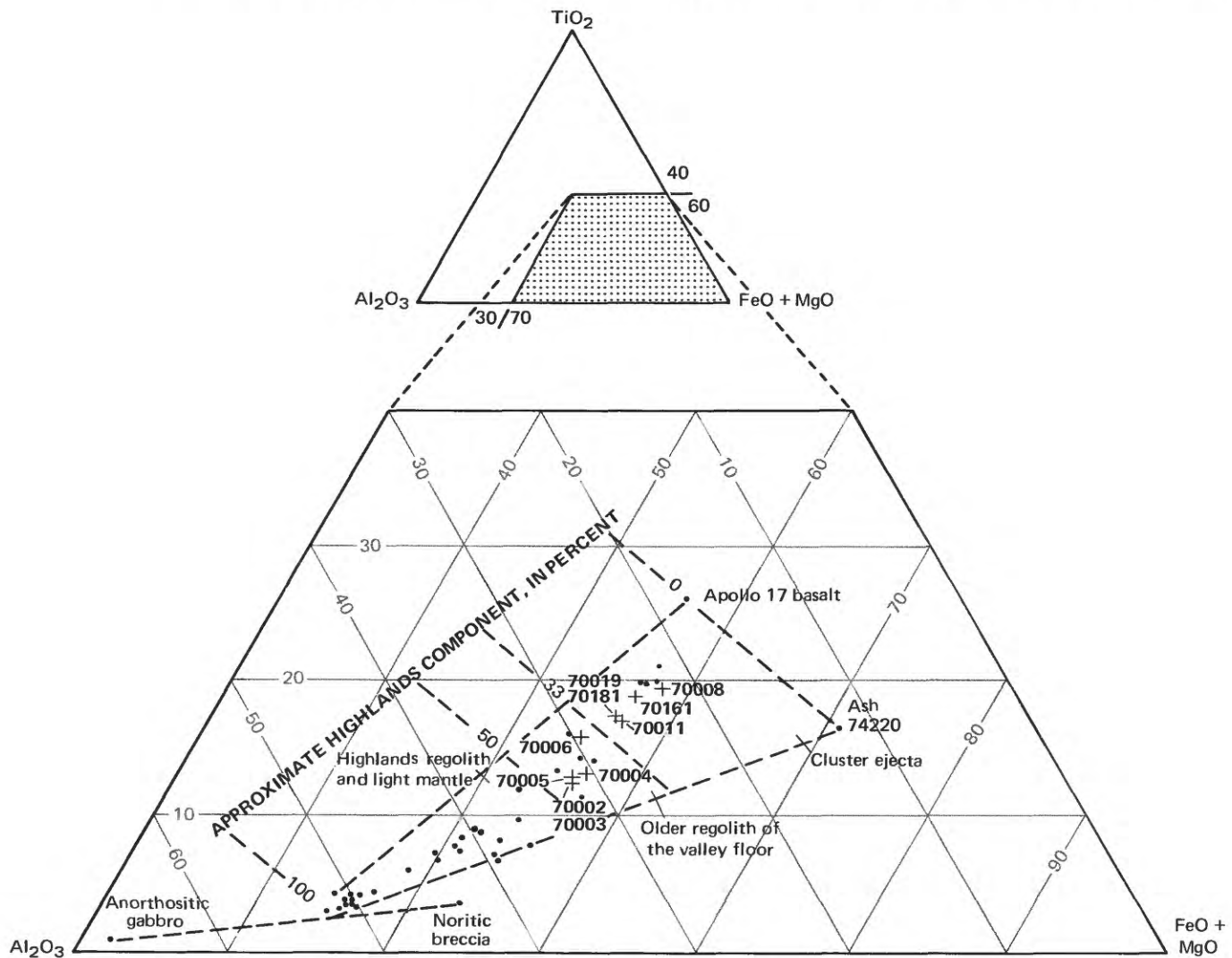


FIGURE 10.—Relative amounts of  $\text{TiO}_2$ ,  $\text{Al}_2\text{O}_3$ , and  $\text{FeO} + \text{MgO}$  in sediment samples from LM/ALSEP/SEP area (crosses) in comparison with sediment samples from rest of traverse region (dots). Plot includes glassy polymict breccia 70019. Lower two-thirds of deep core (70002-70006) are in compositionally mixed older regolith of valley floor; upper part of deep core (70008) and all surface samples are in basalt-rich cluster ejecta. Apollo 17 basalt, anorthositic gabbro, and noritic breccia values from Rhodes and others (1974).

TABLE 3.—Components, in volume percent, of 90-150- $\mu$ m fractions from approximately 27 to 59 cm depth in the deep core (Heiken and McKay, 1974)

Sample No .....	70008,215	70008,220	70008,228	70008,231	70008,235	70008,239
Approximate depth, in centimeters .....	27 to 29	33 to 33.5	43 to 45	47 to 49	56 to 56.5	57 to 59
Agglutinate .....	7.6	9.0	9.1	8.7	20.3	17.4
Basalt, equigranular .....	19.6	19.0	16.8	18.0	19.7	20.5
Basalt, variolitic .....	4.0	5.0	5.2	5.7	2.7	1.0
Breccia: .....						
Low-grade <sup>1</sup> - brown .....	8.0	4.3	3.2	5.3	1.7	3.7
Low-grade <sup>1</sup> - colorless .....	--	--	.3	.7	--	.7
Medium-high grade <sup>2</sup> .....	1.7	2.7	2.3	1.0	.7	1.3
Anorthosite .....	--	--	.3	--	.3	--
Cataclastic anorthosite .....	--	1.7	1.0	.7	1.7	.7
Plagioclase .....	8.0	11.0	12.3	10.3	10.7	8.4
Clinopyroxene .....	27.9	21.7	28.2	32.0	22.0	17.1
Orthopyroxene .....	--	--	.3	--	--	--
Olivine .....	--	1.0	--	.3	--	--
Ilmenite .....	4.3	3.7	3.9	3.3	1.7	3.3
Glass: .....						
Orange .....	5.0	7.7	3.9	3.7	5.3	4.3
"Black" .....	9.3	12.0	11.7	7.7	11.0	15.0
Colorless .....	1.3	1.0	.7	1.0	--	.7
Brown .....	1.3	1.0	.3	1.0	1.3	.7
Gray, "ropy" .....	--	--	.3	.7	1.0	1.0
Other .....	.6	.3	--	--	--	1.0
Total grains counted .....	301	300	309	300	300	298

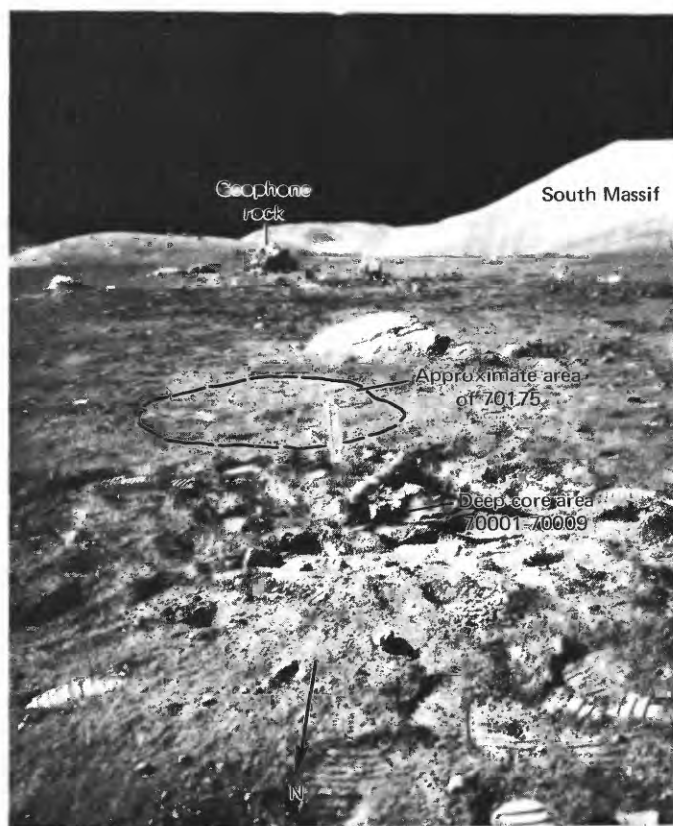
<sup>1</sup> Metamorphic groups 1-3 of Warner (1972).<sup>2</sup> Metamorphic groups 4-8 of Warner (1972).

FIGURE 11.—Deep core (sample 70001-70009) site, with neutron flux probe in deep core hole. Approximate area from which sample 70175 was collected is behind handle of core stem extractor. (NASA photograph AS 17-134-20504.)

the lower part of the unit, and bedrock, represented by abundant fresh rock fragments, were excavated. The glass coatings in the upper part might have formed from melt generated at the impact target.

Of the remaining 2.1 m of core, only the upper 10 cm has so far been dissected and examined directly. This portion consists of subunits of various grain sizes. Composition is similar to the uppermost 18 cm of the core in that basalt fragments are relatively few except in coarser subunits.

X-ray examination (Butler, 1973) of the lower 2 m of the core and studies of fragments from the bit and from the joints between individual core stems indicate that the lower two-thirds of the core is largely finer grained, layered in part, and is compositionally distinct from the upper basalt-rich portion.

The major-element chemistry of samples from core stem 70008 and from the bit and core stem junctions is shown in table 4. The lower five samples, ranging in depth from 133 to 294 cm, represent a uniform mixture of highlands and basaltic components in which the highlands contribution is between one-third and one-half (fig. 10). The upper part of the core, represented by a sample from approximately 31 cm depth (in core stem 70008), has much more basalt; the highlands component is about 20 percent. The sample from the top of core stem 70006, at a depth of 93 cm, is transitional in major-element chemistry between the upper and lower parts of the core. In general agreement with the major-element data, Silver (1974) interpreted a significant compo-

TABLE 4.—Chemical analyses of deep core samples

[Analyses 1-6 from Helmske and others (1973); no. 7 from Laul and others (1974); --, not determined]

	1	2	3	4	5	6	7
SiO <sub>2</sub> .....	42.1	43.4	42.9	42.6	42.6	41.6	--
Al <sub>2</sub> O <sub>3</sub> .....	14.1	14.0	13.9	13.7	14.1	13.3	10.8
FeO .....	14.5	14.5	14.5	14.9	14.7	15.2	18.0
MgO .....	10.3	9.94	10.3	10.1	9.97	9.56	10
CaO .....	11.2	10.9	11.0	11.2	11.2	10.9	10.3
Na <sub>2</sub> O .....	.43	.48	.46	.44	.42	.46	.46
K <sub>2</sub> O .....	.120	.227	.149	.114	.118	.101	.085
TiO <sub>2</sub> .....	5.85	5.56	5.44	6.00	5.80	7.23	9.4
MnO .....	.200	.199	.203	.209	.207	.213	.231
Cr <sub>2</sub> O <sub>3</sub> .....	--	--	--	--	--	--	.463
Total .....	98.80	99.206	98.85	99.26	99.115	98.56	

1. 70001,12; bit; depth-294 cm.

2. 70002,12; top of 70002; depth-253 cm.

3. 70003,12; top of 70003; depth-213 cm.

4. 70004,12; top of 70004; depth-173 cm.

5. 70005,12; top of 70005; depth-133 cm.

6. 70006,12; top of 70006; depth-93 cm.

7. 70008,218; 5.7 to 6.2 cm below top of 70008; depth-31 cm; &lt;1 mm size fraction.

sitional discontinuity between 93 and 133 cm depths from U-Th-Pb measurements. Curtis and Wasserburg (1975a) reported a significant distinction in trace-element compositions between the samples from deeper than 93 cm and those from shallower than 52 cm. A sample at 64 cm was chemically transitional. Interpreting neutron fluence from isotopic ratios of Sm and Gd, Curtis and Wasserburg found that uniformly low irradiation characterizes the upper 52 cm of the deep core and uniformly high irradiation characterizes the core from 93 cm downward. As with the trace-element data, neutron fluence data for the sample from 64 cm suggest that it lies in a transition zone between the distinct upper and lower parts of the core.

**Exposure history:** Combining their neutron fluence data and the available compositional data, Curtis and Wasserburg (1975a) proposed that the entire interval sampled by the deep core was deposited within the past 100 to 200 m.y. The lowest part was derived from materials that had undergone heavy preirradiation and the upper part from materials with relatively little preirradiation. This contrasts with the earlier interpretation of Dragon and others (1975), based on measurements of argon, that the lower interval accumulated in two depositional events, the older of which occurred nearly 1 b.y. ago. Spallation profiles for the other rare gases (Pepin and others, 1975), like the neutron fluence results, are not compatible with lengthy in-place radiation of the lower two-thirds of the core.

Both the neutron-fluence and rare-gas data are compatible with models wherein the upper basalt-rich interval is relatively young. Dragon and others (1975) suggested that a 90-m.y. age best fit the Ar measurements. Crozaz and others (1974) interpreted a 10-m.y. track age for material in the inter-

val from 40 to 60 cm. However, this age is unreasonably young. Possibly material from the upper part of the deep core was lost or disturbed (Waltz and Nagle, 1976); hence the measured track density may reflect an age greater than 10 m.y. (Arvidson and others, 1976a; Crozaz and Plachy, 1976a). More recently, Crozaz and Plachy (1976b) suggested that the anomalously young 10-m.y. age might be explained by the following model: (1) deposition of the upper basalt-rich interval approximately 100 m.y. ago; (2) removal of approximately 25 cm of sediment from the lunar surface within the past 2 m.y. by an impact that formed the shallow depression in which the deep core was drilled; (3) rapid partial filling of the depression by surface-irradiated material.

**Geologic significance:** The deep core sampled regolith material. The upper, basalt-rich interval is a sample of the cluster ejecta, and the lower interval, more enriched in highlands debris, is from the older regolith of the valley floor (Wolfe and others, 1975).

Sample 70011 (fuel products contamination sample)

**Type:** Sedimentary, unconsolidated.

**Weight:** 440.7 g.

**Depth:** 0-3 cm.

**Location:** Beneath LM, near -Z (eastern) footpad.

**Illustrations:** Pan 7, fig. 12.



FIGURE 12.—Postsampling view of sample 70011 area beneath LM. (NASA photograph AS17-143-21929.)

**Comments:** Sample 70011 was collected from a level surface that was slightly disturbed by the LM engine exhaust on descent. The surface material is fine grained with scattered pebbles up to about 2 cm in size. There are no craters in the immediate sample site. Sample is regolith material from the valley floor surface.

**Major-element composition:**

*Chemical analyses of 70011*

	1	2	3
SiO <sub>2</sub> .....	41.5	41.03	41.3
Al <sub>2</sub> O <sub>3</sub> .....	12.43	11.98	12.2
FeO.....	16.0	16.24	16.1
MgO.....	9.93	10.08	10.0
CaO.....	11.1	11.08	11.09
Na <sub>2</sub> O.....	.375	.31	.34
K <sub>2</sub> O.....	.078	.08	.08
TiO <sub>2</sub> .....	7.36	8.30	7.83
P <sub>2</sub> O <sub>5</sub> .....	.048	.10	.07
MnO.....	.216	.23	.22
Cr <sub>2</sub> O <sub>3</sub> .....	.384	.41	.40
Total.....	99.421	99.84	99.67

1. 70011.12 (Wänke and others, 1974).
2. 70011.25 (Rose and others, 1974).
3. Average of 1 and 2.

**Sample 70012**

**Type:** Single drive tube.

**Length:** 18.8 cm.

**Depth:** Approximately 28 cm.

**Net weight:** 485.0 g.

**Location:** Beneath LM approximately 0.5 m behind the +Y (northern) footpad.

**Illustrations:** Pans 5, 6.

**Comments:** The sample area is level and relatively smooth. Small fragments, up to about 4 cm in diameter, litter less than 1 to 2 percent of the local surface, which was swept by the LM descent engine exhaust. Because the bottom cap came loose, part of the sample spilled from the drive tube in transit.

**Petrographic description:** Unconsolidated sedimentary material; dominantly basalt fragments.

**Sample 70017**

**Type:** Olivine basalt.

**Size:** 18×14×10 cm.

**Weight:** 2,957 g.

**Location:** Exact source unknown; sample was most probably collected near the LM on its west side.

**Illustration:** Figure 13 (LRL).

**Petrographic description:** Medium-grained vesicular porphyritic olivine basalt. Aggregates of clinopyroxene and ilmenite in a locally plumose groundmass of plagioclase, clinopyroxene, ilmenite, and accessory minerals.

**Major-element composition:**

*Chemical analyses of 70017*

	1	2	3	4	5	6
SiO <sub>2</sub> .....	38.37	38.8	38.80	38.07	38.68	38.5
Al <sub>2</sub> O <sub>3</sub> .....	8.78	9.73	8.54	8.79	7.40	8.65
FeO.....	18.71	17.60	18.12	18.07	18.77	18.25
MgO.....	9.41	8.89	10.16	9.81	10.45	9.74
CaO.....	10.43	10.04	10.56	10.30	10.05	10.28
Na <sub>2</sub> O.....	.43	.43	.33	.40	.34	.39
K <sub>2</sub> O.....	.047	.036	.07	.04	.07	.05
TiO <sub>2</sub> .....	12.83	12.44	12.84	13.10	13.75	12.99
P <sub>2</sub> O <sub>5</sub> .....	.052	.048	.04	.05	.04	.05
MnO.....	.247	.232	.24	.27	.25	.25
Cr <sub>2</sub> O <sub>3</sub> .....	.577	.45	.49	--	.49	.50
Total.....	99.883	99.70	100.19	98.90	100.29	99.65

1. 70017.18 (Duncan and others, 1974).
2. 70017.23 (Nava, 1974).
3. 70017.30 (Rose and others, 1974).
4. 70017.35 (Rhodes and others, 1974).
5. 70017.50 (Rhodes and others, 1974).
6. Average of 1 through 5.

**Age:**

Rb-Sr isochron: 70017,35,  $3.68 \pm 0.18$  b.y. ( $2\sigma$ ) (Nyquist and others, 1975)

<sup>40</sup>-<sup>39</sup>Ar: 70017,65, no well-defined plateau;  $3.80 \pm 0.03$  b.y. may be an older limit on crystallization age;  $3.63 \pm 0.03$  K-Ar age should be the younger limit (Phinney and others, 1975).

**Exposure age:**

Ar:

70017, 126 m.y. (Arvidson and others, 1975).  
70017,65,  $220 \pm 20$  m.y. (Phinney and others, 1975).

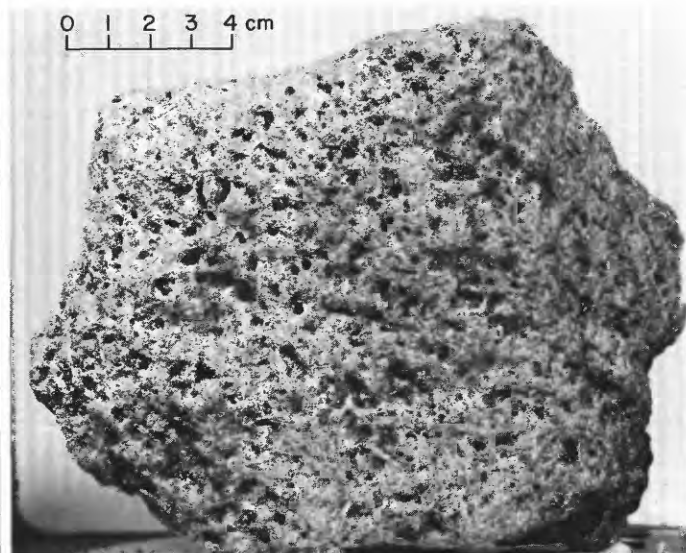


FIGURE 13.—Sample 70017. Medium-grained vesicular olivine basalt. (NASA photograph S-73-15720.)

## Sample 70018

*Type:* Sedimentary, impact-consolidated polymict breccia.

*Size:* 5.5×4.5×1.8 cm.

*Weight:* 51.58 g.

*Location:* Near the LM, possibly from the floor of a 1.5-m crater located about 10 m southwest of the LM.

*Illustrations:* Pans, 6, 7, 8, 10; figure 14 (LRL).

*Comments:* A fragment tentatively identified as sample 70018 is visible in panorama 8, taken from the LM window prior to EVA 1, and is missing in panorama 10, taken from the same position after completion of EVA 3. The 1.5-m crater from which the sample may have come is the largest in the immediate area. A 60-cm white boulder is largely buried in the crater wall. The sampled rock may also have been largely buried. Similar-looking dark rocks are visible on the eastern crater rim. Prior to collecting this sample, the crew described the occurrence near the LM of meter-sized craters with glassy floors. Sample 70018 may be representative of such glassy crater floor material, which is most probably sediment consolidated by the impacts that formed the craters. Alternatively, the sample could be part of a secondary projectile that formed the small crater.

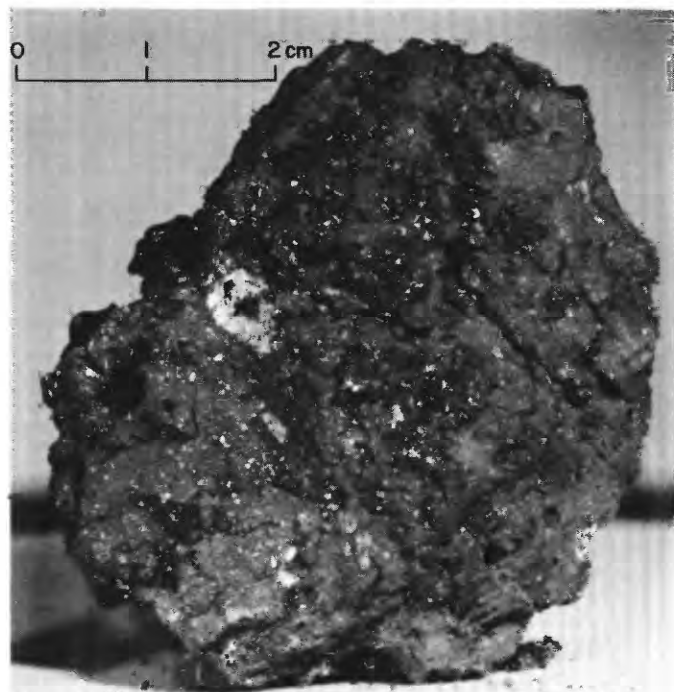


FIGURE 14.—Sample 70018. Impact-consolidated polymict breccia. Irregular glass selvage. (NASA photograph S-73-15330.)

*Petrographic description:* Polymict breccia with clasts of basalt, glass, and mineral fragments in a fine-grained moderately coherent matrix.

## Sample 70019

*Type:* Impact-fused, polymict breccia with a glassy matrix.

*Size:* 13×6×6 cm.

*Weight:* 159.9 g.

*Location:* About 100 m west of the LM on the floor of a 3-m crater. Precise location of the crater is unknown.

*Illustrations:* Figures 15, 16 (LRL).

*Comments:* Sample is from the floor of a shallow 3-m crater; the floor, wall, and rim are covered by glassy clods approximately 2 to 8 cm in diameter. The clods were formed from local regolith by the impact that produced the small crater. This is one of a number of such small glassy craters noted by the crew.

*Petrographic description:* Polymict breccia with a glassy matrix. Clasts in the size range 0.1 to 1.0 mm are in the approximate proportions: 7 percent glass, 12 percent plagioclase, 40 percent clinopyroxene, 2 percent olivine, 15 percent opaque minerals, 13 percent basalt, 7 percent fine-grained feldspathic hornfels, 4 percent recrystallized mineral grains.

## Major-element composition:

## Chemical analyses of 70019

	1	2	3
SiO <sub>2</sub> .....	40.66	41.5	41.1
Al <sub>2</sub> O <sub>3</sub> .....	12.38	12.09	12.24
FeO.....	16.38	16.6	16.5
MgO.....	9.50	9.60	9.55
CaO.....	11.03	11.38	11.20
Na <sub>2</sub> O.....	.47	.400	.44
K <sub>2</sub> O.....	.09	.078	.08
TiO <sub>2</sub> .....	8.26	8.31	8.28
P <sub>2</sub> O <sub>5</sub> .....	.07	.073	.07
MnO.....	.24	.222	.23
Cr <sub>2</sub> O <sub>3</sub> .....	.43	.437	.43
Total.....	99.51	100.690	100.12

1. 70019.28 (Rose and others, 1974).  
 2. 70019.29 (Wänke and others, 1975).  
 3. Average of 1 and 2.

## Sample 70035

*Type:* Olivine basalt.

*Size:* 23×15×10 cm.

*Weight:* 5,765 g.

*Location:* Sample was collected from a large partly buried boulder about 45 m northeast of the LM.

*Illustrations:* Pans 5, 6, 7, 11; figures 17, 18 (LRL), 26.

*Comments:* Sample was broken from a 1.5-m boulder on the rim of a shallow 25-m crater. Only the uppermost part of the boulder, which is coarsely vesicular

basalt with distinct parting planes, projects above the surface.

*Petrographic description:* Coarse-grained vesicular porphyritic olivine basalt. Aggregates of clinopyroxene and ilmenite set in a locally plumose groundmass of

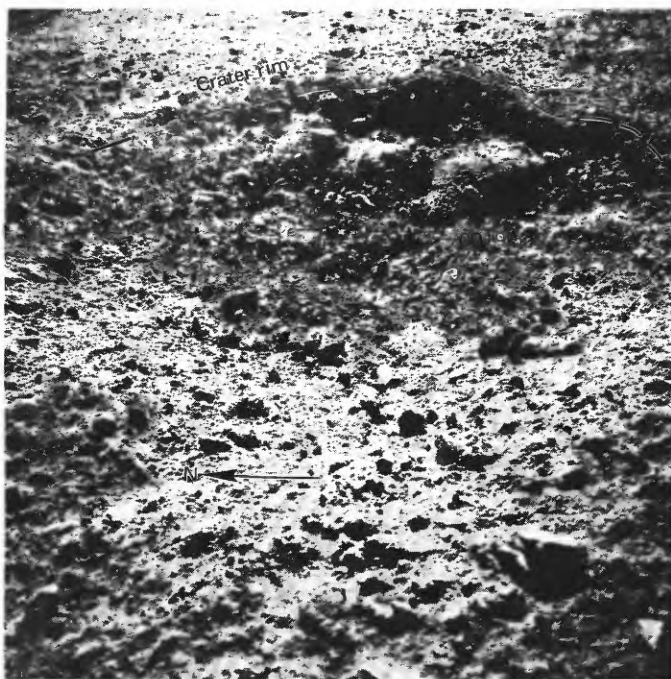


FIGURE 15.—Presampling photograph showing glassy polymict breccia fragment 70019 on floor of shallow 3-m crater. (NASA photograph AS 17-145-22186.)

plagioclase, clinopyroxene, ilmenite, and accessory minerals.

*Major-element composition:*

*Chemical analysis of 70035*

SiO <sub>2</sub> .....	37.84
Al <sub>2</sub> O <sub>3</sub> .....	8.85
FeO.....	18.46
MgO.....	9.89
CaO.....	10.07
Na <sub>2</sub> O.....	.35
K <sub>2</sub> O.....	.06
TiO <sub>2</sub> .....	12.97
P <sub>2</sub> O <sub>5</sub> .....	.05
MnO.....	.28
Cr <sub>2</sub> O <sub>3</sub> .....	.61
Total.....	99.43

70035,1 (Apollo 17 PET, 1973)

*Age:*

*Rb-Sr isochron:*

70035,9,  $3.82 \pm 0.06$  b.y. ( $2\sigma$ ) (Evensen and others, 1973).

70035,6,  $3.73 \pm 0.11$  b.y. ( $2\sigma$ ) (Nyquist and others, 1974).

<sup>40</sup>-<sup>39</sup>Ar:

70035,6,  $3.72 \pm 0.07$  b.y. ( $\geq 2\sigma$ ) (Stettler and others, 1973).

70035,6,  $3.75 \pm 0.07$  b.y. ( $\geq 2\sigma$ ) (Stettler and others, 1973).

70035, 3.74 b.y. (Eberhardt and others, 1973).

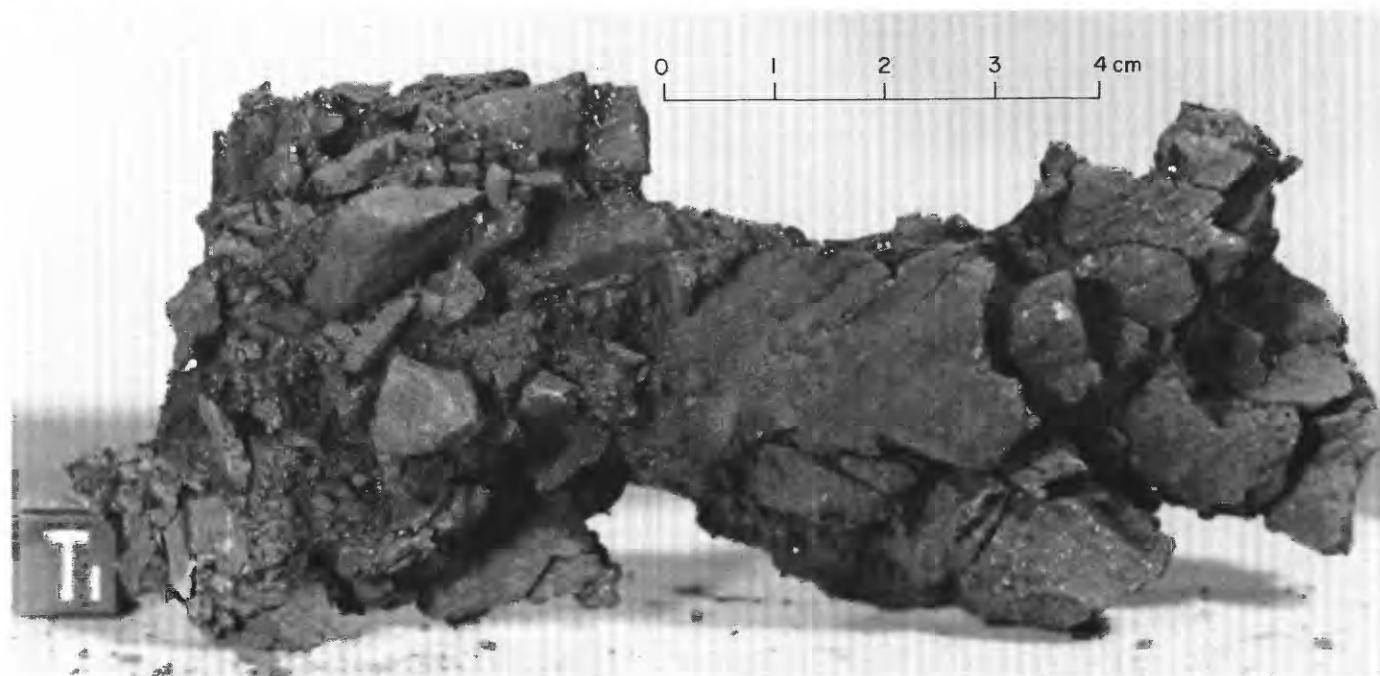


FIGURE 16.—Sample 70019. Impact-fused rock; polymict breccia with glass matrix. (NASA photograph S-73-15333.)

*Exposure age:**Ar:*

70035,6, 100 m.y. (Stettler and others, 1973).

70035,6, 95 m.y. (Stettler and others, 1973).

*Ar and Kr:*

70035, 100 m.y. (Eberhardt and others, 1973).

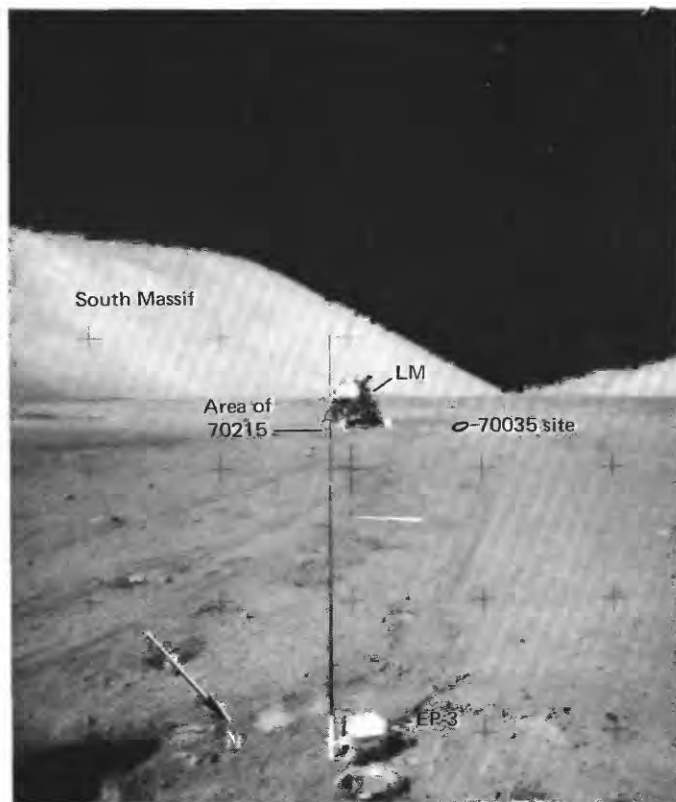
*Sample 70075**Type:* Olivine basalt.*Size:* 3×1.7×1 cm.*Weight:* 5.64 g.*Location:* Unknown.*Illustrations:* Figure 19 (LRL).*Comments:* 70075 is an aphanitic olivine basalt fragment found in the LM after departure from the lunar surface. Its source at the landing site is unknown.*Sample 70135-39, 45-49, 55-57**Type:* Basalt.*Size:* 70135, 10.5×6×3.5 cm; 12 additional smaller fragments.*Weight:* 70135, 446.3 g; 479.90 g total.

FIGURE 17.—Partly buried 1.5-m boulder from which sample 70035 was collected, and postsampling view of 70215 locality. Explosive package 3 in foreground. (NASA photograph AS17-143-21937.)

*Location:* "Geophone rock," 190 m west of the LM in the ALSEP area.*Illustrations:* Pans 1, 2, 3; figures 20, 21 (photomicrograph of 70135).*Comments:* The samples were collected from a large basalt boulder, Geophone rock, that may have been ejected from Camelot crater to the west or from one of the large craters to the south or east. The boulder, which is one of a small number of basalt boulders in the vicinity of the ALSEP, projects about 3 m above the surface.*Petrographic descriptions:*

70135, coarse-grained vesicular porphyritic basalt.

Aggregates of clinopyroxene-ilmenite in an ophitic groundmass of plagioclase, clinopyroxene, ilmenite, and accessory minerals.

70136 and 70137, medium-grained porphyritic basalt. Aggregates of clinopyroxene-ilmenite in a locally plumose(?) groundmass of plagioclase, clinopyroxene, and ilmenite.

*Major-element composition:**Chemical analyses of 70135*

	1	2	3	4
SiO <sub>2</sub> .....	38.60	37.68	37.85	38.04
Al <sub>2</sub> O <sub>3</sub> .....	8.88	7.53	7.34	7.92
FeO.....	18.97	19.74	19.68	19.46
MgO.....	9.45	10.00	9.29	9.58
CaO.....	9.82	9.80	10.18	9.93
Na <sub>2</sub> O.....	.36	.40	.34	.37
K <sub>2</sub> O.....	.06	.051	.09	.07
TiO <sub>2</sub> .....	13.33	13.83	13.34	13.50
P <sub>2</sub> O <sub>5</sub> .....	.04	.077	.07	.06
MnO.....	.29	.260	.29	.28
Cr <sub>2</sub> O <sub>3</sub> .....	.49	.636	.55	.56
Total.....	100.29	100.004	99.02	99.77

1. 70135.33 (Rose and others, 1975).
2. 70135.41 (Duncan and others, 1976).
3. 70135.27 (Rhodes and others, 1976).
4. Average of 1 through 3.

*Age:* Rb-Sr isochron: 70135,27,  $3.75 \pm 0.06$  b.y. ( $2\sigma$ ) (Nyquist and others, 1975).*Exposure age:* Kr-Kr:  $106 \pm 4$  m.y. (Arvidson and others, 1976a).*Sample 70160-64, 65**Type:* Sedimentary, unconsolidated (70160-64) and basalt fragment (70165).*Weight:* 316.17 g, including 2.14-g basalt fragment (70165).*Depth:* Estimated 0-5 cm.*Location:* Collected from the fillet of sediment banked against the east base of a boulder in the ALSEP area.

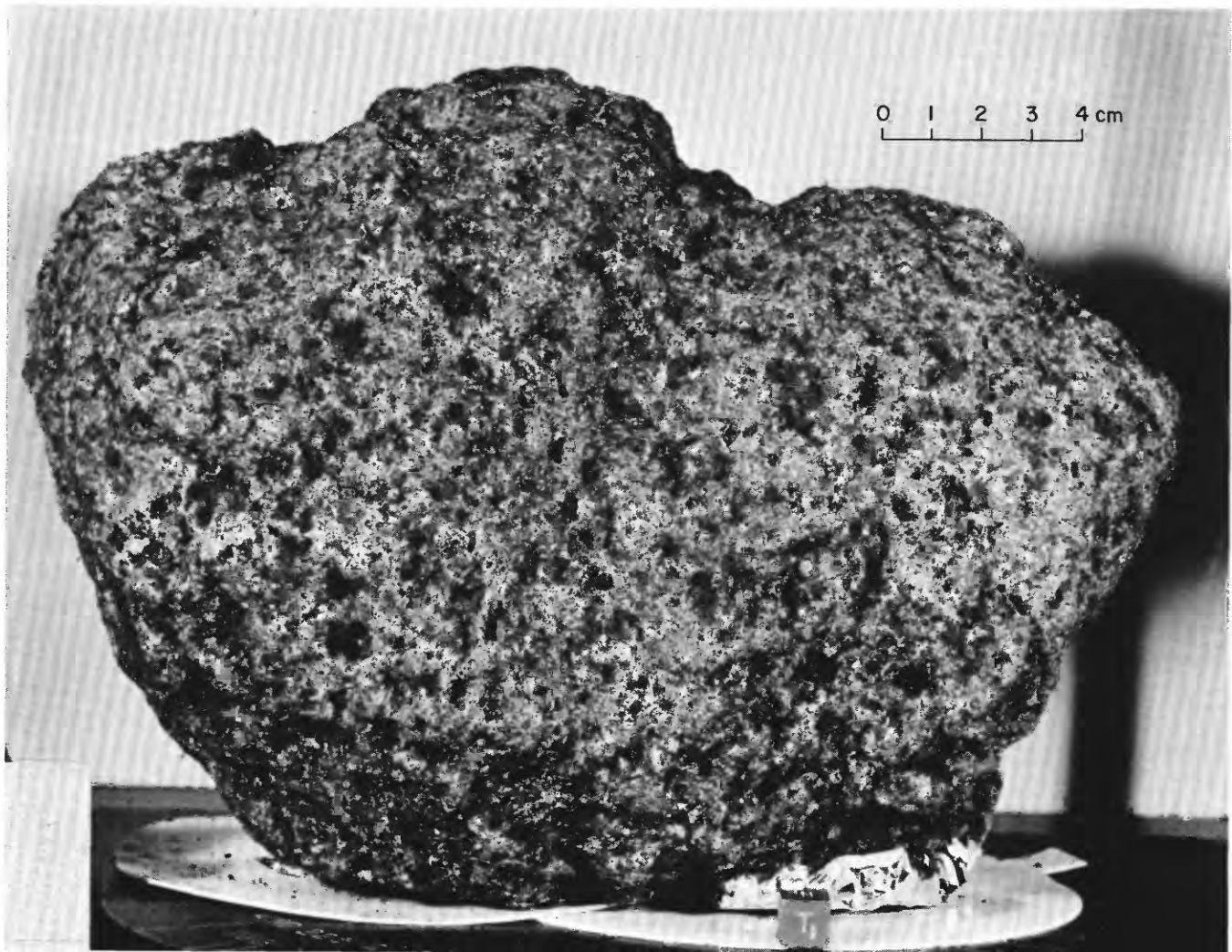


FIGURE 18.—Sample 70035. Coarse-grained vesicular olivine basalt. (NASA photograph S-72-56441.)

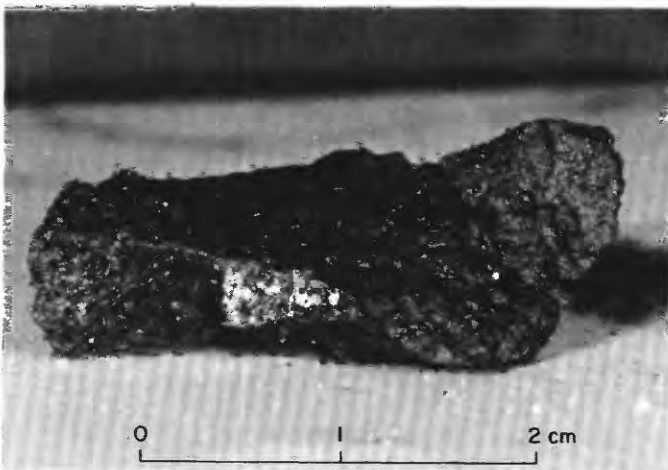


FIGURE 19.—Sample 70075. Aphanitic olivine basalt. (NASA photograph S-73-21768.)

*Illustrations:* Pans 1, 2, 3; figure 22.

*Comments:* The fillet probably represents regolith material, including basalt fragments, that has been heaped against the boulder as ballistic ejecta from nearby impacts.

*Petrographic description:* 7016064, dominantly basalt with feldspar plutonic derivatives, breccia, and agglutinate fragments.

*Components of 90-150- $\mu$ m fraction of 70161,1 (Heiken and McKay, 1974)*

Components	Volume percent
Agglutinate.....	34.0
Basalt, equigranular } .....	15.0
Basalt, variolitic } .....	
Breccia:	
Low grade <sup>1</sup> - brown .....	5.0
Low grade <sup>1</sup> - colorless .....	--
Medium to high grade <sup>2</sup> .....	2.0
Anorthosite.....	--

*Components of 90-150- $\mu$ m fraction of 70161,1 (Heiken and McKay, 1974)—Continued*

<i>Components</i>	<i>Volume percent</i>
Cataclastic anorthosite <sup>3</sup> .....	--
Norite .....	--
Gabbro .....	--
Plagioclase .....	9.0
Clinopyroxene .....	21.6
Orthopyroxene .....	--
Olivine .....	.3
Ilmenite .....	5.0
Glass:	
Orange .....	2.0
"Black" .....	5.2
Colorless .....	.3
Brown .....	.6
Gray, "ropy" .....	--
Other .....	--
Total number grains .....	300

<sup>1</sup>Metamorphic groups 1-3 of Warner (1972).

<sup>2</sup>Metamorphic groups 4-8 of Warner (1972).

<sup>3</sup>Includes crushed or shocked feldspar grains.

*Major-element composition:*

*Chemical analyses of 70161*

SiO <sub>2</sub> .....	40.34
Al <sub>2</sub> O <sub>3</sub> .....	11.60
FeO .....	17.01
MgO .....	9.79
CaO .....	10.98
Na <sub>2</sub> O .....	.32
K <sub>2</sub> O .....	.08
TiO <sub>2</sub> .....	8.99
P <sub>2</sub> O <sub>5</sub> .....	.08
MnO .....	.23
Cr <sub>2</sub> O <sub>3</sub> .....	.46
Total .....	99.88

70161,3 (Apollo 17 PET, 1973).

*Sample 70175*

*Type:* Sedimentary, impact-consolidated polymict breccia.

*Size:* 9×6×6 cm.

*Weight:* 339.6 g.

*Location:* ALSEP area, approximately 5 m south of deep core site.

*Illustrations:* Pans 1, 2, 3; figures 11, 23 (LRL).

*Petrographic description:* Polymict breccia with dominantly basalt clasts, some feldspathic plutonic derivatives, and mineral fragments in a friable matrix.

*Sample 70180-84, 85*

*Type:* Sedimentary, unconsolidated (70180-84); basalt (70185).

*Size:* 70185, two pieces, 9×7.5×5.5 cm; 3.2×2.3×1.5 cm.

*Weight:* 70180-84, 259.78 g; 70185, 466.6 g.

*Depth:* 70180-84, 0-5 cm.

*Location:* ALSEP area, 3 m east of deep core site.

*Illustrations:* Pans 1, 2, 3; figures 24, 25 (LRL).

*Comments:* The samples come from the predominantly fine sediment of the valley floor regolith near the

rim of a 0.5-m crater and just outside of the trampled area surrounding the deep core site. The sediment (70180-84) was collected specifically for comparison with the deep core. The rock (70185), one of



FIGURE 20.—Geophone rock before sampling, showing probable area from which basalt fragments 70135-57 were collected. (NASA photograph AS 17-147-22536.)

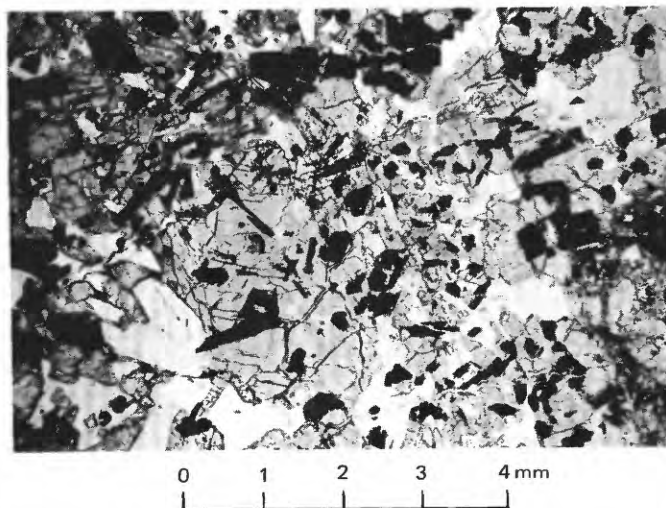


FIGURE 21.—Sample 70135. Photomicrograph showing aggregate of clinopyroxene-ilmenite (left center) in groundmass with plumose intergrowths of plagioclase and clinopyroxene.

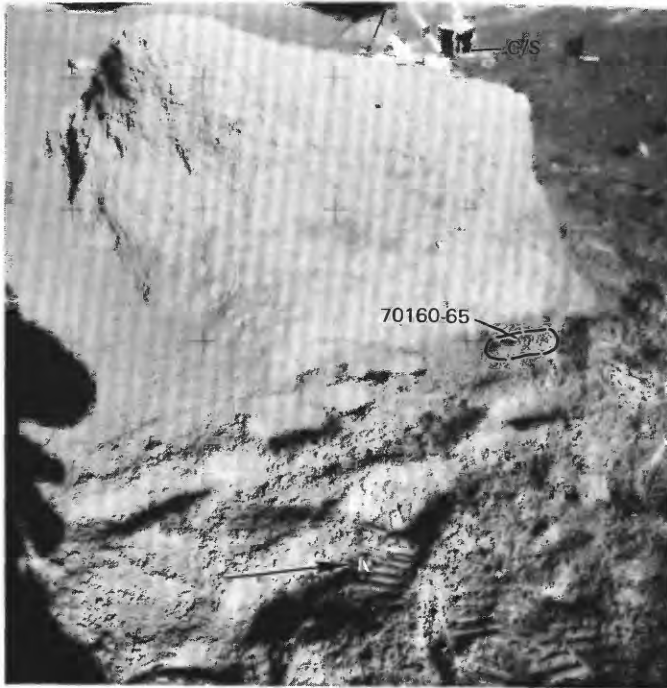


FIGURE 22.—Sample 70160-65 site, after sampling, in fillet at base of 1.5-m boulder near ALSEP central station (C/S). Sediment near boulder has been trampled, and some may have been kicked up onto boulder. (NASA photograph AS 17-136-20718.)

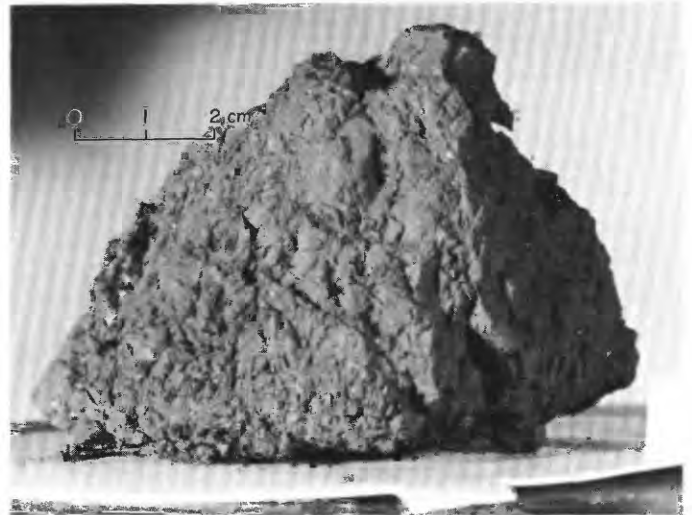


FIGURE 23.—Sample 70175. Impact-consolidated polymict breccia with distinctive fracture pattern. (NASA photograph S-73-15345.)

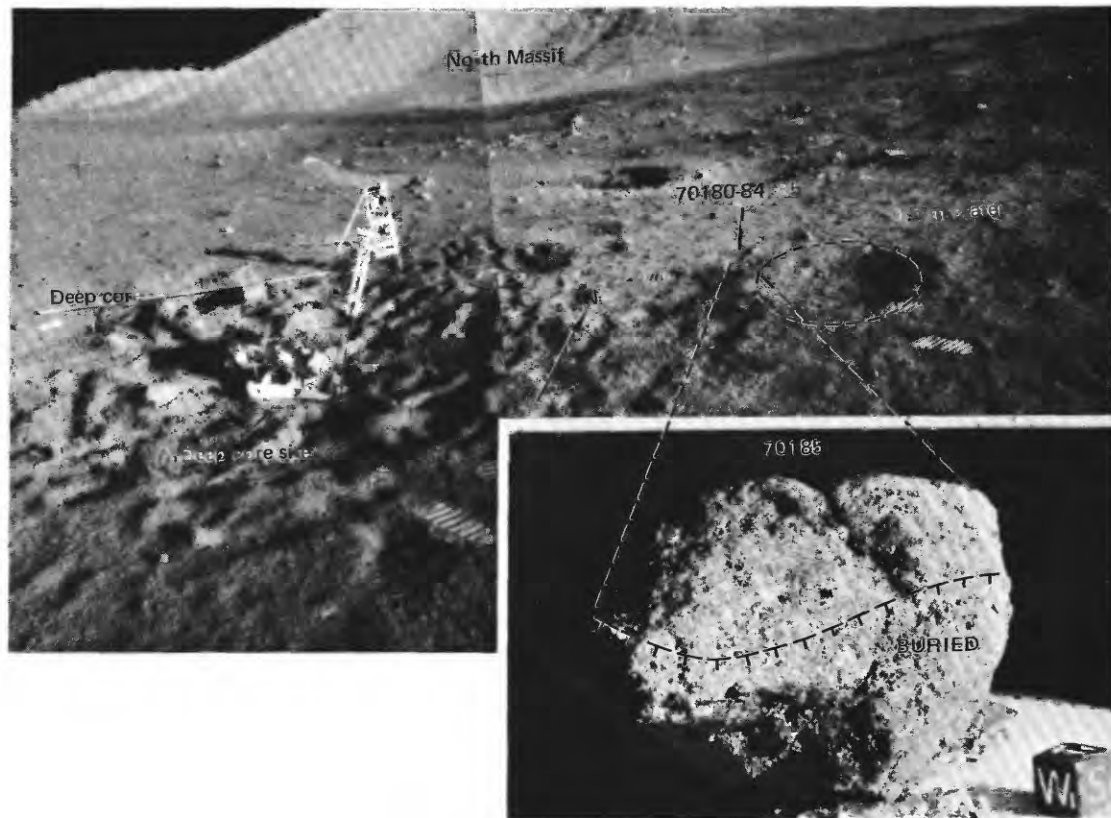


FIGURE 24.—Sample 70180-85 before collection, 3 m east of deep core (sample 70001-70009) site. Inset is LRL view showing 70185 with reconstructed lunar surface orientation and lighting. (NASA photographs AS17-136-20720 and 20721; S-73-17797.)

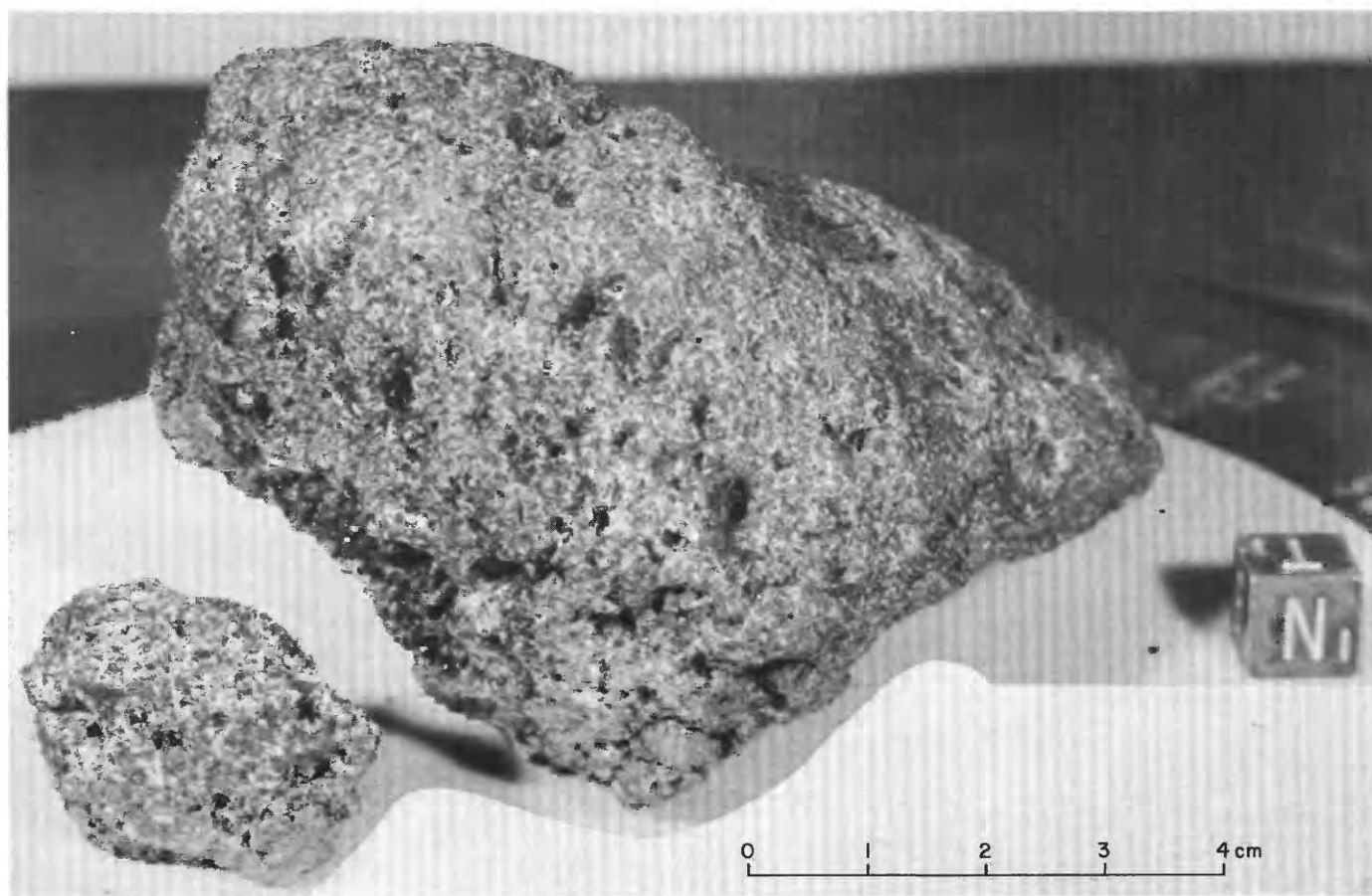


FIGURE 25.—Sample 70185. Fine-grained vesicular basalt. (NASA photograph S-73-15872.)

the many basalt fragments in the valley floor regolith, broke into two pieces before unpacking in the Lunar Receiving Laboratory.

*Petrographic descriptions:*

70180-84, dominantly basalt and agglutinate fragments.

*Components of 90-150- $\mu$ m fraction of 70181,1 (Heiken and McKay, 1974)*

Components	Volume percent
Agglutinate.....	56.0
Basalt, equigranular } .....	14.0
Basalt, variolitic } .....	
Breccia:	
Low grade <sup>1</sup> -brown.....	4.6
Low grade <sup>1</sup> -colorless.....	.3
Medium to high grade <sup>2</sup> .....	2.6
Anorthosite.....	..
Cataclastic anorthosite <sup>3</sup> .....	.3
Norite.....	..
Gabbro.....	..
Plagioclase.....	4.3
Clinopyroxene.....	10.3
Orthopyroxene.....	.3
Olivine.....	..
Ilmenite.....	2.3
Glass:	
Orange.....	3.0
"Black".....	.6

*Components of 90-150- $\mu$ m fraction of 70181,1 (Heiken and McKay, 1974) —Continued*

Components	Volume percent
Glass—Continued	
Colorless.....	.3
Brown.....	.6
Gray, "ropy".....	..
Total number grains.....	300

<sup>1</sup>Metamorphic groups 1-3 of Warner (1972).

<sup>2</sup>Metamorphic groups 4-8 of Warner (1972).

<sup>3</sup>Includes crushed or shocked feldspar grains.

70185, fine-grained vesicular basalt. Scarce aggregates of clinopyroxene-ilmenite in a subophitic(?) groundmass of plagioclase, clinopyroxene, ilmenite, and accessory minerals.

*Major-element compositions:*

*Chemical analyses of 70181 and 70185*

	1	2	3	4
SiO <sub>2</sub> .....	40.87	40.90	40.88	40.18
Al <sub>2</sub> O <sub>3</sub> .....	12.30	12.40	12.35	9.04
FeO.....	16.37	16.55	16.46	17.64
MgO.....	9.82	9.76	9.79	8.11
CaO.....	11.05	10.97	11.01	11.95

## Chemical analyses of 70181 and 70185 — Continued

	1	2	3	4
Na <sub>2</sub> O .....	.35	.38	.36	.39
K <sub>2</sub> O .....	.08	.09	.08	.04
TiO <sub>2</sub> .....	8.11	8.40	8.26	11.52
P <sub>2</sub> O <sub>5</sub> .....	.06	.07	.06	.02
MnO .....	.24	.21	.22	.26
Cr <sub>2</sub> O <sub>3</sub> .....	.44	.46	.45	.40
Total .....	99.69	100.19	99.92	99.55

1. 71081.3 (Apollo 17 PET, 1973).  
 2. 70181.18 (Rose and others, 1974).  
 3. Average of 1 and 2.  
 4. 70185.32 (Rhodes and others, 1976).

**Exposure age:** Minimum track density: 70181, 100 m.y. (Fleischer and Hart, 1974).

## Sample 70215

**Type:** Olivine basalt.

**Size:** 23×13×10.5 cm.

**Weight:** 8,110 g.

**Location:** Approximately 65 m east of the LM, between the LM and the SEP site.

**Illustrations:** Pans 6, 7, 11; figures 17, 26, 27 (photomicrograph).

**Comments:** The largest rock collected on the mission, 70215 is a boulder of subfloor basalt from the regolith.

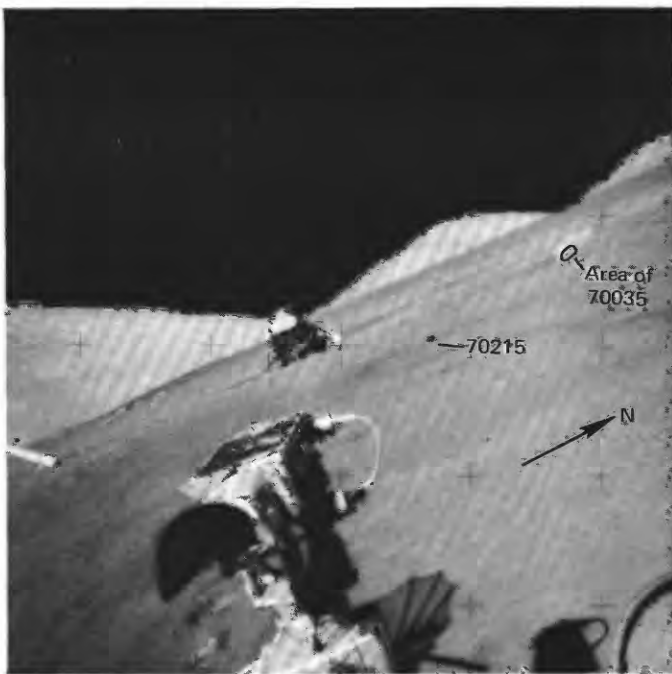


FIGURE 26.—Tilted view from LRV (television camera in foreground) of LM area and 70035 and 70215 sample sites. Astronaut had up-ended rock 70215 before taking photograph. (NASA photograph AS17-143-21926.)

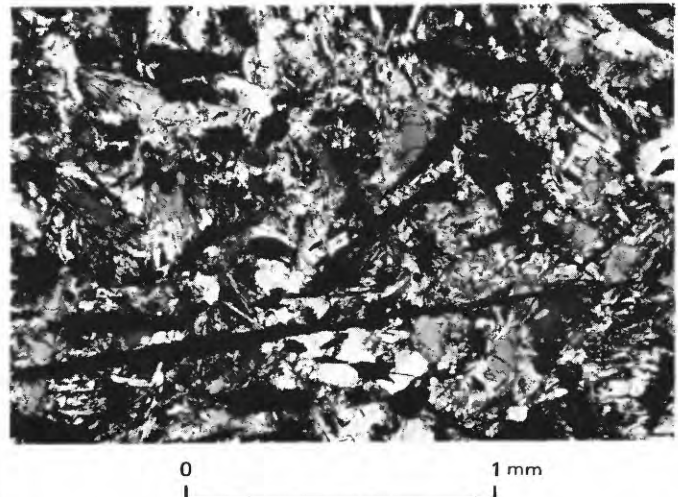


FIGURE 27.—Sample 70215. Photomicrograph showing subvolcanic texture of basalt. Minerals are olivine, clinopyroxene, plagioclase, and thin plates of ilmenite.

**Petrographic description:** Fine-grained olivine basalt with microphenocrysts of olivine, ilmenite, and clinopyroxene in a subvolcanic groundmass of plagioclase, clinopyroxene, ilmenite, and accessory minerals.

## Major-element composition:

## Chemical analyses of 70215

	1	2	3	4	5	6
SiO <sub>2</sub> .....	37.19	37.91	38.46	38.3	37.62	37.9
Al <sub>2</sub> O <sub>3</sub> .....	8.67	8.86	9.01	8.71	8.79	8.81
FeO .....	19.62	19.96	19.40	19.9	19.22	19.62
MgO .....	8.52	7.99	7.91	8.32	9.34	8.42
CaO .....	10.43	10.77	10.94	10.63	10.82	10.72
Na <sub>2</sub> O .....	.32	.38	.42	.369	.31	.36
K <sub>2</sub> O .....	.04	.041	.05	.045	.08	.05
TiO <sub>2</sub> .....	13.14	13.08	12.48	12.53	13.20	12.89
P <sub>2</sub> O <sub>5</sub> .....	.09	.114	.10	.101	.07	.10
MnO .....	.28	.264	.29	.252	.27	.27
Cr <sub>2</sub> O <sub>3</sub> .....	.42	.431	.39	.396	.41	.41
Total .....	99.72	99.800	99.45	99.553	100.13	99.55

1. 70215.2 (Apollo 17 PET, 1973).  
 2. 70215.55 (Duncan and others, 1974).  
 3. 70215.56 (Rhodes and others, 1974).  
 4. 70215.61 (Wänke and others, 1975).  
 5. 70215.73 (Rose and others, 1974).  
 6. Average of 1 through 5.

**Age:** <sup>40</sup>Ar: 70215.21, 3.84±0.04 b.y. (Kirsten and Horn, 1974).

**Exposure age:** Ar: 70215.21, 100±12 m.y. (Kirsten and Horn, 1974).

## Sample 70255

**Type:** Olivine basalt.

**Size:** Two mated pieces, 7.5×5.5×4.5 cm; 5.5×3.5×3 cm.

Weight: 277.2 g.

Location: 2 m south of SEP.

Illustrations: Pan 11, figures 28, 29 (LRL).

Comments: Sample was collected from the rim of a 0.5-m crater. The rock may have been excavated from the regolith when the crater was formed.

Petrographic description: Fine-grained olivine basalt. Scarce olivine microphenocrysts in an intersertal or vitrophyric groundmass.

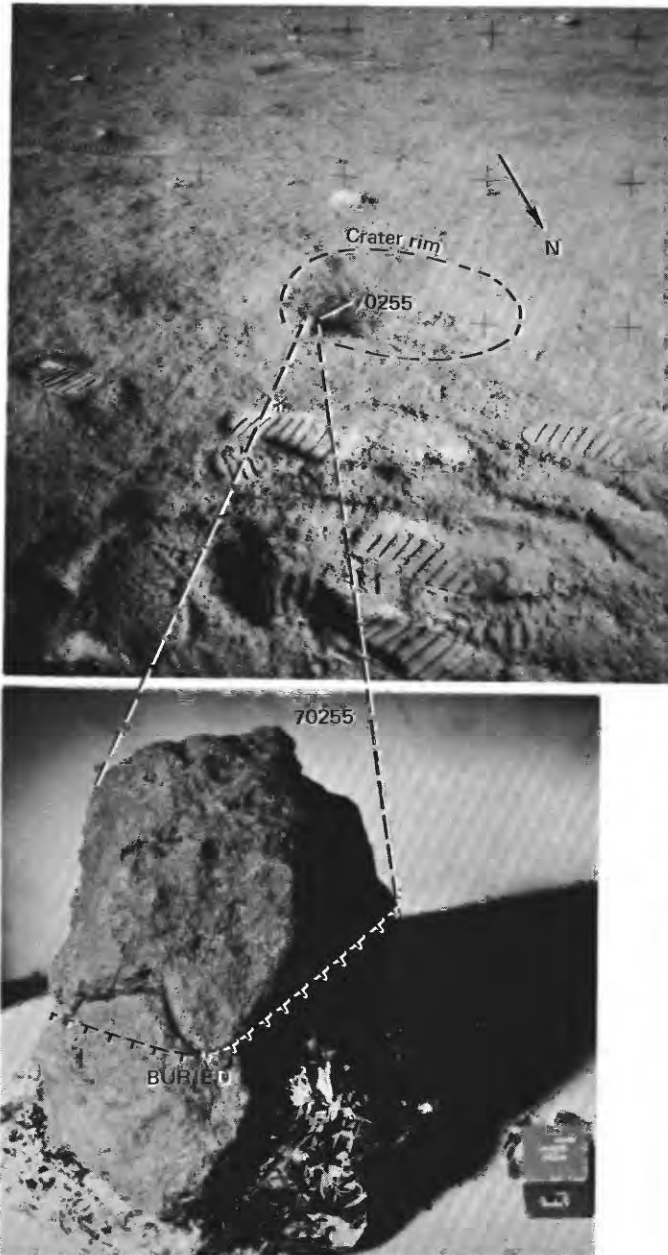


FIGURE 28.—Top, view of sample 70255 before collection from rim of small crater. Bottom, LRL view showing sample with reconstructed lunar surface orientation and lighting. (NASA photographs AS 17-135-20535; S-73-21974.)

#### Major-element composition:

##### Chemical analysis of 70255

SiO <sub>2</sub> .....	40.11
Al <sub>2</sub> O <sub>3</sub> .....	9.02
FeO.....	18.73
MgO.....	7.63
CaO.....	11.30
Na <sub>2</sub> O.....	.39
K <sub>2</sub> O.....	.05
TiO <sub>2</sub> .....	11.41
P <sub>2</sub> O <sub>5</sub> .....	.04
MnO.....	.29
Cr <sub>2</sub> O <sub>3</sub> .....	.34
Total.....	99.31

70255,3 (Rhodes and others, 1976).

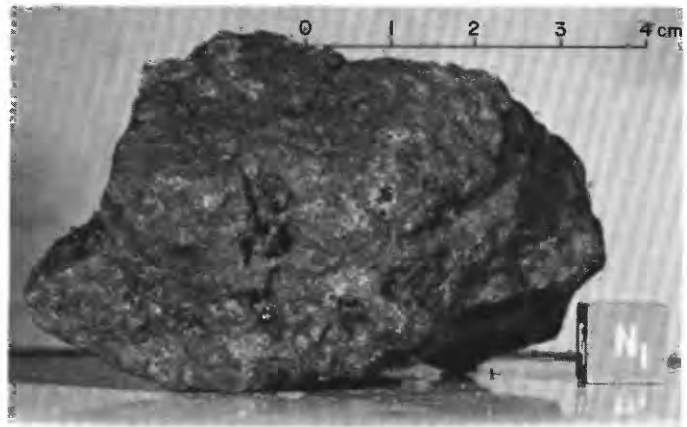


FIGURE 29.—Sample 70255. Fine-grained olivine basalt. (NASA photograph S-73-24088.)

#### Sample 70270-74, 75

Type: Sedimentary, unconsolidated (70270-74) and olivine basalt (70275).

Size: 70275, 6.5×5.0×3.5 cm.

Weight: 70270-74, 193.32 g; 70275, 171.4 g.

Location: About 10 m southeast of SEP.

Illustrations: Pan 11, figures 30, 31 (photomicrograph).

Comments: Rock 70275 is a basalt fragment from the regolith; sediment 70270-74 was scooped with the rock.

#### Petrographic descriptions:

70270-74, unconsolidated sediment, dominantly basalt with agglutinate, glass, and breccia fragments.

70275, medium-grained olivine basalt. Microphenocrysts of olivine and ilmenite in a variolitic groundmass of plagioclase, clinopyroxene, ilmenite, and accessory minerals.

#### Major-element composition:

##### Chemical analysis of 70275

SiO <sub>2</sub> .....	39.37
Al <sub>2</sub> O <sub>3</sub> .....	10.23
FeO.....	18.61

## Chemical analysis of 70275—Continued

MgO .....	6.09
CaO .....	11.65
Na <sub>2</sub> O .....	.38
K <sub>2</sub> O .....	.06
TiO <sub>2</sub> .....	11.90
P <sub>2</sub> O <sub>5</sub> .....	.08
MnO .....	.28
Cr <sub>2</sub> O <sub>3</sub> .....	.26
Total .....	98.91

70275,3 (Rhodes and others, 1976).

## Sample 70295

*Type:* Sedimentary, weakly lithified polymict breccia.*Size:* 12×6×4.8 cm.*Weight:* 361.2 g.*Illustration:* Figure 32 (LRL).*Location:* Collected near the SEP. The precise location is unknown.*Petrographic description:* Polymict breccia with clasts of basalt, feldspathic metaclastic rock, feldspathic cataclasite, and mineral debris in a fine-grained friable matrix.

## STATION 1

## LOCATION

Station 1 is located on the northwestern flank of Steno crater, approximately 150 m from the rim crest (figs. 6, 7E; pl. 2). The station was planned for the east rim of 600-m Emory crater. However, shortage of time after completion of activities in the LM/ALSEP/SEP

area during EVA-1 required selection of a station area nearer to the LM than had been planned.

## OBJECTIVES

The originally planned station was interpreted to be in an area where blocky subfloor material, represented in the Emory crater ejecta, was exposed in a window in the dark mantle. Unusually dark local patches in the Emory area were considered to represent possibly

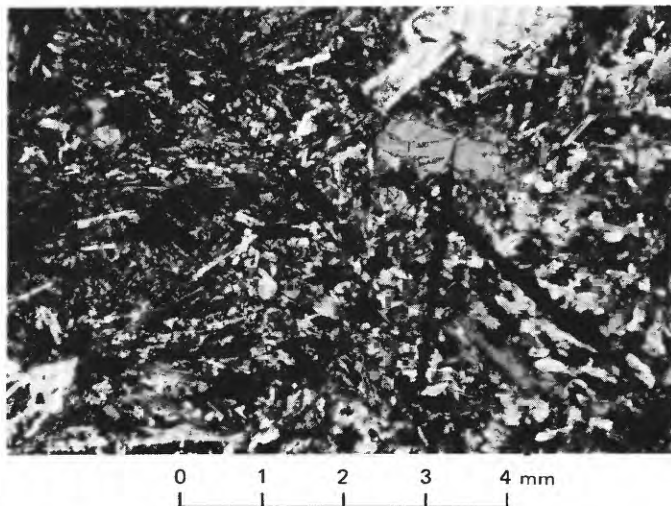


FIGURE 31.—Sample 70275. Photomicrograph showing variolitic texture with fan-shaped intergrowths of clinopyroxene, plagioclase, and ilmenite, larger microphenocrysts of olivine, and thin plates of ilmenite.



FIGURE 30.—Left, sample 70275 on lunar surface. (NASA photograph AS17-135-20540.) Right, LRL view showing 70275 with reconstructed lunar surface orientation and lighting. (NASA photograph S-73-21388.)

younger or thicker deposits of dark mantle material. Observation and sampling were planned to (1) characterize the rock types of the subfloor and dark mantle units, (2) investigate contact relations exposed in the crater rim and wall, and (3) interpret, if possible, the modes of origin of the units (Sevier, 1972).

#### GENERAL OBSERVATIONS

The station area is in gently rolling terrain with abundant rocks up to about a meter in size. Larger blocks, up to several meters in size, can be seen to the south on the rim of Steno crater (pans 12, 13). In part, the rocks are concentrated around small craters in the station area, but some concentrations are not apparently related to craters. The rocks are buried to various degrees, from perched on the surface to nearly completely buried. Generally, fillets of sediment are not developed adjacent to the rocks.

Most of the sampling was done near the distinctly raised rim of a blocky 10-m crater (fig. 33). In particular, fragments were collected from two 0.5-m boulders associated with the crater (pans 12, 13). A rake sample (the rake is a sievelike long-handled scoop designed for gathering a representative collection of fragments of

centimeter size and larger from the upper few centimeters of the regolith) was collected from a relatively flat block-free area 15 m east of the blocky crater. The two sample areas represent the extremes of rock concentrations in the station area. Except for one tiny agglutinate fragment, both sample areas yielded only basalt fragments and soil.

Craters in the station area range from several centimeters to tens of meters in diameter. Most are subdued; some are sharp rimmed and blocky. The 10-m crater where rocks were sampled is one of the sharpest and blockiest craters at station 1.

#### GEOLOGIC DISCUSSION

The basalt-rich surficial material observed and sampled at station 1 is on the ejecta blanket of Steno crater; it represents part of the cluster ejecta (fig. 34). Steno crater is about 600 m in diameter; hence, the maximum depth from which rock might have been excavated is about 120 m. The station area is about one-fourth of a crater diameter out from the crater rim. Therefore, the basalt fragments probably represent subfloor basalt from an intermediate depth in Steno crater.

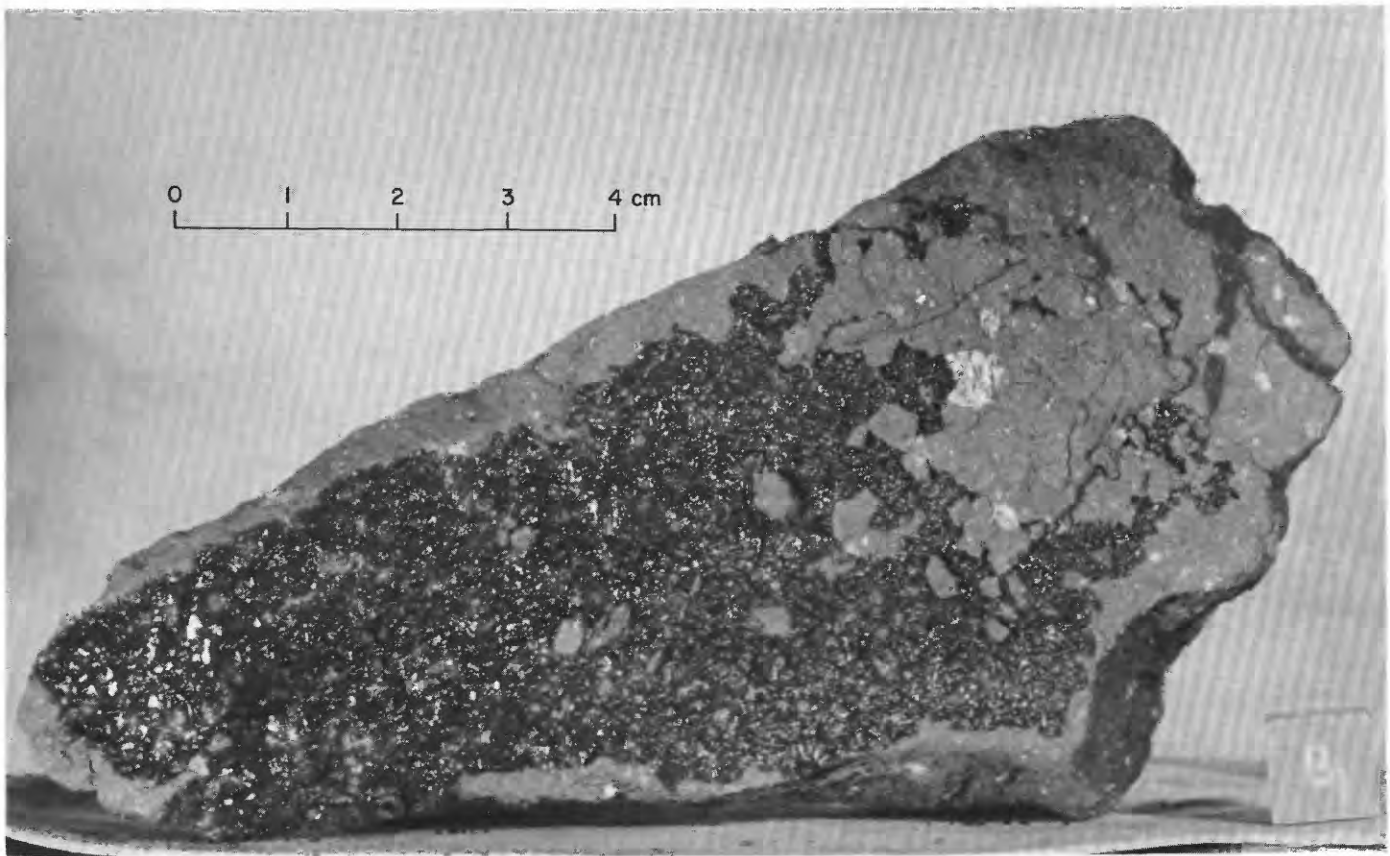


FIGURE 32.—Sample 70295. Weakly lithified polymict breccia. Part of a shiny dark glass vein formed during impact excavation of the rock is exposed on the near surface of the sample. (NASA photograph S-73-17192.)

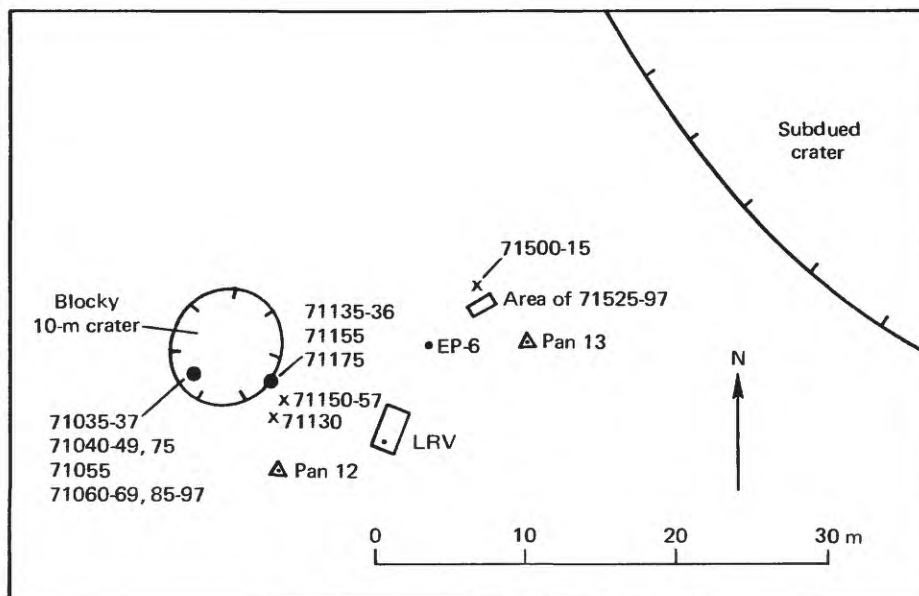


FIGURE 33.—Planimetric map of station 1.

Samples from the two large boulders of the 10-m crater have exposure ages of 102 and 110 m.y. It seems most likely that the boulders were excavated from the subfloor basalt by the impact that formed Steno crater; they were subsequently repositioned by the impact that formed the 10-m crater. Hence, their exposure ages may represent a younger limit for the age of Steno crater. The similarity to exposure ages of 95 to 106 m.y. determined for boulders near the LM suggests that the crater cluster was created approximately 100 m.y. ago. Arvidson and others (1976b) reached a similar conclusion.

On the basis of trace-element distributions, Rhodes and others (1976) concluded that the station 1 basalt samples, although similar in petrography and major-element composition, represent at least two separate lava types. The two large boulders, which are the most likely to represent target material excavated for the first time by the Steno crater, are in their group B.

## SUMMARY OF SAMPLING

## Sample 71035-37

*Type:* Olivine basalt.

*Size:* 71035, 8×5×2.5 cm; 71036, 8.5×4×3 cm; 71037, 2.5×2×2 cm.

*Weight:* 71035, 144.8 g; 71036, 118.4 g; 71037, 14.39 g.

*Location:* From 0.5-m boulder on southwestern wall of blocky 10-m crater (same boulder as 71055).

*Illustrations:* Pans 12, 13; figs. 35, 36 (71035, LRL), 37 (71036, LRL), 38 (71037, LRL), 41.

*Comments:* Sampled boulder is subfloor basalt from the ejecta blanket of Steno crater. It presumably was

repositioned by the impact that formed the 10-m crater.

*Petrographic descriptions:*

71035, medium-grained vesicular olivine basalt. Sparse olivine.

71036, 71037, medium-grained vesicular olivine(?) basalt.

*Major-element composition:**Chemical analysis of 71035*

SiO <sub>2</sub> .....	38.25
Al <sub>2</sub> O <sub>3</sub> .....	8.77
FeO .....	19.74
MgO .....	7.98
CaO .....	10.87
Na <sub>2</sub> O .....	.38
K <sub>2</sub> O .....	.03
TiO <sub>2</sub> .....	13.06
P <sub>2</sub> O <sub>5</sub> .....	.10
MnO .....	.29
Cr <sub>2</sub> O <sub>3</sub> .....	.39
Total .....	100.86

71035,4 (Rhodes and others, 1976).

## Sample 71040-44, 45-49, 75

*Type:* Sedimentary, unconsolidated (71040-44) and six basalt fragments (71045-49, 75).

*Weight:* 71040-44, 258.93 g; 71045-49, 75, total 23.617 g.

*Depth:* 1-2 cm.

*Location:* In shadowed area on west side of 0.5-m boulder on southwestern wall of blocky 10-m crater.

*Illustrations:* Pans 12, 13; figures 35, 41.

*Comments:* Ejecta of blocky 10-m crater. Basalt chips were scooped up with soil sample 71040-44. Sample

71060-69, 85-97 was subsequently scooped from 5 to 6-cm depth at same locality.

*Petrographic descriptions:*

71040-44, dominantly basalt with minor feldspathic plutonic derivatives and agglutinate.

*Components of 90-150- $\mu$ m fraction of 71041,1 (Heiken and McKay, 1974)*

Components	Volume percent
Agglutinates.....	27.4
Basalt, equigranular.....	12.7
Basalt, variolitic.....	1.0
Breccia:	
Low grade <sup>1</sup> - brown.....	1.0
Low grade <sup>1</sup> - colorless.....	1.0
Medium to high grade <sup>2</sup> .....	2.5
Anorthosite.....	--
Cataclastic anorthosite <sup>3</sup> .....	1.0

*Components of 90-150- $\mu$ m fraction of 71041,1 (Heiken and McKay, 1974)—Continued*

Components	Volume percent
Norite.....	--
Gabbro.....	--
Plagioclase.....	12.2
Clinopyroxene.....	17.3
Orthopyroxene.....	--
Olivine.....	.5
Ilmenite.....	5.6
Glass:	
Orange.....	3.6
"Black".....	8.1
Colorless.....	2.0
Brown.....	4.1
Gray, "ropy".....	--
Other.....	--
Total number grains.....	197

<sup>1</sup>Metamorphic groups 1-3 of Warner (1972).

<sup>2</sup>Metamorphic groups 4-8 of Warner (1972).

<sup>3</sup>Includes crushed or shocked feldspar grains.

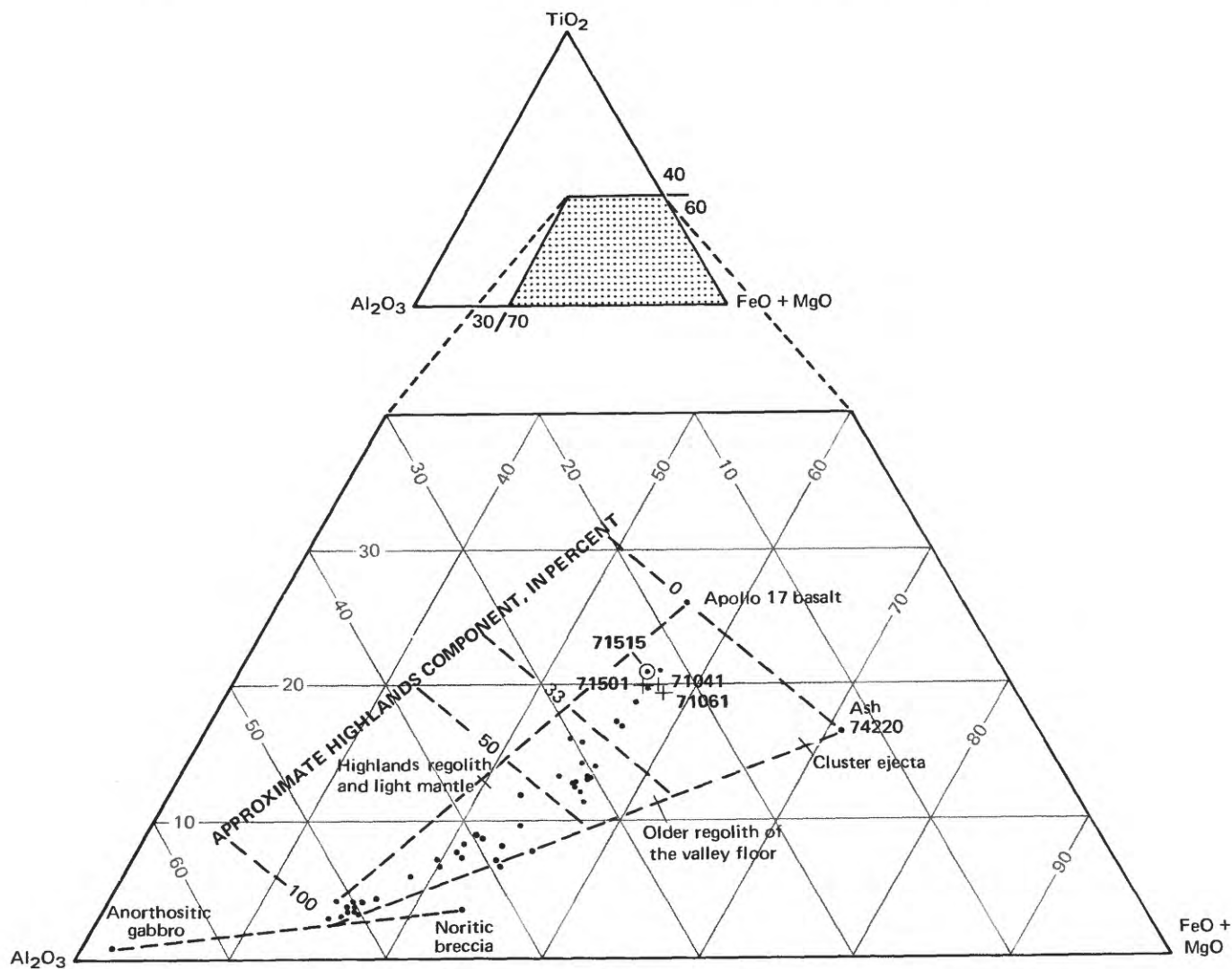


FIGURE 34.—Relative amounts of  $\text{TiO}_2$ ,  $\text{Al}_2\text{O}_3$ , and  $\text{FeO} + \text{MgO}$  in sediment samples from station 1 (crosses) and agglutinate fragment 71515 (circle) in comparison with sediment samples from rest of traverse region (dots). Apollo 17 basalt, anorthositic gabbro, and noritic breccia values from Rhodes and others (1974).

71045, medium-grained vesicular porphyritic olivine basalt. Aggregates of clinopyroxene-ilmenite in an ophitic groundmass of plagioclase, clinopyroxene, ilmenite, and accessory minerals.

*Major-element composition:*

*Chemical analysis of 71041*

SiO <sub>2</sub> .....	39.74
Al <sub>2</sub> O <sub>3</sub> .....	10.80
FeO .....	17.73
MgO .....	9.72
CaO .....	10.72
Na <sub>2</sub> O .....	.35
K <sub>2</sub> O .....	.08

*Chemical analysis of 71041—Continued*

TiO <sub>2</sub> .....	9.57
P <sub>2</sub> O <sub>5</sub> .....	.07
MnO .....	.24
Cr <sub>2</sub> O <sub>3</sub> .....	.47
Total .....	99.49

71041,3 (Apollo 17 PET, 1973).

*Sample 71055*

*Type:* Olivine(?) basalt.

*Size:* 19.5×9.5×2.5 cm.

*Weight:* 669.6 g.

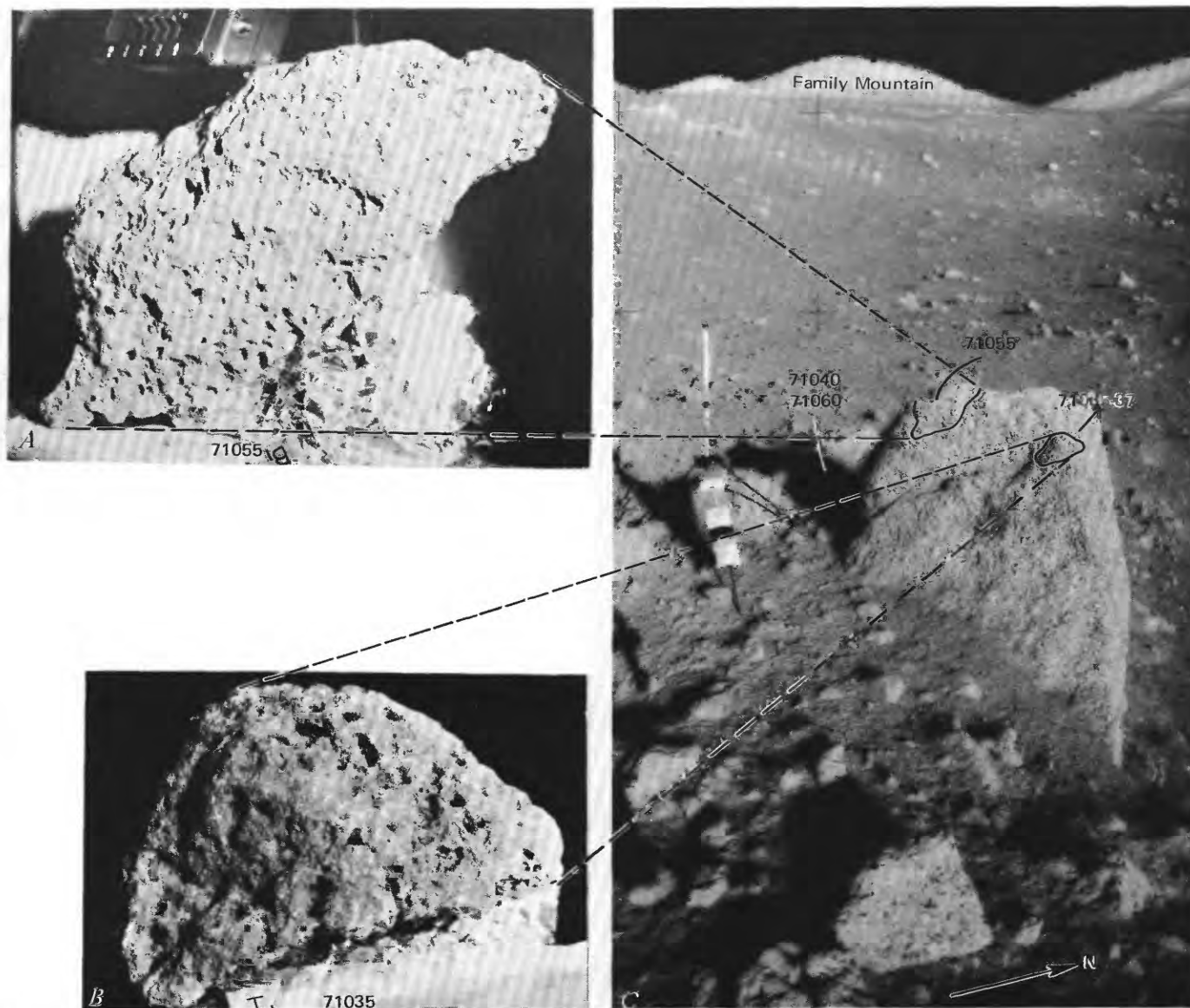


FIGURE 35.—A, Sample 71055 with reconstructed lunar surface orientation and lighting (LRL polaroid photograph). B, Sample 71035 with reconstructed lunar surface orientation and lighting (NASA photograph S-73-17804); C, Samples 71035 and 71055 before collection from 0.5-m boulder in southwest wall of blocky 10-m crater. Samples 71040-49, 75 and 71060-69, 85, 97 collected in shadowed area adjacent to boulder. (NASA photograph AS17-136-20739.)

**Location:** From 0.5-m boulder on southwestern wall of blocky 10-m crater (same boulder as 71035).

**Illustrations:** Pans 12, 13; figures 35, 39 (photomicrograph), 41.

**Comments:** Sampled boulder is subfloor basalt reexcavated from the Steno ejecta blanket by the impact that formed the 10-m crater.

**Petrographic description:** Medium-grained vesicular olivine(?) basalt with a locally plumose groundmass of plagioclase, clinopyroxene, ilmenite, and accessory minerals.

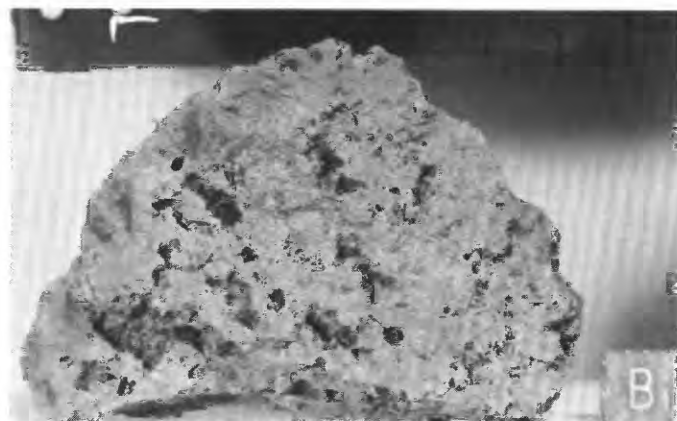


FIGURE 36.—Sample 71035. Medium-grained vesicular basalt. (NASA photograph S-73-15672.)

#### Major-element composition:

##### Chemical analysis of 71055

SiO <sub>2</sub> .....	38.14
Al <sub>2</sub> O <sub>3</sub> .....	8.62
FeO .....	19.20
MgO .....	9.04
CaO .....	10.77
Na <sub>2</sub> O .....	.31
K <sub>2</sub> O .....	.06
TiO <sub>2</sub> .....	13.41
P <sub>2</sub> O <sub>5</sub> .....	.08
MnO .....	.26
Cr <sub>2</sub> O <sub>3</sub> .....	.41
Total .....	100.30

71055,51 (Rose and others, 1974).

**Age:** Rb-Sr isochron: 71055,  $3.64 \pm 0.09$  b.y. (Terra and others, 1974a).

**Exposure age:** Kr-Kr: 71055,  $110 \pm 7$  m.y. (Arvidson and others, 1976b).

Sample 71060-64, 65-69, 85-89, 95-97

**Type:** Sedimentary, unconsolidated (71060-64) and 13 basalt fragments (71065-69, 85-89, 95-97).

**Weight:** 71060-64, 506.48 g; 71065-69, 85-89, 95-97, total 78.235 g.

**Depth:** 5-6 cm.

**Location:** In shadowed area on west side of 0.5-m boulder on southwestern wall of blocky 10-m crater.

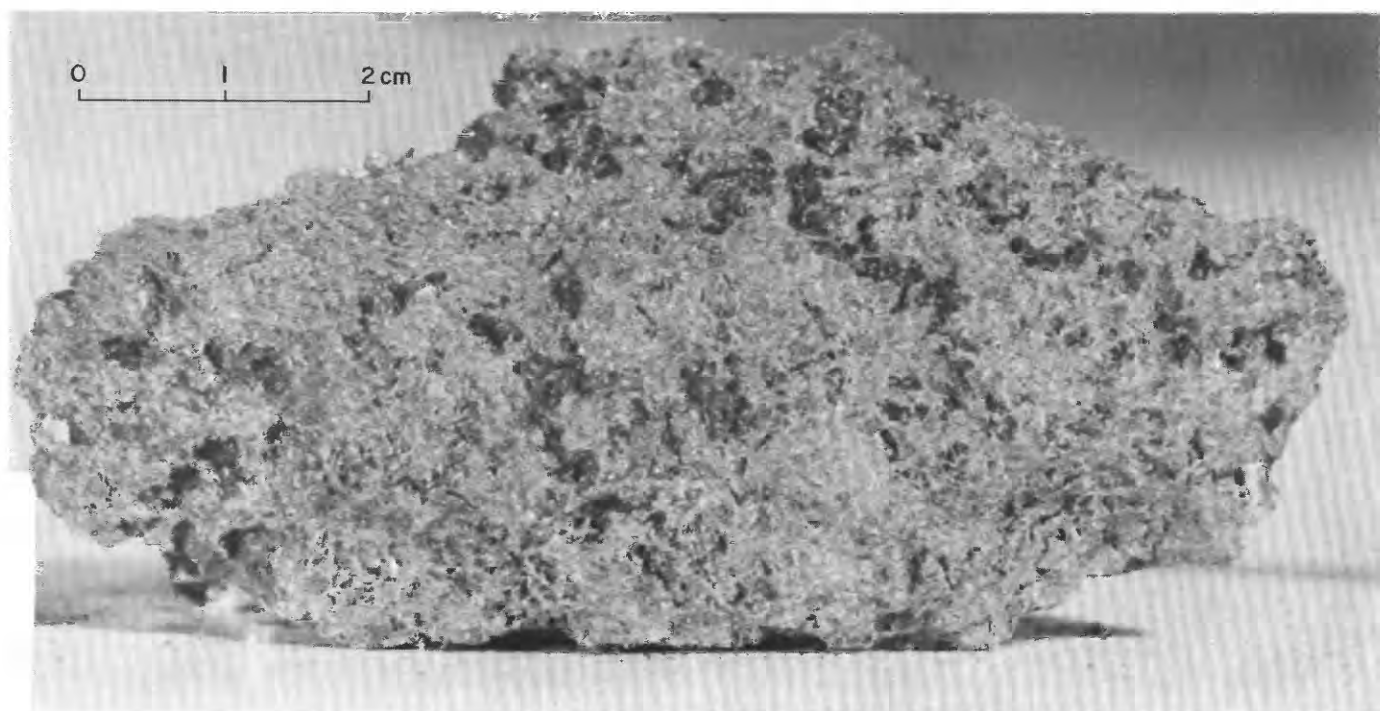


FIGURE 37.—Sample 71036. Medium-grained vesicular olivine(?) basalt. Pyroxene and ilmenite crystals line cavities. (NASA photograph S-73-15675.)

*Illustrations:* Pans 12, 13; figures 35, 40 (71065, LRL), 41.

*Comments:* Ejecta of blocky 10-m crater. Basalt chips were scooped up with sediment 71060-64. Sample 71040-49, 75 was previously scooped from 1 to 2-cm depth at same locality.

*Petrographic descriptions:*

71060-64, Dominantly basalt fragments.

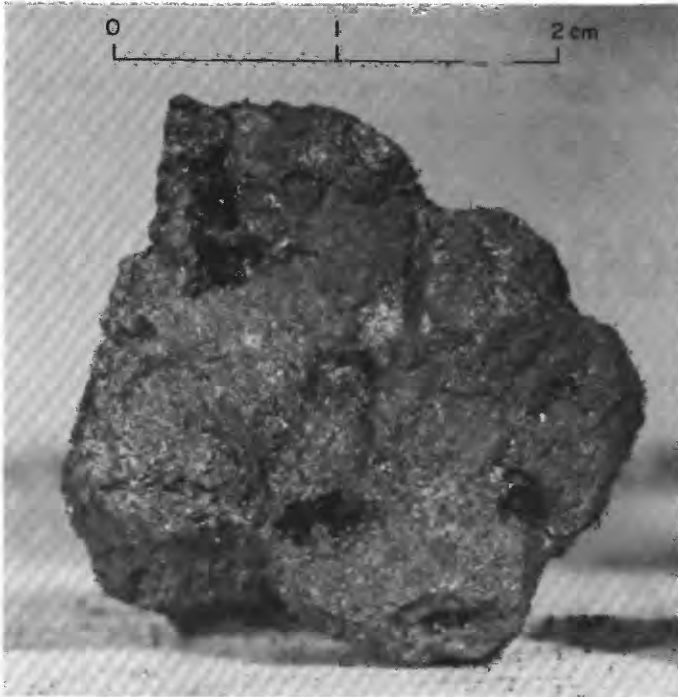


FIGURE 38.—Sample 71037. Medium-grained vesicular olivine(?) basalt. (NASA photograph S-73-15697.)

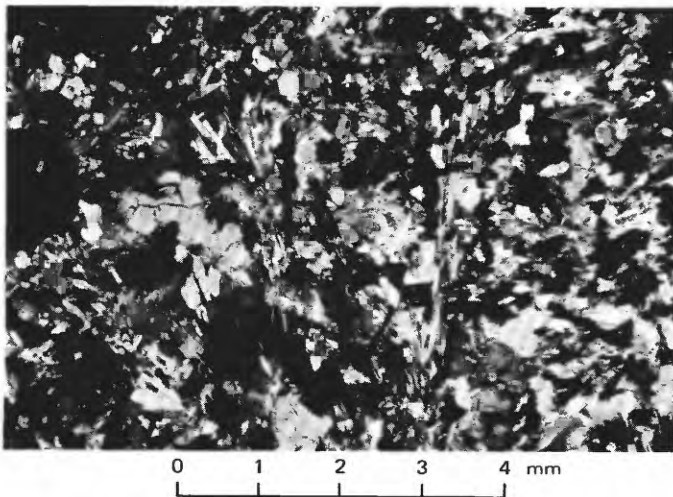


FIGURE 39.—Sample 71055. Photomicrograph showing plumose intergrowths of plagioclase, clinopyroxene, and ilmenite. Crossed polarizers.

*Components of 90-150- $\mu$ m fraction of 71061,1 (Heiken and McKay, 1974)*

Components	Volume percent
Agglutinate.....	9.3
Basalt, equigranular )	
Basalt, variolitic )	19.6
Breccia:	
Low grade <sup>1</sup> - brown.....	3.6
Low grade <sup>1</sup> - colorless.....	.6
Medium to high grade <sup>2</sup> .....	1.6
Anorthosite.....	.3
Cataclastic anorthosite <sup>1</sup> .....	--
Norite.....	--
Gabbro.....	--
Plagioclase.....	17.3
Clinopyroxene.....	21.0
Orthopyroxene.....	--
Olivine.....	--
Ilmenite.....	4.6
Glass:	
Orange.....	6.3
"Black".....	9.6
Colorless.....	1.3
Brown.....	4.6
Gray, "ropy".....	--
Other.....	--
Total number grains.....	300

<sup>1</sup>Metamorphic groups 1-3 of Warner (1972).

<sup>2</sup>Metamorphic groups 4-8 of Warner (1972).

<sup>3</sup>Includes crushed or shocked feldspar grains.

71065, fine-grained olivine basalt.

71066, aphanitic olivine basalt.

*Major-element composition:*

*Chemical analysis of 71061*

SiO <sub>2</sub> .....	40.09
Al <sub>2</sub> O <sub>3</sub> .....	10.70
FeO.....	17.85
MgO.....	9.92
CaO.....	10.59
Na <sub>2</sub> O.....	.36
K <sub>2</sub> O.....	.08
TiO <sub>2</sub> .....	9.32
P <sub>2</sub> O <sub>5</sub> .....	.07
MnO.....	.24
Cr <sub>2</sub> O <sub>3</sub> .....	.49
Total.....	99.71

71061.3 (Apollo 17 PET, 1973).

*Sample 71130-34, 35, 36*

*Type:* Sedimentary, unconsolidated (71130-34) and olivine basalt fragments (71135, 36).

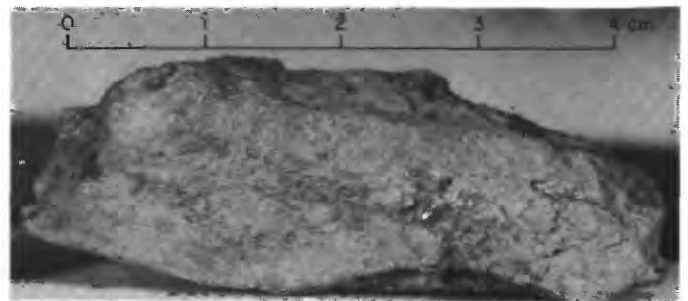


FIGURE 40.—Sample 71065. Fine-grained olivine basalt. (NASA photograph S-73-16932.)

**Size:** 71135, 6×4.5×1.5 cm; 71136, 4×2×2 cm.

**Weight:** 71130-34, 144.03 g; 71135, 36.85 g; 71136, 25.39 g.

**Location:** 71135 and 71136 chipped from 0.5-m boulder on southeast rim of 10-m blocky crater; 71130-34, sediment from near the boulder.

**Illustrations:** Pans 12, 13; figures 41, 42 (71135, LRL), 43 (71136, LRL).

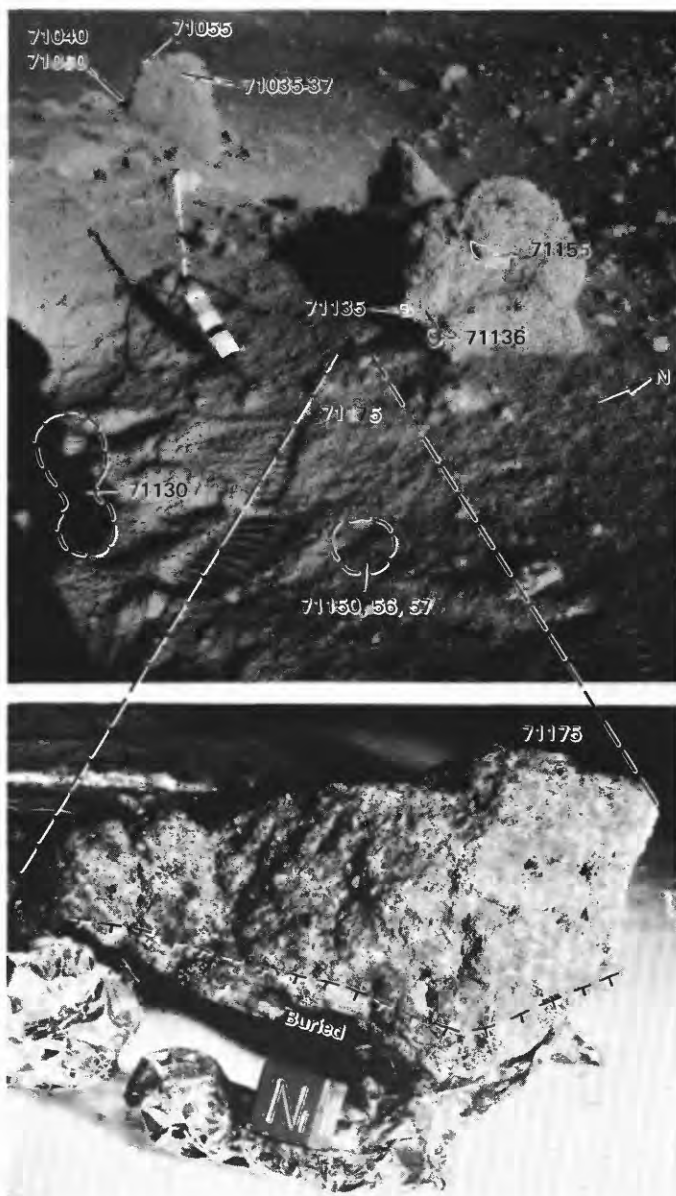


FIGURE 41.—Top, Samples 71135, 71136, 71155 before collection from boulder on southeast rim of blocky 10-m crater. 71135 and 71136 fell to lunar surface, and sediment 71130-34 was scooped up with them. 71175, half-buried near the boulder, is also shown before collection. Samples 71035-37; 71040-49, 75; 71055; 71060-69, 85-97 collected from boulder in upper left and nearby regolith. (NASA photograph AS17-136-20741.) Bottom, LRL view showing 71175 with reconstructed lunar surface orientation and lighting. (NASA photograph S-73-17803.)

**Comments:** Boulder was reexcavated from the Steno ejecta blanket by the impact that formed the 10-m crater. 71135 and 71136 were knocked off the boulder during hammering; when they were picked up, the underlying sediment (71130-34) was collected with them.

**Petrographic descriptions:**

71130-34, dominantly basalt with minor agglutinate and breccia fragments.

71135, medium-grained vesicular olivine basalt with a locally plumose groundmass of plagioclase, clinopyroxene, ilmenite, and accessory minerals.

71136, fine-grained vesicular olivine basalt.

**Major-element compositions:**

*Chemical analyses of 71135 and 71136*

	1	2
SiO <sub>2</sub> .....	39.71	40.30
Al <sub>2</sub> O <sub>3</sub> .....	10.10	10.21
FeO.....	18.57	18.44
MgO.....	7.31	7.03
CaO.....	11.62	11.73
Na <sub>2</sub> O.....	.38	.37
K <sub>2</sub> O.....	.05	.03
TiO <sub>2</sub> .....	10.74	11.12
P <sub>2</sub> O <sub>5</sub> .....	.06	.06
MnO.....	.28	.28
Cr <sub>2</sub> O <sub>3</sub> .....	.31	.28
Total.....	99.13	99.85

1. 71135.5 (Rhodes and others, 1976).

2. 71136.1 (Rhodes and others, 1976).

**Exposure age:** Kr-Kr: 71135, 102 m.y. (Arvidson and others, 1976b).

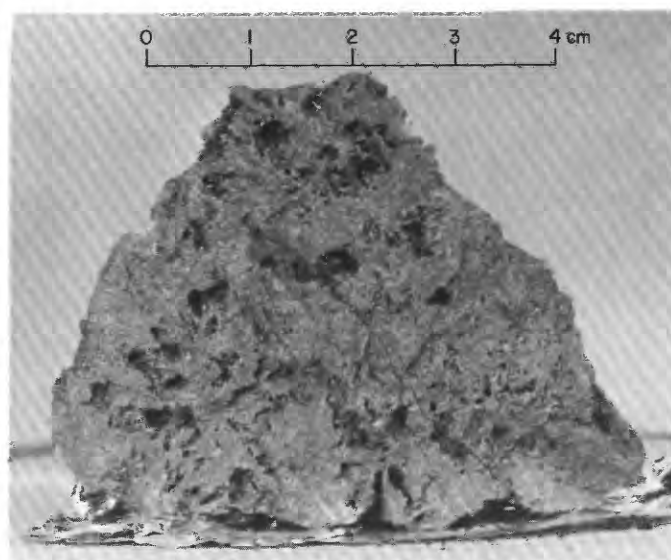


FIGURE 42.—Sample 71135. Medium-grained vesicular olivine basalt. Pyroxene and ilmenite crystals line cavities. (NASA photograph S-73-15686.)

## Sample 71150-54, 55-57

**Type:** Sedimentary, unconsolidated (71150-54), olivine(?) basalt (71155-56), and basalt (71157).

**Size:** 71155, 5×2.5×2.5 cm; 71156, 2.2×1.5×1 cm; 71157, 1.2×1.0×0.8 cm.

**Weight:** 71150-54, 63.93 g; 71155, 26.15 g; 71156, 5.42 g; 71157, 1.466 g.

**Location:** 71155 chipped from the boulder on the south-east rim of the 10-m blocky crater; 71150-54, sediment with two basalt fragments (71156, 71157) from near the boulder.

**Illustrations:** Pans 12, 13; figures 41, 44 (71155, LRL).

**Comments:** Boulder was reexcavated from the ejecta blanket of Steno crater by the impact that formed the 10-m crater. 71155 was knocked off the boulder during hammering; when it was picked up, the underlying sediment (71150-54), including two small basalt fragments (71156, 71157), was collected with it.

**Petrographic descriptions:**

71150-54, dominantly basalt and breccia fragments, minor agglutinate.

71155, fine-grained vesicular olivine(?) basalt.

71156, fine-grained vesicular olivine(?) basalt.

## Sample 71175

**Type:** Olivine basalt.

**Size:** 8×5×4 cm.

**Weight:** 207.8 g.

**Location:** Sample is a cobble from the regolith near the boulder on the southeast rim of the 10-m blocky crater.

**Illustrations:** Pans 12, 13; figures 41, 45 (LRL).

**Comments:** Sample was half buried. It is probably part of the ejecta from the 10-m crater.

**Petrographic description:** Medium-grained vesicular olivine basalt.

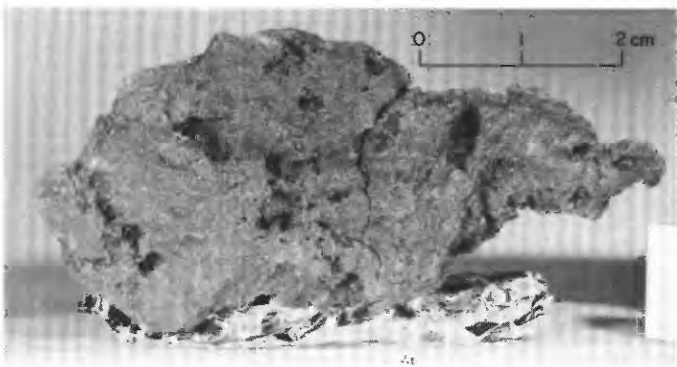


FIGURE 43.—Sample 71136. Fine-grained vesicular olivine basalt. Pyroxene and ilmenite crystals line cavities. (NASA photograph S-73-16424.)

**Major-element composition:***Chemical analysis of 71175*

SiO <sub>2</sub> .....	37.93
Al <sub>2</sub> O <sub>3</sub> .....	8.47
FeO .....	19.37
MgO .....	9.63
CaO .....	9.79
Na <sub>2</sub> O .....	.38
K <sub>2</sub> O .....	.04
TiO <sub>2</sub> .....	13.08
P <sub>2</sub> O <sub>5</sub> .....	.04
MnO .....	.28
Cr <sub>2</sub> O <sub>3</sub> .....	.54
Total .....	99.55

71175,2 (Rhodes and others, 1976).

## Sample 71500-04, 05-09, 15

**Type:** Sedimentary, unconsolidated (71500-04) with five basalt fragments (71505-09) and a glass-bonded agglutinate fragment (71515).

**Weight:** 71500-04, 1,013.79 g; 71505-09 and 71515, 52.57 g.

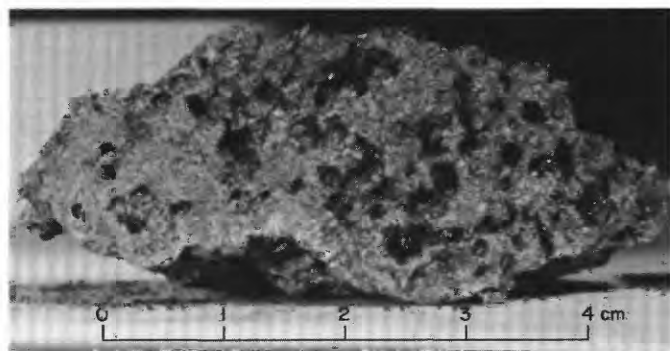


FIGURE 44.—Sample 71155. Fine-grained vesicular olivine(?) basalt. (NASA photograph S-73-15860.)

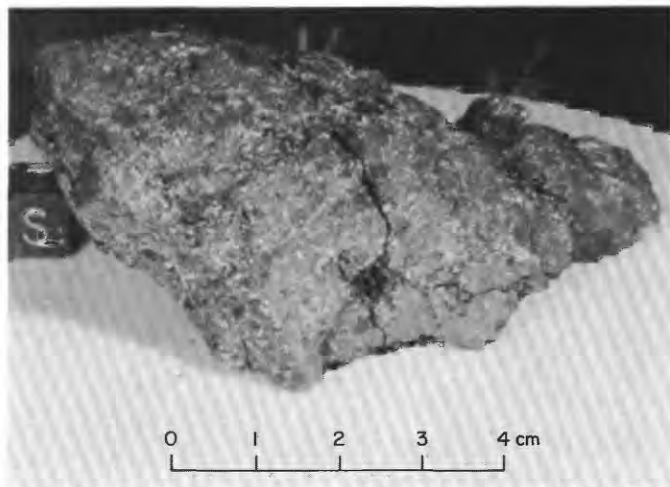


FIGURE 45.—Sample 71175. Medium-grained vesicular olivine basalt. (NASA photograph S-73-15727.)

**Location:** 15 m east of blocky 10-m crater.

**Illustrations:** Pans 12, 13; figure 46.

**Comments:** Sample is unconsolidated sediment collected from the rake sample site; it is regolith developed on Steno crater ejecta. Compositional similarity of agglutinate fragment 71515 to sediment samples (fig. 34) implies that the agglutinate formed from local regolith material.

**Petrographic descriptions:**

71500-04, dominantly basalt and breccia fragments with minor agglutinates.

**Components of 90-150- $\mu$ m fraction of 71501.1 (Heiken and McKay, 1974)**

Components	Volume percent
Agglutinate.....	35.0
Basalt, equigranular }.....	24.6
Basalt, variolitic }.....	
Breccia:	
Low grade <sup>1</sup> - brown.....	2.3
Low grade <sup>1</sup> - colorless.....	.6
Medium to high grade <sup>2</sup> .....	2.3
Anorthosite.....	--
Cataclastic anorthosite <sup>3</sup> .....	--
Norite.....	--
Gabbro.....	--
Plagioclase.....	5.0
Clinopyroxene.....	17.3
Orthopyroxene.....	.6
Olivine.....	--
Ilmenite.....	8.0
Glass:	
Orange.....	1.3
"Black".....	1.3
Colorless.....	.6
Brown.....	.3
Gray, "ropy".....	--
Other.....	--
Total number grains.....	300

<sup>1</sup>Metamorphic groups 1-3 of Warner (1972).

<sup>2</sup>Metamorphic groups 4-8 of Warner (1972).

<sup>3</sup>Includes crushed or shocked feldspar grains.

71505, medium-grained olivine basalt.

71506, coarse-grained olivine basalt.

**Major-element compositions:**

**Chemical analyses of 71501, 71509, 71515**

	1	2	3
SiO <sub>2</sub> .....	39.82	--	--
Al <sub>2</sub> O <sub>3</sub> .....	11.13	7.3	11.2
FeO.....	17.41	20.6	18.2
MgO.....	9.51	10.3	9.3
CaO.....	10.85	9.6	10.4
Na <sub>2</sub> O.....	.32	.314	.37
K <sub>2</sub> O.....	.07	.054	.065
TiO <sub>2</sub> .....	9.52	13.7	10.3
P <sub>2</sub> O <sub>5</sub> .....	.06	--	--
MnO.....	.25	.258	.222
Cr <sub>2</sub> O <sub>3</sub> .....	.46	.647	.458
Total.....	99.40		

1. 71501.3 (Apollo 17 PET, 1973).

2. 71509.2 (Warner and others, 1975a).

3. 71515.0 (Laul and others, 1975).

Samples 71525-29, 35-39, 45-49, 55-59, 65-69, 75-79, 85-89, 95-97

**Type:** 38 rake fragments, all basalt.

**Weight:** Total, 2,220.16 g; range, 2.113 to 415.4 g.

**Location:** 15 m east of blocky 10-m crater.

**Illustrations:** Pans 12, 13; figures 46, 47-54 (LRL), 55 (photomicrograph), 56-63 (LRL).

**Comments:** Subfloor basalt fragments from regolith developed on Steno crater ejecta.

**Petrographic descriptions:**

71525, fine-grained basalt.

71526, fine-grained basalt.

71528, fine-grained basalt.

71529, fine-grained vesicular basalt.

71535, fine-grained vesicular basalt.

71536, medium-grained basalt.

71537, aphanitic basalt.

71538, fine-grained basalt.

71539, fine-grained basalt.

71545, fine-grained basalt.

71546, fine-grained vesicular basalt.

71547, fine-grained vesicular basalt.

71548, medium-grained vesicular basalt.

71549, medium-grained basalt.

71556, medium-grained vesicular basalt.

71557, medium-grained basalt.

71558, medium-grained vesicular olivine basalt.

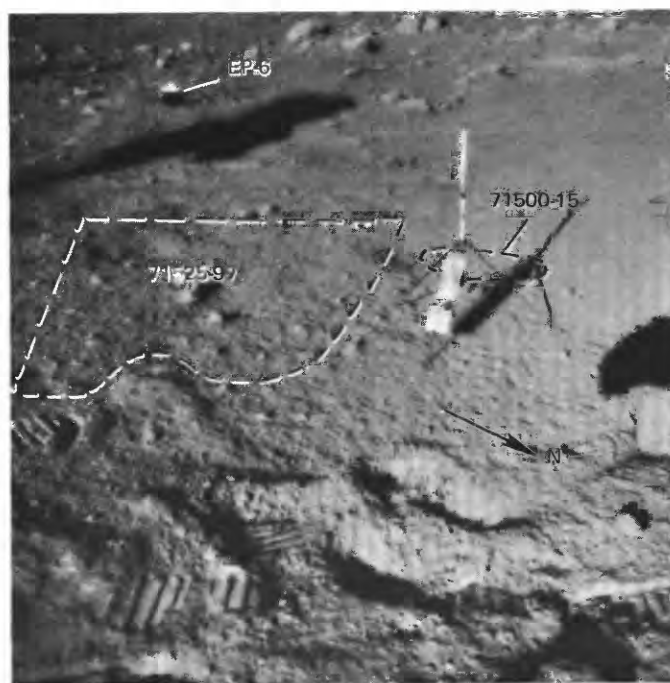


FIGURE 46.—Approximate locations of rake sample (71525-97) and associated sediment sample (71500-15), before collection. (NASA photograph AS17-136-20742.)

71559, medium-grained basalt.  
 71565, medium-grained vesicular olivine basalt with a subophitic(?) groundmass.  
 71566, medium-grained vesicular basalt.  
 71567, medium-grained vesicular olivine basalt.  
 71568, medium-grained olivine basalt.  
 71569, fine-grained olivine basalt. Microphenocrysts of olivine in an intergranular groundmass of plagioclase, clinopyroxene, ilmenite, and accessory minerals.  
 71576, fine-grained olivine basalt.  
 71577, fine-grained vesicular olivine basalt.  
 71578, fine-grained vesicular olivine basalt.  
 71579, fine-grained vesicular basalt.  
 71585, fine-grained vesicular olivine basalt.  
 71586, fine-grained olivine basalt.  
 71587, fine-grained vesicular olivine basalt.  
 71588, fine-grained olivine basalt.  
 71589, fine-grained olivine basalt.

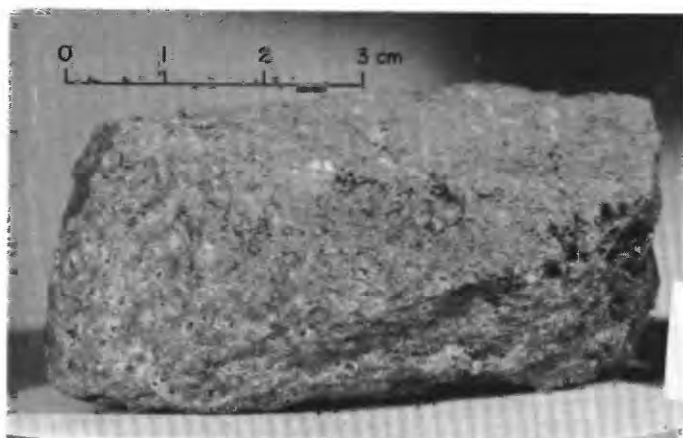


FIGURE 47.—Sample 71546. Fine-grained vesicular basalt. (NASA photograph S-73-16131.)

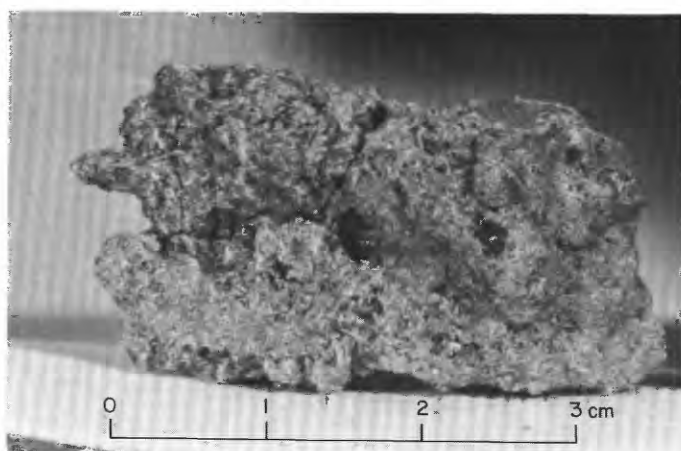


FIGURE 48.—Sample 71548. Medium-grained vesicular basalt. Pyroxene and ilmenite crystals line cavities. (NASA photograph S-73-16136.)

71595, fine-grained olivine basalt.  
 71596, fine-grained olivine basalt.  
 71597, medium-grained vesicular olivine basalt.

#### Major-element compositions:

Chemical analyses of 71546, 71566, 71567, 71569, 71577

	1	2	3	4	5	6	7
SiO <sub>2</sub> .....	39.14	39.27	38.06	39.97	39.4	39.7	39.18
Al <sub>2</sub> O <sub>3</sub> .....	8.91	9.22	8.59	9.08	8.58	8.83	8.92
FeO .....	19.11	18.73	19.40	18.85	18.9	18.9	18.90
MgO .....	8.34	8.40	8.83	7.66	8.47	8.06	8.15
CaO .....	10.79	10.89	10.57	11.27	10.58	10.92	10.95
Na <sub>2</sub> O .....	.40	.40	.38	.41	.388	.40	.39
K <sub>2</sub> O .....	.05	.03	.03	.06	.067	.06	.06
TiO <sub>2</sub> .....	12.33	12.01	12.98	11.57	12.18	11.88	12.04
P <sub>2</sub> O <sub>5</sub> .....	.05	.03	.02	.06	.066	.06	.05
MnO .....	.028	.27	.28	.28	.245	.26	.28
Cr <sub>2</sub> O <sub>3</sub> .....	.41	.38	.43	.36	.465	.41	.41
Total .....	99.81	99.63	99.57	99.57	99.341	99.48	99.33

1. 71546,5 (Rhodes and others, 1976).  
 2. 71566,10 (Rhodes and others, 1976).  
 3. 71567,9 (Rhodes and others, 1976).  
 4. 71569,11 (Rhodes and others, 1976).  
 5. 71569,24 (Wänke and others, 1975).  
 6. Average of 4 and 5.  
 7. 71577,4 (Rhodes and others, 1976).

Exposure age: Kr-Kr: 71569, 134 m.y. (Arvidson, 1976b).

#### STATION LRV-1

##### LOCATION

Station LRV-1 is located approximately 250 m east of Bronte crater (fig. 7C) near a small fresh crater 10 to 15 m in diameter (fig. 64).

##### OBJECTIVES

LRV-1 was an unscheduled stop to sample ejecta from the 10-15-m crater.

##### GENERAL OBSERVATIONS

The station area is in generally flat terrain that rises to the west. Craters are sparse, subdued, and generally

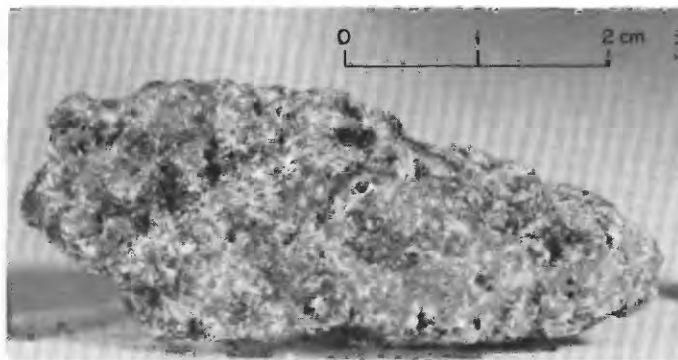


FIGURE 49.—Sample 71556. Medium-grained vesicular basalt. (NASA photograph S-73-16239.)

without blocks. They range in size from a few centimeters to about 30 m in diameter. The sampling was done in a ray associated with one of the rare block-rimmed craters in the area. Blocks from this crater range in size from a few tenths of a meter or less in the sample area (fig. 65) to about 1 meter at the crater rim (fig. 64). Most of the blocks are perched on the surface; they do not appear to be filleted or dust covered.

#### SUMMARY OF SAMPLING

Sample 72130-34, 35

*Type:* Sedimentary, unconsolidated (72130-34), and basalt cataclasite (72135).

*Size:* 72135, 8×6×5.5 cm.



FIGURE 50.—Sample 71557. Medium-grained basalt. (NASA photograph S-73-16245.)

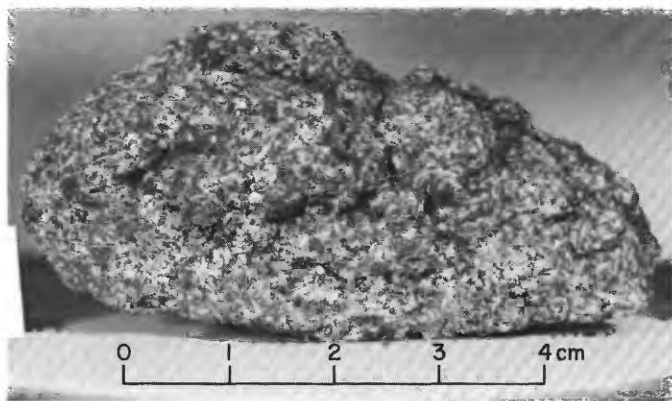


FIGURE 51.—Sample 71559. Medium-grained basalt. (NASA photograph S-73-16456.)

*Weight:* 72130-34, 220.47 g; 72135, 336.9 g.

*Location:* 72135 and associated sediment (72130-34) were collected about three-fourths of a crater diameter out from the rim of the 10-15-m crater.

*Illustrations:* Figures 64, 65, 66 (LRL).

*Comments:* Sample 72135 is a fragment of subfloor basalt that may have been excavated from the regolith by the impact that formed the fresh 10-15-m crater. Its cataclastic texture presumably resulted from an impact, possibly but not necessarily the one that formed the nearby small crater.

*Petrographic description:* 72135, variolitic olivine basalt cataclasite. Fragmental matrix dominant, but some glass present.

#### STATION LRV-2

##### LOCATION

Station LRV-2 is located on a narrow tongue of the light mantle approximately 1.6 km west of Horatio crater and about 1.2 km west of station LRV-1 (fig. 7C).

##### OBJECTIVES

Station LRV-2 was a planned LRV stop to sample and photograph the light mantle.

##### GENERAL OBSERVATIONS

The station area is generally flat with scattered 1-10-m craters (fig. 67). Blocks are sparse and range in size from a few centimeters to a few tenths of a meter.

The craters are subdued and relatively free of blocks. The astronauts noted a higher albedo in the crater walls and rims than on darker parts of the valley floor. They also reported some crater rims with fragments of "instant rock" (regolith breccia).

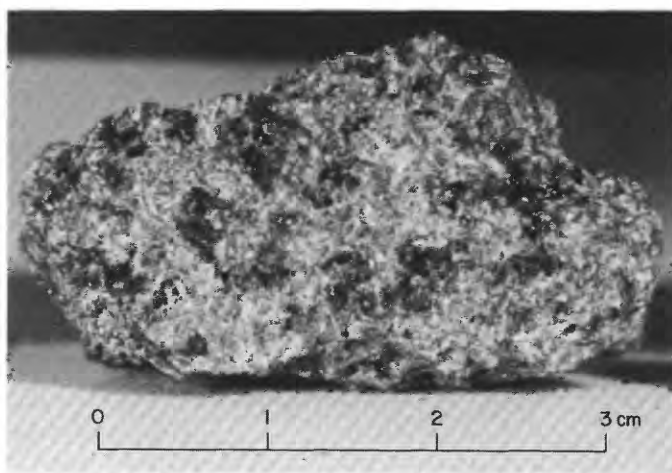


FIGURE 52.—Sample 71565. Medium-grained vesicular olivine basalt. (NASA photograph S-73-16451.)

## SUMMARY OF SAMPLING

Sample 72140-44, 45

*Type:* Sedimentary, unconsolidated (72140-44) and small included breccia fragment (72145).

*Size:* 72145, 1.3×1.3×1 cm.

*Weight:* 72140-44, 350.83 g; 72145, 1.25 g.

*Location:* From the rim of a small crater approximately 5 m in diameter. The small rock (72145) collected with the sediment (72140-44) has not been located

in photographs of the sample area.

*Illustrations:* Figure 67.

*Comments:* The material sampled represents light mantle material probably ejected from the nearby 5-m crater. Its composition reflects the presence of appreciably more highlands material than is in the dark sediment of the valley floor (fig. 68). However, admixed basaltic sediment from the valley floor is much more abundant than in light-mantle samples from stations closer to the South Massif.

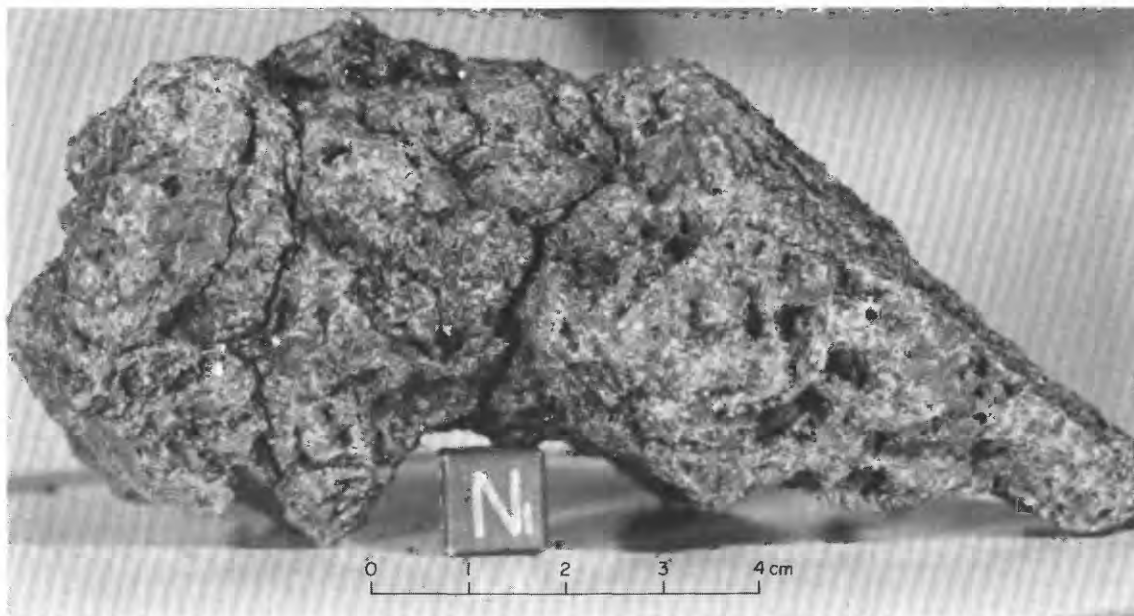


FIGURE 53.—Sample 71566. Medium-grained vesicular basalt. (NASA photograph S-73-16461.)

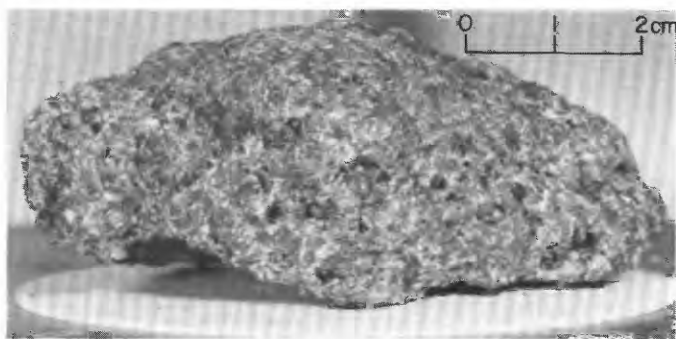


FIGURE 54.—Sample 71567. Medium-grained vesicular olivine basalt. (NASA photograph S-73-16458.)

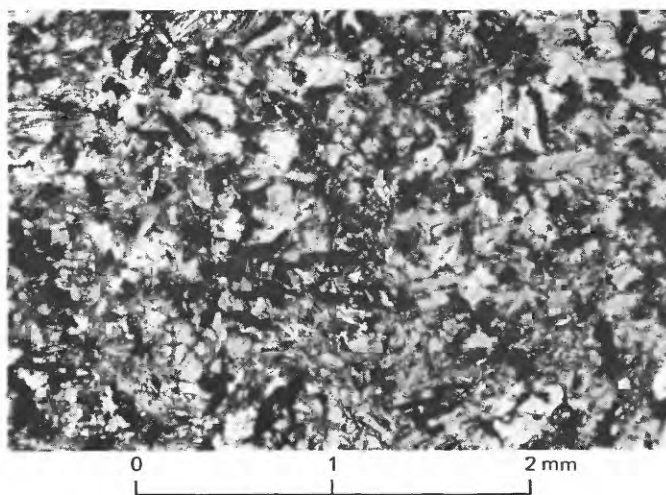


FIGURE 55.—Sample 71569. Photomicrograph showing microphenocrysts of olivine in intergranular groundmass of clinopyroxene, plagioclase, and ilmenite. Crossed polarizers.

*Petrographic description:* 72140-44, dominantly basalt and glass fragments with some agglutinate and breccia.

*Components of 90-150- $\mu$ m fraction of 72141,15 (Heiken and McKay, 1974)*

Components	Volume percent
Agglutinate.....	50.6
Basalt, equigranular .....	6.6
Basalt, variolitic .....	.6
Breccia:	
Low grade <sup>1</sup> - brown.....	4.0
Low grade <sup>1</sup> - colorless.....	4.0
Medium to high grade <sup>2</sup> .....	1.6
Anorthosite.....	..
Cataclastic anorthosite <sup>3</sup> .....	1.3
Norite.....	.3
Gabbro.....	.3

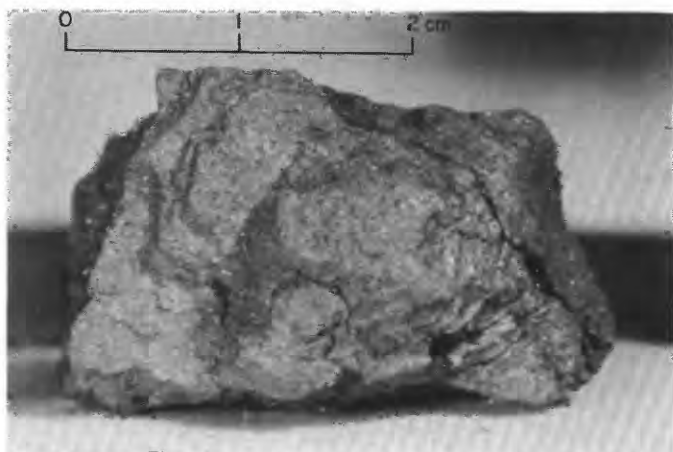


FIGURE 56.—Sample 71576. Fine-grained olivine basalt. (NASA photograph S-73-16617.)

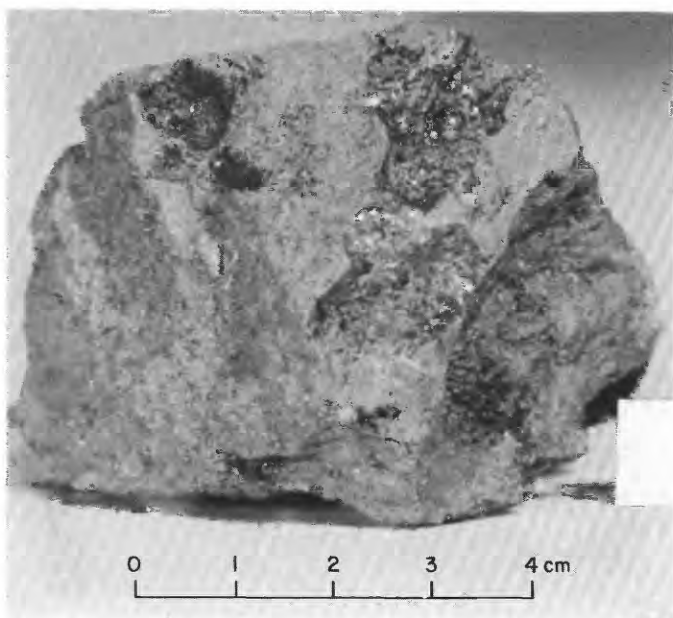


FIGURE 57.—Sample 71577. Fine-grained vesicular olivine basalt. (NASA photograph S-73-16589.)

*Components of 90-150- $\mu$ m fraction of 72141,15 (Heiken and McKay, 1974)—Continued*

Components	Volume percent
Plagioclase .....	9.0
Clinopyroxene .....	7.0
Orthopyroxene .....	..
Olivine .....	..
Ilmenite.....	.6
Glass:	
Orange .....	1.3
"Black".....	5.0
Colorless .....	1.6
Brown .....	3.9
Gray, "ropy".....	1.3
Other.....	..
Total number grains .....	300

<sup>1</sup>Metamorphic groups 1-3 of Warner (1972).

<sup>2</sup>Metamorphic groups 4-8 of Warner (1972).

<sup>3</sup>Includes crushed or shocked feldspar grains.

*Major-element composition:*

*Chemical analyses of 72141*

	1	2	3
SiO <sub>2</sub> .....	43.11	43.0	43.1
Al <sub>2</sub> O <sub>3</sub> .....	16.10	15.78	15.94
FeO.....	13.45	13.35	13.40
MgO.....	10.25	9.88	10.06
CaO.....	11.83	11.8	11.8
Na <sub>2</sub> O.....	.40	.402	.40
K <sub>2</sub> O.....	.12	.106	.11
TiO <sub>2</sub> .....	4.37	4.39	4.38
P <sub>2</sub> O <sub>5</sub> .....	.10	.096	.10
MnO.....	.19	.176	.18
Cr <sub>2</sub> O <sub>3</sub> .....	.37	.346	.36
Total.....	100.29	99.326	99.83

1. 72141,9 (Rhodes and others, 1974).

2. 72141,22 (Wänke and others, 1974).

3. Average of 1 and 2.

STATION LRV-3

LOCATION

Station LRV-3 is approximately 500 m west of station LRV-2 and 2.2 km west of Horatio crater in

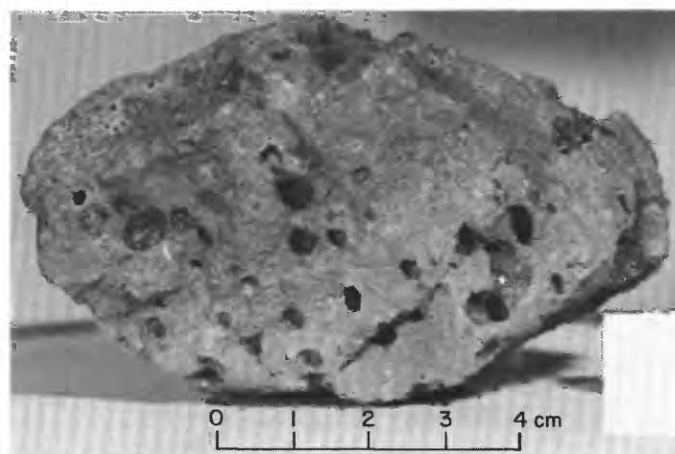


FIGURE 58.—Sample 71578. Fine-grained vesicular olivine basalt. (NASA photograph S-73-16592.)

Tortilla Flat, the dark area between the main body of light mantle and the finger of light mantle to the southeast (figs. 6, 7A; pl. 2).

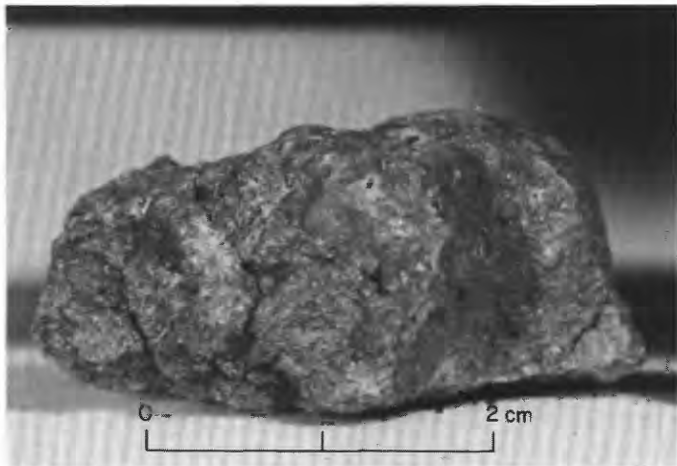


FIGURE 59.—Sample 71586. Fine-grained olivine basalt. (NASA photograph S-73-16594.)

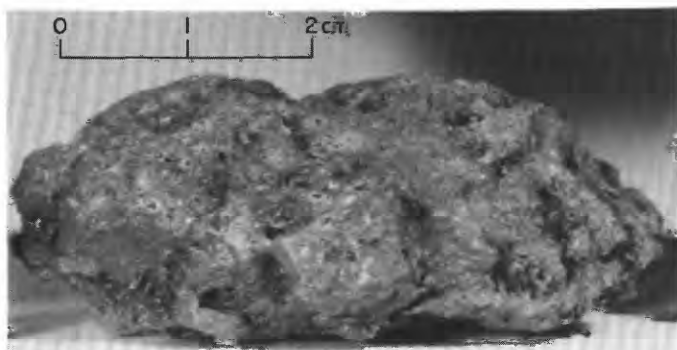


FIGURE 60.—Sample 71587. Fine-grained vesicular olivine basalt. Pyroxene and ilmenite crystals line cavities. (NASA photograph S-73-16598.)

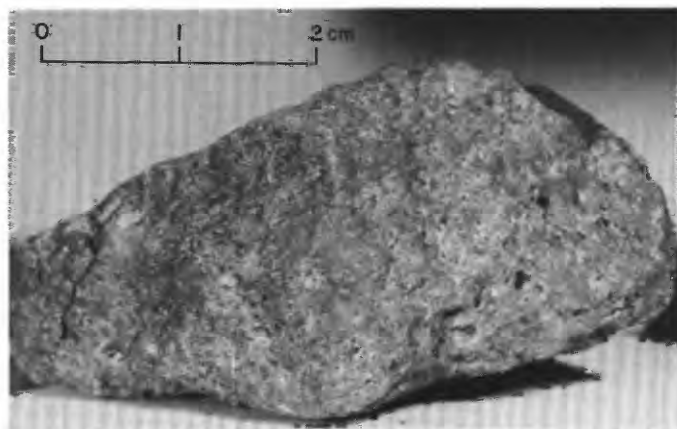


FIGURE 61.—Sample 71588. Fine-grained olivine basalt. (NASA photograph S-73-16602.)

## OBJECTIVES

Station LRV-3 was a planned LRV stop to sample and photograph the dark mantle.

## GENERAL OBSERVATIONS

The station area is flat with scattered craters up to 10 m in diameter (fig. 69) that are widely spaced and generally have subdued, relatively block-free rims. However, clods are present on the rims of a few craters smaller than 3 m. The surface between craters is smooth but has a pitted "raindrop" texture. Scattered small blocks range in size from a few centimeters to a few tenths of a meter.

## SUMMARY OF SAMPLING

Sample 72150, 55

Type: Sedimentary, unconsolidated (72150) and olivine

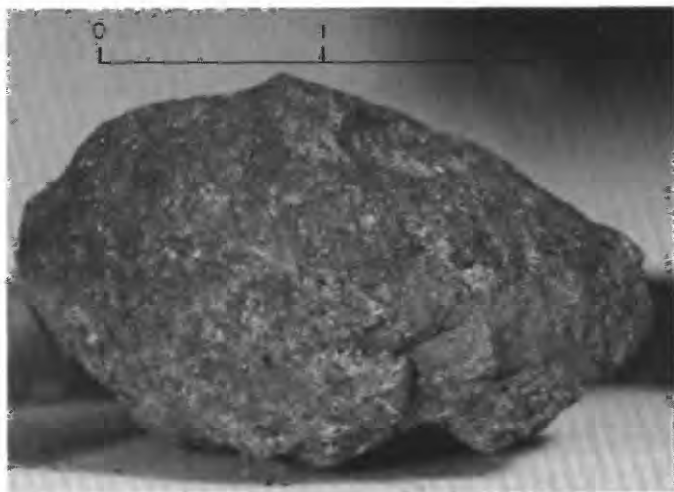


FIGURE 62.—Sample 71595. Fine-grained olivine basalt. (NASA photograph S-73-16608.)



FIGURE 63.—Sample 71596. Fine-grained olivine basalt. (NASA photograph S-73-16613.)

basalt (72155).

Size: 72155, 7×5×4 cm.

Weight: 72150, 53.29 g; 72155, 238.5 g.

Location: Station LRV-3, between two tongues of the light mantle.



FIGURE 64.—View from LRV toward station LRV-1 area showing sample 72130-35 area in ejecta of blocky 10-15-m crater. (NASA photograph AS17-135-20623.)

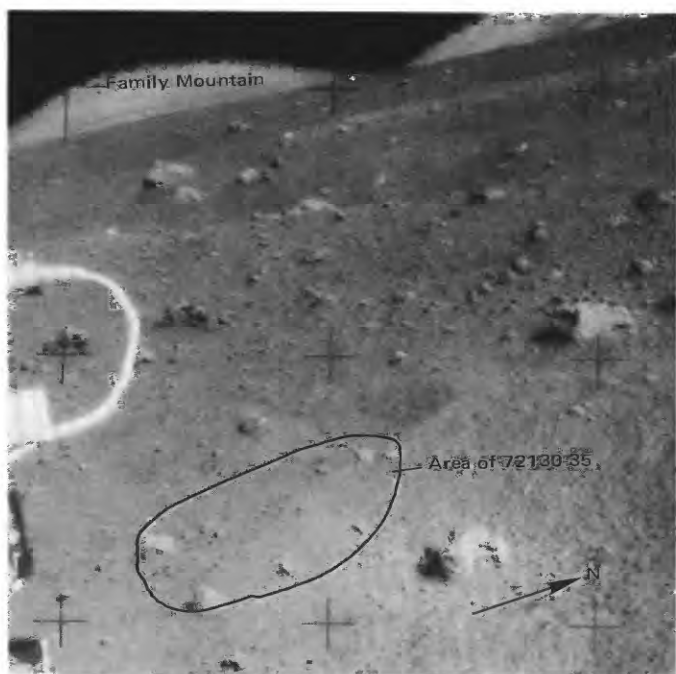


FIGURE 65.—72130-35 sample area; exact sample location is not known. (NASA photograph AS17-135-20625.)

Illustrations: Figures 69, 70 (72155, LRL).

Comments: Collected from the smooth flat intercrater surface; the rock (72155) is not clearly related to any nearby crater. It is a fragment of subfloor basalt from the regolith.

#### Petrographic descriptions:

Components of 90-150- $\mu$ m fraction of 72150,2 (Heiken and McKay, 1974)

Components	Volume percent
Agglutinate.....	52.6
Basalt, equigranular .....	8.3
Basalt, variolitic .....	1.3
Breccia:	
Low grade <sup>1</sup> - brown .....	5.3
Low grade <sup>1</sup> - colorless .....	1.6
Medium to high grade <sup>2</sup> .....	4.0
Anorthosite.....	--
Cataclastic anorthosite <sup>3</sup> .....	.3
Norite .....	--
Gabbro .....	--
Plagioclase .....	5.3
Clinopyroxene .....	5.3
Orthopyroxene .....	--
Olivine .....	--
Ilmenite.....	.6
Glass:	
Orange .....	3.9
"Black" .....	5.3
Colorless .....	1.3
Brown .....	2.8
Gray, "ropy" .....	.6
Other.....	.3
Total number grains .....	300

<sup>1</sup>Metamorphic groups 1-3 of Warner (1972).

<sup>2</sup>Metamorphic groups 4-8 of Warner (1972).

<sup>3</sup>Includes crushed or shocked feldspar grains.

72155, fine-grained vesicular olivine basalt with a variolitic groundmass.



FIGURE 66.—Sample 72135. Olivine basalt cataclastite. (NASA photograph S-73-16206.)

*Major-element composition:**Chemical analyses of 72155*

	1	2	3
SiO <sub>2</sub> .....	38.67	38.9	38.78
Al <sub>2</sub> O <sub>3</sub> .....	8.64	8.54	8.59
FeO.....	18.77	19.4	19.08
MgO.....	8.47	8.72	8.60
CaO.....	10.69	10.42	10.56
Na <sub>2</sub> O.....	.40	.384	.39
K <sub>2</sub> O.....	.07	.067	.07
TiO <sub>2</sub> .....	12.32	12.23	12.28
P <sub>2</sub> O <sub>5</sub> .....	.05	.071	.06
MnO.....	.28	.252	.27
Cr <sub>2</sub> O <sub>3</sub> .....	.43	.468	.45
Total.....	98.79	99.452	99.13

1. 72155.23 (Rhodes and others, 1976).  
 2. 72155.30 (Wänke and others, 1975).  
 3. Average of 1 and 2.

## Sample 72160-64

*Type:* Sedimentary, unconsolidated.

*Weight:* 250.00 g.

*Depth:* 1-2 cm.

*Location:* From the smooth flat intercrater surface near sample 72155.

*Illustrations:* Figure 66.

*Comments:* The composition of the unconsolidated sediment indicates that station LRV-3 is in the older regolith of the valley floor (fig. 71) beyond the limits of the younger, basalt-rich cluster ejecta.

*Petrographic description:* 72160-64, dominantly dark fine-grained breccia fragments and agglutinate with some feldspathic breccia.

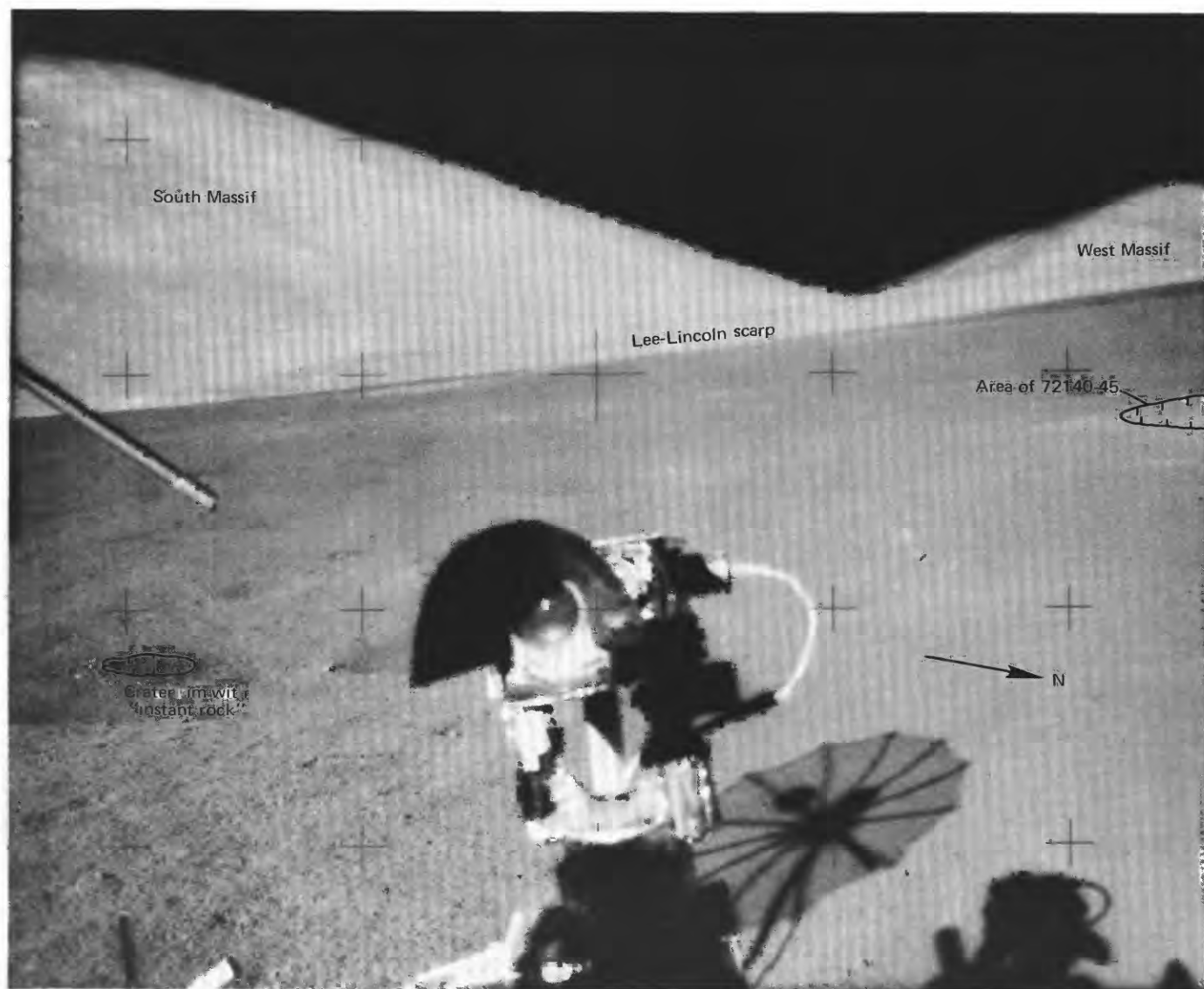


FIGURE 67.—Approximate location of samples 72140-45 before collection at station LRV-2. (NASA photograph AS17-135-20641.)

*Major-element composition:**Chemical analysis of 72161*

SiO <sub>2</sub> .....	42.12
Al <sub>2</sub> O <sub>3</sub> .....	14.22
FeO .....	14.86
MgO .....	10.54
CaO .....	11.17
Na <sub>2</sub> O .....	.41
K <sub>2</sub> O .....	.11
TiO <sub>2</sub> .....	5.21
P <sub>2</sub> O <sub>5</sub> .....	.08
MnO .....	.22
Cr <sub>2</sub> O <sub>3</sub> .....	.42
Total .....	99.36

72161.6 (Rhodes and others, 1974).

**STATION 2****LOCATION**

Station 2 is at the foot of South Massif where it inter-

sects the southeast rim of Nansen crater (fig. 7B); it is near the contact between the light mantle and the materials of the South Massif (pls. 1 and 2).

**OBJECTIVES**

The objectives at station 2 were to characterize South Massif bedrock and the light mantle and to investigate features indicative of the origin of the light mantle (Sevier, 1972).

**GENERAL OBSERVATIONS**

The station area includes the flat to gently rolling southeastern rim crest of Nansen crater and the lower slope of the South Massif (pans 14 and 15, pls. 5 and 6).

The smaller craters in the station area range in size from several centimeters to 20 m. Nansen crater is ap-

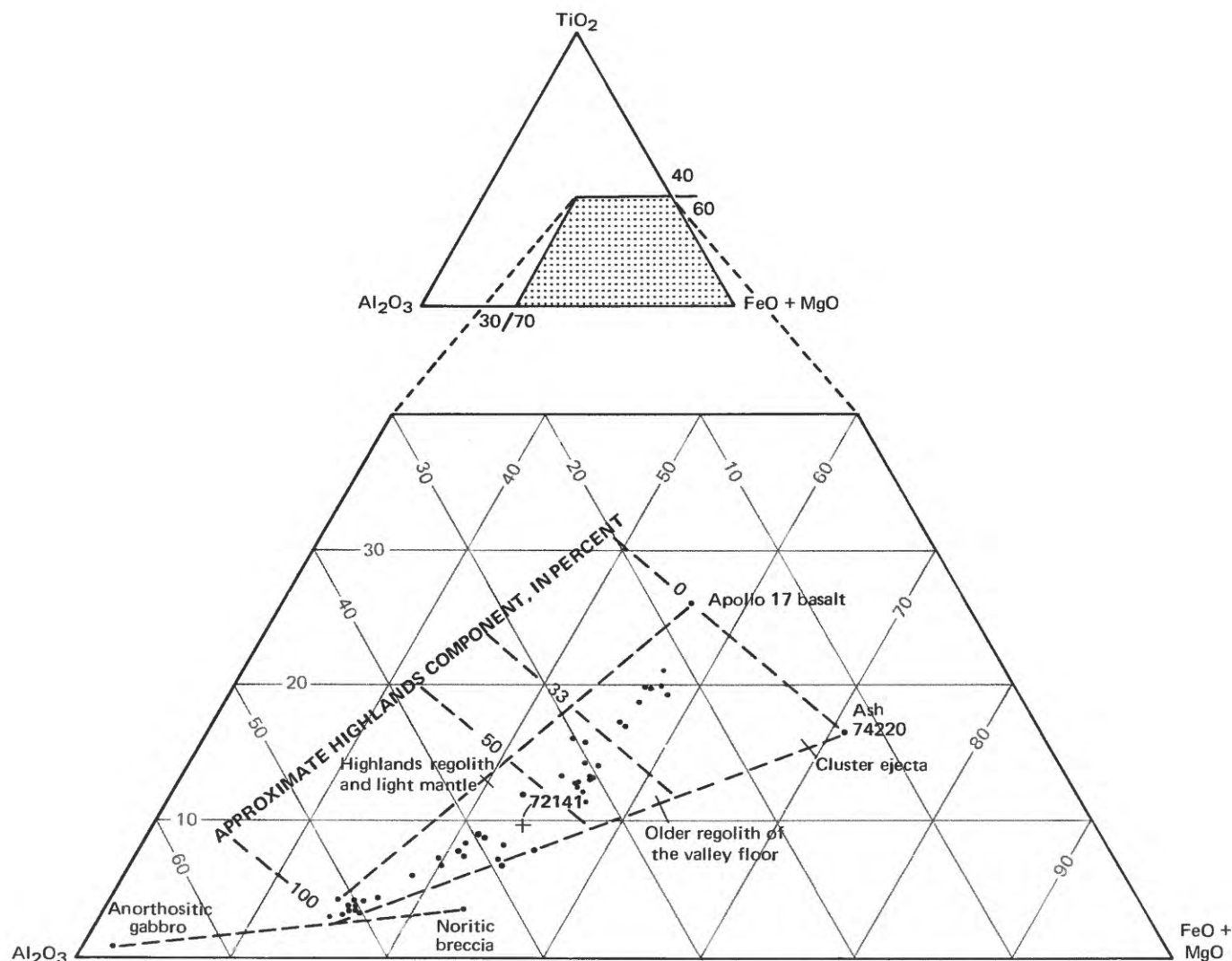


FIGURE 68.—Relative amounts of TiO<sub>2</sub>, Al<sub>2</sub>O<sub>3</sub>, and FeO + MgO in sediment sample 72141 (cross), collected at station LRV-2, in comparison with sediment samples from rest of traverse region (dots). Apollo 17 basalt, anorthositic gabbro, and noritic breccia values from Rhodes and others (1974).

proximately 1 km long across its northwest-southeast axis and 0.5 km across its northeast-southwest axis. Craters near station 2 on the South Massif appear to have blockier and higher rims than those on the rim of Nansen, but overall the crater abundance in the two areas is similar.

Near the station, the area between craters on the South Massif is moderately blocky. The Nansen crater rim is less blocky in comparison, and the average block size is much smaller. Blocks on the South Massif range in size from a few centimeters to several meters, those on the Nansen crater rim from a few centimeters to 1 m.

Fillets are well developed on the uphill sides of blocks on the massif slope and are not present on the downhill

sides. Blocks on the Nansen rim have poorly developed fillets. The degree of block burial ranges from almost none to almost total burial.

The astronauts reported that lobes of unconsolidated material extend from the slopes of South Massif onto the light mantle and encroach onto the north wall of Nansen crater. The lobes suggest that downslope movement of South Massif materials has occurred. Visible lobes do not extend as far as the rake sample area (72735-38) in the light mantle on the southeast rim of Nansen crater (fig. 72).

Most of the rock samples collected from the lower slopes of South Massif were chipped from three boulders, two of which are about 2 m across and the third about two-thirds meter across (fig. 72). Sediment was

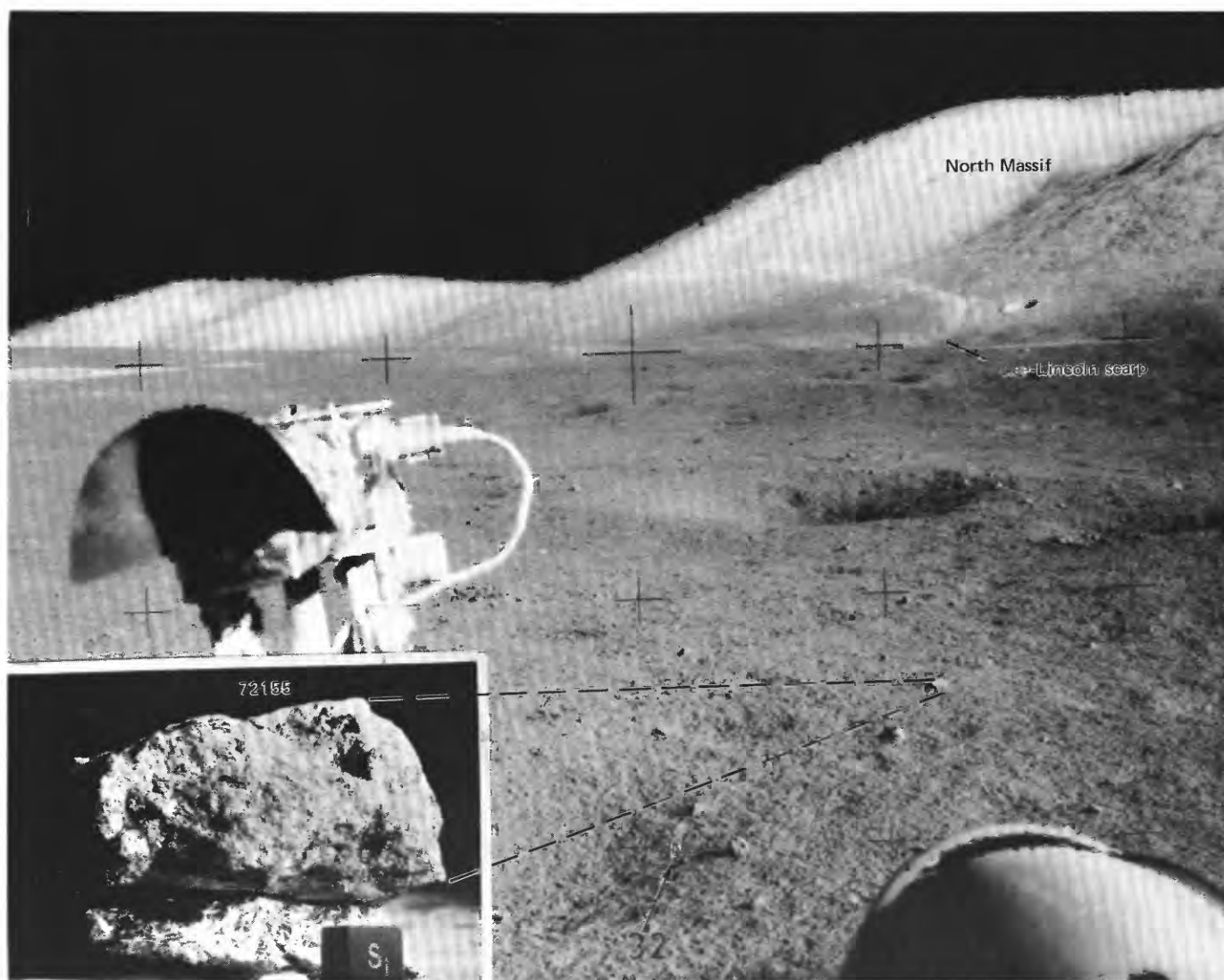


FIGURE 69. — Station LRV-3 sampling area, before sampling, and probable location of sample 72155. Inset shows 72155 with tentatively reconstructed lunar surface orientation and lighting. Sediment sample 72150 was collected with 72155. Sediment sample 72160-64 was collected in same general area. (NASA photographs AS17-135-20649; S-73-18406.)

collected from beneath overhangs on the two larger boulders and from beneath the smaller boulder after it was rolled. Sediment was also collected from the fillet of the southernmost large boulder, and a rake sample was collected about 5 m east of this boulder. Another rake sample was taken from the surface of the light mantle about 50 m north of the break in slope at the base of South Massif.

The three sampled boulders are in a field of boulders near the base of the massif (fig. 73). Most of the boulders may have rolled from a blocky area about two-thirds of the way up the massif. Schmitt (1973) observed that in the upper part of the massif above station 2 blue-gray material overlies tan-gray material and that the hue of boulder 1 as seen from a distance resembled the blue-gray hue seen near the top of the massif. Boulders 2 and 3 resembled the tan-gray hue of the upper massif. Some of the boulders, although not the sampled ones, are at the ends of visible tracks.

Boulder 1 is layered and foliated rock (fig. 74), the only one of this type seen by the crew. The boulder is approximately 2 m across and 1 m high as measured from the lunar surface. It has a well-developed fillet approximately 30 cm high on its uphill side and no fillet on its downhill side. The boulder appears to be highly eroded and has a hackly and knobby surface. The knobs range from less than 1 to about 15 cm across and were reported by the crew to be mostly fine-grained clasts eroded from a more friable fine-grained matrix. The crew also reported dark elongate clasts parallel to the layering; however, these are not discernible in the photographs.

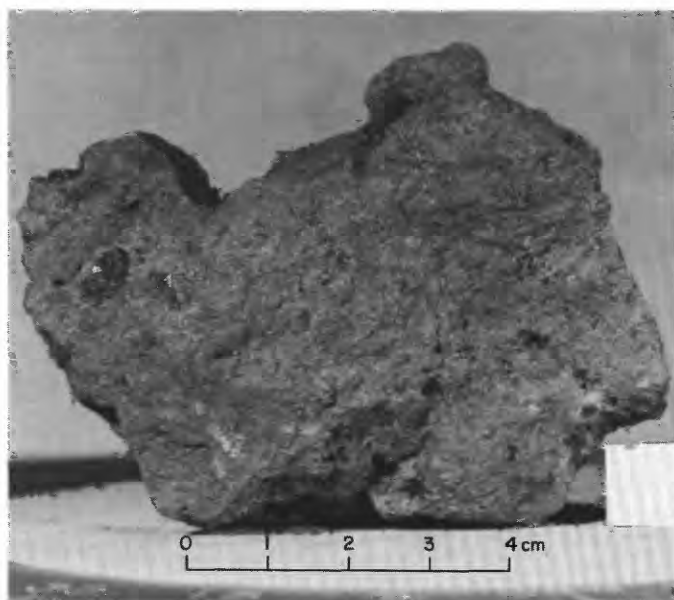


FIGURE 70.—Sample 72155. Fine-grained vesicular olivine basalt. (NASA photograph S-73-16918.)

Four samples, 72215, 72235, 72255, and 72275, were taken from boulder 1.

Boulder 2, a greenish-gray breccia, is approximately 2 m wide and 2 m high as measured from the lunar surface. It is rounded and smoother than boulder 1. Although several sets of fractures can be recognized (Muehlberger and others, 1973), no layering is visible. The boulder has a fillet about 25 cm high on its uphill side but overhangs the ground surface on its downhill side.

Five samples, 72315, 72335, 72355, 72375, and 72395, were taken from boulder 2.

Boulder 3 is an equant subangular breccia boulder about 40 cm across. Clasts as large as 10 cm are visible in lunar surface photographs. Three fractures transecting the boulder are recognized (Muehlberger and others, 1973), but no well-developed fracture or cleavage sets are visible. The boulder has a poorly developed fillet. Two samples, a metadunite clast (72415-18) and matrix material (72435), were collected from boulder 3.

#### GEOLOGIC DISCUSSION

The lower slopes of the South Massif at station 2 are interpreted as the surface of a thick wedge of colluvium (fig. 242) onto which boulders from the upper part of the massif have rolled. The boulders are samples of feldspar-rich breccia emplaced as ejecta from the impact that formed the southern Serenitatis basin (Wolfe and Reed, 1976; Reed and Wolfe, 1975).

The four samples of boulder 1 are polymict breccia. Fragments of metaclastic rock with aphanitic to granoblastic matrix make up about 40 to 70 percent of the matrix materials of the four samples. Fragments of plagioclase, olivine, and pyroxene, with plagioclase about twice as abundant as olivine and pyroxene combined, make up about 20 to 45 percent of the matrix materials. Metagabbro and metatroctolite as well as small amounts of quartz-potassium feldspar rock occur in all four samples. Fragments of ophitic basalt and basalt cataclasite are present in 72275.

Petrographers of the boulder 1 consortium (Consortium Indomitabile) concluded that the boulder includes two lithologically distinct associations (Marvin, 1975; Ryder and others, 1975): (1) light-gray friable feldspar-rich matrix interfingering with crushed pigeonite basalt and (2) dark-gray to black competent microbreccia that is commonly interlayered with cataclastic anorthositic breccia. The competent microbreccia, represented according to the consortium interpretation by samples 72215 and 72255 and by clasts in 72235 and 72275, is interpreted as fragments of older impact breccia incorporated in the light-gray friable breccia matrix by a later impact. The matrix of the competent

breccia records thermal metamorphism and local partial melting not seen in the matrix of the light-gray friable breccia. Some grains of olivine in the competent breccia have equilibration rims 10 to 15  $\mu\text{m}$  wide, which also were not seen in the light-gray friable breccia. Hence, Ryder and others (1975) believe the competent breccia records older high-temperature thermal events to which the entire boulder was not subjected.

We suggest that boulder 1 is a fragment of the ejecta from the impact that created the southern Serenitatis basin. The target, as represented by the materials of the boulder, was heterogeneous. It included gabbroic, noritic, troctolitic, and anorthositic plutonic rocks and their coarsely metamorphosed equivalents, and rocks of "granitic" composition. Although preexisting impact breccia was undoubtedly present near the surface in the target region, much of the target material was

probably excavated for the first time by the southern Serenitatis impact. The clasts of pigeonite basalt in sample 72275 may represent a lava flow in the target area or a fragment of pigeonite basalt introduced to the target by some distant earlier impact. An alternate hypothesis is that they came from local subsurface partial melt zones formed in the target plutonic rocks by some earlier impact but not previously excavated. The spectrum of dynamic and thermal metamorphism—pulverization, heating, melting—represented by various phases in both clasts and matrix of the four samples were the product of a continuous complex process of impact, excavation, and deposition as outlined by Wilshire and Moore (1974). At the depositional stage the mass consisted of relics of the target rock and variously fused, quenched, and pulverized rock debris undergoing cataclastic flow. When it came to rest, the

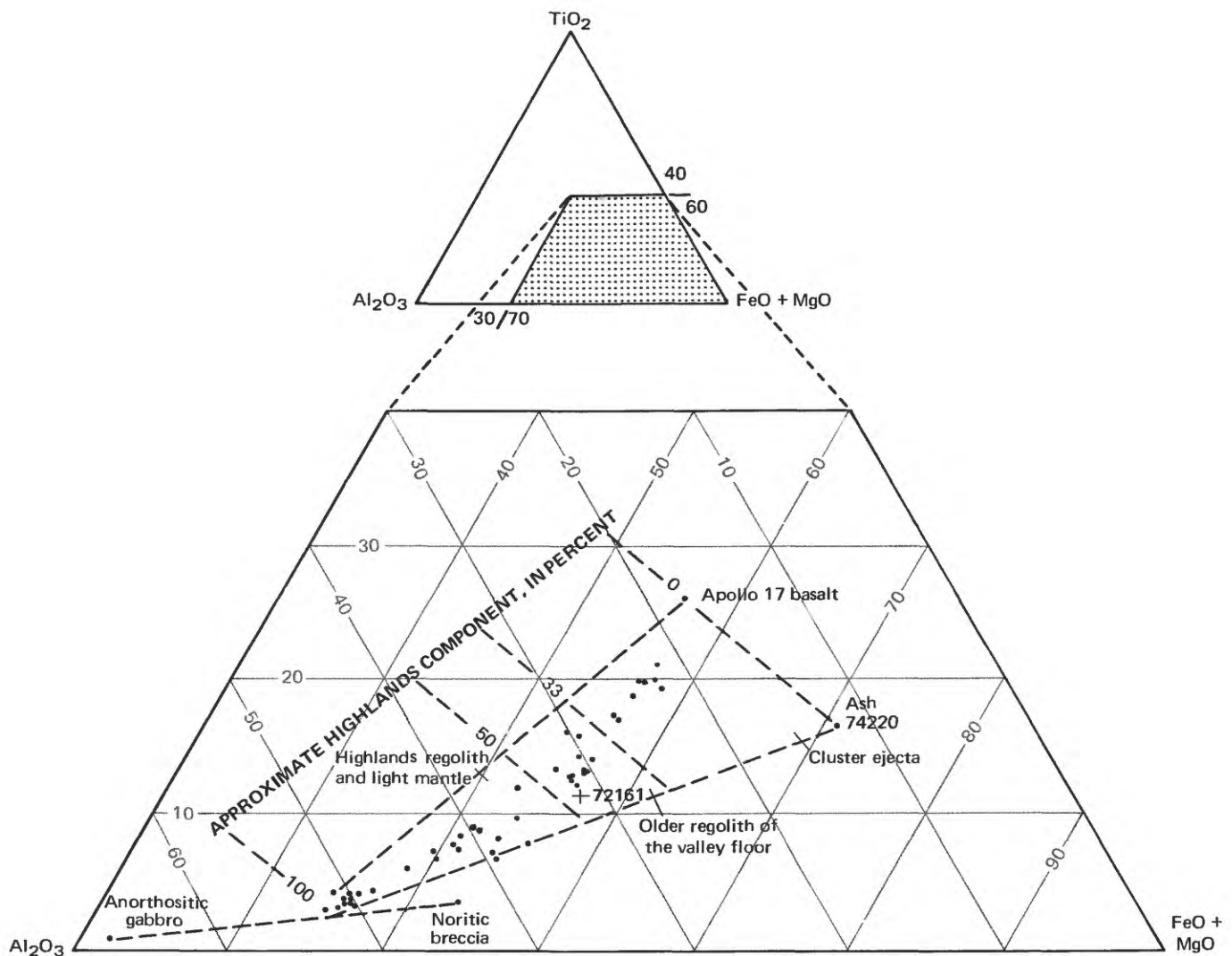


FIGURE 71.—Relative amounts of  $\text{TiO}_2$ ,  $\text{Al}_2\text{O}_3$ , and  $\text{FeO} + \text{MgO}$  in sediment sample 72161 (cross), collected at station LRV-3, in comparison with sediment samples from rest of traverse region (dots). Apollo 17 basalt, anorthositic gabbro, and noritic breccia values from Rhodes and others (1974).

heterogeneous distribution of strongly heated to fused material and colder pulverized material dictated whether the final product had a granoblastic-melt matrix (for example, samples 72215, 72255) or a friable matrix (for example, sample 72275). In this view, the dominant clast type—polymict breccia with very fine grained matrix—was assembled by the same event that excavated its components and the components of the groundmass that encloses it and does not necessarily represent earlier impact brecciation as is commonly held.

Ryder and others (1975) suggested that the light-gray friable breccia had a provenance different at least in part from that of the competent breccia (that is, the friable breccia is not simply the crushed equivalent of

the competent breccia). They cite two lines of evidence: (1) the occurrence of distinctive pigeonite basalt clasts in the friable breccia but not in the competent breccia and (2) chemical differences, particularly in meteoritic materials, between their two breccia types.

The pigeonite basalt clasts have been found only in friable breccia sample 72275 (Ryder and others, 1975). Variation diagrams of major elements (fig. 75) show that the compositions of the matrix and of some clast samples of 72275 diverge from the nearly linear trend characteristic of Apollo 17 highlands rocks toward the composition of the iron-rich pigeonite basalt. We infer from these data that the boulder 1 breccia, except for mechanical admixture of pigeonite basalt, is compositionally like the rest of the Apollo 17 highlands suite.

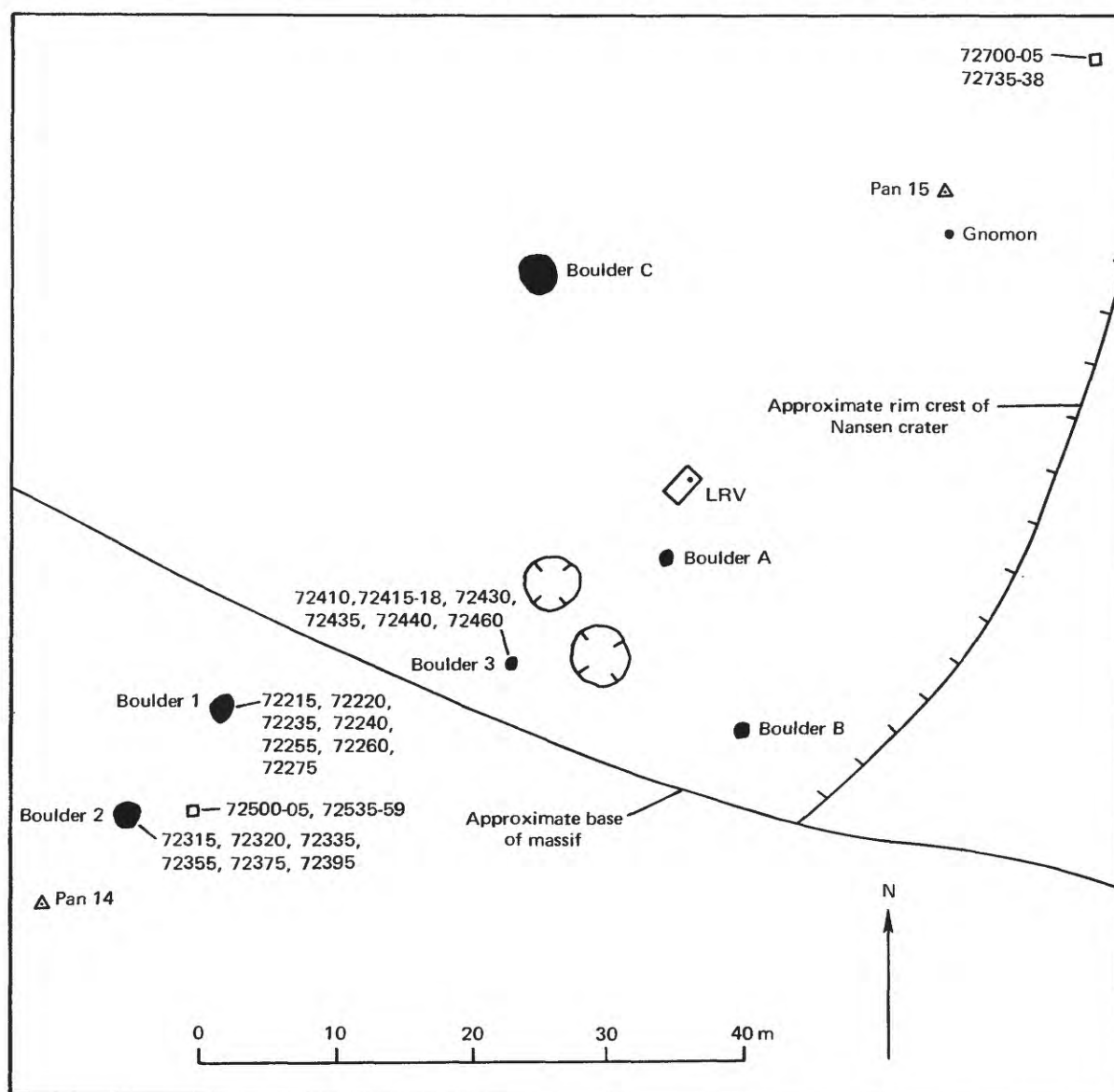


FIGURE 72.—Planimetric map of station 2.

The restricted occurrence of pigeonite basalt in 72275 reflects the inhomogeneous distribution of the basalt within the target area.

Chemical data (fig. 75) suggest that pigeonite basalt has been incorporated in the dark rind of the so-called Marble Cake clast, described by Ryder and others as a 3-cm clast consisting of "cataclastic gabbroic anorthosite crudely interlayered with gray breccia and [vesicular] dark rim material\*\*\*. The rim and core have been

fluidized and interlayered in a rather complex manner to form a 'marble cake' pattern." We suggest that the dark rim material with its pigeonite basalt component was formed simultaneously with the 72275 matrix in a local zone within the mobilized ejecta where more intense cataclasis and perhaps partial melting occurred. Similar relations have been described by Wilshire and Moore (1974) for the large clast in sample 72235 (fig. 79) as well as a model for cataclasis and mobiliza-

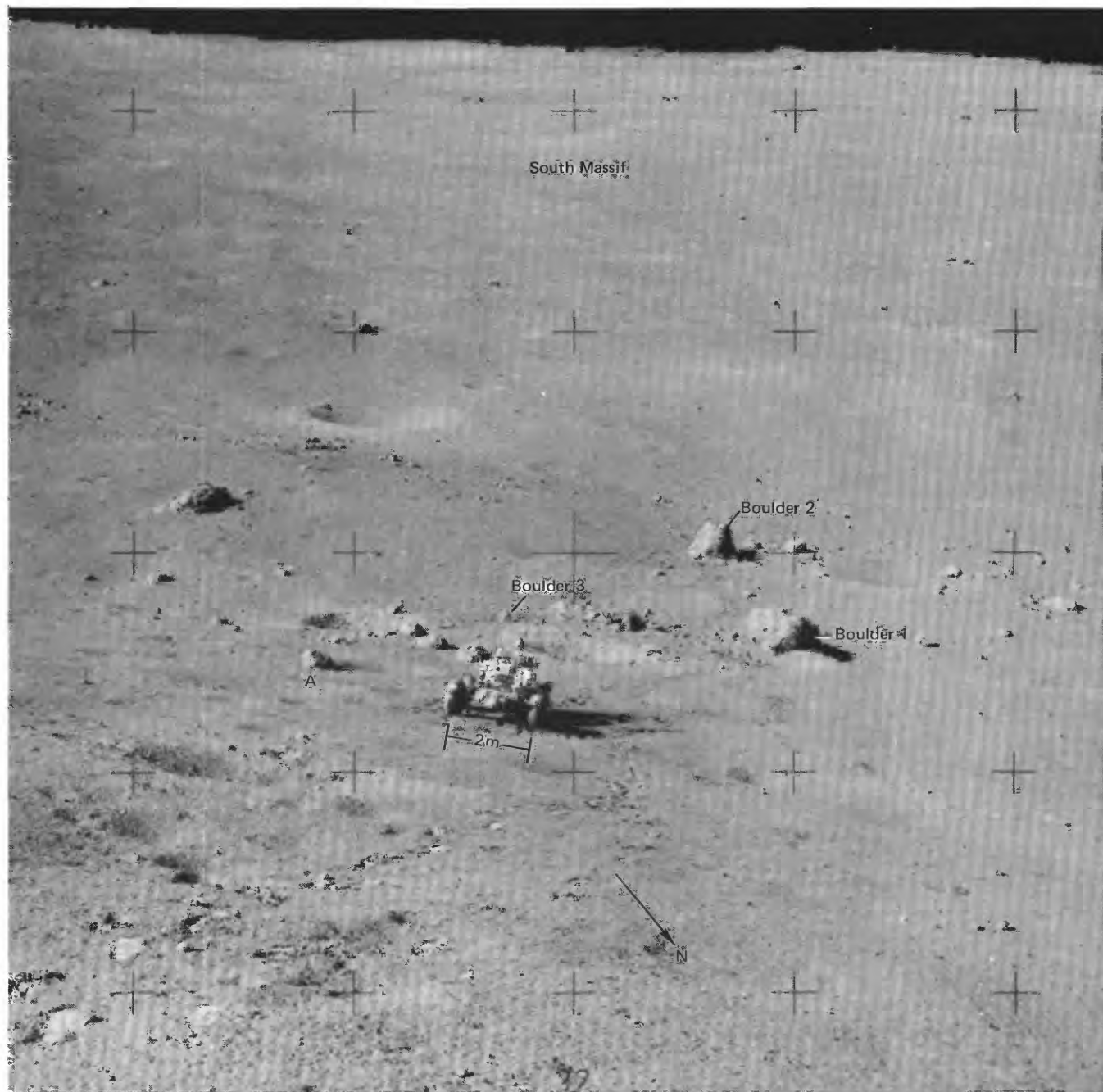


FIGURE 73.—Station 2 area. Distance from LRV to boulder 2 is about 50 m. A denotes boulder identified on station map (fig. 72) and in pans 14 and 15 (pls. 5 and 6). (NASA photograph AS17-138-21072.)

tion of ejecta in impacts to produce such layered and coated clasts.

Samples of both matrix and clasts of boulder 1, excluding the pigeonite basalt and a few clasts interpreted as plutonic fragments, are characterized by a distinctive meteoritic trace-element distribution (group 3) that is different from the equally distinctive pattern (group 2) shared by most of the Apollo 17 highlands breccia (Morgan and others, 1975). The data suggest that differences between the 72275 trace-element distribution and that of the other boulder 1 samples are due at least in part to the admixture of pigeonite basalt in 72275. Because of the predominance of the group 2 pattern in the Apollo 17 highlands breccia, Morgan and others (1975) concluded that it represents the trace-element signature of the projectile that formed the Serenitatis Basin (southern Serenitatis basin of this report). They suggested that the boulder 1 materials were excavated in the same impact but that they came from a position in the basin distant enough from the projectile itself to avoid detectable admixture of materials of the projectile. Supporting evidence that the trace-element distributions of groups 2 and 3 may each represent ejecta of the same basin impact comes from station 3. Two of three matrix samples from rock 73215 contain the group 2 meteoritic component. The third matrix sample, taken about a centimeter from the first two and not visibly different, contains the group 3

cia, Morgan and others (1975) concluded that it represents the trace-element signature of the projectile that formed the Serenitatis Basin (southern Serenitatis basin of this report). They suggested that the boulder 1 materials were excavated in the same impact but that they came from a position in the basin distant enough from the projectile itself to avoid detectable admixture of materials of the projectile. Supporting evidence that the trace-element distributions of groups 2 and 3 may each represent ejecta of the same basin impact comes from station 3. Two of three matrix samples from rock 73215 contain the group 2 meteoritic component. The third matrix sample, taken about a centimeter from the first two and not visibly different, contains the group 3

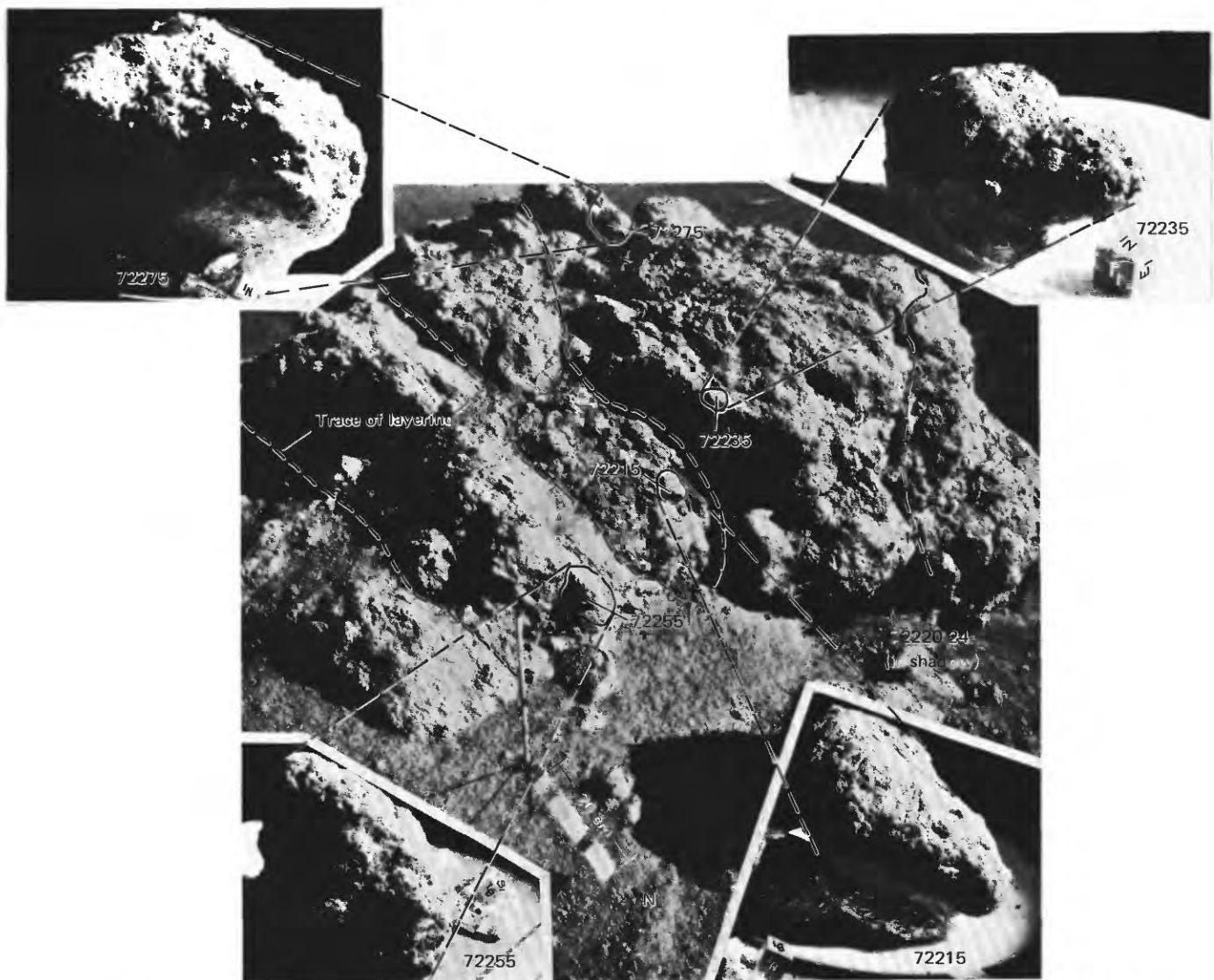


FIGURE 74.—Boulder 1 at station 2 before sampling, showing locations of rock samples 72215, 72235, 72255, and 72275, and sediment sample 72220-24. Boulder is about 2 m across and 1 m high. Insets are laboratory photographs showing four rock samples with reconstructed lunar surface orientations and lighting. (NASA photographs AS17-137-20901; S-73-17987 (72215), S-73-17963 (72235), S-73-17989 (72255), and S-73-17988 (72275).)

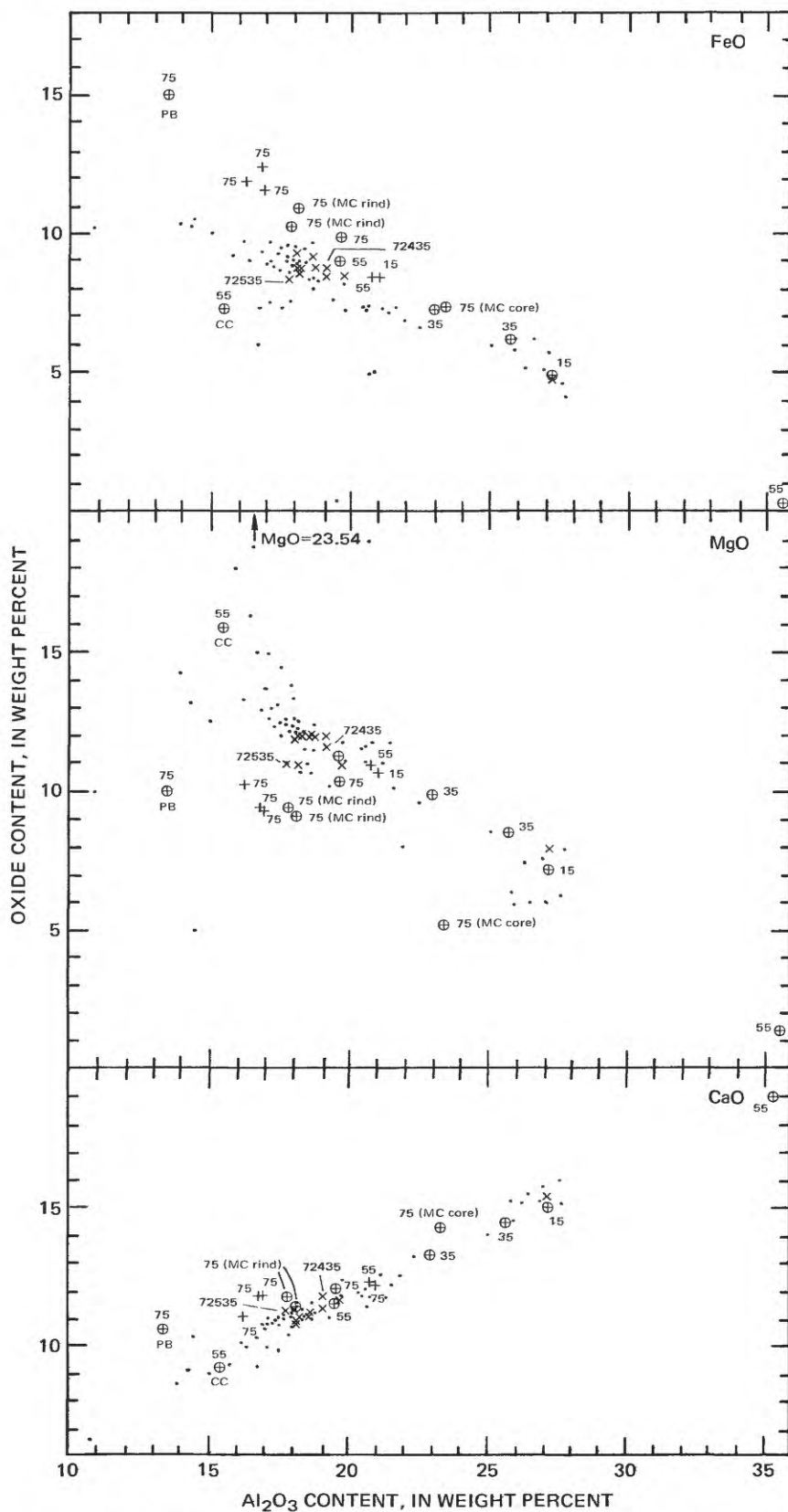


FIGURE 75.—Plots of FeO, MgO, and CaO contents in relation to  $Al_2O_3$  content for analyzed rocks from station 2 (excluding metadunite 72415-18) in comparison with all analyzed Apollo 17 highlands rocks. Cross, boulder 1 matrix sample; circled cross, boulder 1 clast sample (those with  $Al_2O_3$  contents ranging from 17.9 through 23.1 percent are competent breccia from distinct clasts within individual samples); 15, 35, 55, 75 identify last two digits of boulder 1 sample numbers; PB, pigeonite basalt; MC, Marble Cake clast; CC, Civet Cat norite clast; x, sample from boulder 2 except where identified as 72435 (boulder 3) and 72535 (rake fragment).

meteoritic component (James and others, 1975a).

Boulder 2 samples and sample 72435, which represents the matrix material of boulder 3, are polymict breccia. Modal analyses by Wilshire (this report) show that the matrix, in the 0.1–1.0-mm size range, is dominated by clasts of plagioclase (49–65 percent), with smaller amounts of olivine (6–28 percent) and pyroxene (1–4 percent). Metagabbroid fragments (10–21 percent) are the dominant lithic type in this size range. Larger lithic clasts, up to about 2 cm in diameter, have been classified by Dymek and others (1976b) as members of the dunite-anorthosite-norite-troctolite suite.

Matrix textures in boulders 2 and 3 are described by Wilshire (this report) as aphanitic to granoblastic to poikilitic, implying that thermal metamorphism in an ejecta blanket at least in part recrystallized a matrix that may have ranged initially from fragmental to partly melted. In contrast, Dymek and others (1976b) have described no textures indicative of thermal metamorphism; they have interpreted the matrices of boulders 2 and 3 as aggregates of abundant microclasts within a poikilitic to subophitic groundmass that crystallized from a melt. In their model, the breccia was formed by violent mixing of predominantly unshocked cold clasts with impact melt generated in the formation of a lunar basin.

Analyzed subsamples from boulders 2 and 3 show a high degree of chemical homogeneity (fig. 75). Except for a single clast that is unusually rich in plagioclase (72335,2;  $\text{Al}_2\text{O}_3=27.3$  percent), all of the analyzed samples are tightly clustered ( $\text{Al}_2\text{O}_3$  values between 18 and 20 percent) within the compositionally restricted Apollo 17 breccia suite. However, Dymek and others (1976b) have reported on the basis of microprobe analyses that the “igneous” groundmass in boulders 2 and 3 differs from the bulk breccia compositions. In addition, the dominant plagioclase in the clasts is significantly more calcic than that in the groundmass, and olivine and pyroxene clasts tend to be more magnesian than their groundmass counterparts. Hence they have concluded that the groundmass melt and the clasts were derived from slightly different sources; that is, the groundmass was not produced by crushing, grinding, melting, or recrystallization of the observed clast assemblage.

Sample 72415-18, the clast of metadunite from boulder 3, has been interpreted as a sample of a cumulate igneous rock (Albee and others, 1975); its relict granoblastic fabric may represent prolonged deep-seated thermal metamorphism. Snee and Ahrens (1975) found evidence of shock deformation from which they inferred shock pressures in the range of 330–440 kb. Before or during incorporation into the

ejecta of which boulder 3 is a sample, the metadunite fragment underwent cataclasis. Papanastassiou and Wasserburg (1975) inferred a crystallization age of  $4.55 \pm 0.10$  b.y. and suggested that the metadunite clast was derived from an early lunar differentiate; its mineralogy is appropriate for it to be related by fractional crystallization to norite 78235 and metatroctolite 76535 (Dymek and others, 1975).

Both the chemical composition (fig. 76) and the petrography of sediment samples from station 2 reflect their derivation from the feldspar-rich rocks of the South Massif. All are samples of unconsolidated colluvium derived from impact-generated regolith on the surface of the massif. Sample 72700-04, collected more than 50 m out from the base of the South Massif, is the most likely sample from station 2 to represent pure light mantle material. However, the other analyzed samples (fig. 76), from the lowest part of the massif slope, are indistinguishable from 72700-04 in figure 76; they could all represent light mantle material.

The boulders near the base of the massif probably rolled to their present positions after emplacement of the light mantle. Some, although not the three sampled boulders, are at the ends of tracks that probably would have been obliterated by subsequent deposition of light mantle, and all would probably have been buried by the boulder-poor light mantle if they had been there first. Evaluating exposure ages determined for boulder 1, Leich and others (1975) concluded that the boulder has been in its present position at the base of the massif for about 42 m.y.

#### SUMMARY OF SAMPLING

##### Sample 72215

*Type:* Polymict breccia with an aphanitic matrix.

*Size:*  $9.7 \times 6.6 \times 5.0$  cm.

*Weight:* 379.2 g.

*Location:* From 2-m boulder 1 on lower slopes of South Massif approximately 35 m southwest of the LRV.

*Illustrations:* Pans 14, 15, figures 73, 74, 77 (LRL).

*Comments:* Boulder 1 represents bedrock from the upper part of the South Massif.

*Petrographic description:* Polymict breccia with an aphanitic matrix. Clasts in the size range 0.1 to 1.0 mm are in the approximate proportions: 32 percent plagioclase, 3 percent pyroxene, 12 percent olivine, 33 percent dark metaclastic rocks with aphanitic matrices, 5 percent light metaclastic rocks with granoblastic matrices, 5 percent quartz-potassium feldspar fragments, 6 percent metagabbro, 1 percent metatroctolite, 2 percent recrystallized olivine, and 8 percent recrystallized plagioclase. The dominant source rock is probably troctolite-metatroctolite.

In the classification of the boulder 1 consortium

(Consortium Indomitable), sample 72215 is dominantly gray competent breccia, interpreted as representing the matrix of many of the clasts that are themselves incorporated within the light-gray friable breccia of sample 72275 (Marvin, 1975).

*Major-element composition:*

*Chemical analyses of 72215*

	1	2
SiO <sub>2</sub> .....	45.2	44.7
Al <sub>2</sub> O <sub>3</sub> .....	21.1	27.3
FeO .....	8.43	4.80
MgO .....	10.7	7.19
CaO .....	12.1	14.9
Na <sub>2</sub> O .....	.52	.48
K <sub>2</sub> O .....	.25	.11
TiO <sub>2</sub> .....	.9	.5

*Chemical analyses of 72215—Continued*

	1	2
P <sub>2</sub> O <sub>5</sub> .....	..	..
MnO .....	.128	.067
Cr <sub>2</sub> O <sub>3</sub> .....	.25	.126
Total .....	99.578	100.18

1. Average of 4 analyses of gray competent breccia matrix (Blanchard and others, 1975). Original analyses (72215,47; 60; 64; 92) in Blanchard and others, 1974).

2. 72215,76, anorthostic breccia clast (Blanchard and others, 1975).

Age: Rb-Sr:  $4.03 \pm 0.03$  b.y. determined for Rb-rich microgranite clasts in competent breccia matrices of 72215,104 and 72255,59 (Compston and others, 1975). Microgranite fragments show reaction-rim relation to enclosing breccia, and some have been partially melted; hence, they predate the high-

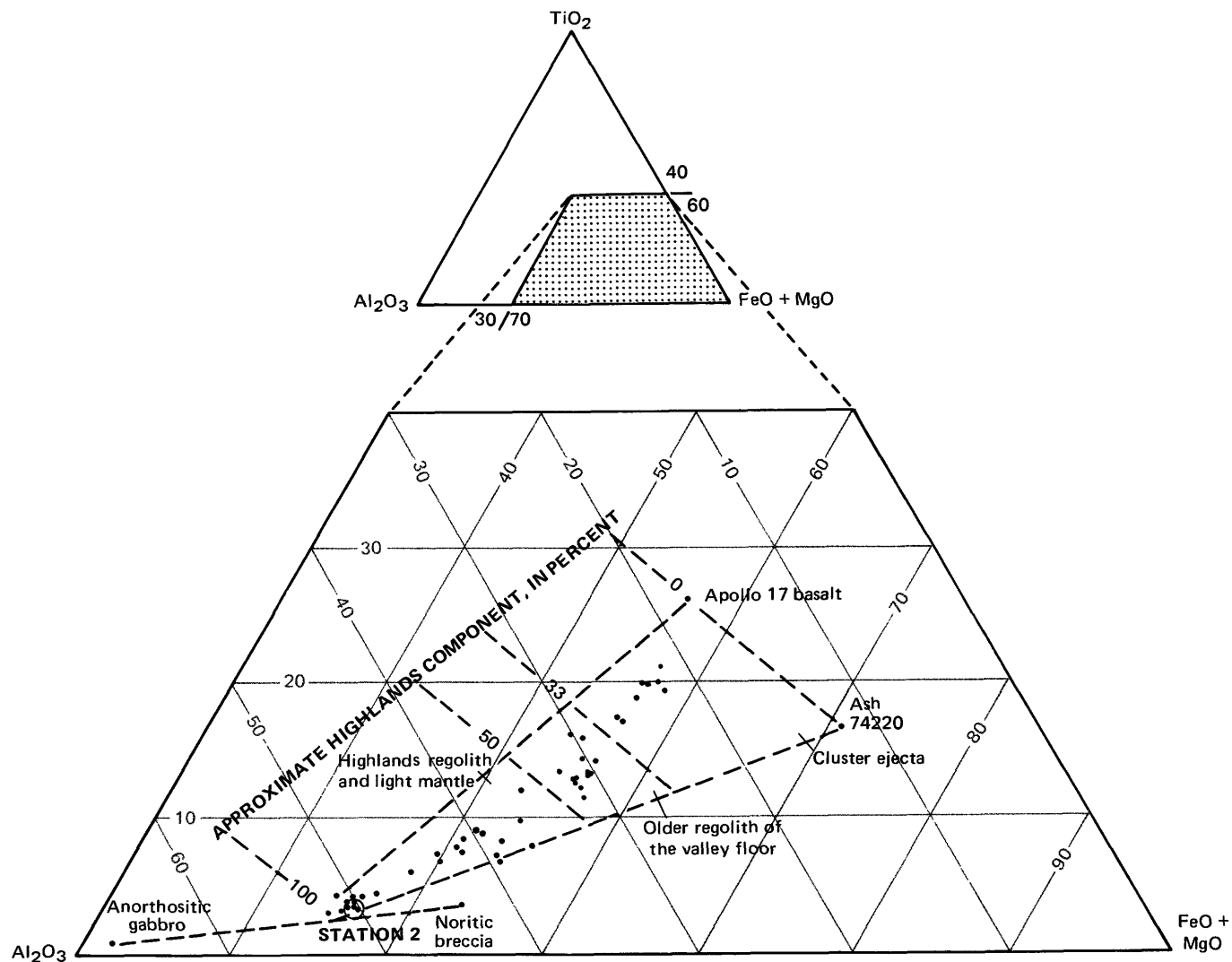


FIGURE 76.—Relative amounts of TiO<sub>2</sub>, Al<sub>2</sub>O<sub>3</sub>, and FeO+MgO in sediment samples 72321, 72441, 72461, 72501, and 72701 (circled) from station 2, in comparison with sediment samples from rest of traverse region. Apollo 17 basalt, anorthositic gabbro, and noritic breccia values from Rhodes and others (1974).

temperature high-pressure assembly of the matrix inferred by Stoesser and others (1974a). Rb-Sr age of microgranite clasts is an older limit for consolidation of the competent breccia matrix and may be the crystallization age of the microgranite.

*Exposure age:* Kr:  $41.4 \pm 1.4$  m.y. (Leich and others, 1975).

Sample 72220-24

*Type:* Sedimentary, unconsolidated.

*Weight:* 388.56 g.

*Depth:* 0-3 cm.

*Location:* From fillet underneath the east-facing overhang on boulder 1.

*Illustrations:* Pans 14, 15; figures 73, 74, 78.

*Petrographic description:* 72220-24, dominantly breccia, some agglutinate, some feldspar fragments.

Sample 72235

*Type:* Polymict breccia with a cataclastic matrix.

*Size:*  $7 \times 4 \times 3$  cm.

*Weight:* 61.91 g.

*Location:* From boulder 1 on lower slopes of South Massif approximately 35 m southwest of the LRV.

*Illustration:* Pans 14, 15; figures 73, 74, 79.

*Comments:* Boulder 1 represents bedrock from the upper part of the South Massif.

*Petrographic description:* Polymict breccia with a cataclastic matrix. The specimen is dominated by a  $2.5 \times 4$  cm clast (fig. 79) of interlayered troctolitic(?) cataclasite and dark finely pulverized material. Clasts in the size range 0.1 to 1.0 mm are in the approximate proportions: 15 percent plagioclase, 9 percent pyroxene, 1 percent olivine, 1 percent opaque minerals, 57 percent dark metaclastic rocks with aphanitic matrix, 3 percent light metaclastic rocks with granoblastic matrix, 1 percent quartz-potassium feldspar rocks, 11 percent metagabbro, 2 percent recrystallized plagioclase.

The boulder 1 consortium described 72235 as a coherent knob (the large  $2.5 \times 4$  cm clast) of interlayered black competent breccia and anorthositic breccia with an adhering matrix of light-gray friable breccia similar to the matrix of 72275 (Marvin, 1975).

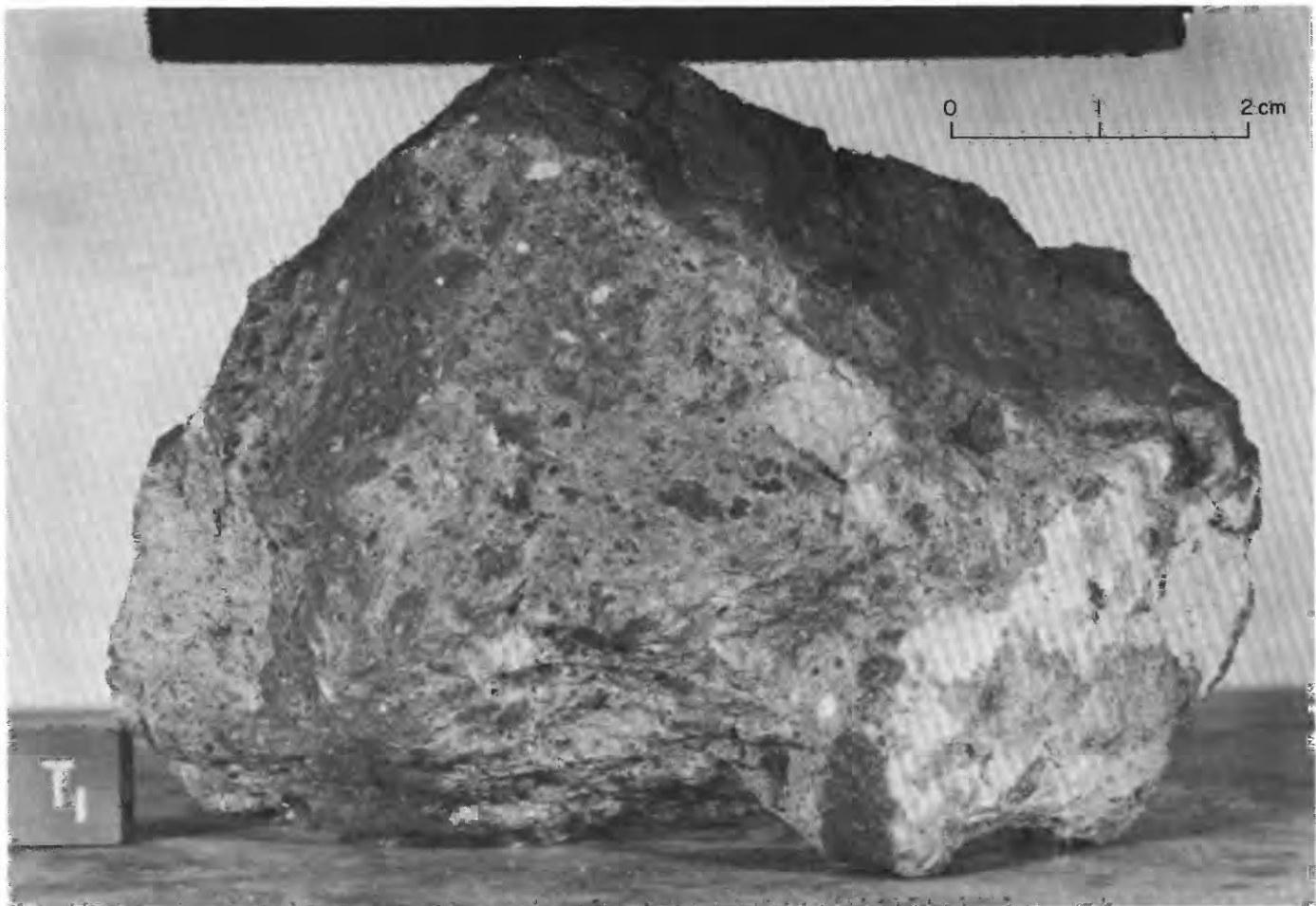


FIGURE 77.—Sample 72215. Polymict breccia with aphanitic matrix. (NASA photograph S-73-16661.)

*Major-element composition:**Chemical analyses of 72235*

	1	2
SiO <sub>2</sub> .....	44.6	44.5
Al <sub>2</sub> O <sub>3</sub> .....	23.1	25.8
FeO .....	7.28	6.19
MgO .....	9.9	8.52
CaO .....	13.2	14.4
Na <sub>2</sub> O .....	.514	.42
K <sub>2</sub> O .....	.20	.11
TiO <sub>2</sub> .....	.8	.8
P <sub>2</sub> O <sub>5</sub> .....	..	..
MnO .....	.111	.080
Cr <sub>2</sub> O <sub>3</sub> .....	.21	.146
Total .....	99.92	100.97

1. 72235,46, competent breccia matrix of 72235. Composition, intermediate between the more typical competent breccia matrix of the boulder (for example, average matrix of 72255) and anorthositic breccia clasts (for example, 72215,76 and 72235,36), is interpreted as a mechanical mixture of components that were abundant at the source region and that are identifiable in the boulder 1 samples (Blanchard and others, 1975).
2. 72235,36, anorthositic breccia clast (Blanchard and others, 1975).
- Additional analyses, by defocused beam microprobe, have been published by Stoesser and others (1974a) and Ryder and others (1975).

*Sample 72240-44*

*Type:* Sedimentary, unconsolidated.

*Weight:* 322.42 g.

*Depth:* 0-5 cm.

*Location:* From fillet on east of boulder 1 on lower slopes of South Massif, approximately 35 m southwest of LRV.

*Illustrations:* Pans 14, 15; figures 73, 78.

*Comments:* Sample 72240-44 represents regolith developed on the talus at the base of South Massif.

*Petrographic description:* 72240-44, dominantly breccia and agglutinate.

*Sample 72255*

*Type:* Polymict breccia with an aphanitic matrix.

*Size:* 10.5×9×2.5 cm.

*Weight:* 461.2 g.

*Location:* From boulder 1 on lower slopes of South Massif approximately 35 m southwest of LRV.

*Illustrations:* Pans 14, 15; figures 73, 74, 80 (LRV).

*Comments:* Source rock (boulder 1) is from high on the slope of South Massif.

*Petrographic description:* Polymict breccia with an aphanitic matrix. Clasts in the size range 0.1 to 1.0 mm are in the approximate proportions: 19 percent plagioclase, 2 percent olivine, 8 percent pyroxene, 60 percent dark metaclastic rocks with aphanitic matrices, 3 percent light metaclastic rocks with granoblastic matrices, 1 percent quartz-potassium feldspar rocks, 4 percent metagabbro, 1 percent metatroctolite, 1 percent recrystallized olivine, 2

percent recrystallized plagioclase, trace noritic cataclastite.

The boulder 1 consortium has interpreted 72255 as a polymict breccia with a competent matrix (in contrast to the friable-matrix breccia of 72275 type). Hence they believe it may represent a clast within boulder 1. Numerous clasts within 72255 include some described as gray aphanitic microbreccia, white anorthosite with and without black rims, crystalline gabbroic clasts, and the particularly conspicuous 2-cm "Civet Cat" clast (fig. 80) interpreted as a norite fragment with relict plutonic texture visible through shock features (Marvin, 1975).

*Major-element composition:**Chemical analyses of 72255*

	1	2	3	4
SiO <sub>2</sub> .....	45.0	52.0	43.0	46.0
Al <sub>2</sub> O <sub>3</sub> .....	20.9	15.5	35.8	19.7
FeO .....	8.45	7.4	0.13	9.05
MgO .....	11.0	15.9	1.43	11.3
CaO .....	12.2	9.1	18.9	11.5
Na <sub>2</sub> O .....	.51	.33	.63	.54
K <sub>2</sub> O .....	.25	.08	.12	.28
TiO <sub>2</sub> .....	.8	.3	.7	1.2
P <sub>2</sub> O <sub>5</sub> .....	..	..	..	..
MnO .....	.122	.122	.003	.136
Cr <sub>2</sub> O <sub>3</sub> .....	.25	.16	.003	.263
Total .....	99.482	100.89	100.72	99.97

1. Average of four analyses of gray competent breccia matrix (Blanchard and others, 1975); original analyses (72255,52, 64, 69, 79) from Blanchard and others (1974).
2. Coarse norite clast ("Civet Cat") 72255,42 (Blanchard and others, 1975).
- 3,4. 72255,45, clast of interlayered white anorthositic breccia (column 3) and black competent breccia (column 4) (Blanchard and others, 1975).
- Additional analyses by defocused beam microprobe have been published by Stoesser and others (1974a) and Ryder and others (1975).

*Age:*

<sup>40-39</sup>Ar: 72255,42,  $3.99 \pm 0.03$  b.y., Civet Cat norite clast; 72255,52,  $4.01 \pm 0.03$  b.y., matrix adjacent to Civet Cat clast (Leich and others, 1975). Mean value of  $4.00 \pm 0.03$  is interpreted as an accurate measure of the time that 72255 began retention of argon and as the time when the competent breccias, such as the 72255 matrix, were assembled. It may represent an older limit for the formation of the Serenitatis basin (Leich and others, 1975).

Rb-Sr isochron: 72255,41,  $4.17 \pm 0.05$  (2 $\sigma$ ) b.y., Civet Cat norite clast; may represent original igneous age or at least a younger limit on original crystallization (Compston and others, 1975). Data also show a Rb-Sr disturbance at  $\sim 3.9 \pm 0.1$  b.y., which may represent the high-temperature event in which the competent breccia of boulder 1 was formed.

Fission track: Whitlockite crystal in 72255,30,  $3.96^{+0.04}_{-0.07}$  b.y., interpreted as representing the last high-temperature metamorphic event

experienced by the boulder 1 materials (Goswami and Hutcheon, 1975).

*Exposure age:*

Kr:  $44.1 \pm 3.3$  m.y. (Leich and others, 1975).

Track age:  $\sim 40$  m.y. (Goswami and Hutcheon, 1975) apparently supersedes an earlier track age determination of  $19 \pm 2$  m.y. by Hutcheon and others (1974b).

Sample 72260-64

*Type:* Sedimentary, unconsolidated.

*Weight:* 279.0 g.

*Depth:* 0-1 cm.

*Location:* From fillet on east side of boulder 1 on lower slopes of South Massif, approximately 35 m southwest of LRV.

*Illustrations:* Pans 14, 15; figures 73, 78.

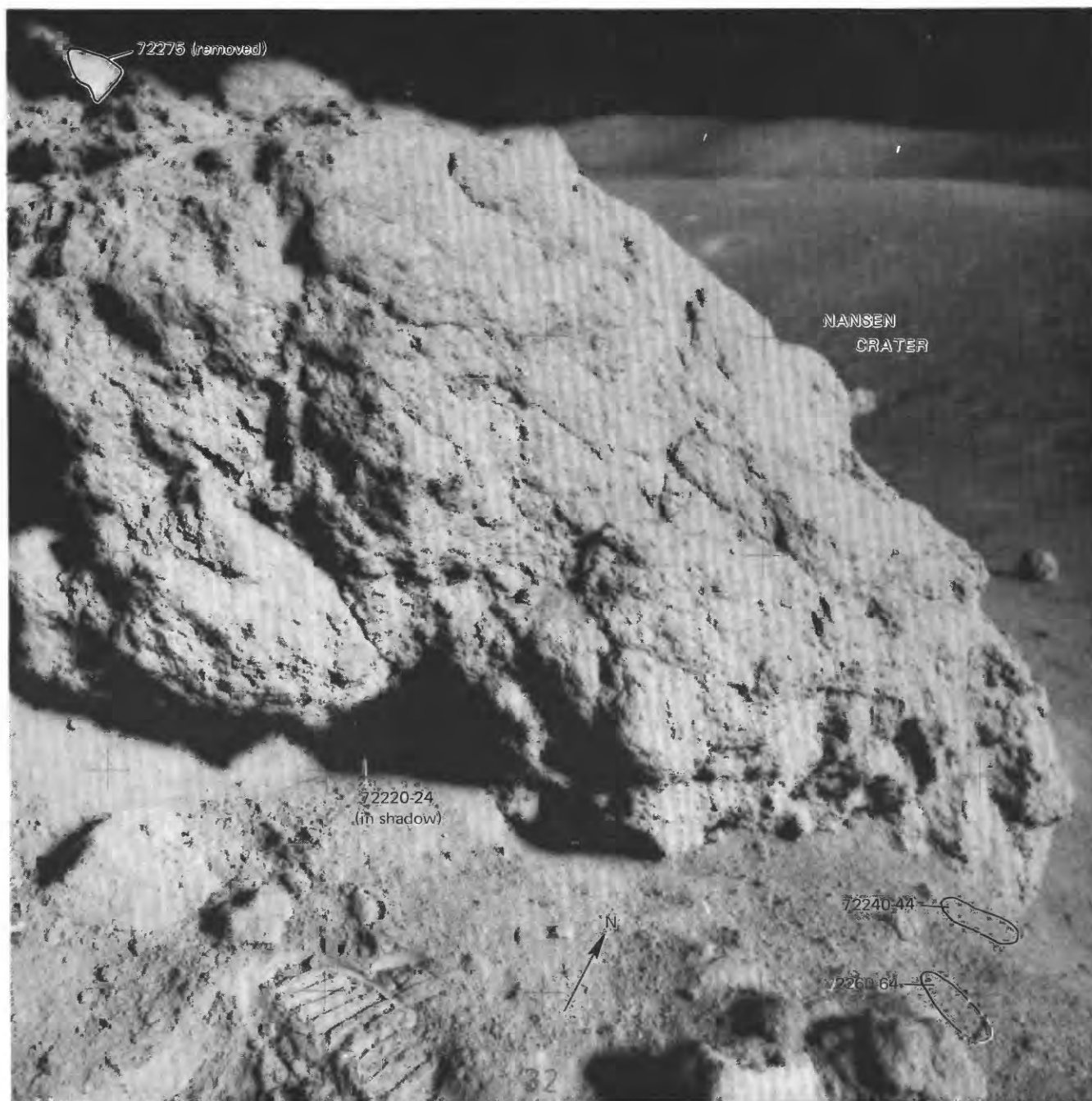


FIGURE 78.—Boulder 1 at station 2 showing 72275 after collection and 72220-24, 72240-44, and 72260-64 before collection. (NASA photograph AS17-138-21031.)

**Comments:** Skim sample 72260-64 represents regolith developed on the talus at the base of South Massif.

#### Sample 72275

**Type:** Polymict breccia with cataclastic matrix.

**Size:** 17×14×12 cm.

**Weight:** 3,640 g.

**Location:** From boulder 1 on lower slopes of South Massif approximately 35 m southwest of LRV.

**Illustrations:** Pans 14, 15; figures 73, 74, 78, 81 (LRL).

**Comments:** Source rock (boulder 1) is from upper part of South Massif.

**Petrographic description:** Polymict breccia with a fine-grained cataclastic matrix. Clast types in the size range 0.1 to 1.0 mm are in the approximate proportions: 13 percent plagioclase, 2 percent olivine, 5 percent pyroxene, 65 percent dark metaclastic rocks with aphanitic matrix, 5 percent light metaclastic rocks with granoblastic matrix, 1 percent ophitic basaltic rock, 1 percent anorthosite, 4 percent metagabbro, 1 percent metatroctolite, 3 percent recrystallized plagioclase, 1 percent anorthosite cataclasite, 1 percent basalt cataclasite, trace quartz-potassium feldspar rock.

The boulder 1 consortium has described 72275 as predominantly light-gray friable matrix material in which the most conspicuous clast types are (1) gray and black competent breccia; (2) anorthositic breccia, commonly cataclastic, sometimes with rims of black competent breccia as in the 2-cm "Marble

Cake" clast from 72275; (3) felty pigeonite basalt clast that occur as clots of basalt within lenses and bands of basaltic debris interfingering with the light-gray friable matrix. Pigeonite basalt occurs only within the light friable matrix, never within the clasts of gray or black competent breccia (Marvin, 1975).

#### Major-element composition:

##### Chemical analyses of 72275

	1	2	3	4	5	6	7	8	9
SiO <sub>2</sub> ....	47.54	47.31	48.3	48.0	47.0	47.0	47.0	46.0	47.7
Al <sub>2</sub> O <sub>3</sub> ....	17.01	16.90	16.3	13.5	17.9	18.2	23.5	19.7	16.7
FeO ..... 11.58	12.45	11.9	15.0	10.3	10.9	7.4	9.9	12.0	
MgO ..... 9.35	9.47	10.3	10.0	9.43	9.14	5.24	10.4	9.7	
CaO ..... 11.71	11.72	11.0	10.5	11.7	11.2	14.2	12.0	11.5	
Na <sub>2</sub> O ....	.38	.35	.44	.29	.39	.63	.36	.30	.39
K <sub>2</sub> O ..... .28	.22	.25	.25	.47	.49	.32	.25	.25	
TiO <sub>2</sub> ....	.91	.94	1.0	1.4	1.8	1.1	1.8	.8	1.0
P <sub>2</sub> O <sub>5</sub> ....	.35	.38	--	--	--	--	--	--	.36
MnO ..... .18	.19	.17	.156	.104	.167	.077	.111	.18	
Cr <sub>2</sub> O <sub>3</sub> ..	.36	.34	.35	.46	.27	.20	.24	.35	
Total...	99.65	100.27	100.01	99.56	99.55	99.41	100.10	99.70	100.13

*Note.*—Additional analyses by defocused beam microprobe have been published by Stoesser and others (1974a, b) and Ryder and others (1975).

1. 72275.2, representative nortite breccia from 72275 (Apollo 17 PET, 1973).
2. 72275.90, matrix (Rose and others, 1974).
3. 72275.57, light-gray friable breccia matrix (Blanchard and others, 1975).
4. 72275.91, pigeonite basalt clast (Blanchard and others, 1975).
5. 72275.80, black competent breccia rind of Marble Cake clast (Blanchard and others, 1975).
6. 72275.166, black competent breccia rind of Marble Cake clast (Blanchard and others, 1975).
7. 72275.76, anorthositic breccia core of Marble Cake clast (Blanchard and others, 1975).
8. 72275.83, gray competent breccia clast (Blanchard and others, 1975).
9. Average matrix composition (average of columns 1, 2, and 3).

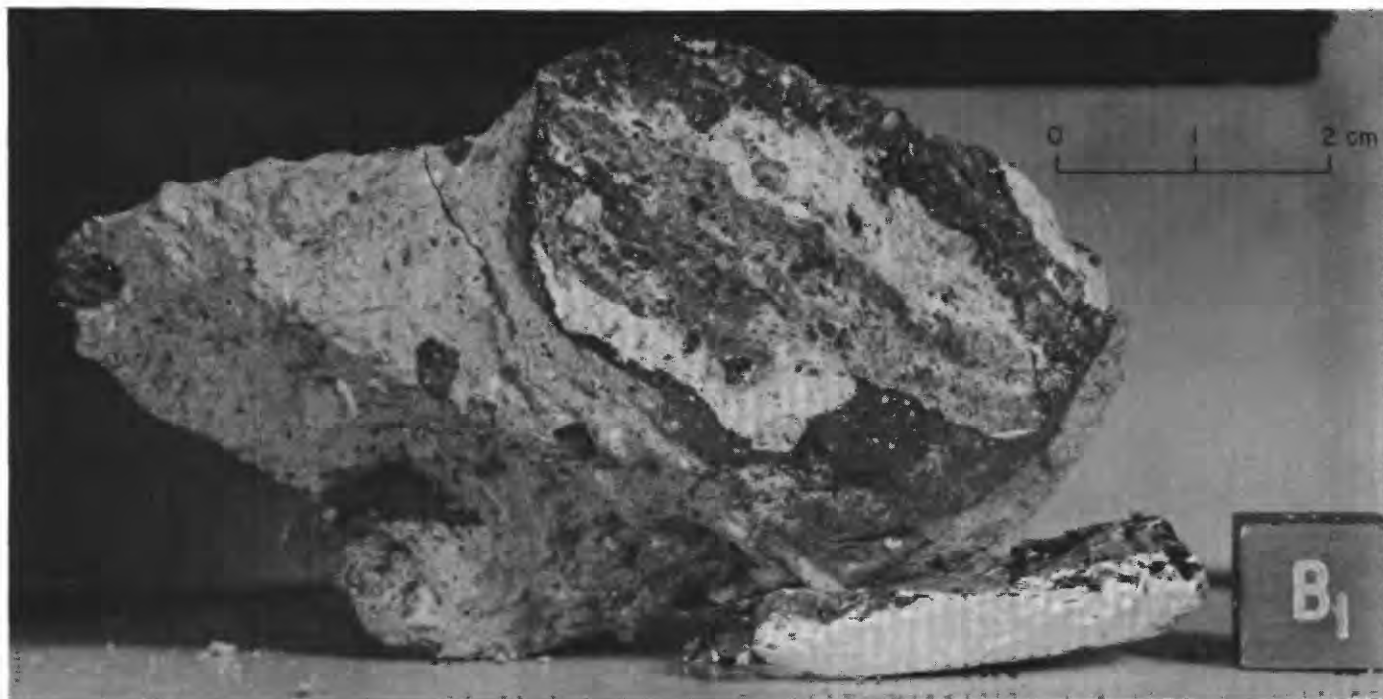


FIGURE 79.—Sample 72235. Polymict breccia with cataclastic matrix. At right is large (2.5×4 cm) clast of interlayered troctolitic(?) cataclasite and dark finely pulverized material. (NASA photograph S-73-16772.)

**Age:**

$^{40}\text{Ar}$ - $^{39}\text{Ar}$ : 72275,80,  $3.99 \pm 0.03$  b.y., black competent breccia rim of Marble Cake clast (Leich and others, 1975).

Rb-Sr isochron: 72275,171,  $4.01 \pm 0.04$  b.y., pigeonite basalt clast; interpreted as age of original crystallization because of absence of petrographic evidence for either thermal metamorphism or extensive shock effects on the pigeonite basalt fragments (Compston and others, 1975).

Fission track: Whitlockite crystal in 72275,  $3.98^{+0.04}_{-0.06}$  b.y. (Goswami and others, 1976b).

**Exposure age:**

Kr:  $52.5 \pm 1.4$  m.y. (Leich and others, 1975). This exposure age may represent the time since first exposure of boulder 1 material to irradiation, perhaps while the sampled mate-

rial was still in place high on the South Massif. Slightly younger Kr ages determined for 72215 and 72275 give a mean value of  $41.8 \pm 1.3$  m.y., which may represent the time of emplacement of the boulder in its present position (Leich and others, 1975). The ~40-m.y. track age of 72255 (Goswami and Hutcheon, 1975) is compatible with the suggested ~42-m.y. life of the boulder at the base of the massif.

**Sample 72315**

*Type:* Polymict breccia with granoblastic matrix.

*Size:*  $10 \times 5.5 \times 2$  cm.

*Weight:* 131.4 g.

*Location:* From boulder 2 on lower slopes of South Massif approximately 50 m southwest of LRV.

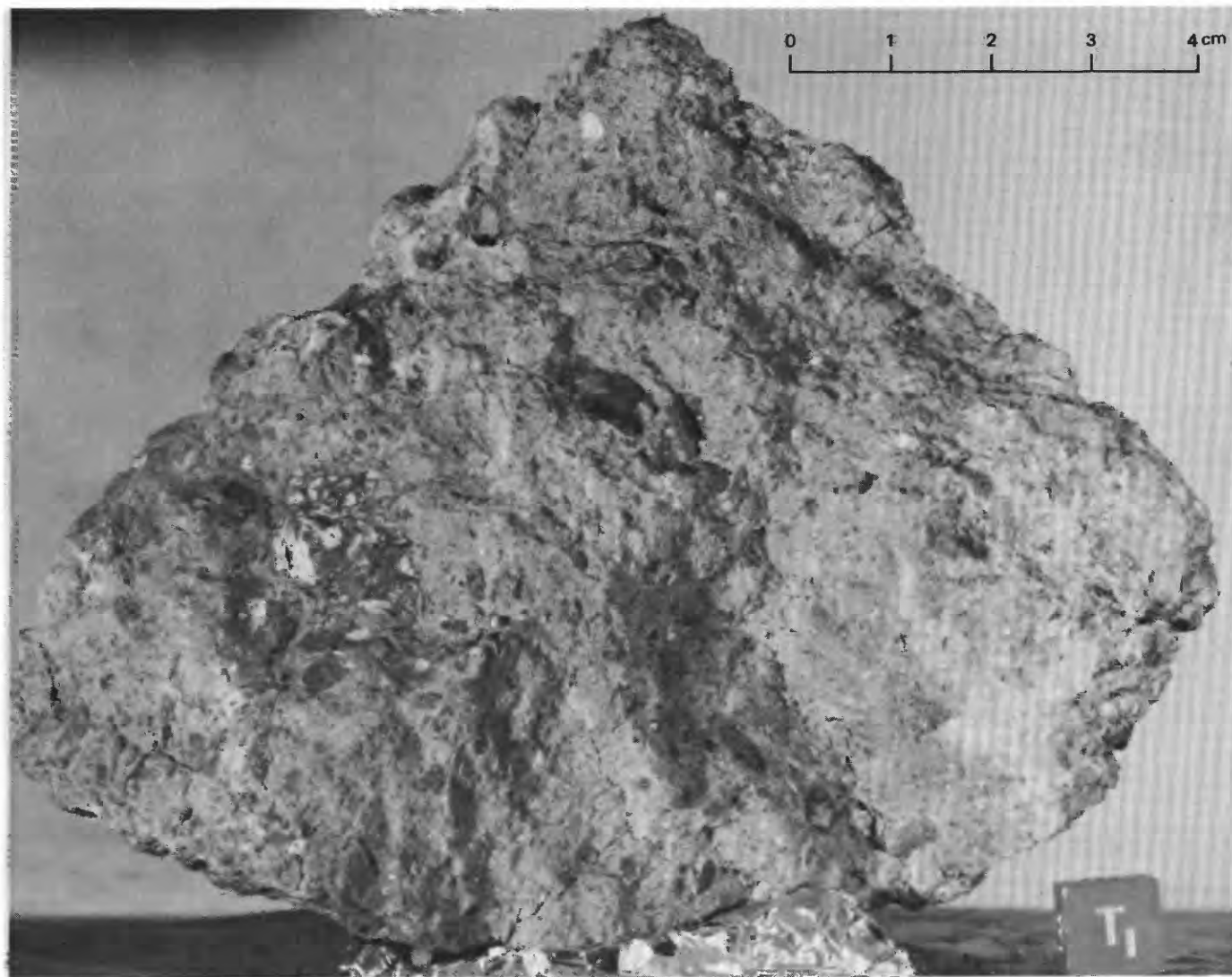


FIGURE 80.—Sample 72255. Polymict breccia with aphanitic matrix. Conspicuous black and white clast at left center is the 2-cm norite "Civet Cat" clast (Marvin, 1975). (NASA photograph S-73-16010.)

*Illustrations:* Pans 14, 15; Figures 73, 82, 83, (LRL).

*Comments:* Boulder 2 represents bedrock from high on the South Massif.

*Petrographic description:* Polymict breccia with a granoblastic matrix. Locally vuggy with vug linings of coarse plagioclase and brown pyroxene; similar minerals occurs as clasts in the breccia. Clasts in the size range 0.1 to 1.0 mm are in the approximate

proportions: 63 percent plagioclase, 7 percent olivine, 2 percent pyroxene, 21 percent metagabbroid rock, 1 percent metatroctolite, 4 percent recrystallized olivine, 2 percent recrystallized plagioclase.

Dymek and others (1976b) have interpreted the matrix as an aggregate of microclasts with a very fine interstitial groundmass that crystallized from a melt.

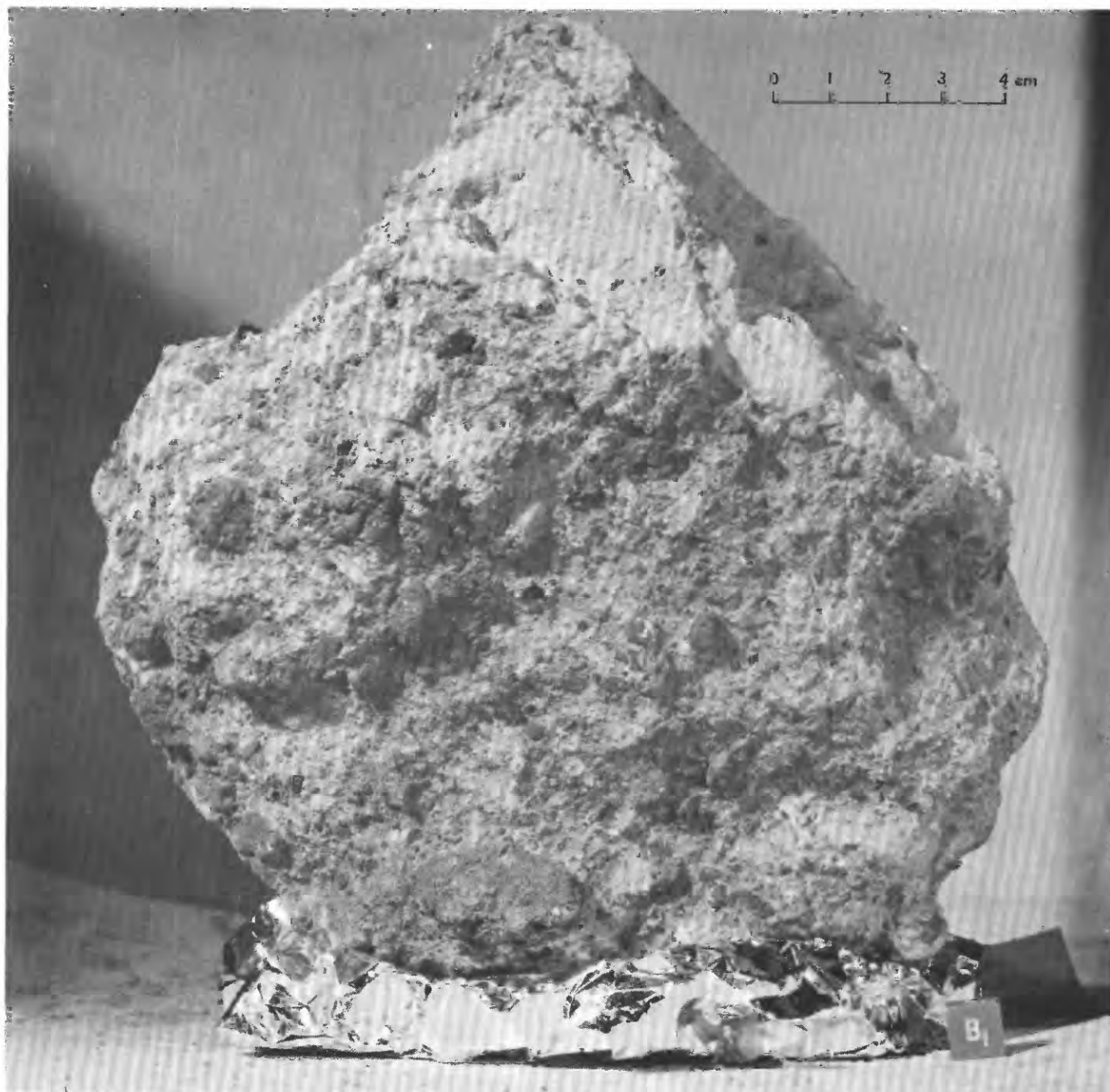


FIGURE 81.—Sample 72275. Polymict breccia with cataclastic matrix. (NASA photograph S-73-16056.)

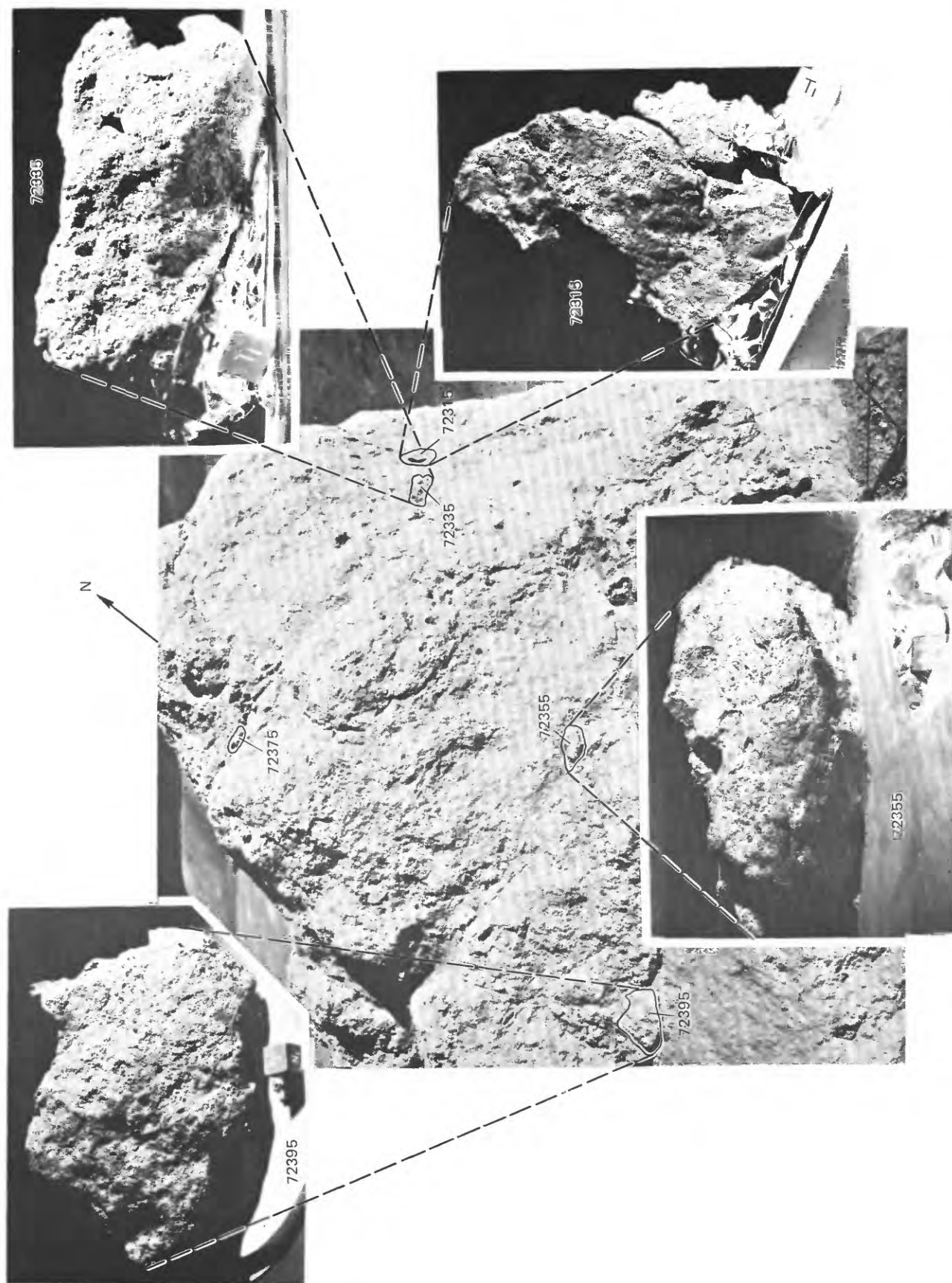


FIGURE 82.—Boulder 2, station 2, showing locations of samples 72315, 72335, 72355, 72375, and 72395 before collection. Boulder is approximately 2 m high. Insets show samples 72315, 72335, 72355, and 72395 with reconstructed lunar surface orientations and lighting. (NASA photographs AS17-137-20913; S-73-18408 (72315), S-73-21389 (72335), S-73-17799 (72355), and S-73-19586 (72395).) (Modified from Muehlberger and others, 1973.)

*Major-element composition:**Chemical analyses of 72315*

	1	2
SiO <sub>2</sub> .....	--	--
Al <sub>2</sub> O <sub>3</sub> .....	19.8	19.2
FeO.....	8.5	8.5
MgO.....	11.0	12.0
CaO.....	11.6	11.3
Na <sub>2</sub> O.....	.61	.70
K <sub>2</sub> O.....	.32	.35
TiO <sub>2</sub> .....	1.4	1.4
P <sub>2</sub> O <sub>5</sub> .....	--	--
MnO.....	.111	.111
Cr <sub>2</sub> O <sub>3</sub> .....	.186	.187

1. 72315,3 (Laul and Schmitt, 1974).

1. 72315,4 (Laul and Schmitt, 1974).

*Exposure age:* Track measurements and micrometeorite crater counts:  $\sim 10^5$  years. The lighter (fresher) appearance of this part of the boulder surface, which presumably was exposed by local spalling  $\sim 10^5$  years ago, may have been the cause for the crew's interpreting this part of boulder 2 as a clast (Hutcheon and others, 1974a).

## Sample 72320-24

*Type:* Sedimentary, unconsolidated.

*Weight:* 106.31 g.

*Depth:* Upper few centimeters.

*Location:* From about 20 cm under an east-west overhang on the southwest side of boulder 2.

*Illustrations:* Pans 14, 15.

*Comments:* Sediments accumulated by mass wasting from South Massif.

*Petrographic description:* 72320-24, dominantly agglutinate and fine-grained breccia and (or) metaclastic rock.

*Components of 90-150- $\mu$ m fraction of 72321,7 (Heiken and McKay, 1974)*

Components	Volume percent
Agglutinate.....	45.3
Basalt, equigranular.....	2.3
Basalt, variolitic.....	.7
Breccia:	
Low grade <sup>1</sup> - brown.....	5.3
Low grade <sup>1</sup> - colorless.....	7.3
Medium to high grade <sup>2</sup> .....	15.6
Anorthosite.....	.7
Cataclastic anorthosite <sup>3</sup> .....	1.7
Norite.....	2.0
Gabbro.....	--
Plagioclase.....	9.3
Clinopyroxene.....	2.7
Orthopyroxene.....	.3
Olivine.....	.3
Ilmenite.....	Trace
Glass:	
Orange.....	Trace
"Black".....	1.3
Colorless.....	1.0
Brown.....	2.0
Gray, "ropy".....	.7
Other.....	--
Total number grains.....	300

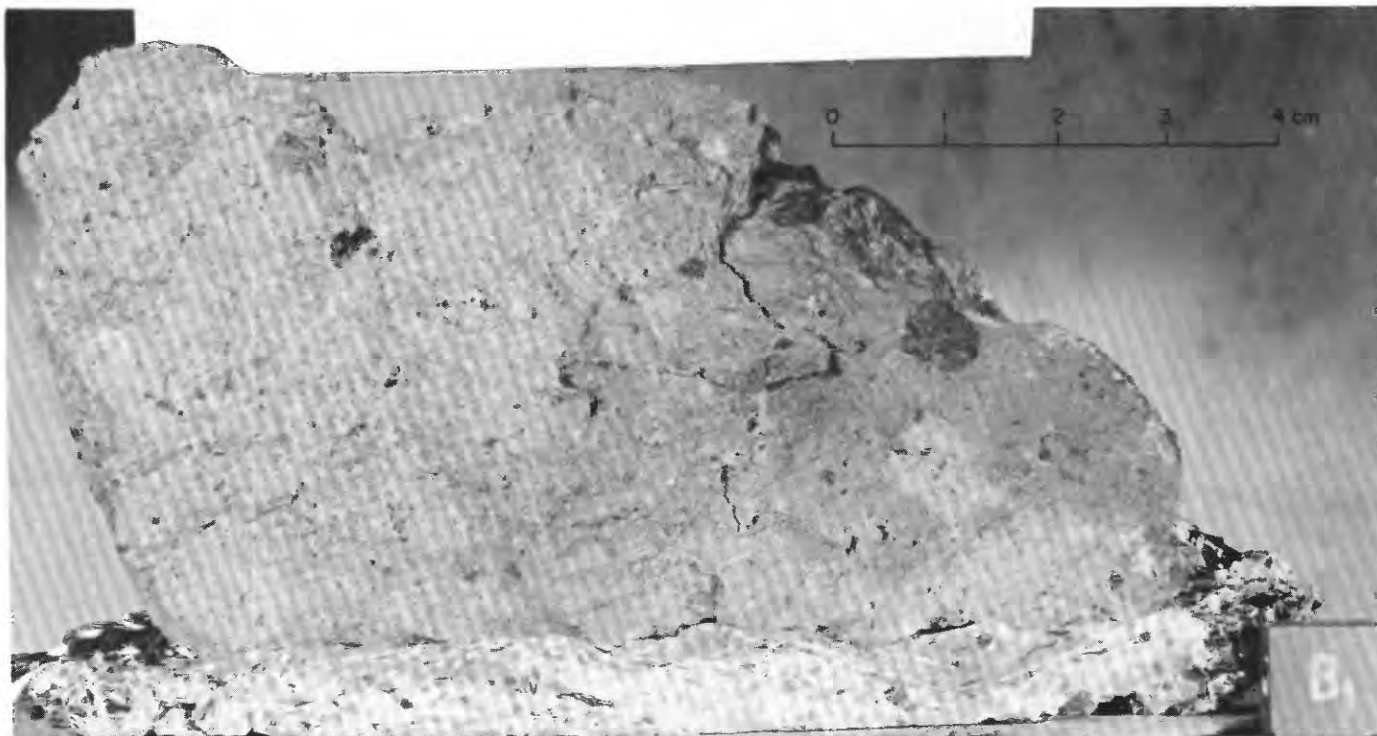
<sup>1</sup> Metamorphic groups 1-3 of Warner (1972).<sup>2</sup> Metamorphic groups 4-8 of Warner (1972).<sup>3</sup> Includes crushed or shocked feldspar grains.

FIGURE 83.—Sample 72315. Polymict breccia with granoblastic matrix. (NASA photograph S-73-16657.)

**Major-element composition:***Chemical analysis of 72321*

SiO <sub>2</sub> .....	44.91
Al <sub>2</sub> O <sub>3</sub> .....	20.57
FeO .....	8.65
MgO .....	9.84
CaO .....	12.82
Na <sub>2</sub> O .....	.47
K <sub>2</sub> O .....	.16
TiO <sub>2</sub> .....	1.56
P <sub>2</sub> O <sub>5</sub> .....	.15
MnO .....	.13
Cr <sub>2</sub> O <sub>3</sub> .....	..
Total .....	99.26

72321.5 (Rhodes and others, 1974).

**Sample 72335****Type:** Polymict breccia with a poikilitic(?) matrix.**Size:** 8×1.5×1.5 cm.**Weight:** 108.9 g.**Location:** From boulder 2 on lower slopes of South Massif approximately 50 m southwest of the LRV.**Illustrations:** Pans 14, 15; figures 73, 82, 84 (LRL).**Comments:** Boulder 2 represents bedrock from the upper part of South Massif.**Petrographic description:** Polymict breccia with a poikilitic(?) matrix. Clast types include plagioclase, olivine pyroxene, and fine-grained metaclastic rock.

Dymek and others (1976b) have interpreted the matrix as an aggregate of microclasts with a very fine interstitial groundmass that crystallized from a melt.

**Major-element composition:***Chemical analyses of 72335*

	1	2	3
SiO <sub>2</sub> .....	..	..	..
Al <sub>2</sub> O <sub>3</sub> .....	27.3	18.2	18.3
FeO .....	4.8	8.6	8.8
MgO .....	8.0	11.0	12.0
CaO .....	15.4	10.7	11.0
Na <sub>2</sub> O .....	.45	.61	.60
K <sub>2</sub> O .....	.12	.27	.34
TiO <sub>2</sub> .....	.60	1.6	1.6
P <sub>2</sub> O <sub>5</sub> .....	..	..	..
MnO .....	.060	.112	.114
Cr <sub>2</sub> O <sub>3</sub> .....	.100	.190	.200

1. 72335.2 (Laul and Schmitt, 1974); analysis is of ~1-cm clast that has more plagioclase than normal 72335 breccia (Dymek and others, 1976a).

2. 72335.6 (Laul and Schmitt, 1975a).

3. 72335.7 (Laul and Schmitt, 1975a).

Columns 2 and 3 are representative of bulk of boulder 2 samples (Dymek and others, 1976a); presumably they represent the boulder matrix.

**Sample 72355****Type:** Polymict breccia with a granoblastic matrix.**Size:** 10×6.5×5.5 cm.**Weight:** 367.4 g.**Location:** From boulder 2 on lower slopes of South Massif approximately 50 m southwest of the LRV.**Illustrations:** Pans 14, 15; figures 73, 82, 85 (LRL).**Comments:** Source rock (boulder 2) is from high on the slope of South Massif.**Petrographic description:** Polymict breccia with a granoblastic matrix. Locally vuggy with vug linings of distinctive spongy plagioclase and brown pyroxene; both minerals also occur as clasts in the breccia. Clasts in the size range 0.1 to 1.0 mm are in the approximate proportions: 62 percent plagioclase, 4 percent pyroxene, 21 percent olivine, 10 percent metagabbroid rock, 1 percent metatroctolite, 2 percent recrystallized olivine, 1 percent recrystallized plagioclase.

Dymek and others (1976b) have interpreted the matrix as an aggregate of microclasts with a very fine interstitial groundmass that crystallized from a melt.

**Major-element composition:***Chemical analysis of 72355*

SiO <sub>2</sub> .....	..
Al <sub>2</sub> O <sub>3</sub> .....	18.8
FeO .....	8.7
MgO .....	12.0
CaO .....	11.1
Na <sub>2</sub> O .....	.70
K <sub>2</sub> O .....	.33
TiO <sub>2</sub> .....	1.6

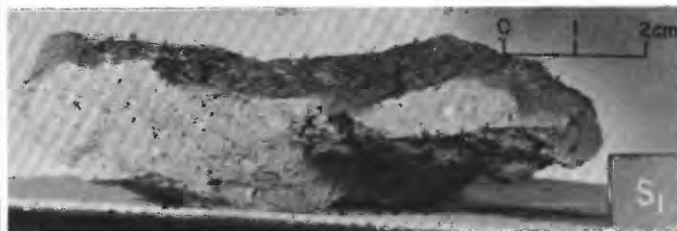


FIGURE 84.—Sample 72335. Polymict breccia with poikilitic(?) matrix. (NASA photograph S-73-16250.)

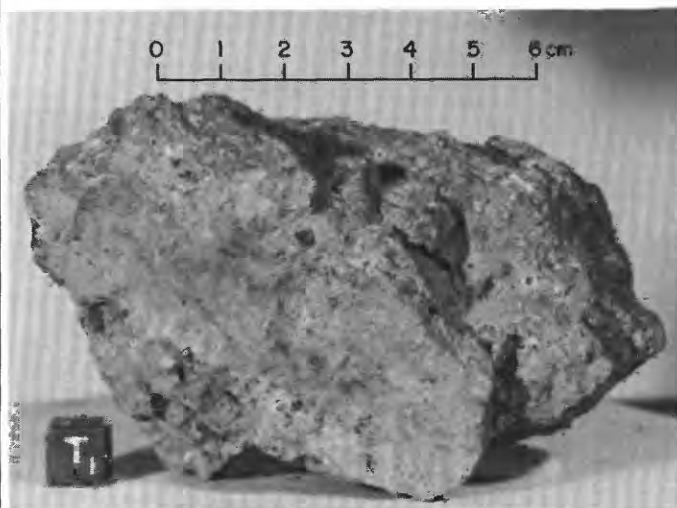


FIGURE 85.—Sample 72355. Polymict breccia with granoblastic matrix. (NASA photograph S-73-15352.)

## Chemical analysis of 72355—Continued

P <sub>2</sub> O <sub>5</sub> .....	--
MnO .....	.114
Cr <sub>2</sub> O <sub>3</sub> .....	.193

72355.7 (Laul and Schmitt, 1974).

## Sample 72375

*Type:* Polymict breccia with a poikilitic(?) matrix.*Size:* 5×4×3 cm (estimated from LRL photos).*Weight:* 18.16 g.*Location:* From boulder 2 on lower slopes of South Massif approximately 50 m southwest of the LRV.*Illustrations:* Pans 14, 15; figures 73, 82, 86 (LRL).*Comments:* Source rock (boulder 2) is from high on the slope of South Massif.

*Petrographic description:* Polymict breccia with a poikilitic(?) matrix. Clasts in the size range 0.1 to 1.0 mm are in the approximate proportions: 48 percent plagioclase, 5 percent olivine, 1 percent pyroxene, 1 percent brown pyroxene-plagioclase vug lining, 1 percent light metaclastic rock with granoblastic matrix, 19 percent metagabbroid rock, 1 percent recrystallized olivine, 1 percent recrystallized plagioclase.

Dymek and others (1976b) have interpreted the matrix as an aggregate of microclasts with a very fine interstitial groundmass that crystallized from a melt.

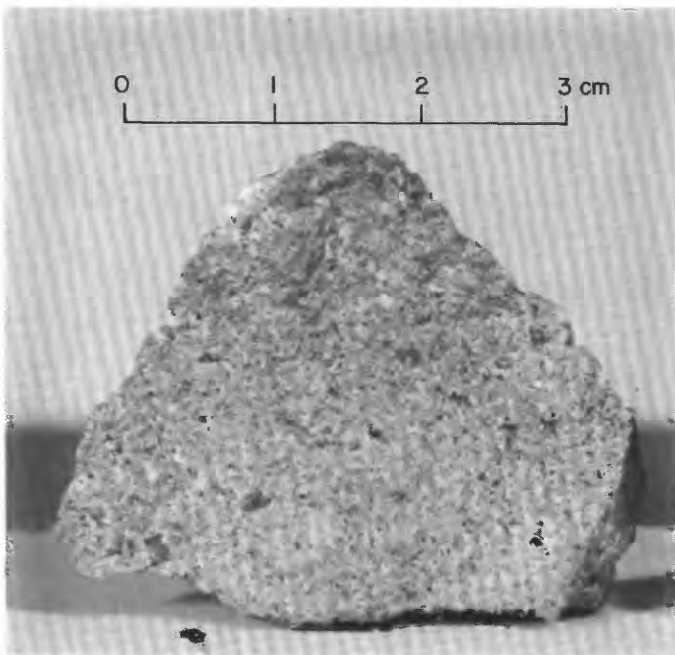


FIGURE 86.—Sample 72375. Polymict breccia with poikilitic(?) matrix. (NASA photograph S-73-15358.)

## Major-element composition:

## Chemical analysis of 72375

SiO <sub>2</sub> .....	--
Al <sub>2</sub> O <sub>3</sub> .....	18.2
FeO .....	8.8
MgO .....	12.0
CaO .....	10.8
Na <sub>2</sub> O .....	.67
K <sub>2</sub> O .....	.27
TiO <sub>2</sub> .....	1.5
P <sub>2</sub> O <sub>5</sub> .....	--
MnO .....	.112
Cr <sub>2</sub> O <sub>3</sub> .....	.178

72375.2 (Laul and Schmitt, 1974).

## Sample 72395

*Type:* Polymict breccia with an aphanitic matrix.*Size:* 12×9×5.5 cm.*Weight:* 536.4 g.*Location:* From boulder 2 on lower slopes of South Massif approximately 50 m southwest of the LRV.*Illustrations:* Pans 14, 15; figures 73, 82, 87 (LRL).*Comments:* Boulder 2 represents bedrock from high on the slope of South Massif.

*Petrographic description:* Polymict breccia with an aphanitic matrix. Fragments of brown pyroxene from vug linings; scarce fragments of moderately dark metaclastic rocks. Clasts in the size range 0.1 to 1.0 mm are in the approximate proportions: 56 percent plagioclase, 27 percent olivine, 1 percent pyroxene, 15 percent metagabbroid rock, 1 percent metatroctolite, 1 percent recrystallized olivine, 3 percent recrystallized plagioclase.

Dymek and others (1976b) considered 72395 typical of the samples from boulder 2 and described it as follows:

Sample 72395 is\*\*\*a sugary-textured, light greenish-gray "metaclastic" rock with only a few clasts larger than a few mm. The most abundant clasts are clear white plagioclase and pale green olivine, although shocked, glassy plagioclase is also present. Each type occurs as subangular to rounded fragments 1-3 mm across. The few large lithic clasts are typically fine-grained "felsites," probably shocked anorthosite. The sample is highly vesicular, containing very small spherical vesicles (<50μm), irregular vesicles, and "slit" vesicles.

In addition, they interpreted the matrix as an aggregate of microclasts with a very fine interstitial groundmass that crystallized from a melt.

## Major-element composition:

## Chemical analyses of 72395

	1	2
SiO <sub>2</sub> .....	--	46.8
Al <sub>2</sub> O <sub>3</sub> .....	18.7	18.1
FeO .....	9.2	9.26
MgO .....	12.0	11.95
CaO .....	11.0	11.26
Na <sub>2</sub> O .....	.67	.693

## Chemical analyses of 72395—Continued

	1	2
K <sub>2</sub> O .....	.32	.287
TiO <sub>2</sub> .....	1.7	1.75
P <sub>2</sub> O <sub>5</sub> .....	—	.325
MnO .....	.166	.120
Cr <sub>2</sub> O <sub>3</sub> .....	.210	.205
Total .....		100.75

1. 72395.3 (Laul and Schmitt, 1974).  
 2. 72395.46 (Wänke and others, 1975).

**Exposure age:** Track age: ~27 m.y. (Hutcheon and others, 1974b).

## Sample 72410

**Type:** Sedimentary, unconsolidated.

**Weight:** 52.0 g.

**Depth:** 0-1 cm.

**Location:** From approximately one-half meter southeast of boulder 3.

**Illustrations:** Pans 14, 15; figures 73, 88.

**Comments:** Sediment collected with samples 72415-18.

## Sample 72415-18

**Type:** Metadunite cataclasite.

**Size:** 72415, 4×2×0.8 cm; 72416, 2.1×1.2×0.9 cm; 72417, 3.2×2.1×1.2 cm; 72418, 4×2.5×1 cm.

**Weight:** 72415, 32.34 g; 72416, 11.53 g; 72417, 11.32 g; 72418, 3.55 g.

**Location:** From light clast in boulder 3 at base of South Massif approximately 15 m southwest of LRV.

**Illustrations:** Pans 14, 15; figures 73, 88, 89 (LRL).

**Comments:** Boulder 3 represents bedrock from the upper part of the South Massif.

**Petrographic description:** Metadunite cataclasite. Relict clasts have granoblastic-polygonal texture. One to 2 percent spinel-plagioclase-pyroxene intergrowths, the remainder partly recrystallized olivine.

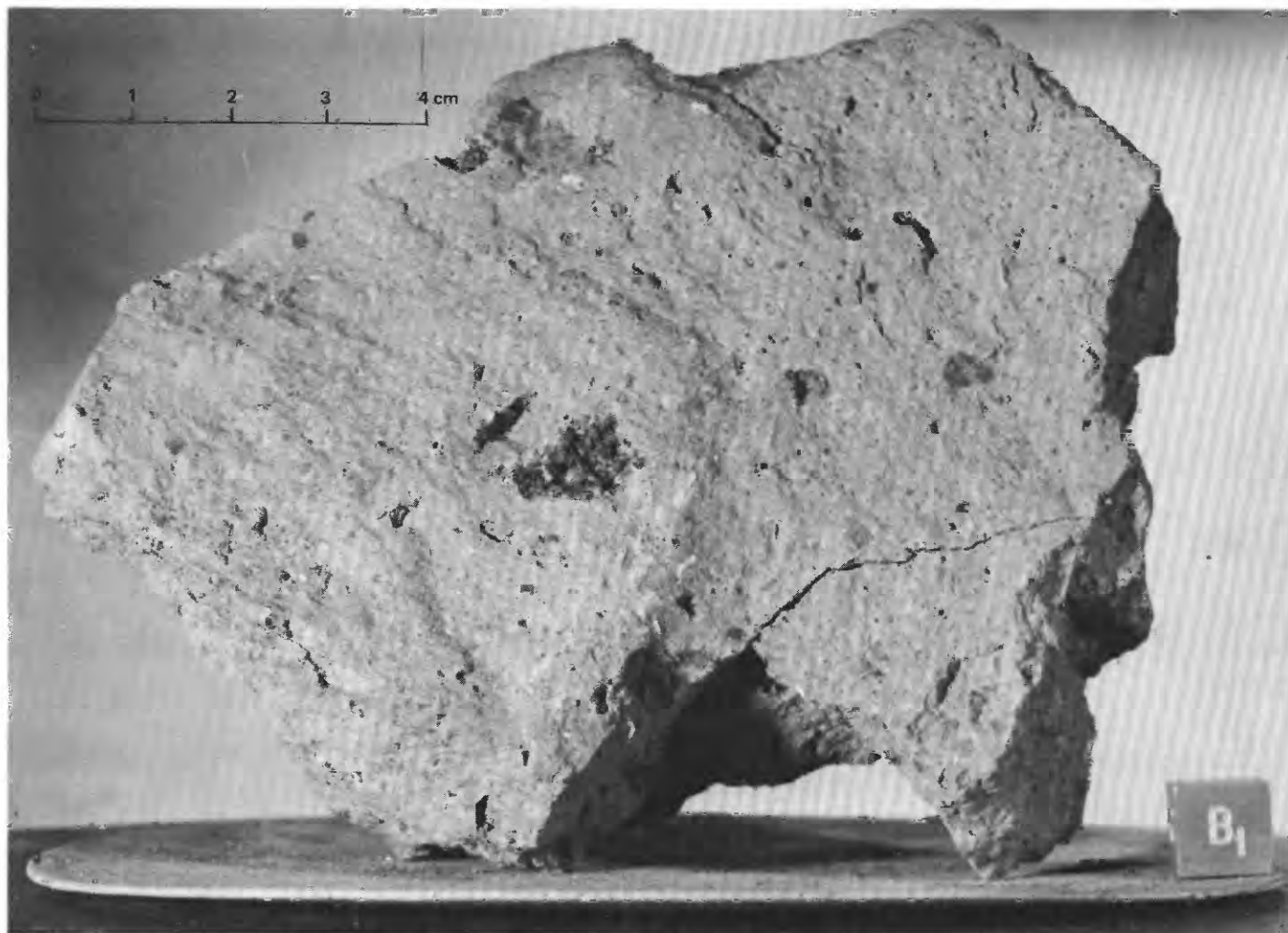


FIGURE 87.—Sample 72395. Polymict breccia with aphanitic matrix. (NASA photograph S-73-16052.)

Major-element composition:

Chemical analyses of 72415 and 72417

	1	2
SiO <sub>2</sub> .....	39.93	--
Al <sub>2</sub> O <sub>3</sub> .....	1.53	1.3
FeO.....	11.34	11.9
MgO.....	43.61	45.4
CaO.....	1.14	1.1
Na <sub>2</sub> O.....	<.02	.013
K <sub>2</sub> O.....	.00	.0024
TiO <sub>2</sub> .....	.03	--

Chemical analyses of 72415 and 72417—Continued

	1	2
P <sub>2</sub> O <sub>5</sub> .....	.04	--
MnO.....	.13	.113
Cr <sub>2</sub> O <sub>3</sub> .....	.34	.34
Total.....	98.11	

1. 72415.2 (Apollo 17 PET, 1973).  
2. 72417 (Laul and Schmitt, 1975b).

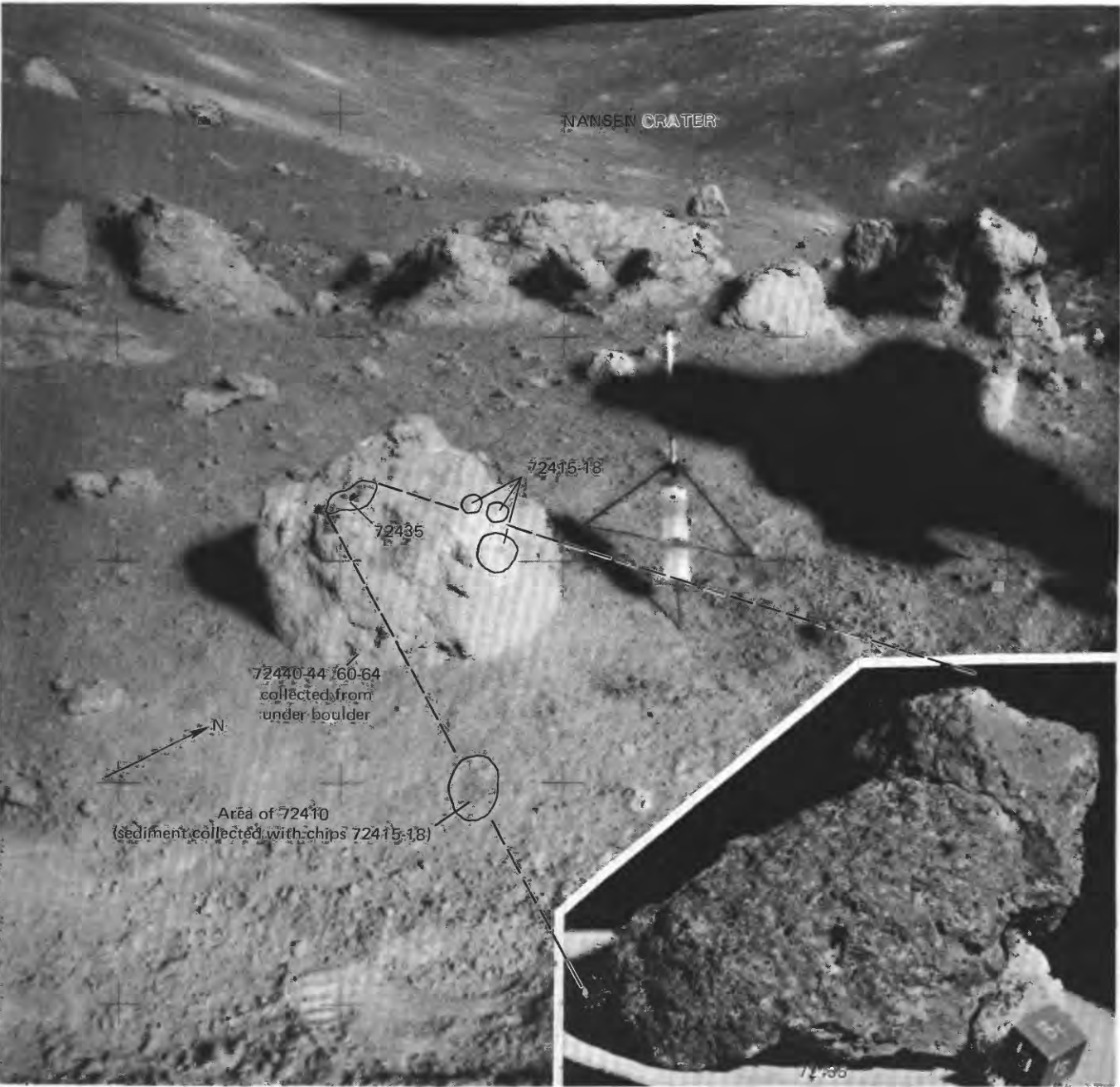


FIGURE 88.—Boulder 3 at station 2 showing locations of samples 72410, 72415-18, 72435, 72440-44, and 72460-64 before collection. Inset shows 72435 with reconstructed lunar surface orientation and lighting. (NASA photographs AS17-138-21049; S-73-19389.)

**Age:**

Rb-Sr isochron: 72417,  $4.55 \pm 0.10$  ( $2\sigma$ ) b.y. (Papanastassiou and Wasserburg, 1975).

$^{40}\text{-}^{39}\text{Ar}$ : 72417,  $\sim 3.95 \pm 0.01$  b.y.  $^{40}\text{-}^{39}\text{Ar}$  release pattern is complicated but indicates argon loss at about  $3.95 \pm 0.01$  b.y. (Dymek and others, 1975).

**Sample 72430-34**

**Type:** Sedimentary, unconsolidated.

**Weight:** 80.87 g.

**Depth:** Unknown—scooped up with sample 72435.

**Location:** In area of boulder 3.

**Illustrations:** Pans 14, 15, figures 73, 88.

**Comments:** Sediment derived from South Massif by mass wasting.

**Petrographic description:** 72430-34, dominantly breccia.

**Sample 72435**

**Type:** Polymict breccia with a poorly developed poikilitic matrix.

**Size:**  $5 \times 4 \times 3$  cm,  $5 \times 4 \times 3$  cm (2 mated pieces).

**Weight:** 160.6 g.

**Location:** From matrix of boulder 3.

**Illustrations:** Pans 14, 15; figures 73, 88, 90 (LRL).

**Comments:** Source rock (boulder 3) is from high on the slope of South Massif.

**Petrographic description:** Polymict breccia with a poorly developed poikilitic matrix. Probable local fusion in areas of vesicles; crystallization yielded intergrowths of brown pyroxene and spongy plagioclase that appear as clasts in samples 72355, 72375, 72395. Clasts in the size range 0.1 to 1.0 mm are in the approximate proportions: 53 percent plagioclase, 3

percent pyroxene, 24 percent olivine, 2 percent dark metaclastic rocks with aphanitic matrix, 1 percent light metaclastic rocks with granoblastic matrix, 1 percent troctolite, 13 percent metagabbroid rock, 1 percent recrystallized olivine, 4 percent recrystallized plagioclase.

Dymek and others (1976b) have described 72435 as similar to the samples from boulder 2. It consists of 5-10 percent megacrysts (1 mm-2 cm) set in an extremely fine grained partially clastic matrix that consists of microclasts (<1 mm) in a very fine grained (<50  $\mu\text{m}$ ) groundmass crystallized from a melt. They have identified the larger lithic clasts as anorthosite (predominant), dunite, and troctolite(?).

**Major-element composition:****Chemical analysis of 72435**

SiO <sub>2</sub> .....	45.76
Al <sub>2</sub> O <sub>3</sub> .....	19.23
FeO .....	8.70
MgO .....	11.63
CaO .....	11.72
Na <sub>2</sub> O .....	.52
K <sub>2</sub> O .....	.23
TiO <sub>2</sub> .....	1.54
P <sub>2</sub> O <sub>5</sub> .....	.27
MnO .....	.11
Cr <sub>2</sub> O <sub>3</sub> .....	.20
Total .....	99.91

72435.1 (Apollo 17 PET, 1973)

**Age:**

Rb-Sr: <4.10 b.y.; lowest model age determined for any breccia component is  $4.10 \pm 0.05$  b.y. for a single clast; hence 4.10 b.y. is an older limit for breccia formation (Papanastassiou and Wasserburg, 1975).

Rb-Sr isochron:  $3.85 \pm 0.18$  ( $2\sigma$ ) b.y.; defined by five samples from interior of same clast as above; surrounding matrix, not equilibrated with clast, gives older Rb-Sr age (Papanastassiou and Wasserburg, 1975).

Fission track: <4.05 b.y.; tracks measured in plagioclase crystal from decay of Pu, U, and Th in the adjacent matrix suggest 4.05 b.y. is older limit for assembly of the breccia (Goswami and others, 1976a).

**Sample 72440-44**

**Type:** Sedimentary, unconsolidated.

**Weight:** 450.39 g.

**Depth:** 0-4 cm.

**Location:** Collected from beneath boulder 3 after boulder was rolled.

**Illustrations:** Pans 14, 15; figures 73, 88.

**Comments:** Material derived from South Massif by mass wasting.

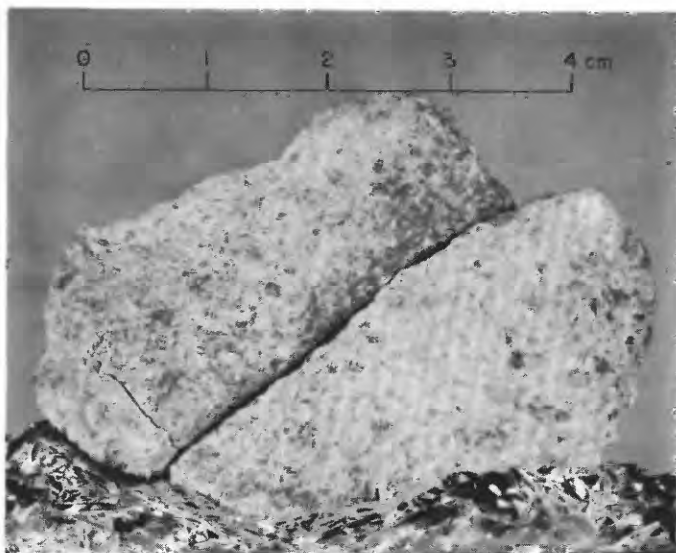


FIGURE 89.—Sample 72415. Metadunite cataclasite. (NASA photograph S-73-16199.)

**Petrographic description:** 72440-44, dominantly metaclastic rock and breccia, some agglutinate, minor feldspathic plutonic derivatives.

*Components of 90-150- $\mu$ m fraction of 72441.7 (Heiken and McKay, 1974)*

Components	Volume percent
Agglutinate.....	41.7
Basalt, equigranular .....	1.3
Basalt, variolitic .....	1.3
Breccia:	
Low grade <sup>1</sup> - brown .....	9.3
Low grade <sup>1</sup> - colorless .....	6.3
Medium to high grade <sup>2</sup> .....	19.3
Anorthosite .....	1.0
Cataclastic anorthosite <sup>3</sup> .....	1.3
Norite .....	.7
Gabbro .....	..
Plagioclase .....	6.7
Clinopyroxene .....	3.0
Orthopyroxene .....	3.3
Olivine .....	.7
Ilmenite .....	.3
Glass:	
Orange .....	.3
"Black" .....	.3
Colorless .....	1.3
Brown .....	1.0
Gray, "ropy" .....	.3
Other .....	..
Total number grains .....	300

<sup>1</sup> Metamorphic groups 1-3 of Warner (1972).

<sup>2</sup> Metamorphic groups 4-8 of Warner (1972).

<sup>3</sup> Includes crushed or shocked feldspar grains.

*Major-element composition:*

*Chemical analyses of 72441*

	1	2	3	4
SiO <sub>2</sub> .....	44.84	45.03	45.17	45.01
Al <sub>2</sub> O <sub>3</sub> .....	21.06	20.51	20.25	20.61
FeO .....	8.54	8.85	8.68	8.69
MgO .....	9.99	9.89	10.78	10.22
CaO .....	12.59	12.83	12.75	12.72
Na <sub>2</sub> O .....	.34	.46	.40	.40
K <sub>2</sub> O .....	.27	.17	.16	.20
TiO <sub>2</sub> .....	1.42	1.53	1.53	1.49
P <sub>2</sub> O <sub>5</sub> .....	.20	.17	.15	.17
MnO .....	.18	.13	.11	.14
Cr <sub>2</sub> O <sub>3</sub> .....	.28	.22	.28	.26
Total .....	99.71	99.81	100.26	99.91

1. 72441 (Mason and others, 1974).

2. 72441.3 (Rhodes and others, 1974).

3. 72441.9 (Rose and others, 1974).

4. Average of 1-3.

**Sample 72460-64**

**Type:** Sedimentary, unconsolidated.

**Weight:** 125.01 g.

**Depth:** 0-1 cm (skim sample).

**Location:** Collected from beneath boulder 3 after boulder was rolled.

**Illustrations:** Pans 14, 15; figures 73, 88.

**Comments:** Material derived from South Massif by mass wasting.

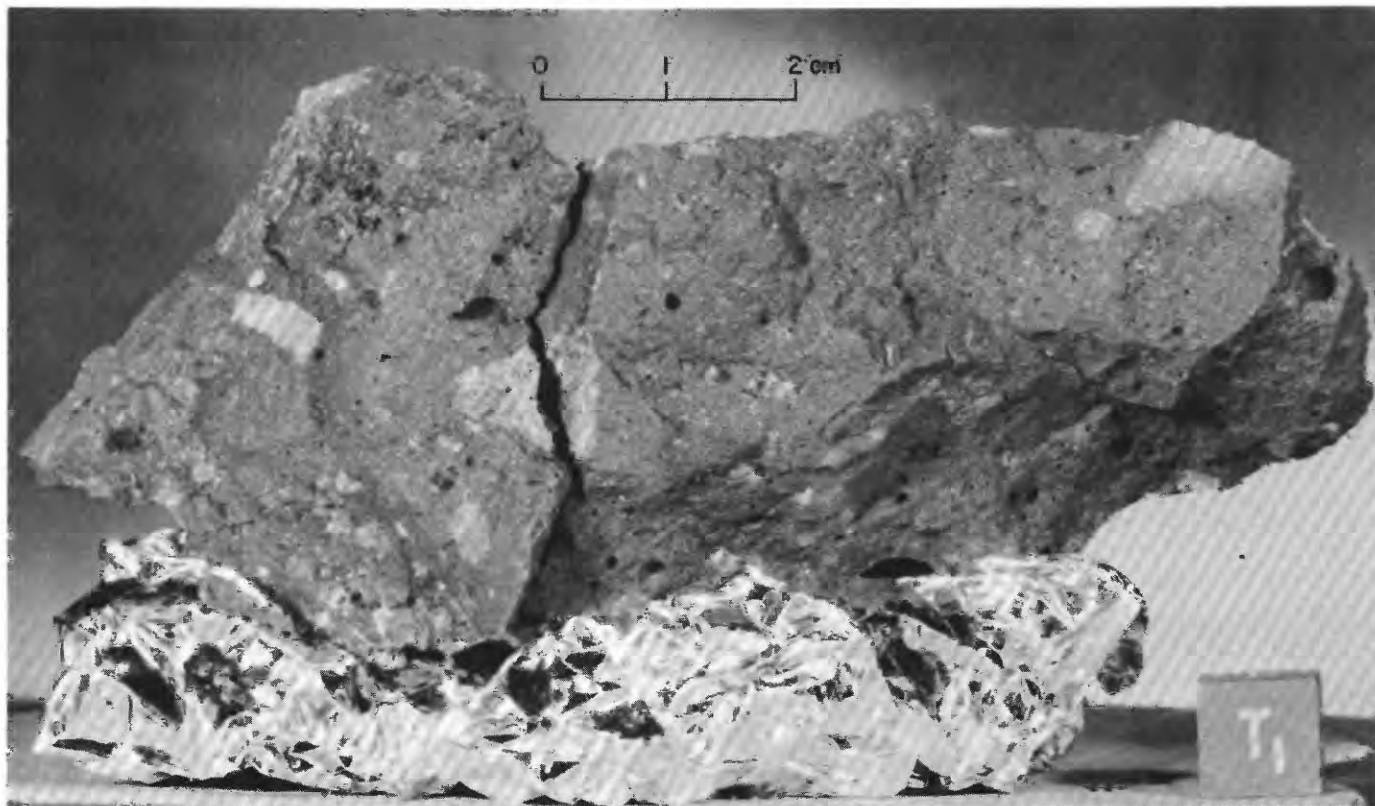


FIGURE 90.—Sample 72435. Polymict breccia with poorly developed poikilitic matrix. (NASA photograph S-73-16187.)

**Petrographic description:** 72460-64, dominantly metaclastic rock and breccia, some agglutinate, minor feldspathic plutonic derivatives.

*Components of 90-150- $\mu$ m fraction of 72461,5 (Heiken and McKay, 1974)*

Components	Volume percent
Agglutinate.....	43.0
Basalt, equigranular .....	2.7
Basalt, variolitic .....	.3
Breccia:	
Low grade <sup>1</sup> - brown .....	8.3
Low grade <sup>1</sup> - colorless .....	5.7
Medium to high grade <sup>2</sup> .....	15.3
Anorthosite .....	2.0
Cataclastic anorthosite <sup>3</sup> .....	1.3
Norite .....	.3
Gabbro .....	--
Plagioclase .....	11.0
Clinopyroxene .....	3.0
Orthopyroxene .....	3.0
Olivine .....	.3
Ilmenite .....	.6
Glass:	
Orange .....	.7
"Black" .....	1.0
Colorless .....	1.0
Brown .....	1.3
Gray, "ropy" .....	--
Other .....	--
Total number grains .....	300

<sup>1</sup>Metamorphic groups 1-3 of Warner (1972).

<sup>2</sup>Metamorphic groups 4-8 of Warner (1972).

<sup>3</sup>Includes crushed or shocked feldspar grains.

**Major-element composition:**

*Chemical analyses of 72461*

	1	2	3
SiO <sub>2</sub> .....	44.98	44.79	44.88
Al <sub>2</sub> O <sub>3</sub> .....	20.87	20.63	20.75
FeO.....	8.58	8.61	8.60
MgO.....	9.69	10.52	10.10
CaO.....	12.97	12.87	12.92
Na <sub>2</sub> O.....	.47	.43	.45
K <sub>2</sub> O.....	.17	.17	.17
TiO <sub>2</sub> .....	1.50	1.56	1.53
P <sub>2</sub> O <sub>5</sub> .....	.16	.16	.16
MnO.....	.12	.11	.12
Cr <sub>2</sub> O <sub>3</sub> .....	.21	.28	.24
Total.....	99.72	100.13	99.92

1. 72461,3 (Rhodes and others, 1974).

2. 72461,7 (Rose and others, 1974).

3. Average of 1 and 2.

**Sample 72500-05**

**Type:** Sedimentary, unconsolidated (72500-04) with breccia fragment (72505).

**Weight:** 72500-04, 1,057.73 g; 72505, 3.09 g.

**Size:** 72505, 1.7×1.5×1 cm.

**Depth:** 0-4 cm.

**Location:** From lower slopes of South Massif approximately 45 m southwest of LRV.

**Illustrations:** Pans 14, 15; figures 73, 91.

**Comments:** Material derived from South Massif by mass wasting; sediment sample to complement rake sample 72535-59.

**Petrographic description:** 72500-04, dominantly metaclastic rock and breccia, some agglutinate, minor basalt, and feldspathic plutonic derivatives.

*Components of 90-150- $\mu$ m fraction of 72501, 1 (Heiken and McKay, 1974)*

Components	Volume percent
Agglutinate.....	48.0
Basalt, equigranular .....	3.3
Basalt, variolitic .....	--
Breccia:	
Low grade <sup>1</sup> - brown .....	8.3
Low grade <sup>1</sup> - colorless .....	8.7
Medium to high grade <sup>2</sup> .....	12.6
Anorthosite .....	.7
Cataclastic anorthosite <sup>3</sup> .....	1.7
Norite .....	.3
Gabbro .....	--
Plagioclase .....	6.3
Clinopyroxene .....	3.3
Orthopyroxene .....	2.0
Olivine .....	.7
Ilmenite .....	.3
Glass:	
Orange .....	1.0
"Black" .....	1.0
Colorless .....	.7
Brown .....	.7
Gray, "ropy" .....	--
Other .....	.3
Total number grains .....	300

<sup>1</sup>Metamorphic groups 1-3 of Warner (1972).

<sup>2</sup>Metamorphic groups 4-8 of Warner (1972).

<sup>3</sup>Includes crushed or shocked feldspar grains.

**Major-element composition:**

*Chemical analyses of 72501*

	1	2	3	4
SiO <sub>2</sub> .....	45.12	45.17	45.52	45.27
Al <sub>2</sub> O <sub>3</sub> .....	20.64	20.63	20.52	20.60
FeO.....	8.77	8.74	8.98	8.83
MgO.....	10.08	9.87	9.90	9.95
CaO.....	12.86	12.84	12.69	12.80
Na <sub>2</sub> O.....	.40	.46	.50	.45
K <sub>2</sub> O.....	.16	.17	.17	.17
TiO <sub>2</sub> .....	1.56	1.55	1.62	1.58
P <sub>2</sub> O <sub>5</sub> .....	.13	.15	.14	.14
MnO.....	.11	.13	.12	.12
Cr <sub>2</sub> O <sub>3</sub> .....	.23	.23	.17	.21
Total.....	100.06	99.94	100.33	100.12

1. 72501,2 (Rhodes and others, 1974).

2. 72501,22 (Rhodes and others, 1974).

3. 72501,36 (Seon, 1974).

4. Average of 1-3.

**Age:**

<sup>40</sup>-<sup>39</sup>Ar:

72503,8,12, 3.96±0.02 b.y. (Schaeffer and Husain, 1974); fragment from 2-4-mm fraction: recrystallized melt rock with plagioclase, olivine and lithic fragments in groundmass of plagioclase, poikilitic pigeonite, and opaque minerals (Bence and others, 1974).

72503,8,5, 3.974±0.011 b.y. (Schaeffer and others, 1976); fragment from 2-4-mm fraction, described as coarse-grained recrystallized noritic breccia with a troctolite clast.

72503, 86,  $3.982 \pm 0.006$  b.y. (Schaeffer and others, 1976); fragment from 2-4-mm fraction, described as fine-grained recrystallized noritic breccia.

Sample 72535-39, 45-49, 55-59

*Type:* Fifteen breccia fragments from rake sample.

*Size:* Largest, 72535, is  $7.6 \times 6.8 \times 5.9$  cm; others are much smaller.

*Weight:* 417.901 g total (largest is 72535, 221.4 g).

*Depth:* 0-1 cm.

*Location:* From lower slopes of South Massif approximately 45 m southwest of LRV.

*Illustrations:* Pans 14, 15; figures 73, 91.

*Comments:* 72535-39, 45-48 are blue-gray breccia.

72549, 55-58 are green-gray breccia.

72559 is light-gray breccia.

*Petrographic descriptions:*

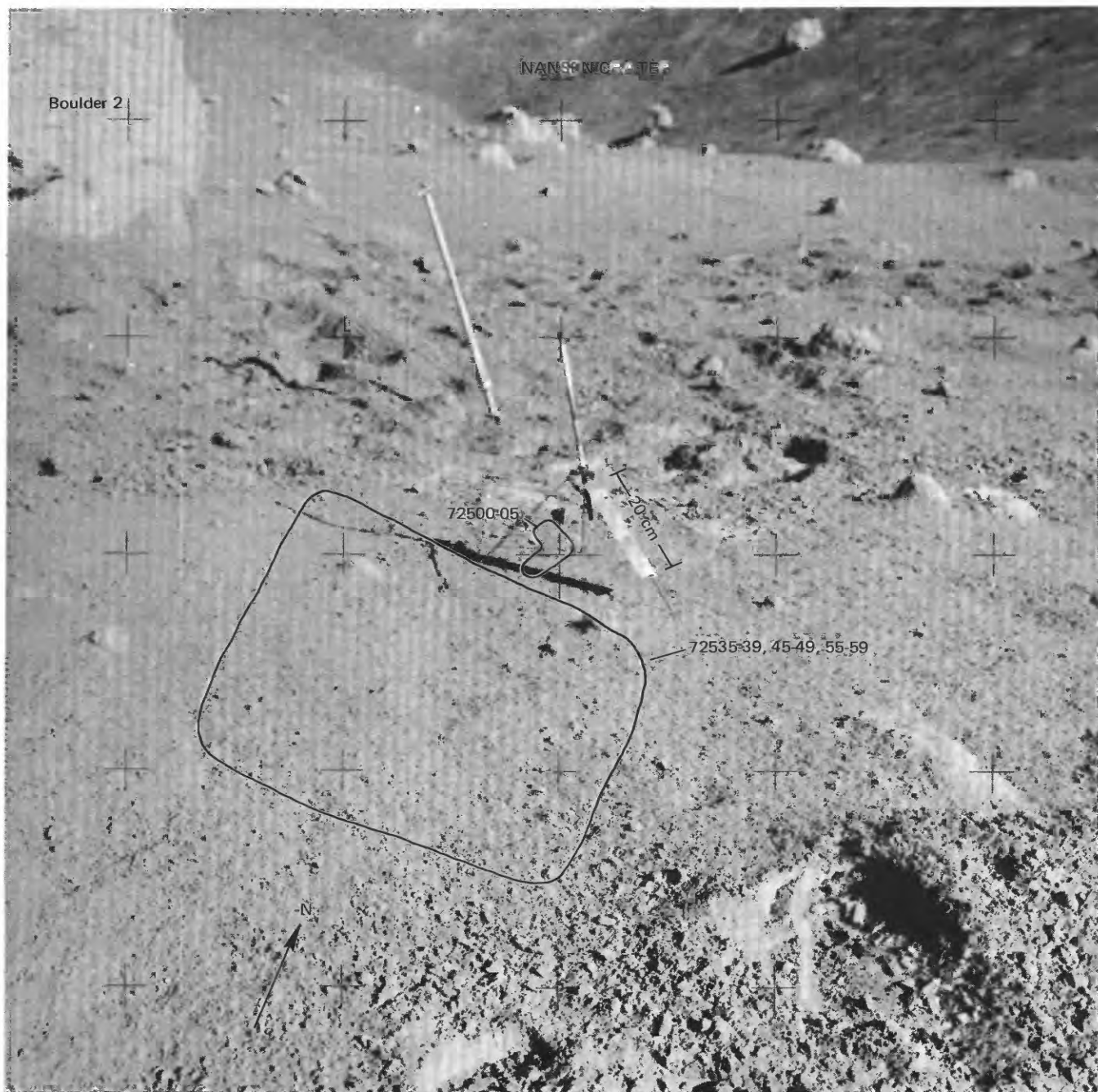


FIGURE 91.—First rake area at station 2 showing areas from which samples 72500-05 and 72535-59 were collected, before sampling. (NASA photograph AS17-138-21045.)

72535, polymict breccia with an aphanitic matrix. Possible local fusion in areas of spherical vesicles. Cavity-rich zones contain angular clasts similar to the dominant rock type of the whole rock. Light metaclastic fragments with granoblastic(?) texture and mineral debris.

72536-39, same as 72535.

72547, like 72535, but cavities are lined or filled with intergrowths of brown pyroxene and spongy plagioclase.

72548, polymict(?) breccia with an aphanitic matrix. Skin of metagabbroid or gabbroid cataclasite on one side.

72549, metaclastic rock with a fine-grained poikilitic(?) matrix. Mineral debris, no lithic clasts.

72555, metaclastic rock with a fine-grained poikilitic(?) matrix. Mineral debris, no lithic clasts.

72558, metaclastic rock with a fine-grained poikilitic(?) matrix. No lithic clasts. Vugs lined by intergrowths of brown pyroxene and plagioclase. Mineral porphyroclasts.

72559, metaclastic rock with an aphanitic matrix. No lithic clasts, scarce mineral clasts.

#### Major-element composition:

##### Chemical analysis of 72535

SiO <sub>2</sub> .....	--
Al <sub>2</sub> O <sub>3</sub> .....	17.8
FeO.....	8.4
MgO.....	11.0
CaO.....	11.2
Na <sub>2</sub> O.....	.58
K <sub>2</sub> O.....	.13
TiO <sub>2</sub> .....	1.4
P <sub>2</sub> O <sub>5</sub> .....	--
MnO.....	.099
Cr <sub>2</sub> O <sub>3</sub> .....	.190

72535,1 rake fragment, blue-gray breccia  
(Laul and Schmitt, 1975a).

Exposure age: Kr-Kr: 107±4 m.y. (Arvidson and others, 1976b).

#### Sample 72700-05

Type: Sedimentary, unconsolidated (72700-04) and breccia fragment (72705).

Size: 72705, 1.3×1×1 cm.

Weight: 72700-04, 883.01 g; 72705, 2.39 g.

Depth: 0-5 cm.

Location: On southeast rim of Nansen crater approximately 42 m northeast of LRV.

Illustrations: Pans 14, 15; figure 92.

Comments: Collected from surface of light mantle adjacent to South Massif. Sediment sample to complement rake sample 72735-38.

Petrographic description: 72700-04, dominantly metaclastic rock and breccia, some agglutinate, minor feldspathic plutonic derivatives.

#### Components of 90-150-μm fraction of 72701,1 (Heiken and McKay, 1974)

Components	Volume percent
Agglutinate.....	43.6
Basalt, equigranular.....	1.7
Basalt, variolitic.....	--
Breccia:	
Low grade <sup>1</sup> - brown.....	12.6
Low grade <sup>1</sup> - colorless.....	9.7
Medium to high grade <sup>2</sup> .....	11.7
Anorthosite.....	1.3
Cataclastic anorthosite <sup>3</sup> .....	1.0
Norite.....	.3
Gabbro.....	--
Plagioclase.....	7.7
Clinopyroxene.....	3.0
Orthopyroxene.....	.7
Olivine.....	1.7
Ilmenite.....	--
Glass:	
Orange.....	1.0
"Black".....	1.7
Colorless.....	.7
Brown.....	1.3
Gray. "ropy".....	--
Other.....	--
Total number grains.....	300

<sup>1</sup>Metamorphic groups 1-3 of Warner (1972).

<sup>2</sup>Metamorphic groups 4-8 of Warner (1972).

<sup>3</sup>Includes crushed or shocked feldspar grains.

#### Major-element composition:

##### Chemical analyses of 72701

	1	2	3	4	5	6
SiO <sub>2</sub> .....	44.87	45.24	44.96	45.45	45.8	45.3
Al <sub>2</sub> O <sub>3</sub> .....	20.60	20.70	20.55	20.70	21.0	20.7
FeO.....	8.65	8.78	8.94	8.99	8.6	8.8
MgO.....	9.97	9.99	9.98	9.86	9.98	9.96
CaO.....	12.80	12.74	12.83	12.69	12.3	12.7
Na <sub>2</sub> O.....	.40	.44	.51	.49	.435	.46
K <sub>2</sub> O.....	.16	.154	.17	.17	.132	.16
TiO <sub>2</sub> .....	1.52	1.50	1.53	1.59	1.55	1.54
P <sub>2</sub> O <sub>5</sub> .....	.15	.153	.14	.14	--	.15
MnO.....	.12	.116	.13	.12	.110	.12
Cr <sub>2</sub> O <sub>3</sub> .....	.23	.229	.23	.18	.200	.21
Total.....	99.47	100.042	99.97	100.38	100.127	100.10

1. 72701.2 (Rhodes and others, 1974).
2. 72701.12 (Duncan and others, 1974).
3. 72701.21 (Rhodes and others, 1974).
4. 72701.23 (Scoon, 1974).
5. 72701.37 (Wänke and others, 1973).
6. Average of 1-5.

#### Sample 72735-38

Type: Four breccia fragments from rake sample.

Size: 72735, 5×3.5×2 cm; 72736, 5.5×2.5×2 cm; 72737, 1.5×1.1×1.1 cm; 72738, 4×2.5×2.5 cm.

Weight: 72735, 51.11 g; 72736, 28.73 g; 72737, 3.33 g; 72738, 23.75 g.

Depth: 0-2 cm.

Location: Southeast rim of Nansen crater approximately 42 m northeast of LRV.

Illustrations: Pans 14, 15; figure 92.

Comments: Fragments were derived from the South

Massif; they probably were emplaced on the rim of Nansen crater by deposition of the light mantle.

*Petrographic descriptions:*

72735, metaclastic rock with an aphanitic matrix. Plagioclase and olivine(?) mineral clasts, no lithic clasts.

72736, metanorite(?) with clasts of norite(?) in a fine-grained poikilitic(?) matrix.

72738, polymict(?) breccia with clasts of fine-grained metaclastic rock in an aphanitic matrix.

STATION 2A (LRV-4)

LOCATION

Station 2a is located on the light mantle about 600 m northeast of Nansen crater (fig. 7B).

OBJECTIVES

Station 2a was originally planned as an LRV sample stop to sample the light mantle; it was decided during the mission to add a traverse gravimeter reading, which permitted more comprehensive sampling than at a normal LRV sample stop.

GENERAL OBSERVATIONS

The station area is flat to gently rolling with scattered craters up to about 5 m in diameter. Most of the craters are subdued or have only slightly raised rims. None have blocky ejecta, but most have clods of "instant rock" (figs. 94, 95). The crew described the intercrater surface as blue-gray material overlying lighter colored material. The surface is saturated with small craters up to 5 cm in diameter.

Rock fragments up to several centimeters in diameter cover less than one percent of the surface. Many appear to be only slightly buried, and fillets are poorly

developed.

Samples include two surface sediment samples, a sediment sample from a depth of 15 cm in a trench, a clod that came from a crater wall and disintegrated to loose sediment by the time it reached the LRL, two breccia fragments from the surface, and two more breccia fragments from the trench.

GEOLOGIC DISCUSSION

The light mantle is interpreted as South Massif regolith material transported to the valley floor either as an avalanche (Scott and Carr, 1972; Howard, 1973; Muehlberger and others, 1973) that may have been triggered by impacting secondary projectiles from Tycho, or as the ejecta of the secondary craters themselves (Lucchitta, 1977). The hypothesis that the light mantle formed from South Massif regolith is supported by (1) the predominance of fine-grained material and near-absence in the light mantle of cobble- and boulder-size fragments, reported by the crew and shown in figures 94 through 96, (2) the predominance of breccia fragments and near-absence of basalt in the samples, and (3) the obvious highlands provenance shown in the chemical composition of the sediment samples (fig. 93).

SUMMARY OF SAMPLING

Sample 73120-24

*Type:* Sedimentary, unconsolidated.

*Weight:* 287.68 g.

*Depth:* From upper few centimeters.

*Location:* On light mantle at station 2a.

*Illustrations:* Figure 94.

*Comments:* Light mantle material.

*Petrographic description:* 73120-24, dominantly breccia and agglutinate.

Components of 90-150- $\mu$ m fraction of 73121,10 (Heiken and McKay, 1974)

Components	Volume percent
Agglutinate.....	41.7
Basalt, equigranular.....	--
Basalt, variolitic.....	--
Breccia:	
Low grade <sup>1</sup> - brown.....	8.7
Low grade <sup>1</sup> - colorless.....	7.7
Medium to high grade <sup>2</sup> .....	15.6
Anorthosite.....	.3
Cataclastic anorthosite <sup>3</sup> .....	1.0
Norite.....	.3
Gabbro.....	--
Plagioclase.....	8.3
Clinopyroxene.....	4.3
Orthopyroxene.....	2.3
Olivine.....	1.0
Ilmenite.....	2.0
Glass:	
Orange.....	1.7
"Black".....	.7
Colorless.....	2.3
Brown.....	2.0



FIGURE 92.—Photomosaic of second rake area at station 2 showing areas from which samples 72700-05 and 72735-38 were collected, before sampling. (NASA photographs AS17-137-20974 and 20975.)

*Components of 90-150- $\mu$ m fraction of 73121,10 (Heiken and McKay, 1974)—Continued*

Components	Volume percent
Glass—Continued	
Gray, "ropy" .....	--
Other .....	--
Total number grains .....	300

<sup>1</sup>Metamorphic groups 1-3 of Warner (1972).<sup>2</sup>Metamorphic groups 4-8 of Warner (1972).<sup>3</sup>Includes crushed or shocked feldspar grains.*Major-element composition:**Chemical analyses of 73121*

	1	2	3	4
SiO <sub>2</sub> .....	44.60	45.56	45.6	45.3
Al <sub>2</sub> O <sub>3</sub> .....	20.83	21.23	20.8	21.0
FeO .....	8.59	8.45	8.58	8.54
MgO .....	10.00	9.73	10.18	9.97
CaO .....	12.87	12.82	13.2	13.0
Na <sub>2</sub> O .....	.44	.39	.427	.42
K <sub>2</sub> O .....	.15	.17	.141	.15
TiO <sub>2</sub> .....	1.42	1.39	1.38	1.40
P <sub>2</sub> O <sub>5</sub> .....	.13	.15	.135	.14
MnO .....	.13	.11	.109	.12
Cr <sub>2</sub> O <sub>3</sub> .....	.22	.26	.210	.23
Total .....	99.38	100.26	100.762	100.27

1. 73121.6 (Rhodes and others, 1974).

2. 73121.16 (Rose and others, 1974).

3. 73121.18 (Wänke and others, 1974).

4. Average of 1 through 3.

*Sample 73130-34**Type:* Sedimentary, unconsolidated.*Weight:* 238.07 g.*Depth:* Disintegrated surface fragment.*Location:* Collected about 30 cm down from rim on wall of 2-m crater at station 2a.*Illustrations:* Figures 94, 95.*Comments:* Collected as "instant rock" sample, but disintegrated in transit to the LRL.*Petrographic description:* 73130-34, dominantly breccia.*Exposure age:* <sup>22</sup>Na-<sup>26</sup>Al: 73131, minimum, 0.1 m.y.; maximum, 0.5 $\pm$ 0.1 m.y. May limit age of the small fresh crater (Yokoyama and others, 1976).*Sample 73140-46**Type:* Sedimentary, unconsolidated (73140-44) and two breccia fragments (73145, 73146).*Size:* 73145, 2.5 $\times$ 2 $\times$ 1 cm.*Weight:* 73140-44, 337.0 g; 73145, 5.6 g; 73146, 3.01 g.*Depth:* 15 cm below surface.*Location:* From bottom of trench at station 2a.*Illustrations:* Figure 94.*Comments:* May be most representative of light mantle material because of the absence of nearby large craters, distance from South Massif, and location from below surface.*Petrographic descriptions:*

73140-44, dominantly fine-grained breccia and (or) metaclastic rock, some agglutinate.

*Components of 90-150- $\mu$ m fraction of 73141,4 (Heiken and McKay, 1974)*

Components	Volume percent
Agglutinate .....	32.0
Basalt, equigranular .....	2.6
Basalt, variolitic .....	--
Breccia:	
Low grade <sup>1</sup> - brown .....	18.3
Low grade <sup>1</sup> - colorless .....	4.9
Medium to high grade <sup>2</sup> .....	15.3
Anorthosite .....	.3
Cataclastic anorthosite <sup>3</sup> .....	2.0
Norite .....	.3
Gabbro .....	--
Plagioclase .....	14.0
Clinopyroxene .....	4.2
Orthopyroxene .....	1.0
Olivine .....	1.0
Ilmenite .....	.7
Glass:	
Orange .....	Trace
"Black" .....	.6
Colorless .....	.6
Brown .....	1.6
Gray, "ropy" .....	--
Other .....	.3
Total number grains .....	306

<sup>1</sup>Metamorphic groups 1-3 of Warner (1972).<sup>2</sup>Metamorphic groups 4-8 of Warner (1972).<sup>3</sup>Includes crushed or shocked feldspar grains.

73145, metagabbroid(?) breccia with abundant plagioclase debris in an aphanitic matrix.

*Major-element composition:**Chemical analyses of 73141*

	1	2	3	4	5
SiO <sub>2</sub> .....	45.06	44.91	45.35	45.8	45.3
Al <sub>2</sub> O <sub>3</sub> .....	21.52	21.42	21.56	21.2	21.4
FeO .....	8.10	8.14	8.02	8.12	8.10
MgO .....	10.04	9.94	10.28	10.10	10.09
CaO .....	13.04	13.06	12.91	12.9	13.0
Na <sub>2</sub> O .....	.38	.44	.38	.431	.41
K <sub>2</sub> O .....	.15	.15	.14	.134	.14
TiO <sub>2</sub> .....	1.29	1.24	1.26	1.23	1.26
P <sub>2</sub> O <sub>5</sub> .....	.12	.12	.12	.119	.12
MnO .....	.11	.12	.11	.108	.11
Cr <sub>2</sub> O <sub>3</sub> .....	.21	.21	.24	.213	.22
Total .....	100.02	99.75	100.37	100.355	100.15

1. 73141.1 (Rhodes and others, 1974).

2. 73141.7 (Rhodes and others, 1974).

3. 73141.21 (Rose and others, 1974).

4. 73141.23 (Wänke and others, 1974).

5. Average of 1 through 4.

*Sample 73150-56**Type:* Sedimentary, unconsolidated (73150-54); polymict breccia with a cataclastic matrix (73155); and small breccia fragment (73156).*Size:* 73155, 5.5 $\times$ 4.2 $\times$ 3.8 cm; 73156, 1.5 $\times$ 1 $\times$ 1 cm.*Weight:* 73150-54, 158.95 g; 73155, 79.3 g; 73156, 3.15 g.*Depth:* 0-1 cm.*Location:* On surface of light mantle at station 2a.*Illustrations:* Figures 96, 97 (LRL).

*Comments:* Sediment (73150-54) including a small breccia fragment (73156) scooped up with sample 73155.

*Petrographic descriptions:*

73150-54, dominantly fine-grained breccia and (or) metaclastic rock, some agglutinate.

73155, polymict breccia with fine-grained metaclastic clasts with variable proportions of minerals in an aphanitic matrix. This matrix has been locally shattered and invaded by coarser feldspathic debris.

STATION 3

LOCATION

Station 3 is located on the light mantle approximately

50 m east of the rim of Lara crater and just above the base of the Lee-Lincoln scarp (fig.7A).

OBJECTIVES

Analysis of orbital photographs before the mission indicated that the light mantle covered the scarp, which is probably the topographic expression of a fault upthrown on the west (Lucchitta, 1976). It was hoped that depositional structures indicative of the mode of origin might be seen where the light mantle was draped over the earlier formed scarp. Observation and sampling were planned to determine the interrelations and chronology of the scarp and light-mantle materials and to sample the light mantle near the base of the scarp.

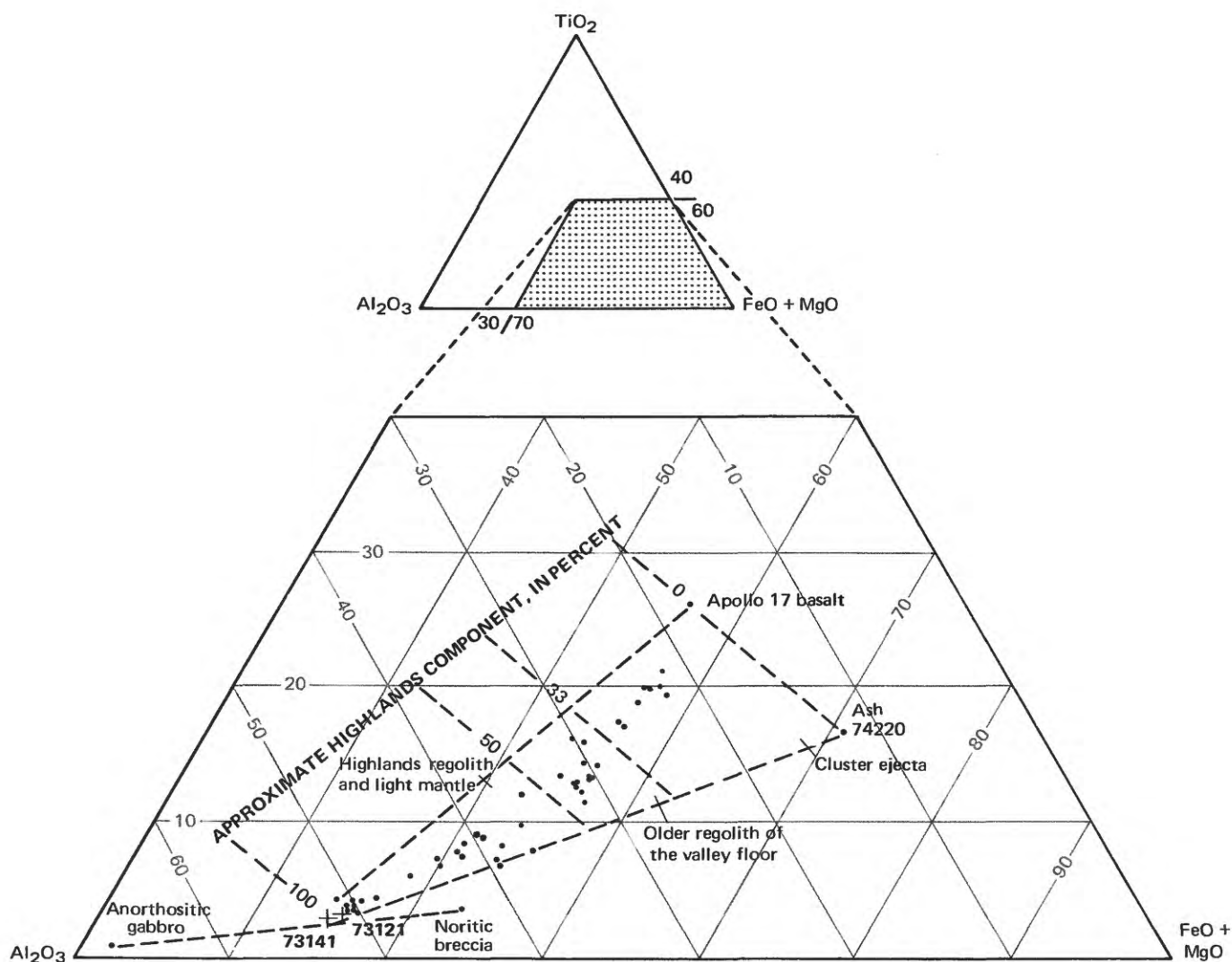


FIGURE 93.—Relative amounts of  $\text{TiO}_2$ ,  $\text{Al}_2\text{O}_3$ , and  $\text{FeO}+\text{MgO}$  in sediment samples 73121 and 73141 (crosses), collected at station 2a, in comparison with sediment samples from rest of traverse region (dots). Apollo 17 basalt, anorthositic gabbro, and noritic breccia values from Rhodes and others (1974).

## GENERAL OBSERVATIONS

The station area is on a northeast-facing slope of the scarp, which the crew had described earlier as being a series of hummocky lobes with north-south trends where the scarp crosses the light-mantle area.

Craters ranging in size from 4 cm to 15 m are common in the station area (pan 16). Those less than 2

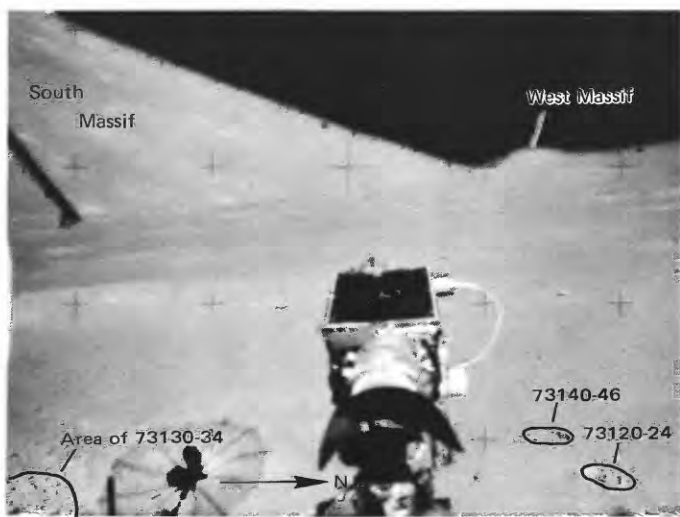


FIGURE 94.—Area of station 2a, from LRV, after samples 73120-24, 73130-34, and 73140-46 were collected. (NASA photograph AS17-138-21103.)



FIGURE 95.—The 2-m crater from which sample 73130-34 at station 2a was collected, before sampling. (NASA photograph AS17-138-21097.)

m in diameter appear to be subdued and shallow; some have cloddy ejecta. Several of the craters larger than 2 m in diameter have blocky raised rims. The largest crater in the area is the 500-m Lara crater, which is covered by light mantle.

Rock fragments up to 25 cm across are common but cover less than 1 percent of the surface. Boulders up to 1 m across appear to be concentrated on and near the rims of the larger craters. Most of the rock fragments and boulders are perched on the surface or are only slightly buried. Fillets are poorly developed.

The surface sediment was described as medium gray in color. Footprints and LRV tracks in the photographs of the station area reveal lighter gray material just below the surface. A shallow trench showed that medium-gray surface material about 0.5 cm thick overlies a light-gray layer 3 cm thick, which in turn overlies marbled or mottled light- and medium-gray material.

Samples at station 3 consisted of a double drive tube, eight rock samples, and five sediment samples, four of which were collected from a trench (fig. 98). All of the samples except the drive tube were collected from the raised rim of a 10-m crater. The drive tube was taken near the base of the scarp, about 20 m south-southeast of the 10-m crater.

## GEOLOGIC DISCUSSION

Except for one small fragment of olivine basalt (sample 73219), rocks collected at station 3 are breccias presumably transported from the surface of the South Massif during emplacement of the light mantle. Only one rock, polymict breccia sample 73215, has been studied in detail (James consortium; see discussion of 73215 for citations). It consists of flow-banded dark aphanite and lighter colored granulated clastic debris. The aphanite has been interpreted by the consortium as clast-laden melt assembled in a basin-forming impact; flow banding was produced during transport of the ejecta from the transient cavity.

In preliminary examination (Wilshire, this report), polymict breccia 73235 resembled 73215. Major-element data for the two rocks (fig. 99) show that they are very much alike and that they fall within the narrow compositional spectrum of the Apollo 17 highlands materials.

The station 3 samples came largely from near the rim crest of a 10-m crater, which apparently penetrated only light-mantle material. Sediment samples from the trench dug in the crater rim show chemically (fig. 100) and petrographically the preponderance of highlands material and the near absence of admixed basaltic debris. Measurements of  $^{22}\text{Na}$  and  $^{26}\text{Al}$  in the four trench samples (73231, 73241, 73261, 73281) suggest that the 10-m crater may have formed within the last 2 m.y. (Yokoyama and others, 1976). Alternately, the track age of  $4.7 \pm 1$  m.y. determined for 73275 could repre-

sent the age of the small crater (Croaz and others, 1974).

Rocks from station 3 record a complex range of noble-gas exposure ages, all older than 100 m.y. These ages presumably reflect exposure that occurred either (1) in the regolith of the South Massif before the light mantle was deposited or (2) in the light mantle since its emplacement on the valley floor.

#### SUMMARY OF SAMPLING

Sample 73002/73001 (upper/lower)

*Type:* Double drive tube.

*Length:* 56.9 cm (73001, 34.9 cm; 73002, 22.0 cm).

*Depth:* Approximately 70.6 cm.

*Weight:* 1,238.7 g (73001, 809 g; 73002, 429.7 g).

*Location:* On light mantle near base of scarp.



FIGURE 96.—Location of sample 73155 before collection. Sediment sample 73150-54, including small fragment 73156, was scooped up with 73155. Inset shows 73155 with reconstructed lunar surface orientation and lighting. (NASA photographs AS17-138-21099; S-73-19595.)

*Illustrations:* Pan 16; figure 101.

*Comments:* Light mantle material apparently undisturbed by recent cratering. About 4 cm of sample was spilled from the bottom of the upper drive tube (73002).

#### Sample 73210-14

*Type:* Sedimentary, unconsolidated.

*Weight:* 98.58 g.

*Depth:* From surface.

*Location:* From rim of 10-m crater at station 3.

*Illustrations:* Pan 16; figures 102, 103.

*Comments:* Surface sediment collected with five rock fragments (73215-19).

*Petrographic description:* 73210-14, dominantly breccia.

#### Sample 73215

*Type:* Polymict breccia with a cataclastic matrix.

*Size:* 12×11×8.5 cm.

*Weight:* 1,062 g.

*Location:* From rim of 10-m crater at station 3.

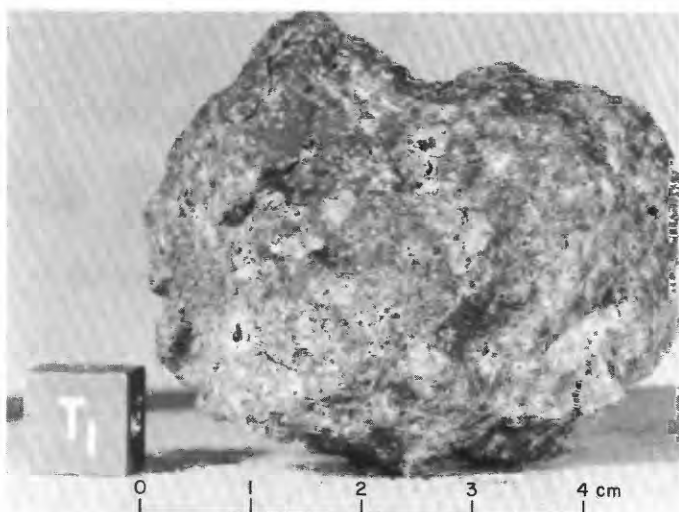


FIGURE 97.—Sample 73155. Polymict breccia with locally cataclastic matrix. (NASA photograph S-73-17056.)

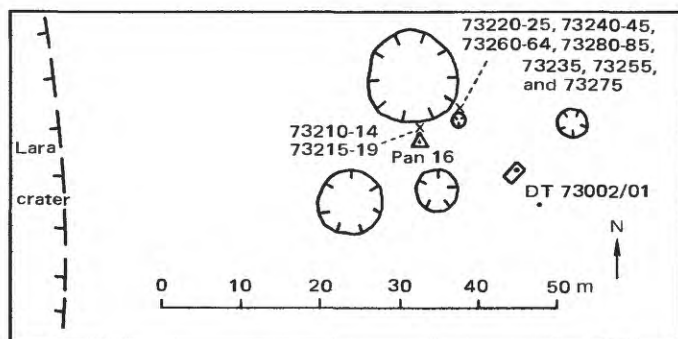


FIGURE 98.—Planimetric map of station 3.

*Illustrations:* Pan 16; figures 102, 103, 104 (LRL), 105 (photomicrograph).

*Comments:* Light-gray breccia, probably from the South Massif.

*Petrographic description:* Polymict breccia with crudely banded light and dark clastic material; light material (weakly annealed?) injected into broken dark polymict breccia. Light material is coarse metaclastic debris derived from troctolite or metatroctolite and other sources. In the dark breccia, clasts in the size range 0.1 to 1.0 mm are in the following approximate proportions: 52 percent plagioclase, 4 percent pyroxene, 1 percent pink spinel, 19 percent olivine, 4 percent light metaclastic rocks, 11 percent dark metaclastic rocks, 2 percent recrystallized olivine, 10 percent recrystallized plagioclase.

Sample 73215 has been studied by a consortium whose major petrographic and petrologic conclusions (James, 1975, 1976a, b; James and others, 1975a, b, 1976; James and Blanchard, 1976) are:

(1) The rock consists of subparallel bands of different types of aphanite interspersed with bands of granulated clastic material; this fabric was produced by flow of the constituents during aggregation. Flow and subsequent shearing also formed small faults at high angles to the banding, small schlieren derived from granulated clasts, and several sets of finely spaced fractures.

(2) The bulk of 73215 is gray to black aphanite that occurs not only as "matrix" but as clasts within aphanite matrix and within zones of granulated clastic material. The aphanite, considered equivalent to the gray and black competent breccias of boulder 1 at station 2, is an aggregate of mineral (mainly plagioclase, olivine, pyroxene) and lithic (dominated by anorthosite-norite-troctolite suite) clasts enclosed in a very fine groundmass. The groundmass, interpreted as having crystallized from a melt, is described as microintergranular to microsubophitic; most grains are 1-8  $\mu\text{m}$  in size. Dominant constituents are plagioclase and low-calcium pyroxene, with minor amounts of olivine, opaque minerals, iron metal, and troilite. As shown by microprobe analyses (not given in this report), the groundmass is less rich in  $\text{CaO}$  and  $\text{Al}_2\text{O}_3$  (that is, more mafic) than is the bulk aphanite; hence, the presumed melt from which it crystallized was not simply derived by melting of the clast suite it contains.

(3) Melt and clasts, now aggregated as the aphanite, presumably were produced and violently mixed in a basin-forming impact. The clasts represent rock crushed within and beneath the growing crater cavity and ejected along with melt (now the very fine groundmass) generated in the same impact. Most

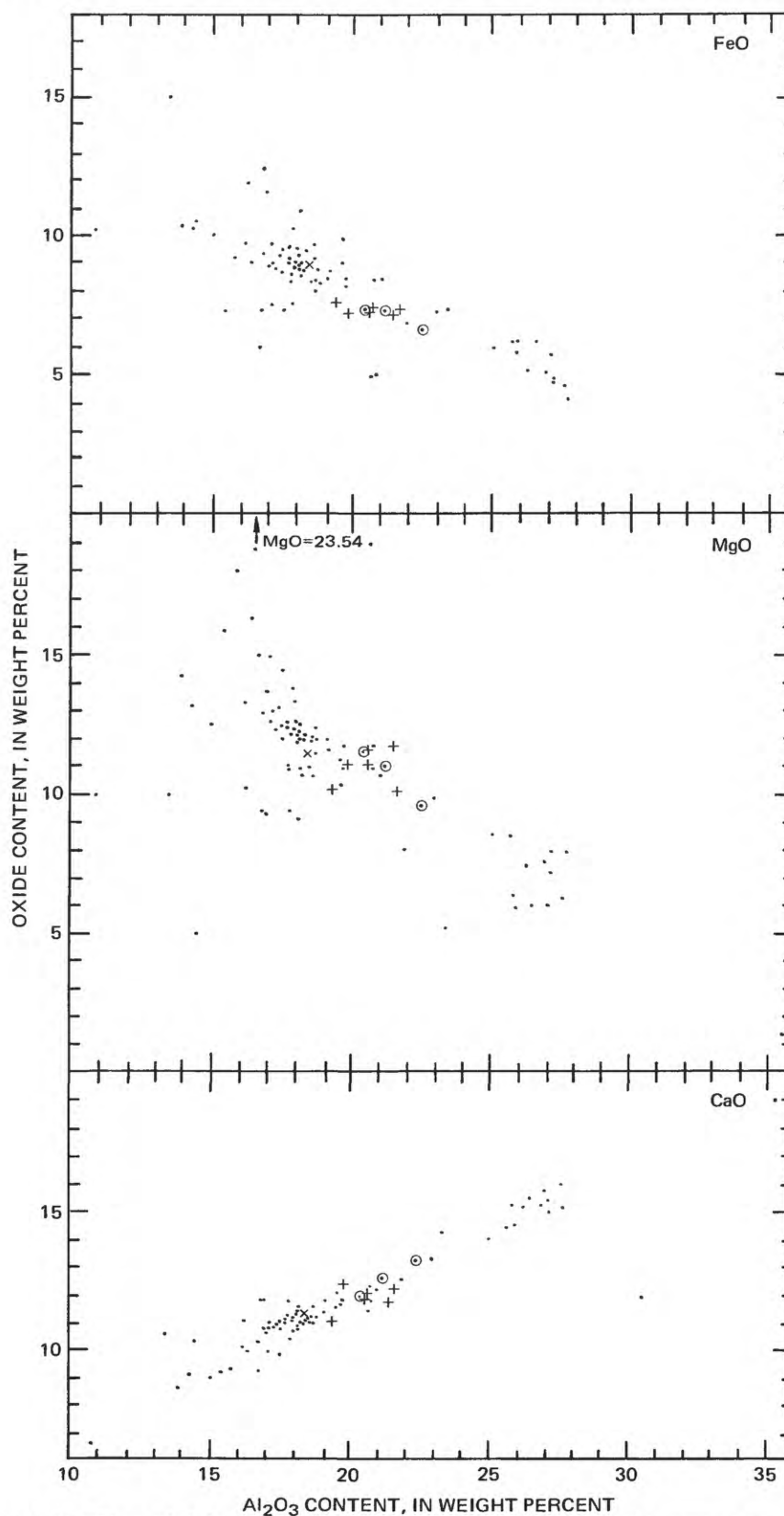


FIGURE 99.—Plots of FeO, MgO, and CaO contents in relation to  $\text{Al}_2\text{O}_3$  content for analyzed rocks from station 3 in comparison with all analyzed Apollo 17 highlands rocks (dots). Cross, 73215 aphanitic "matrix;" circled dot, 73235; x, 73275.

clasts were not strongly shocked or heated in the impact, but some had been shocked, and some were at high temperatures. The melt cooled rapidly and crystallized as it was mixed with the relatively cold clasts. Lithologic banding, schlieren, and preferred orientation of elongate clasts were produced by flow during aggregation of the breccia.

#### Major-element composition:

##### Chemical analyses of aphanite "matrix" from 73215

	1	2	3	4	5	6
SiO <sub>2</sub> .....	46.1	48.1	46.1	46.8	46.4	45.9
Al <sub>2</sub> O <sub>3</sub> .....	21.7	19.4	19.9	21.5	20.7	20.6
FeO .....	7.39	7.64	7.28	7.20	7.43	7.34
MgO .....	10.2	10.2	11.1	11.8	11.1	11.6
CaO .....	12.2	11.0	12.3	11.8	12.0	11.8

##### Chemical analyses of aphanite "matrix" from 73215—Continued

	1	2	3	4	5	6
Na <sub>2</sub> O .....	.495	.624	.487	.488	.520	.52
K <sub>2</sub> O .....	.167	.656	.191	.170	.273	.205
TiO <sub>2</sub> .....	1.1	.8	1.1	.4	.81	.7
P <sub>2</sub> O <sub>5</sub> .....	..	..	..	..	..	..
MnO .....	.104	.123	.119	.099	.107	.104
Cr <sub>2</sub> O <sub>3</sub> .....	.200	.168	.221	.230	.211	.250
Total .....	99.7	98.7	98.8	100.4	99.6	99.0

1. 73215.74 homogeneous gray matrix (James and others, 1975a).
2. 73215.161 homogeneous black matrix (James and others, 1975a).
3. 73215.177 schlieren-rich gray matrix (James and others, 1975a).
4. 73215.184 heterogeneous black matrix (James and others, 1975a).
5. 73215 average of eight typical matrix samples (James and others, 1975b).
6. 73215 average of matrix samples 73215.74; 151; 170B; 177; 184; 159; 185; 209; 262 (James and others, 1976).

#### Age:

Fission track: Whitlockite crystal  $4.05^{+0.05}_{-0.08}$  b.y.,  
(Braddy and others, 1975).

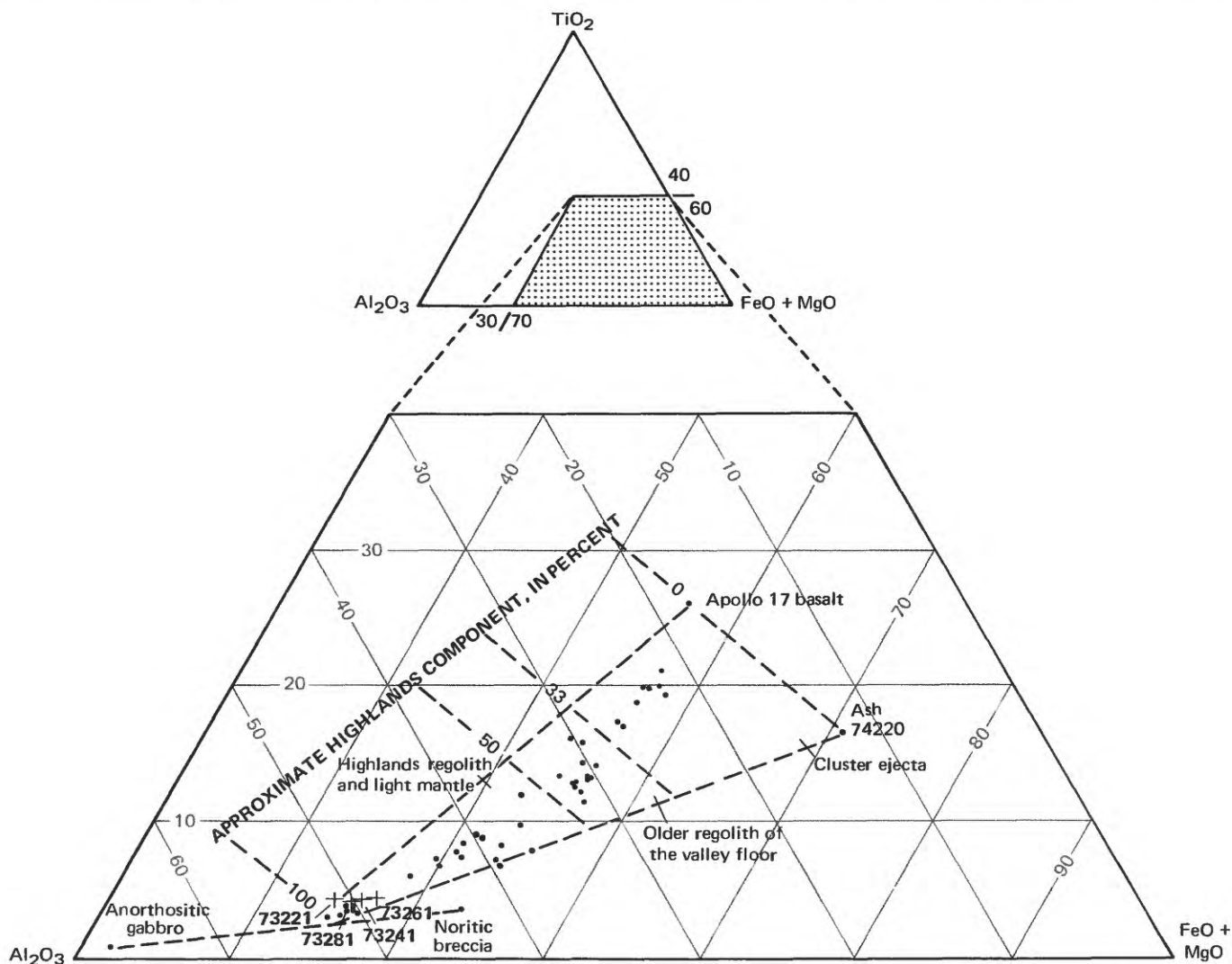


FIGURE 100.—Relative amounts of TiO<sub>2</sub>, Al<sub>2</sub>O<sub>3</sub>, and FeO + MgO in sediment samples 73221, 73241, 73261, and 73281 from trench at station 3 (crosses) in comparison with sediment samples from rest of traverse region (dots). Apollo 17 basalt, anorthositic gabbro, and noritic breccia values from Rhodes and others (1974).

Compaction age: tracks in plagioclase crystal from radioactive decay in adjacent ground-mass —  $4.08^{+0.07}_{-0.2}$  b.y. (Goswami and others, 1976b).



FIGURE 101.—Drive-tube sample 73002/73001 during sampling. (NASA photograph AS17-137-20981.)

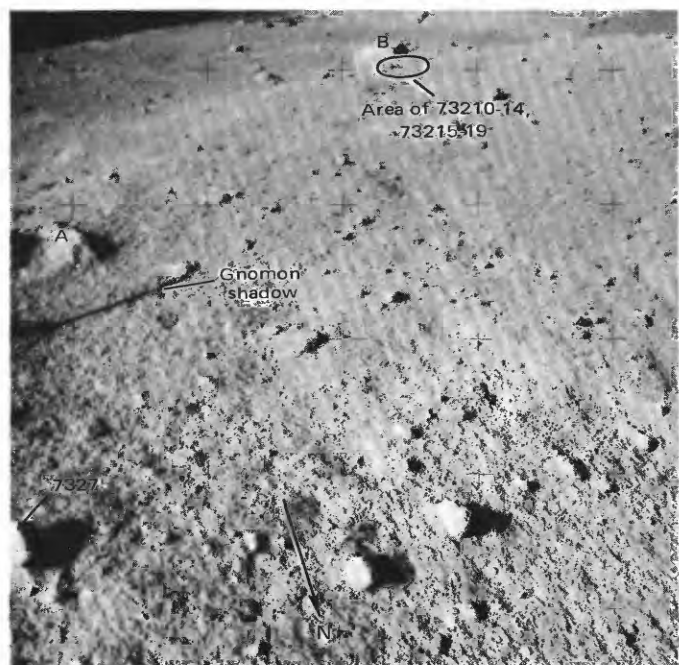


FIGURE 102.—Locations of samples 73210-14, 15-19, and 73275, before collection. Letters A and B indicate same boulders seen in figures 103, 109, and 110. (NASA photograph AS17-138-21145.)

Pb-U-Th data suggest that 73215 matrix was strongly modified by extensive outgassing of Pb approximately 4.0 b.y. ago (James and others, 1975a).

$^{40-39}\text{Ar}$  (Jessberger and others, 1976b):

- 73215,41.1, black matrix,  $4.04 \pm .03$  b.y.
- 73215,73.1, gray matrix,  $4.15 \pm .01$  b.y.
- 73215,177.1, schlieren-rich gray matrix,  $4.13 \pm .04$  b.y.
- 73215,38.57, gray aphanite spheroid,  $4.16 \pm .03$  b.y.
- 73215,46,10,7, black aphanite clast,  $4.24 \pm .01$  b.y.
- 73215,46,6,1, dark-gray aphanitic clast,  $4.17 \pm .07$  b.y.
- 73215,38,39,1,2, feldspathic clast,  $4.11 \pm .05$  b.y.,  $4.28 \pm .03$  b.y.
- 73215,38,39,1,1, troctolite vein,  $4.00 \pm .06$  b.y.
- 73215,29,9,6, anorthositic gabbro clast,  $4.06 \pm .02$  b.y.,  $4.24 \pm .01$  b.y.
- 73215,46,25,5, anorthositic gabbro clast,  $4.07 \pm .01$  b.y.,  $4.26 \pm .01$  b.y.
- 73215,46,33,4, anorthositic gabbro clast,  $4.07 \pm .01$  b.y.,  $4.22 \pm .01$  b.y.

An age of  $\sim 4.05$  b.y. is interpreted as an older limit on the event that aggregated the aphanite "matrix," because the abundant small clasts presumably were incom-



FIGURE 103.—Area of samples 73210-14 and 15-19 after collection, and the eastern part of the 10-m crater at station 3. Scoop and sample collection bag at right. B refers to boulder seen in figures 102 and 110. (NASA photograph AS17-138-21160.)

pletely outgassed. An age of  $\sim 4.25$  b.y. is interpreted as a younger limit for the age of crystallization or metamorphism of preimpact rocks of the target, because they probably were partially outgassed during formation of the 73215 breccia (Jessberger and others, 1976b).

Rb-Sr isochron: anorthositic gabbro,  $4.24 \pm 0.31$  ( $2\sigma$ ) b.y. Age is interpreted as a younger limit for crystallization of the anorthositic gabbro parent rock (James and others, 1976a).

*Exposure age:*

Kr:  $243 \pm 7$  m.y. (matrix) (James and others, 1975a).

Ar: (Jessberger and others, 1976b):

73215,41.1, black matrix,  $254 \pm 9$  m.y.

73215,73.1, gray matrix,  $238 \pm 12$  m.y.

73215,177.1, schlieren-rich gray matrix,  $257 \pm 11$  m.y.

73215,38.57, gray aphanite spheroid,  $259 \pm 12$  m.y.

73215,46,10,7, black aphanite clast,  $252 \pm 22$  m.y.

73215,46,6,1, dark-gray aphanitic clast,  $256 \pm 24$  m.y.

73215,38,39,1,2, feldspathic clast,  $228 \pm 40$  m.y.

73215,38,39,1,1, troctolite vein,  $247 \pm 62$  m.y.

73215,29,9,6, anorthositic gabbro clast,  $268 \pm 6$  m.y.

73215,46,25,5, anorthositic gabbro clast,  $250 \pm 12$  m.y.

73215,46,33,4, anorthositic gabbro clast,  $244 \pm 10$  m.y.

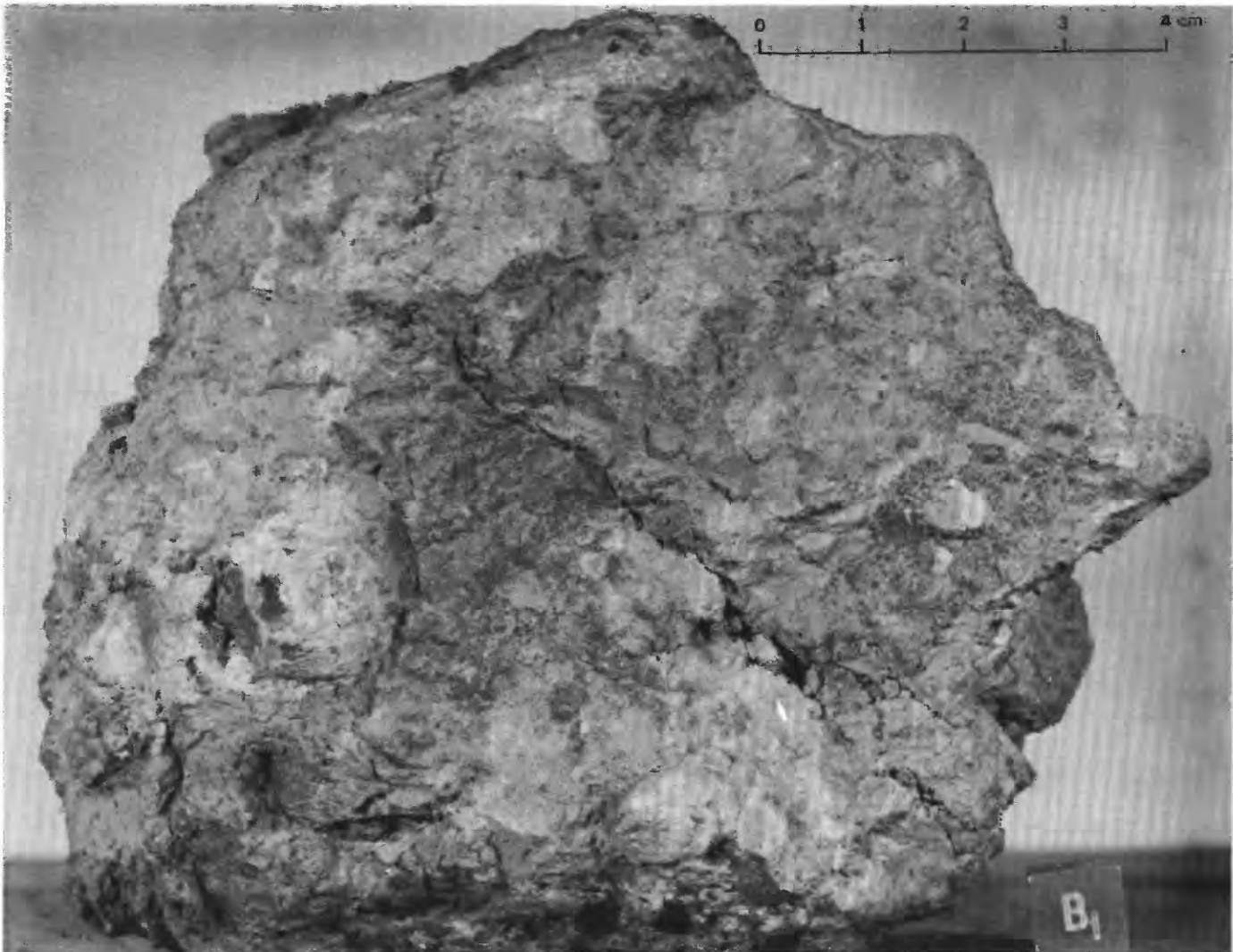


FIGURE 104.—Sample 73215. Polymict breccia with cataclastic matrix. (NASA photograph S-73-16663.)

Agreement of clast exposure ages with the Kr exposure age for the matrix is evidence against irradiation of clasts in the regolith before aggregation of the breccia (Jessberger and others, 1976a).

#### Sample 73216

*Type:* Polymict breccia with a granoblastic matrix.

*Size:* 7×5×3 cm.

*Weight:* 162.2 g.

*Location:* From rim of 10-m crater at station 3.

*Illustrations:* Pan 16; figures 102, 103, 106 (LRL).

*Comments:* Greenish-gray breccia, probably from the South Massif.

*Petrographic description:* Polymict breccia with clasts of metaclastic rock and feldspathic plutonic derivatives in a fine-grained granoblastic matrix. Moderately abundant plagioclase and olivine clasts.

#### Sample 73217

*Type:* Polymict breccia with an aphanitic matrix.

*Size:* 6.5×4.5×3.0 cm.

*Weight:* 138.8 g.

*Location:* From rim of 10-m crater at station 3.

*Illustrations:* Pan 16; figures 102, 103, 107 (LRL).

*Comments:* Blue-gray breccia, probably from the South Massif.

*Petrographic description:* Polymict breccia with clasts of dark metaclastic rock, light feldspathic cataclasite, and mineral debris (dominantly plagioclase) in an aphanitic matrix.

#### Sample 73218

*Type:* Polymict breccia with an aphanitic matrix.

*Size:* 4×3×2.5 cm.

*Weight:* 39.67 g.

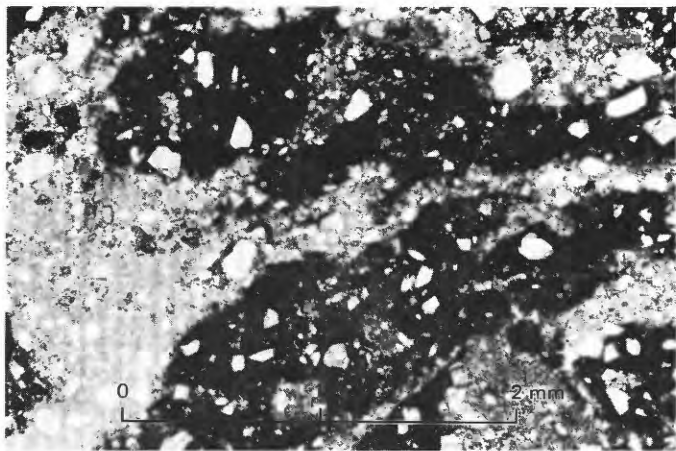


FIGURE 105.—Sample 73215. Photomicrograph showing clasts of polymict breccia with dark aphanitic matrices in matrix of fragmented feldspathic debris.

*Location:* From rim of 10-m crater at station 3.

*Illustrations:* Pan 16; figures 102, 103, 108 (LRL).

*Comments:* Greenish-gray breccia, probably from the South Massif.

*Petrographic description:* Polymict breccia with clasts of light metaclastic rock, metagabbroid rock, and plagioclase, pyroxene, and olivine mineral debris.

#### Sample 73219

*Type:* Olivine basalt.

*Size:* 1.5×1.3×1.0 cm.

*Weight:* 2.88 g.

*Location:* From rim of 10-m crater at station 3.

*Illustrations:* Pan 16; figures 102, 103.

*Comments:* Presumably subfloor basalt ejected from some distant crater.

#### Sample 73220-25

*Type:* Sedimentary, unconsolidated (73220-24), including rock fragment (73225).

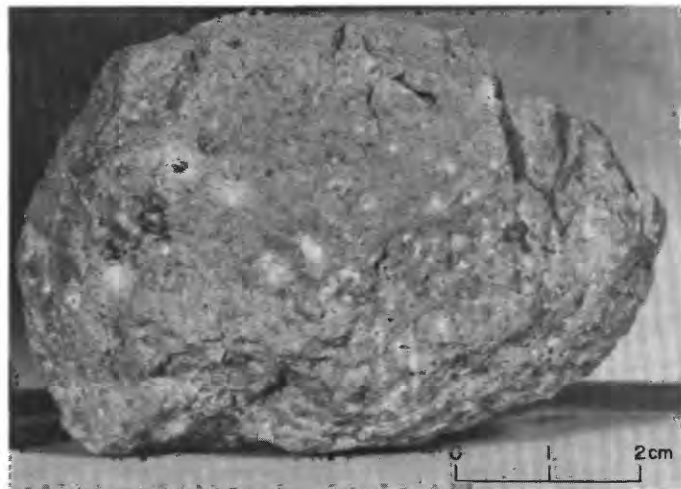


FIGURE 106.—Sample 73216. Polymict breccia with granoblastic matrix. (NASA photograph S-73-16780.)

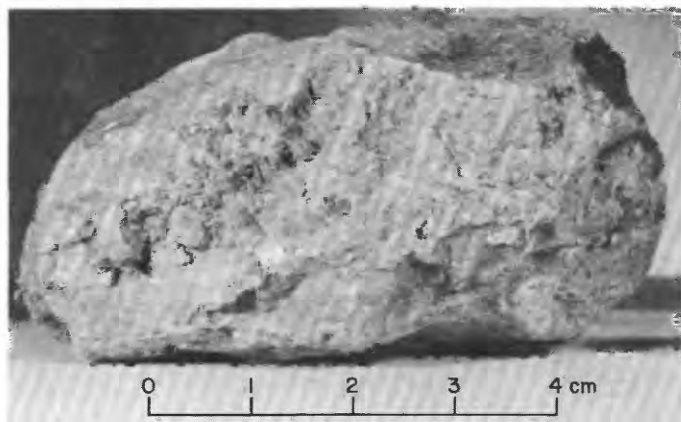


FIGURE 107.—Sample 73217. Polymict breccia with aphanitic matrix. (NASA photograph S-73-16785.)

Size: 73225, 1.7×1.5×1.3 cm.

Weight: 73220-24, 75.88 g; 73225, 3.66 g.

Depth: Upper one-half cm of trench wall.

Location: From trench on rim of 10-m crater at station 3.

Illustrations: Pan 16; figures 109, 111.

Comments: Ejecta from the 10-m crater.

Petrographic description: 73220-24, dominantly fine-grained breccia and (or) metaclastic rock, some unannealed feldspar cataclasite, scarce glass.

Components of 90-150- $\mu$ m fraction of 73221,1 (Heiken and McKay, 1974)

Components	Volume percent
Agglutinate.....	26.3
Basalt, equigranular }	3.0
Basalt, variolitic }	
Breccia:	
Low grade <sup>1-2</sup> brown.....	18.3
Low grade <sup>1-2</sup> colorless.....	10.3
Medium to high grade <sup>2</sup> .....	18.0
Anorthosite.....	.3
Cataclastic anorthosite <sup>3</sup> .....	.3
Norite.....	—
Gabbro.....	—
Plagioclase.....	11.3
Clinopyroxene.....	8.0
Orthopyroxene.....	Trace
Olivine.....	1.3
Ilmenite.....	.3
Glass:	
Orange.....	—
"Black".....	2.6
Colorless.....	.3
Brown.....	.6
Gray, "ropy".....	—
Other.....	—
Total number grains.....	300

<sup>1</sup>Metamorphic groups 1-3 of Warner (1972).

<sup>2</sup>Metamorphic groups 4-8 of Warner (1972).

<sup>3</sup>Includes crushed or shocked feldspar grains.



FIGURE 108.—Sample 73218. Polymict breccia with aphanitic matrix. (NASA photograph S-73-16911.)

Major-element composition:

Chemical analyses of 73221

	1	2	3
SiO <sub>2</sub> .....	45.20	45.1	45.2
Al <sub>2</sub> O <sub>3</sub> .....	21.03	20.6	20.8
FeO.....	8.85	8.75	8.80
MgO.....	8.97	9.38	9.18
CaO.....	12.86	12.5	12.7
Na <sub>2</sub> O.....	.41	.461	.44
K <sub>2</sub> O.....	.16	.142	.15
TiO <sub>2</sub> .....	1.86	1.82	1.84
P <sub>2</sub> O <sub>5</sub> .....	.15	—	.15
MnO.....	.11	.116	.11
Cr <sub>2</sub> O <sub>3</sub> .....	.27	.219	.24
Total.....	99.87	99.088	99.61

1. 73221.13 (Rose and others, 1974).

2. 73221.16 (Wänke and others, 1974).

3. Average of 1 and 2.

Exposure age: <sup>22</sup>Na/<sup>26</sup>Al: 73221, minimum 0.8±0.2 m.y.; maximum 1.1±0.2 m.y. (Yokoyama and others, 1976).

Sample 73235

Type: Polymict breccia with a cataclastic matrix.

Size: 12×10×8 cm.

Weight: 878.3 g.

Location: From surface on rim of 10-m crater at station 3.

Illustrations: Pan 16; figures 109, 110, 111, 112 (LRL), 113 (photomicrograph).

Comments: Ejecta from the 10-m crater.

Petrographic description: Polymict breccia with clasts of metagabbroid rocks, and plagioclase, pyroxene, and olivine porphyroclasts in a dark aphanitic matrix. The matrix has been shattered and invaded by coarse angular fragments of minerals, mostly feldspar, and some brown spinel-plagioclase symplectite.

Major-element composition:

Chemical analyses of 73235

	1	2	3
SiO <sub>2</sub> .....	45.96	46.20	46.6
Al <sub>2</sub> O <sub>3</sub> .....	22.57	21.28	20.50
FeO.....	6.68	7.32	7.38
MgO.....	9.61	11.05	11.54
CaO.....	13.18	12.55	11.9
Na <sub>2</sub> O.....	.44	.48	.456
K <sub>2</sub> O.....	.200	.20	.198
TiO <sub>2</sub> .....	.60	.67	.65
P <sub>2</sub> O <sub>5</sub> .....	.192	.20	.186
MnO.....	.091	.11	.100
Cr <sub>2</sub> O <sub>3</sub> .....	.196	—	.199
Total.....	99.719	100.06	99.709

1. 73235.53 (Duncan and others, 1974).

2. 73235.55 (Rhodes and others, 1974).

3. 73235.91 (Wänke and others, 1974).

## Age:

<sup>40-39</sup>Ar:73235,  $3.96^{+0.04}_{-0.08}$  b.y., (Turner and Cadogan, 1975).73235,27,  $3.98 \pm 0.04$  b.y., (Phinney and others, 1975).

## Exposure age:

Ar:

111 m.y. (Arvidson and others, 1974).

110 m.y. (Turner and Cadogan, 1975).

 $195 \pm 20$  m.y. (Phinney and others, 1975).

FIGURE 109.—Trench, 10-15 cm deep, at station 3, showing areas from which samples 73220-25, 73240-45, 73260-64, and 73280-85 were collected, before sampling. Samples 73235 and 73255 also shown. A designates boulder also seen in figures 102, 103, and 110. (NASA photograph AS17-138-21148.)

## Sample 73240-45

*Type:* Sedimentary, unconsolidated (73240-44) and breccia fragment (73245).

*Size:* 73245, 1×1×0.8 cm.

*Weight:* 73240-44, 358.97 g; 73245, 1.6 g.

*Depth:* Upper 5 cm of soil in trench.

*Location:* From trench on rim of 10-m crater at station 3.

*Illustrations:* Pan 16; figures 109, 111.

*Comments:* Ejecta from 10-m crater.

*Petrographic description:* 73240-44, dominantly fine-grained breccia and (or) metaclastic rock, some agglutinate.

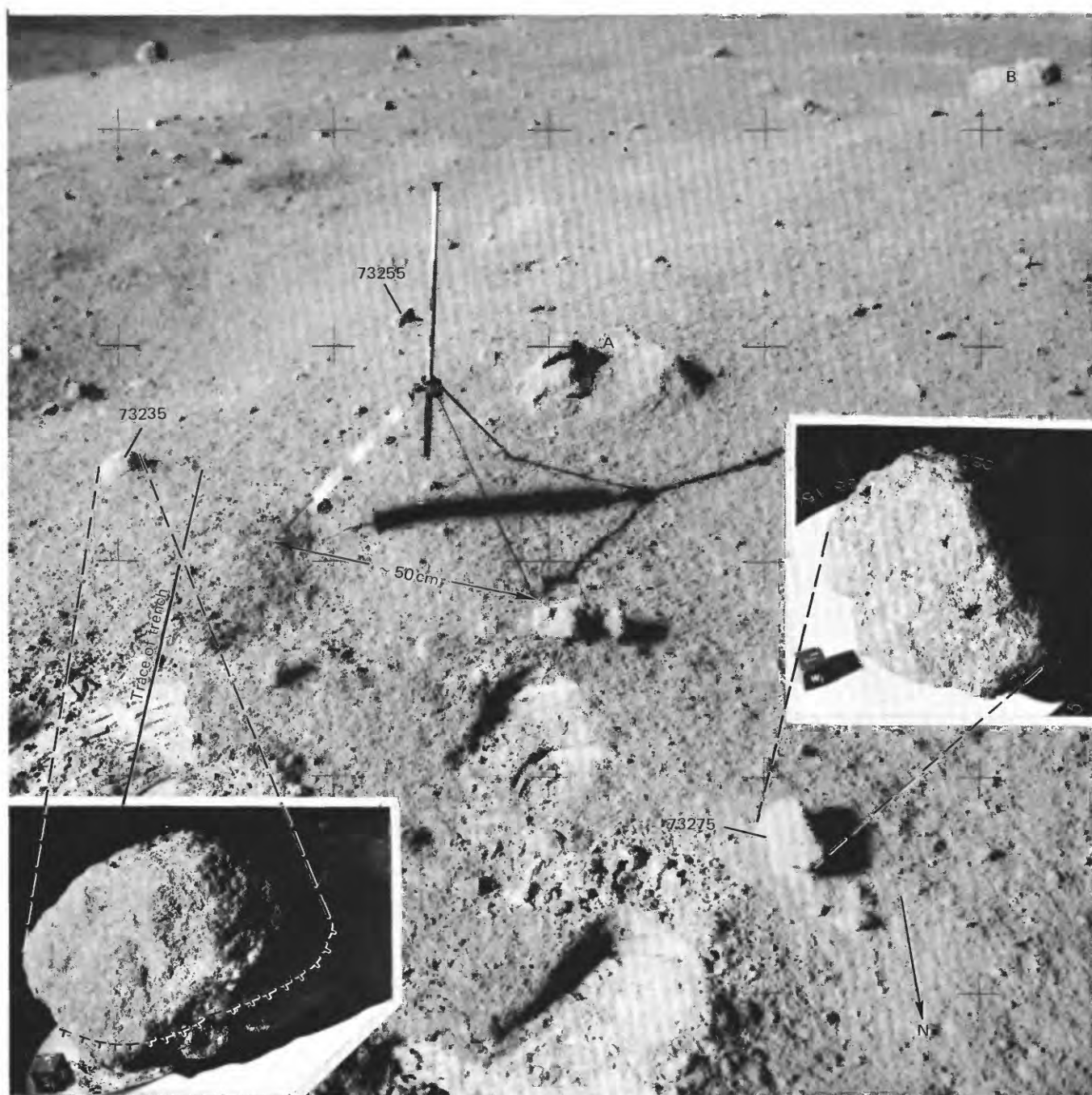


FIGURE 110.—Samples 73235, 73255, and 73275 before collection, and approximate trace of west edge of trench shown in figure 111. Insets show 73235 and 73275 with reconstructed lunar surface orientations and lighting. A and B designate boulders shown in figures 102, 103, and 109. (NASA photographs AS17-138-21144; S-73-16968 (73235), S-73-16969 (73275).)

*Components of 90-150- $\mu$ m fraction of 73241,9 (Heiken and McKay, 1974)*

Components	Volume percent
Agglutinate.....	8.4
Basalt, equigranular .....	1.0
Basalt, variolitic .....	--
Breccia:	
Low grade <sup>1</sup> - brown.....	35.8
Low grade <sup>1</sup> - colorless.....	.3
Medium to high grade <sup>2</sup> .....	25.4
Anorthosite.....	.3
Cataclastic anorthosite <sup>3</sup> .....	2.7
Norite.....	--
Gabbro.....	--
Plagioclase.....	11.4
Clinopyroxene .....	3.3
Orthopyroxene.....	2.0
Olivine.....	.7
Ilmenite.....	--
Glass:	
Orange .....	.3
"Black".....	5.7
Colorless .....	1.0
Brown .....	--
Gray, "ropy" .....	1.0
Other.....	--
Total number grains .....	299

<sup>1</sup>Metamorphic groups 1-3 of Warner (1972).

<sup>2</sup>Metamorphic groups 4-8 of Warner (1972).

<sup>3</sup>Includes crushed or shocked feldspar grains.

*Major-element composition:*

*Chemical analyses of 73241*

	1	2	3
SiO <sub>2</sub> .....	44.55	45.4	45.0
Al <sub>2</sub> O <sub>3</sub> .....	20.20	20.56	20.38
FeO.....	8.45	8.39	8.42
MgO.....	11.11	9.65	10.38
CaO.....	12.90	12.6	12.8
Na <sub>2</sub> O.....	.46	.448	.45
K <sub>2</sub> O.....	.16	.146	.15
TiO <sub>2</sub> .....	1.73	1.68	1.70
P <sub>2</sub> O <sub>5</sub> .....	.15	.126	.14
MnO.....	.11	.109	.11
Cr <sub>2</sub> O <sub>3</sub> .....	.25	.200	.22
Total.....	100.07	99.309	99.75

1. 73241.14 (Rose and others, 1974).

2. 73241.17 (Wänke and others, 1974).

3. Average of 1 and 2.

*Exposure age:*

<sup>22</sup>Na-<sup>26</sup>Al: 73241, minimum  $0.6 \pm 0.6$  m.y.; maximum  $1.5 \pm 0.5$  m.y. (Yokoyama and others, 1976).

Tracks: 85 percent of feldspar crystals have low track density; these crystals are interpreted as having had maximum exposure of 20 m.y. Hence, the 10-m crater is 20 m.y. old or less (Croaz and others, 1974).

*Sample 73255*

*Type:* Polymict breccia with an aphanitic matrix.

*Size:* 8×7.5×5 cm.

*Weight:* 394.1 g.

*Location:* From surface on rim of 10-m crater at station 3.

*Illustrations:* Pan 16; figures 109, 110, 111, 114 (LRL).

*Comments:* Light-gray breccia, probably from the South Massif.

*Petrographic description:* Polymict breccia with clasts of metaclastic and metagabbroid rocks and mineral clasts of plagioclase and olivine in an aphanitic matrix.

*Sample 73260-64*

*Type:* Sedimentary, unconsolidated.

*Weight:* 326.23 g.

*Depth:* About 5-10 cm below surface in trench.

*Location:* From trench on rim of 10-m crater at station 3.

*Illustrations:* Pan 16; figures 109, 110.

*Comments:* The medium-gray part of the "marbled" zone described by the crew. May also include material from the small patch of light sediment visible in the presampling trench photograph (fig. 109).

*Petrographic description:* 73260-64, dominantly fine-grained breccia and (or) metaclastic rock, some glass, and agglutinate.

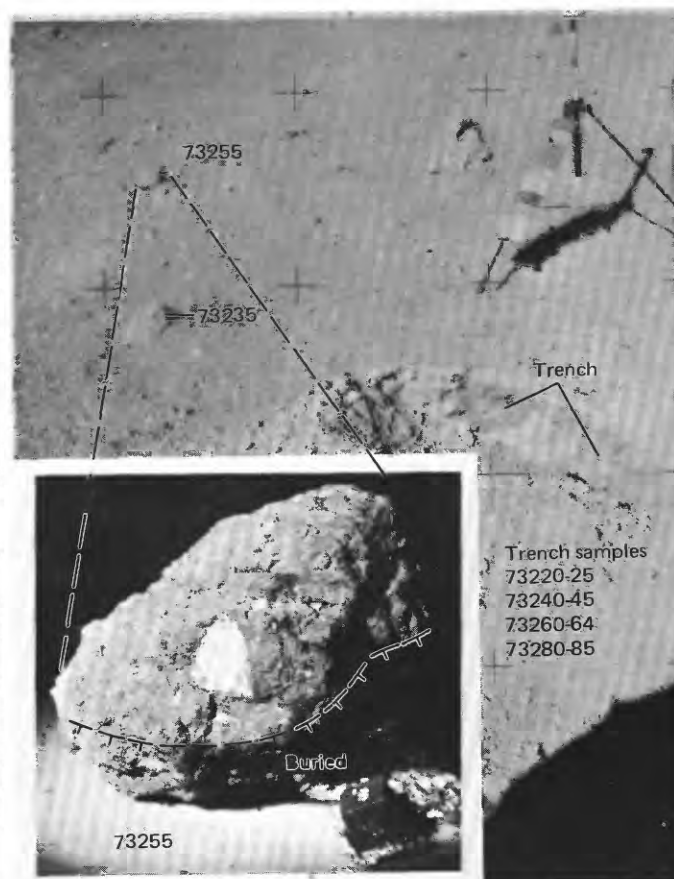


FIGURE 111.—Trench at station 3 from which samples 73220-25, 73240-45, 73260-64, and 73280-85 had been collected and samples 73235 and 73255 before collection. Inset shows 73255 with reconstructed lunar surface orientation and lighting. (NASA photographs AS17-138-21148; S-73-19592.)

*Components of 90-150- $\mu$ m fraction of 73261.1 (Heiken and McKay, 1974)*

Components	Volume percent
Agglutinate.....	34.3
Basalt, equigranular } .....	2.0
Basalt, variolitic } .....	
Breccia:	
Low grade <sup>1</sup> - brown.....	18.7
Low grade <sup>1</sup> - colorless.....	4.7
Medium to high grade <sup>2</sup> .....	15.7
Anorthosite.....	.3
Cataclastic anorthosite <sup>1</sup> .....	1.6
Norite.....	..
Gabbro.....	..
Plagioclase.....	9.7
Clinopyroxene.....	7.0
Orthopyroxene.....	..
Olivine.....	..
Ilmenite.....	.6
Glass:	
Orange.....	1.7
"Black".....	.6
Colorless.....	.6
Brown.....	1.3
Gray, "ropy".....	1.0
Other.....	..
Total number grains.....	300

<sup>1</sup>Metamorphic groups 1-3 of Warner (1972).<sup>2</sup>Metamorphic groups 4-8 of Warner (1972).

Includes crushed or shocked feldspar grains.

*Major-element composition:**Chemical analyses of 73261*

	1	2	3
SiO <sub>2</sub> .....	44.71	45.1	44.9
Al <sub>2</sub> O <sub>3</sub> .....	19.69	20.2	19.9
FeO.....	8.86	8.84	8.85
MgO.....	10.95	9.65	10.30
CaO.....	12.90	12.7	12.8
Na <sub>2</sub> O.....	.40	.458	.43
K <sub>2</sub> O.....	.16	.151	.16
TiO <sub>2</sub> .....	1.90	1.82	1.86
P <sub>2</sub> O <sub>5</sub> .....	.14	.134	.14
MnO.....	.11	.117	.11
Cr <sub>2</sub> O <sub>3</sub> .....	.24	.212	.23
Total.....	100.06	99.382	99.68

1. 73261.14 (Rose and others, 1974).

2. 73261.17 (Wanke and others, 1974).

3. Average of 1 and 2.

*Exposure age:* <sup>22</sup>Na-<sup>26</sup>Al: 73261, maximum  $1.8 \pm 0.8$  m.y. (Yokoyama and others, 1976).

## Sample 73275

*Type:* Metaclastic, with a granoblastic matrix.*Size:* 10×7×7 cm.*Weight:* 429.6 g.*Location:* From surface on rim of 10-m crater at station 3.*Illustrations:* Pan 16; figures 102, 110, 115 (LRL).*Comments:* Ejected from 10-m crater.*Petrographic description:* Metaclastic rock with clasts of plagioclase, pyroxene, olivine, and scarce 2- and 3-grain lithic clasts of plagioclase, pyroxene, and

olivine in a fine-grained granoblastic matrix.

*Major-element composition:**Chemical analysis of 73275*

SiO <sub>2</sub> .....	46.16
Al <sub>2</sub> O <sub>3</sub> .....	18.49
FeO.....	9.05
MgO.....	11.54
CaO.....	11.30
Na <sub>2</sub> O.....	.67
K <sub>2</sub> O.....	.27
TiO <sub>2</sub> .....	1.43
P <sub>2</sub> O <sub>5</sub> .....	.26
MnO.....	.13
Cr <sub>2</sub> O <sub>3</sub> .....	..
Total.....	99.30

73275.30 (Rhodes and others, 1974).

*Age:* <sup>40</sup>-<sup>39</sup>Ar: 73275,22,  $3.96 \pm 0.05$  b.y. (Turner and Cadogan, 1975).*Exposure age:*

Ar: 160 m.y. (Turner and Cadogan, 1975).

Kr: 139 m.y. (Croaz and others, 1974).

Tracks:  $4.7 \pm 1$  m.y. (Croaz and others, 1974).

## Sample 73280-85

*Type:* Sedimentary, unconsolidated (73280-84) and breccia fragment (73285).*Size:* 73285, 2.5×1×1 cm.*Weight:* 73280-84, 166.55 g; 73285, 2.58 g.*Depth:* About 5-10 cm below surface in trench.*Location:* From trench on rim of 10-m crater at station 3.*Illustrations:* Pan 16; figures 109, 110.*Comments:* The white part of the "marbled" zone described by the crew.*Petrographic description:* 73280-84, dominantly fine-grained breccia and (or) metaclastic(?) rock, some fine-grained feldspathic cataclasite.*Components of 90-150- $\mu$ m fraction of 73281.1 (Heiken and McKay, 1974)*

Components	Volume percent
Agglutinate.....	24.6
Basalt, equigranular } .....	3.7
Basalt, variolitic } .....	
Breccia:	
Low grade <sup>1</sup> - brown.....	23.7
Low grade <sup>1</sup> - colorless.....	2.3
Medium to high grade <sup>2</sup> .....	20.6
Anorthosite.....	.3
Cataclastic anorthosite <sup>1</sup> .....	1.6
Norite.....	..
Gabbro.....	..
Plagioclase.....	9.3
Clinopyroxene.....	.3
Orthopyroxene.....	Trace
Olivine.....	.3
Ilmenite.....	1.3
Glass:	
Orange.....	1.3
"Black".....	.3
Colorless.....	.6

*Components of 90-150- $\mu$ m fraction of 73281,1 (Heiken and McKay, 1974)—Continued*

Components	Volume percent
Glass—Continued	
Brown .....	2.0
Gray, "ropy" .....	.3
Other .....	..
Total number grains .....	300

<sup>1</sup>Metamorphic groups 1-3 of Warner (1972).

<sup>2</sup>Metamorphic groups 4-8 of Warner (1972).

<sup>3</sup>Includes crushed or shocked feldspar grains.

*Major-element composition:*

*Chemical analyses of 73281*

	1	2	3
SiO <sub>2</sub> .....	45.31	46.0	45.7
Al <sub>2</sub> O <sub>3</sub> .....	20.23	20.8	20.5
FeO .....	8.82	8.54	8.68
MgO .....	9.95	9.98	9.96
CaO .....	12.91	11.8	12.4
Na <sub>2</sub> O .....	.41	.445	.43
K <sub>2</sub> O .....	.16	.137	.15
TiO <sub>2</sub> .....	1.76	1.75	1.76
P <sub>2</sub> O <sub>5</sub> .....	.14	..	.14
MnO .....	.11	.110	.11
Cr <sub>2</sub> O <sub>3</sub> .....	.27	.206	.24
Total .....	100.07	99.768	100.07

1. 73281,12 (Rose and others, 1974).

2. 73281,18 (Wänke and others, 1974).

3. Average of 1 and 2.

*Exposure age:* <sup>22</sup>Na-<sup>26</sup>Al: 73281, maximum  $1.1 \pm 0.3$  m.y. (Yokoyama and others, 1976).

**STATION LRV-5**

**LOCATION**

Station LRV-5 is located on the light mantle 700 m northeast of station 3 (fig. 7A).

**OBJECTIVES**

Station LRV-5 was an unplanned LRV stop to sample a crater with abundant fragmental ejecta.

**GENERAL OBSERVATIONS**

The station area is flat to gently rolling with scattered craters up to 15 m in diameter (fig. 116). Most of the craters are subdued or have only slightly raised rims. The one exception is the 15-m crater whose ejecta was sampled. That crater has a raised blocky rim, a high concentration of blocks and fragments on the inner crater wall, and a very blocky ejecta blanket.

Rock fragments or clods range in size from 1 to 50 cm and cover 15 to 20 percent of the ejecta blanket surface. The fragments are dominantly angular and partially buried. No fillets are visible in the photographs.

The LRV sample was collected from the ejecta blanket less than one crater diameter from the rim of the

blocky crater.

**SUMMARY OF SAMPLING**

**Sample 74110-19**

*Type:* Sedimentary, unconsolidated (74110-14) and sedimentary, weakly lithified polymict breccia (74115-19).

*Size:* Not available.

*Weight:* 74110-14, 245.41 g; 74115-19, 37.11 g total.

*Location:* From the ejecta blanket of a 15-m crater in the light mantle at station LRV-5.

*Illustration:* Figure 116.

*Comments:* Samples represent light mantle material.

The polymict breccia (74115-19) represents the abundant blocks of the crater ejecta, which were probably indurated by the impact that formed the 15-m crater.

*Petrographic descriptions:*

74110-14, dominantly breccia of several types, fine-grained feldspathic cataclasite, agglutinate, and glass.

74115, 16, polymict breccia with clasts of metaclastic rock, fine-grained breccia, orange glass, and mineral debris in a fine-grained friable matrix.

**STATION LRV-6**

**LOCATION**

Station LRV-6 is located on the light mantle about 1.1 km northeast of station 3 (fig. 7A).

**OBJECTIVES**

Station LRV-6 was a planned LRV stop to sample the light mantle.

**GENERAL OBSERVATIONS**

The station area is flat to gently rolling with scattered craters up to 30 m in diameter. Craters from 5 cm to 2 m are most common; they are mainly shallow and subdued (fig. 117). The surface is saturated with craters less than 5 cm across.

There are scattered rock fragments 1-5 cm in size and a few larger fragments and boulders up to 1 or 2 m in size. Fragments are either perched on the surface or are only slightly buried. Fillets are poorly developed.

**SUMMARY OF SAMPLING**

**Sample 74120-24**

*Type:* Sedimentary, unconsolidated.

*Weight:* 385.87 g.

*Depth:* From the upper few centimeters.

**Location:** Light mantle at station LRV-6.

**Illustration:** Figure 117.

**Comments:** Highlands material is dominant (fig. 118), although there is a slightly greater admixture of valley-floor material at station LRV-6 than in sediment samples from closer to the South Massif.

**Petrographic description:** 74120-24, dominantly breccia of several types, metaclastic(?) rock, agglutinate, possibly some basalt.

*Components of 90-150- $\mu$ m fraction of 74121.12 (Heiken and McKay, 1974)*

Components	Volume percent
Agglutinate.....	51.7
Basalt, equigranular.....	2.0
Basalt, variolitic.....	..
Breccia:	
Low grade <sup>1</sup> - brown.....	7.0
Low grade <sup>1</sup> - colorless.....	5.7
Medium to high grade <sup>2</sup> .....	12.0
Anorthosite.....	.7
Cataclastic anorthosite <sup>1</sup> .....	.7
Norite.....	.7
Gabbro.....	..
Plagioclase.....	7.3
Clinopyroxene.....	3.7
Orthopyroxene.....	1.0
Olivine.....	.3
Ilmenite.....	.7
Glass:	
Orange.....	.3
"Black".....	2.3
Colorless.....	1.7
Brown.....	1.8
Gray, "ropy".....	..
Other.....	.3
Total number grains.....	300

<sup>1</sup>Metamorphic groups 1-3 of Warner (1972).

<sup>2</sup>Metamorphic groups 4-8 of Warner (1972).

<sup>3</sup>Includes crushed or shocked feldspar grains.

### Major-element composition:

*Chemical analyses of 74121*

	1	2	3	4	5
SiO <sub>2</sub> .....	43.51	44.51	44.9	44.9	44.5
Al <sub>2</sub> O <sub>3</sub> .....	19.41	19.36	18.75	18.97	19.12
FeO.....	10.00	10.24	10.43	10.34	10.25
MgO.....	9.84	9.93	10.20	9.86	9.96
CaO.....	12.11	12.44	11.73	12.2	12.1
Na <sub>2</sub> O.....	.31	.40	.44	.427	.39
K <sub>2</sub> O.....	.19	.134	.136	.135	.15
TiO <sub>2</sub> .....	2.58	2.56	2.47	2.57	2.54
P <sub>2</sub> O <sub>5</sub> .....	.11	.136	.120	.117	.12
MnO.....	.18	.132	.128	.134	.14
Cr <sub>2</sub> O <sub>3</sub> .....	.29	.269	.23	.248	.26
Total.....	98.53	100.111	99.53	99.901	99.53

1. 74121 (Mason and others, 1974).

2. 74121.2 (Duncan and others, 1974).

3. 74121.16 (Nava, 1974).

4. 74121.18 (Wänke and others, 1974).

5. Average of 1 through 4.

### STATION 4

#### LOCATION

Station 4 is located on the southern rim crest of the 110-m crater, Shorty, near the northern terminus of the light mantle (fig. 7A; pl. 2).

### OBJECTIVES

Analysis of orbital photographs before the mission suggested that Shorty is a young, rayed, dark-haloed crater formed by an impact that excavated thick dark mantle material from below the light mantle. An alternate hypothesis was that Shorty is a volcanic vent that produced a small amount of dark mantle material after the emplacement of the light mantle. Observation and sampling were planned to examine Shorty crater, to determine its origin, to sample its ejecta, and to examine the distal end of the light mantle and sample its variety of rock types. Because of shortage of time and because of the unique character of the materials found at Shorty, observation and sampling were confined to the crater rim.

### GENERAL OBSERVATIONS

Shorty crater has the distinctly raised rim that characterizes the younger impact craters at the Taurus-Littrow site. Its floor is hummocky, with a low central mound and with marginal hummocks that resemble slumps forming discontinuous benches along the lower parts of the crater wall. The central mound is blocky and jagged as are the marginal hummocks or benches.

The walls, rim, and ejecta blanket consist largely of dark material that is much finer grained than the crater floor materials, although blocks occur locally on the crater wall and rim. The dark ejecta blanket is similar in albedo to the nearby dark parts of the valley floor. Fragments up to about 15 cm in diameter cover less than 3 percent of the surface on the crater rim. Scattered larger blocks reach more than 5 m in size. Rock burial ranges from none to almost complete. The rocks range in shape from angular to subrounded. Some of them are filleted, especially on the upslope sides of a few of the larger boulders on the crater walls.

Small craters up to several meters in diameter with rims ranging from sharp to subdued are scattered around the rim and flanks of Shorty crater. Their ejecta are no blockier, except for clods, than the adjacent surfaces.

Samples were collected from a low place on the southern rim crest of Shorty just east of a 5-m boulder of fractured basalt (figs. 119 and 120; pans 17 and 18, pl. 6). Debris that may have been shed from the boulder lies on the nearby surface, and blocks are abundant on this part of the inner crater wall. All of the rocks examined are basalt. They are commonly intensely fractured and some show irregular knobby surfaces that resemble the surfaces of terrestrial flow breccias.

A trench dug in the rim crest exposed orange volcanic ash buried beneath a one-half-cm-thick layer

of gray sediment typical of the general surface material at the station. The orange ash forms a 1-meter-wide unit that trends parallel to the crater rim crest for about 2 m. Color zoning within the ash, as seen in the trench, occurs as 10-cm-wide yellowish bands along the margins of the orange deposit. The yellow bands are in steep sharp contact with gray sediment exposed at each end of the trench, and they grade inward to the more reddish ash that makes up the major part of the zone. A drive tube in the axial part of the colored zone bottomed in black ash. Similar orange material has been excavated by a small fresh crater high on the northwest interior wall of Shorty and perhaps also on the rim crest a short distance southeast of the LRV.

Samples included three sediment samples from the

trench, a double drive tube 69.2 cm deep, two rock samples broken from boulders, and one ejecta fragment from the surface of the crater rim.

#### GEOLOGIC DISCUSSION

Cratering experiments have shown that craters with flat floors or central mounds may form in targets where unconsolidated material overlies coherent material; the difference in elevation between the precrater surface and the crater floor in such craters is approximately equivalent to the thickness of the unconsolidated layer (Oberbeck and Quaide, 1967; Quaide and Oberbeck, 1968). Topographic profiles made by analytical stereoplotter show that the rocky floor of Shorty crater is approximately 14 m lower than the precrater



FIGURE 112.—Sample 73235. Polymict breccia with cataclastic matrix. (NASA photograph S-73-16961.)

surface. Applying the experimental results and noting the blockiness of the crater floor and the occurrence of a few basalt blocks on the rim, we suggest that the sub-floor basalt in the Shorty target area was overlain by about 14 m of unconsolidated or poorly consolidated material.

The overburden consisted, in ascending order, of volcanic ash, older regolith of the valley floor, and light

mantle. We interpret the volcanic ash of the trench and double drive tube as a clod of ejecta excavated from a remnant of an ash blanket deposited on the surface of the subfloor basalt about 3.5 b.y. ago. The light-gray sediment of the trench is typical (fig. 121) of the mixture of highlands and valley floor debris that makes up

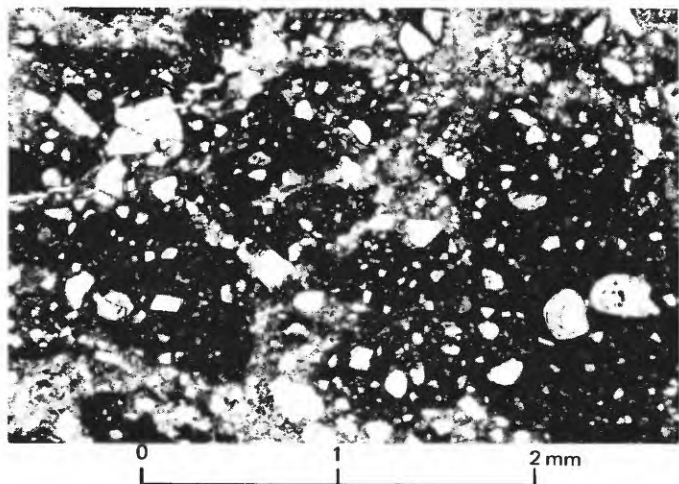


FIGURE 113.—Sample 73235. Photomicrograph showing clasts of aphanitic breccia in matrix of broken, dominantly feldspathic mineral debris.

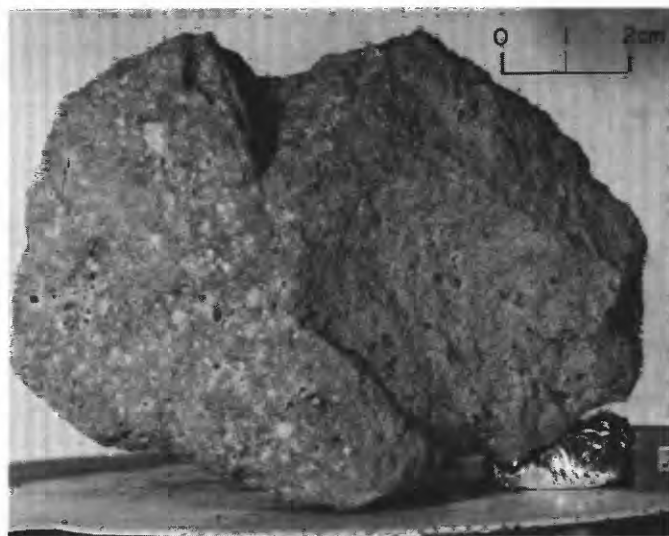


FIGURE 115.—Sample 73275. Metaclastic rock with granoblastic matrix. (NASA photograph S-73-16929.)

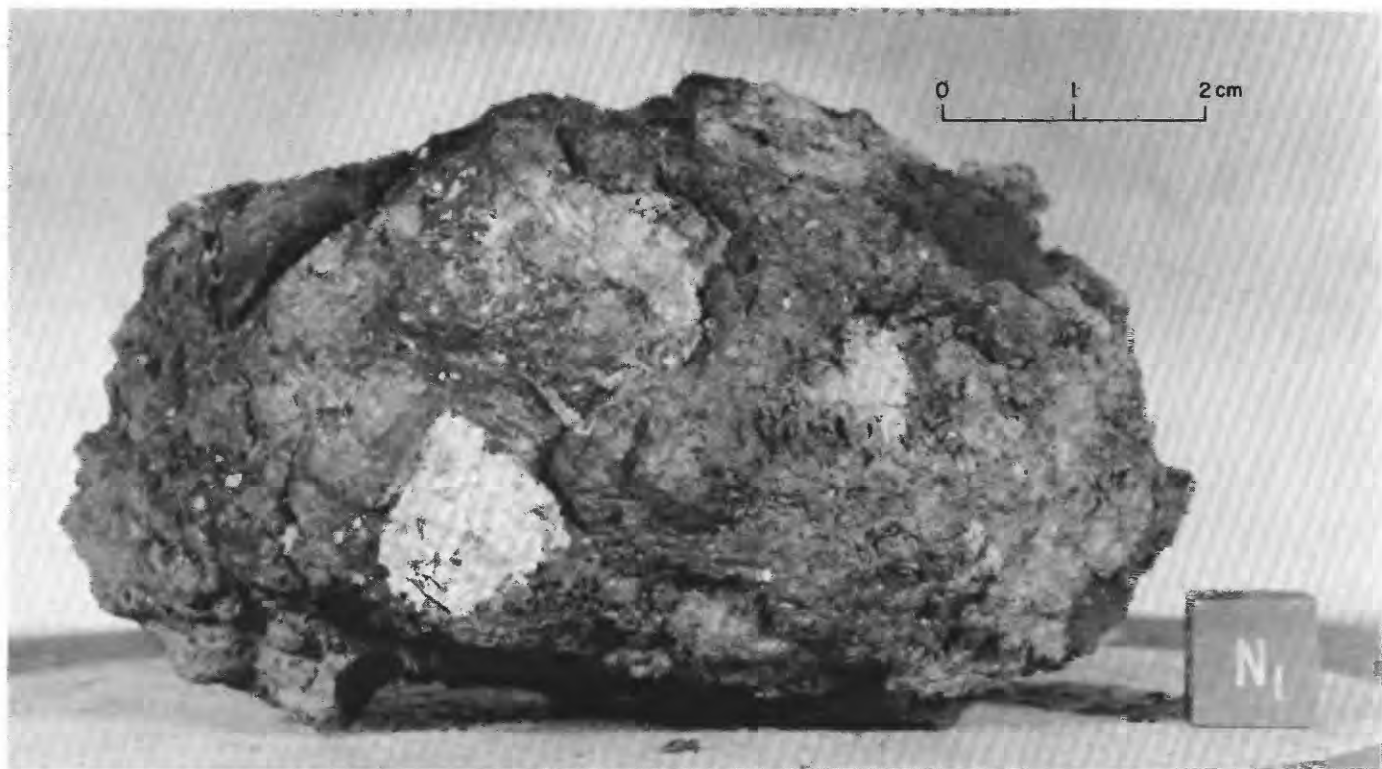


FIGURE 114.—Sample 73255. Polymict breccia with aphanitic matrix. (NASA photograph S-73-16951.)

the older regolith of the valley floor. Light mantle, which was at the surface where Shorty formed, is not recognized in the samples. It presumably is buried within the ejecta by material excavated from greater depth.

On the basis of major-element composition, station 4 basalt is generally similar to that from the LM and station 1. However, on the basis of trace-element distributions, particularly the uniquely low Ba/Rb ratio, Rhodes and others (1976) concluded that the station 4 basalt samples (74245, 74255, and 74275) were from a distinct flow not sampled at other stations.

Shorty crater was probably excavated between about 10 and 30 m.y. ago. Noble-gas exposure ages determined for the orange volcanic ash and for basalt sample 74275 are about 30 m.y. An exposure age of approximately 17 m.y. was determined for basalt sample 74255. Track ages of about 10 m.y. have been determined for the orange volcanic ash by several investigators, some of whom have suggested that the slightly older noble-gas ages record a brief irradiation of the ash between its initial deposition and subsequent burial about 3.5 b.y. ago.

#### SUMMARY OF SAMPLING

Sample 74002/74001 (upper/lower)

*Type:* Double drive tube.

*Length:* 69.2 cm (74001, 35.7 cm; 74002, 33.5 cm).

*Depth:* Approximately 71 cm.

*Weight:* 1,981.6 g net.

*Location:* East of 5-m boulder on south rim of Shorty crater.

*Illustrations:* Pans 17, 18; figures 120, 122, 122.1.

*Comments:* The cored material is unusually compact.

The lower tube (74001) has recently been opened and consists of poorly bedded layers of black ash (G. H. Heiken, written commun., 1977). The contact between the black ash and the overlying orange ash, which is exposed in the trench, occurs within the upper drive tube (74002) at a depth estimated from the debris smeared on the exterior of the tube to be approximately 25 cm (fig. 122). The ash on the crater rim probably represents a clod of ejecta excavated in the Shorty impact from remnants of a once-continuous ash deposit overlying the subfloor basalt.

*Petrographic description:* (bottom of lower drive tube) volcanic ash, fine-grained, dark to opaque and black spheres and conchoidal fragments.

*Components of 90-150- $\mu$ m fraction of 74001,2 (bottom of double drive tube) (Heiken and McKay, 1974)*

Components	Volume percent
Agglutinate.....	--
Basalt, equigranular.....	--
Basalt, variolitic.....	--
Breccia:	
Low grade <sup>1</sup> - brown.....	--
Low grade <sup>1</sup> - colorless.....	--
Medium to high grade <sup>2</sup> .....	--

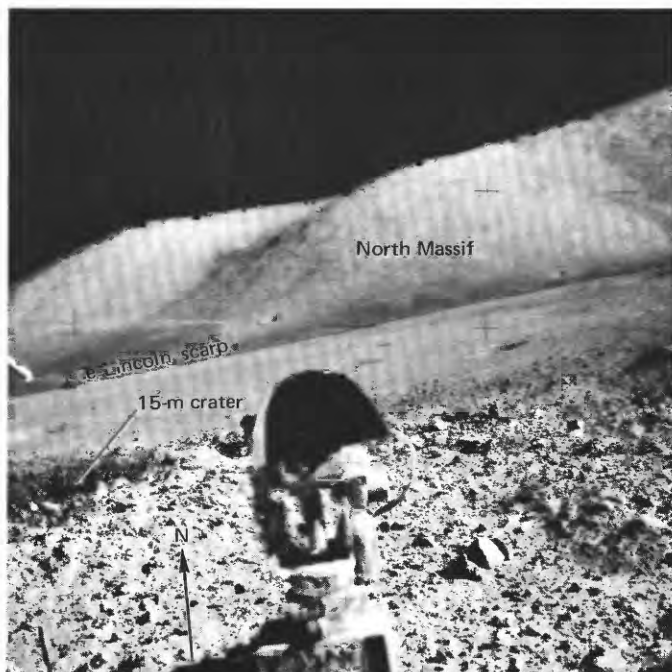


FIGURE 116.—Station LRV-5 area before sampling. Sample 74110-19 was probably collected from blocky ejecta in near field. (NASA photograph AS17-133-20208.)



FIGURE 117.—Station LRV-6 area. Sample 74120-24 may have been collected in near-field area of this view. (NASA photograph AS17-133-20212.)

Components of 90-150- $\mu$ m fraction of 74001.2 (bottom of double drive tube) (Heiken and McKay, 1974)—Continued

Components	Volume percent
Anorthosite.....	..
Cataclastic anorthosite <sup>1</sup> .....	..
Norite.....	..
Gabbro.....	..
Plagioclase.....	1.6
Clinopyroxene.....	.3
Orthopyroxene.....	..
Olivine.....	..
Ilmenite.....	..
Glass:	
Orange.....	8.0
"Black".....	73.3
Colorless.....	..
Brown.....	16.6
Gray, "ropy".....	..
Other.....	..
Total number grains.....	300

<sup>1</sup>Metamorphic groups 1-3 of Warner (1972).

<sup>2</sup>Metamorphic groups 4-8 of Warner (1972).

<sup>3</sup>Includes crushed or shocked feldspar grains.

### Major-element composition:

Chemical analyses of 74001 (Heiken and others, 1974)

	1	2	3	4	5	6
SiO <sub>2</sub> .....	39.38	38.38	39.14	38.61	38.16	38.73
Al <sub>2</sub> O <sub>3</sub> .....	6.06	5.91	5.82	6.33	5.78	5.98
FeO.....	22.44	22.25	23.29	22.84	22.16	22.60
MgO.....	10.29	14.87	14.54	16.16	15.12	14.20
CaO.....	9.55	7.40	7.32	7.08	7.29	7.73
Na <sub>2</sub> O.....	.32	.40	.37	.25	.40	.35
K <sub>2</sub> O.....	.06	.07	.07	.06	.08	.07
TiO <sub>2</sub> .....	10.34	9.19	9.03	9.81	8.95	9.46
P <sub>2</sub> O <sub>5</sub> .....	..	..	..	..	..	..
MnO.....	..	..	..	..	..	..
Cr <sub>2</sub> O <sub>3</sub> .....	.56	.59	.54	.71	.56	.59
Total.....	99.00	99.06	100.12	101.85	98.50	99.71

1. 74001.2-4, black droplets, 95 percent crystallized.

2. 74001.2-5, clear orange glass.

3. 74001.2-6, surface droplets.

4. 74001.2-7, surface droplets.

5. 74001.2-8, clear orange glass.

6. Average of 1 through 5.

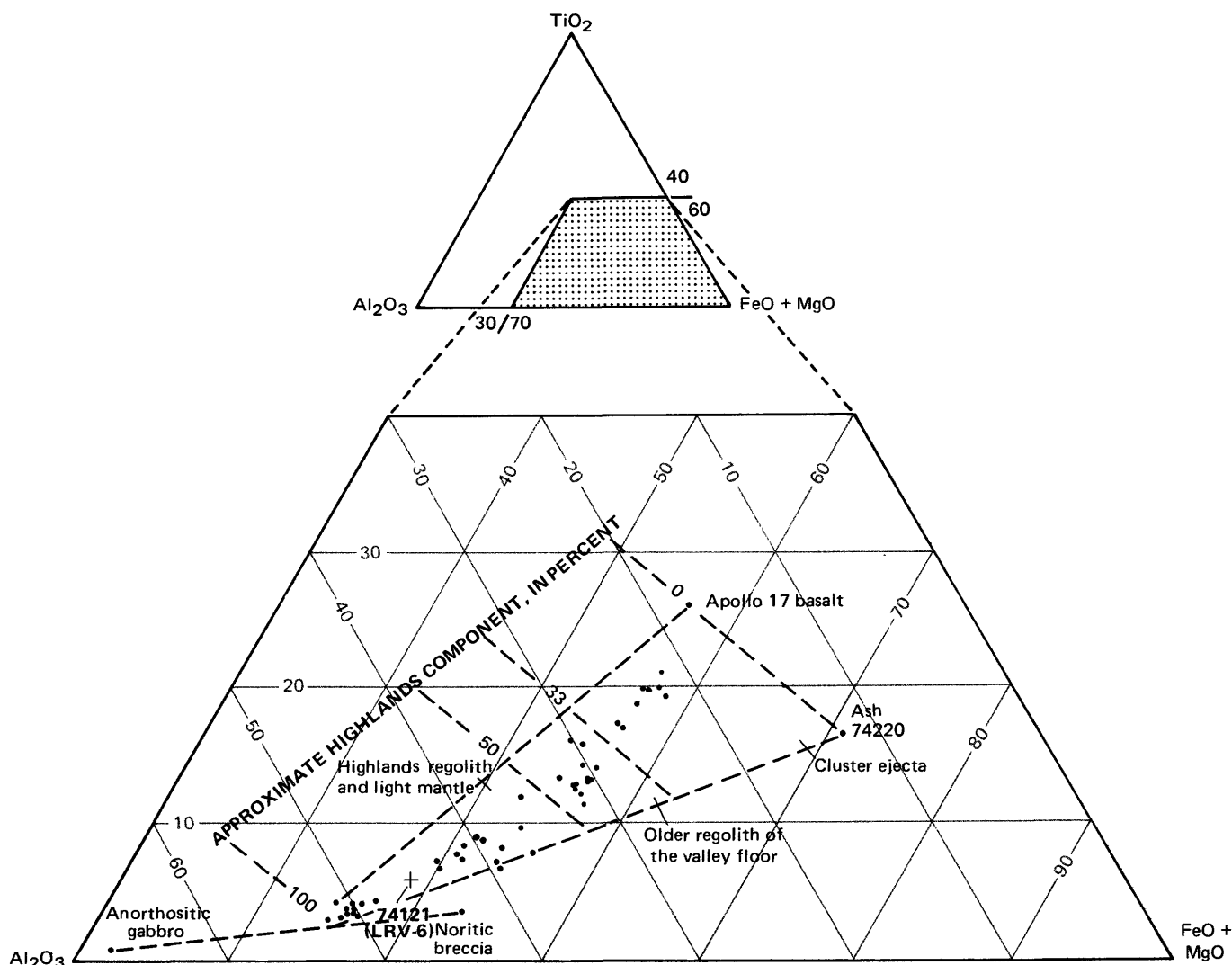


FIGURE 118.—Relative amounts of TiO<sub>2</sub>, Al<sub>2</sub>O<sub>3</sub>, and FeO+MgO in sediment sample 74121 (cross), collected at station LRV-6, in comparison with sediment samples from rest of traverse region (dots).

*Exposure age:* Ne and Ar: 45 m.y. on sample from bottom of double drive tube at approximately 70 cm depth (Eberhardt and others, 1974).

#### Sample 74220

*Type:* Volcanic ash.

*Weight:* 1,180 g.

*Depth:* 5-8 cm.

*Location:* From center of meter-long trench east of the 5-m boulder on the south rim of Shorty crater.

*Illustrations:* Pans 17, 18; figures 120, 122, 123 (photomicrograph).

*Comments:* The reddish zone in the trench, about 80 cm wide, grades laterally into yellowish zones, each about 10 cm wide. These are in turn in sharp steep contact with light-gray sediment exposed at each end of the trench. Figure 122 shows the inferred relations between the materials of the trench and double drive tube (74002/74001). The ash is more coherent than normal sediment from the regolith surface; it has fractured, in the trench wall, to form chunks 1 to 6 cm long. Some of the chunks are color zoned, becoming darker inward, within the outer 2 cm (Butler, 1973).

Orange and black ash of the trench and double drive tube are interpreted as samples of weakly indurated ash from an ejected clod that was deposited on the rim of Shorty during formation of the crater. Presumably the clod was excavated from a layer of

ash that once formed a continuous deposit overlying the subfloor basalt.

*Petrographic description:* Poorly consolidated ash composed of orange glass spherules and partly crystallized spherules and glass shards.

*Components of 90-150- $\mu$ m fraction of 74220 (Heiken and McKay, 1974)*

Components	Volume percent	
	1	2
Agglutinate .....	1.3	2.7
Basalt, equigranular) {	1.6	2.0
Basalt, variolitic {		
Breccia:		
Low grade <sup>1</sup> - brown .....	.3	..
Low grade <sup>1</sup> - colorless .....	..	1.3
Medium to high grade <sup>2</sup> .....	..	..
Anorthosite .....	..	..
Cataclastic anorthosite <sup>1</sup> .....	..	..
Norite .....	..	..
Gabbro .....	..	..
Plagioclase .....	..	1.0
Clinopyroxene .....	.3	.3
Orthopyroxene .....	..	..
Olivine .....	..	..
Ilmenite .....	..	.3
Glass:		
Orange .....	66.3	83.6
"Black" .....	29.3	6.7
Colorless .....	.3	..
Brown .....	..	1.3
Gray, "ropy" .....	..	.7
Other .....	..	..
Total number grains .....	300	300

<sup>1</sup>Metamorphic groups 1-3 of Warner (1972).

<sup>2</sup>Metamorphic groups 4-8 of Warner (1972).

<sup>3</sup>Includes crushed or shocked feldspar grains.

1. 74220.6

2. 74220.82

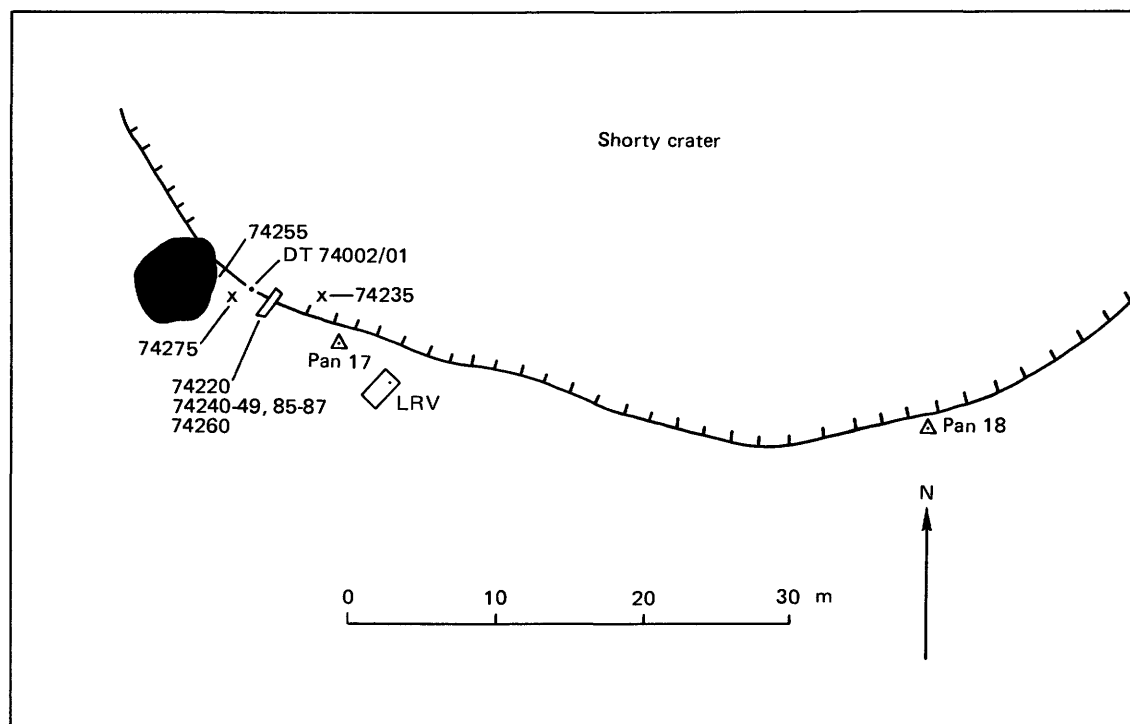


FIGURE 119.—Planimetric map of station 4.

Modes are from loose material around the clods and show contamination from thin surface sediment layer. Thin sections of a clod show 100 percent orange glass or its equivalent, the partly crystallized black spheres (G. H. Heiken, written commun., 1977).

#### Major-element composition:

##### Chemical analyses of 74220

	1	2	3	4	5	6
SiO <sub>2</sub> .....	38.55	38.0	39.4	39.13	39.5	37.6 -43.5
Al <sub>2</sub> O <sub>3</sub> .....	5.85	5.51	6.02	6.18	6.0	1.49 -9.05
FeO.....	21.96	22.4	22.7	22.38	23.0	22.0 -24.8
MgO.....	14.99	14.5	15.5	16.79	15.5	5.08 -35.3
CaO.....	7.16	6.99	6.42	6.94	6.5	1.33 -10.6
Na <sub>2</sub> O.....	.33	.39	.69	.34	.65	.19 -1.03
K <sub>2</sub> O.....	..	.06	.0	.03	.0	.0 -0.7
TiO <sub>2</sub> .....	8.87	8.87	9.30	8.33	9.0	2.32 -13.7
P <sub>2</sub> O <sub>5</sub> .....	..	..	..	..	..	.. ..
MnO.....	..	..	.30	..	.28	.05 -.48
Cr <sub>2</sub> O <sub>3</sub> .....	.55	.70	..	.53	..	.. ..
Total	98.26	97.42	100.33	100.65	100.43	

	7	8	9	10	11	12
SiO <sub>2</sub> .....	38.57	39.03	39.4	38.9	39.0	38.6
Al <sub>2</sub> O <sub>3</sub> .....	6.32	6.47	6.52	6.38	6.42	5.79
FeO.....	22.04	22.13	21.9	22.34	22.1	22.4
MgO.....	14.44	14.44	14.01	14.76	14.41	15.0
CaO.....	7.68	7.62	7.4	7.01	7.4	6.86
Na <sub>2</sub> O.....	.36	.34	.396	.43	.38	.47
K <sub>2</sub> O.....	.09	.077	.076	.076	.80	.03
TiO <sub>2</sub> .....	8.81	8.72	8.09	8.96	8.64	9.01
P <sub>2</sub> O <sub>5</sub> .....	.04	.043	.048	.097	.06	..
MnO.....	.30	.273	.252	.255	.27	.3
Cr <sub>2</sub> O <sub>3</sub> .....	.75	.684	.589	.68	.68	.62
Total.....	99.40	99.827	98.681	99.89	100.16	99.08

1. 74220, microprobe analyses of orange glass, 47 analyses of relatively homogeneous orange glass; largest standard deviation, for MgO, is 0.44 (Reid and others, 1973).
2. 74220.87, microprobe analyses of orange glass, 16 analyses (Carter and others, 1973).
3. 74220.89, microprobe analyses of orange glass, 19 analyses (Glass, 1973).
4. 74220, microprobe analyses of black opaque crystalline fragments, 33 analyses of relatively heterogeneous fragments (larger standard deviations are: Al<sub>2</sub>O<sub>3</sub>, 1.05; MgO, 4.79; CaO, 1.45; TiO<sub>2</sub>, 1.64). Average (column 4) is similar to orange glass values (Reid and others, 1973).
5. 74220.89, mode of 40 microprobe analyses of heterogeneous black opaque fragments; modal value is similar to composition of orange glass; heterogeneity interpreted as due to addition or subtraction of olivine (Glass, 1973).
6. 74220.89, ranges for values given in column 5.
7. 74220.3, bulk sample (Apollo 17 PET, 1973).
8. 74220.31, bulk sample (Duncan and others, 1974).
9. 74220.36, bulk sample (Wanke and others, 1973).
10. 74220.40, bulk sample (Nava, 1974).
11. Average for bulk sample, columns 7 through 10.
12. Average for orange glass, columns 1 through 3.

#### Age:

##### <sup>40</sup>Ar:

74220,39, 3.71±0.06 b.y. (Husain and Schaeffer, 1973).

74220, 3.67 b.y., mean of four determinations ranging from 3.60 to 3.71 b.y. (Eberhardt and others, 1973).

##### K-Ar:

74220,47, 3.5±0.3 b.y. (Hintenberger and Weber, 1973).

##### Fission track:

74220, 3.7 b.y. (Hutcheon and others, 1974b).

##### U-Pb:

74220, 3.63 b.y. (Tatsumoto and others, 1973).

##### Pb-Pb:

74220, 3.48±0.03 b.y.; determined for carefully separated and cleaned glass spheres; determinations of greater age (above) attributed to Ar entrapment and Pb contamination by components other than orange glass in 74220 (Tera and Wasserburg, 1976).

##### Exposure age:

##### Ar:

74220,13, 30±6 m.y. (Huneke and others, 1973).

74220,15, 30 m.y. (Eberhardt and others, 1974).

74220,39, 32±4 m.y. (Husain and Schaeffer, 1973).

74220, 30 m.y. (Kirsten and others, 1973).

##### Ne:

74220, 29 m.y. (Kirsten and others, 1973).

##### Tracks:

74220, 20-35 m.y. maximum residence time at 5.0-7.5-cm depth (Fleischer and others, 1974); 4-7 m.y. since last disturbance of material at 5.0-7.5-cm depth suggested by minimum track densities (Fleischer and others, 1974).

74220,68, ~9-11 m.y. (Storzer and others, 1973).

74220, 9.1-13.6 m.y.; inferred as maximum for residence in sampling position; 30-m.y. noble-gas ages (above) interpreted as indicative of two-stage exposure history (Hutcheon and others, 1974b).

74220,10 m.y.; interpreted as age of Shorty Crater (Kirsten and others, 1973); 30-m.y. rare-gas ages (above) may imply brief period of irradiation immediately after initial deposition on the lunar surface (~3.5 b.y. ago).

##### Sample 74235

Type: Olivine basalt.

Size: 4.3×3.4×3.3 cm.

Weight: 59.04 g.

Location: East of the 5-m boulder on the south rim of Shorty crater.

Illustrations: Pans 17, 18; figure 124 (photomicrograph).

Comments: Ejecta fragment.

**Petrographic description:** Very fine grained vesicular olivine basalt. Quench olivine in variolitic groundmass of abundant opaque needles and intergrowths of pyroxene and plagioclase.

**Major-element composition:**

*Chemical analyses of 74235*

	1	2	3
SiO <sub>2</sub> .....	39.42	38.62	39.02
Al <sub>2</sub> O <sub>3</sub> .....	9.21	8.61	8.91
FeO.....	18.55	19.31	18.93
MgO.....	8.67	8.35	8.51
CaO.....	10.85	10.70	10.78
Na <sub>2</sub> O.....	.37	.40	.38
K <sub>2</sub> O.....	.08	.07	.08
TiO <sub>2</sub> .....	12.39	12.17	12.28
P <sub>2</sub> O <sub>5</sub> .....	.05	.05	.05
MnO.....	.27	.28	.28
Cr <sub>2</sub> O <sub>3</sub> .....	.47	.51	.49
Total.....	100.33	99.07	99.71

1. 74235.18 (Rose and others, 1975).  
 2. 74235.21 (Rhodes and others, 1976).  
 3. Average of 1 and 2.

**Exposure age:**

Kr: 74235.9,  $188 \pm 20$  m.y. (Eberhardt and others, 1975).

Ar: 74235.9,  $180 \pm 20$  m.y. (Eberhardt and others, 1975).

Sample 74240-49, 85-87

**Type:** Sedimentary, unconsolidated (74240-44), basalt fragments (74245, 47-49, 85-87), and weakly lithified polymict breccia (74246).

**Weight:** 74240-44, 924.32 g; 74245-49, 85-87, 116.66 g.

**Depth:** 5-8 cm.

**Location:** Southwest end of trench on the south rim of Shorty crater.

**Illustrations:** Pans 17, 18; figures 120, 122.

**Comments:** From the gray sediment adjacent to the 1-m-wide band of orange volcanic ash.

**Petrographic descriptions:**

74240-44, dominantly basalt, some glass, minor friable feldspathic clastic rocks.

*Components of 90-150- $\mu$ m fraction of 74240,6 (Heiken and McKay, 1974)*

Components	Volume percent
Agglutinate .....	8.0
Basalt, equigranular { .....	30.0
Basalt, variolitic { .....	
Breccia:	
Low grade <sup>1</sup> - brown .....	1.6
Low grade <sup>1</sup> - colorless .....	13.3
Medium to high grade <sup>2</sup> .....	2.0
Anorthosite .....	..
Cataclastic anorthosite <sup>1</sup> .....	.6
Norite .....	..
Gabbro .....	..
Plagioclase .....	4.6
Clinopyroxene .....	11.3
Orthopyroxene .....	..

*Components of 90-150- $\mu$ m fraction of 74240,6 (Heiken and McKay, 1974)—Continued*

Components	Volume percent
Olivine .....	..
Ilmenite .....	1.3
Glass:	
Orange .....	4.0
"Black" .....	..
Colorless .....	4.6
Brown .....	3.6
Gray, "ropy" .....	14.3
Other .....	.3
Total number grains .....	300

<sup>1</sup>Metamorphic groups 1-3 of Warner (1972).

<sup>2</sup>Metamorphic groups 4-8 of Warner (1972).

<sup>3</sup>Includes crushed or shocked feldspar grains.

74245, aphanitic vesicular olivine basalt.

74246, polymict(?) breccia with clasts of basalt in a fine-grained friable matrix.

74247, aphanitic vesicular olivine(?) basalt.

74248, aphanitic basalt.

**Major-element compositions:**

*Chemical analyses of 74240 and 74241*

	1	2	3	4	5	6
SiO <sub>2</sub> .....	40.78	42.4	42.3	42.00	41.55	42.1
Al <sub>2</sub> O <sub>3</sub> .....	12.54	13.91	13.69	13.19	13.35	13.54
FeO.....	15.84	15.2	14.66	14.84	14.89	14.90
MgO.....	9.15	9.27	9.88	9.17	9.19	9.38
CaO.....	11.36	11.42	10.89	11.56	11.54	11.35
Na <sub>2</sub> O.....	.38	.453	.48	.43	.48	.46
K <sub>2</sub> O.....	.12	.104	.123	.14	.12	.12
TiO <sub>2</sub> .....	8.61	6.49	7.33	7.90	7.45	7.29
P <sub>2</sub> O <sub>5</sub> .....	.09	.099	.124	.10	.10	.11
MnO.....	.24	.192	.202	.20	.22	.20
Cr <sub>2</sub> O <sub>3</sub> .....	.41	.339	.38	.42	.41	.39
Total.....	99.52	99.877	100.06	99.95	99.30	99.84

1. 74240.3 (Apollo 17 PET, 1973).  
 2. 74241.19 (Wänke and others, 1973).  
 3. 74241.20 (Nava, 1974).  
 4. 74241.29 (Rose and others, 1974).  
 5. 74241.50 (Rhodes and others, 1974).  
 6. Average of 2 through 5.

*Chemical analysis of 74245*

SiO <sub>2</sub> .....	38.59
Al <sub>2</sub> O <sub>3</sub> .....	8.72
FeO.....	18.06
MgO.....	9.65
CaO.....	10.59
Na <sub>2</sub> O.....	.36
K <sub>2</sub> O.....	.06
TiO <sub>2</sub> .....	11.92
P <sub>2</sub> O <sub>5</sub> .....	.04
MnO.....	.27
Cr <sub>2</sub> O <sub>3</sub> .....	.54
Total .....	98.80

74245.4-7 (Rhodes and others, 1976).

**Age:**

40-39Ar:

74243.4,A (2-4-mm basalt fragment),  
 $3.78 \pm 0.04$  b.y. (Kirsten and Horn, 1974).

74243.4,C (2-4-mm basalt fragment), 3.93

b.y. interpreted as tentative older age limit (Kirsten and Horn, 1974).

Sample 74255

Type: Olivine basalt.

Size: 13×7×6 cm.

Weight: 737.3 g.

Location: Base of 5-m boulder on south rim of Shorty

crater.

Illustrations: Pans 17, 18; figures 120, 125 (LRL).

Comments: Subfloor basalt.

Petrographic description: Medium-grained vesicular porphyritic olivine basalt. Aggregates of clinopyroxene-ilmenite in a poorly developed subophitic groundmass of plagioclase, clinopyroxene, ilmenite, olivine, and accessory minerals.



FIGURE 120.—Station 4 area showing locations of drive tube (74002/74001), trench samples (74220, 74240-49, 85-87, 74260), and basalt samples 74255 and 74275 before collection. Inset shows 74255 with reconstructed lunar surface orientation and lighting. (NASA photographs AS17-137-20990; S-73-18404.)

*Major-element composition:**Chemical analyses of 74255*

	1	2	3
SiO <sub>2</sub> .....	37.96	38.40	38.18
Al <sub>2</sub> O <sub>3</sub> .....	8.55	8.84	8.70
FeO.....	18.11	17.98	18.04
MgO.....	10.50	10.72	10.61
CaO.....	10.35	10.20	10.28
Na <sub>2</sub> O.....	.36	.37	.36
K <sub>2</sub> O.....	.08	.10	.09
TiO <sub>2</sub> .....	12.17	12.76	12.46
P <sub>2</sub> O <sub>5</sub> .....	.05	.06	.06
MnO.....	.27	.28	.28
Cr <sub>2</sub> O <sub>3</sub> .....	.58	.60	.59
Total.....	98.98	100.31	99.65

1. 74255,25 (Rhodes and others, 1976).  
 2. 74255,42 (Rose and others, 1975).  
 3. Average of 1 and 2.

*Age:**Rb-Sr isochron:*

74255,25,  $3.83 \pm 0.07$  b.y. (Bansal and others, 1975).

74255,25,  $3.70 \pm 0.12$  ( $2\sigma$ ) b.y. (Murthy, 1976).

*Exposure age:* Kr: 74255,18,  $17.3 \pm 1.0$  m.y. (Eberhardt and others, 1975).

Sample 74260

*Type:* Sedimentary, unconsolidated.

*Weight:* 526.7 g.

*Depth:* 5-8 cm.

*Location:* Northeast end of trench on the south rim of

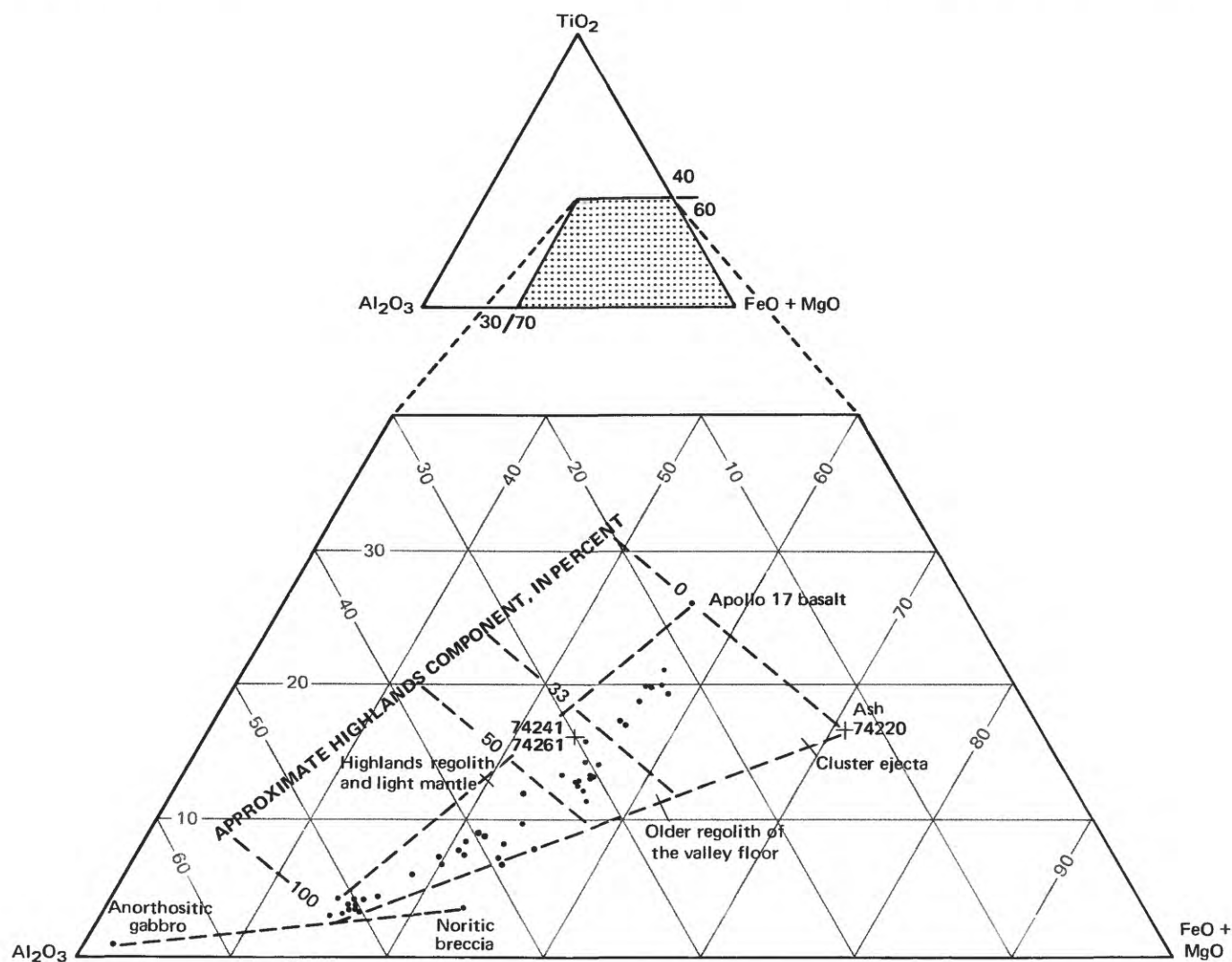


FIGURE 121.—Relative amounts of TiO<sub>2</sub>, Al<sub>2</sub>O<sub>3</sub>, and FeO+MgO in volcanic ash 74220 and sediment samples 74241 and 74261 (crosses), collected from trench at station 4, in comparison with sediment samples from rest of traverse region (dots). Apollo 17 basalt, anorthositic gabbro, and noritic breccia values from Rhodes and others (1974).

**Shorty crater.**

*Illustrations:* Pans 17, 18: figures 120, 122.

*Comments:* From the light-gray sediment northeast of the orange volcanic ash in the trench exposure.

*Petrographic description:* 74260, dominantly basalt, breccia, glass, and agglutinate.

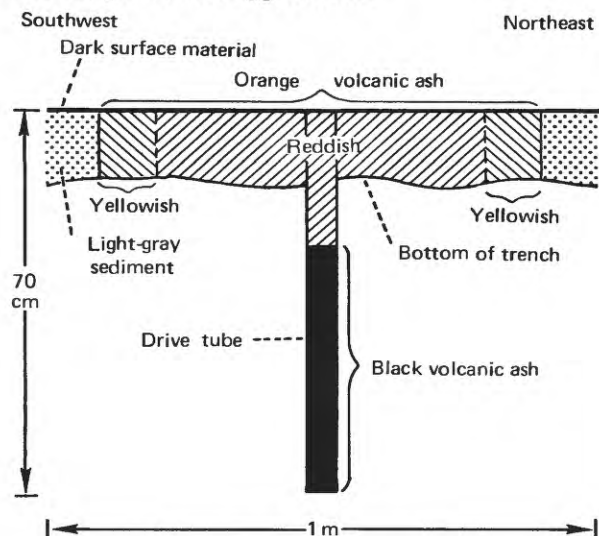


FIGURE 122.—Schematic cross section showing materials in trench and double drive tube on rim crest of Shorty crater (modified from Muehlberger and others, 1973).

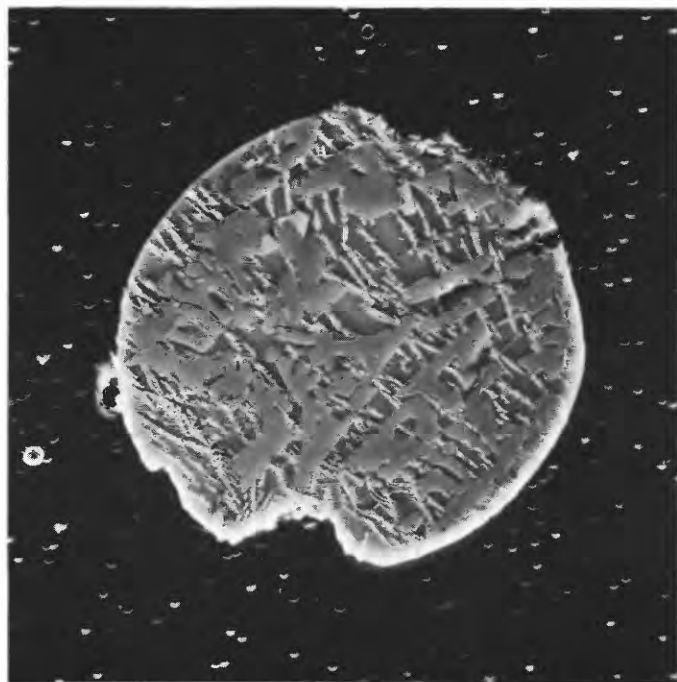


FIGURE 122.1.—Scanning electron micrograph of ion-etched 40-μm sphere from sample 74001.2. Exhibiting a quench texture typical of black droplets, it consists of olivine (largest, best developed crystals) and minor spinel (blocky bright crystals). Low-relief area is orange glass, similar in composition to other orange glass. (NASA photograph S77-21580.)

*Components of 90-150-μm fraction of 74260,5 (Heiken and McKay, 1974)*

Components	Volume percent
Agglutinate.....	7.7
Basalt, equigranular } .....	23.7
Basalt, variolitic } .....	
Breccia:	
Low grade <sup>1</sup> —brown.....	7.4
Low grade <sup>1</sup> —colorless.....	5.4
Medium to high grade <sup>2</sup> .....	3.3
Anorthosite.....	..
Cataclastic anorthosite <sup>3</sup> .....	..
Norite.....	..
Gabbro.....	..
Plagioclase.....	2.7
Clinopyroxene.....	13.7
Orthopyroxene.....	..
Olivine.....	.3
Ilmenite.....	2.3
Glass:	
Orange.....	7.7
"Black".....	2.0
Colorless.....	3.7
Brown.....	1.7
Gray, "ropy".....	18.1
Other.....	.3
Total number grains.....	300

<sup>1</sup>Metamorphic groups 1-3 of Warner (1972).

<sup>2</sup>Metamorphic groups 4-8 of Warner (1972).

<sup>3</sup>Includes crushed or shocked feldspar grains.

*Major-element compositions:*

*Chemical analyses of 74260 and 74261*

	1	2
SiO <sub>2</sub> .....	41.22	42.08
Al <sub>2</sub> O <sub>3</sub> .....	13.25	13.70
FeO.....	15.31	14.96
MgO.....	9.47	9.56
CaO.....	11.37	11.25
Na <sub>2</sub> O.....	.38	.42
K <sub>2</sub> O.....	.12	.13
TiO <sub>2</sub> .....	7.68	7.45
P <sub>2</sub> O <sub>5</sub> .....	.09	.09
MnO.....	.23	.19
Cr <sub>2</sub> O <sub>3</sub> .....	.41	.48
Total.....	99.53	100.31

1. 74260.2 (Apollo 17 PET, 1973).

2. 74261.16 (Rose and others, 1974).

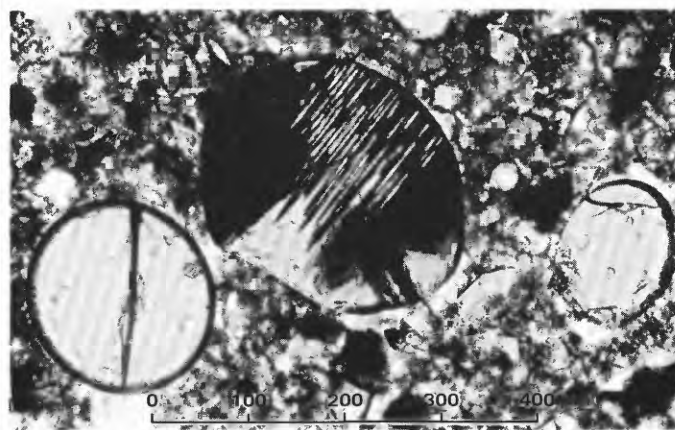


FIGURE 123.—Sample 74220. Photomicrograph showing partly crystallized (to olivine and opaque material) spheres and ellipsoids of orange glass in matrix of orange glass shards.

Sample 74275

Type: Olivine basalt.

Size: 17×12×4 cm.

Weight: 1,493 g.

Location: From 20-cm boulder east of the 5-m boulder on the south rim of Shorty crater.

Illustrations: Pans 17, 18; figures 120, 126, 127 (photomicrograph).

Petrographic description: Medium-grained vesicular porphyritic olivine basalt with olivine phenocrysts and scarce small "dunite" xenoliths in an inter-

granular groundmass of plagioclase, pyroxene, ilmenite, and accessory minerals.

Major-element composition:

Chemical analyses of 74275

	1	2	3	4
SiO <sub>2</sub> .....	38.43	38.7	38.44	38.5
Al <sub>2</sub> O <sub>3</sub> .....	8.51	8.39	8.93	8.61
FeO.....	18.25	18.24	18.03	18.17
MgO.....	10.26	10.15	10.46	10.29
CaO.....	10.38	10.1	10.26	10.2
Na <sub>2</sub> O.....	.37	.370	.33	.36
K <sub>2</sub> O.....	.075	.080	.09	.08
TiO <sub>2</sub> .....	12.66	11.84	12.75	12.42
P <sub>2</sub> O <sub>5</sub> .....	.074	.063	.06	.07
MnO.....	.247	.241	.27	.25
Cr <sub>2</sub> O <sub>3</sub> .....	.639	.539	.65	.61
Total.....	99.895	98.713	100.27	99.56

- 1. 74275.58 (Duncan and others, 1974).
- 2. 74275.69 (Wänke and others, 1974).
- 3. 74275.98 (Rose and others, 1975).
- 4. Average of 1 through 3.

Age: Rb-Sr isochron: 74275,56, 3.81±0.32 b.y. (Nyquist and others, 1976).

Exposure age: Kr: 74275,24, 32±1 m.y. (Eberhardt and others, 1975).

STATION LRV-7

LOCATION

Station LRV-7 is located on the south rim of the Victory crater cluster approximately 1.3 km east of Shorty crater and station 4 (fig. 7C).

OBJECTIVES

The stop at Victory was planned to collect a regolith

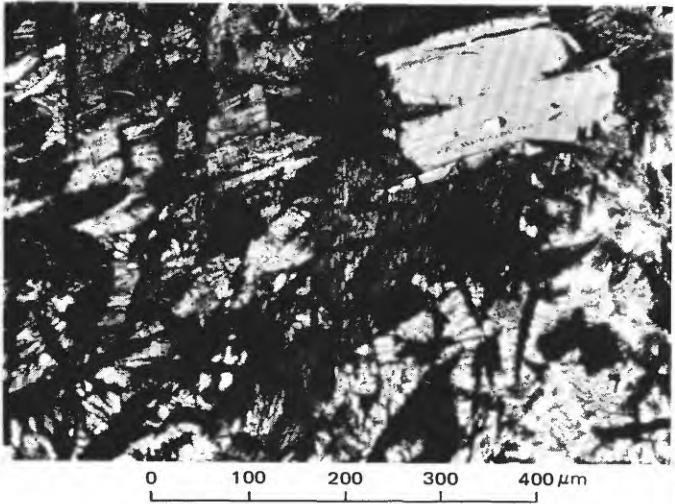


FIGURE 124.—Sample 74235. Photomicrograph showing quenched olivine in variolitic groundmass of ilmenite, clinopyroxene, and plagioclase.

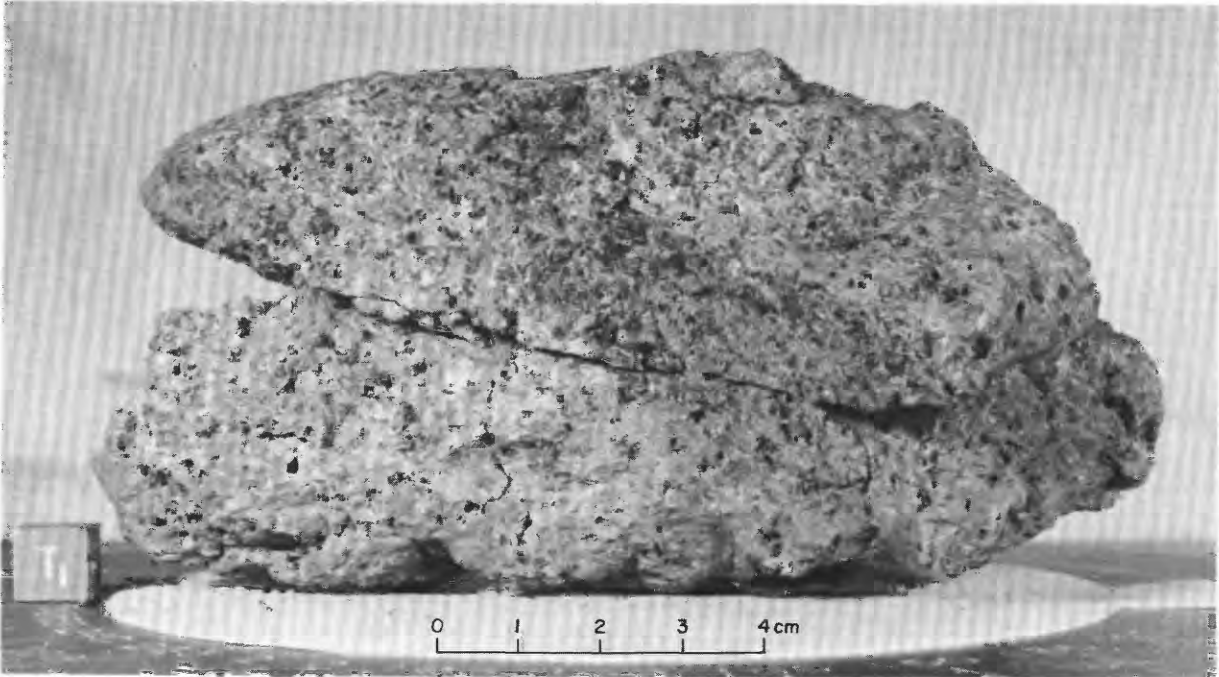


FIGURE 125.—Sample 74255. Medium-grained vesicular olivine basalt. (NASA photograph S-73-16904.)

sample, take a photographic panorama from the LRV, and place explosive package number 1 on the surface.

#### GENERAL OBSERVATIONS

The station area is on the gently sloping rim crest (fig. 128) of Victory crater. Scattered subdued craters in the sampling area range in size from 1 to 5 m. Blocks

up to 1 m in diameter cover 2 to 3 percent of the surface. The blocks are slightly to moderately buried, and fillets are rare. A sediment sample was collected.

#### SUMMARY OF SAMPLING

##### Sample 75110-15

*Type:* Sedimentary, unconsolidated (75110-14) and basalt (75115).

*Size:* 75115, 2×1.3×1 cm.

*Weight:* 75110-14, 381.33 g; 75115, 2.60 g.

*Depth:* From upper few centimeters.

*Location:* South rim crest of Victory crater.

*Illustration:* Figure 128.

*Petrographic description:* 75110-14, dominantly basalt, some fine-grained breccia and (or) metaclastic rock, minor agglutinate.

*Components of 90-150- $\mu$ m fraction of 75111,13 (Heiken and McKay, 1974)*

Components	Volume percent
Agglutinate .....	52.2
Basalt, equigranular .....	5.6
Basalt, variolitic .....	2.7
Breccia:	
Low grade <sup>1</sup> - brown .....	2.3
Low grade <sup>1</sup> - colorless .....	..
Medium to high grade <sup>2</sup> .....	5.6
Anorthosite .....	..
Cataclastic anorthosite <sup>3</sup> .....	.7
Norite .....	..
Gabbro .....	..
Plagioclase .....	2.0
Clinopyroxene .....	8.3
Orthopyroxene .....	..
Olivine .....	..
Ilmenite .....	.7
Glass:	
Orange .....	5.0
"Black" .....	11.6
Colorless .....	1.0
Brown .....	1.0



FIGURE 126.—Top, sample 74275 before collection (NASA photograph AS17-137-20984) and, bottom, reconstructed lunar surface orientation and lighting (NASA photograph S-73-18405).

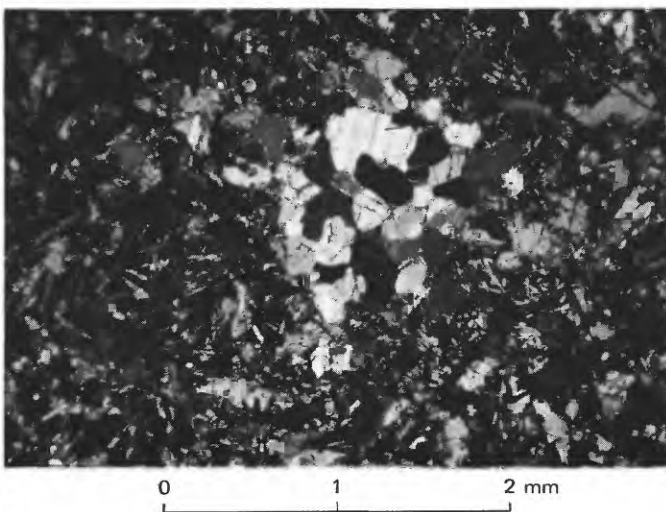


FIGURE 127.—Sample 74275. Photomicrograph showing small "dunite" in intergranular groundmass of plagioclase, ilmenite, and clinopyroxene. Crossed polarizers.

*Components of 90-150- $\mu$ m fraction of 75111,13 (Heiken and McKay, 1974)—Continued*

<i>Components</i>	<i>Volume</i>
Glass—Continued	
Gray, "ropy" .....	1.0
Other .....	.3
Total number grains .....	300

<sup>1</sup>Metamorphic groups 1-3 of Warner (1972).

<sup>2</sup>Metamorphic groups 4-8 of Warner (1972).

<sup>3</sup>Includes crushed or shocked feldspar grains.

*Major-element composition:*

*Chemical analysis of 75115*

SiO <sub>2</sub> .....	--
Al <sub>2</sub> O <sub>3</sub> .....	8.9
FeO .....	20.9
MgO .....	9.3
CaO .....	10.5
Na <sub>2</sub> O .....	.386
K <sub>2</sub> O .....	.069
TiO <sub>2</sub> .....	12.6
P <sub>2</sub> O <sub>5</sub> .....	--
MnO .....	.250
Cr <sub>2</sub> O <sub>3</sub> .....	.444

75115,1 (Warner and others, 1975a).

**STATION LRV-8**

**LOCATION**

Station LRV-8 is located between Victory and Horatio craters approximately 0.7 km east-southeast of station LRV-7 (fig. 7C).

**OBJECTIVES**

Station LRV-8 was a planned LRV stop to collect a surface sample and to take photographs.

**GENERAL OBSERVATIONS**

The station area is on a flat to gently rolling area of the valley floor west of the major concentration of fresh clustered craters. Scattered subdued craters range from 1 to 5 m in size. At least three small craters with cloddy ejecta blankets are near the site.

The surface (fig. 129) generally resembles that at LRV stops 1, 3, and 7. Distinguishable fragments cover less than one percent of the surface; in the sample area



FIGURE 128.—Station LRV-7 area and probable location of sample 75110-15 collection site. (NASA photograph AS17-133-20281.)

they are less than 10 cm in size.

A sediment sample was collected from an area between craters.

#### SUMMARY OF SAMPLING

##### Sample 75120-24

*Type:* Sedimentary, unconsolidated.

*Weight:* 375.21 g.

*Depth:* From upper few centimeters.

*Location:* Between Victory and Horatio craters on the valley floor.

*Illustration:* Figure 129.

*Petrographic description:* 75120-24, dominantly basalt, some fine-grained breccia and (or) metaclastic rock, and glass.

*Components of 90-150- $\mu$ m fraction of 75121,14 (Heiken and McKay, 1974)*

Components	Volume percent
Agglutinate.....	63.0
Basalt, equigranular .....	5.7
Basalt, variolitic .....	2.3
Breccia:	
Low grade <sup>1</sup> - brown .....	2.0
Low grade <sup>1</sup> - colorless .....	.3
Medium to high grade <sup>2</sup> .....	3.7
Anorthosite.....	--
Cataclastic anorthosite <sup>1</sup> .....	--
Norite.....	--
Gabbro.....	--
Plagioclase .....	4.0
Clinopyroxene .....	8.7
Orthopyroxene.....	--
Olivine.....	--
Ilmenite.....	.7
Glass:	
Orange .....	3.0
"Black" .....	3.7
Colorless .....	1.7
Brown .....	1.0
Gray, "ropy" .....	--
Other.....	.3
Total number grains .....	301

<sup>1</sup>Metamorphic groups 1-3 of Warner (1972).

<sup>2</sup>Metamorphic groups 4-8 of Warner (1972).

<sup>3</sup>Includes crushed or shocked feldspar grains.

#### STATION 5

#### LOCATION

Station 5 is located on the blocky southwest rim of Camelot crater (figs. 7C and 130).

#### OBJECTIVES

Exploration objectives at station 5 were to observe subfloor and dark mantle materials in the floor, rim, and walls of Camelot crater and to sample them on the rim.

#### GENERAL OBSERVATIONS

Camelot is a low-rimmed 650-m crater. Abundant blocks are exposed in a few places around the crater rim. They extend downward on the crater walls but are absent from the crater floor. The block abundance decreases markedly within a few meters outward from the

rim crest, where the terrain is smooth and undulating. In the station area, the rocks of the blocky rim cover about 30 percent of the surface (pans 19, 20). They range in size from a few centimeters to over 3 m, are subrounded to subangular, and are moderately to deeply buried. Filletting appears to be minimal. The crew described the boulder tops as free of sediment except for one flat 3-m boulder.

Younger craters up to 20 m in size are scattered around the rim and on the floor of Camelot, and a 100-m crater is superposed on the north rim. Most of the younger craters have subdued smooth rims and shallow floors.

Undisturbed fine regolith material at station 5 displays the "raindrop" pattern observed at some of the previous stations such as LRV-2 and LRV-3.

Samples from station 5 were four basalt fragments chipped from boulders and two sediment samples, one from on top of a boulder and one from between boulders.

#### GEOLOGIC DISCUSSION

Camelot crater is the largest crater visited by the Apollo 17 crew. Boulders on its rim most probably represent the deepest sampled part of the subfloor basalt, perhaps from a depth of more than 100 m.

The three boulder samples (75015, 75035, and 75055) are chemically unique among the Apollo 17 basalt samples; they have higher than normal concentrations of SiO<sub>2</sub>, Al<sub>2</sub>O<sub>3</sub>, and CaO, and lower than normal concentrations of FeO, MgO, TiO<sub>2</sub>, and Cr<sub>2</sub>O<sub>3</sub>. Interpreting trace-element as well as major-element distributions, Rhodes and others (1976) suggested that the major-element variations in the Apollo 17 basalt were produced largely by shallow-level fractional crys-



FIGURE 129.—Station LRV-8 area and probable location of sample 75120-24 collection site. (NASA photograph AS17-133-20315.)

tallization in three or more lava flows. They viewed the relatively coarse and chemically unique Camelot boulders as samples of highly fractionated basalt from deep within a thick, slowly cooled lava flow; samples from other stations include less fractionated basalt of the same magma type.

Sediment samples from station 5 are rich in basaltic debris. Their chemical compositions (fig. 131) are like those associated with the basalt-rich cluster ejecta.

The rim of Camelot looks smoother than the rims of craters in the large cluster south and east of the landing point. Hence, on photogeologic grounds, Camelot was interpreted as older (Lucchitta, 1972). However, topographic profiles made by analytical stereoplotter show that the depth-to-diameter ratio for Camelot is similar to that for the clustered craters to the southeast. Their appearance of greater freshness may be due to the abundant smaller craters, not present at Camelot, that have distinctly roughened the topography.

The many exposures ages determined for the three boulder samples from station 5 range from 70 to 95 m.y. Because of their unusual composition and their occurrence among the large concentration of boulders on the crater rim, we confidently interpret the three sampled boulders as excavated from the subfloor basalt by the Camelot impact. Hence 70-95 m.y. approximates or is at least a younger limit for the age of Camelot crater. Arvidson and others (1976b) discussed the possibility that 75015 and 75035 (exposure ages approximately 72-92 m.y.) had undergone a pronounced shielding change, perhaps due to catastrophic rupture of a single boulder to form the two sampled boulders. If so, the exposure ages of these two samples are less than the age of Camelot crater.

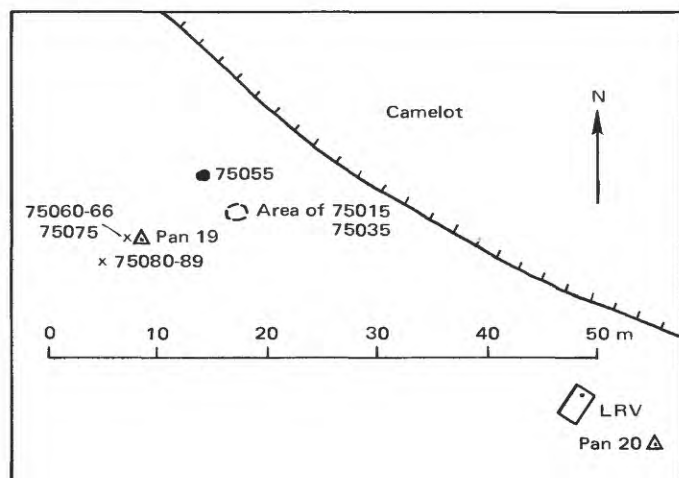


FIGURE 130.—Planimetric map of station 5.

## SUMMARY OF SAMPLING

### Sample 75015

*Type:* Basalt.

*Size:* 10×9×6 cm.

*Weight:* 1,006 g.

*Location:* From boulder in block field on southwest rim of Camelot.

*Illustrations:* Pan 19; figures 132, 133 (LRL).

*Comments:* Subfloor basalt ejected from Camelot crater.

*Petrographic description:* Coarse-grained vesicular basalt. Intergranular to subophitic groundmass.

### Major-element composition:

#### Chemical analysis of 75015

SiO <sub>2</sub> .....	41.92
Al <sub>2</sub> O <sub>3</sub> .....	10.06
FeO .....	18.77
MgO .....	6.20
CaO .....	12.15
Na <sub>2</sub> O .....	.48
K <sub>2</sub> O .....	.06
TiO <sub>2</sub> .....	9.56
P <sub>2</sub> O <sub>5</sub> .....	.05
MnO .....	.29
Cr <sub>2</sub> O <sub>3</sub> .....	.17
Total .....	99.71
75015,2 (Rhodes and others, 1976).	

*Exposure age:* Kr-Kr: 92±4 m.y. (Arvidson and others, 1976b).

### Sample 75035

*Type:* Basalt.

*Size:* 16×14×7 cm.

*Weight:* 1,235 g.

*Location:* From boulder in block field on southwest rim of Camelot.

*Illustrations:* Pan 19; figures 132, 134 (LRL).

*Comments:* Subfloor basalt ejected from Camelot crater.

*Petrographic description:* Medium-grained basalt with plumose to subophitic(?) groundmass.

### Major-element composition:

#### Chemical analyses of 75035

	1	2	3	4
SiO <sub>2</sub> .....	42.31	41.1	42.61	42.01
Al <sub>2</sub> O <sub>3</sub> .....	10.30	9.24	10.05	9.86
FeO .....	18.57	19.2	18.08	18.6
MgO .....	6.28	6.12	6.25	6.22
CaO .....	12.15	11.68	12.53	12.12
Na <sub>2</sub> O .....	.53	.460	.39	.46
K <sub>2</sub> O .....	.061	.084	.08	.08
TiO <sub>2</sub> .....	8.95	10.09	9.59	9.54
P <sub>2</sub> O <sub>5</sub> .....	.084	.080	.06	.07
MnO .....	.262	.269	.27	.27

## Chemical analyses of 75035—Continued

	1	2	3	4
Cr <sub>2</sub> O <sub>3</sub> .....	.207	.235	.26	.23
Total.....	99.704	98.558	100.17	99.46

1. 75035, 19 (Duncan and others, 1976).  
 2. 75035, 46 (Wänke and others, 1975).  
 3. 75035, 65 (Rose and others, 1975).  
 4. Average of 1 through 3.

## Age:

<sup>40</sup>-<sup>39</sup>Ar: 75035,21,  $3.77 \pm 0.04$  b.y. (Turner and Cadogan, 1975).  
 Rb-Sr isochron: 75035,43,  $3.81 \pm 0.14$  (2 $\sigma$ ) b.y. (Murthy, 1976).

## Exposure age:

Ar: 75035,21, 80 m.y. (Turner and Cadogan, 1975).  
 Kr: 75035,  $71.7 \pm 1.8$  m.y. (Croaz and others, 1974).

## Sample 75055

Type: Olivine basalt.

Size: 21×14×1.8 cm.

Weight: 949.4 g.

Location: From boulder in block field on southwest rim of Camelot.

Illustrations: Pan 19; figures 135, 136 (photomicrograph).

Comments: Subfloor basalt ejected from Camelot crater.

Petrographic description: Coarse-grained olivine basalt

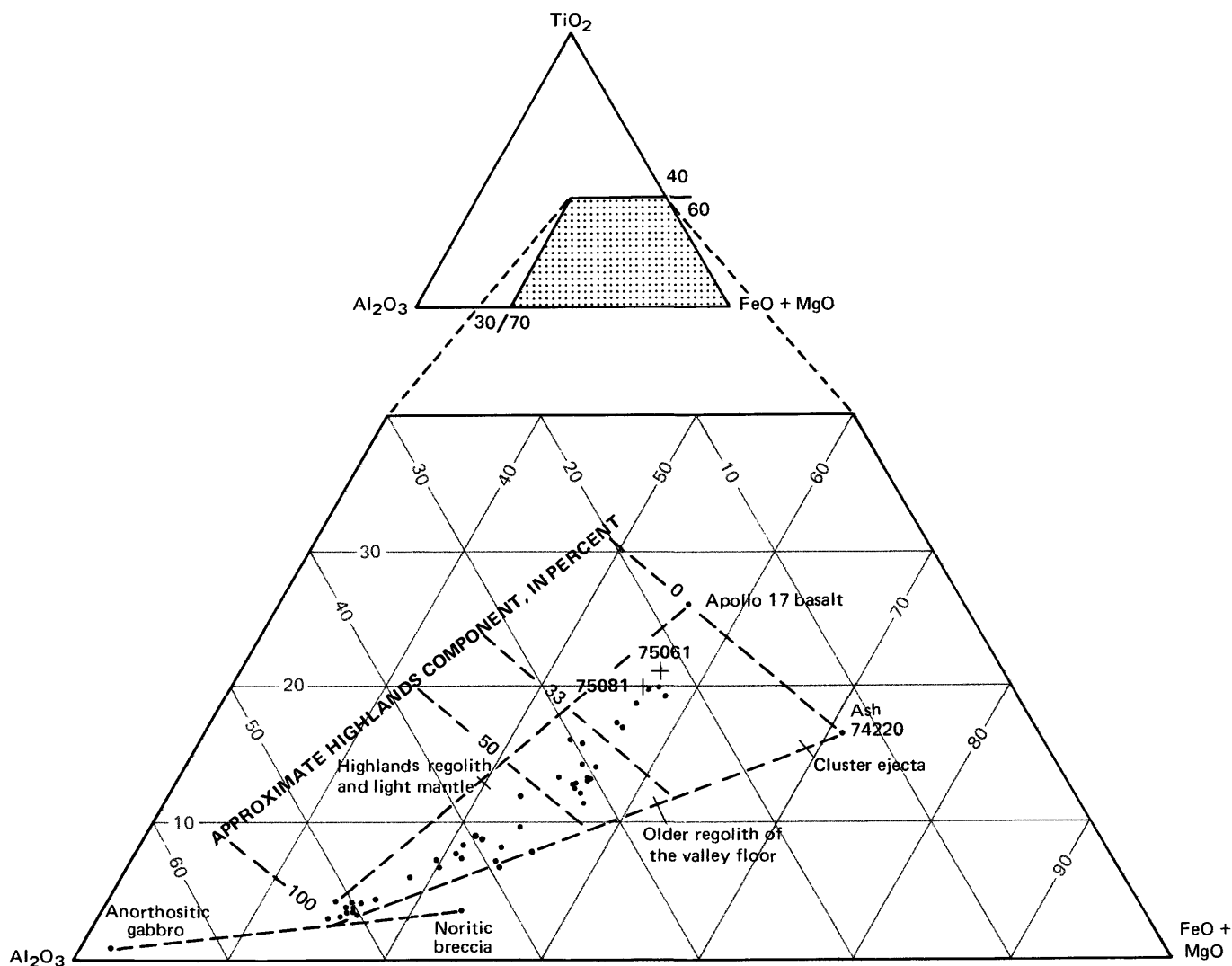


FIGURE 131.—Relative amounts of TiO<sub>2</sub>, Al<sub>2</sub>O<sub>3</sub>, and FeO+MgO in sediment samples 75061 and 75081 (crosses), from station 5, in comparison with sediment samples from rest of traverse region (dots). Apollo 17 basalt, anorthositic gabbro, and noritic breccia values from Rhodes and others (1974).

with a subophitic groundmass composed of plagioclase, clinopyroxene, ilmenite, and accessory minerals.

#### Major-element composition:

##### Chemical analyses of 75055

	1	2	3
SiO <sub>2</sub> .....	41.27	39.93	40.60
Al <sub>2</sub> O <sub>3</sub> .....	9.75	9.58	9.66
FeO.....	18.24	17.77	18.00
MgO.....	6.84	7.26	7.05
CaO.....	12.30	12.40	12.35
Na <sub>2</sub> O.....	.44	.42	.43
K <sub>2</sub> O.....	.09	.06	.08
TiO <sub>2</sub> .....	10.17	11.41	10.79
P <sub>2</sub> O <sub>5</sub> .....	.07	.06	.06
MnO.....	.29	.27	.28
Cr <sub>2</sub> O <sub>3</sub> .....	.27	.31	.29
Total.....	99.73	99.47	99.59

1. 75055.6 (Apollo 17 PET, 1973).

2. 75055.75 (Rhodes and others, 1976).

3. Average of 1 and 2.

#### Age:

##### Rb-Sr isochron:

75055,  $3.77 \pm 0.06$  (2 $\sigma$ ) b.y. (Tera and others, 1974b).

75055,  $3.83 \pm 0.10$  (2 $\sigma$ ) b.y. (Tatsumoto and others, 1973).

##### <sup>40</sup>Ar:

75055, 11.2,  $3.82 \pm 0.05$  b.y. (Kirsten and Horn, 1974).

75055,  $3.78 \pm 0.04$  b.y. (Huneke and others, 1973).

75055,  $3.76 \pm 0.05$  b.y. (Turner and others, 1973).

#### Exposure age:

##### Ar:

75055, 11.2,  $85 \pm 10$  m.y. (Kirsten and Horn, 1974).

75055, 95 m.y. (Huneke and others, 1973).

75055, 90 m.y. (Turner and others, 1973).

##### Tracks:

75055, 70 m.y. (Kirsten and others, 1973).

#### Sample 75060-66

Type: Sedimentary, unconsolidated (75060-64), basalt (75065), and breccia (75066).

Size: 75065, 1×1×1 cm; 75066, 1.2×1×0.5 cm.

Weight: 75060-64, 184.86 g; 75065, 1.263 g; 75066, 0.98 g.

Depth: 0-1 cm.

Location: Top of boulder in block field on southwest rim of Camelot.

Illustrations: Pan 19; figure 137.

Comments: Mantling material from small centimeter-deep hollow in the upper surface of a flat 3-m boulder; sample collected one-half m in from east side of boulder.

der; sample collected one-half m in from east side of boulder.

Petrographic description: 75060-64, dominantly basalt with minor metaclastic rock and (or) breccia, rare glass.

##### Components of 90-150- $\mu$ m fraction of 75061,2 (Heiken and McKay, 1974)

Components	Volume percent
Agglutinate.....	24.0
Basalt, equigranular { .....	26.6
Basalt, variolitic { .....	
Breccia: .....	
Low grade <sup>1</sup> -brown .....	2.6
Low grade <sup>1</sup> -colorless .....	2.0
Medium to high grade <sup>2</sup> .....	.3
Anorthosite.....	..
Cataclastic anorthosite <sup>3</sup> .....	..
Norite .....	..
Gabbro .....	..
Plagioclase .....	4.6
Clinopyroxene .....	29.6
Orthopyroxene.....	..
Olivine .....	.3
Ilmenite.....	5.3
Glass: .....	
Orange .....	1.0
"Black" .....	..
Colorless .....	1.6
Brown .....	1.6
Gray, "ropy" .....	..
Other .....	..
Total number grains.....	299

<sup>1</sup> Metamorphic groups 1-3 of Warner (1972).

<sup>2</sup> Metamorphic groups 4-8 of Warner (1972).

<sup>3</sup> Includes crushed or shocked feldspar grains.

#### Major-element composition:

##### Chemical analyses of 75061

	1	2	3
SiO <sub>2</sub> .....	39.32	39.70	39.51
Al <sub>2</sub> O <sub>3</sub> .....	10.42	10.60	10.51
FeO.....	18.19	17.86	18.02
MgO.....	9.53	9.65	9.59
CaO.....	10.72	10.72	10.72
Na <sub>2</sub> O.....	.33	.37	.35
K <sub>2</sub> O.....	.08	.08	.08
TiO <sub>2</sub> .....	10.31	10.46	10.38
P <sub>2</sub> O <sub>5</sub> .....	.06	.06	.06
MnO.....	.25	.24	.24
Cr <sub>2</sub> O <sub>3</sub> .....	.48	.48	.48
Total.....	99.69	100.22	99.94

1. 75061.4 (Apollo 17 PET, 1973).

2. 75061.27 (Rose and others, 1974).

3. Average of 1 and 2.

#### Exposure age:

##### Minimum track density:

75061, 32 m.y.

75062, 40 m.y., interpreted as concordant ages of  $36 \pm 4$  m.y. for the top centimeter of sediment mantling the 75075 boulder (Fleischer and Hart, 1974).

#### Sample 75075

Type: Olivine basalt.

Size: 15×12×5 cm.

*Weight:* 1,008 g.

*Location:* Top of boulder in block field on southwest rim of Camelot.

*Illustrations:* Pan 19; figures 137, 138 (photomicrograph), 139.

*Comments:* Sample 75075 was a loose fragment on top of a 3-m flat boulder. It differs significantly from the three station 5 boulder samples (75015, 75035, and 75055) in both composition and exposure history; hence, it is probably a fragment ejected from the



FIGURE 132.—Locations of samples 75015 and 75035 before collection. Inset shows 75035 with reconstructed lunar surface orientation and lighting. (NASA photographs AS17-145-22138; S-73-19593.)

regolith by a post-Camelot impact.

**Petrographic description:** Medium-grained vesicular porphyritic olivine basalt. Scarce clinopyroxene-ilmenite aggregates in a locally plumose groundmass of plagioclase, clinopyroxene, ilmenite, and accessory minerals.

**Major-element composition:**

*Chemical analyses of 75075*

	1	2	3
SiO <sub>2</sub> .....	37.64	38.51	38.08
Al <sub>2</sub> O <sub>3</sub> .....	8.20	8.29	8.24
FeO.....	18.78	18.85	18.82
MgO.....	9.49	9.68	9.58
CaO.....	10.29	10.17	10.23
Na <sub>2</sub> O.....	.40	.37	.38
K <sub>2</sub> O.....	.05	.11	.08
TiO <sub>2</sub> .....	13.45	13.33	13.39
P <sub>2</sub> O <sub>5</sub> .....	.05	.12	.08
MnO.....	.28	.25	.26
Cr <sub>2</sub> O <sub>3</sub> .....	.57	.55	.56
Total.....	99.26	100.23	99.70

1. 75075.58 (Rhodes and others, 1974).

2. 75075.72 (Rose and others, 1974).

3. Average of 1 and 2.

**Age:**

**Rb-Sr isochron:**

75075.57,  $3.82 \pm 0.06$  (2 $\sigma$ ) b.y. (Murthy, 1976).

75075.58,  $3.84 \pm 0.12$  (2 $\sigma$ ) b.y. (Nyquist and others, 1975).

**<sup>40</sup>Ar-<sup>39</sup>Ar:**

75075,  $3.74 \pm 0.06$  b.y. ( Jessberger and others, 1975).

**Sm-Nd isochron:**

75075,  $3.69 \pm 0.08$  (2 $\sigma$ ) b.y. (Lugmair and others, 1975a).

**Exposure age:**

**Ar:**

144 m.y. (Lugmair and others, 1975b).

$120 \pm 15$  m.y. (Jessberger and others, 1975).

**Kr:**

$143 \pm 5$  m.y. (Lugmair and others, 1975b).

143 m.y. (Arvidson and others, 1975).

Sample 75080-89

**Type:** Sedimentary, unconsolidated (75080-84) and basalt fragments (75085-89).



FIGURE 133.—Sample 75015. Coarse-grained vesicular basalt. (NASA photograph S-73-16666.)

**Size:** Largest fragment (75087) is 2×2×1 cm.  
**Weight:** 75080-84, 1,549.71 g; 75085-89, 12.65 g.  
**Depth:** 0-5 cm.

**Location:** Between boulders in block field on southwest rim of Camelot.

**Illustrations:** Pan 19; figure 139.

**Comments:** Collected from regolith surface adjacent to boulder from which samples 75060-66 and 75075 were collected.

**Petrographic description:** 75080-84, dominantly basalt with some glass, possible agglutinates.

*Components of 90-150- $\mu$ m fraction of 75081,36 (Heiken and McKay, 1974)*

Components	Volume percent
Agglutinate.....	35.3
Basalt, equigranular .....	15.7
Basalt, variolitic .....	4.0
Breccia:	
Low grade <sup>1</sup> - brown .....	.7
Low grade <sup>1</sup> - colorless .....	.7
Medium to high grade <sup>2</sup> .....	2.0
Anorthosite .....	.3
Cataclastic anorthosite <sup>3</sup> .....	..
Norite .....	..
Gabbro .....	..
Plagioclase .....	9.0
Clinopyroxene .....	20.3
Orthopyroxene .....	..
Olivine .....	.7
Ilmenite .....	5.7
Glass:	
Orange .....	.7
"Black" .....	3.0
Colorless .....	1.3
Brown .....	.6
Gray, "ropy" .....	..
Other .....	..
Total number grains .....	300

<sup>1</sup>Metamorphic groups 1-3 of Warner (1972).

<sup>2</sup>Metamorphic groups 4-8 of Warner (1972).

<sup>3</sup>Includes crushed or shocked feldspar grains.

*Major-element compositions:*

*Chemical analyses of 75081*

	1	2	3	4
SiO <sub>2</sub> .....	40.27	40.00	40.12	40.13
Al <sub>2</sub> O <sub>3</sub> .....	11.31	11.18	11.31	11.27
FeO .....	17.20	17.30	17.29	17.26
MgO .....	9.59	9.42	9.44	9.48
CaO .....	10.97	10.87	10.89	10.91
Na <sub>2</sub> O .....	.33	.38	.36	.36
K <sub>2</sub> O .....	.08	.08	.074	.08
TiO <sub>2</sub> .....	9.41	9.40	9.60	9.47
P <sub>2</sub> O <sub>5</sub> .....	.07	.07	.082	.07
MnO .....	.25	.25	.228	.24
Cr <sub>2</sub> O <sub>3</sub> .....	.46	.45	.470	.46
Total .....	99.94	99.40	99.864	99.73

1. 75081,3 (Apollo 17 PET, 1973).

2. 75081,56 (Rhodes and others, 1974).

3. 75081,66, average of four analyzed size fractions (Duncan and others, 1974).

4. Average of 1 through 3.

*Chemical analyses of 75088 and 75089*

	1	2
SiO <sub>2</sub> .....	..	..
Al <sub>2</sub> O <sub>3</sub> .....	10.4	8.7
FeO .....	20.4	20.6
MgO .....	8.9	9.8
CaO .....	11.8	10.0
Na <sub>2</sub> O .....	.379	.394
K <sub>2</sub> O .....	.060	.065
TiO <sub>2</sub> .....	11.9	13.2
P <sub>2</sub> O <sub>5</sub> .....	..	..
MnO .....	.255	.240
Cr <sub>2</sub> O <sub>3</sub> .....	.310	.531

1. 75088,1 (Warner and others, 1975a).

2. 75089,1 (Warner and others, 1975a).

*Ages of 2-4-mm basalt fragments in 75083:*

<sup>40-30</sup>Ar:

75083,2,1, olivine-porphyritic ilmenite basalt,  $3.77 \pm 0.05$  b.y.

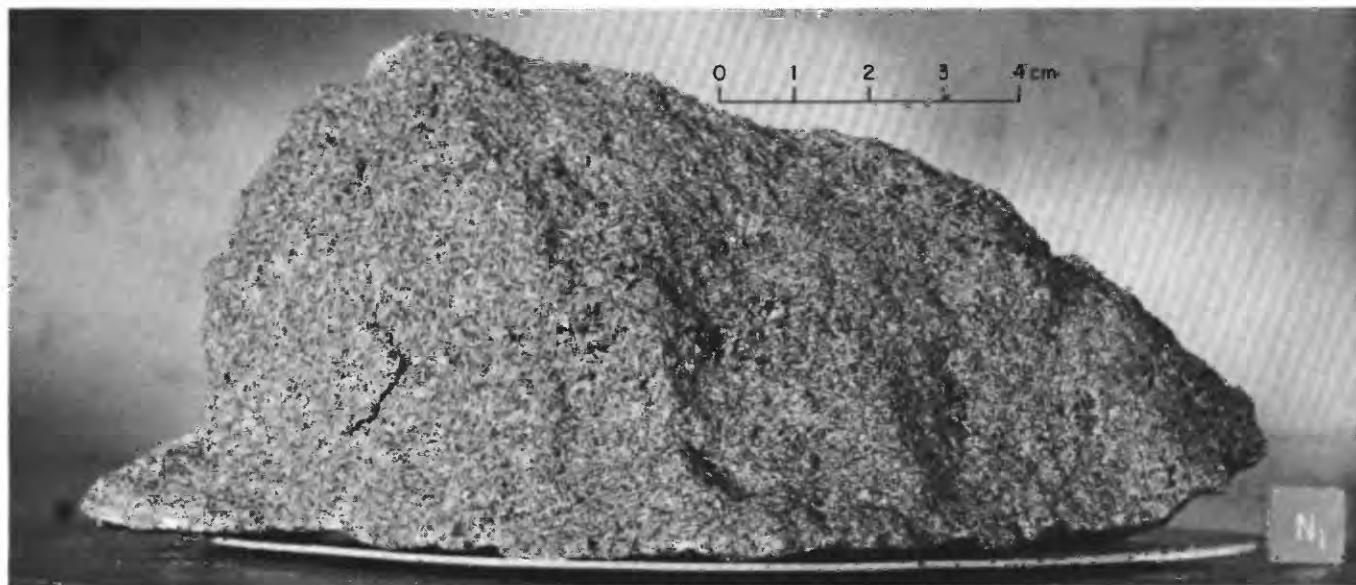


FIGURE 134.—Sample 75035. Medium-grained basalt. (NASA photograph S-73-16252.)

75083,2,3, Apollo 11 type basalt,  $3.75 \pm 0.04$  b.y.

75083,2,4, olivine-porphyrific ilmenite basalt,  $3.67 \pm 0.10$  b.y.

75083,2,5, intermediate between olivine-porphyrific ilmenite basalt and plagioclase-poikilitic ilmenite basalt,  $3.74 \pm 0.04$  b.y.

75083,2,8, plagioclase-poikilitic ilmenite

basalt,  $3.68 \pm 0.10$  b.y.

75083,2,9, plagioclase-poikilitic ilmenite basalt,  $3.68 \pm 0.07$  b.y.

75083,2,15, plagioclase-poikilitic ilmenite basalt,  $3.75 \pm 0.05$  b.y.

Above dates by Schaeffer and Husain, reported in Papike and others (1974); basalt classification of Papike and others (1974).

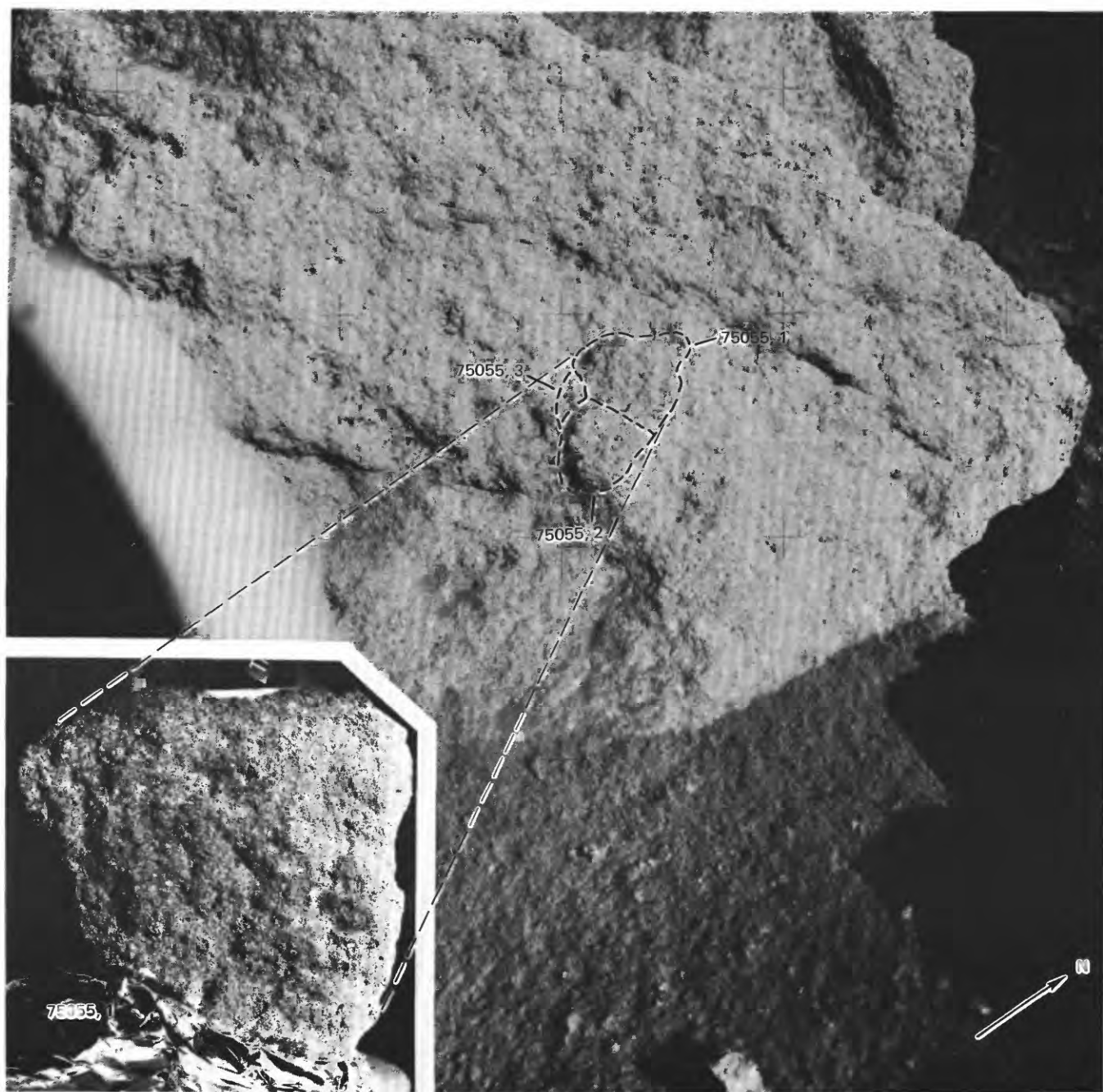


FIGURE 135.—Location of sample 75055 before collection. Inset shows 75055,1 with reconstructed lunar surface orientation and lighting. (NASA photographs AS17-145-22149; S-73-17796.)

75083,3,3,  $3.70 \pm 0.09$  b.y. (Huneke and others, 1973).

*Exposure age of 75081:*

Tracks:

Estimate for 5 cm burial, 97 m.y.

Estimate for 3 cm burial, 56 m.y. (Bull and Durrani, 1976).

Minimum track density:

Estimate for 5 cm burial, ~146 m.y., based on 110-m.y. exposure at 4-cm depth prior to being covered by 1 cm ~36 m.y. ago (75061, 75062 data) (Fleischer and Hart, 1974).

#### STATION LRV-9

##### LOCATION

Station LRV-9 is about 1.5 km north of the LM/ALSEP/SEP area, about halfway between the LM and station 6, and about 500 m, slightly less than a crater diameter, south of Henry crater (figs. 6 and 7D).

##### OBJECTIVES

LRV-9 was a planned Rover sample and photography stop.

##### GENERAL OBSERVATIONS

The surface in the area of LRV-9 is flat to gently rolling. There are scattered craters up to 10 m in size and smaller rimless depressions in the area. Rock fragments up to a few tens of centimeters in size are sparse and appear to have been excavated from the local craters. The fragments cover less than 1 percent of the surface, are angular to subrounded, and are slightly to mostly buried. Filletting is rare in the area.

The sample came from a small crater with abundant clods on its rim.

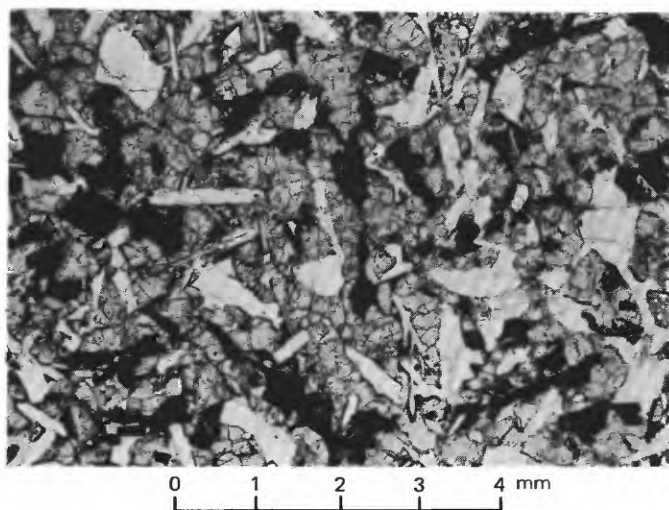


FIGURE 136.—Sample 75055. Photomicrograph showing coarse-grained ophitic intergrowths of clinopyroxene, plagioclase, and ilmenite.

#### SUMMARY OF SAMPLING

Sample 76120-24

*Type:* Sedimentary, unconsolidated.

*Weight:* 303.92 g.

*Depth:* From upper few centimeters.

*Location:* Meter-size crater at LRV-9.

*Illustration:* Figure 140.

*Comments:* Sample 76120-24 represents local regolith material that may include ejecta from Henry crater.

*Petrographic description:* 76120-24, dominantly fine-grained breccia and (or) metaclastic rock, some agglutinate.

#### STATION LRV-10

##### LOCATION

Station LRV-10 is located adjacent to Turning Point rock (fig. 144), about 2.8 km north of the LM/ALSEP/SEP area (figs. 6 and 7D).

##### OBJECTIVES

Station LRV-10 was an unplanned sampling and photography stop.

##### GENERAL OBSERVATIONS

The station area is near the gradational contact between valley floor and North Massif; it is on a moderate slope of about  $10^\circ$  to the south with fairly distinct breaks in slope both above and below the sampling site.

Turning Point rock is about 6 m high and perhaps 10 m across in its longest dimension. It is surrounded by a halo of smaller boulders and rock fragments that are rounded, partly buried, and filleted on their uphill sides. Outside the halo of boulders around Turning Point rock, fragments large enough to be recognized in photographs make up less than 1 percent of the surface material.

Sparse subdued 1-5-m craters, generally without blocks or clods, are scattered around the sample area.

Samples included sediment and three rock fragments collected about 4 m north of Turning Point rock.

#### SUMMARY OF SAMPLING

Sample 76130-37

*Type:* Sedimentary, unconsolidated (76130-34); metaclastic rock with a poikilitic matrix (76135); olivine basalt (76136), and small rock fragment (76137).

*Size:* 76135,  $7 \times 6 \times 4$  cm; 76136,  $6 \times 4 \times 3$  cm; 76137,  $1.8 \times 1.5 \times 1$  cm.

*Weight:* 76130-34, 180.77 g; 76135, 133.5 g; 76136, 86.6 g; 76137, 2.46 g.

*Depth:* From upper few centimeters.

*Location:* Approximately 4 m north of Turning Point

rock at LRV-10.

*Illustrations:* Figures 141, 142 (LRL, 76135), 143 (photomicrograph, 76136).

*Comments:* LRV-10 is in a zone where North Massif and valley floor material, represented respectively by samples 76135 and 76136, are mixed.

*Petrographic descriptions:*

76130-34, no description available.

76135, vesicular metaclastic rock with scarce metatrolitic clasts in poikilitic matrix of

pyroxene oikocrysts enclosing both newly crystallized plagioclase and abundant mineral clasts of plagioclase and olivine. Clusters and fragments of intergrown spongy plagioclase and brown pyroxene that line cavities in other rocks are present.

76136, medium-grained olivine basalt with a variolitic groundmass composed of plagioclase, clinopyroxene, ilmenite, and accessory minerals.

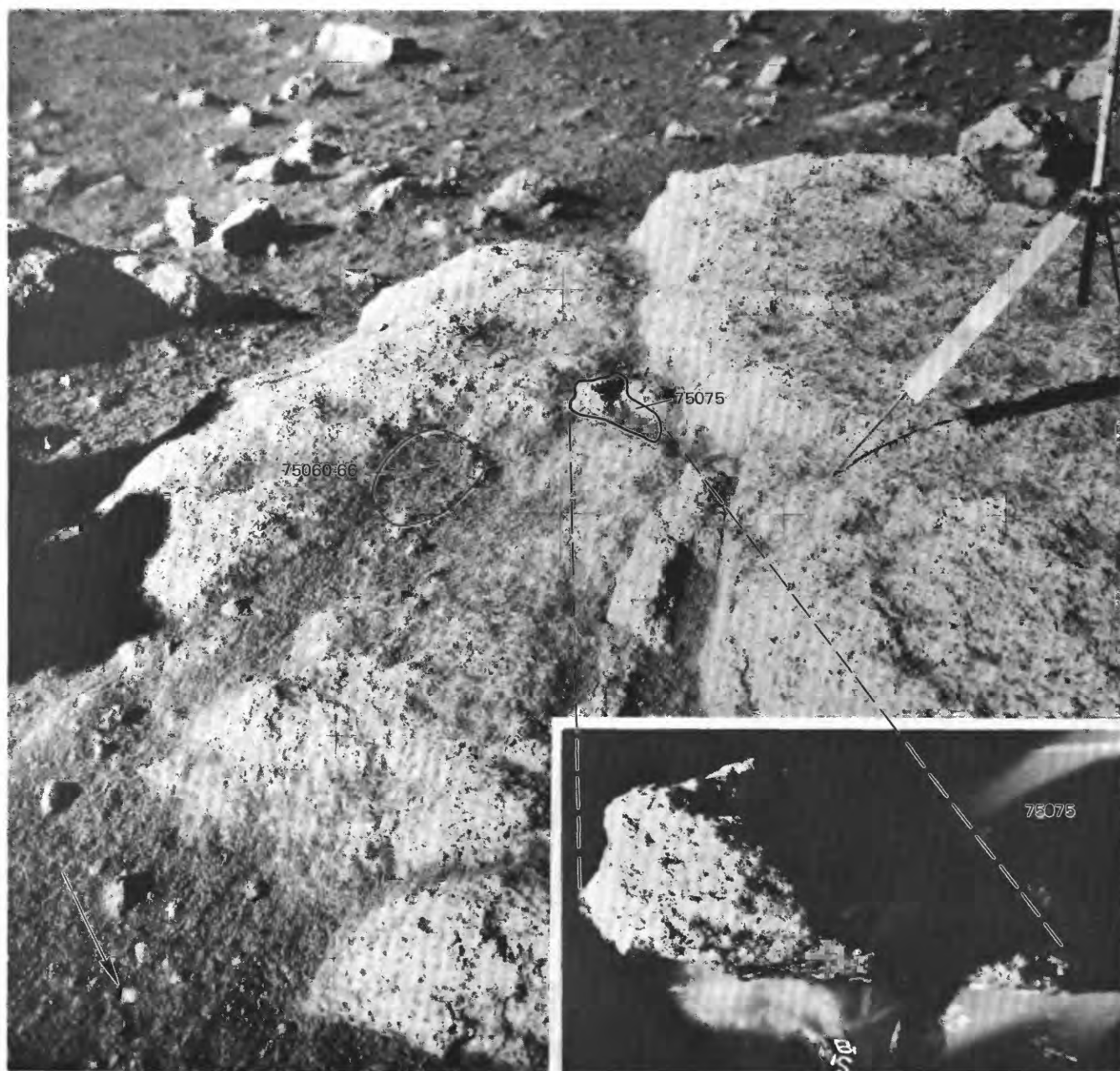


FIGURE 137.—Locations of samples 75060-66 and 75075 before collection. Inset shows 75075 with reconstructed lunar surface orientation and lighting. (NASA photographs AS17-145-22155; S-73-17800.)

*Major-element composition:**Chemical analysis of 76136*

SiO <sub>2</sub> .....	38.60
Al <sub>2</sub> O <sub>3</sub> .....	8.65
FeO.....	19.12
MgO.....	8.61
CaO.....	10.53
Na <sub>2</sub> O.....	.38
K <sub>2</sub> O.....	.06
TiO <sub>2</sub> .....	12.64
P <sub>2</sub> O <sub>5</sub> .....	.06
MnO.....	.28
Cr <sub>2</sub> O <sub>3</sub> .....	.44
Total.....	99.37

76136.8 (Rhodes and others, 1976).

**STATION 6****LOCATION**

Station 6 is in a blocky area on the south slope of the North Massif about 0.4 km northeast of Turning Point rock (figs. 7D and 144).

**OBJECTIVES**

The objectives at station 6 were to characterize and sample (1) the blocks and sediment of the North Massif and (2) dark mantle materials that extend upward locally onto the lower slopes of the massif.

**GENERAL OBSERVATIONS**

Station 6 is on an 11° slope, about 250 m north of the break in slope between the valley floor and the massif. The most prominent local feature is a cluster of five large blocks alined downslope from the end of a single boulder track that originates from a point about one-third of the way up the face of the massif (figs. 144, 145). Several other tracks originating near the same level, about 500 m above the valley floor, can be seen

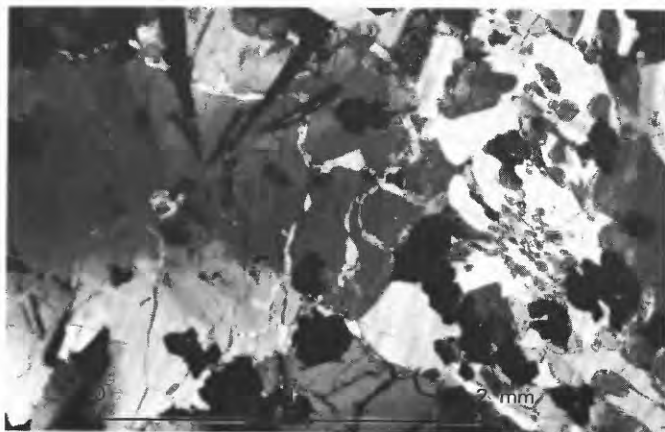


FIGURE 138.—Sample 75075. Photomicrograph showing large aggregate of clinopyroxene-ilmenite with small olivine core (left half) in groundmass that is locally plumose intergrowth of plagioclase, clinopyroxene, and ilmenite. Crossed polarizers.

in figure 145. Fields of blocks are abundant from this level upward; at about this same level the slope increases from about 21.5° in the lower one-third to about 25° in the upper two-thirds of the massif.

Fragment distribution is bimodal in the station area. There are relatively few fragments in the 3-15-cm size range. Blocks greater than one-half meter in size are generally gathered in clusters, but fragments less than one-half meter in size are scattered over the area. Most of the blocks are subrounded to rounded, but a few are angular. Some of the larger boulders have well-developed fillets on the uphill sides, but fillets are absent or only slightly developed on the smaller blocks. Smooth-rimmed and relatively block free craters up to 10 m in size appear randomly scattered over the surface in the station area. A few small fresh craters have blocky rims with the ejecta deposited preferentially downslope. Near crater rims, bootprints and LRV wheel marks indicate that the sediment is relatively soft; however, the regolith surface between craters is moderately firm.

Samples at station 6 include a single drive tube, ten rock samples, seven sediment samples, and one rake sample (fig. 146). Of the ten rock samples, three were from the surface, four were from block 1, and one each came from blocks 2, 4, and 5. Three of the sediment samples were taken from between major blocks. One sediment sample was collected downslope from the blocks, another from the boulder track, another from on top of block 1, and the last from the ejecta blanket of a small crater. The rake collected 23 chips from the ejecta blanket of the small crater.

**GEOLOGIC DISCUSSION**

The North Massif, like the South Massif, is interpreted as a fault-bounded block of ejecta deposited and faulted by the impact that formed the southern Serenitatis basin. In the upper two-thirds of the massif, where concentrations of boulders abound (fig. 145), bedrock is probably close to the surface. The less steep slope of the lower one-third is probably the surface of a thick colluvial wedge (fig. 242) onto which boulders from the upper part of the massif have rolled.

The five large blocks at station 6 are alined and probably represent a single fragmented boulder (fig. 146). Blocks 1 and 2 and 2 and 3 can be pieced back together as shown in figures 147 and 148. Blocks 4 and 5 can also be easily rejoined with minimal manipulation. However, fit between the blocks 1-2-3 reconstruction and the blocks 4-5 reconstruction is uncertain. Block 2, the largest of the five, is about 10 m across. Reassembled, the whole boulder would measure approximately 18×10×6 m.

On the basis of lunar surface photographs and de-

scriptions as well as preliminary sample descriptions, Muehlberger and others (1973) distinguished two major breccia types, greenish-gray and blue-gray breccia. Blocks 3, 4, and 5 and part of block 2 are greenish-gray breccia. Block 2 shows an irregular contact zone about 50 cm wide between greenish-gray breccia to the southwest and blue-gray breccia to the northeast. Block 1 is also blue-gray breccia. Light-colored inclusions occur in both breccia types.

A modified classification (fig. 149), utilizing, in particular, differences in degree of vesicularity and foliation, was developed by Heiken and others (1973); it provides the stratigraphic frame of reference used in subsequent reports by members of the consortium to study the station 6 boulder (for example, Simonds, 1975).

In spite of variable vesicularity, color, and degree of foliation, the station 6 boulder consists of a chemically



FIGURE 139.—Locations from which samples 75075 and 75080-89 were collected. (NASA photograph AS17-145-22158.)

uniform matrix (fig. 150) with clasts up to about a meter in size of anorthosite-norite-troctolite suite rocks or their impact-modified derivatives. According to Simonds (1975), the matrix is a clast-bearing rock formed from a mechanical mixture of cold, generally little shocked clasts and superheated impact melt that was quenched to form a very fine subophitic to ophitic crystalline groundmass. The approximate mode of the groundmass is 50 percent plagioclase, 30 percent pigeonite, 13 percent olivine, 5 percent augite, and 2 percent ilmenite and accessory minerals. Clast abundance ranges from about 2 to 40 percent (Simonds, 1975; Warner and others, 1976).

Simonds (1975) has described several properties of the clasts and the crystallized groundmass that vary systematically with the groundmass grain size. With increasing groundmass grain size, (1) clast abundance decreases, (2) the ratios of mafic to feldspathic clasts and of pyroxene to olivine clasts decrease, and (3) groundmass pyroxene and plagioclase become, respectively, more magnesian and more calcic. Simonds has interpreted these systematic variations as related to initial clast content in the clast-melt mixture. Where the clast-melt ratio was high, the matrix was rapidly quenched; its grain size is extremely fine; little or no digestion of clasts occurred. Where there was initially more melt, the melt was less rapidly quenched; its grain size is coarser, and its composition was modified by digestion of the smaller and less refractory clasts. Modeling the cooling of the clast-melt mixture inferred

by Simonds for the station 6 boulder, Onorato and others (1976) have suggested that thermal equilibrium between clasts and melt is achieved in a time on the order of 100 seconds, with 90 percent of the change from initial melt temperature to the equilibrium temperature occurring within about 1 second.

The  $^{40}\text{--}^{39}\text{Ar}$  age of the station 6 boulder has been intensively examined by Cadogan and Turner (1976), who concluded that the impact event that aggregated the boulder occurred  $3.96 \pm 0.04$  b.y. ago. Exposure age measurements by Crozaz and others (1974) suggest that the boulder rolled to its present position, forming its prominent track, about 22 m.y. ago.

Other rocks collected at station 6 include breccia, a few subfloor basalt fragments, and a metatroctolite (76535) that has been interpreted as a metamorphosed derivative of a deep-seated plutonic rock that could have been an early lunar differentiate formed during the same magmatic event as the one represented by dunite sample 72415-18 from station 2.

Unconsolidated sediment of the station 6 regolith is highlands debris like that of the South Massif and light mantle with a 20 to 30 percent admixture of basalt debris and ash from the valley floor (fig. 151).

#### SUMMARY OF SAMPLING

##### Sample 76001

Type: Single drive tube.

Weight: 711.6 g.

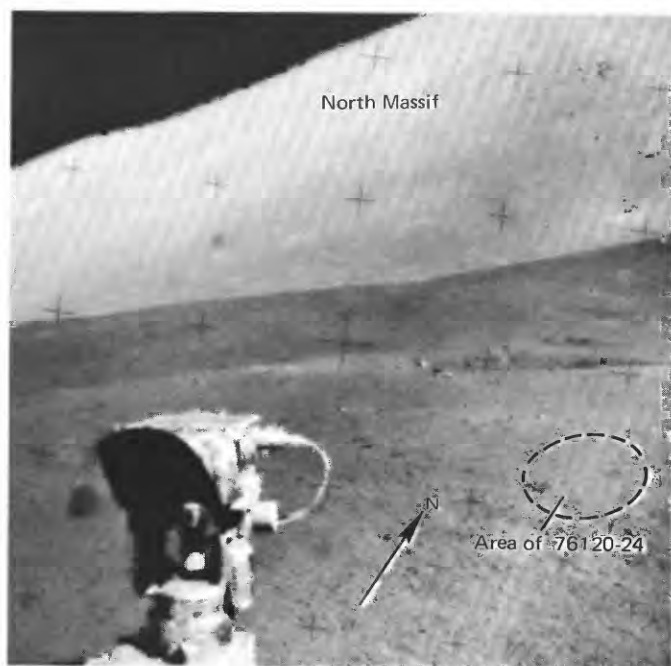


FIGURE 140.—Station LRV-9 sampling area. (NASA photograph AS17-141-21543.)

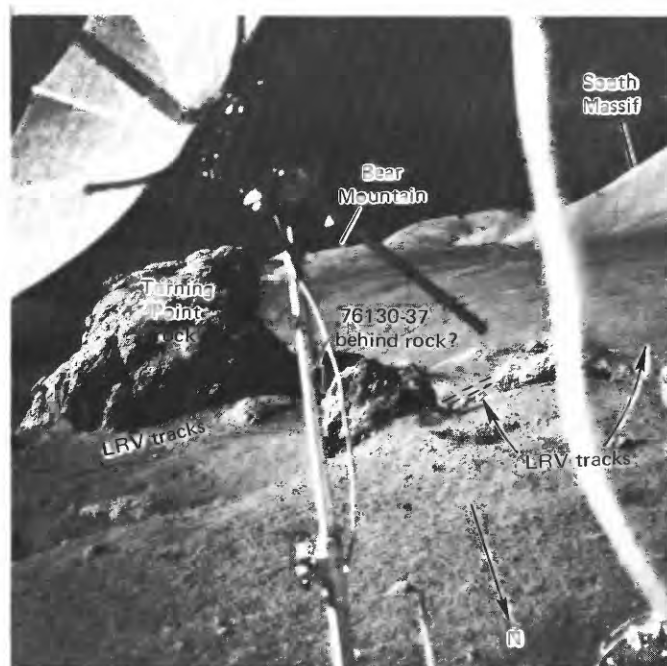


FIGURE 141.—Station LRV-10 area after sampling. Sample 76130-37 was probably collected from behind rock in foreground. (NASA photograph AS17-140-21396.)

*Length:* 35.5 cm.

*Depth:* Approximately 37.1 cm.

*Location:* 3-4 m southeast of the LRV at station 6.

*Illustrations:* Pans 21, 22; figure 152.

*Comments:* Drive tube has not been opened.

#### Sample 76015

*Type:* Metaclastic rock with a poikilitic matrix.

*Size:* 20×16×14 cm.

*Weight:* 2,819 g.

*Location:* North side of block 5 at station 6.

*Illustrations:* Pans 21, 22; figures 153, 154 (LRL).

*Comments:* Sample 76015 is a greenish-gray breccia similar in texture and color to sample 76215 from block 4. Both are from well-foliated unit B (fig. 149) defined by Heiken and others (1973).

*Petrographic description:* Vesicular metaclastic rock with scarce lithic clasts of plagioclase-, pyroxene-, or (rare) olivine-rich hornfels and mineral clasts of plagioclase and some olivine in a poikilitic matrix with low-calcium pyroxene oikocrysts enclosing newly crystallized plagioclase and broken mineral debris. Cavities are irregular to spherical.

Simonds (1975) interpreted sample 76015 as a clast-bearing poikilitic impact melt. The crystallized melt is now represented by a continuous network of interlocking pigeonite oikocrysts enclosing small plagioclase crystals. Mineral and lithic clasts make up about 14 volume percent of the sample. Most mineral clasts lack definitive shock features. Larger plagioclase fragments commonly have overgrowths up to 20  $\mu\text{m}$  wide that tend to make them euhedral. As determined by

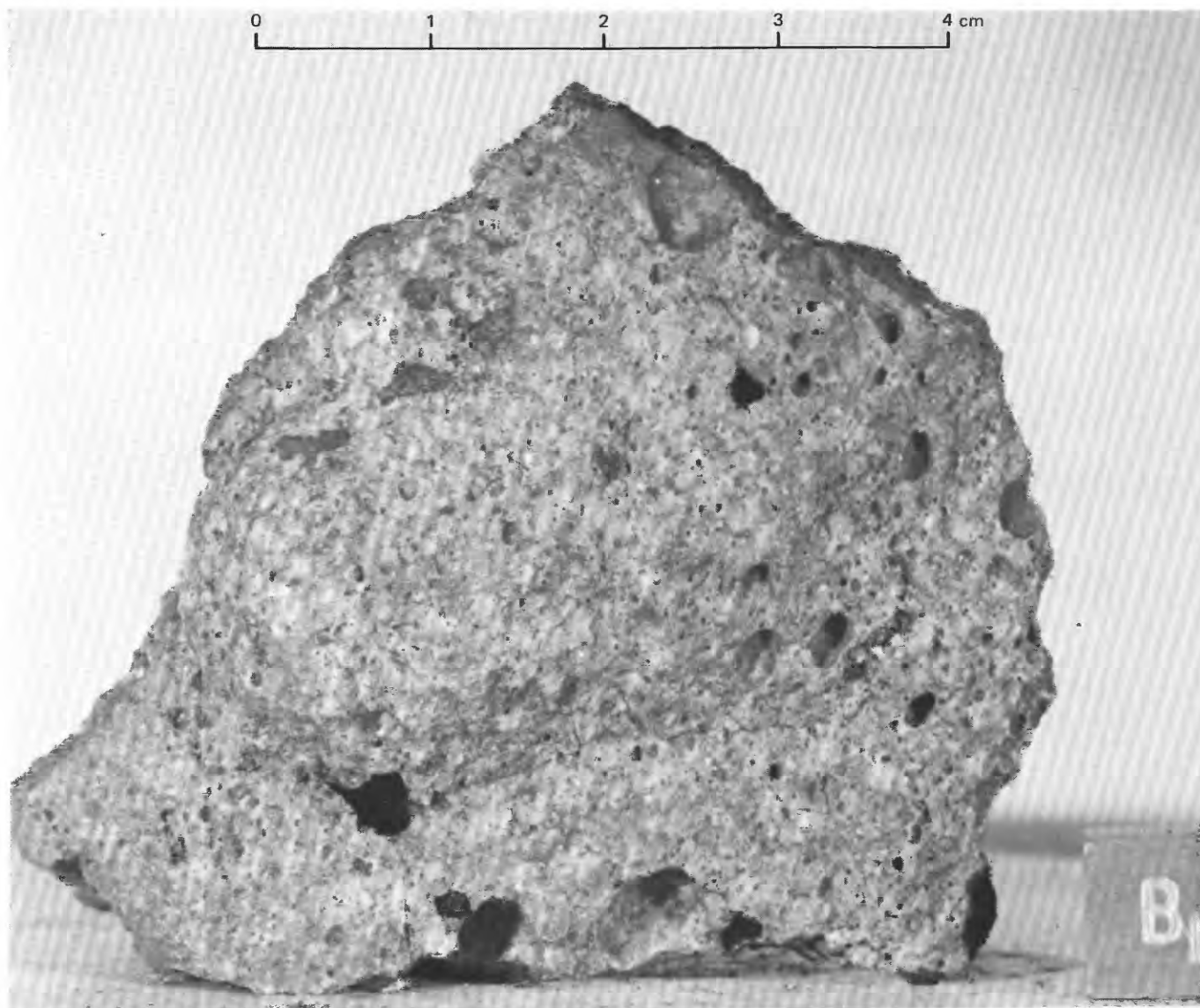
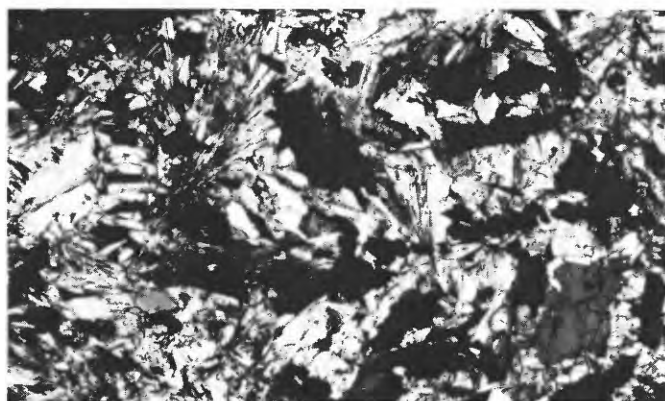


FIGURE 142.—Sample 76135. Metaclastic rock with poikilitic matrix. (NASA photograph S-73-15405.)

Simonds (1975), lithic clasts include annealed dunite, anorthosite, anorthositic troctolite, norite, troctolite, and basalt.



0 1 mm

FIGURE 143.—Sample 76136. Photomicrograph showing medium-grained olivine basalt with variolitic texture. Crossed polarizers.

### Major-element composition:

#### Chemical analyses of 76015

	1	2	3	4
SiO <sub>2</sub> .....	46.16	46.38	46.38	46.59
Al <sub>2</sub> O <sub>3</sub> .....	17.17	17.78	17.77	18.00
FeO.....	9.81	9.65	9.07	9.10
MgO.....	13.03	12.40	12.67	12.43
CaO.....	10.77	11.13	11.11	11.10
Na <sub>2</sub> O.....	.70	.72	.69	.75
K <sub>2</sub> O.....	.26	.26	.26	.29
TiO <sub>2</sub> .....	1.52	1.55	1.53	1.48
P <sub>2</sub> O <sub>5</sub> .....	.27	.29	.29	.28
MnO.....	.13	.13	.12	.12
Cr <sub>2</sub> O <sub>3</sub> .....	--	--	--	--
Total.....	99.82	100.29	99.89	100.14

1. 76015,22, matrix (Rhodes and others, 1974).
2. 76015,37, matrix (Rhodes and others, 1974).
3. 76015,41, matrix (Rhodes and others, 1974).
4. 76015,64, matrix (Rhodes and others, 1974).

### Age:

<sup>40</sup>Ar:

76015,38 (matrix),  $3.93 \pm 0.04$  b.y. (Cado-  
gan and Turner, 1976).

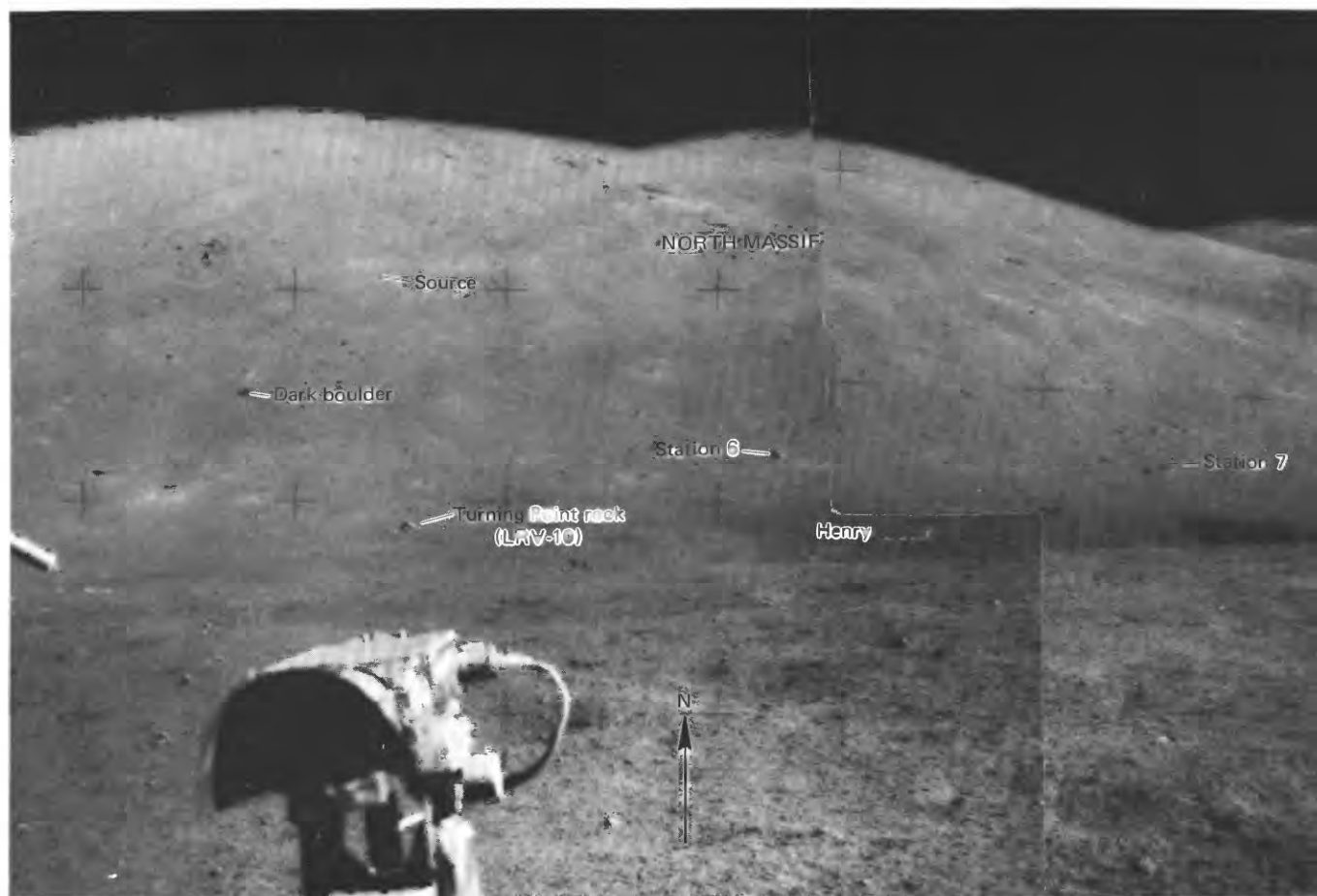


FIGURE 144.—View from LRV of North Massif showing Turning Point rock (LRV-10) and stations 6 and 7. Dark boulder is at end of boulder track originating high on massif, and station 6 boulder is at end of barely visible track originating at point labeled "source." Figure 145 gives a telephoto view of some of these features. (NASA photographs AS17-141-21549, 21550.)

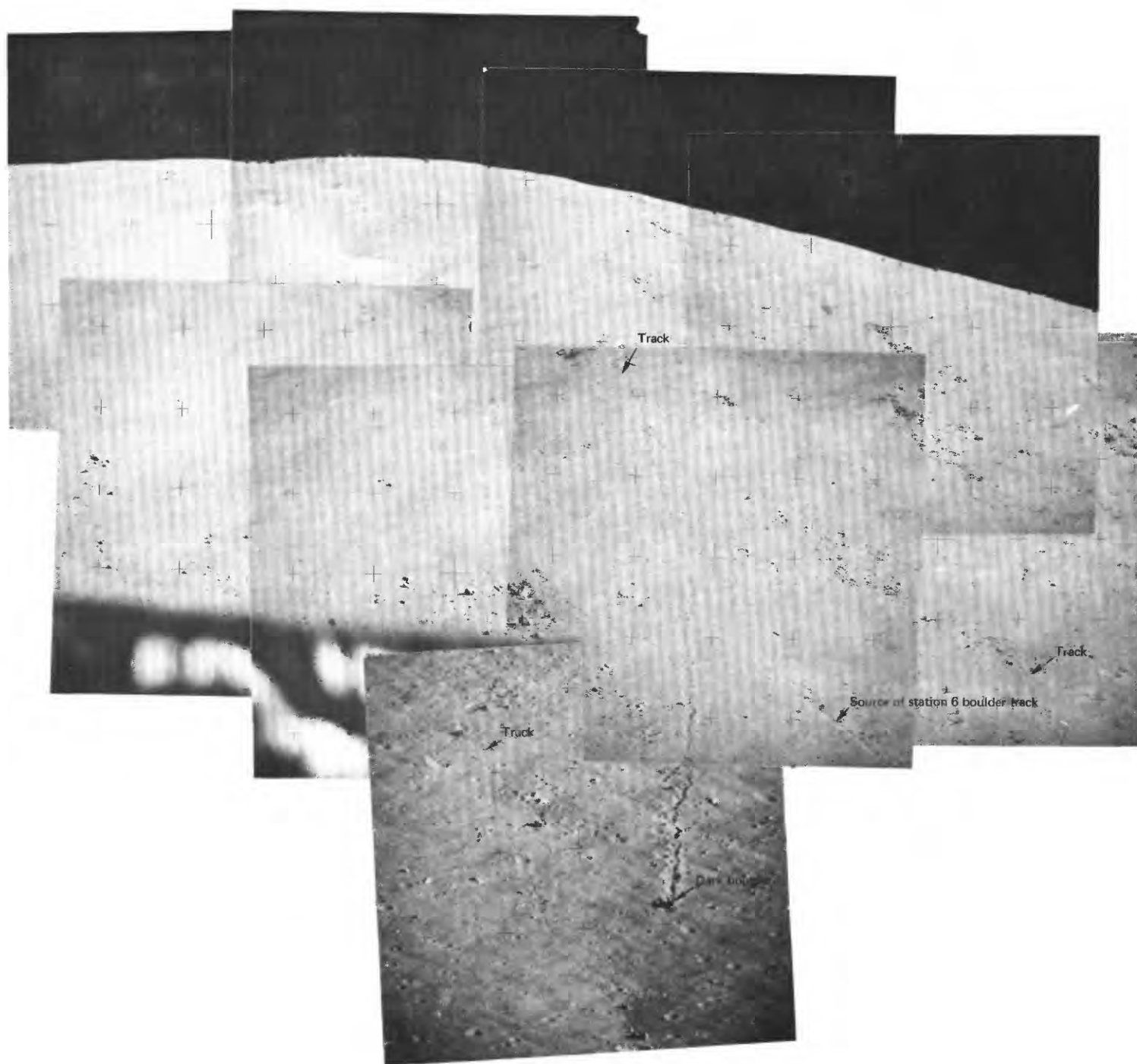


FIGURE 145.—Telephoto view of North Massif, taken from LM area, shows scattered fields of blocks on massif face and source of track made by station 6 boulder. Upper ends of three other boulder tracks are identified by the word "track." (NASA photographs AS17-144-21991, 22119 to 22122, and 22127 to 22130.)

76015,38 (plagioclase concentrate),  
 $3.96 \pm 0.06$  b.y. (Cadogan and Turner,  
 1976).

76015,36 (plagioclase concentrate),  
 $3.96 \pm 0.04$  b.y. (Cadogan and Turner,  
 1976).

*Exposure age:*

Kr:  $17.5 \pm 0.5$  m.y. (Croaz and others, 1974).

Track:  $18.3 \pm 3$  m.y. (Croaz and others, 1974).

The difference between this exposure age and the slightly greater exposure age measured on 76351 is interpreted as due to a change in shielding, perhaps in the event that separated block 5 from the rest of the station 6 boulder. On the basis of solar flare track measurements, Croaz and others (1974) estimate that block 5 was broken away about 1 m.y. ago.

Sample 76030-37

*Type:* Sedimentary, unconsolidated (76030-34);

polymict breccia with an aphanitic matrix (76035); breccia (76036); and basalt (76037).

*Size:* 76035,  $12 \times 5.5 \times 5$  cm; 76036,  $2.5 \times 2 \times 0.6$  cm; 76037,  $1.7 \times 1.2 \times 0.8$  cm.

*Weight:* 76030-34, 180.96 g; 76035, 376.2 g; 76036, 3.95 g; 76037, 2.52 g.

*Depth:* Upper few centimeters.

*Location:* Small crater about 20 m east of blocks. 76035 and possibly 76036 from a one-third-meter boulder in the small crater.

*Illustrations:* Pan 21, 22; figures 155, 156 (photomicrograph, 76035), 166.

*Comments:* Sample 76035 was chipped from a one-third-meter boulder that may represent ejecta from a crater higher up on the North Massif. Sample 76036 may also have been chipped from the boulder or may be a regolith fragment. Sample 76037 is probably a chip of subfloor basalt from the local regolith. Sediment sample 76030-34 represents the local regolith, presumably a mixture of North Massif and valley floor material.

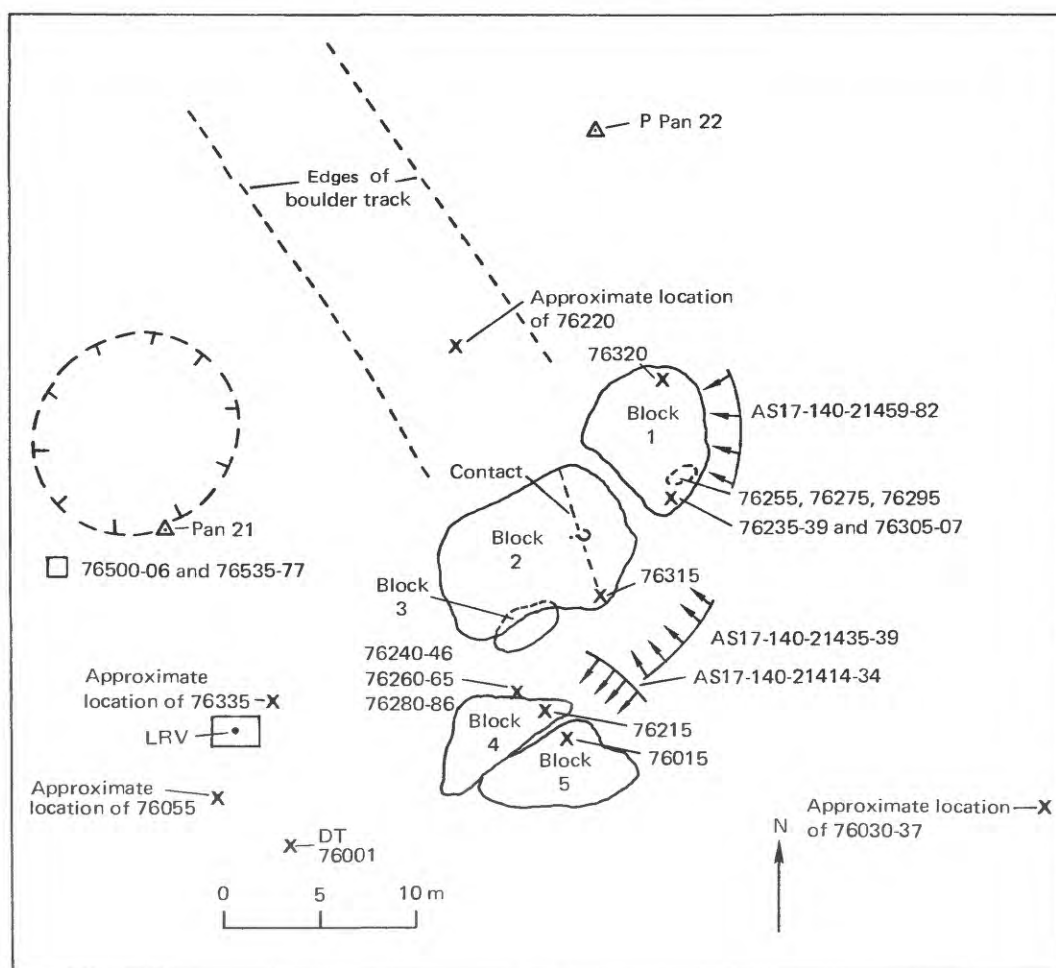


FIGURE 146.—Planimetric map of station 6.

*Petrographic description:*

76030-34, no description available.

76035, vesicular polymict breccia with clasts of metatroctolitic rocks with relict plagioclase and olivine in a poikilitic matrix, polycrystalline olivine aggregates, fine-grained intersertal rocks of basaltic mineralogy, and fine-grained plagioclase-rich metaclastic rocks in an aphanitic matrix of recrystallized pyroxene, plagioclase, and abundant plagioclase and olivine mineral clasts with scarce spinel clasts.

Sample 76055

*Type:* Polymict breccia with a granoblastic matrix.

*Size:* 23×13×13 cm.

*Weight:* 6,412 g.

*Location:* Regolith surface within a few meters of the south side of the LRV at station 6.

*Illustrations:* Pans 21, 22; figures 157 (LRL), 166.

*Comments:* Sample 76055 is a greenish-gray breccia fragment from the North Massif.

*Petrographic description:* Polymict breccia with a fine-grained vesicular granoblastic matrix. Lithic clasts include (1) metatroctolite with a poikiloblastic matrix that is much coarser grained than the breccia matrix, (2) "dunite" cataclasite, (3) "anorthosite" cataclasite, and (4) felsic melt rock with an uneven ophitic to intersertal texture. Mineral clasts include plagioclase, olivine, and pink spinel. Cavities in youngest matrix are slitlike en echelon openings with drusy linings.

*Major-element composition:*

*Chemical analyses of 76055*

	1	2
SiO <sub>2</sub> .....	45.7	44.65
Al <sub>2</sub> O <sub>3</sub> .....	15.84	16.47
FeO.....	9.27	9.11



FIGURE 147.—Blocks 1 and 2 of station 6 boulder. Arrows indicate probable matchpoints between two blocks. Sample 76320-24 was collected from sediment deposited on near surface of block 1. (NASA photograph AS17-140-21496.)

## Chemical analyses of 76055—Continued

	1	2
MgO .....	17.89	16.33
CaO .....	9.13	9.93
Na <sub>2</sub> O .....	.55	.48
K <sub>2</sub> O .....	.223	.20
TiO <sub>2</sub> .....	1.38	1.24
P <sub>2</sub> O <sub>5</sub> .....	.220	.19
MnO .....	.122	.11
Cr <sub>2</sub> O <sub>3</sub> .....	.19	.19
Total .....	100.52	98.90

1. 76055,3 (Nava, 1974).

2. 76055,5 (Apollo 17 PET, 1973).

## Age:

<sup>40</sup>Ar—<sup>39</sup>Ar:

76055, 3.98±0.05 b.y. (Turner and others, 1973).

76055,4,1, 4.05±0.07 b.y. (Kirsten and Horn, 1973).

76055,6, 3.97±0.04 b.y. (Huneke and others, 1973).

## Rb-Sr isochron:

76055,6, 3.86±0.04 b.y. (Tera and others, 1974b). Two-point isochron based on Rb-Sr measurements for total rock and for a separate dominated by fine-grained potassium-rich phases. Plagioclase separates are off of this isochron and were interpreted as not equilibrated with the finer grained recrystallized matrix. Model age for potassium-rich fine-grained material, calculated with respect to BABI (basaltic achondrite best initial) is 4.08 b.y., interpreted as a strict older limit on the age of metamorphism (Tera and others, 1974b).

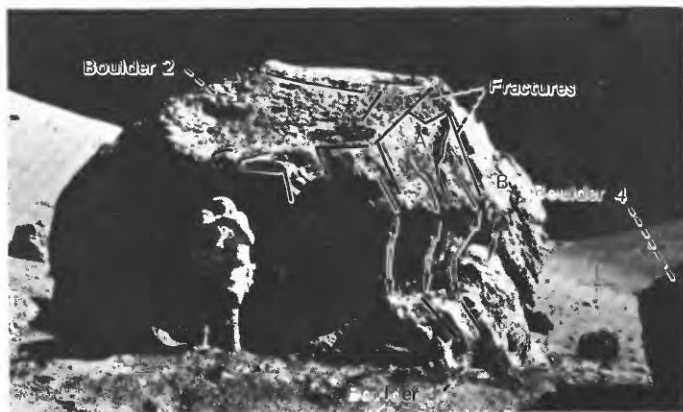


FIGURE 148.—Blocks 2 and 3 at station 6. Arrows connect fractures that would be aligned if blocks were fitted together. (NASA photograph AS17-146-22293.) (After Muehlberger and others, 1973.)

## Exposure age:

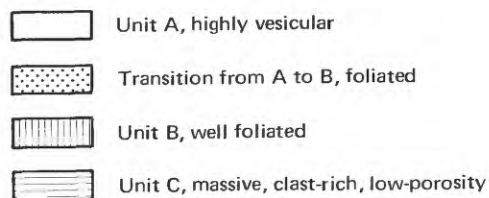
Ar:

76055, 125 m.y. (Turner and others, 1973).

76055,4,1, 120±15 m.y. (Kirsten and Horn, 1974).

76055,6, 140 m.y. (Huneke and others, 1973).

## Sample 76215

*Type:* Metaclastic rock with a dominantly poikilitic matrix.*Size:* 10.5×8×6 cm.*Weight:* 643.9 g.*Location:* From rock lying on surface at northeast corner of block 4 at station 6.*Illustrations:* Pan 21; figures 158, 159, 160 (LRL), 161 (photomicrograph).*Comments:* Sample 76215, a greenish-gray breccia, was broken from a rock that the crew identified as having spalled from block 4. The sample is from theN  
↑

0 5 10 m

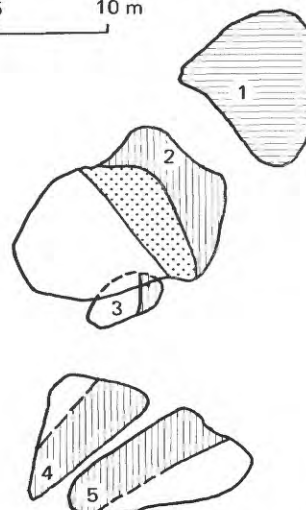


FIGURE 149.—Map showing lithologic divisions inferred by Heiken and others (1973) for station 6 boulder.

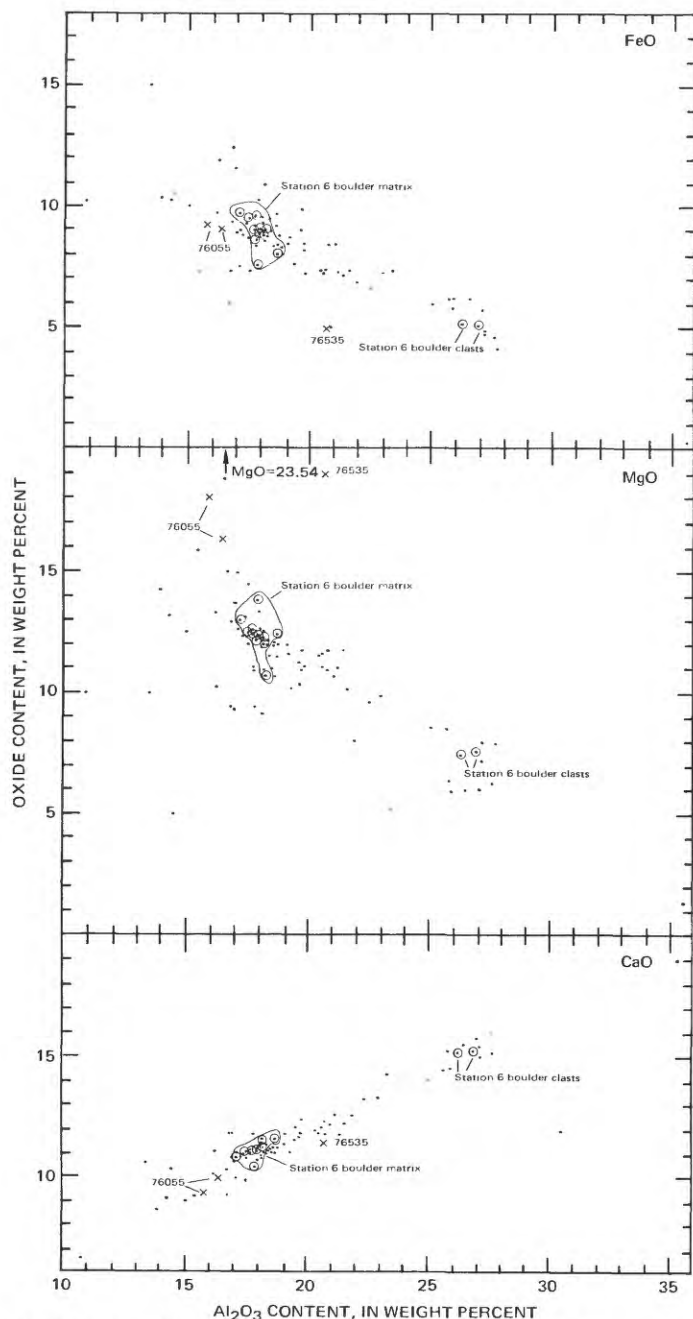


FIGURE 150.—Plots of FeO, MgO, and CaO contents in relation to  $\text{Al}_2\text{O}_3$  content for analyzed highlands rocks at station 6 (circled dots, station 6 boulder; x, other station 6 rocks) in comparison with all analyzed Apollo 17 highlands rocks (dots).

well-foliated unit B of Heiken and others (1973).  
*Petrographic description:* Vesicular metaclastic rock with scarce lithic clasts of fine-grained feldspathic hornfels and mineral clasts of plagioclase and olivine in a poikilitic matrix that grades, toward vesicles, to an ophitic melt texture. Poikilitic part is dominant and has oikocrysts of low-calcium pyroxene enclosing newly crystallized plagioclase as well as relict broken grains of plagioclase and olivine.

Simonds (1975) interpreted sample 76215 as a poikilitic and ophitic impact melt largely represented by clast-laden poikilitic rock consisting of a network of pigeonite and subordinate augite oikocrysts enclosing abundant tiny feldspar grains and some olivine. Mineral clasts, largely with no evidence of shock metamorphism, are feldspar, pyroxene, and olivine; overgrowths tend to make the feldspars euhedral. Lithic clasts are anorthosite and dunite.

#### Major-element composition:

##### Chemical analyses of 76215

	1	2
$\text{SiO}_2$ .....	46.13	46.02
$\text{Al}_2\text{O}_3$ .....	18.73	17.83
$\text{FeO}$ .....	8.08	8.70
$\text{MgO}$ .....	12.43	12.21
$\text{CaO}$ .....	11.50	11.10
$\text{Na}_2\text{O}$ .....	--	--
$\text{K}_2\text{O}$ .....	.25	.27
$\text{TiO}_2$ .....	1.24	1.52
$\text{P}_2\text{O}_5$ .....	.24	.28
$\text{MnO}$ .....	--	--
$\text{Cr}_2\text{O}_3$ .....	--	--

1. 76215, 28, 29, and 48, matrix (Simonds, 1975).  
 2. 76215, 26, and 27, matrix (Simonds, 1975).

Age:  $^{40}\text{Ar}$ : 76215, 30 (matrix),  $3.94 \pm 0.04$  b.y. (Cadogan and Turner, 1976).

#### Sample 76220-24

Type: Sedimentary, unconsolidated.

Weight: 612.84 g.

Depth: From upper few centimeters.

Location: Station 6 boulder track depression approximately 10 m north of boulder area.

Illustrations: Pans 21, 22; figure 162.

Comments: Sample 76220-24 is probably a mixture of North Massif and valley floor material.

#### Sample 76235-39, 76305-07

Type: Olivine metanorite cataclasite.

Sizes:  $1.5 \times 1.5 \times 0.5$  cm to  $5 \times 3 \times 2$  cm.

Weight: 81.24 g total.

Location: From light-gray clast on southeast side of block 1 at station 6.

*Illustrations:* Pans 21, 22; figures 163, 164 (LRL), 167.

*Comments:* From clast incorporated in blue-gray breccia of massive low-porosity unit C of Heiken and others (1973).

*Petrographic description:* Metatroctolite or olivine metanorite cataclasite. Unshattered relics have a poikiloblastic to granoblastic-polygonal texture.

Simonds (1975) described 76235 as olivine-bearing feldspathic norite with poikilitic pyroxene. The rock contains 70 percent plagioclase, 20 percent pigeonite, and 10 percent olivine.

*Major-element composition:*

*Chemical analysis of 76230*

SiO <sub>2</sub> .....	44.52
Al <sub>2</sub> O <sub>3</sub> .....	27.01

*Chemical analysis of 76230 —Continued*

FeO .....	5.14
MgO .....	7.63
CaO .....	15.17
Na <sub>2</sub> O .....	.35
K <sub>2</sub> O .....	.06
TiO <sub>2</sub> .....	.20
P <sub>2</sub> O <sub>5</sub> .....	.05
MnO .....	.06
Cr <sub>2</sub> O <sub>3</sub> .....	.11
Total .....	100.30
76230.4 (Apollo 17 PET, 1973).	

The analysis was made of a small chip from the sample residue; according to Butler (1973), the 76230 chip is representative of the larger 76235-39, 76305-07 collection of chips from the light-gray clast in block 1.

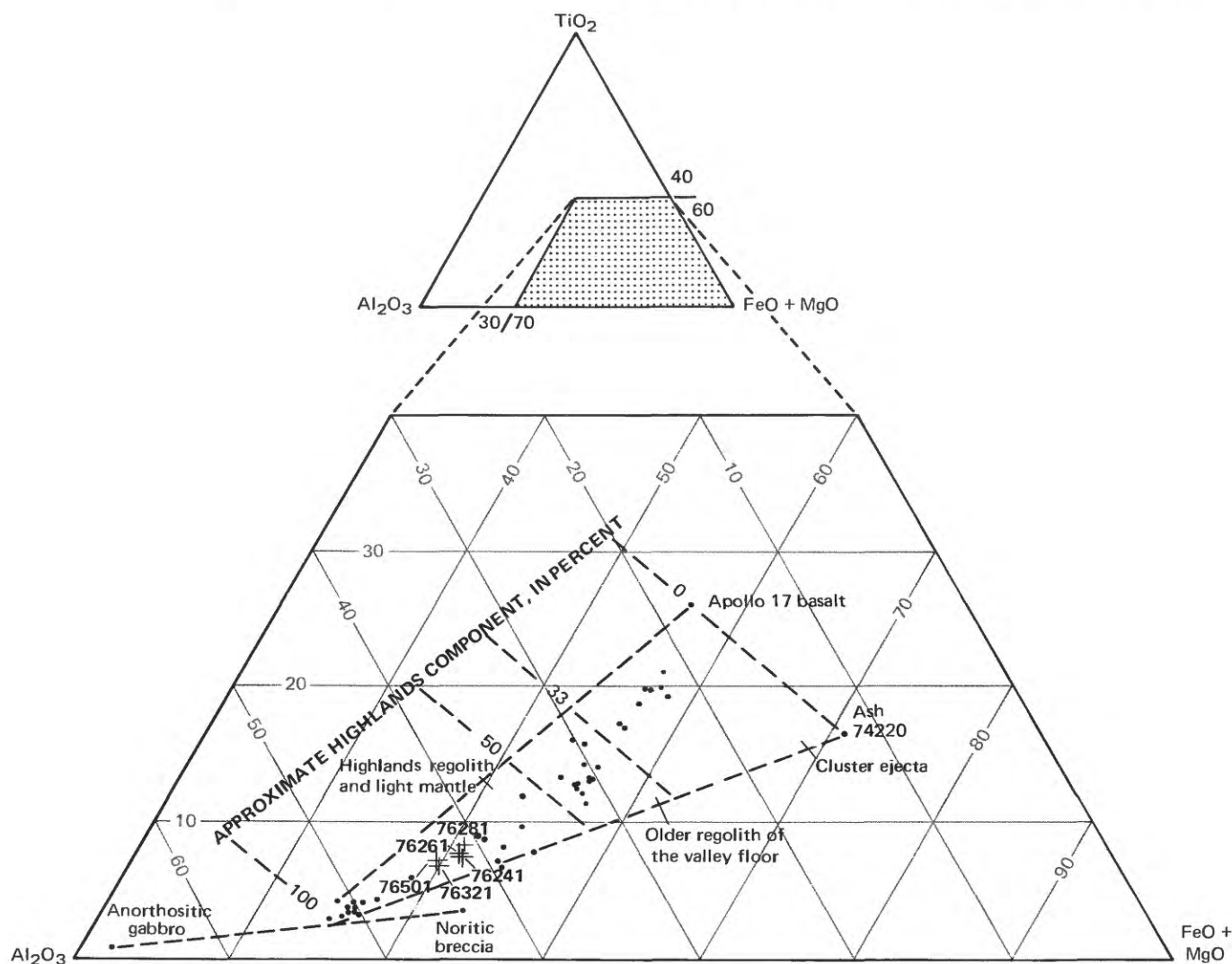


FIGURE 151.—Relative amounts of TiO<sub>2</sub>, Al<sub>2</sub>O<sub>3</sub>, and FeO + MgO in sediment samples 76241, 76261, 76281, 76321, and 76501 (crosses) from station 6, in comparison with sediment samples from rest of traverse region (dots). Apollo 17 basalt, anorthositic gabbro, and noritic breccia values from Rhodes and others (1974).

Age:

$^{40}\text{-}^{39}\text{Ar}$ :

76235,3,  $3.93 \pm 0.06$  b.y. (Cadogan and Turner, 1976).

76235,3,  $3.95 \pm 0.06$  b.y.

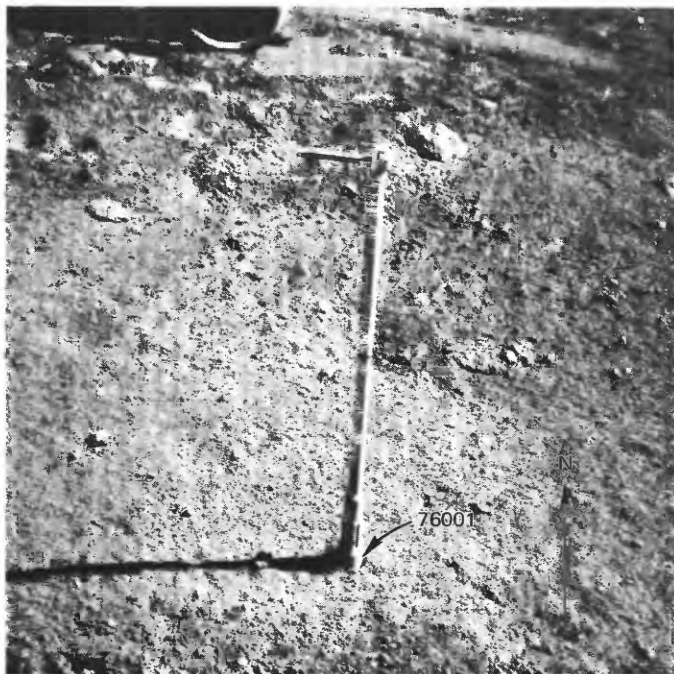
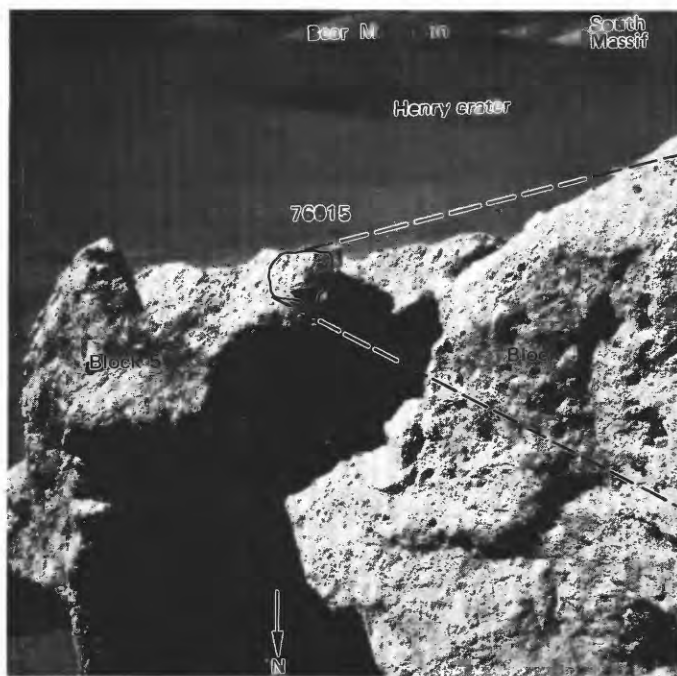


FIGURE 152.—Drive tube sample 76001 during sampling. (NASA photograph AS17-146-22292.)



Ages from two separate runs are in agreement with each other and with ages determined for the enclosing breccia. Strong heating and complete outgassing of argon during the impact that assembled the station 6 boulder materials are inferred (Cadogan and Turner, 1976).

#### Sample 76240-46

*Type:* Sedimentary, unconsolidated (76240-44) and metaclastic rock with a poikilitic(?) matrix (76245-46).

*Size:* 76245, two pieces,  $2 \times 2 \times 1$  cm and  $1 \times 1 \times 0.5$  cm; 76246,  $3 \times 2 \times 2$  cm.

*Weight:* 76240-44, 475.8 g; 76245, 8.24 g; 76246, 6.5 g.

*Depth:* 0 to 5 cm.

*Location:* From shadowed area immediately north of block 4 at station 6.

*Illustrations:* Pan 21; figures 165, 166.

*Comments:* Sediment sample 76240-44 is a mixture of North Massif and valley floor material. The two breccia fragments (76245-46) presumably came from the North Massif.

#### *Petrographic description:*

76240-44, basalt, some feldspathic metaclastic rocks.

*Components of 90-150- $\mu$ m fraction of 76241,24 (Heiken and McKay, 1974)*

Components	Volume percent
Agglutinate .....	48.0
Basalt, equigranular .....	2.3
Basalt, variolitic .....	1.0

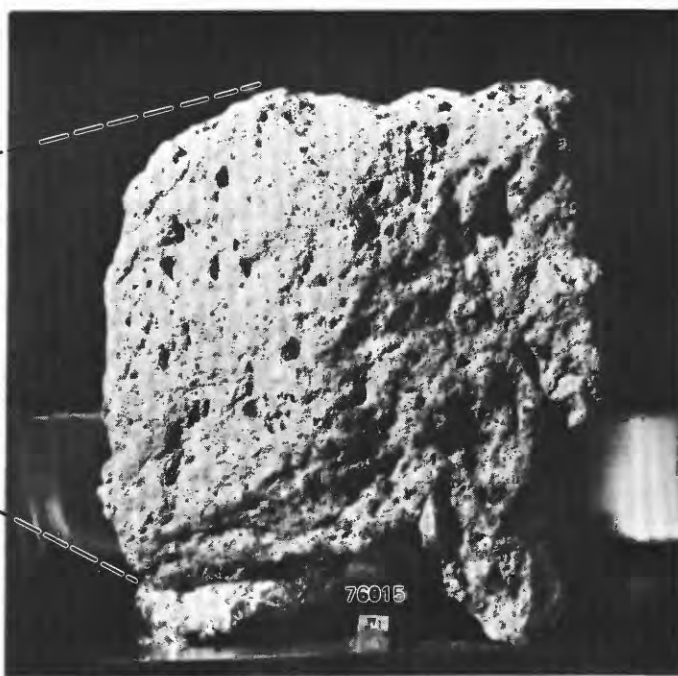


FIGURE 153.—Left, Location of sample 76015 on block 5 before collection. Shadowed area marks northeast-southwest split between blocks 4 and 5. (NASA photograph AS17-140-21411.) Right, Sample 76015 with reconstructed lunar surface orientation and lighting. (NASA photograph S-73-19376.)

Components of 90-150- $\mu$ m fraction of 76241,24 (Heiken and McKay, 1974)—Continued

Components	Volume percent
Breccia:	
Low grade <sup>1</sup> - brown	4.7
Low grade <sup>1</sup> - colorless	2.7
Medium to high grade <sup>2</sup>	12.3
Anorthosite	.3
Cataclastic anorthosite <sup>3</sup>	1.3
Norite	..
Gabbro	..
Plagioclase	12.0
Clinopyroxene	5.0
Orthopyroxene	2.0
Olivine	1.3
Ilmenite	2.0
Glass:	
Orange	.7
"Black"	2.3
Colorless	.7
Brown	1.3
Gray, "ropy"	..
Other	..
Total number grains	300

<sup>1</sup>Metamorphic groups 1-3 of Warner (1972).

<sup>2</sup>Metamorphic groups 4-8 of Warner (1972).

<sup>3</sup>Includes crushed or shocked feldspar grains.

76245,76246, vesicular metaclastic(?) rocks with scarce mineral relics in a poikilitic(?) matrix. No thin sections available.

Major-element composition:

Chemical analysis of 76241

SiO <sub>2</sub>	43.20
Al <sub>2</sub> O <sub>3</sub>	17.85
FeO	10.92
MgO	11.05
CaO	11.97
Na <sub>2</sub> O	.43
K <sub>2</sub> O	.12
TiO <sub>2</sub>	3.31
P <sub>2</sub> O <sub>5</sub>	.09
MnO	.16
Cr <sub>2</sub> O <sub>3</sub>	..
Total	99.10

76241.14 (Rhodes and others, 1974).

Sample 76255

Type: Polymict breccia with a cataclastic matrix.

Size: 11×8×6 cm.

Weight: 406.6 g.

Location: Southeast side of block 1 at station 6.

Illustrations: Pans 21, 22; figures 163, 167, 168 (LRL), 169 (map of slab).

Comments: Sample 76255 was collected from the contact zone between a large tan clast (fig. 167) and the blue-gray breccia of the massive low-porosity unit C of Heiken and others (1973).

Petrographic description: Polymict breccia formed by disruption of an older polymict breccia with large clasts of olivine norite or olivine metanorite. Resultant rock is banded polymict breccia (older matrix, reworked) and olivine-norite cataclasite containing fragments of the older polymict breccia. The resulting polymict breccia has clasts of fine-grained

feldspathic metaclastic rock and elongate cavities with linings of delicate brown pyroxene-spongy plagioclase intergrowths. Some vug linings were disrupted and incorporated in the cataclasite but were formed by local melting of the older polymict breccia.

Warner and others (1976), members of the consortium studying the station 6 boulder in detail, have described sample 76255 as predominantly a clast of norite cataclasite (unit 3 in fig. 169) in a matrix of fine-grained polymict breccia (unit 1 in fig. 169), with a zone of mixed lithology (unit 2 in fig. 169) separating the two units. They have interpreted the polymict breccia as crystallized clast-laden impact melt and regard it as a portion of the matrix of the massive unit C (fig. 149). Additional small clasts in the sample include gabbro, troctolite, and two basalt fragments that resemble mare basalt. Age: <sup>40-39</sup>Ar: 76255,46 (clast, presumably norite cataclasite),  $4.02 \pm 0.04$  b.y. (Cadogan and Turner, 1976).

Sample 76260-65

Type: Sedimentary, unconsolidated (76260-64) and breccia fragment (76265).

Size: 76265, 2×1.5×0.7 cm.

Weight: 76260-64, 291.18 g; 76265, 1.75 g.

Depth: From 0 to 2 cm.

Location: Regolith surface north of block 4 at station 6.

Same site as sample 76280-86.

Illustrations: Pan 21; figures 165, 166.

Comments: Sediment sample 76260-64 is regolith derived from the North Massif with some admixed valley floor material. Sample 76265 is presumably a chip of North Massif material.

Petrographic description: 76260-64, dominantly fine-grained breccia and (or) metaclastic rock, scarce glass.

Components of 90-150- $\mu$ m fraction of 76261,26 (Heiken and McKay, 1974)

Components	Volume percent
Agglutinate	45.3
Basalt, equigranular	3.3
Basalt, varjolitic	1.0
Breccia:	
Low grade <sup>1</sup> - brown	2.3
Low grade <sup>1</sup> - colorless	3.3
Medium to high grade <sup>2</sup>	12.6
Anorthosite	1.0
Cataclastic anorthosite <sup>3</sup>	..
Norite	.3
Gabbro	..
Plagioclase	10.3
Clinopyroxene	9.3
Orthopyroxene	3.3
Olivine	.7
Ilmenite	1.0
Glass:	
Orange	.7

*Components of 90-150- $\mu$ m fraction of 76261,26 (Heiken and McKay, 1974) — Continued*

<i>Components</i>	<i>Volume percent</i>
Glass—Continued	
"Black" .....	1.3
Colorless .....	2.0
Brown .....	1.9
Gray, "ropy" .....	--
Other .....	--
Total number grains .....	300

<sup>1</sup>Metamorphic groups 1-3 of Warner (1972).

<sup>2</sup>Metamorphic groups 4-8 of Warner (1972).

<sup>3</sup>Includes crushed or shocked feldspar grains.

*Major-element composition:*

*Chemical analysis of 76261*

SiO <sub>2</sub> .....	43.64
Al <sub>2</sub> O <sub>3</sub> .....	17.96
FeO .....	10.93
MgO .....	10.75
CaO .....	12.11
Na <sub>2</sub> O .....	.45
K <sub>2</sub> O .....	.12
TiO <sub>2</sub> .....	3.38
P <sub>2</sub> O <sub>5</sub> .....	.11
MnO .....	.16
Cr <sub>2</sub> O <sub>3</sub> .....	.28
Total .....	99.89
76261.15 (Rhodes and others, 1974).	



FIGURE 154.—Sample 76015. Metaclastic rock with poikilitic matrix. (NASA photograph S-73-15014.)

## Sample 76275

*Type:* Polymict breccia with an aphanitic matrix.

*Size:* 6.8×4×3 cm.

*Weight:* 55.93 g.

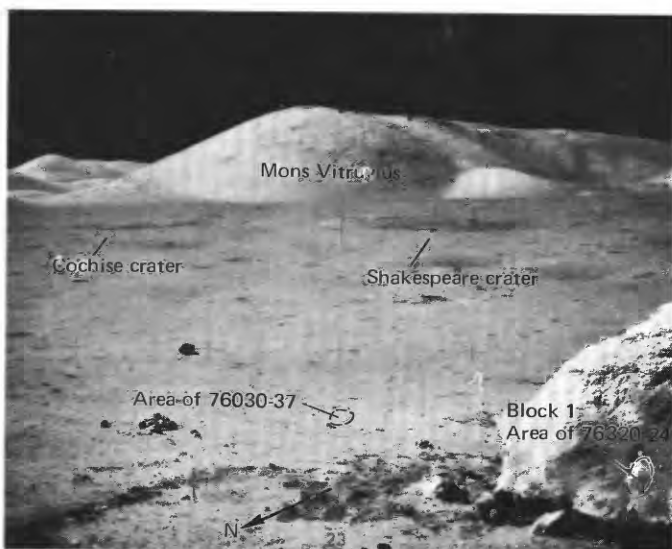


FIGURE 155.—Sample 76030-37 area (before collection) and sample 76320-24 site (after collection.) (NASA photograph AS17-140-21500.)

*Location:* From southeast side of block 1 at station 6.

*Illustrations:* Pans 21, 22; figures 163, 170 (LRL).

*Comments:* Sample 76275 is blue-gray breccia from the massive clast-rich low-porosity unit C (Heiken and others, 1973) that makes up block 1 (fig. 149).

*Petrographic description:* Polymict breccia with clasts of

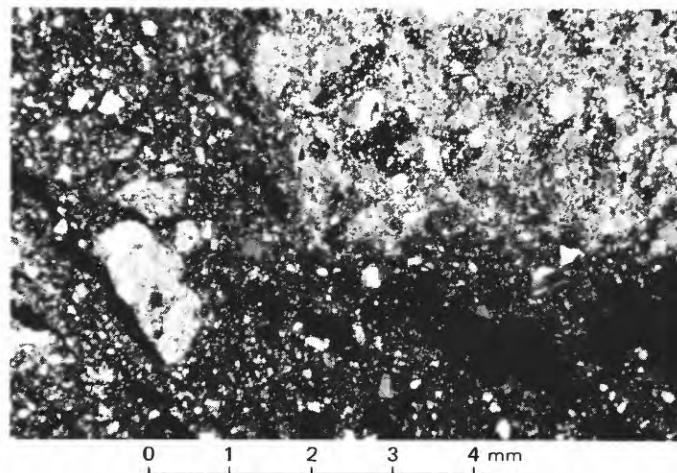


FIGURE 156.—Sample 76035. Photomicrograph showing clast with coarse poikilitic texture and porphyroclasts of plagioclase and olivine in aphanitic matrix with abundant slit cavities. Crossed polarizers.

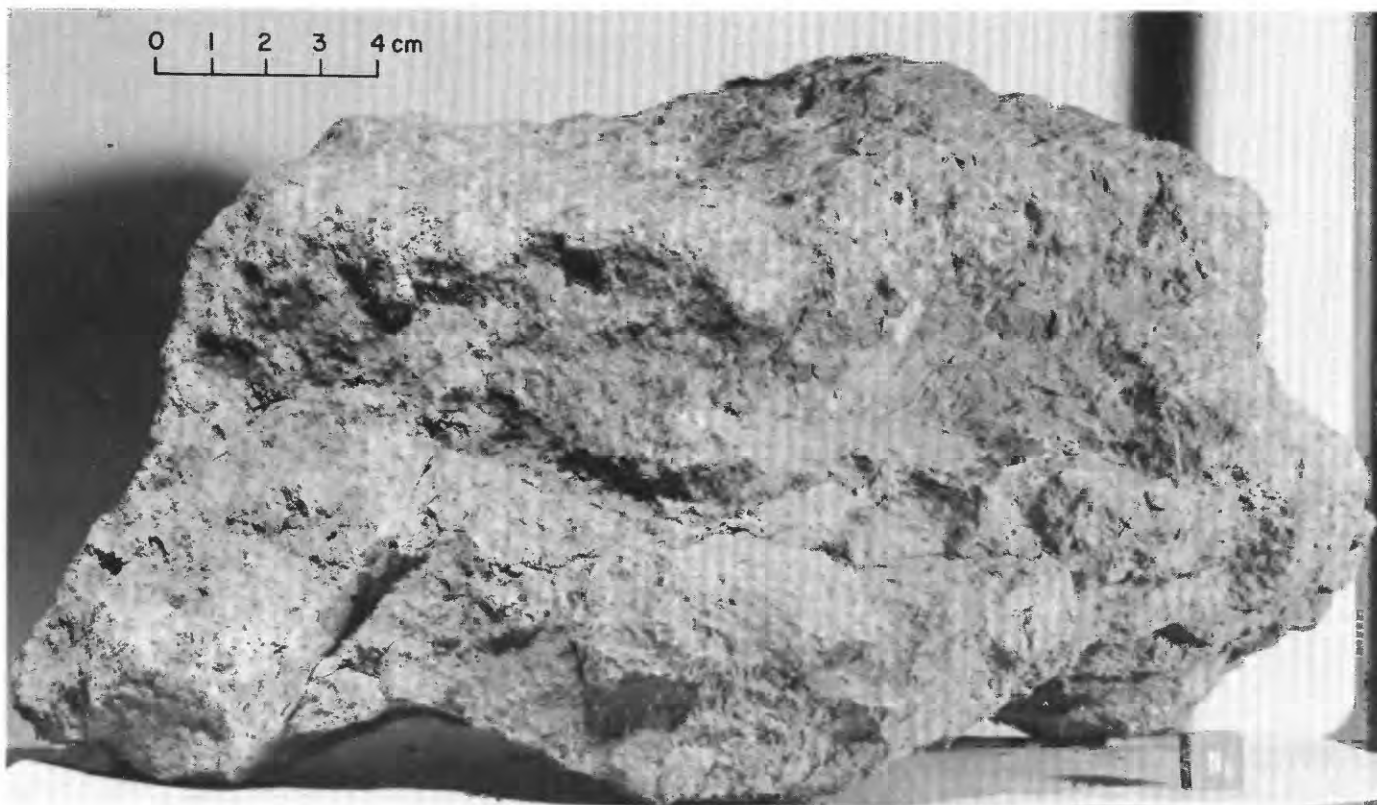


FIGURE 157.—Sample 76055. Polymict breccia with fine-grained vesicular granoblastic matrix. (NASA photograph S-73-15714.)

fine-grained breccia or metaclastic rock with an aphanitic matrix, breccia with a highly vesicular matrix, noritic(?) cataclasite, and mineral fragments in an aphanitic matrix. Intergrowths of brown pyroxene and spongy plagioclase occur as clasts. Youngest matrix may be impact fused.

Simonds (1975) has described 76275 as a clast-bearing fine subophitic melt rock identical in petrography to sample 76295.

Age:  $^{40-39}\text{Ar}$ : 76275, 39,  $4.02 \pm 0.04$  b.y. (Cadogan and Turner, 1976).

#### Sample 76280-86

*Type:* Sedimentary, unconsolidated (76280-84), with two small rock fragments (76285, 86).

*Size:* 76285,  $3 \times 1.5 \times 1.5$  cm; 76286,  $1.5 \times 1 \times 1$  cm.

*Weight:* 76280-84, 442.47 g; 76285, 2.208 g; 76286, 1.704 g.

*Depth:* From 2 to 8 cm.

*Location:* Regolith surface north of block 4 at station 6.

Same site as sample 76260-65.

*Illustrations:* Pan 21; figures 165, 166.

*Comments:* Sample is regolith derived from the North Massif with some admixed valley floor material.

*Petrographic description:* 76280-84, dominantly fine-grained breccia and (or) metaclastic rock, scarce glass, agglutinate.



FIGURE 158.—Area of block 4 from which source rock for sample 76215 was spalled. (NASA photograph AS17-140-21416.)

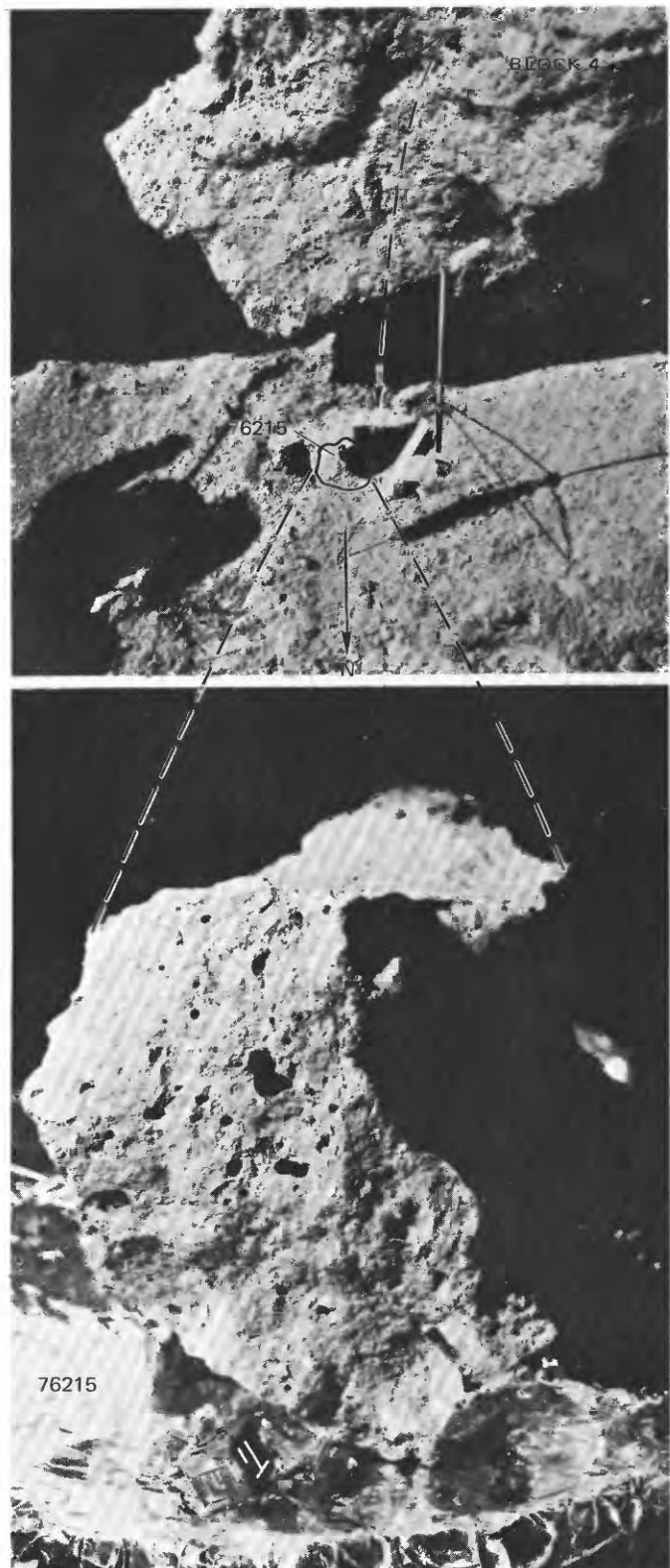


FIGURE 159.—Top, Location of sample 76215, before sampling, on rock spalled from block 4. (NASA photograph AS17-140-21410.) Bottom, Sample 76215 with reconstructed lunar surface orientation and lighting. (NASA photograph S-73-33506.)

Components of 90-150- $\mu$ m fraction of 76281,6 (Heiken and McKay, 1974)

Components	Volume percent
Agglutinate.....	45.3
Basalt, equigranular.....	5.0
Basalt, variolitic.....	1.7
Breccia:	
Low grade <sup>1</sup> - brown.....	5.3
Low grade <sup>1</sup> - colorless.....	.7
Medium to high grade <sup>2</sup> .....	10.3
Anorthosite.....	1.0
Cataclastic anorthosite <sup>3</sup> .....	.3
Norite.....	..
Gabbro.....	..
Plagioclase.....	10.7
Clinopyroxene.....	6.3
Orthopyroxene.....	4.7
Olivine.....	..
Ilmenite.....	1.3
Glass:	
Orange.....	1.3
"Black".....	3.7
Colorless.....	1.7
Brown.....	..
Gray, "ropy".....	.3
Other.....	.3
Total number grains.....	300

<sup>1</sup>Metamorphic groups 1-3 of Warner (1972).<sup>2</sup>Metamorphic groups 4-8 of Warner (1972).<sup>3</sup>Includes crushed or shocked feldspar grains.

## Major-element composition:

## Chemical analysis of 76281

SiO <sub>2</sub> .....	43.56
Al <sub>2</sub> O <sub>3</sub> .....	17.80
FeO.....	11.26
MgO.....	10.55
CaO.....	12.18
Na <sub>2</sub> O.....	.43
K <sub>2</sub> O.....	.11
TiO <sub>2</sub> .....	3.83

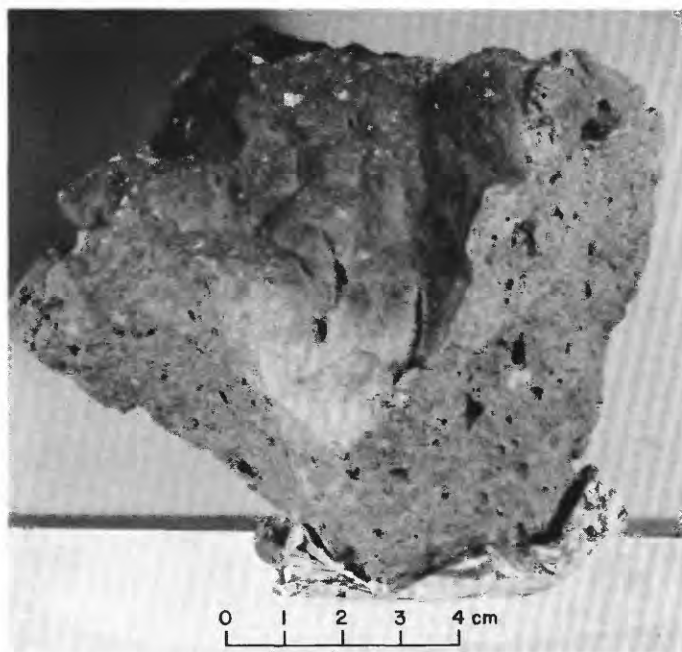


FIGURE 160.—Sample 76215. Metaclastic rock with poikilitic matrix. (NASA photograph S-72-56373.)

## Chemical analysis of 76281—Continued

P <sub>2</sub> O <sub>5</sub> .....	.09
MnO.....	.16
Cr <sub>2</sub> O <sub>3</sub> .....	.29
Total.....	100.26

76281,4 (Rhodes and others, 1974).

## Sample 76295

Type: Polymict breccia with an aphanitic matrix.

Size: 10×6×3.5 cm.

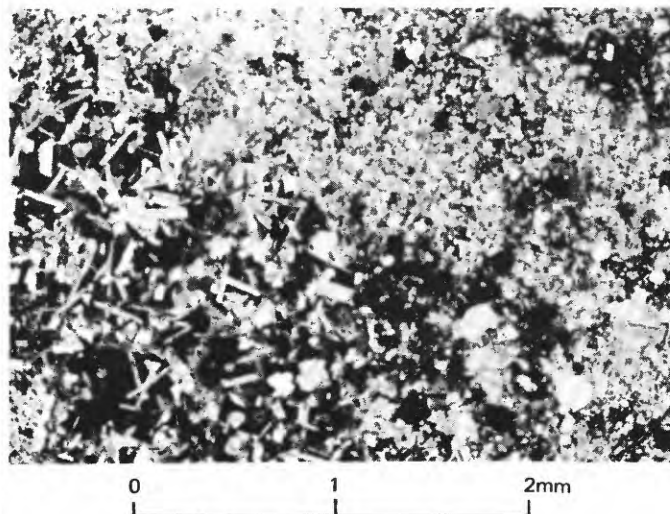


FIGURE 161.—Sample 76215. Photomicrograph showing abrupt transition from ophitic texture (lower left) to poikilitic texture (upper right). Ophitic texture is best developed around vesicles. Poikilitic part has much more abundant broken mineral debris than ophitic part. Crossed polarizers.

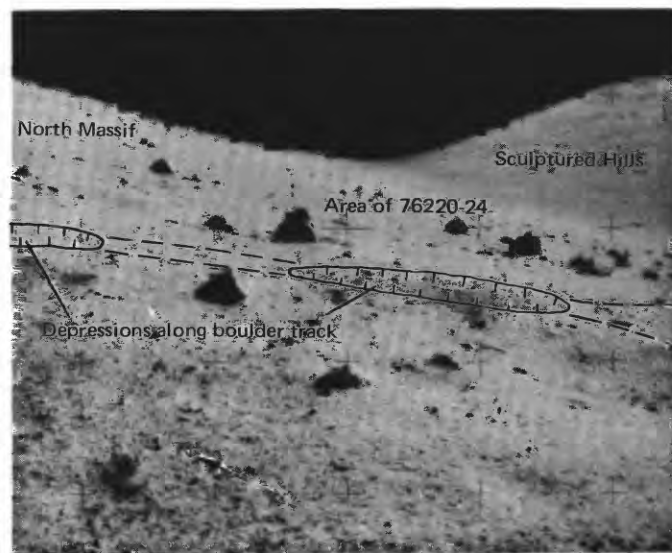


FIGURE 162.—Boulder track depression from which sample 76220-24 was collected, before sampling. (NASA photograph AS17-141-21588.)

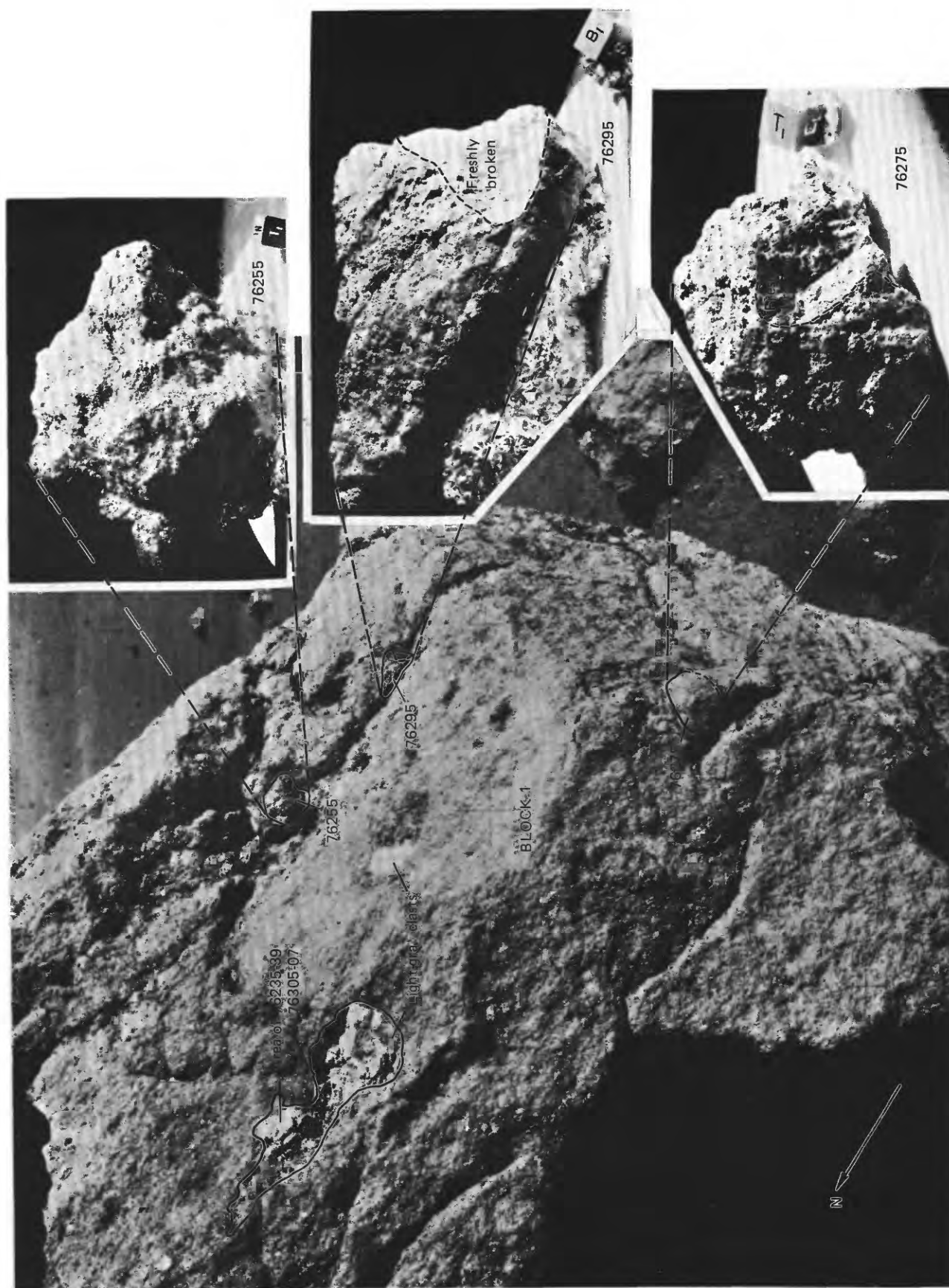


FIGURE 163.—Block 1 at station 6 before sampling. Shows locations of samples 76235-39, 76305-07, 76255, 76275, and 76295. Insets show samples 76255, 76275, and 76295 with reconstructed lunar surface orientations and lighting. (NASA photographs AS17-140-214443; S-73-19375 (76255); S-73-19385 (76275); S-73-19387 (76295).)

*Weight:* 260.7 g.

*Location:* From southeast side of block 1 at station 6.

*Illustrations:* Pans 21, 22; figures 163, 167, 171 (LRL).

*Comments:* Sample 76295 is blue-gray breccia of the clast-rich low-porosity unit C (Heiken and others, 1973) of block 1 (fig. 149).

*Petrographic description:* Polymict breccia with an

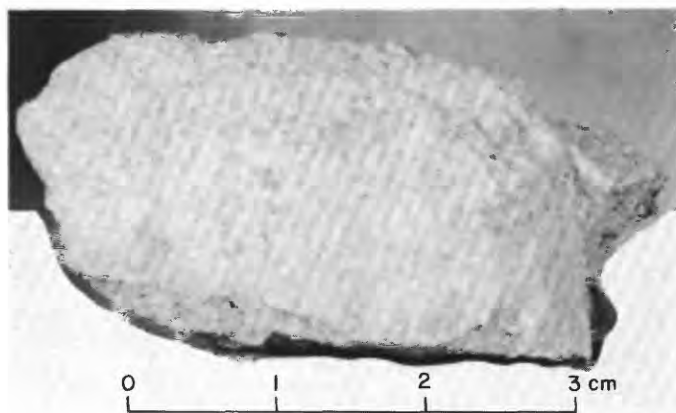


FIGURE 164.—Sample 76235. Metatroctolite cataclasite or olivine metanorite cataclasite. (NASA photograph S-73-16733.)



FIGURE 165.—Locations of samples 76240-46, 76260-65 and 76280-86, after collection. (NASA photograph AS17-141-21606.)

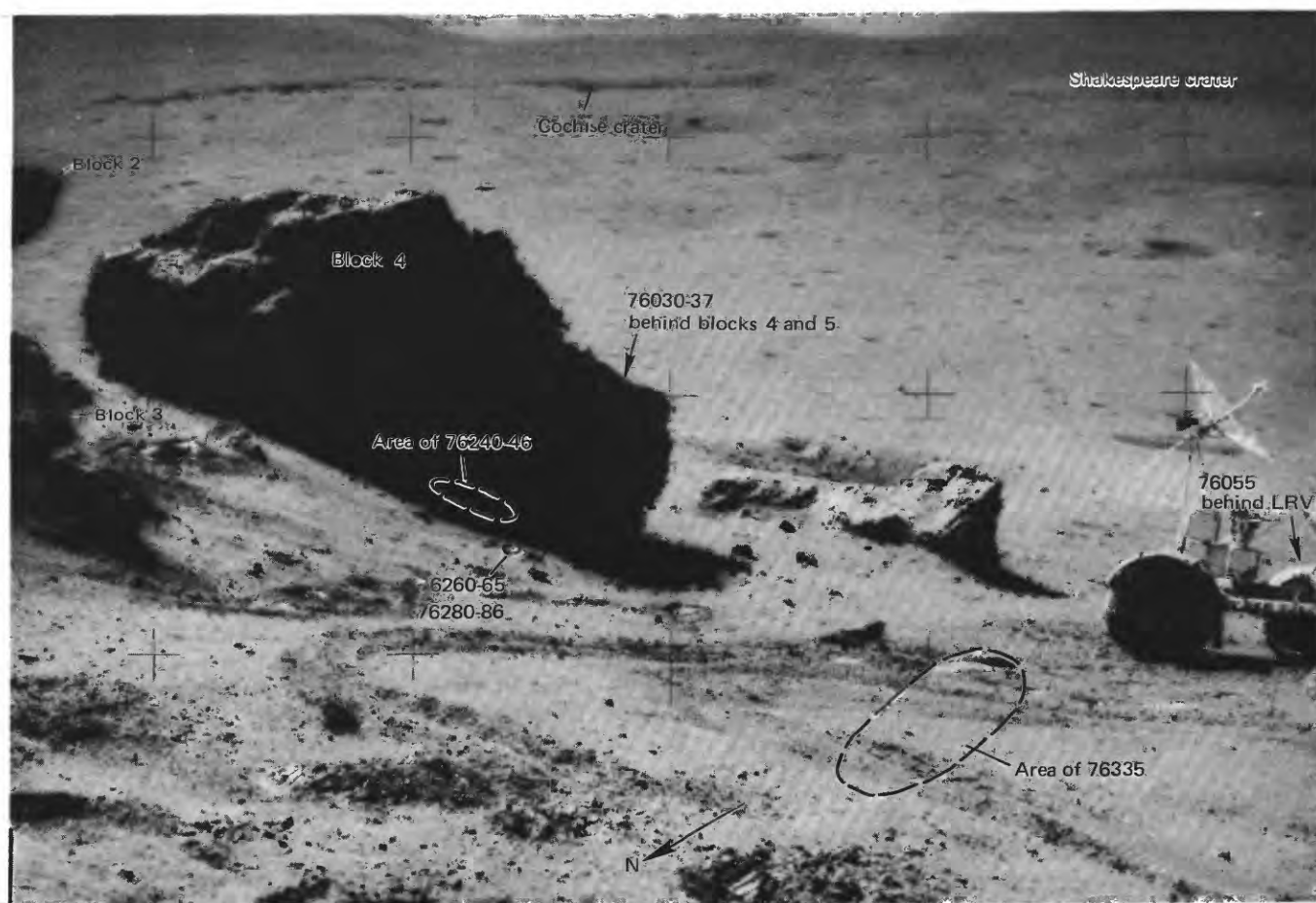


FIGURE 166.—View, southeastward, of block 4, LRV area at station 6. (NASA photograph AS17-141-21597.)

aphanitic matrix. Clasts are (1) aphanitic breccia containing feldspathic metaclastic clasts and abundant plagioclase and olivine mineral debris, (2) feldspathic metaclastic rocks, and (3) abundant plagioclase and olivine. Younger matrix is lighter colored than that of the breccia clasts.

Simonds (1975) has described 76295 as nonvesicular crystalline rock that consists of mineral and noritic lithic clasts in a matrix that crystallized from an

impact melt. The matrix is predominantly blue-gray, very fine grained, and subophitic with pyroxene oikocrysts. A second matrix type occurs as tan vein-like bodies in which mineral clasts are at least twice as abundant as they are in the blue-gray matrix. Both matrix types contain about 50 percent feldspar; the tan matrix material has abundant augite and no olivine, whereas the blue-gray matrix has abundant olivine and little augite.

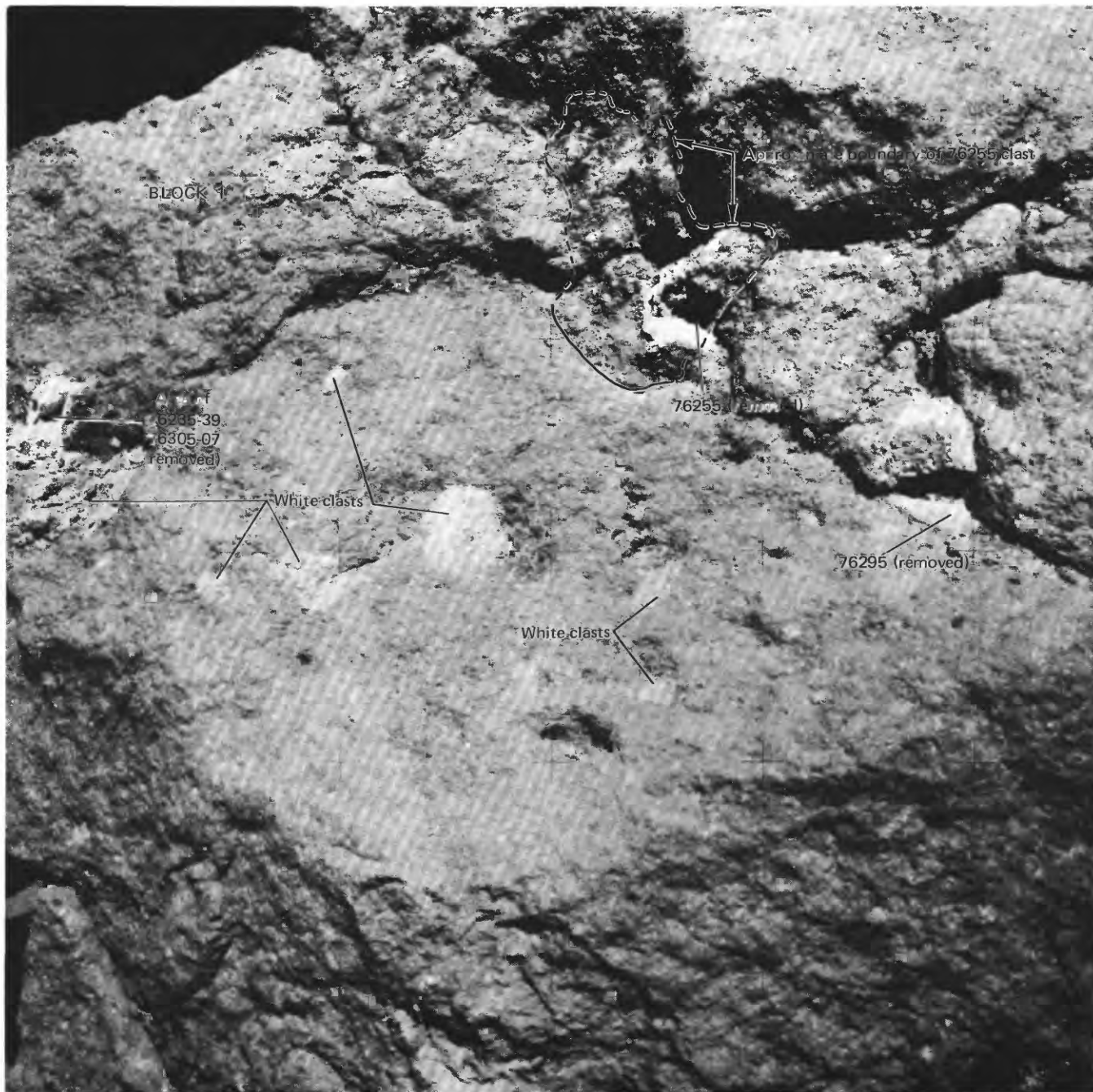


FIGURE 167.—View, northeastward, of block 1 after sampling, showing scattered clasts, locations from which samples 76235-39, 76305-07, 76255, and 76295 were collected, and approximate outline of large clast sampled by 76255. (NASA photograph AS17-140-21456.)

*Major-element composition:**Chemical analysis of 76295*

SiO <sub>2</sub> .....	47.03
Al <sub>2</sub> O <sub>3</sub> .....	18.25
FeO .....	9.09
MgO .....	10.78
CaO .....	11.54
Na <sub>2</sub> O .....	..
K <sub>2</sub> O .....	.26
TiO <sub>2</sub> .....	1.39
P <sub>2</sub> O <sub>5</sub> .....	.32
MnO .....	..
Cr <sub>2</sub> O <sub>3</sub> .....	..

76295,14 and 37, matrix (Simonds, 1975).

*Age:*

<sup>40-39</sup>Ar:

76295,1 (tan matrix),  $3.95 \pm 0.04$  b.y.  
(Cadogan and Turner, 1976).

76295,3 (blue matrix),  $3.96 \pm 0.04$  b.y.  
(Cadogan and Turner, 1976).

*Sample 76315*

*Type:* Polymict breccia with an aphanitic matrix.

*Size:* 12×10×4.5 cm.

*Weight:* 671.1 g.

*Location:* Southeast side of block 2 at station 6.

*Illustrations:* Pans 21, 22; figures 172, 173 (LRL).



FIGURE 168.—Sample 76255. Polymict breccia with cataclastic matrix. Large (approximately 3×4 cm) dark oval patch at left is dark polymict breccia or fine subophitic impact melt of Warner and others (1976; see fig. 169). Remainder of rock (light-colored part) is mainly norite cataclasite. (NASA photograph S-72-56415.)

Comments: Sample 76315 is a fragment of blue-gray breccia from the contact zone between greenish-gray and blue-gray parts of boulder 2. Heiken and others (1973) have described the zone as the foliated tran-

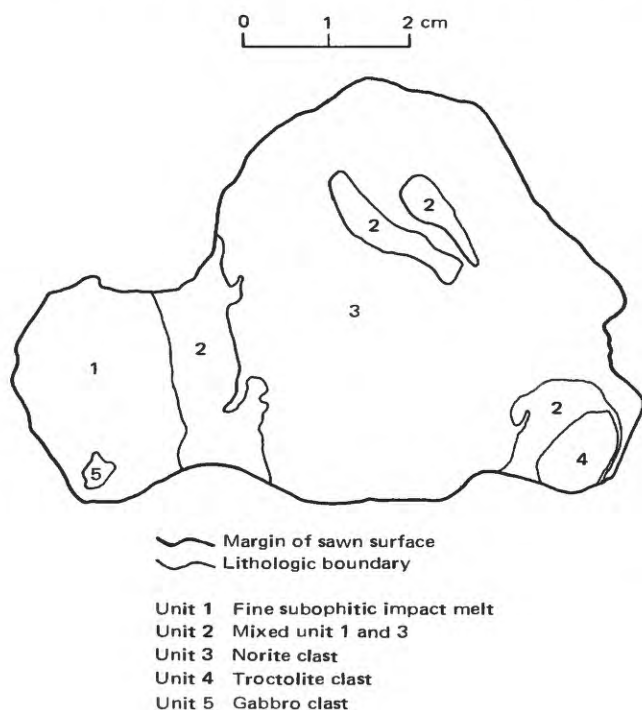


FIGURE 169.—Sample 76255. Map of slab cut parallel to  $N_1$  face (that is, parallel to top view of rock shown in side view in figure 168). (From Warner and others, 1976.)

sition zone between highly vesicular unit A (green-gray breccia of fig. 172) and well-foliated unit B (blue-gray breccia of fig. 172).

*Petrographic description:* Polymict breccia with clasts of feldspathic metaclastic rock, spinel-troctolite cataclasite, intersertal basalt with relict spinel, and plagioclase, olivine, and scarce quartz mineral fragments in an aphanitic matrix. A large feldspathic cataclasite clast appears to have been locally fused and is veined by the dark aphanitic matrix material (fig. 173).

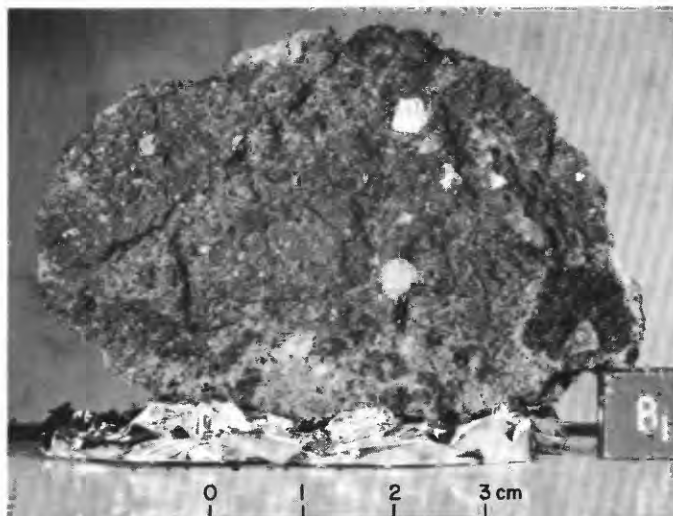


FIGURE 170.—Sample 76275. Polymict breccia with aphanitic matrix. (NASA photograph S-73-24035B.)

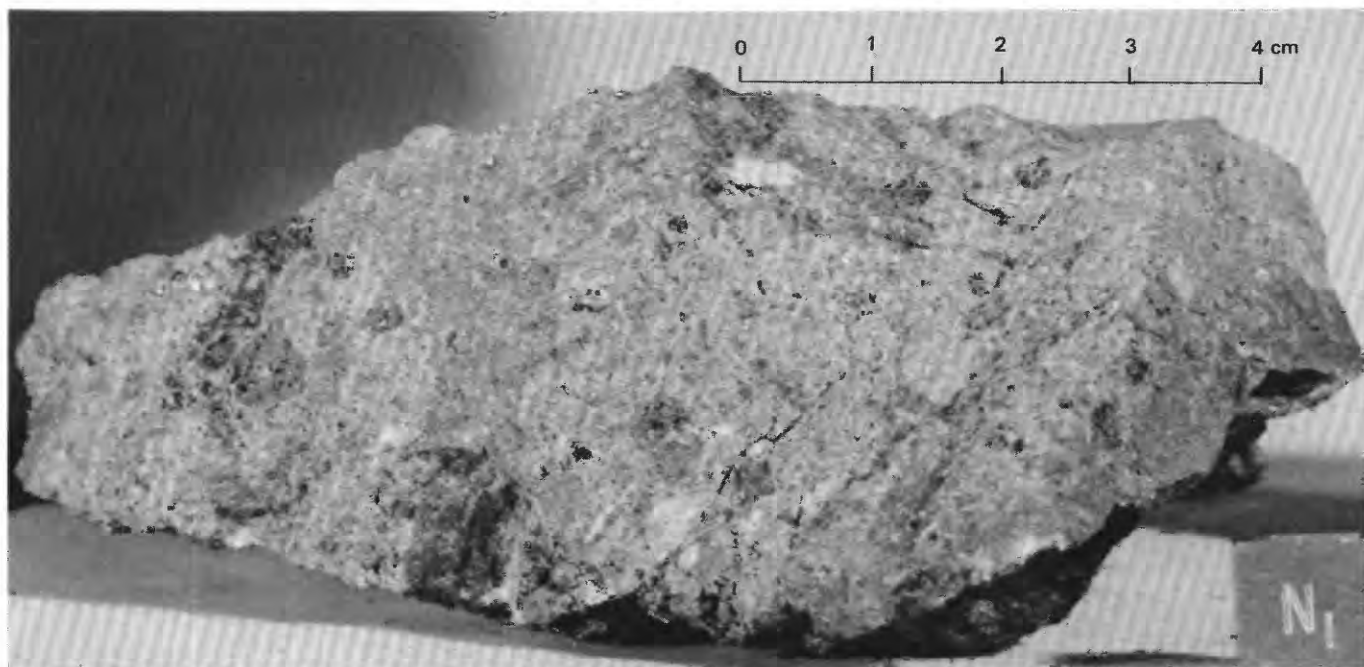


FIGURE 171.—Sample 76295. Polymict breccia with aphanitic matrix. (NASA photograph S-72-56409.)

Simonds (1975) has described 76315 as nonvesicular blue-gray rock that consists of mineral and lithic clasts in a matrix crystallized from impact melt. The mineral clasts, feldspar, olivine, pyroxene, and minor spinel, generally appear unshocked. Lithic clasts are derivatives of anorthosite-norite-troctolite-suite rocks. The matrix is micropoikilitic to subophitic, with olivine and pyroxene enclosing feldspar. A foliation is defined by lines of small (<1 mm) vesicles and by variations in the matrix color.

#### Major-element composition:

##### Chemical analyses of 76315

	1	2	3	4	5	6
SiO <sub>2</sub> .....	45.82	45.64	46.45	46.21	48.57	45.10
Al <sub>2</sub> O <sub>3</sub> .....	18.01	17.53	18.18	18.14	17.91	26.37
FeO .....	8.94	9.53	8.83	8.95	7.66	5.29
MgO .....	12.41	12.50	12.34	12.02	13.84	7.46
CaO .....	11.06	10.97	11.30	11.32	10.36	15.12
Na <sub>2</sub> O .....	.57	.70	.64	.60	.47	.47
K <sub>2</sub> O .....	.27	.26	.22	.26	.15	.10
TiO <sub>2</sub> .....	1.47	1.50	1.43	1.50	.32	.36
P <sub>2</sub> O <sub>5</sub> .....	.29	.30	.29	.29	.12	.06
MnO .....	.11	.13	.13	.12	.13	.07
Cr <sub>2</sub> O <sub>3</sub> .....	.19	.19	.20	.19	--	--
Total .....	99.14	99.25	100.01	99.60	99.53	100.40

1. 76315.2 (Apollo 17 PET. 1973); identified as matrix sample by Phinney and others (1974).

2. 76315.30M. matrix (Rhodes and others, 1974).

3. 76315.30, 3, clast (Rhodes and others, 1974).

4. 76315.35, matrix (Rhodes and others, 1974).

5. 76315.52, clast (Rhodes and others, 1974).

6. 76315.62, clast (Rhodes and others, 1974).

Described by Simonds (1975) as 2-cm light-gray clast with 70 percent plagioclase, 17 percent pigeonite, and 13 percent olivine.

#### Age:

<sup>40</sup>Ar-<sup>39</sup>Ar:

76315.36 (matrix),  $3.98 \pm 0.04$  b.y. (Turner and Cadogan, 1975).

76315.67 (dark clast),  $3.97 \pm 0.04$  b.y. (Turner and Cadogan, 1975).

76315.61 (white clast),  $3.98 \pm 0.04$  b.y. (Turner and Cadogan, 1975).

K-Ar:

76315 (matrix), 4.0 b.y. (Bogard and Nyquist, 1974).

#### Exposure age:

Kr:  $21.7 \pm 1.2$  m.y. (Croaz and others, 1974).

Tracks:  $21 \pm 3$  m.y. (Croaz and others, 1974).

Croaz and others (1974) have interpreted the time since emplacement of station 6 boulder to be  $22 \pm 1$  m.y.

Smaller rare-gas exposure ages have been determined by Bogard and Nyquist (1974) and Turner and Cadogan (1975). Both sets of investigators indicate that their exposure ages are too low because of partial shielding or incorrect assumed <sup>38</sup>Ar production rate.

Sample 76320-24

Type: Sedimentary, unconsolidated.

Weight: 813.74 g.

Depth: From upper few centimeters.

Location: Flat upper surface of the north side of block 1 at station 6.

Illustrations: Pans 21, 22; figures 147, 155, 174.

Comments: Sample 76320-24 is probably ejecta deposited on block 1 by some nearby impact.

Petrographic description: 76320-24, dominantly fine-grained breccia and (or) metaclastic rock, scarce basalt, agglutinate.

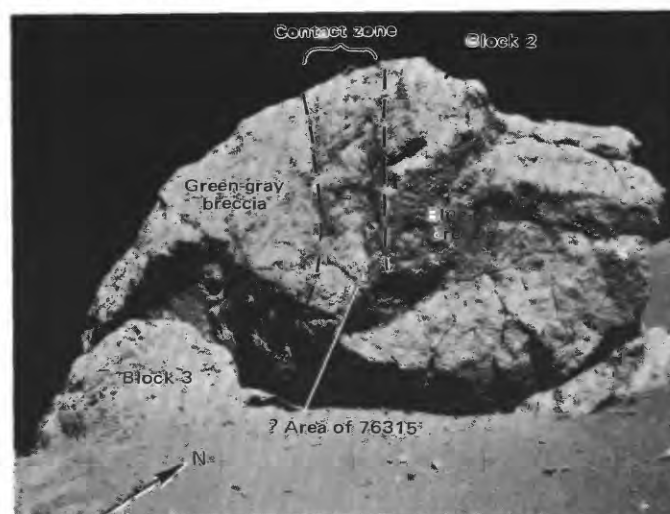


FIGURE 172.—Blocks 2 and 3 at station 6 before sampling. Exact location of sample 76315 is uncertain but is probably within contact zone. (NASA photograph AS 17-140-21436.)

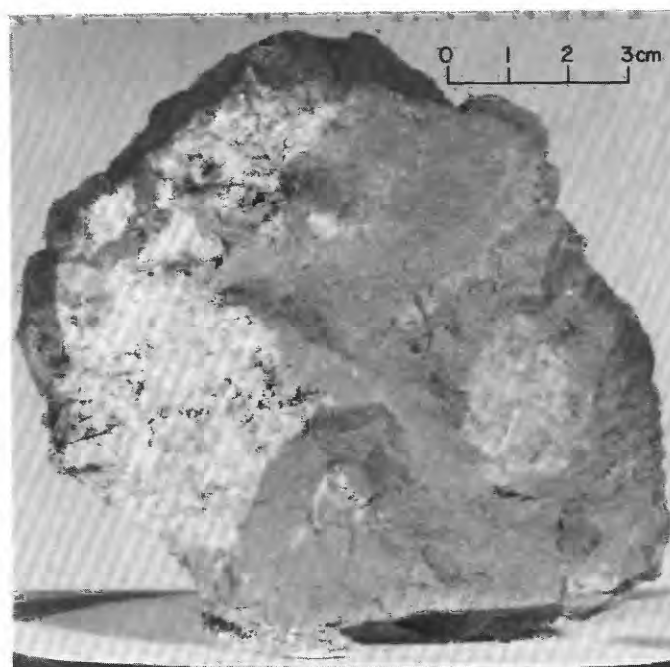


FIGURE 173.—Sample 76315. Polymict breccia with aphanitic matrix. Large feldspathic cataclastic clast at left is veined by dark aphanitic matrix material. (NASA photograph S-73-17109.)

*Components of 90-150- $\mu$ m fraction of 76321,10 (Heiken and McKay, 1974)*

Components	Volume percent
Agglutinate.....	39.1
Basalt, equigranular.....	2.7
Basalt, variolitic.....	..
Breccia:	
Low grade <sup>1</sup> - brown.....	4.3
Low grade <sup>1</sup> - colorless.....	..
Medium to high grade <sup>2</sup> .....	14.4
Anorthosite.....	..
Cataclastic anorthosite <sup>3</sup> .....	1.0
Norite.....	..
Gabbro.....	..
Plagioclase.....	15.7
Clinopyroxene.....	6.7
Orthopyroxene.....	5.7
Olivine.....	..
Ilmenite.....	.3
Glass:	
Orange.....	1.3
"Black".....	2.3
Colorless.....	2.3
Brown.....	4.0
Gray, "ropy".....	..
Other.....	..
Total number grains.....	299

<sup>1</sup>Metamorphic groups 1-3 of Warner (1972).

<sup>2</sup>Metamorphic groups 4-8 of Warner (1972).

<sup>3</sup>Includes crushed or shocked feldspar grains.

**Major-element composition:**

*Chemical analyses of 76321*

	1	2	3
SiO <sub>2</sub> .....	44.19	44.08	44.14
Al <sub>2</sub> O <sub>3</sub> .....	18.68	18.41	18.54
FeO.....	10.36	10.53	10.44
MgO.....	10.82	10.82	10.82
CaO.....	12.24	12.23	12.24
Na <sub>2</sub> O.....	.40	.46	.43
K <sub>2</sub> O.....	.124	.13	.13
TiO <sub>2</sub> .....	2.95	3.00	2.98
P <sub>2</sub> O <sub>5</sub> .....	.113	.09	.10
MnO.....	.135	.15	.14
Cr <sub>2</sub> O <sub>3</sub> .....	.272	.26	.27
Total.....	100.284	100.16	100.23

1. 76321.3 (Duncan and others, 1974).

2. 76321.7 (Rhodes and others, 1974).

3. Average of 1 and 2.

**Sample 76335**

**Type:** Troctolite cataclasite.

**Size:** Largest fragment, 8×6.5×5 cm.

**Weight:** 352.9 g.

**Location:** From the south slope of the North Massif about 1-2 m northeast of the LRV at station 6,

**Illustrations:** Pans 21, 22; figures 166, 175 (photomicrograph).

**Comments:** Sample 76335 is presumably a clast from North Massif breccia.

**Petrographic description:** Troctolite cataclasite. Relics of partly crushed troctolite with olivine interstitial to plagioclase.

**Sample 76500-06**

**Type:** Sedimentary, unconsolidated (76500-04) with

two breccia fragments (76505, 06).

**Size:** 76505, less than 1 cm; 76506, 1.3×1×1 cm.

**Weight:** 76500-04, 1,019.47 g; 76505, 4.69 g; 76506, 2.81 g.

**Depth:** From upper few centimeters.

**Location:** Ejecta blanket of a 10-m crater about 15 m northwest of the LRV at station 6.

**Illustrations:** Pans 21, 22; figure 176.

**Comments:** Sediment sample, from the rake area, rep-

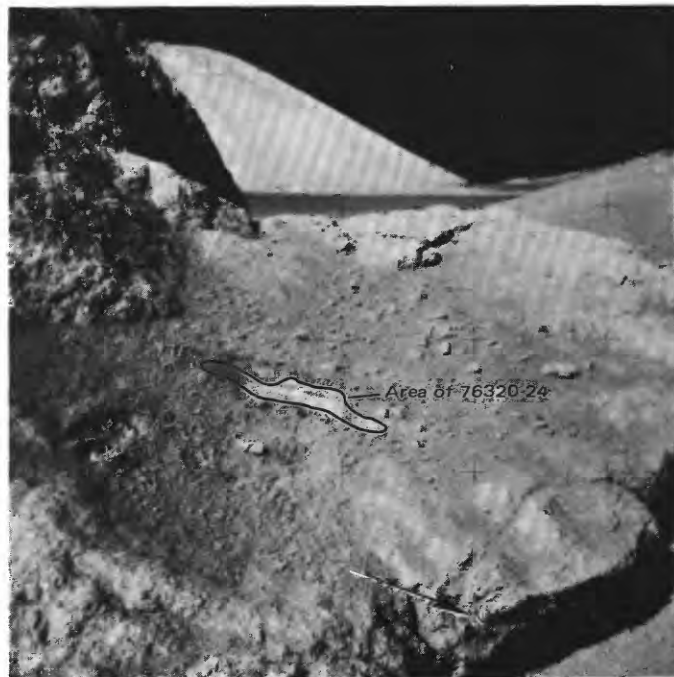


FIGURE 174.—Sample 76320-24 site after collection. (NASA photograph AS17-140-21482.)

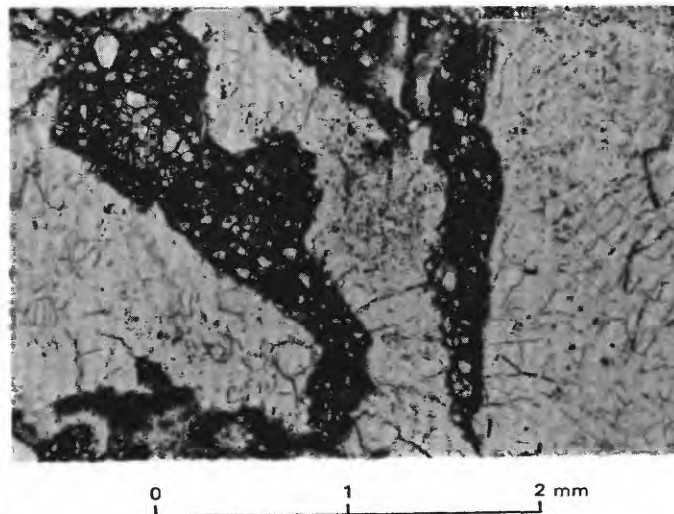


FIGURE 175.—Sample 76335. Photomicrograph showing texture of troctolite cataclasite. Olivine (dark) has been finely pulverized, whereas larger relict plagioclase grains (light) have survived.

resents material derived from the North Massif with some admixture of valley floor debris.

*Petrographic description:* 76500-04, dominantly fine-grained breccia and (or) metaclastic rock, some agglutinate, minor glass.

*Components of 90-150- $\mu$ m fraction of 76501,1 (Heiken and McKay, 1974)*

Components	Volume percent
Agglutinate.....	47.2
Basalt, equigranular }	
Basalt, variolitic }	1.7
Breccia:	
Low grade <sup>1</sup> - brown.....	3.8
Low grade <sup>1</sup> - colorless.....	--
Medium to high grade <sup>2</sup> .....	8.3
Anorthosite.....	--
Cataclastic anorthosite <sup>3</sup> .....	1.4
Norite.....	--
Gabbro.....	--
Plagioclase.....	17.2
Clinopyroxene.....	7.6
Orthopyroxene.....	7.9
Olivine.....	.7
Ilmenite.....	1.7
Glass:	
Orange.....	.7
"Black".....	.3
Colorless.....	1.4
Brown.....	--
Gray, "ropy".....	--
Other.....	--
Total number grains.....	290

<sup>1</sup>Metamorphic groups 1-3 of Warner (1972).

<sup>2</sup>Metamorphic groups 4-8 of Warner (1972).

<sup>3</sup>Includes crushed or shocked feldspar grains.

*Major-element compositions:*

*Chemical analyses of 76501*

	1	2	3	4
SiO <sub>2</sub> .....	43.41	43.71	43.34	43.49
Al <sub>2</sub> O <sub>3</sub> .....	18.63	18.83	18.41	18.62
FeO.....	10.32	10.35	10.39	10.35
MgO.....	11.08	10.71	11.08	10.96
CaO.....	12.28	12.06	12.24	12.19
Na <sub>2</sub> O.....	.35	.38	.40	.38
K <sub>2</sub> O.....	.10	.11	.11	.11
TiO <sub>2</sub> .....	3.15	3.20	3.15	3.17
P <sub>2</sub> O <sub>5</sub> .....	.08	.08	.09	.08
MnO.....	.14	.13	.15	.14
Cr <sub>2</sub> O <sub>3</sub> .....	.26	.26	.27	.26
Total.....	99.80	99.82	99.63	99.75

1. 76501,2 (Apollo 17 PET, 1973).

2. 76501,30 (Rose and others, 1974).

3. 76501,42 (Rhodes and others, 1974).

4. Average of 1 through 3.

*Age:*

40-39Ar:

76503,6,4 (2-4-mm fragment-"recrystallized anorthositic" rock),  $3.970 \pm 0.013$  b.y. (Schaeffer and others, 1976).

76503,6,9 (2-4-mm fragment-"highland basalt"),  $\sim 3.97$  b.y. (Schaeffer and others, 1976).

76503,6,13 (2-4-mm fragment-"recrystallized anorthositic" rock),  $4.227 \pm 0.008$  b.y. (Schaeffer and others, 1976).

*Exposure age:*

Ar:

76503,6,4 (2-4-mm fragment-"recrystallized anorthositic" rock),  $160 \pm 7$  m.y. (Schaeffer and others, 1976).

76503,6,9 (2-4-mm fragment-"highland basalt"),  $83 \pm 5$  m.y. (Schaeffer and others, 1976).

76503,6,13 (2-4-mm fragment-"recrystallized anorthositic" rock),  $106 \pm 6$  m.y. (Schaeffer and others, 1976).

Sample 76535-39, 45-49, 55-59, 65-69, 75-77

*Type:* 23 rock fragments from rake sample:

76535, metatroctolite.

76536, olivine (?) norite cataclasite.

76537, olivine basalt.

76538, basalt.

76539, basalt.

76545

76546

76547 } polymict breccia with glassy matrix.

76548

76549

76555 } polymict breccia with an aphanitic matrix.

76556

76557

76558, breccia.

76559, breccia.

76565, sedimentary, weakly lithified polymict breccia.

76566, friable dark breccia.

76567, sedimentary, weakly lithified polymict breccia.

76568, basalt cataclasite.

76569, breccia.

76575, polymict breccia with an aphanitic matrix.

76576, breccia with an aphanitic matrix.

76577, metaclastic breccia with an aphanitic matrix.

*Sizes:* 76535, >6 cm maximum dimension; other fragments range up to about 4 cm.

*Weight:* 358.031 g total; 76535, 155.5 g.

*Location:* Ejecta blanket of a 10-m crater about 15 m northwest of the LRV station 6.

*Illustrations:* Pans 21, 22; figures 176, 177 (76535, LRL).

*Comments:* The basalt fragments are probably

from subfloor basalt; the rest were presumably derived from the North Massif.

*Petrographic descriptions:*

76535, metatroctolite with symplectite intergrowths along some olivine-plagioclase boundaries; partial recrystallization to a coarse-granoblastic-polygonal texture (fig. 177).

Sample 76535 has been described as coarse-grained troctolite with 35 percent plagioclase, 60 percent olivine, and 5 percent low-calcium pyroxene (Dymek and others, 1975) and as coarse-grained troctolite granulite with 58 percent plagioclase ( $An_{96}$ ), 37 percent olivine ( $For_{88}$ ), and 4 percent orthopyroxene ( $En_{86}$ ) (Gooley and others, 1974).

Gooley and others suggested that the rock formed as a cumulate and cooled slowly at a depth inferred from the occurrence of chromian spinel-bronzite-diopside symplectites to be between 10 and 30 km. Dymek and others (1975) agreed that the rock crystallized at relatively great depth, but they objected to the specific depth calculation of Gooley and others (1974) because of the large uncertainties in applying experimental thermodynamic data to sample 76535. Stewart (1975) related the granular-polygonal texture to his "Apollonian metamorphism" and inferred an annealing time on the order of  $10^8$  years at a depth greater than 7 km for rock 76535.

76536, olivine(?) norite cataclasite.

76537, aphanitic olivine basalt.

76538, coarse-grained porphyritic basalt with aggregates of clinopyroxene-ilmenite in a subophitic(?) groundmass of plagioclase, clinopyroxene, ilmenite, and accessory minerals.

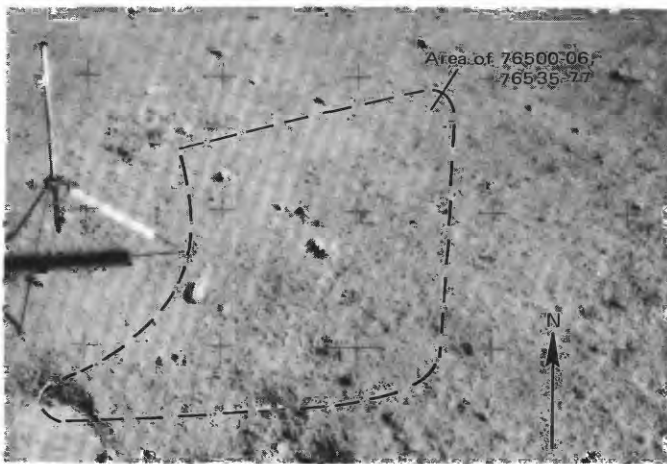


FIGURE 176.—Rake area at station 6 before sampling. (NASA photograph AS17-141-21622.)

76539, aphanitic basalt with a vitrophyric(?) groundmass.

76545-47, 49, polymict breccia with clasts of fine-grained feldspathic metaclastic rock, basalt, and mineral fragments in a vitreous matrix that is frothy along fractures. Prominent flow foliation.

76555, polymict breccia with clasts of fine-grained metaclastic rock and troctolite or metatroctolite and mineral fragments in an aphanitic matrix.

76556, polymict breccia with clasts of aphanitic breccia and metatroctolite(?) with granoblastic-polygonal texture and mineral fragments in an aphanitic matrix.

76557, polymict(?) breccia with clasts of metatroctolite(?) and mineral fragments in an aphanitic matrix with slitlike cavities.

76565, polymict breccia with clasts of basalt, fine-grained metaclastic rock, feldspathic cataclasite, possible glass, and mineral debris in a fine-grained friable matrix.

76567, polymict breccia with clasts of fine-grained metaclastic rock, spinel troctolite or metatroctolite, and mineral debris in a moderately coherent fine-grained matrix.

76568, basalt cataclasite with uncrushed relict aphanitic basalt in finely comminuted basalt matrix; adhering sediment contains glass.

76575, polymict breccia with clasts of breccia and fine-grained feldspathic metaclastic rocks and mineral clasts of olivine(?) and plagioclase in an aphanitic matrix.

76576, breccia with fragments of aphanitic breccia in a feldspathic aphanitic matrix.

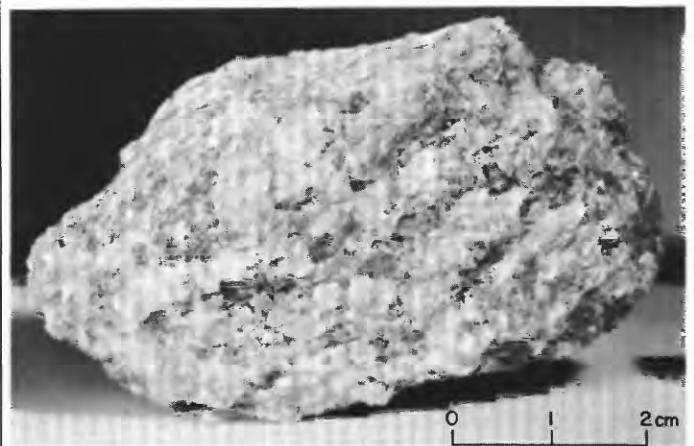


FIGURE 177.—Sample 76535. Metatroctolite; partially recrystallized to coarse granoblastic-polygonal texture. (NASA photograph S-73-19460.)

76577, metaclastic rock with porphyroclasts of olivine and plagioclase (and a possible "dunite" cataclasite) in an aphanitic matrix.

#### Major-element compositions:

Chemical analyses of 76535, 76537, and 76539

	1	2	3
SiO <sub>2</sub> .....	42.88	38.25	38.21
Al <sub>2</sub> O <sub>3</sub> .....	20.73	8.69	8.80
FeO.....	4.99	19.60	19.42
MgO.....	19.09	8.01	7.87
CaO.....	11.41	10.67	10.91
Na <sub>2</sub> O.....	.23	.40	.39
K <sub>2</sub> O.....	.03	.05	.06
TiO <sub>2</sub> .....	.05	13.05	12.65
P <sub>2</sub> O <sub>5</sub> .....	.03	.11	.10
MnO.....	.07	.29	.29
Cr <sub>2</sub> O <sub>3</sub> .....	.11	.37	.34
Total.....	99.62	99.49	99.04

1. 76535,21 (Rhodes and others, 1974).

2. 76537,1 (Rhodes and others, 1976).

3. 76539,3 (Rhodes and others, 1976).

#### Age:

##### K-Ar:

76535,  $4.34 \pm 0.08$  b.y.; determined for plagioclase, includes attempted correction for trapped Ar (Bogard and others, 1974).  
76535 (plagioclase), 4.23 b.y.; actual age is less if trapped <sup>40</sup>Ar is present (Huneke and Wasserburg, 1975).

##### <sup>40</sup>Ar:

76535,  $4.26 \pm 0.02$  b.y. (Husain and Schaeffer, 1975).  
76535, Ar release patterns complex, possibly complicated by trapped Ar. Rock may have been subjected to a metamorphic event <4.08 b.y. ago (Huneke and Wasserburg, 1975).

##### Sm-Nd isochron:

76535,  $4.26 \pm 0.06$  (2σ) b.y., interpreted as crystallization age (Lugmair and others, 1976).

##### Rb-Sr isochron:

76535,  $4.61 \pm 0.07$  (2σ) b.y. Preferred interpretation is that this is the age of formation of the troctolite, possibly in a major magmatic differentiation event that also produced the dunite represented by sample 72415-18. One out of five olivine separates is discordant and was not included in defining the isochron; its model age,  $4.09 \pm 0.12$  b.y., may indicate a disturbance at a time later than 4.09 b.y. ago (Papanastassiou and Wasserburg, 1976).

##### <sup>207</sup>Pb/<sup>206</sup>Pb:

76535, baddeleyite,  $4.271 \pm 0.029$  (2σ) b.y. (Hintherne and others, 1975).

76535, "pyrochlore,"  $4.274 \pm 0.021$  (2σ) b.y. (Hintherne and others, 1975).

##### U-Pb:

76535, rock was recrystallized or isotopically homogenized approximately 4.0 b.y. ago (Tera and others, 1974a).

##### Fission track:

76535, apatite, 4.07 b.y.; may record metamorphic event. A possible complication arises, however, from laboratory data that suggest that fission tracks in apatite may be partially annealed over long periods of time at lunar surface temperatures; hence, it may be unlikely that tracks formed in the interval since a 4.07-b.y. event would be fully preserved (Braddy and others, 1975).

Papanastassiou and Wasserburg (1976) suggested that the seemingly disparate age determinations (4.61 b.y. and ~4.25 b.y.) might be accounted for if the troctolite formed initially 4.61 b.y. ago but remained, until 4.25 b.y. ago, at temperatures sufficiently high to permit degassing of argon and chemical and isotopic exchange of Sm and Nd. Rb-Sr systems, in small inclusions within olivine, were sealed to exchange by the impervious (with respect to Rb and Sr) jacket of olivine that enclosed them during magmatic crystallization 4.61 b.y. ago.

##### Exposure age:

##### Ar:

200 m.y. (Bogard and others, 1974).  
200 m.y. (Huneke and Wasserburg, 1975).  
 $156 \pm 8$  m.y. (Husain and Schaeffer, 1975).  
221 m.y. (Lugmair and others, 1976).

##### Kr:

$211 \pm 7$  m.y. (Croaz and others, 1974).  
 $223 \pm 16$  m.y. (Lugmair and others, 1976).

##### Tracks:

$2.0 \pm 1$  m.y. (Croaz and others, 1974).

Lugmair and others (1976) have interpreted the spallation and neutron-capture record as indicative of exposure at an average shielding depth in the regolith of ~30 cm for  $223 \pm 16$  m.y.

#### STATION 7

##### LOCATION

Station 7 is located one-half km east of station 6 on the lower slope of North Massif just above the break in slope between the massif and valley floor (figs. 7D and 144).

##### OBJECTIVES

The objectives at station 7 were the same as those for station 6—to characterize and sample the massif and dark mantle materials.

## GENERAL OBSERVATIONS

The southward slope toward the valley at station 7 is about  $9^\circ$ . Less than one percent of the surface is covered by blocks and fragments, which appear to have a bimodal distribution (pans 23, 24). Fragments up to 2 or 3 cm in size are abundant, and blocks 30 cm or larger are common, but rock fragments in the 3-30-cm size range are scarce. Blocks larger than 30 cm are in clusters, whereas the smaller fragments are randomly scattered over the surface.

Blocks range from angular to rounded and their burial from none to nearly complete. The sampled 3-m breccia boulder overhangs the surface on three sides. Nearby half-meter boulders are almost totally buried, and most fragments less than 1 m in size are at least partially buried. Fillets are restricted to the uphill sides of the blocks; they are well developed on blocks larger than one-half meter but poorly developed or absent on smaller blocks.

Scattered craters are up to about 4 m in size. Most are less than one-half meter in diameter; some of those have raised blocky rims with the ejecta deposited preferentially downslope. Ejecta deposits are indistinguishable around the subdued nonblocky craters.

Samples at station 7 consisted of four rocks from the 3-m breccia boulder, seventeen rocks from the surface, and two surface sediment samples (fig. 178).

## GEOLOGIC DISCUSSION

We interpret the massifs as fault blocks composed of southern Serenitatis basin ejecta that was faulted as part of the basin-forming process. Slumping from the fault scarps produced thick colluvial wedges against the lower parts of the massifs. The colluvial wedges were later partly buried by subfloor basalt; additional material has been added to their surfaces by mass

wasting and deposition of ejecta since extrusion of the subfloor basalt. Station 7, like station 6, is on the surface of a colluvial wedge that extends about one-third of the way up the massif. Above the wedge, bedrock (southern Serenitatis basin ejecta) is close to the surface although mantled by impact-generated regolith.

The major feature of interest at station 7 is a 3-m breccia boulder. There is no visible boulder track. However, it is so like the station 6 boulder in lithology and in chemical composition (fig. 179) there is little doubt of its North Massif origin. Repeated exposure age determinations suggest that it was emplaced near the base of the massif 25 to 30 m.y. ago.

Three major lithologic types are recognized in the station 7 boulder. In order of decreasing age, as interpreted from geologic relations in the boulder (fig. 180), these are light-gray, blue-gray, and greenish-gray breccia. Light-gray breccia is represented primarily by a clast of norite cataclasite approximately  $0.5 \times 1.5$  m in size. Blue-gray breccia envelops and intrudes (dikes of fig. 180) the large clast of norite cataclasite. Systematic fractures cut both the clast and the blue-gray breccia. Vesicular greenish-gray breccia in contact with blue-gray breccia is interpreted as the youngest matrix of the boulder because (1) the fracture sets of the light-gray clast and the blue-gray breccia are not recognized in the greenish-gray breccia and (2) the vesicles of the greenish-gray breccia are both elongated and aligned in trains parallel to the contact with the blue-gray breccia (fig. 190).

The greenish-gray breccia and the blue-gray breccia (both envelope and dike) are texturally similar. Like the matrices of boulders 2 and 3 at station 2, sample 73215 from station 3, and the station 6 boulder, they consist of mineral and lithic clasts in fine-grained crystalline groundmasses, which Chao and others (1974, 1975) have interpreted as having crystallized from melts.

The greenish-gray and blue-gray matrix samples have a narrow range of major-element composition (fig. 179) that is similar to the compositions of most of the other highlands boulder matrices and virtually identical to the station 6 boulder matrix (fig. 150). Winzer and others (1975a) concluded that in large-ion lithophile-element composition, the station 7 boulder matrix samples are so similar to each other and to samples from the other breccia boulders of the Apollo 17 site that they appear to be identical.

The chemical similarity of the greenish-gray and blue-gray breccias of the station 7 boulder implies that they formed from identical target materials. Their textural similarity implies similar histories of mobilization, aggregation, and cooling; that is, the two breccia types represent similar ejecta facies. The blue-gray

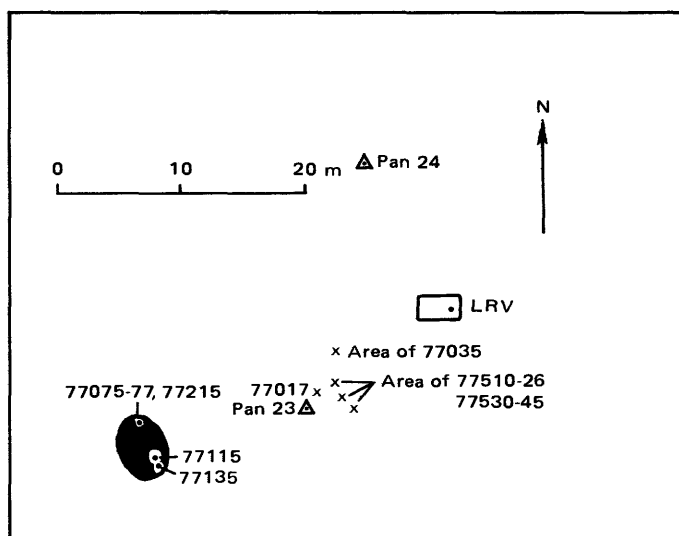


FIGURE 178.—Planimetric map of station 7.

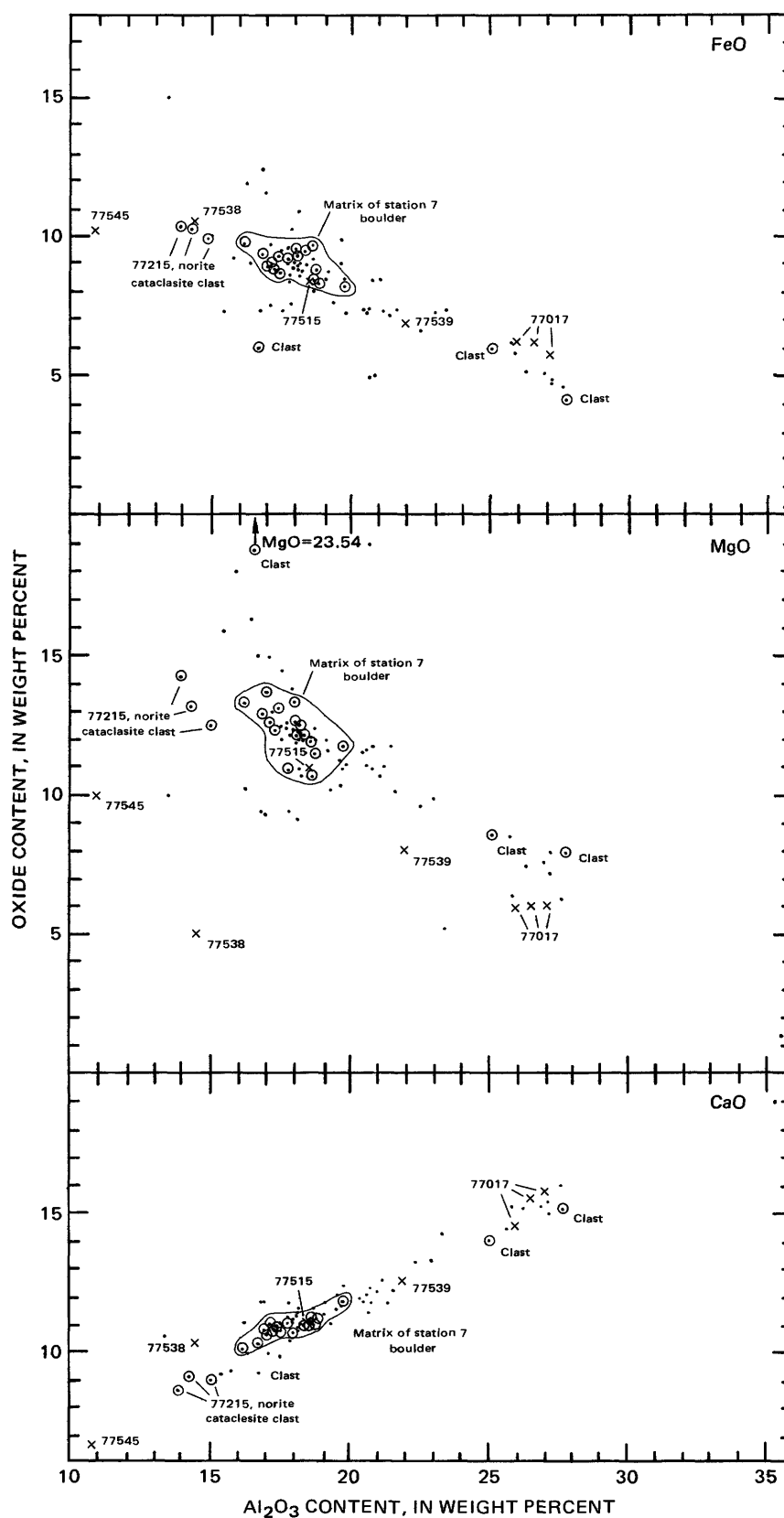


FIGURE 179.—Plots of FeO, MgO, and CaO contents in relation to  $\text{Al}_2\text{O}_3$  content for analyzed highlands rocks, at station 7 in comparison with all analyzed Apollo 17 highlands rocks. Circled dots, station 7 boulder (matrix samples except where identified as clasts);  $\times$ , other station 7 highlands rocks; dots, all other Apollo 17 highlands rocks.

breccia, although fractured, does not record the cataclasis that might be expected if it were a sample of older rock excavated by the impact that formed the greenish-gray breccia, as previously suggested (Chao and others, 1974; Chao and others, 1975b; Reed and Wolfe, 1975). We believe that a model in which the two breccias were produced by the same impact is more likely.

Norite and troctolite, included among the target rocks, were crushed and partly disaggregated to form some of the mineral and lithic clasts; the large light-gray norite cataclasite clast is one of the larger observed remnants of preexisting noritic target rock. The mobilized ejecta consisted of a mixture of dust- to boulder-sized clasts and impact melt. Parts of it aggregated during transport and formed clots sufficiently coherent to sustain systematic fractures (as in the

blue-gray breccia and its large noritic clast) while being incorporated in more highly mobile ejecta (unfractured vesicular greenish-gray breccia).

Radiometric age determinations for samples from the station 7 boulder are summarized graphically in figure 181. Crystallization about 4.4 b.y. ago or earlier is clearly implied for the norite parent of the large cataclasite clast.

Chronological interpretation of the enclosing breccias is less straightforward. Rb-Sr isochron ages with mean values of 3.75 and 3.8 b.y. have been reported for the blue-gray and greenish-gray breccias; the same workers have reported a 3.8-b.y. Pb disturbance in the cataclasite clast. Although the geologic significance of these determinations is unclear, it is improbable that they are related to formation of the breccia for three reasons. (1) They overlap many of the ages determined

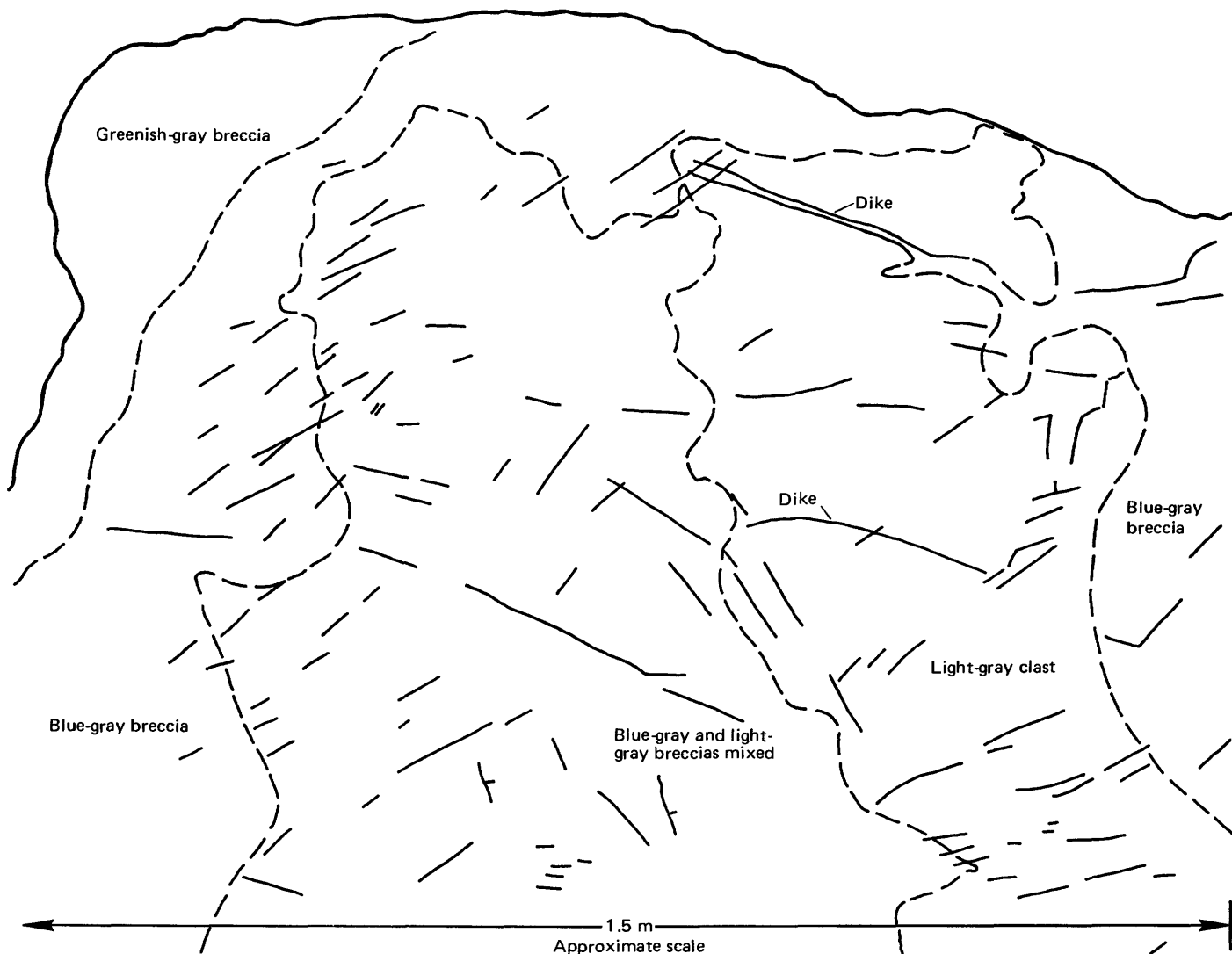


FIGURE 180.—Map of station 7 boulder. Same view as in figure 185. Dashed lines are contacts between lithologic units mapped from color photographs taken on lunar surface. Solid lines show fractures, outline of boulder, and dikes (labeled). (From Muehlberger and others, 1973.)

for subfloor basalt. Photogeologic and field evidence exclude the possibility that North Massif materials are younger than the sampled part of the subfloor basalt. (2) The station 7 boulder breccias are texturally and compositionally part of the Apollo 17 massif breccia suite. With few exceptions, ages determined for many samples from this suite are  $\geq 3.92$  b.y. It is improbable that breccia of the station 7 boulder was deposited in the same area  $\sim 200$  m.y. later than identical breccia represented by samples from the other stations. (3) Acceptance of the young Rb-Sr ages as geologically significant requires the improbable condition of an event that caused Rb-Sr equilibration without resetting the argon clock.

Two  $^{40}\text{Ar}$  ages of  $\sim 3.8$  b.y. were interpreted for the greenish-gray breccia by Stettler and others (1974), who regarded them as uncertain results based on short poorly defined high-temperature plateaus. At the older end of the spectrum, Nakamura and others (1976) have disavowed their 4.14-b.y. Rb-Sr age for the greenish-gray breccia on the grounds that its apparently excessive antiquity might be due to contamination by older xenocrysts. Disregarding the doubtfully young and doubtfully old ages, we are left with five argon ages and one Rb-Sr age that suggest that the breccia represented by the station 7 boulder was probably assembled between  $\sim 3.9$  and 4.0 b.y., a result compatible with the ages generally inferred for other massif breccia samples.

The single analyzed sediment sample from station 7 (fig. 182) is approximately a 2:1 mixture of massif debris and valley floor debris. The valley-floor component, basaltic debris with some ash, presumably was emplaced in the station 7 area as ejecta from some of the many valley-floor craters. The massif component is chemically identical to sediment derived from the South Massif at station 2 and in the light mantle.

## SUMMARY OF SAMPLING

## Sample 77017

*Type:* Olivine gabbro breccia with a glassy matrix.

*Size:*  $17 \times 12.5 \times 9$  cm.

*Weight:* 1,730 g.

*Location:* From surface approximately 10 m southwest of the LRV.

*Illustrations:* Pans 23, 24; figure 183 (LRL).

*Comments:* Sample 77017 is a regolith fragment.

*Petrographic description:* Monomict breccia with clasts of olivine gabbro or metagabbro in a matrix of vesicular glass.

With respect to major elements, glass of sample 77017 (cols. 4-6 of table below) is inhomogeneous. The least aluminous glassy material (col. 6) is chemically like the older regolith of the valley floor, which is highlands debris with about 30 to 50 percent basalt and ash debris from the valley floor. Major elements of the glassy portions of the sample (cols. 4-6) and of the gabbro itself (cols. 1-3) have ap-

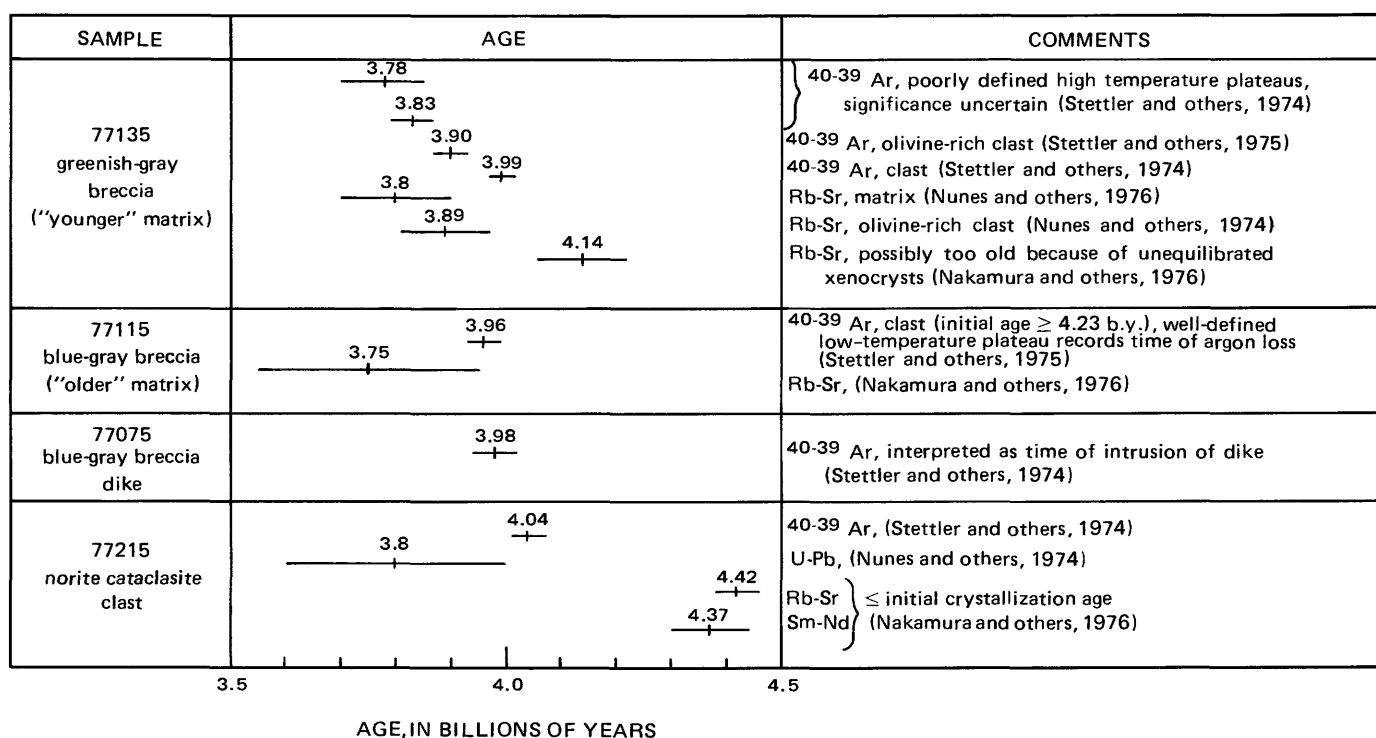


FIGURE 181.—Summary of radiometric ages for station 7 boulder.

proximately linear distributions with respect to  $\text{Al}_2\text{O}_3$ . The linear distributions are mixing lines indicative of incomplete mixing of impact melts derived from the older regolith of the valley floor and from the gabbro fragment, which apparently was a clast in the regolith. At one time the gabbro presumably was a clast in highlands breccia. Kirsten and Horn (1974) also interpreted the glassy matrix as regolith material fused approximately 1.5 b.y. ago.

*Major-element composition:*

*Chemical analyses of 77017*

	1	2	3	4	5	6
$\text{SiO}_2$ .....	44.09	--	--	43.17	--	42.82
$\text{Al}_2\text{O}_3$ .....	26.59	26.0	27.1	23.11	18.9	13.67

*Chemical analyses of 77017—Continued*

	1	2	3	4	5	6
FeO .....	6.19	6.2	5.7	9.02	12.1	14.91
MgO .....	6.06	6	6	7.77	8	9.29
CaO .....	15.43	14.5	15.7	13.96	11.7	12.29
Na <sub>2</sub> O .....	.30	.31	.36	.37	.39	.41
K <sub>2</sub> O .....	.06	.050	.076	.20	.10	.22
TiO <sub>2</sub> .....	.41	.75	.35	2.31	5.3	6.01
P <sub>2</sub> O <sub>5</sub> .....	.03	--	--	.07	--	.09
MnO .....	.08	.085	.077	.12	.155	.19
Cr <sub>2</sub> O <sub>3</sub> .....	.13	.140	.126	.26	.290	.45
Total .....	99.37			100.36		100.35

1. 77017.2 (Apollo 17 PET, 1973).
  2. 77017.57, bulk composition (Laul and others, 1974).
  3. 77017, gray fragment (Laul and others, 1974).
  4. 77017, glass veinlet, microprobe analyses (Helz and Appelman, 1974).
  5. 77017, dark matrix (Laul and others, 1974).
  6. 77017, glass rim, microprobe analyses (Helz and Appelman, 1974).
- Data from columns 4-6 not included in figure 179.

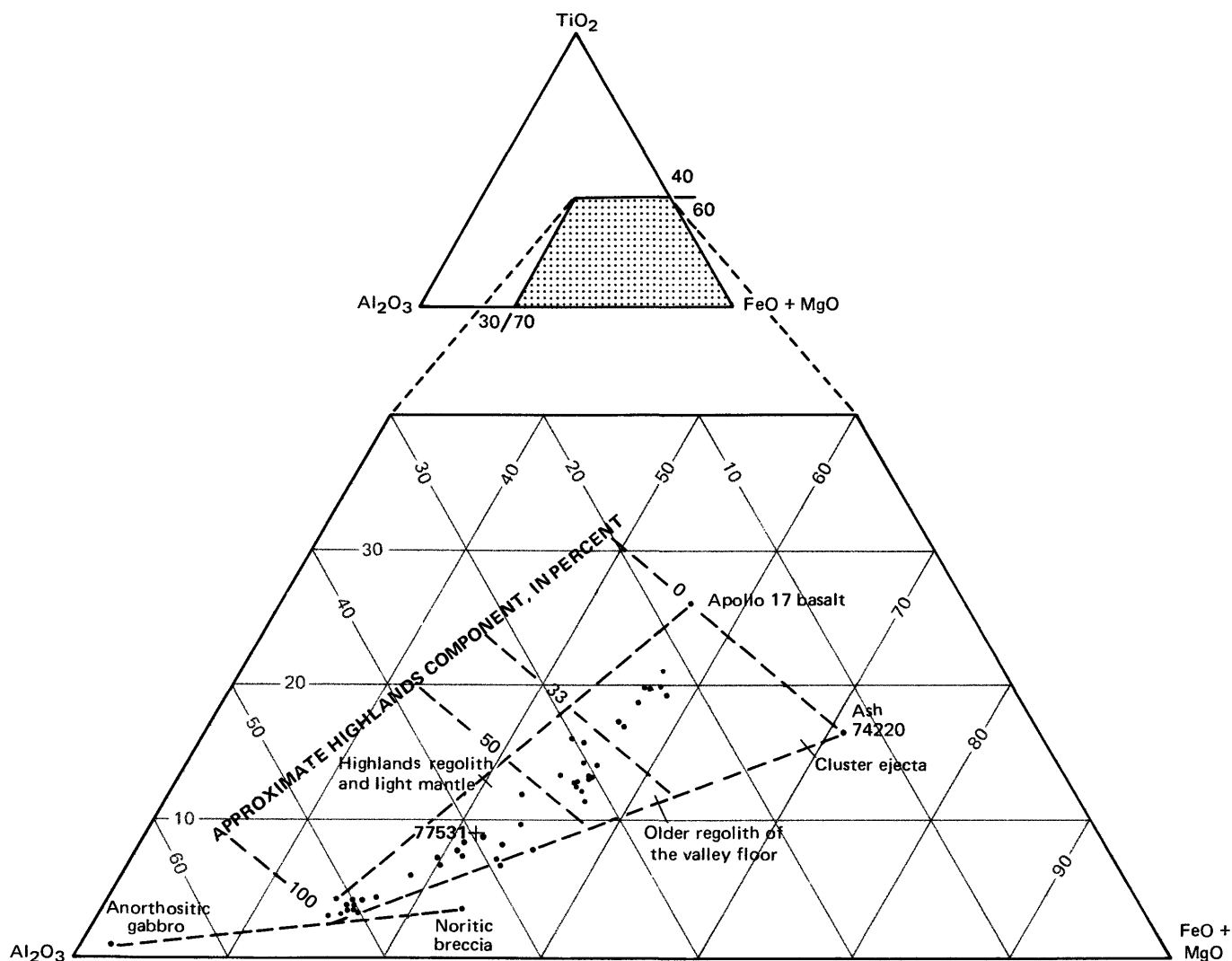


FIGURE 182.—Relative amounts of  $\text{TiO}_2$ ,  $\text{Al}_2\text{O}_3$ , and  $\text{FeO}+\text{MgO}$  in sediment sample 77531, from station 7 (cross), in comparison with sediment samples from rest of traverse region (dots). Apollo 17 basalt, anorthositic gabbro, and noritic breccia values from Rhodes and others (1974).

## Age:

<sup>40-39</sup>Ar:

77017,32A, anorthositic breccia (carefully separated from black glass vein material),  $4.04 \pm 0.05$  b.y.; interpreted as dating the time when the augite and pigeonite poikiloblasts crystallized (Kirsten and Horn, 1974).

77017,32B, black glass vein,  $1.5 \pm 0.3$  b.y. (Kirsten and Horn, 1974).

Trapped solar-wind gases indicate that the glass and the host rock of sample 77017 are genetically unrelated; glass is interpreted as impact-melted regolith injected into fractures in host rock  $\sim 1.5$  b.y. ago without obliterating the previous metamorphic record (Kirsten and Horn, 1974).

77017,46,  $3.97 \pm 0.02$  b.y. (Phinney and others, 1975).

## Exposure age:

Ar:

77017,32A, anorthositic breccia,  $80 \pm 10$  m.y. (Kirsten and Horn, 1974).

77017,32B, black glass vein,  $90 \pm 40$  m.y. (Kirsten and Horn, 1974).

77017,46,  $224 \pm 20$  m.y. (Phinney and others, 1975).

## Sample 77035

*Type:* Polymict breccia with an aphanitic matrix.

*Size:*  $22 \times 15.5 \times 15$  cm.

*Weight:* 5,727 g.

*Location:* From surface about 6 m southwest of the LRV.

*Illustrations:* Pans 23, 24; figure 184 (LRL).

*Comments:* Sample 77035, a fragment from the regolith

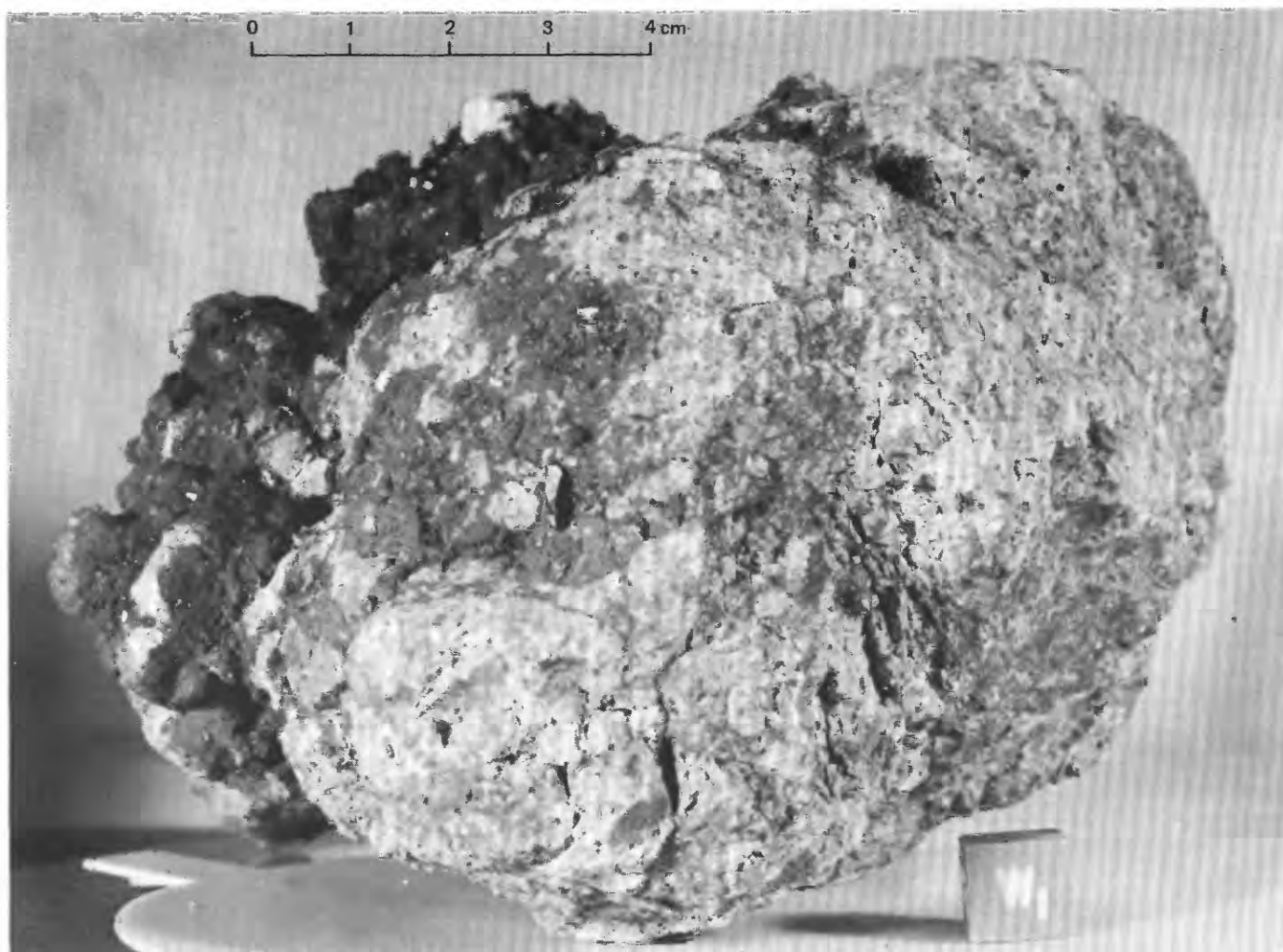


FIGURE 183.—Sample 77017. Monomict breccia with clasts of olivine gabbro in glassy matrix. (NASA photograph S-73-17771.)

at station 7, is presumably North Massif material.

**Petrographic description:** Polymict breccia with clasts of gabbro(?) or metagabbro(?), fine-grained metaclastic or breccia fragments, vitreous(?) fragments, feldspathic metaclastic rocks, and plagioclase and olivine in an irregularly and faintly banded aphanitic matrix with slitlike cavities.

**Major-element composition:**

*Chemical analysis of 77035*

SiO <sub>2</sub> .....	46.8
Al <sub>2</sub> O <sub>3</sub> .....	18.1
FeO .....	8.88
MgO .....	12.19
CaO .....	11.22
Na <sub>2</sub> O .....	.623
K <sub>2</sub> O .....	.261
TiO <sub>2</sub> .....	1.50
P <sub>2</sub> O <sub>5</sub> .....	.264

*Chemical analysis of 77035*

MnO .....	.112
Cr <sub>2</sub> O <sub>3</sub> .....	.197
Total .....	100.147

77035.61 (Wänke and others, 1975).

**Sample 77075-77**

**Type:** Monomict(?) breccia with an aphanitic matrix; includes adhering norite cataclasite.

**Sizes:** 77075, three fragments, 4×4×4 cm, 1.5×1.5×1.2 cm, 1×1×0.5 cm; 77076, 3×2×2 cm; 77077, 2×2×1.5 cm.

**Weights:** 77075, 172.4 g total; 77076, 13.97 g; 77077, 5.45 g.

**Location:** 3-m boulder.

**Illustrations:** Pan 24; figures 185, 186 (LRL).

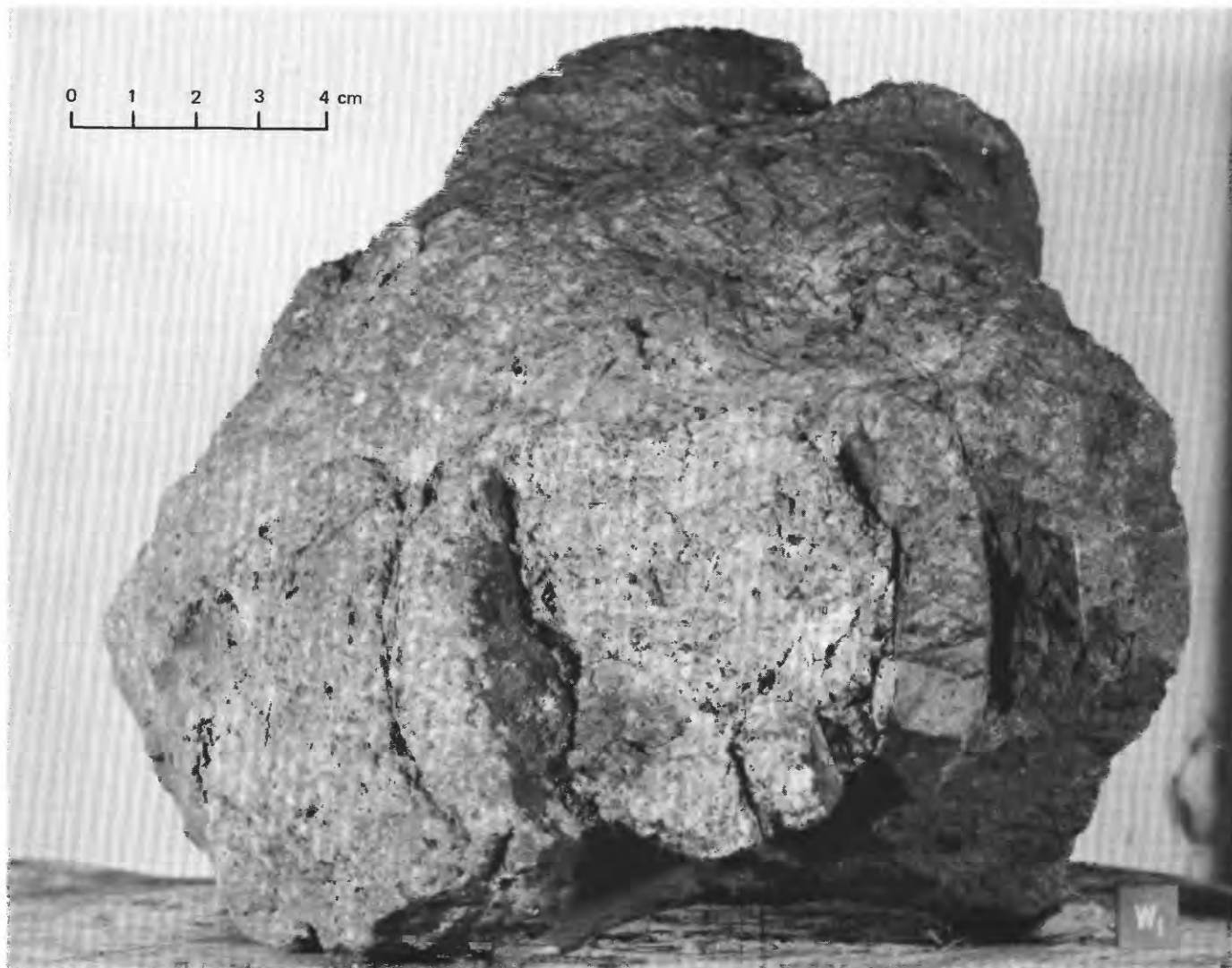


FIGURE 184.—Sample 77035. Polymict breccia with aphanitic matrix. Faint banding and slitlike cavities are aligned parallel to margin of light-gray gabbroid(?) clast. (NASA photograph S-73-15902.)

**Comments:** Samples 77075-77 are from a blue-gray breccia dike that intrudes a light-gray 1.5-m inclusion enveloped by blue-gray breccia that is continuous with the dike. The blue-gray breccia is in turn enclosed in greenish-gray vesicular breccia.

**Petrographic description:** Breccia dike in norite cataclastite. The dike has plagioclase, olivine, and orthopyroxene porphyroclasts and rare metaclastic fragments in an aphanitic matrix.

According to Chao and others (1974), the black dike material of sample 77075 consists of xenocrysts of calcic plagioclase, olivine, and rare orthopyroxene in a very fine holocrystalline matrix composed of

#### Major-element composition:

##### Chemical analysis of 77075

SiO <sub>2</sub> .....	46.4
Al <sub>2</sub> O <sub>3</sub> .....	18.17
FeO .....	9.31
MgO .....	12.57
CaO .....	10.55
Na <sub>2</sub> O .....	.65
K <sub>2</sub> O .....	.23
TiO <sub>2</sub> .....	1.38
MnO .....	.11
P <sub>2</sub> O <sub>5</sub> .....	.26
Cr <sub>2</sub> O <sub>3</sub> .....	.17
Total .....	99.90

77075.21 dark vein, matrix (Winzer and others, 1974).



FIGURE 185.—Distribution of rock types and locations of samples 77075-77 and 77215 in 3-m breccia boulder at station 7, before sampling. Light-gray clast is enclosed in blue-gray breccia, which is in turn enclosed in greenish-gray vesicular breccia. Dashed lines separate rock units. View is to southwest. (NASA photograph AS17-146-22305.)

intimately intergrown plagioclase and pyroxene with subordinate olivine and ilmenite.

*Age:*  $^{40}\text{--}^{39}\text{Ar}$ : 77075, 18,  $3.98 \pm 0.04$  b.y., interpreted as representing time of intrusion of the veinlet (Stettler and others, 1974).

*Exposure age:* Ar: 77075, 18, 25.5 m.y., includes correction for shielding effects (Stettler and others, 1974).

#### Sample 77115

*Type:* Polymict breccia with an aphanitic matrix.

*Size:* 6.5×5.5×3.5 cm.

*Weight:* 115.9 g.

*Location:* 3-m boulder.

*Illustrations:* Pan 24; figures 187, 188 (LRL), 189 (photomicrograph), 190.

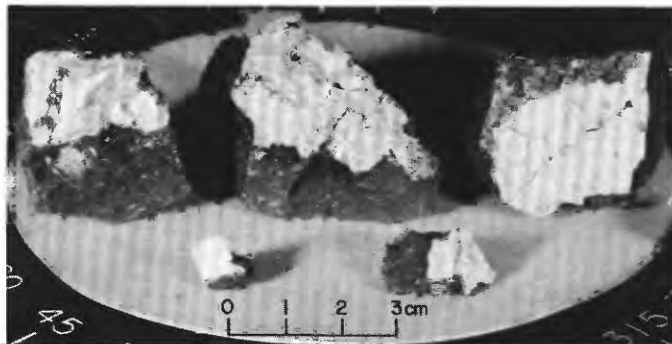


FIGURE 186.—Sample 77075. Fragments of dark, fine-grained breccia dike in norite cataclasite. (NASA photograph S-73-17186.)

*Comments:* Sample 77115 is from blue-gray breccia that contains conspicuous clasts including the 1.5-m-long light-gray clast represented by norite cataclasite sample 77215. The blue-gray breccia, which is highly fractured, is in turn incorporated in relatively unfractured greenish-gray breccia.

*Petrographic description:* Polymict breccia with clasts of very fine grained feldspathic metaclastic rock, fine-grained dark breccia or metaclastic rocks, and plagioclase, orthopyroxene, and olivine porphyroclasts in an irregularly banded inhomogeneous aphanitic matrix. Irregular banding is in part the result of disaggregation and cataclastic flow of troctolite cataclasite.

Chao and others (1974, 1975a, 1975b) classified and described rock 77115 as fragment-laden feldspathic pigeonite basalt consisting of a vuggy microsubophitic to micropoikilitic matrix with scattered xenocrysts and xenoliths that are coarser than the matrix crystals. The matrix shows chill effects against the inclusions. Matrix minerals, generally smaller than 0.2 mm, are mainly plagioclase, clinopyroxene (mainly pigeonite), olivine, and ilmenite. Xenocrysts, commonly with zoned rims, are dominantly plagioclase (65 percent), clinopyroxene (4 percent), orthopyroxene (7 percent), and olivine (20 percent); xenoliths are fragments of anorthosite-troctolite-norite rocks that commonly have been brecciated and recrystallized.

Chao and others (1975b) argued that 77115 is not metamorphic but crystallized from a melt that was

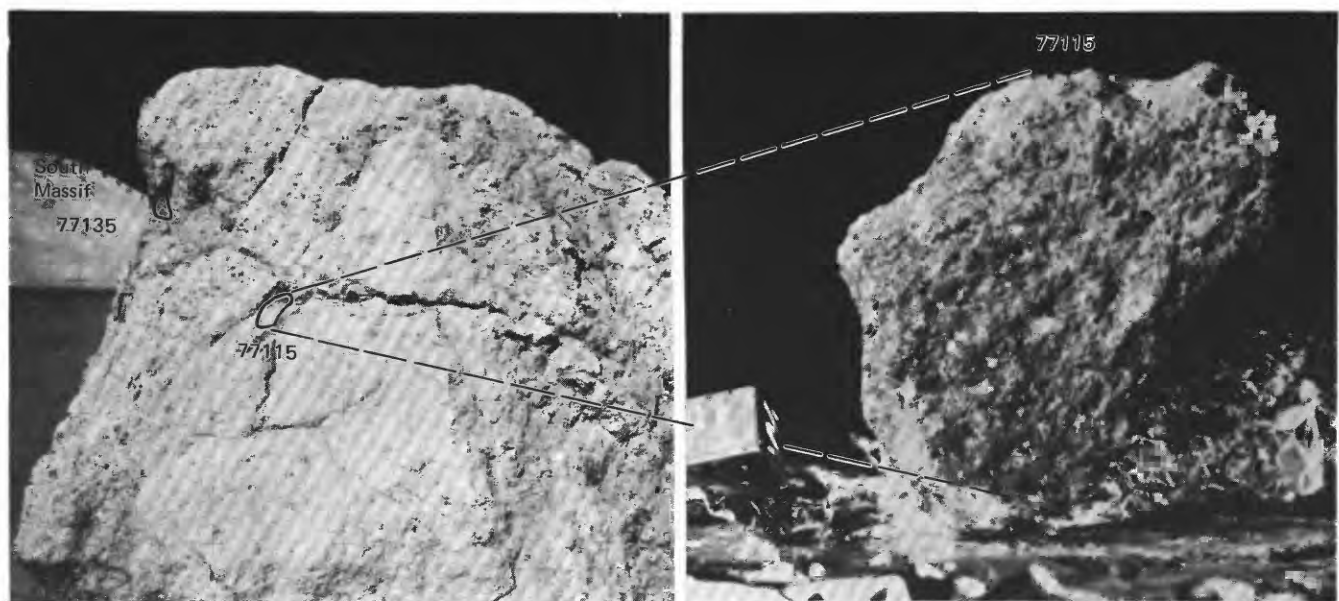


FIGURE 187.—Left, Locations of samples 77115 and 77135 in 3-m breccia boulder at station 7, before sampling. View is to southwest. (NASA photograph AS17-146-22299.) Right, Sample 77115 with reconstructed lunar surface orientation and lighting. (View similar to NASA photograph S-73-33505.)

inferred from the fine matrix grain size ( $\sim 10 \mu\text{m}$ ) and from the abundance of vugs and vesicles to have crystallized rapidly near the surface. They suggested a two-stage cooling history: (1) a period of slow cooling during which xenocrysts reacted with the melt to form zoned rims and (2) a rapid quench to form the fine matrix. Igneous rather than impact origin for the melt was suggested because (1) 99 percent of the xenoliths and xenocrysts show no evidence of shock and (2) the inferred two-stage cooling history seemed more likely for a melt of endogenous igneous origin than for impact melt that might be expected to cool at a uniform rate.

Huebner (in Chao and others, 1975b) gave an alternate interpretation that the xenocryst rims were formed by subsolidus reaction with the matrix rather than by reaction with a melt. He cited the following arguments:

1. Olivine xenocrysts become more fayalitic toward the rims, pyroxene becomes more magnesian; hence the mafic silicates approach supposed equilibrium from opposite directions.
2. Plagioclase xenocrysts form two populations ( $\text{An}_{71-79}$  and  $\text{An}_{93-95}$ ). Both types are zoned outward to margins that are  $\text{An}_{86}$ ; thus "equilibrium" appears to have been approached from both more sodic and more calcic directions. Textural evidence indicates that xenocrysts were neither mantled nor resorbed as a result of contact with a melt.
3. Experimental data suggest that the matrix is too magnesian to have been in equilibrium as a melt with the pyroxene and olivine rims; the rims should have been resorbed by a melt of the matrix composition.
4. Phase-equilibrium data suggest that the pigeonite

and orthopyroxene xenocrysts would have been resorbed by a liquid of the composition of the matrix of 77115; instead, the low-calcium pyroxene xenocrysts survived and developed rims.

#### Major-element composition:

##### Chemical analyses of 77115

	1	2	3	4	5	6	7	8	9	10
$\text{SiO}_2$ .....	41.8	46.6	47.0	46.5	47.1	47.1	47.2	47.1	46.1	46.1
$\text{Al}_2\text{O}_3$ .....	16.78	18.63	17.59	17.06	17.35	18.86	17.55	16.26	18.8	18.7
$\text{FeO}$ .....	6.08	8.44	8.73	8.99	8.90	8.39	9.51	9.74	8.8	9.7
$\text{MgO}$ .....	23.54	11.96	12.01	13.77	12.33	10.98	12.43	13.34	11.5	10.7
$\text{CaO}$ .....	10.24	11.01	10.74	10.60	10.79	11.11	10.89	10.07	11.1	11.0
$\text{Na}_2\text{O}$ .....	.31	.67	.66	.66	.66	.69	.67	.61	.68	.65
$\text{K}_2\text{O}$ .....	.08	.25	--	.26	.26	.32	.24	--	.15	.16
$\text{TiO}_2$ .....	.17	1.15	1.26	1.30	1.31	1.23	1.34	1.21	2.48	3.03
$\text{P}_2\text{O}_5$ .....	.53	.37	.31	.29	.33	.31	.31	.24	.09	--
$\text{MnO}$ .....	.06	.11	.11	.12	.11	.11	.11	.12	.07	--
$\text{Cr}_2\text{O}_3$ ...	.04	.19	.16	.17	.17	.16	.18	.17	.21	--
Total	99.63	99.38	98.57	99.72	99.31	99.26	100.43	98.86	99.98	100.04

1. 77115, 19 clast, classified as troctolite by Winzer and others (1977).
  2. 77115, 19.
  3. 77115, 69, 70, 71.  
Cols. 2 and 3, contact zone between clast (col. 1) and matrix (col. 4-8).
  4. 77115, 19.
  5. 77115, 69.
  6. 77115, 70.
  7. 77115, 71.
  8. 77115, 72.  
Col. 4-8, matrix
  9. 77115, bulk composition, matrix plus xenocrysts.
  10. 77115, matrix only, does not include xenocrysts ( $\sim 19$  volume percent). Samples 9 and 10, calculated from mineral modes and microprobe analyses from three thin sections (Chao and others, 1975b).
- Analyses 1-8 from splits from a single 2.44-g chip (Winzer and others, 1974).  
NOTE.—Additional analyses by defocused beam microprobe have been published by Stoessner and others (1974a,b) and Ryder and others (1975).

#### Age:

$^{40}\text{Ar}$ : 77115, 75, plagioclase from clast shows well-defined low-temperature plateau at  $3.96 \pm 0.03$  b.y., which records a time of argon

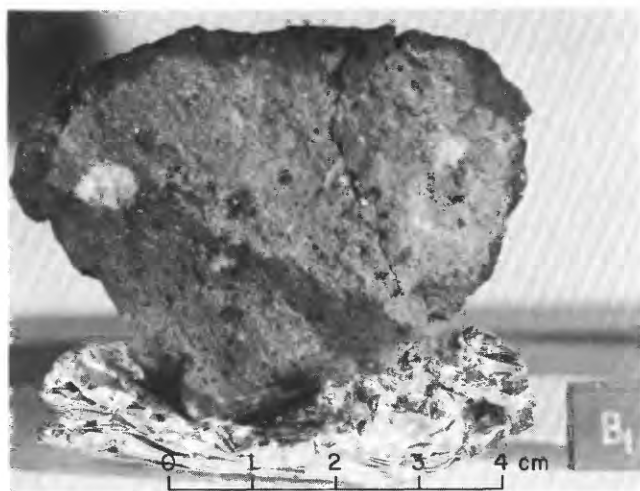


FIGURE 188.—Sample 77115. Polymict breccia with aphanitic matrix. (NASA photograph S-73-15011.)

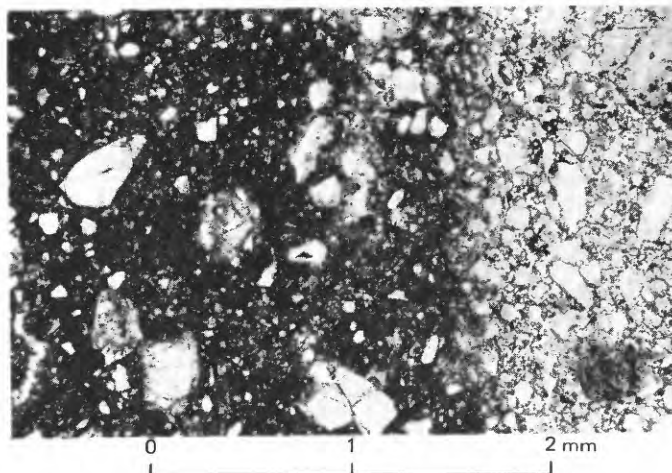


FIGURE 189.—Sample 77115. Photomicrograph showing contact between pink spinel troctolite cataclastic clast (right) and aphanitic matrix with mineral and lithic debris (left).

loss. Argon loss was incomplete at 3.96 b.y.; additional heating shows clast formed  $\geq 4.23$  b.y. ago (Stettler and others, 1975).

Rb-Sr isochron: 77115,35,  $3.75 \pm 0.20$  b.y. (Nakamura and others, 1976).

#### Sample 77135

*Type:* Polymict breccia with a poikilitic matrix.

*Size:* 10.3×8×4 cm.

*Weight:* 337.4 g.

*Location:* 3-m boulder.

*Illustrations:* Pan 24; figures 187, 190, 191 (LRL).

*Comments:* Sample 77135 is from the vesicular greenish-gray breccia matrix that encloses the blue-gray breccia represented by sample 77115. Fracture sets developed in the blue-gray breccia are not seen in the greenish-gray breccia, and vesicles of the greenish-gray breccia are elongated and alined in trains parallel to the contact with the blue-gray breccia.

*Petrographic description:* Polymict breccia with small clasts of "dunite," feldspathic metaclastic rocks, and abundant porphyroclasts of olivine and plagioclase in a highly vesicular poikilitic matrix.

According to Chao and Minkin (1974) and Chao and others (1974), 77135 is a fragment-laden pigeon-

ite basalt that originated from a melt of either impact or igneous origin. The melt crystallized to a fine poikilitic aggregate of plagioclase, pigeonite, and olivine, with minor augite and ilmenite. Both pigeon-

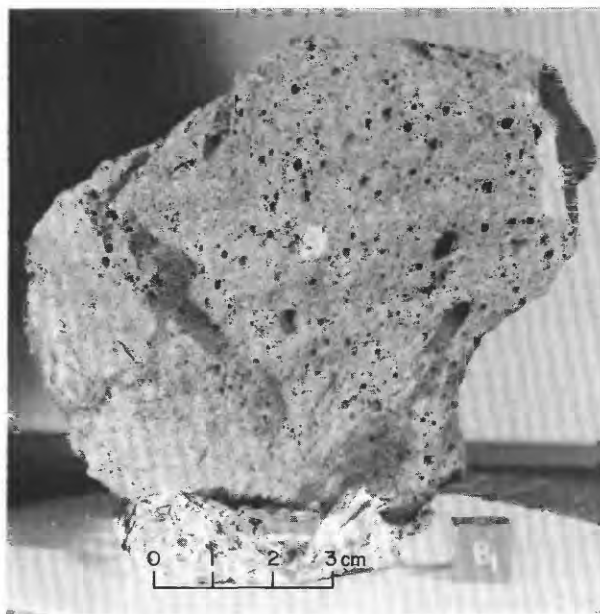


FIGURE 191.—Sample 77135. Polymict breccia with poikilitic matrix. (NASA photograph S-72-56391.)

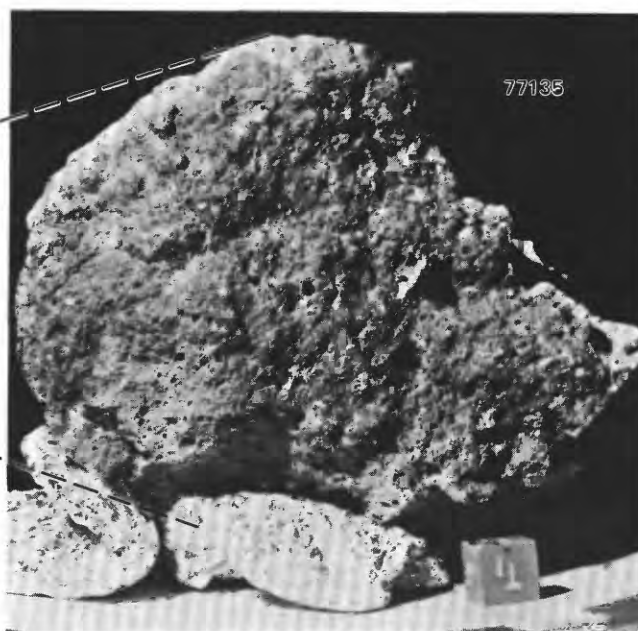


FIGURE 190.—Left, Sample 77135 (before collection) and location from which sample 77115 was collected. Irregular dashed line is contact between fractured blue-gray breccia and vesicular greenish-gray breccia. Note preferred orientation and alinement of vesicles parallel to contact. View is to southwest. (NASA photograph AS17-146-22338.) Right, Sample 77135 with reconstructed lunar surface orientation and lighting. (NASA photograph S-73-19386.)

ite and augite form oikocrysts enclosing plagioclase and olivine. Xenoliths are highly feldspathic crystalline rocks; most of the xenocrysts, dominantly olivine and plagioclase, may be mineral fragments disaggregated by crushing of rocks like those of the xenoliths.

#### Major-element composition:

Chemical analyses of 77135

	1	2	3	4	5	6	7	8
SiO <sub>2</sub> .....	45.3	44.4	46.13	46.17	45.3	46.3	47.5	46.3
Al <sub>2</sub> O <sub>3</sub> .....	25.13	27.81	18.01	17.83	18.03	18.39	17.18	19.82
FeO.....	5.98	4.19	9.11	9.14	9.56	9.48	9.01	8.28
MgO.....	8.59	7.96	12.63	12.39	13.38	12.19	12.66	11.78
CaO.....	13.95	15.09	11.03	11.08	10.64	10.96	10.91	11.74
Na <sub>2</sub> O.....	.40	.41	.53	.69	.61	.65	.66	.56
K <sub>2</sub> O.....	.09	.07	.30	.27	.22	.23	.41	.21
TiO <sub>2</sub> .....	.43	.24	1.54	1.53	1.72	1.48	1.45	1.31
P <sub>2</sub> O <sub>5</sub> .....	.10	.03	.28	.30	.28	.28	.29	.21
MnO.....	.06	.05	.13	.13	.11	.11	.11	.10
Cr <sub>2</sub> O <sub>3</sub> .....	.13	.09	.20	.21	.18	.18	.18	.16
Total.....	100.16	100.34	99.89	99.74	100.03	100.25	100.36	100.47

1. 77135.41, clast (Winzer and others, 1974).

2. 77135.52, troctolite clast (Winzer and others, 1974).

3. 77135.2 (Apollo 17 PET, 1973).

4. 77135.5 (Rhodes and others, 1974).

5. 77135.66, less vesicular matrix (Winzer and others, 1974).

6. 77135.77, more vesicular matrix (Winzer and others, 1974).

7. 77135.82, matrix (Winzer and others, 1976).

8. 77135.91, matrix (Winzer and others, 1976).

#### Age:

##### Rb-Sr isochron:

77135.34,  $4.14 \pm 0.08$  b.y., regarded as suspect because it seems too old; possibly analyzed separates included older xenocrysts that had not equilibrated with the matrix (Nakamura and others, 1976).

77135.57, clast,  $3.89 \pm 0.08$  (2 $\sigma$ ) b.y. (Tatsumoto and others, 1974; Nunes and others, 1974).

77137.34, vesicular matrix, station 7 boulder,  $3.8 \pm 0.1$  b.y. (Nunes and others, 1976).

##### <sup>40</sup>Ar:

77135.51, clast,  $3.99 \pm 0.02$  b.y. (Stettler and others, 1974).

77135.57, olivine-rich clast,  $3.90 \pm 0.03$  b.y. (Stettler and others, 1975). (Similar to Rb-Sr age, above, on same clast.)

77135.71, vesicular matrix, short poorly defined high-temperature plateaus at  $3.83 \pm 0.04$  b.y.,  $3.78 \pm 0.08$  b.y. (Stettler and others, 1974).

#### Exposure age:

##### Ar:

77135.51, clast, 28.5 m.y. (Stettler and others, 1974).

77135.71, vesicular matrix, 29.6 m.y. (Stettler and others, 1974).

77135.71, vesicular matrix,  $20 \pm 2$  m.y.

(Eberhardt and others, 1975).

Exposure ages of Stettler and others (above) include their recommended 3/2 correction for shielding effects. Application of the same correction to the 20-m.y. result, which Eberhardt and others indicate is too low because of uncorrected shielding effects, produces a concordant age of ~30 m.y.

##### Kr:

77135,  $28.6 \pm 1.4$  m.y. (Croaz and others, 1974).

77135.71,  $31.8 \pm 1.6$  m.y. (Eberhardt and others, 1975).

##### Tracks:

77135,  $5.4 \pm 1$  m.y. (Croaz and others, 1974), discordantly young track age could reflect any minor spalling event; hence it is a firm younger limit but does not necessarily date the emplacement of the station 7 boulder.

#### Sample 77215

Type: Norite cataclasite.

Size: 41 pieces that range from 1 cm to  $6.5 \times 4.5 \times 2.5$  cm.

Weight: 846.4 g total.

Location: From 3-m boulder approximately 22 m southwest of the LRV.

Illustrations: Pan 24, figures 185, 192 (LRL).

Comments: Sample 77215 is from the large (approximately  $0.5 \times 1.5$  m) light-gray clast enclosed in and intruded by blue-gray breccia.

Petrographic description: Norite cataclasite. Sample is in many pieces, some of which contain dark fine-grained breccia veins similar to those of 77075, and some troctolitic cataclasite fragments.

A mode determined by Chao and others (1976b) shows that sample 77215 consists of about 8 percent norite fragments, 10 percent "anorthosite" fragments (aggregated anorthite crystals interpreted as representing orthopyroxene-free portions of the noritic parent rock), 6 percent glass fragments similar in composition to the bulk composition of the noritic breccia itself, rare olivine-plagioclase breccia fragments, and 75 percent mineral fragments. Mineral fragments are dominantly orthopyroxene (31 percent) and plagioclase (40 percent) that are assumed to be largely derived from the norite parent.

Chao and others have interpreted the norite as a plutonic rock that crystallized at a depth of 8 or more kilometers. They suggest that a cratering event delivered crushed norite to the surface, where it was

mixed with noritic glass and olivine-plagioclase breccia (troctolite cataclasite) that are interpreted as probable products of separate cratering events. Subsequently, in their model, the noritic breccia was intruded by the blue-gray breccia dike and later enveloped in the greenish-gray vesicular breccia.

*Major-element composition:*

*Chemical analyses of 77215*

	1	2	3	4	5	6
SiO <sub>2</sub> .....	46.8	47.2	46.0	51.1	51.1	51.3
Al <sub>2</sub> O <sub>3</sub> .....	17.44	16.89	17.75	14.32	13.98	15.06
FeO .....	9.39	9.36	9.04	10.32	10.38	10.07
MgO .....	13.16	12.93	12.74	13.23	14.31	12.56
CaO .....	10.88	10.76	10.94	9.08	8.65	8.96
Na <sub>2</sub> O .....	.65	.68	.68	.55	.39	.43
K <sub>2</sub> O .....	.24	.23	.24	.15	.18	.14
TiO <sub>2</sub> .....	1.37	1.35	1.32	.37	.30	.32
P <sub>2</sub> O <sub>5</sub> .....	.28	.27	.26	.10	.14	.11
MnO .....	.12	.12	.11	.17	.17	.16
Cr <sub>2</sub> O <sub>3</sub> .....	.19	.20	.14	.36	.36	.32
Total .....	100.52	99.99	99.22	99.75	99.96	99.43

1. 77215.115, black dike (Winzer and others, 1976).
2. 77215.119, dike (Winzer and others, 1976).
3. 77215.121, dike (Winzer and others, 1976).
4. 77215.130, gray glass (Winzer and others, 1976); impact-fused equivalent of the norite (Chao and others, 1976b).
5. 77215.152, matrix (Winzer and others, 1976); equals norite breccia (Chao and others, 1976b).
6. 77215.45 (Winzer and others, 1974); represents bulk composition of noritic breccia 77215 (Chao and others, 1976a).

*Age:*

*Rb-Sr isochron:*

77215,37 and 77215,145,  $4.42 \pm 0.04$  ( $2\sigma$ ) b.y. (Nakamura and others, 1976) corresponds with Pb-Pb model age of 4.42 b.y. (Nunes and others, 1974) and may be primary crystallization age of the norite or the age of its cataclasis; crystallization age preferred by Nakamura and others because of concordance with Sm-Nd age.

*Sm-Nd isochron:*

77215,37,  $4.37 \pm 0.07$  ( $2\sigma$ ) b.y. (Nakamura and others, 1976).

*U-Pb isochron:*

77215,37,  $3.8 \pm 0.2$  b.y., interpreted as recording an impact event (Nunes and others, 1974).

*<sup>40</sup>-<sup>39</sup>Ar:*

77215,45A,  $4.04 \pm 0.03$  b.y. (Stettler and others, 1974).

*Exposure age:* Ar: 77215,45A, 27.1 m.y. includes correction calculated to compensate for partial shielding (Stettler and others, 1974).



FIGURE 192.—Sample 77215. Fragments of norite cataclasite with some dark, fine-grained breccia veins similar to sample 77075. Largest fragment is 6.5×4.5×2.5 cm. (NASA photograph S-73-17778.)

## Sample 77510-19, 25-26

*Type:* Sedimentary, unconsolidated (77510-14); breccia or polymict breccia fragments with aphanitic or poikilitic(?) matrices (77515, 77517-19); olivine basalt (77516); and two small breccia fragments (77525-26).

*Size:* 77515, 7.5×6.5×5.5 cm; 77516, 6×4×2.5 cm; 77517, 4×4×3 cm; 77518, 3.5×3.5×2.5 cm; 77519, 3.5×2.5×2 cm; 77525 and 77526, near centimeter size.

*Weight:* 77515, 337.6 g; 77516, 103.7 g; 77517, 45.6 g; 77518, 42.5 g; 77519, 27.4 g; 77525 and 77526, 2.26 g total.

*Depth:* From upper few centimeters.

*Location:* Regolith surface about 10 m southwest of the LRV.

*Illustrations:* Pan 24; figures 193 (LRL, 77515), 194 (LRL, 77516), 195 (LRL, 77517), 196 (LRL, 77519).

*Comments:* Sample is regolith material with breccia fragments probably derived from the North Massif. Sample 77516 is basalt presumably ejected from some crater on the valley floor.

*Petrographic descriptions:*

77510-14, dominantly fine-grained breccia and (or) metaclastic rock, some agglutinate.

77515, polymict breccia with clasts of breccia,

metatroctolite(?), feldspathic metaclastic rock, and porphyroclasts of plagioclase and olivine in a fine-grained poikilitic(?) matrix with slitlike and spherical cavities loosely concentrated in a 1-cm-thick band.

77516, medium-grained olivine basalt with an intersertal or intergranular groundmass.

77517, polymict breccia with fragments of breccia, fine-grained metaclastic rock, and porphyroclasts of olivine and plagioclase in a feldspathic aphanitic matrix..

77518, breccia with few small porphyroclasts of pyroxene(?), olivine(?), and plagioclase in a fine-grained poikilitic(?) matrix.

77519, polymict breccia with small clasts of metatroctolite with granoblastic-polygonal texture, and porphyroclasts of plagioclase, olivine, and pyroxene(?) in a fine-grained poikilitic(?) matrix.

*Major-element composition:*

*Chemical analysis of 77515*

SiO <sub>2</sub> .....	..
Al <sub>2</sub> O <sub>3</sub> .....	18.6
FeO .....	8.4
MgO .....	11
CaO .....	11.0
Na <sub>2</sub> O .....	.68
K <sub>2</sub> O .....	.24
TiO <sub>2</sub> .....	1.4
P <sub>2</sub> O <sub>5</sub> .....	..
MnO .....	.099
Cr <sub>2</sub> O <sub>3</sub> .....	.170

77515,3, tan-gray breccia (Laul and Schmitt, 1975a).

*Sample 77530-39, 45*

*Type:* Sedimentary, unconsolidated (77530-34); basalt



FIGURE 193.—Sample 77515. Polymict breccia with poikilitic(?) matrix. (NASA photograph S-73-19416.)

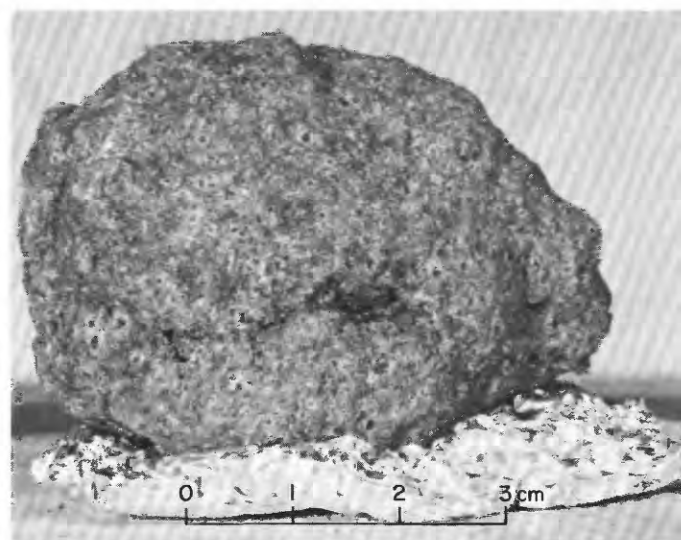


FIGURE 194.—Sample 77516. Medium-grained olivine basalt. (NASA photograph S-73-19409.)

(77535); olivine basalt (77536); and breccia or polymict breccia fragments with aphanitic to poikilitic(?) matrices (77537-39, 45).

*Size:* 77535, 10.5×8.5×3.5 cm; 77536, 11×7×3.5 cm; 77537-39, 45, 3 to 5 cm maximum dimension.

*Weight:* 77530-34, 219.46 g; 77535, 577.8 g; 77536, 355.3 g; 77537-39, 45, 188 g total.

*Depth:* From upper few centimeters.

*Location:* Regolith surface about 10 m southwest of the LRV.

*Illustrations:* Pan 24; figures 197 (LRL, 77535), 198 (LRL, 77536), 199 (LRL, 77537), 200 (LRL, 77538), 201 (LRL, 77539), 202 (LRL, 77545).

*Comments:* Sample is regolith material largely derived from the North Massif and the valley floor. Samples 77535-36 are basalt fragments probably ejected from craters on the valley floor. The breccia samples are highlands material presumably eroded from the North Massif.

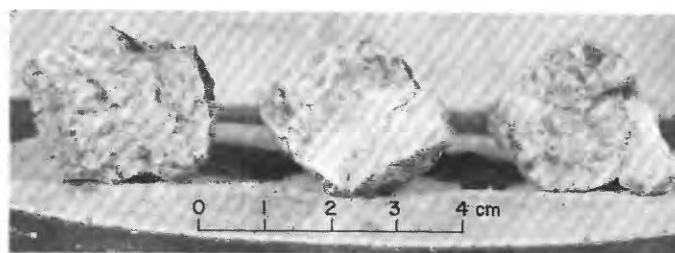


FIGURE 195.—Sample 77517. Polymict breccia with aphanitic matrix. (NASA photograph S-73-19404.)

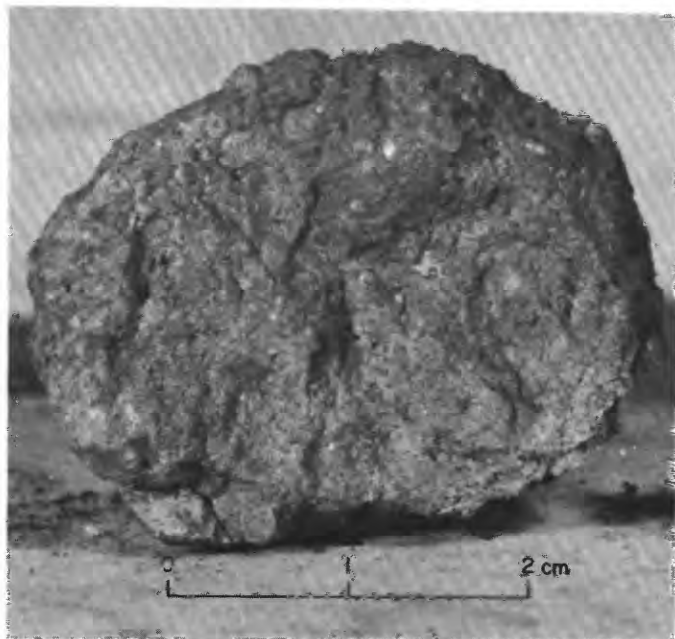


FIGURE 196.—Sample 77519. Polymict breccia with poikilitic(?) matrix. (NASA photograph S-73-19134.)

#### *Petrographic descriptions:*

77530-34, dominantly fine-grained breccia and (or) metaclastic rock, some basalt and agglutinate, minor glass.

*Components of 90-150-μm fraction of 77531,1 (Heiken and McKay, 1974)*

Components	Volume percent
Agglutinate.....	54.0
Basalt, equigranular.....	4.0
Basalt, variolitic.....	.7
Breccia:	
Low grade <sup>1</sup> - brown.....	5.6
Low grade <sup>1</sup> - colorless.....	2.3
Medium to high grade <sup>2</sup> .....	9.7
Anorthosite.....	.7
Cataclastic anorthosite <sup>3</sup> .....	1.0
Norite.....	..
Gabbro.....	..
Plagioclase.....	9.3
Clinopyroxene.....	3.3
Orthopyroxene.....	1.0
Olivine.....	.7
Ilmenite.....	1.3
Glass:	
Orange.....	.3
"Black".....	3.3
Colorless.....	.3
Brown.....	2.0
Gray, "ropy".....	..
Other.....	..
Total number grains.....	300

<sup>1</sup>Metamorphic groups 1-3 of Warner (1972).

<sup>2</sup>Metamorphic groups 4-8 of Warner (1972).

<sup>3</sup>Includes crushed or shocked feldspar grains.

77535, medium-grained slightly vesicular porphyritic basalt. Aggregates of clinopyroxene-ilmenite in a subophitic groundmass of plagioclase, clinopyroxene, ilmenite, and accessory minerals.

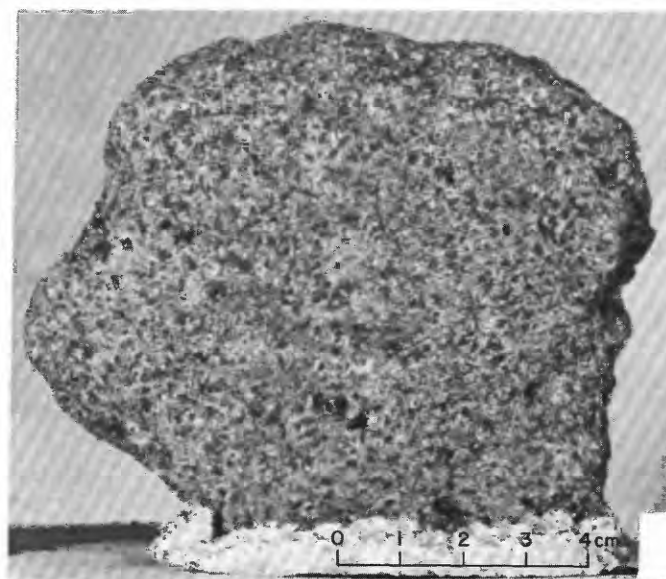


FIGURE 197.—Sample 77535. Medium-grained basalt. (NASA photograph S-73-19122.)

77536, medium-grained vesicular porphyritic olivine basalt. Aggregates of clinopyroxene-ilmenite in a subophitic groundmass of plagioclase, clinopyroxene, ilmenite, and accessory minerals.

77537, breccia with very scarce fine-grained metaclastic rocks and porphyroclasts of olivine(?) and plagioclase in a vesicular fine-grained poikilitic(?) matrix.

77538, polymict breccia with scarce small fine-grained dark metaclastic rocks, feldspathic

cataclasite, and dominantly plagioclase porphyroclasts in an aphanitic matrix.

77539, polymict breccia with clasts of meta-anorthosite, metatroctolite(?) and porphyroclasts of plagioclase in a vesicular fine-grained poikilitic(?) matrix.

77545, polymict breccia with clasts of mafic troctolite or meta-troctolite, "dunite," and porphyroclasts of plagioclase and olivine in a vesicular fine-grained poikilitic(?) matrix.

#### Major-element compositions:

Chemical analyses of 77531, 77535, 77538, 77539, 77545

	1	2	3	4	5
SiO <sub>2</sub> .....	43.07	38.57	--	--	--
Al <sub>2</sub> O <sub>3</sub> .....	17.16	8.95	14.5	22.0	10.9
FeO .....	11.70	18.53	10.6	6.9	10.3
MgO .....	10.19	8.85	5.0	8.0	10
CaO .....	11.93	10.66	10.3	12.5	6.6
Na <sub>2</sub> O .....	.44	.39	.75	.56	.47
K <sub>2</sub> O .....	.11	.05	1.04	.20	.14
TiO <sub>2</sub> .....	3.91	12.39	1.2	1.1	1.2
P <sub>2</sub> O <sub>5</sub> .....	.08	.04	--	--	--
MnO .....	.17	.27	.150	.082	.110
Cr <sub>2</sub> O <sub>3</sub> .....	.31	.43	.240	.136	.520
Total .....	99.07	99.13			

1. 77531.3 (Rhodes and others, 1974).
2. 77535.6 (Rhodes and others, 1976).
3. 77538.2, tan-gray breccia (Laul and Schmitt, 1975a)
4. 77539.8, tan-gray breccia (Laul and Schmitt, 1975a)
5. 77545.1, tan-gray breccia (Laul and Schmitt, 1975a)

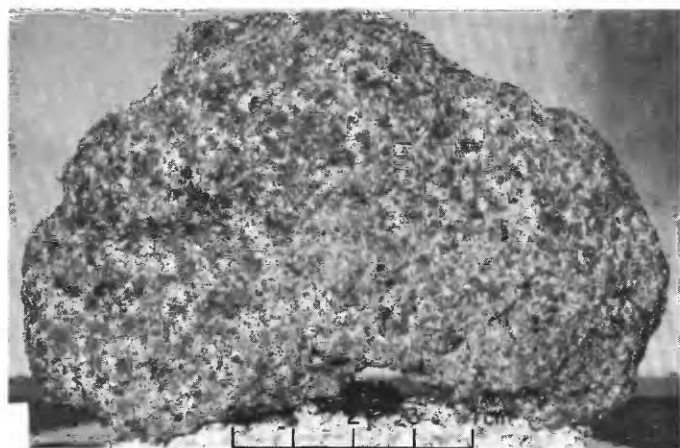


FIGURE 198.—Sample 77536. Medium-grained vesicular olivine basalt. (NASA photograph S-73-19154.)

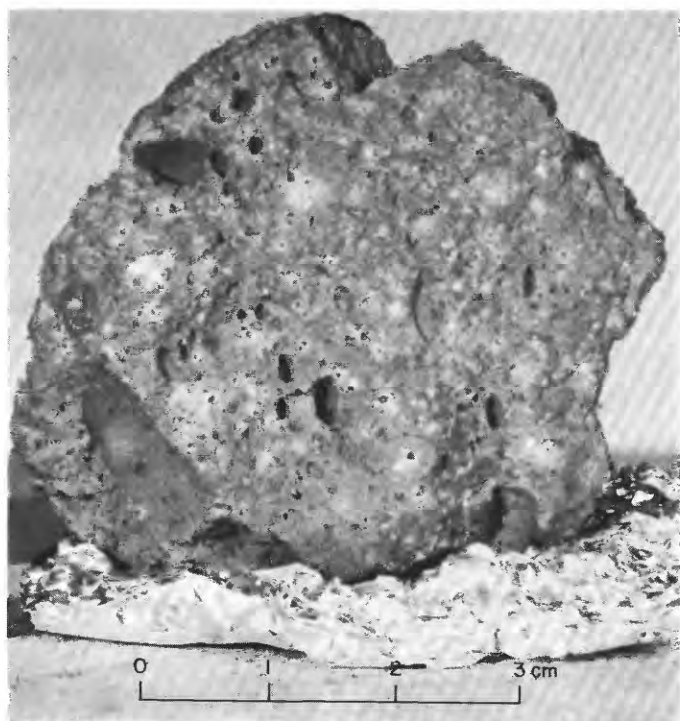


FIGURE 199.—Sample 77537. Polymict breccia with poikilitic(?) matrix. (NASA photograph S-73-19145.)

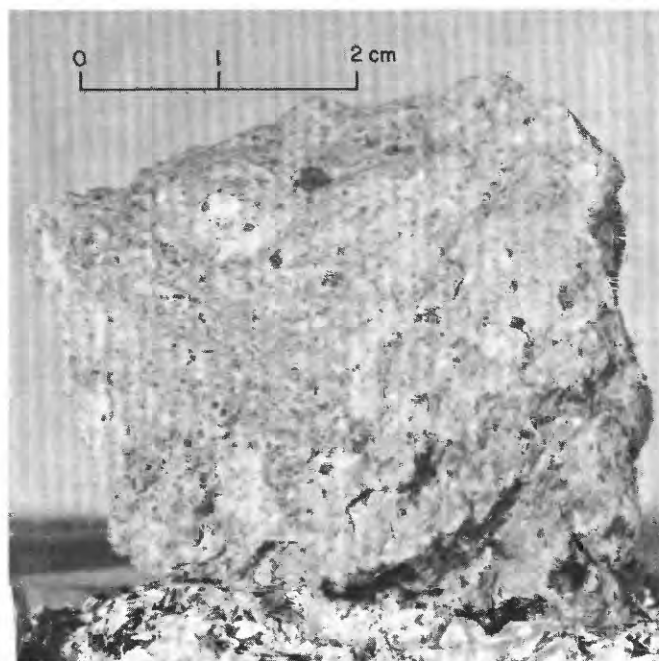


FIGURE 200.—Sample 77538. Polymict breccia with aphanitic matrix. (NASA photograph S-73-19064.)

## STATION LRV-11

## LOCATION

Station LRV-11 (fig. 7D) is located on the southeastern rim of SWP crater (now called "Bowen-Apollo" on NASA lunar photomap, edition 1, sheet 43D1S2(25)).

## OBJECTIVES

Station LRV-11 was an unplanned LRV stop to sample ejecta of a fresh small dark-rimmed crater on the rim of SWP crater.

## GENERAL OBSERVATIONS

The small dark-rimmed crater was estimated to be 30 or 40 m in diameter. It has a raised blocky rim and a

blocky ejecta blanket made up of angular clods (fig. 203) that disintegrated easily under the LRV wheels. The clods cover as much as 70 percent of the surface at the crater rim and up to 50 percent of the surface at the sampling site. They range in size from a few centimeters to about 30 centimeters. Many have rounded tops; some are partly buried.

The sediment between clods is the same color and probably has the same composition as the clods. The area surrounding the ejecta blanket of the small crater appears typical of other dark regolith surfaces on the valley floor, with fragment populations of less than one percent.

## SUMMARY OF SAMPLING

Sample 78120-24

*Type:* Sedimentary, unconsolidated.

*Weight:* 209.94 g.

*Depth:* From upper few centimeters.

*Location:* From ejecta blanket of small crater on the southeastern rim of SWP crater.

*Illustrations:* Pan 26; figure 203.

*Comments:* Sampled sediment was probably excavated from a depth of no more than a few meters in the regolith on the rim of SWP.

## STATION 8

## LOCATION

Station 8 is located near the base of the Sculptured Hills (figs. 7D and 204) and about 4 km northeast of the LM. It is within the zone shown as dark mantle in the premission geologic maps (Scott and others, 1972; Wolfe and Freeman, 1972).

## OBJECTIVES

The objectives at station 8 were to photograph and sample the Sculptured Hills and dark-mantle map units and to compare the materials from these units with massif and subfloor materials.

## GENERAL OBSERVATIONS

The terrain at station 8 is undulating and forms a gently inclined transition zone between the Sculptured Hills to the northeast and the valley floor to the southwest. The Sculptured Hills differ strikingly from the massifs because of the undulating, gentler slopes, greater abundance of dark streaks and patches, distinctive hummocky topographic form, absence of resistant ledges, and near-absence of boulders (fig. 204; pl. 2).

In the immediate station area, craters up to 10 m in diameter are common. They range from fresh to subdued. None have prominently raised or blocky rims, but many of the craters less than 1 m in size are lined

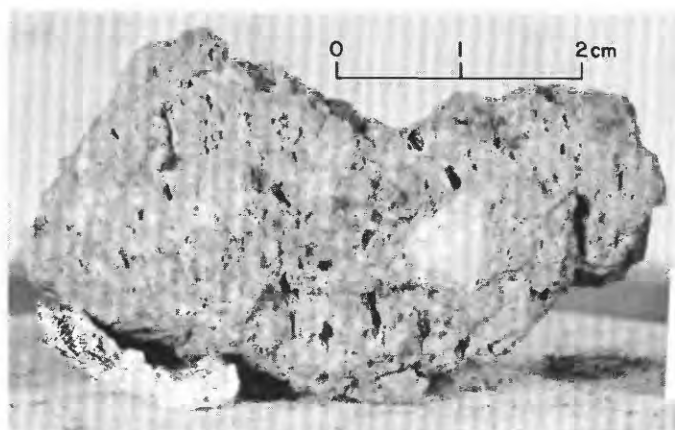


FIGURE 201.—Sample 77539. Polymict breccia with poikilitic(?) matrix. (NASA photograph S-73-19062.)

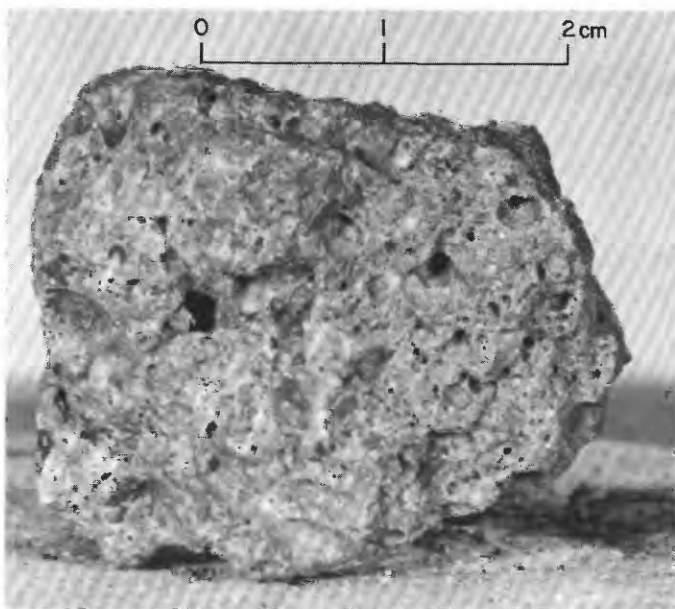


FIGURE 202.—Sample 77545. Polymict breccia with poikilitic(?) matrix. (NASA photograph S-73-19128.)

with small clods.

Pebble-size fragments are common; larger ones are sparse. The largest rock seen is less than 1 m in size. While approaching station 8, the crew noted that rocks larger than 20 cm are rare on the Sculptured Hills slopes compared with the foot of the North and South Massifs. The few visible rocks range from subangular to subrounded. Some are partly buried, but the sampled norite boulder is perched on the surface. The crew thought that except for the norite boulder all of the examined rocks larger than 20 cm were probably sub-floor basalt.

Surface sediment of the station 8 area is dark like the dark sediment of the valley floor; it is fine grained and cohesive on the surface and in the 25-cm-deep trench. Tracks made by the downhill movement of clods were noted by the crew.

Samples at station 8 (fig. 205) consisted of fragments from the norite boulder, sediment from beneath the boulder, four trench samples, a loose rock from the surface, rock fragments from a small crater, and sediment and a suite of small rocks collected by rake from the rim of a 15-m crater.

#### GEOLOGIC DISCUSSION

Sculptured Hills material surrounds the massifs and projects locally through the fill of the Taurus-Littrow valley (pl. 1). Interpreting these relations and drawing support from better preserved analogous features in

the Orientale Basin (Scott and others, 1977), we suggest that the Sculptured Hills material is ejecta emplaced during formation of the southern Serenitatis basin but after initiation of the faulting that formed the Taurus-Littrow graben and the massif blocks.

The morphologic difference between the Sculptured Hills and the massifs, the absence of resistant ledges and boulder clusters on the upper slopes, and the near absence of boulders on the Sculptured Hills slope near station 8 (fig. 204) imply a lithologic difference between the two units. A reasonable interpretation is that the coherent breccia with its clast-laden crystalline matrix is scarce or absent in the Sculptured Hills unit.

Rocks collected at station 8 are dominantly basalt, presumably deposited as ejecta from the valley floor, and fragments of weakly sintered polymict breccia, which are samples of regolith material compacted by impact. Only three highland rocks were sampled: metagabbro cataclasite (78155), the norite (78235, 36, 38, 78255), and a noritic rake fragment (78527) compositionally like the fused norite of 78235 (fig. 206). Any or all of the three could have been introduced to the station 8 area by impacts excavating material from outside of the Sculptured Hills. However, if they are fragments of the Sculptured Hills material and if the coherent breccia so common in the massifs is really absent from the Sculptured Hills, then perhaps the Sculptured Hills unit is dominantly cataclasite formed by crushing of plutonic anorthosite-norite-troctolite-suite rocks in a basin-forming impact.

Sediment compositions (fig. 207) show that the fine regolith material at station 8 is a mixture of highlands and valley-floor debris. Several of the plotted points are close to the join connecting ash 74220 and the alumina-rich sediment samples of the South Massif and light mantle. In agreement with the photogeologic observation that station 8 is in an area of dark surficial material, this suggests that ash may be the dominant valley-floor component represented at station 8. However, a component of relatively magnesian noritic debris similar in composition to rake fragment 78527 and the 78235 glasses would also place the sediment compositions near this join.

Compositions of five of the six analyzed weakly lithified polymict breccia samples plot in the same general region of figure 207 as the sediment samples. They presumably are samples of locally indurated regolith compositionally like the unconsolidated station 8 sediment.

#### SUMMARY OF SAMPLING

##### Sample 78135

Type: Olivine basalt.

Size: 5×4×3 cm.

Weight: 133.9 g.

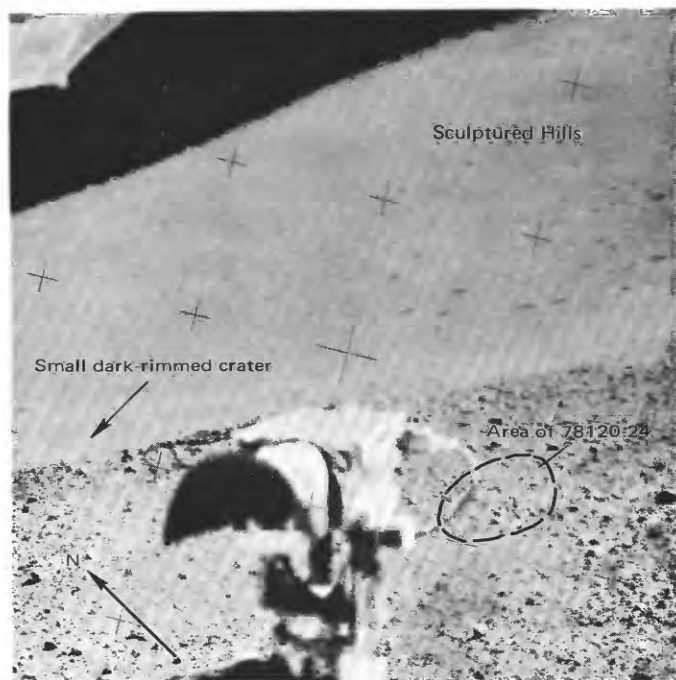


FIGURE 203.—Sampling area at station LRV-11 before sampling. (NASA photograph AS17-142-21693.)

*Location:* About 10 m north of LRV.

*Illustrations:* Pans 25, 26; figures 208, 209 (LRL), 210.

*Comments:* Sample 78135 is a regolith fragment of sub-

floor basalt.

*Petrographic description:* Fine- to medium-grained olivine basalt.

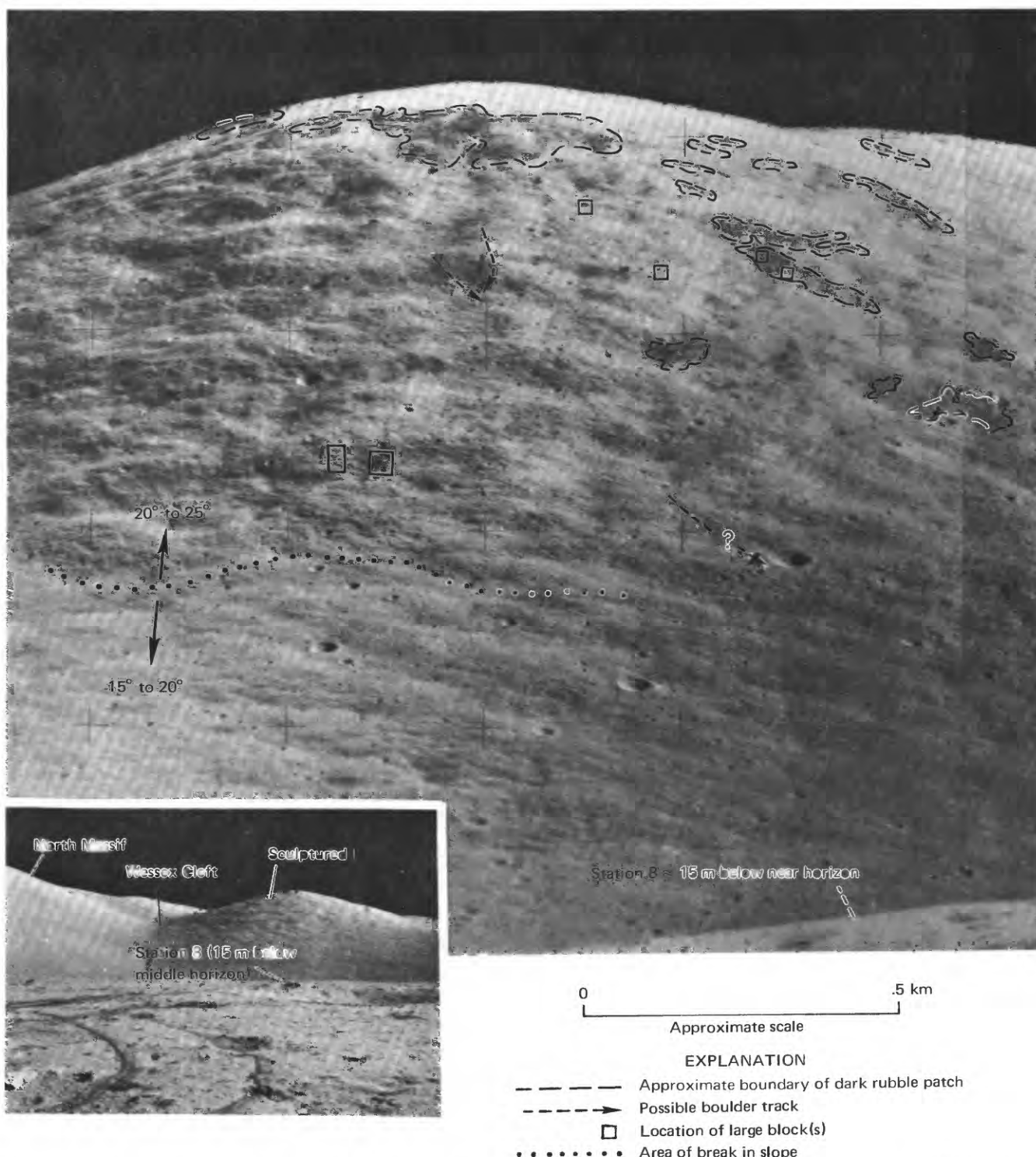


FIGURE 204.—Telephoto mosaic of Sculptured Hills slope above station 8 as viewed from station 2a. Sun elevation is 28°. (NASA photographs AS17-144-22034 and 22035.) (From Muehlberger and others, 1973.) Inset, Station 8 area at Sculptured Hills as viewed from the LM, 4 km away. (NASA photograph AS17-137-20876.)

*Major-element composition:**Chemical analysis of 78135*

SiO <sub>2</sub> .....	37.98
Al <sub>2</sub> O <sub>3</sub> .....	8.38
FeO .....	19.05
MgO .....	8.69
CaO .....	10.71
Na <sub>2</sub> O .....	.36
K <sub>2</sub> O .....	.05
TiO <sub>2</sub> .....	12.89
P <sub>2</sub> O <sub>5</sub> .....	.04
MnO .....	.27
Cr <sub>2</sub> O <sub>3</sub> .....	.45
Total .....	98.87

78135.5 (Rhodes and others, 1976).

*Sample 78155**Type:* Metagabbro cataclasite.*Size:* 52 pieces, largest is 6.5×4.5×3 cm.*Weight:* 401.1 g total.*Location:* From meter-size "pit crater" in southwest wall of a 15-m crater located about 20 m north of the LRV.*Illustrations:* Pans 25, 26; figures 210, 211 (photomicrograph), 217, 221.*Petrographic description:* Metagabbro cataclasite. Relict lithic fragments are dominantly metaclastic rocks with textures ranging from aphanitic to granoblastic-polygonal and, locally, melt texture with newly crystallized plagioclase laths.*Major-element composition:**Chemical analysis of 78155*

SiO <sub>2</sub> .....	45.57
Al <sub>2</sub> O <sub>3</sub> .....	25.94
FeO .....	5.82
MgO .....	6.33
CaO .....	15.18
Na <sub>2</sub> O .....	.33
K <sub>2</sub> O .....	.08
TiO <sub>2</sub> .....	.27
P <sub>2</sub> O <sub>5</sub> .....	.04
MnO .....	.10
Cr <sub>2</sub> O <sub>3</sub> .....	.14
Total .....	99.80

78155.2 (Apollo 17 PET, 1973).

*Age:*

U-Pb: 78155, complex history with three or more events in the U-Th-Pb evolution;  $3.81^{+0.25}_{-0.18}$  (2 $\sigma$ ) b.y. interpreted as age of last resetting (Nunes and Tatsumoto, 1975).

<sup>40</sup>-<sup>39</sup>Ar: 78155,29,  $4.22 \pm 0.04$  b.y.; extremely well defined plateau age, identical to its total argon age (Turner and Cadogan, 1975).

*Exposure age:* Ar: 78155,29, 30 m.y. (Turner and Cadogan, 1975).

*Sample 78220-24**Type:* Sedimentary, unconsolidated.*Weight:* 344.78 g.*Depth:* From upper few centimeters.*Location:* Beneath sampled norite boulder about 50 m northeast of the LRV.*Illustrations:* Pan 26; figure 212.*Comments:* Sample 78220-24, collected after the norite boulder was rolled, is a mixture of highlands and valley-floor debris.*Petrographic description:* 78220-24, dominantly fine-grained breccia and (or) metaclastic rock, some agglutinate.*Components of 90-150- $\mu$ m fraction of 78221,8 (Heiken and McKay, 1974)*

Components	Volume percent
Agglutinate .....	57.0
Basalt, equigranular .....	1.0
Basalt, variolitic .....	--
Breccia:	
Low grade <sup>1</sup> - brown .....	6.3
Low grade <sup>1</sup> - colorless .....	--
Medium to high grade <sup>2</sup> .....	7.0
Anorthosite .....	1.3
Cataclastic anorthosite <sup>1</sup> .....	--
Norite .....	--
Gabbro .....	.3
Plagioclase .....	5.0
Clinopyroxene .....	8.9
Orthopyroxene .....	3.6
Olivine .....	1.7
Ilmenite .....	1.0
Glass:	
Orange .....	.7
"Black" .....	3.0
Colorless .....	1.3
Brown .....	2.0
Gray, "ropy" .....	--
Other .....	--
Total number grains .....	302

<sup>1</sup>Metamorphic groups 1-3 of Warner (1972).<sup>2</sup>Metamorphic groups 4-8 of Warner (1972).

Includes crushed or shocked feldspar grains.

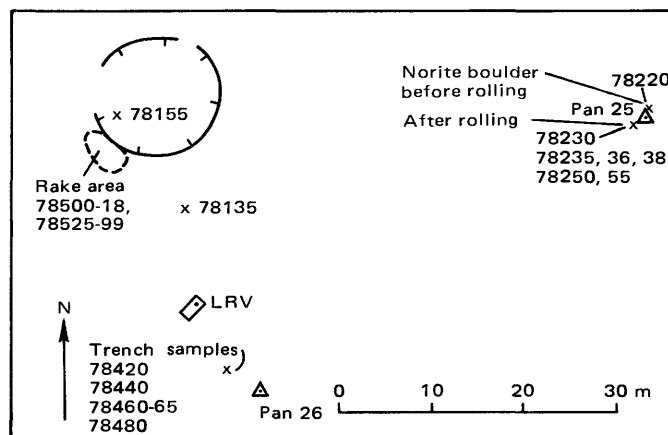


FIGURE 205.—Planimetric map of station 8.

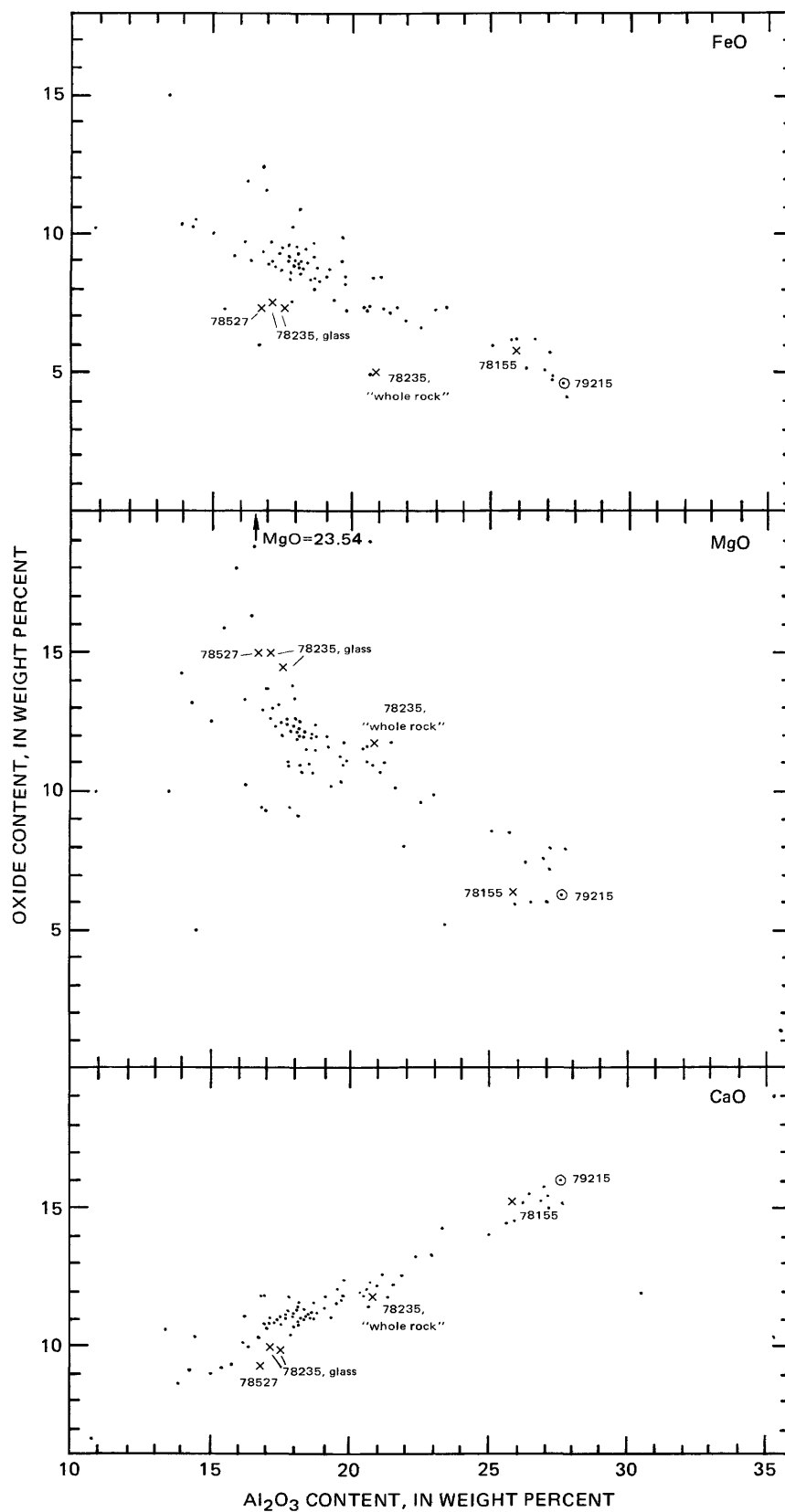


FIGURE 206.—Plots of FeO, MgO, and CaO contents in relation to  $\text{Al}_2\text{O}_3$  content for analyzed highlands rocks from stations 8 (x) and 9 (circled dot) in comparison with all analyzed Apollo 17 highlands rocks (dots).

*Major-element composition:**Chemical analysis of 78221*

SiO <sub>2</sub> .....	43.67
Al <sub>2</sub> O <sub>3</sub> .....	17.13
FeO .....	11.68
MgO .....	10.55
CaO .....	11.79
Na <sub>2</sub> O .....	.37
K <sub>2</sub> O .....	.092
TiO <sub>2</sub> .....	3.84
P <sub>2</sub> O <sub>5</sub> .....	.080
MnO .....	.157
Cr <sub>2</sub> O <sub>3</sub> .....	.321

Total ..... 99.680

78221.1 (Duncan and others, 1974).

Sample 78230-36, 38

Type: Sedimentary, unconsolidated (78230-34) and norite fragments (78235, 36, 38) from boulder.

Size: 78235, 2 pieces, 5×4×3.5 cm and 5.5×5×4 cm; 78236, 7.5×5.5×2 cm; 78238, 5×4.5×3.5 cm.

Weight: 78230-34, 210.5 g; 78235, 199.0 g; 78236, 93.06 g; 78238, 57.58 g.

Location: At half-meter norite boulder about 50 m northwest of the LRV.

Illustrations: Pans 25, 26; figures 213, 214 (LRL, 78236), 215.

Comments: Samples 78230-36, 38 were collected after the norite boulder was rolled downhill; samples came from what had been the boulder top. Sediment sample 78230-34 was scooped up from the surface with rock fragments 78235, 36, and 38. The boulder was perched on the surface; there was no visible boulder track. Presumably it arrived fairly recently in the station 8 area as ejecta from an unidentified crater. A highly detailed account of the field occurrence and

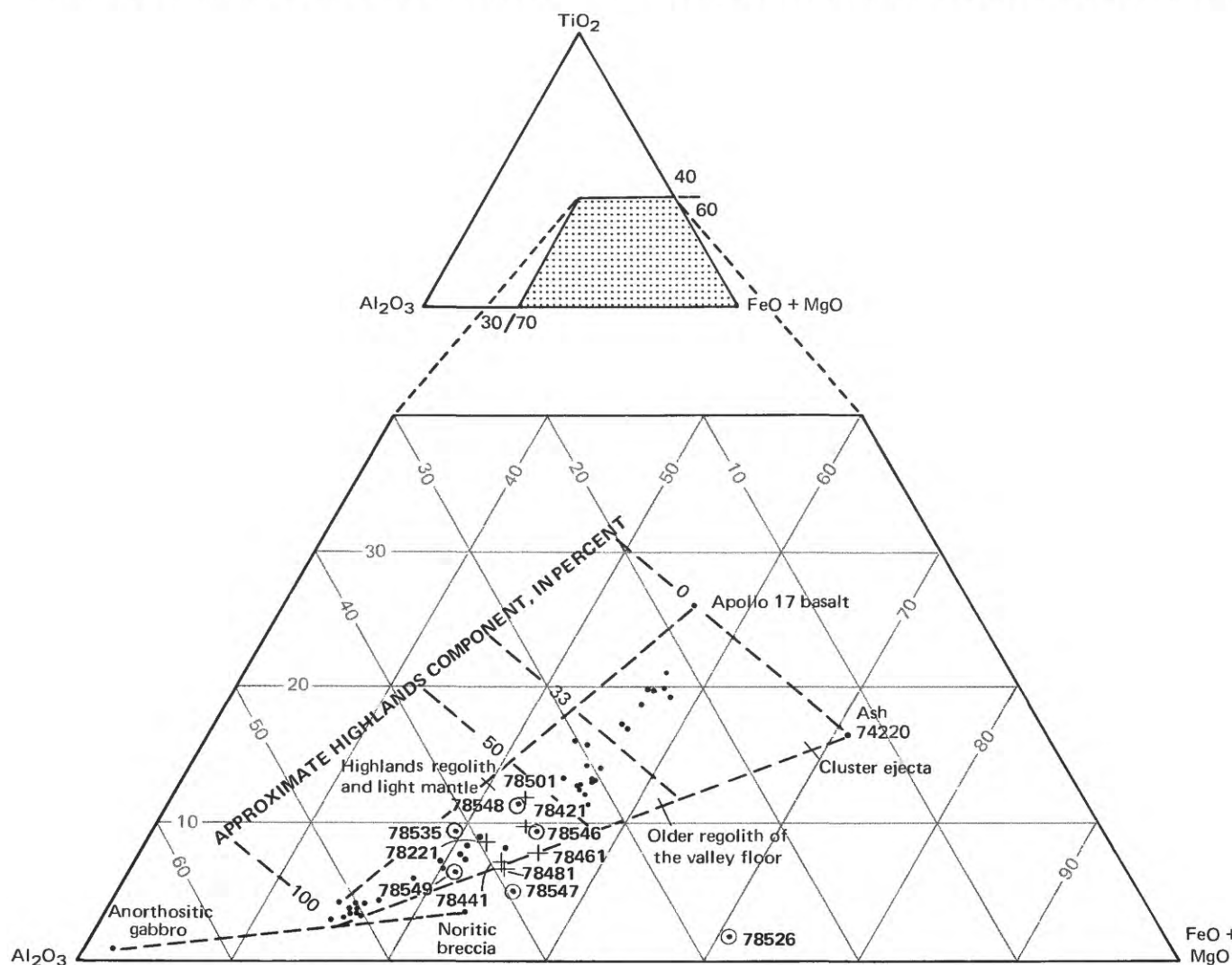


FIGURE 207.—Relative amounts of TiO<sub>2</sub>, Al<sub>2</sub>O<sub>3</sub>, and FeO+MgO in sediment samples (crosses) and weakly lithified polymict breccia (circled dots) from station 8 in comparison with sediment samples from elsewhere in traverse region (dots). Apollo 17 basalt, anorthositic gabbro, and noritic breccia values from Rhodes and others (1974).

sampling has been given by Jackson and others (1975).

**Petrographic description:** Plagioclase-orthopyroxene cumulate. Approximately equal proportions of cumulus plagioclase and orthopyroxene; dominantly plagioclase and orthopyroxene postcumulus material with minor clinopyroxene.

The norite is shocked, with plagioclase partly altered to maskelynite, and fractured. Vesicular black glass coats the samples and forms veins that intrude some of the fracture sets (Jackson and others, 1975).

Major-element data imply that the glass formed by fusion of the norite. As shown in figure 215, glass and "whole-rock" compositions (see table, columns 1-3) lie on or close to mixing lines joining low-calcium pyroxene and plagioclase (see table, columns 4 and 5). The chemical data imply ratios of plagioclase to plagioclase-plus-pyroxene of approximately 0.45 for the glasses and 0.57 for the "whole rock." Modal values for the same ratio are approximately 0.48 (McCallum and Mathez, 1975), 0.50 (Dymek and others, 1975), and 0.67-0.70 (Jackson and others, 1975).

Jackson and others (1975) concluded that the cumulate norite crystallized at a depth of 8 km or more. According to Dymek and others (1975), its mineral compositions are suitable for the station 8 norite to be related by crystal fractionation and liquid line of descent to the plutonic parents of

metatroctolite 76535 and metadunite 72415-18.

### Major-element composition:

#### Chemical analyses of 78235

	1	2	3	4	5
SiO <sub>2</sub> .....	49.7	49.8	49.5	53.9	46.3
Al <sub>2</sub> O <sub>3</sub> .....	17.58	17.15	20.87	3.44	33.85
FeO .....	7.39	7.52	5.05	11.16	.23
MgO .....	14.51	14.98	11.76	27.52	.45
CaO .....	9.86	9.92	11.71	3.26	17.93
Na <sub>2</sub> O .....	.34	.35	.35	.05	.58
K <sub>2</sub> O .....	.058	.060	.061	.015	.102
TiO <sub>2</sub> .....	.16	.19	.16	.32	.08
P <sub>2</sub> O <sub>5</sub> .....	.07	.08	.04	.04	.04
MnO .....	.11	.12	.08	.20	.003
Cr <sub>2</sub> O <sub>3</sub> .....	.33	.35	.23	.52	.01
Total .....	100.11	100.52	99.81	100.43	99.58

1. 78235.34, rind glass (Winzer and others, 1975b).
2. 78235.34, vein glass (Winzer and others, 1975b).
3. 78235.34, "whole rock"; analyzed sample too small with respect to grain size of rock to be necessarily representative (Winzer and others, 1975b).
4. 78235.34, pyroxene (Winzer and others, 1975b).
5. 78235.34, plagioclase (Winzer and others, 1975b).

### Sample 78250, 55

**Type:** Sedimentary, unconsolidated (78250) and two glass-coated norite fragments (78255).

**Size:** 78255, 4.5×4 cm × ?.

**Weight:** 78250, 50.57 g; 78255, 48.31 g.

**Location:** Norite boulder about 50 m northwest of the LRV.

**Illustrations:** Pans 25, 26.

**Comments:** Sample 78255 was collected from the

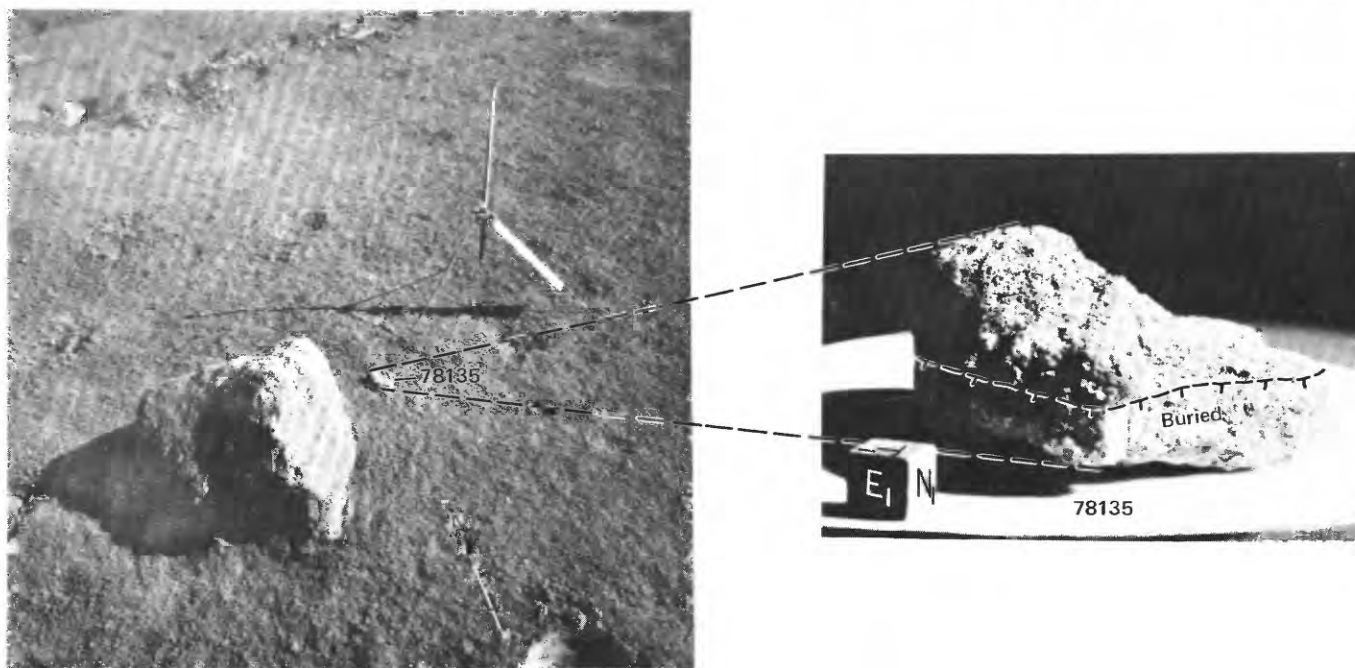


FIGURE 208.—Left, Sample 78135 before sampling. (NASA photograph AS17-146-22365.) Right, Sample 78135 with reconstructed lunar orientation and lighting. (NASA photograph S-73-21073.)

bottom of the one-half-meter norite boulder after it was rolled downhill. Sample 78250 was scooped from the surface with the rock fragments.

*Petrographic description:* 78255, similar to sample 78235 from the same boulder.

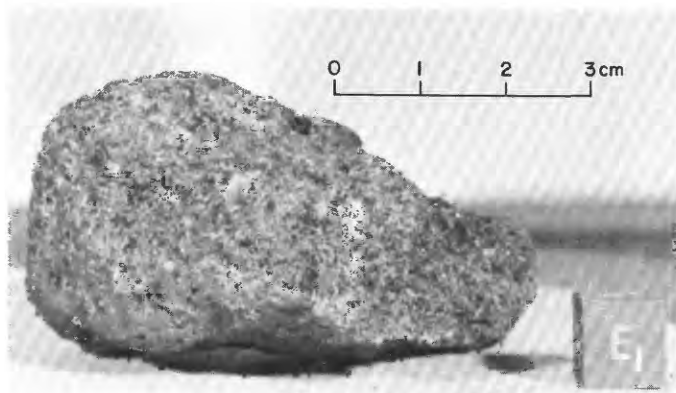


FIGURE 209.—Sample 78135. Fine-grained olivine basalt. (NASA photograph S-73-15006.)

Sample 78420-24

*Type:* Sedimentary, unconsolidated.

*Weight:* 292.62 g.

*Depth:* From lowest 10 cm of 25-cm-deep trench.

*Location:* 7 m southeast of LRV.

*Illustrations:* Pans 25, 26; figure 216.

*Comments:* The lowest 5 cm of the trench exposure was described as slightly coarser than the material from higher in the trench. Sample 78420-24 represents mixed highlands and valley-floor material.

*Petrographic description:* 78420-24, Dominantly fine-grained breccia and (or) metaclastic rock, some glass, minor agglutinate.

*Components of 90-150- $\mu$ m fraction of 78421,1 (Heiken and McKay, 1974)*

Components	Volume percent
Agglutinate	62.6
Basalt, equigranular	5.7
Basalt, variolitic	
Breccia:	
Low grade <sup>1</sup> -brown	7.0

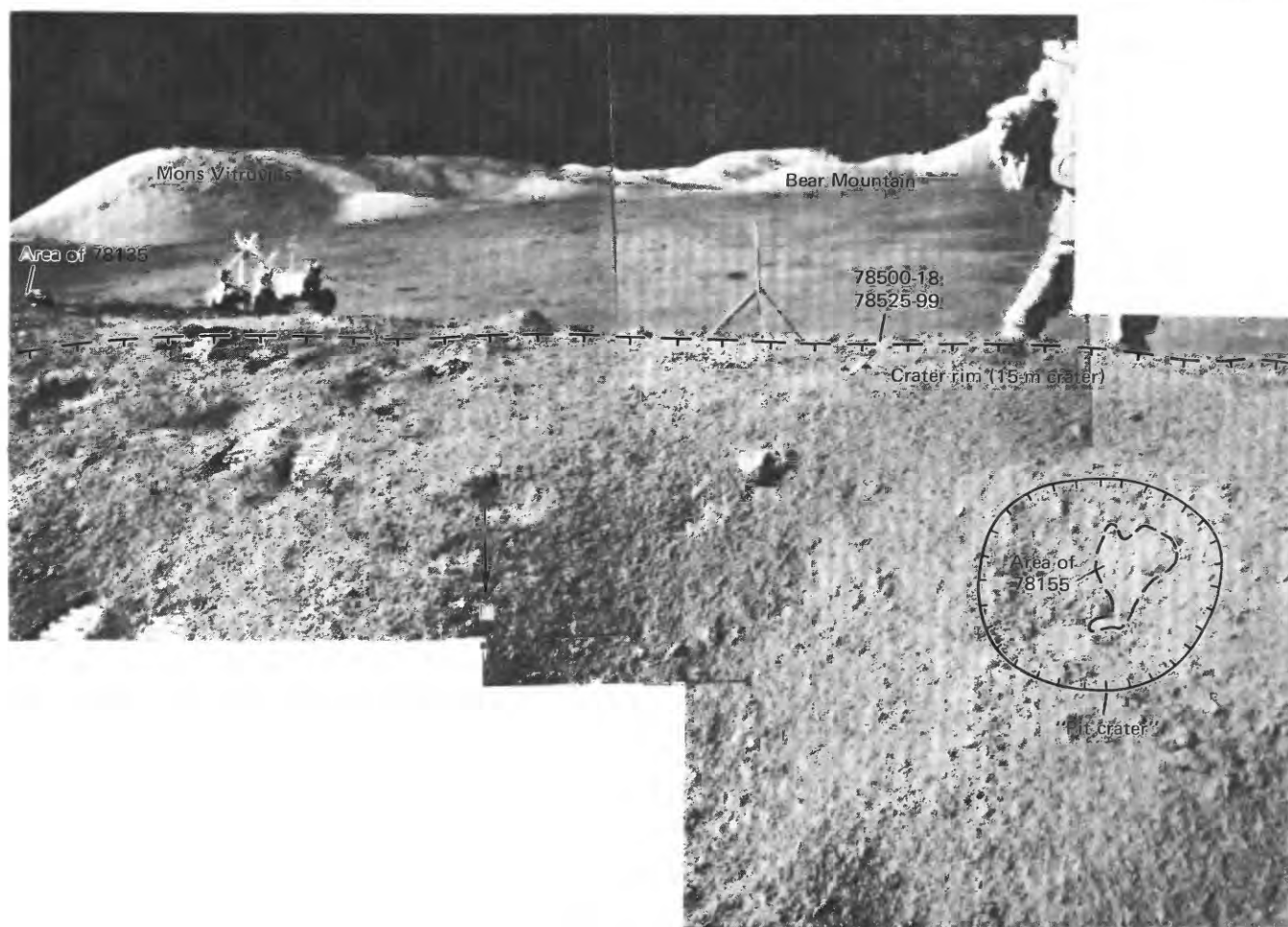


FIGURE 210.—Sample 78155, before collection, in meter-size "pit crater" in southwest wall of 15-m crater at station 8. Samples 78500-18 and 78525-99 were collected from rim of 15-m crater. (NASA photographs AS17-146-22400-22402.)

*Components of 90-150- $\mu$ m fraction of 78421.1 (Heiken and McKay, 1974)—Continued*

Components	Volume percent
Breccia—Continued	
Low grade <sup>1</sup> - colorless	1.3
Medium to high grade <sup>2</sup>	2.6
Anorthosite	.3
Cataclastic anorthosite <sup>3</sup>	.6
Norite	--
Gabbro	--
Plagioclase	7.3
Clinopyroxene	9.0
Orthopyroxene	--
Olivine	.6
Ilmenite	--
Glass:	
Orange	.6
"Black"	.3
Colorless	1.3
Brown	.6
Gray, "ropy"	--
Other	--
Total number grains	300

<sup>1</sup>Metamorphic groups 1-3 of Warner (1972).

<sup>2</sup>Metamorphic groups 4-8 of Warner (1972).

<sup>3</sup>Includes crushed or shocked feldspar grains.

*Major-element composition:*

*Chemical analysis of 78421*

SiO <sub>2</sub>	44.7
Al <sub>2</sub> O <sub>3</sub>	17.4
FeO	12.2
MgO	11.8
CaO	11.8
Na <sub>2</sub> O	.43
K <sub>2</sub> O	--
TiO <sub>2</sub>	3.8
P <sub>2</sub> O <sub>5</sub>	--
MnO	.164
Cr <sub>2</sub> O <sub>3</sub>	--
Total	102.294

78421.23 (Miller and others, 1974).

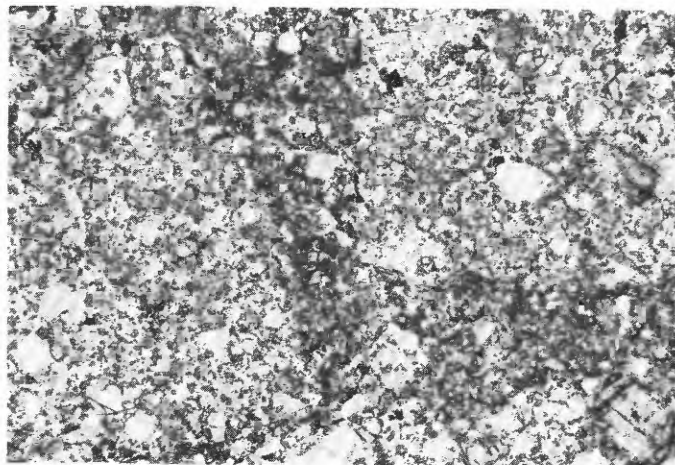


FIGURE 211.—Sample 78155. Photomicrograph showing relict lithic clasts in metagabbro cataclasite. Before crushing, rock was metaclastic with porphyroclasts of plagioclase in aphanitic to granoblastic-polygonal matrix.

Sample 78440-44

*Type:* Sedimentary, unconsolidated.

*Weight:* 251.59 g.

*Depth:* From 6 to 15 cm in 25-cm-deep trench.

*Location:* 7 m southeast of LRV.

*Illustrations:* Pans 25, 26; figure 216.

*Comments:* Sample 78440-44 represents mixed high-lands and valley floor material.

*Petrographic description:* 78440-44, dominantly fine-grained breccia and (or) metaclastic rock and agglutinate, some glass.

*Major-element composition:*

*Chemical analysis of 78441*

SiO <sub>2</sub>	44.1
Al <sub>2</sub> O <sub>3</sub>	17.2
FeO	12.4
MgO	10.9
CaO	11.1
Na <sub>2</sub> O	.49
K <sub>2</sub> O	--
TiO <sub>2</sub>	3.2
P <sub>2</sub> O <sub>5</sub>	--
MnO	.169
Cr <sub>2</sub> O <sub>3</sub>	--
Total	99.559

78441.9 (Miller and others, 1974).

Sample 78460-65

*Type:* Sedimentary, unconsolidated (78460-64) with small breccia fragment (78465).

*Size:* 78465, 1.5×1×1 cm.



FIGURE 212.—Site of sample 78220-24, removed from surface beneath rolled norite boulder. Dashed line outlines impression made by boulder during rolling. (NASA photograph AS17-142-21704.)

*Weight:* 78460-64, 412.02 g; 78465, 1.039 g.

*Depth:* From 1 to 6 cm in 25-cm-deep trench.

*Location:* 7 m southeast of LRV.

*Illustrations:* Pans 25, 26; figure 216.

*Comments:* Sample 78460-65 represents mixed high-lands and valley floor material.

*Petrographic description:* 78460-64, dominantly fine-grained breccia and (or) metaclastic rock and

agglutinate, some glass.

*Major-element composition:*

*Chemical analysis of 78461*

SiO <sub>2</sub> .....	42.6
Al <sub>2</sub> O <sub>3</sub> .....	16.1
FeO .....	12.9
MgO .....	11.1
CaO .....	11.1

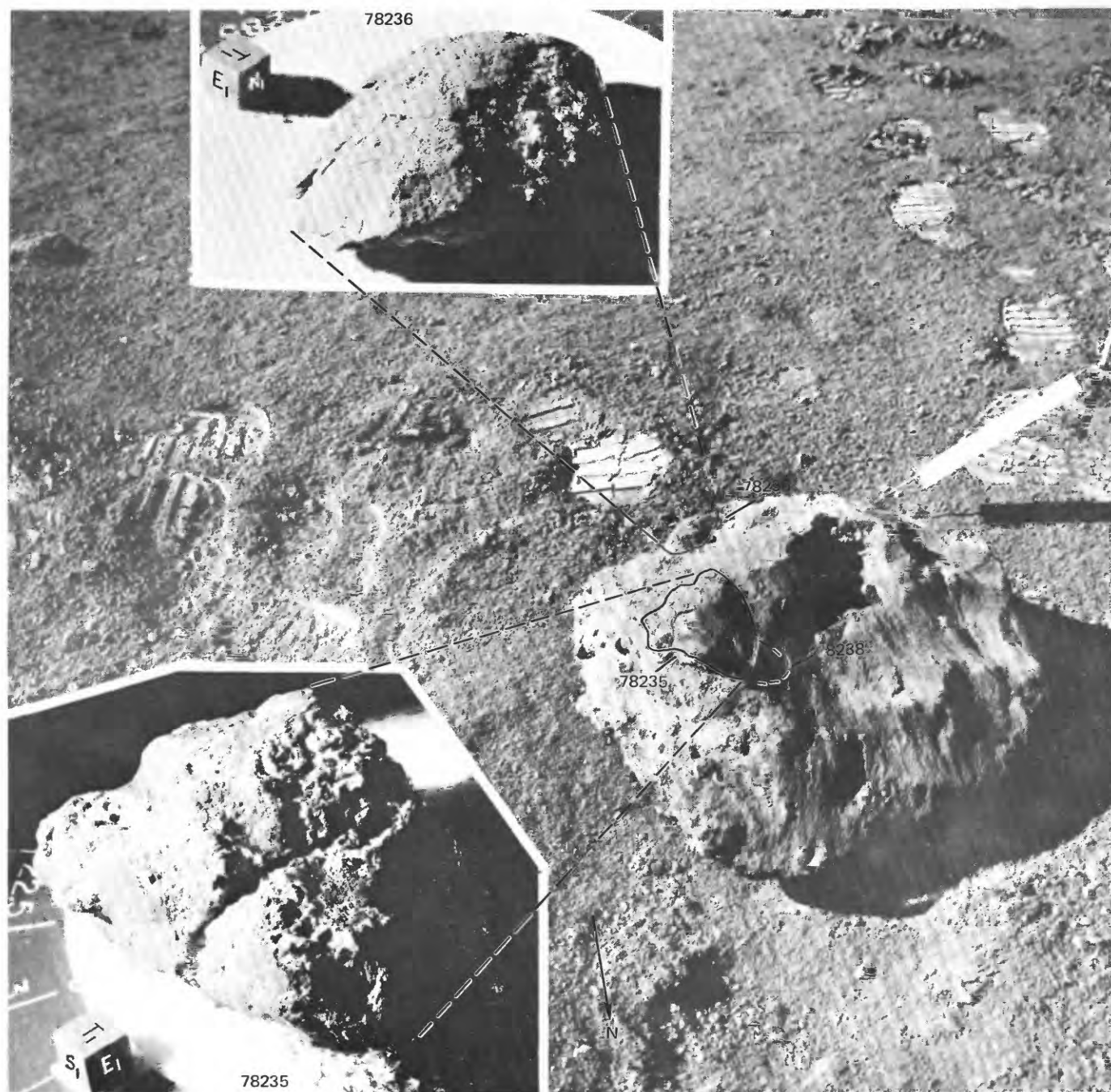


FIGURE 213.—Samples 78235, 78236, and 78238 before rolling of one-half-meter norite boulder at station 8. Insets show samples 78235 and 78236 with reconstructed lunar orientations and lighting. (NASA photographs AS17-146-22370; view similar to S-73-17962 (78235) and S-73-17817 (78236).)

*Chemical analysis of 78461—Continued*

Na <sub>2</sub> O .....	.40
K <sub>2</sub> O .....	--
TiO <sub>2</sub> .....	3.5
P <sub>2</sub> O <sub>5</sub> .....	--
MnO .....	.158
Cr <sub>2</sub> O <sub>3</sub> .....	--

Total .....	97.858
-------------	--------

78461.7 (Miller and others, 1974).

**Sample 78480-84***Type:* Sedimentary, unconsolidated.*Weight:* 267.45 g.*Depth:* Skim sample from top centimeter of 25-cm-deep trench.*Location:* 7 m southeast of LRV.*Illustrations:* Pans 25, 26; figure 216.*Comments:* Sample 78480-84 represents mixed high-lands and valley floor material.*Petrographic description:* 78480-84, dominantly agglutinate, fine-grained breccia and (or) metaclastic rock, glass, and feldspathic cataclasite.*Major-element composition:**Chemical analysis of 78481*

SiO <sub>2</sub> .....	43.2
Al <sub>2</sub> O <sub>3</sub> .....	17.0
FeO .....	12.0
MgO .....	11.3
CaO .....	10.6
Na <sub>2</sub> O .....	.39
K <sub>2</sub> O .....	--
TiO <sub>2</sub> .....	3.0
P <sub>2</sub> O <sub>5</sub> .....	--
MnO .....	.160
Cr <sub>2</sub> O <sub>3</sub> .....	--

Total .....	97.65
-------------	-------

78481.21 (Miller and others, 1974).



FIGURE 214.—Sample 78236. Norite composed of approximately equal proportions of cumulus orthopyroxene and plagioclase. Glass selvages at edges of sample. As seen in this view, sample is approximately 7.5×5.3 cm. (NASA photograph S-73-17813.)

Sample 78500-09, 15-18

Type: Sedimentary, unconsolidated (78500-04);

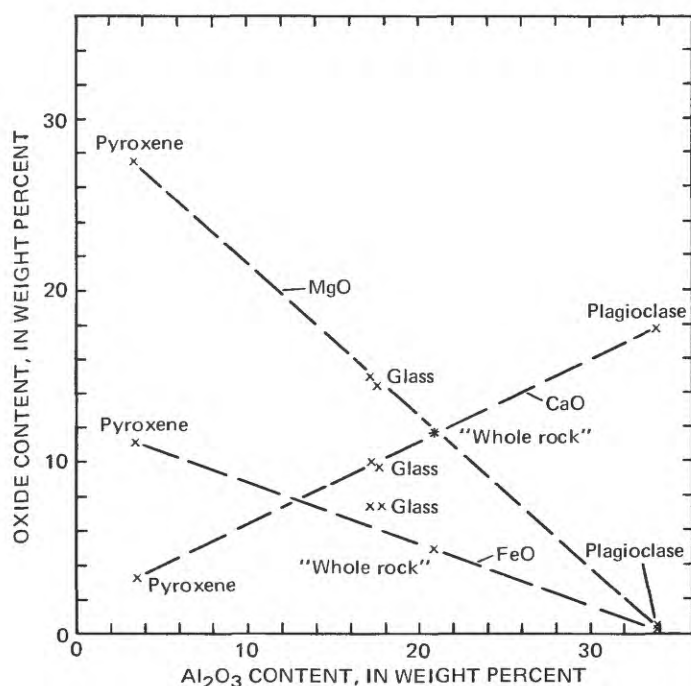


FIGURE 215.—Plot showing MgO, FeO, and CaO contents in relation to  $\text{Al}_2\text{O}_3$  content for analyzed glasses, "whole-rock," low-calcium pyroxene, and plagioclase in sample 78235,34. Dashed lines are plagioclase-pyroxene joins. Plagioclase: pyroxene for glass is  $\sim 45:55$ , for "whole rock" is  $\sim 57:43$ .

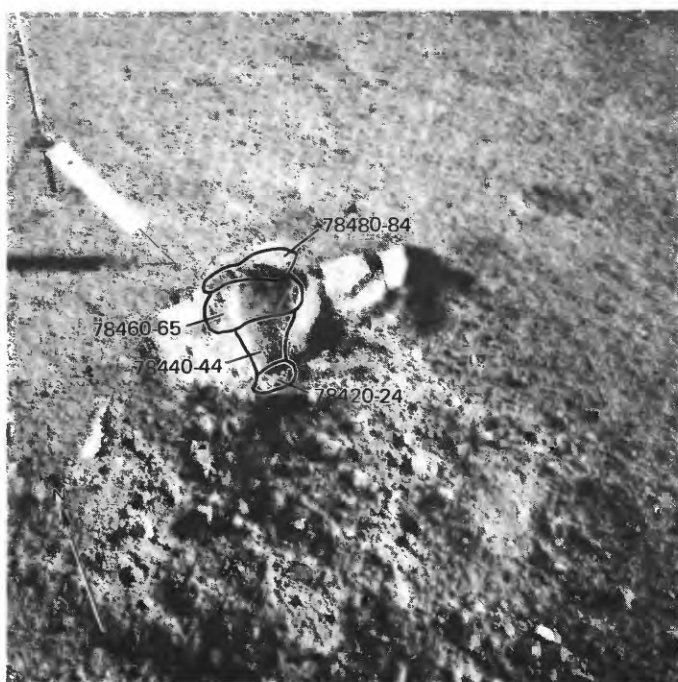


FIGURE 216.—Trench and locations of samples 78420-24, 78440-44, 78460-65, and 78480-84 at station 8. (NASA photograph AS17-142-21725.)

three fragments of olivine basalt (78505-07); sedimentary, weakly lithified polymict breccia (78508); basalt (78509); and four small breccia fragments (78515-18).

Size: 78505,  $8 \times 7.5 \times 6.5$  cm; 78506,  $4.5 \times 4 \times 3$  cm; 78507,  $3.8 \times 3.4 \times 1.5$  cm; 78508-09, 15-18, appreciably smaller.

Weight: 78500-04, 1,166.75 g; 78505, 506.3 g; 78506, 55.97 g; 78507, 23.35 g; 78508-09, 15-18, 29.99 g total.

Depth: From upper few centimeters.

Location: Rim of 15-m crater about 20 m northwest of the LRV.

Illustrations: Pans 25, 26; figures 210, 217, 218 (78505, photomicrograph), 219 (78506, LRL), 220 (78507, LRL).

Comments: Sediment sample, collected to complement rake sample 78525-99, is a mixture of highlands and valley-floor regolith material excavated from the 15-m crater.

#### Petrographic descriptions:

78500-04, dominantly agglutinate, fine-grained breccia and (or) metaclastic rock, glass, and feldspathic cataclasite.

#### Components of 90-150- $\mu\text{m}$ fraction of 78501,1 (Heiken and McKay, 1974)

Components	Volume percent
Agglutinate.....	35.3
Basalt, equigranular } .....	11.0
Basalt, variolitic } .....	
Breccia:	
Low grade <sup>1</sup> - brown.....	2.3
Low grade <sup>1</sup> - colorless.....	.3
Medium to high grade <sup>2</sup> .....	8.0
Anorthosite.....	Trace
Cataclastic anorthosite <sup>3</sup> .....	2.0
Norite.....	Trace
Gabbro.....	..
Plagioclase.....	13.3
Clinopyroxene.....	6.0
Orthopyroxene.....	7.3
Olivine.....	..
Ilmenite.....	3.7
Glass:	
Orange.....	2.0
"Black".....	3.6
Colorless.....	1.0
Brown.....	2.3
Gray, "ropy".....	.3
Other.....	2.0
Total number grains.....	300

<sup>1</sup>Metamorphic groups 1-3 of Warner (1972).

<sup>2</sup>Metamorphic groups 4-8 of Warner (1972).

<sup>3</sup>Includes crushed or shocked feldspar grains.

78505, coarse-grained vesicular porphyritic olivine basalt. Aggregates of clinopyroxene-ilmenite in a locally plumose groundmass of plagioclase, clinopyroxene, ilmenite, and accessory minerals.

78506, medium-grained vesicular porphyritic olivine basalt with aggregates of clinopyroxene-ilmenite in a subophitic(?) groundmass of plagioclase, clinopyroxene, ilmenite, ac-

cessory minerals.

78507, medium-grained vesicular olivine basalt with an intergranular(?) groundmass.

78508, polymict breccia with clasts of basalt, fine-grained feldspathic metaclastic rock, and glass in a moderately coherent fine-grained matrix.

78509, fine-grained vesicular basalt.

#### Major-element compositions:

Chemical analyses of 78501, 78505, and 78506

	1	2	3	4	5	6
SiO <sub>2</sub> .....	42.67	42.83	43.15	42.88	--	38.55
Al <sub>2</sub> O <sub>3</sub> .....	15.73	15.65	15.74	15.71	10.6	8.99
FeO .....	13.15	13.18	13.33	13.22	18.6	19.36
MgO .....	9.91	10.01	9.98	9.97	9.5	9.59
CaO .....	11.77	11.51	11.65	11.64	9.9	9.94
Na <sub>2</sub> O .....	.35	.38	.42	.38	.458	.39
K <sub>2</sub> O .....	.09	.090	.11	.10	.070	.05
TiO <sub>2</sub> .....	5.47	5.28	5.34	5.36	12.0	12.93
P <sub>2</sub> O <sub>5</sub> .....	.05	.082	.06	.06	--	.02
MnO .....	.18	.177	.18	.18	.227	.27
Cr <sub>2</sub> O <sub>3</sub> .....	.37	.355	.31	.34	.436	.51
Total .....	99.74	99.544	100.27	99.84		100.60

1. 78501.2 (Apollo 17 PET, 1973).
2. 78501.12 (Duncan and others, 1974).
3. 78501.37 (Scoon, 1974).
4. Average of 1-3.
5. 78505.32 (Warner and others, 1975a).
6. 78506.29 (Rhodes and others, 1976).

#### Age:

<sup>40</sup>-<sup>39</sup>Ar:

78503,7.1,  $4.13 \pm 0.03$  b.y.; 2-4-mm "gabbroic anorthosite" fragment interpreted by Bence and others (1974) as initially plutonic (Schaeffer and Husain, 1974).

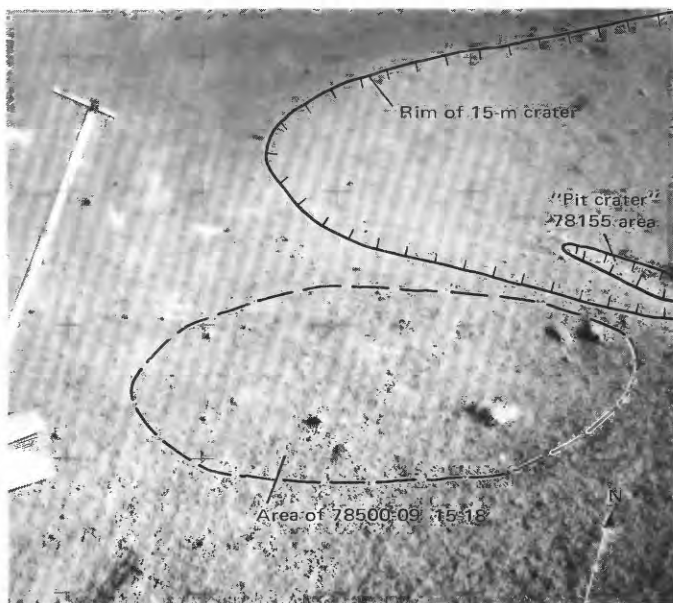


FIGURE 217.—Area of 78500-09, 15-18 before sampling. (NASA photograph AS17-142-21707.)

78500-18

78503,7.6,  $4.118 \pm 0.020$  b.y.; 2-4-mm "re-crystallized anorthositic" fragment (Schaeffer and others, 1976).

78503,13A,  $4.28 \pm 0.05$  b.y.; 2-4-mm "poikilitic gabbro" fragment (Kirsten and Horn, 1974).

78503,13B,  $3.83 \pm 0.05$  b.y.; 2-4-mm basalt fragment (Kirsten and Horn, 1974).

#### Pb-Pb:

78503,13A,  $3.96 \pm 0.03$  b.y.,  $3.98 \pm 0.02$  b.y.,  $3.91 \pm 0.05$  b.y. determined on three zirconolites; may represent an impact melt-

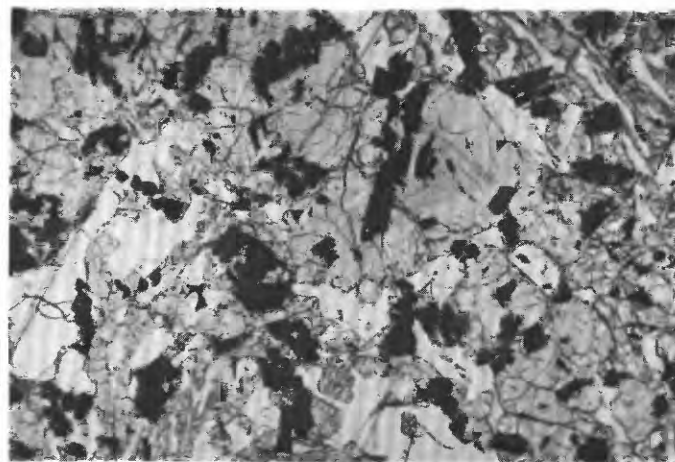


FIGURE 218.—Sample 78505. Photomicrograph showing aggregate of clinopyroxene-ilmenite (top center) in locally plumose groundmass of clinopyroxene, plagioclase, and ilmenite.

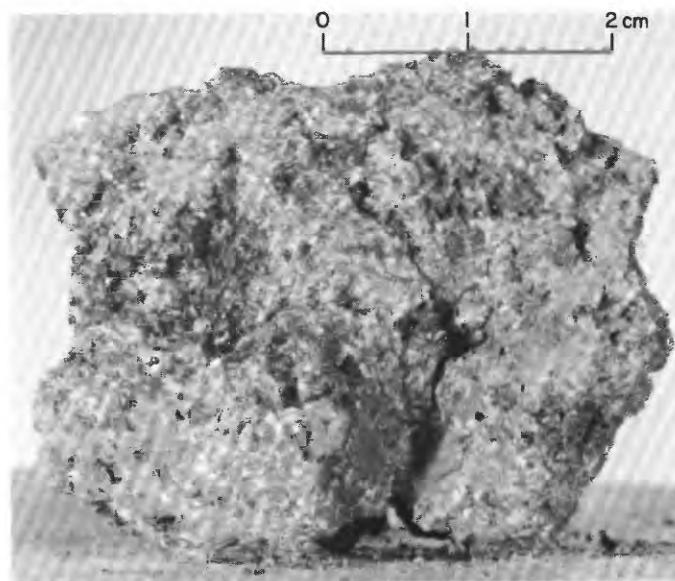


FIGURE 219.—Sample 78506. Medium-grained olivine basalt. (NASA photograph S-73-15467.)

78500-18

ing event at ~3.95 b.y. through which some radiogenic Ar survived (Hinthorne and Conrad, 1976).

*Exposure age:* Ar: 78503,6,7,  $332 \pm 22$  m.y.; 2-4-mm "recrystallized anorthosite" fragment (Schaeffer and others, 1976).

*Sample* 78525-28, 30, 35-39, 45-49, 55-59, 65-69, 75-79, 85-89, 95-99

*Type:* 39 rock fragments, with some associated sediment (78530) from rake sample; 78525,26, sedimentary, weakly lithified polymict breccia; 78527, norite(?); 78528, basalt; 78530, sedimentary, unconsolidated; 78535-39, 45-49, 55-59, 65-68, sedimentary, weakly lithified polymict breccia; 78569, 75-79, 85-89, 95-99, basalt.

*Size:* Rock fragments, largest is less than 6 cm long.

*Weight:* 78530, 88.92 g; 78525-28, 35-39, 45-49, 55-59, 65-69, 75-79, 85-89, 95-99, 1,355.94 g total.

*Depth:* Raked from upper few centimeters.

*Location:* Near rim of 15-m crater about 20 m northwest of the LRV.

*Illustrations:* Pans 25, 26; figure 221.

*Comments:* Except for norite(?) fragment 78527, which is similar in chemical composition to the fused part of norite 78235, all rake fragments are basalt or weakly lithified polymict breccia derived from regolith material.

#### *Petrographic descriptions:*

78527, norite(?) partly glass coated, fractured; 75 percent plagioclase (maskelynite?), 25 per-

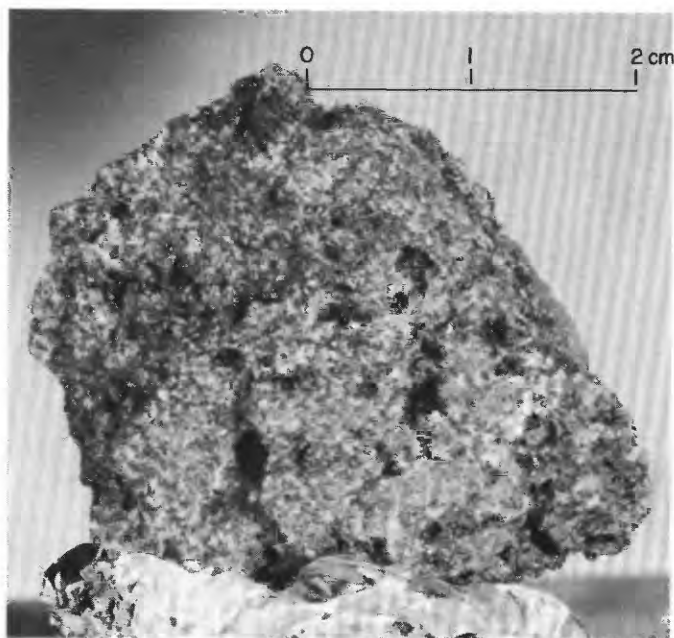


FIGURE 220.—Sample 78507. Medium-grained olivine basalt. (NASA photograph S-73-16144.)

cent orthopyroxene(?).

78528, fine-grained basalt.

78525, 26; 78535-38; 78545, 46, polymict breccia.

Matrix coherent, vitreous.

78547-49; 78555-57; 78567, polymict breccia with fine-grained friable matrix.

78569, fine-grained basalt with an intersertal(?) groundmass.

78575, fine-grained olivine basalt.

78576, medium-grained vesicular basalt.

78577, medium-grained vesicular basalt.

78578, medium-grained vesicular basalt.

78579, medium-grained vesicular olivine basalt.

78585, no description.

78586, aphanitic basalt.

78587, aphanitic basalt.

78596, fine-grained basalt.

78597, fine-grained vesicular olivine basalt.

78598, fine-grained basalt.

78599, fine-grained basalt.

#### *Major-element compositions:*

*Chemical analyses of station 8 rake fragments 78526, 78527, 78535, 78546, 78547, 78548, 78549, 78595, 78597, 78599*

	1	2	3	4	5	6	7	8	9	10
SiO <sub>2</sub> .....	..	..	..	..	..	..	..	..	38.54	38.44
Al <sub>2</sub> O <sub>3</sub> .....	11.1	16.8	17.2	15.3	16.3	16.0	18.0	9.0	8.85	8.67
FeO .....	17.4	7.4	11.3	13.2	11.8	13.2	11.4	19.9	19.67	19.14
MgO .....	11	15	9.7	10	11	10	10	9.1	7.83	8.47
CaO .....	10.0	9.2	11.6	11.0	11.1	11.3	11.9	11.0	10.94	10.48
Na <sub>2</sub> O .....	.15	.42	.38	.45	.36	.41	.39	.387	.39	.38
K <sub>2</sub> O .....	.020	.065	.090	.10	.085	.090	.10	.063	.04	.06
TiO <sub>2</sub> .....	.8	.6	3.9	4.2	2.2	5.2	2.6	12.8	12.39	12.52
P <sub>2</sub> O <sub>5</sub> .....	..	..	..	..	..	..	..	..	.11	.04
MnO .....	.261	.090	.140	.160	.160	.167	.042	.253	.29	.28
Cr <sub>2</sub> O <sub>3</sub> .....	.740	.210	.300	.330	.360	.340	.294	.443	.32	.43
Total .....									99.37	98.91

1. 78526.1, weakly lithified polymict breccia (Laul and Schmitt, 1975a).
2. 78527.2, norite(?) (Laul and Schmitt, 1975a).
3. 78535.3, weakly lithified polymict breccia (Laul and Schmitt, 1975a).
4. 78546.3, weakly lithified polymict breccia (Laul and Schmitt, 1975a).
5. 78547.3, weakly lithified polymict breccia (Laul and Schmitt, 1975a).
6. 78548.3, weakly lithified polymict breccia (Laul and Schmitt, 1975a).
7. 78549.1, weakly lithified polymict breccia (Laul and Schmitt, 1975a).
8. 78595.3, basalt (Warner and others, 1975a).
9. 78597.4, basalt (Rhodes and others, 1976).
10. 78599.3-2, basalt (Rhodes and others, 1976).

#### STATION 9

#### LOCATION

Station 9 is located on the southeast rim and on the ejecta blanket of Van Serg crater (fig. 7D).

#### OBJECTIVES

The objectives at station 9 were to determine the origin of Van Serg crater, to sample the dark mantle and subfloor materials, and to characterize the lithology and stratigraphy of the dark mantle.

## GENERAL OBSERVATIONS

Van Serg crater is 90 m in diameter and has a blocky central mound about 30 m across, discontinuous benches on the inner walls, a raised blocky rim, and a blocky ejecta blanket. The older, subdued crater to the southeast is also about 90 m in diameter, has a much lower and smoother rim, and is covered with blocky ejecta from Van Serg. Craters younger than Van Serg are extremely rare in the station 9 area. A few small (<5 m) craters are present.

Exploration and sampling at station 9 was concentrated in two areas: (1) the southeast rim of Van Serg and (2) an area about 65 m to the southeast near the northeast rim of the subdued crater (fig. 222).

In both sample areas fragment sizes are up to about 30 cm, with a few larger boulders up to approximately 2 m in size. Fragments larger than 2 cm cover about 10 percent of the Van Serg rim crest but no more than 3 percent in the southeastern area. Blocks and fragments in both sampling areas are typically angular. Many are partially buried, but there is little or no development of fillets even on the steep inner walls of Van Serg crater.

Surface sediment is gray, uniformly fine, and has no visible linear patterns. The upper few centimeters is soft and compacts easily to preserve bootprints. A trench in the southeastern sample area exposed a 7-cm upper dark unit underlain by about 10 cm of light-gray sediment.

Samples from the southeast rim of Van Serg crater

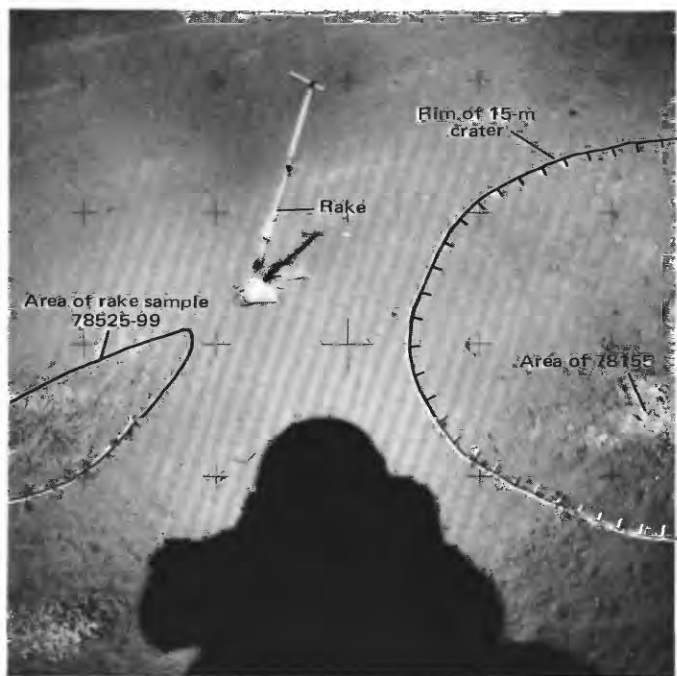


FIGURE 221.—Area of rake sample 78525-99. (NASA photograph AS17-142-21709.)

consisted of three rocks picked up from the surface, two rocks chipped from a boulder, and two sediment samples with associated small rock fragments. Samples from the southeastern site consisted of a double drive tube, two rocks collected from the surface, and three samples from a trench.

## GEOLOGIC DISCUSSION

Because the station 9 area is distinctly more blocky than the surrounding plains, we interpret it as lying entirely within the ejecta of Van Serg crater. The dominant rock type, as seen by the crew at station 9, as interpreted from lunar surface photographs, and as recorded in the sample collection, is dark friable polymict breccia that represents regolith material indurated and excavated by the Van Serg impact. The overwhelming abundance of such regolith breccia and the paucity of basalt blocks imply that subfloor basalt bedrock was not excavated in the formation of Van Serg.

Multiple topographic profiles, made by analytical stereoplotter on orbital Apollo 17 panoramic camera photographs, suggest that the floor of Van Serg is approximately 11 m below the precrater surface. Hence, we suggest that at least 11 m of unconsolidated material overlies the subfloor basalt in the station 9 area.

The regolith material excavated from Van Serg is

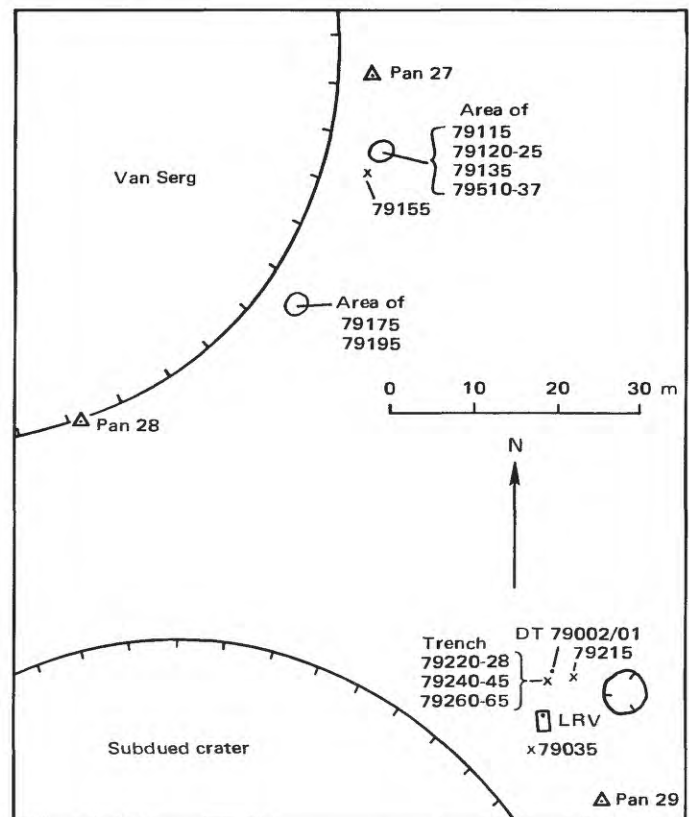


FIGURE 222.—Planimetric map of station 9.

similar in composition to the lower two-thirds of the deep core (LM/ALSEP/SEP area) and to the gray sediment from the Shorty crater (station 4) trench (fig. 223). We interpret these samples as representative of the older regolith of the valley floor, a unit formed by long-term mixing of impact-generated debris from the local highlands, from the subfloor basalt, and from the ash unit. It is likely that the slightly more basaltic character of regolith breccia sample 79035 (fig. 223) reflects local inhomogeneity in the Van Serg target.

Several lines of field evidence suggest that Van Serg crater is very young. These include (1) the abundance and angularity of the relatively friable blocks of regolith breccia, (2) the scarcity of younger craters, (3) the general absence of fillets even on the steep inner crater walls, and (4) the uneroded nature of the crater rim and central mound. Shorty crater, apparently

formed sometime between 10 and 30 m.y. ago, is probably older than Van Serg. Shorty lacks the abundant blocks of regolith breccia; its rim as seen in orbital photographs seems somewhat less sharp, and small craters may be slightly more abundant on the rim of Shorty.

Exposure age measurements for station 9 samples include an estimate of 24 m.y. determined from minimum track densities in mineral grains in the trench samples (Fleischer and Hart, 1974), 3.7 m.y. determined from tracks in rock 79215 from the southeastern sample area (Bhandari and others, 1976), and approximately 1.5 m.y. determined from  $^{22}\text{Na}$ - $^{26}\text{Al}$  measurements in the trench samples (Yokoyama and others, 1976). By comparison with 10-30-m.y.-old Shorty crater, Van Serg's distinctly more youthful appearance suggests that the younger exposure ages (1.5 and 3.7

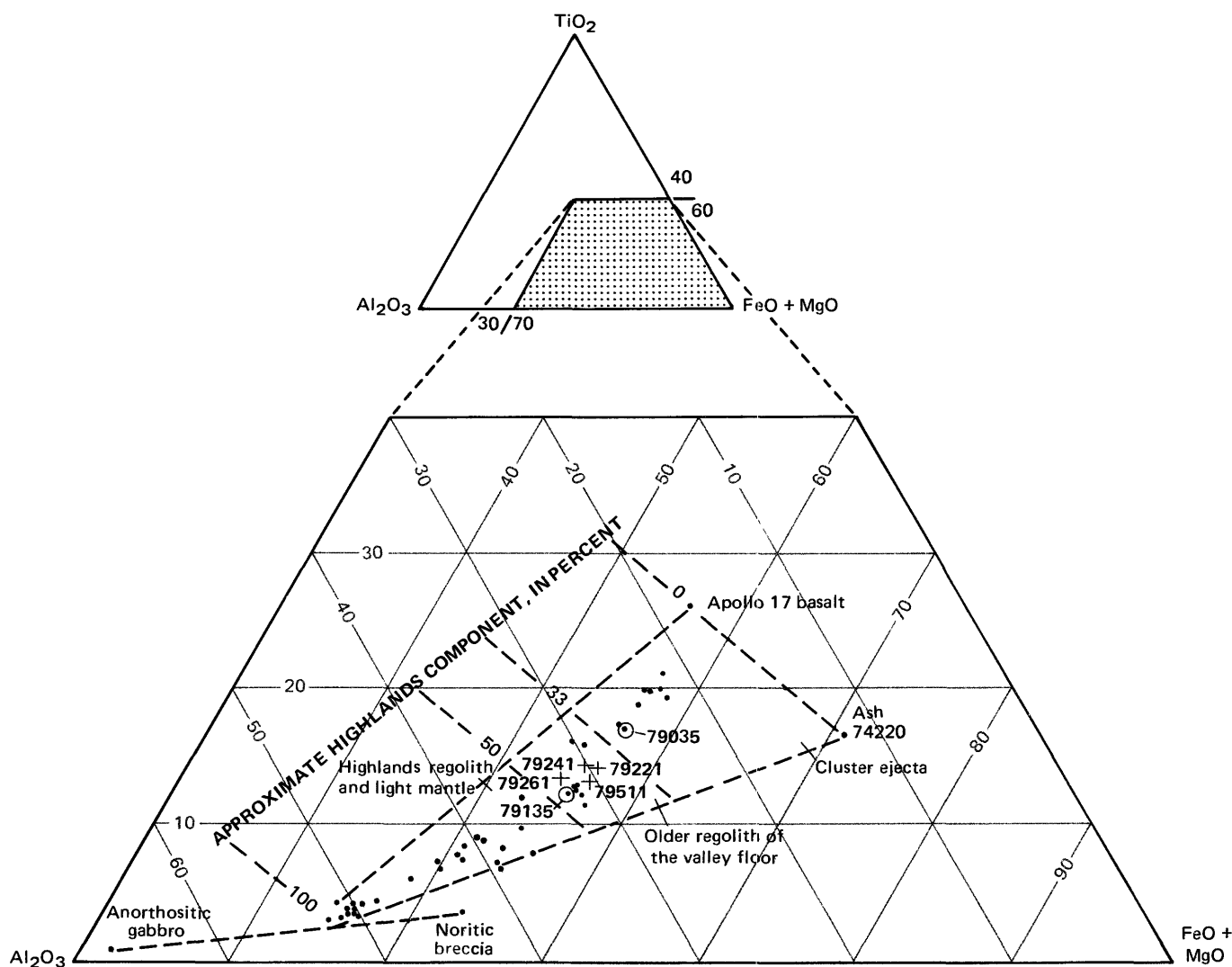


FIGURE 223.—Relative amounts of  $\text{TiO}_2$ ,  $\text{Al}_2\text{O}_3$ , and  $\text{FeO} + \text{MgO}$  in sediment samples (crosses) and in regolith breccia (circled dots) from station 9 in comparison with sediment samples from elsewhere in traverse region (dots). Apollo 17 basalt, anorthositic gabbro, and noritic breccia values from Rhodes and others (1974).

m.y.) may more nearly approximate the age of Van Serg crater.

#### SUMMARY OF SAMPLING

##### Sample 79002/79001 (upper/lower)

*Type:* Double drive tube.

*Length:* 51.7 cm (79001, 32.0 cm; 79002, 19.7 cm).

*Depth:* Approximately 71 cm.

*Net weight:* 1,152.8 g.

*Location:* About 5 m north of the LRV.

*Illustrations:* Pans 28, 29; figure 224.

*Comments:* Drive tube 79001-02 is probably in ejecta from Van Serg crater.

##### Sample 79035

*Type:* Sedimentary, weakly lithified polymict breccia.

*Size:* Three large fragments: 19×14×10 cm, 15×10×6 cm, 15×6×4.5 cm, and three smaller fragments.

*Weight:* 2,806 g total.

*Location:* A few meters from the LRV; precise location unknown.

*Illustrations:* Pans 28, 29; figure 225 (LRL).

*Comments:* Sample 79035 is a sample of indurated regolith material that may have been excavated by the Van Serg impact. Its composition (table; fig. 223) shows it to have more basalt than other analyzed sediment samples from station 9. However, the difference may reflect no more than local inhomogeneity of the regolith.

*Petrographic description:* Polymict breccia with small clasts of metaclastic rock, basalt, glass, maskelynite, and mineral debris in a fine-grained friable matrix.

#### Major-element composition:

##### Chemical analysis of 79035

SiO <sub>2</sub> .....	41.7
Al <sub>2</sub> O <sub>3</sub> .....	12.26
FeO .....	16.51
MgO .....	9.91
CaO .....	11.2
Na <sub>2</sub> O .....	.409
K <sub>2</sub> O .....	.082
TiO <sub>2</sub> .....	7.99
P <sub>2</sub> O <sub>5</sub> .....	.055
MnO .....	.217
Cr <sub>2</sub> O <sub>3</sub> .....	.402
Total .....	100.735

79035.27 (Wänke and others, 1974).

##### Sample 79115

*Type:* Sedimentary, impact-consolidated polymict breccia.

*Size:* 9.5×7.5×5 cm.

*Weight:* 346.3 g.

*Location:* Broken from boulder on southeast rim of Van Serg crater.

*Illustrations:* Pan 28; figures 226, 227 (LRL), 228 (photomicrograph).

*Comments:* Sample 79115 is impact-consolidated regolith material ejected from Van Serg crater.

*Petrographic description:* Polymict breccia with small clasts of metaclastic rock, basalt, glass (including orange glass spheres), maskelynite, and mineral debris in a fine-grained friable matrix.

##### Sample 79120-25

*Type:* Sedimentary, unconsolidated (79120-24) and small breccia fragment (79125).

*Size:* 79125, 2×1.2×1 cm.

*Weight:* 79120-24, 372.39 g; 79125, 1.91 g.

*Depth:* From 0-3 cm.

*Location:* Southeast rim of Van Serg crater.

*Illustrations:* Pan 28; figure 226.

*Comments:* Van Serg ejecta.

*Petrographic description:* 79120-24, dominantly fine-grained breccia and (or) metaclastic rock, some glass.

##### Sample 79135

*Type:* Sedimentary, impact-consolidated polymict breccia.

*Size:* 20×12×10 cm.

*Weight:* 2,283 g.

*Location:* From a breccia boulder on the southeast rim of Van Serg.

*Illustrations:* Pan 28, figures 226, 229 (LRL).

*Comments:* Sample 79135 is impact-consolidated regolith material ejected from Van Serg crater.

*Petrographic description:* Polymict breccia with clasts of basalt, feldspathic metaclastic rock, glass (including orange glass spheres), and mineral debris in a fine-grained moderately coherent matrix.

#### Major-element composition:

##### Chemical analyses of 79135

	1	2	3	4
SiO <sub>2</sub> .....	42.49	42.57	42.6	42.5
Al <sub>2</sub> O <sub>3</sub> .....	15.08	14.74	13.83	14.55
FeO .....	14.01	15.19	14.97	14.72
MgO .....	10.42	9.10	10.81	10.11
CaO .....	11.44	10.91	11.1	11.2
Na <sub>2</sub> O .....	.40	.40	.469	.42
K <sub>2</sub> O .....	.10	.11	.098	.10
TiO <sub>2</sub> .....	5.15	6.33	5.42	5.63
P <sub>2</sub> O <sub>5</sub> .....	.07	.09	.076	.08
MnO .....	.19	.19	.195	.19
Cr <sub>2</sub> O <sub>3</sub> .....	.39	.45	.373	.40
Total .....	99.54	100.08	99.941	99.90

1. 79135.1 (Apollo 17 PET, 1973).

2. 79135.35 (Rose and others, 1974).

3. 79135.38 (Wänke and others, 1974).

4. Average of 1-3.

## Sample 79155

Type: Olivine basalt breccia with a glassy matrix.

Size: 8×6×5 cm.

Weight: 318.8 g.

Location: Southeast rim of Van Serg crater.

Illustrations: Pan 28; figure 230 (LRL).

Comments: Sample 79155 is a piece of impact-brecciated and impact-fused subfloor basalt. Its exposure age implies a long history as a regolith frag-

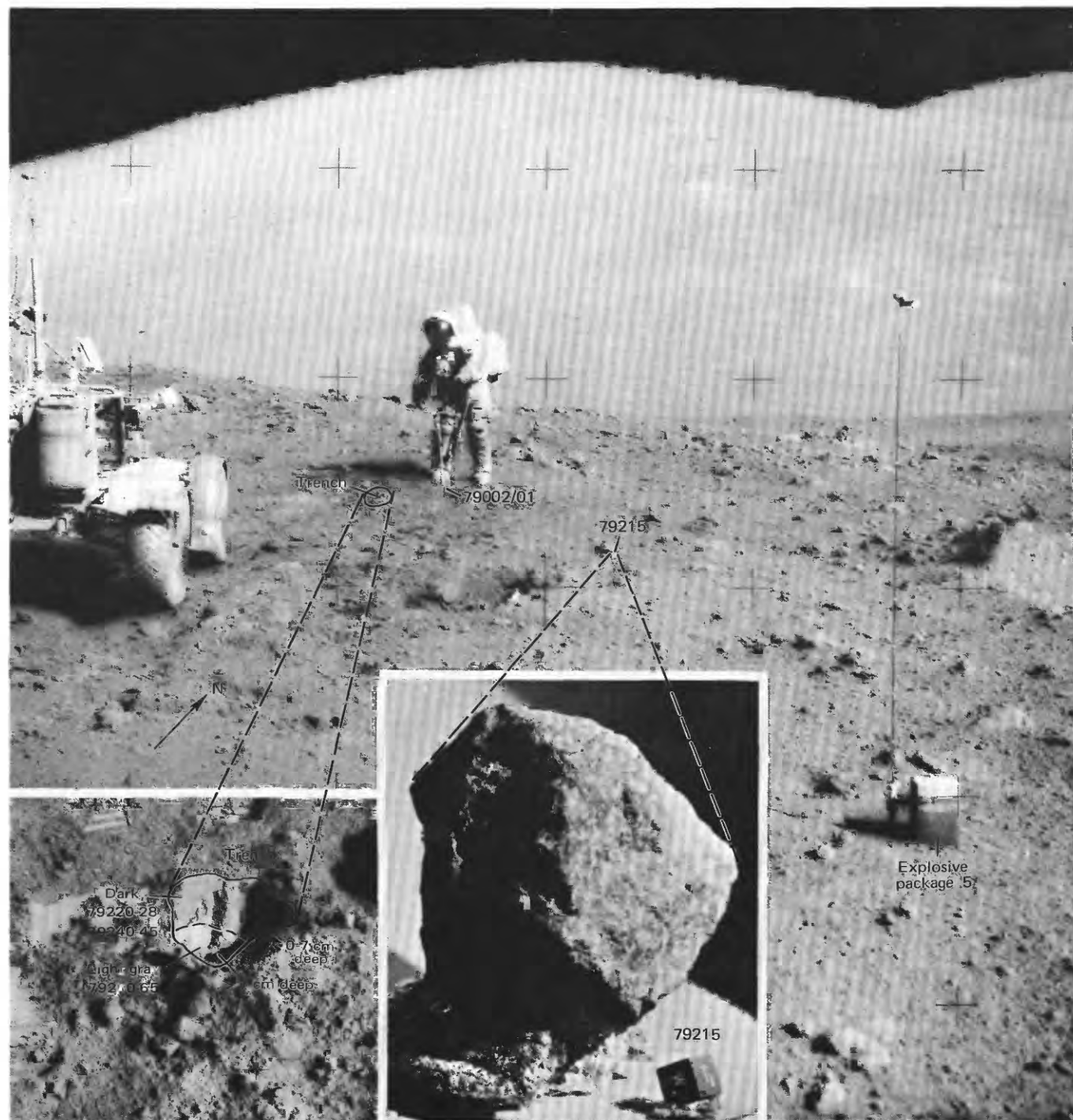


FIGURE 224.—Drive-tube sample 79002/79001, trench samples 79220-28, 79240-45, 79260-65, and rock sample 79215. Astronaut is collecting drive-tube sample. Insets show trench after sampling and rock sample 79215 with reconstructed lunar surface orientation and lighting. (NASA photographs AS17-143-21837; AS17-142-21827, trench closeup; S-73-19590.)

ment. It was probably part of the regolith material of the Van Serg target.

*Petrographic description:* Monomict breccia with clasts of medium-grained olivine basalt with subophitic(?) texture in a dark glass matrix.

*Major-element composition:*

*Chemical analyses of 79155*

	1	2	3
SiO <sub>2</sub> .....	37.50	39.13	38.32
Al <sub>2</sub> O <sub>3</sub> .....	8.58	9.40	8.99
FeO.....	19.04	18.19	18.62
MgO.....	9.14	9.58	9.36
CaO.....	10.29	10.19	10.24
Na <sub>2</sub> O.....	.38	.36	.37
K <sub>2</sub> O.....	.06	.08	.07
TiO <sub>2</sub> .....	12.99	12.56	12.78
P <sub>2</sub> O <sub>5</sub> .....	.05	.04	.04
MnO.....	.28	.27	.28
Cr <sub>2</sub> O <sub>3</sub> .....	.46	.50	.48
Total.....	98.77	100.30	99.55

1. 79155,38 (Rhodes and others, 1976).

2. 79155,39 (Rose and others, 1975).

3. Average of 1 and 2.

*Age:* <sup>40</sup>-<sup>39</sup>Ar: 79155,24, 3.80±0.04 b.y.; intermediate temperature plateau; age is considered an older limit for the basalt (Kirsten and Horn, 1974).

*Exposure age:* Ar: 79155,24, 575±60 m.y. (Kirsten and Horn, 1974).

*Sample 79175*

*Type:* Polymict breccia with a glassy matrix.

*Size:* 14×13×9 cm.

*Weight:* 677.7 g.

*Location:* Southeast rim of Van Serg crater.

*Illustrations:* Pan 28; figures 231, 232 (LRL), 233.

*Comments:* Sample 79175 is impact-fused regolith material from the Van Serg target.

*Petrographic description:* Polymict breccia with clasts of fine-grained polymict breccia, basalt, feldspathic metaclastic rocks, orange glass, and mineral debris in a glass matrix.

*Sample 79195*

*Type:* Sedimentary, weakly lithified polymict breccia.



FIGURE 225.—Sample 79035,1. Weakly lithified polymict breccia. (NASA photograph S-73-15729.)

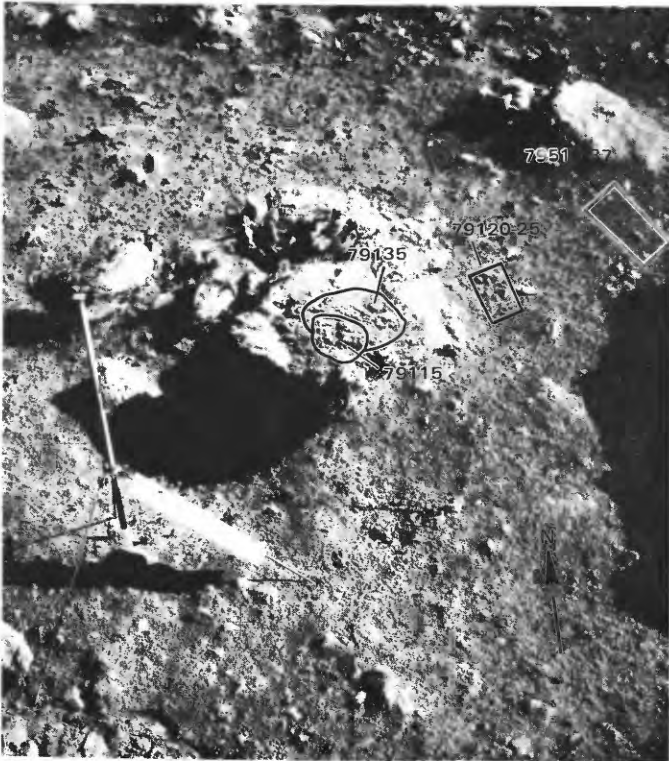


FIGURE 226.—Locations of samples 79115, 79120-25, 79135, and 79510-37 before collection. (NASA photograph AS 17- 147-22413.)

*Size:* Four pieces, 9×6.5×5 cm, 7×5.5×4 cm, 2.5×2×1.5 cm, 1.5×1.5×1 cm.

*Weight:* 368.5 g total.

*Location:* Southeast rim of Van Serg crater.

*Illustrations:* Pan 28; figures 233, 234 (LRL).

*Comments:* Sample 79195 is weakly indurated regolith material ejected from Van Serg crater.

*Petrographic description:* Polymict breccia with clasts of basalt, metaclastic rocks or fine-grained breccia, and mineral debris in a fine-grained friable matrix.

#### Sample 79215

*Type:* Metatroctolite(?) breccia with a granoblastic matrix.

*Size:* 9×8×7.5 cm.

*Weight:* 553.8 g.

*Location:* About 5 m northeast of the LRV.

*Illustrations:* Pans 28, 29; figures 224, 235 (photomicrograph).

*Comments:* Sample 79215 is a highlands rock that may have been a regolith fragment in the Van Serg target.

*Petrographic description:* Metatroctolite(?) breccia. Porphyroclasts, dominantly plagioclase and olivine, and relict lithic clasts of metatroctolite(?) with granoblastic to granoblastic-polygonal texture in a fine-grained granoblastic matrix.

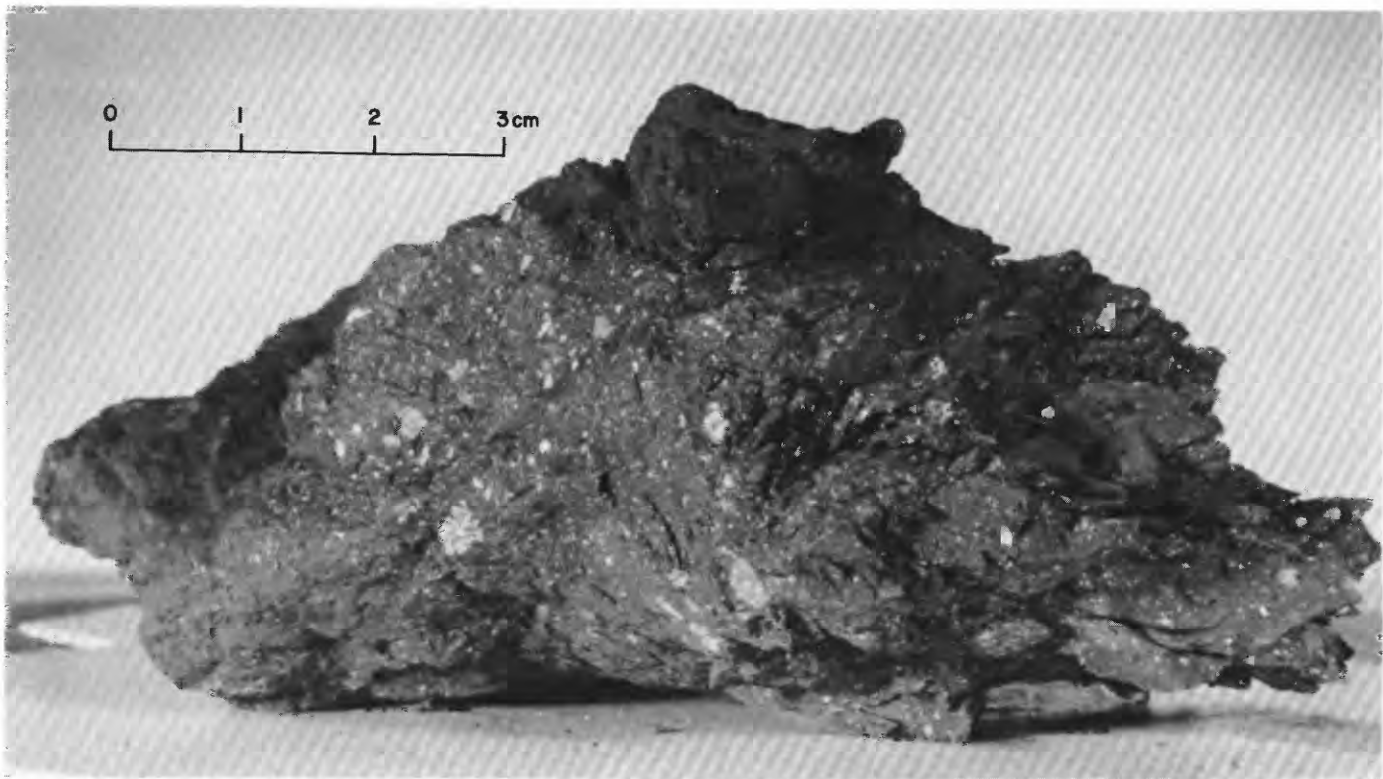


FIGURE 227.—Sample 79115. Impact-consolidated polymict breccia with distinctive fracture pattern. (NASA photograph S-73-15398.)

Bickel and others (1976b) interpreted sample 79215 as a derivative of a plagioclase-olivine cumulate rock that was crushed and finely mixed by meteorite impact and subsequently more intensely annealed than were most lunar breccias.

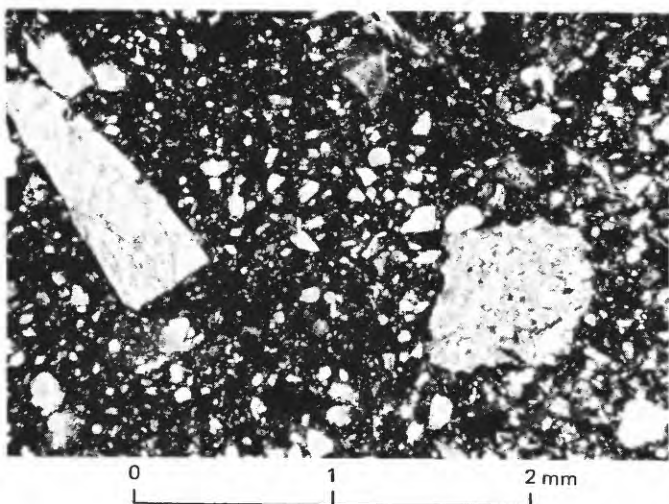


FIGURE 228.—Sample 79115. Photomicrograph showing mineral and lithic debris in very fine grained matrix that has been impact consolidated.

#### Major-element composition:

##### Chemical analysis of 79215

SiO <sub>2</sub> .....	43.8
Al <sub>2</sub> O <sub>3</sub> .....	27.7
FeO .....	4.6
MgO .....	6.3
CaO .....	15.9
Na <sub>2</sub> O .....	.5
K <sub>2</sub> O .....	.1
TiO <sub>2</sub> .....	.3
P <sub>2</sub> O <sub>5</sub> .....	.4
MnO .....	.06
Cr <sub>2</sub> O <sub>3</sub> .....	.2
Total .....	99.86

79215, whole rock composition calculated from microprobe point counts (Bickel and others, 1976a).

*Exposure age:* Tracks: 79215,75, 3.7 m.y. (Bhandari and others, 1976).

#### Sample 79220-28

*Type:* Sedimentary, unconsolidated (79220-24) and sedimentary, weakly lithified polymict breccias (79225-28).

*Size:* 79225, 3.5×2×1 cm, is the largest.

*Weight:* 79220-24, 269.3 g; 79225, 7.42 g; 79226, 6.73 g; 79227, 5.57 g; 79228, 2.5 g.

*Depth:* From 0 to 2 cm in trench.

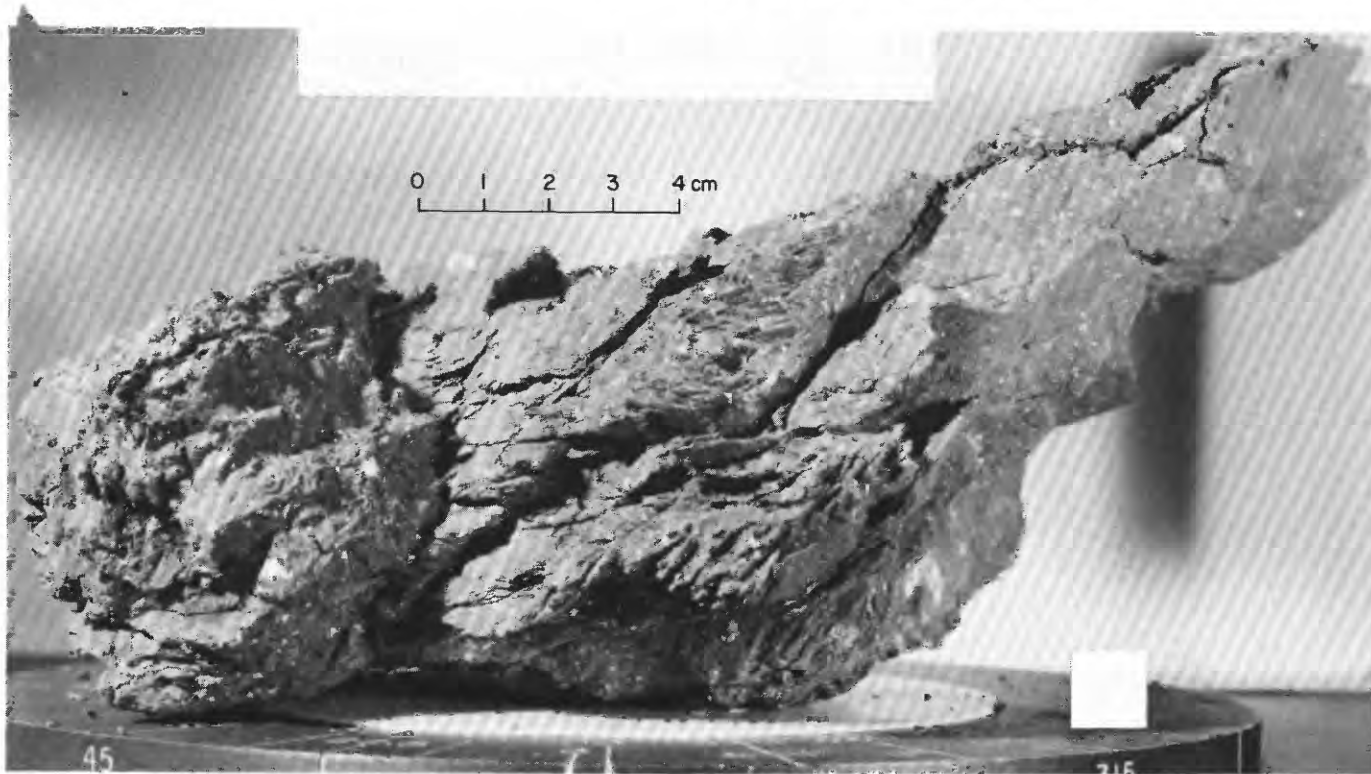


FIGURE 229.—Sample 79135. Impact-consolidated polymict breccia with distinctive fracture pattern. (NASA photograph S-73-15447.)

*Location:* About 65 m southeast of the Van Serg crater rim crest.

*Illustrations:* Pans 28, 29; figure 224.

*Comments:* Sample 79220-28 is from the upper dark unit exposed in the trench. The material is probably ejecta from Van Serg crater.

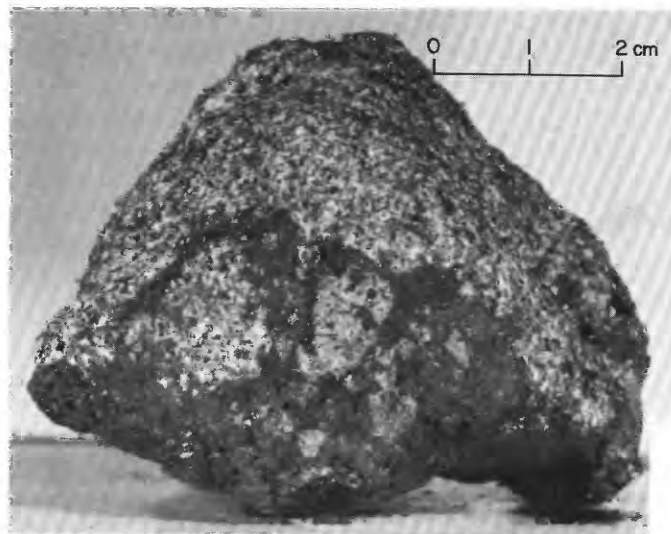


FIGURE 230.—Sample 79155. Monomict breccia with clasts of olivine basalt in glassy matrix. (NASA photograph S-73-15321.)

*Petrographic descriptions:*

79220-24, dominantly fine-grained breccia and (or) metaclastic rock, some glass, basalt.

*Components of 90-150- $\mu$ m fraction of 79221,2 (Heiken and McKay, 1974)*

Components	Volume percent
Agglutinate.....	44.4
Basalt, equigranular } .....	14.4
Basalt, variolitic } .....	
Breccia:	
Low grade <sup>1</sup> - brown .....	8.5
Low grade <sup>1</sup> - colorless .....	1.0
Medium to high grade <sup>2</sup> .....	1.0
Anorthosite.....	..
Cataclastic anorthosite <sup>1</sup> .....	.03
Norite.....	..
Gabbro.....	..
Plagioclase.....	6.9
Clinopyroxene.....	6.5
Orthopyroxene.....	..
Olivine.....	..
Ilmenite.....	1.3
Glass:	
Orange.....	4.2
"Black".....	3.3
Colorless .....	2.3
Brown.....	2.3
Gray, "ropy".....	3.6
Other .....	..
Total number grains .....	306

<sup>1</sup>Metamorphic groups 1-3 of Warner (1972).

<sup>2</sup>Metamorphic groups 4-8 of Warner (1972).

<sup>3</sup>Includes crushed or shocked feldspar grains.

79225-27, polymict breccia with very small lithic and mineral clasts in a fine-grained friable matrix.

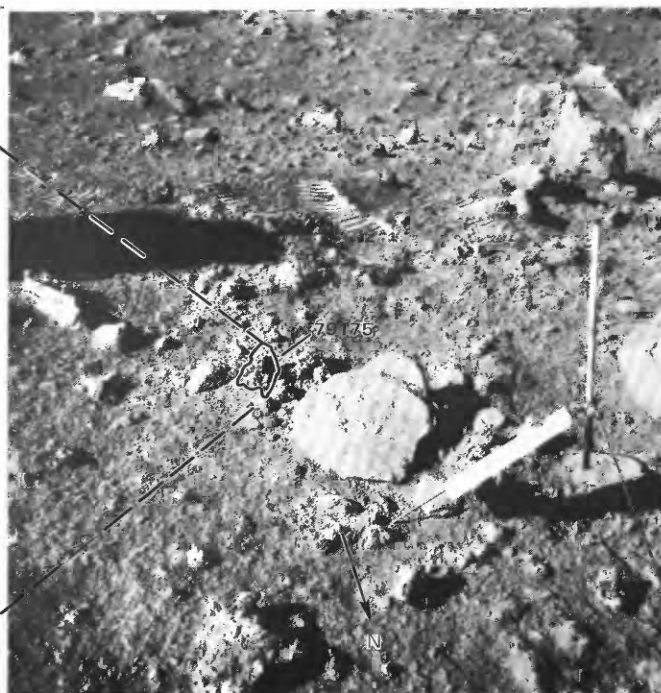
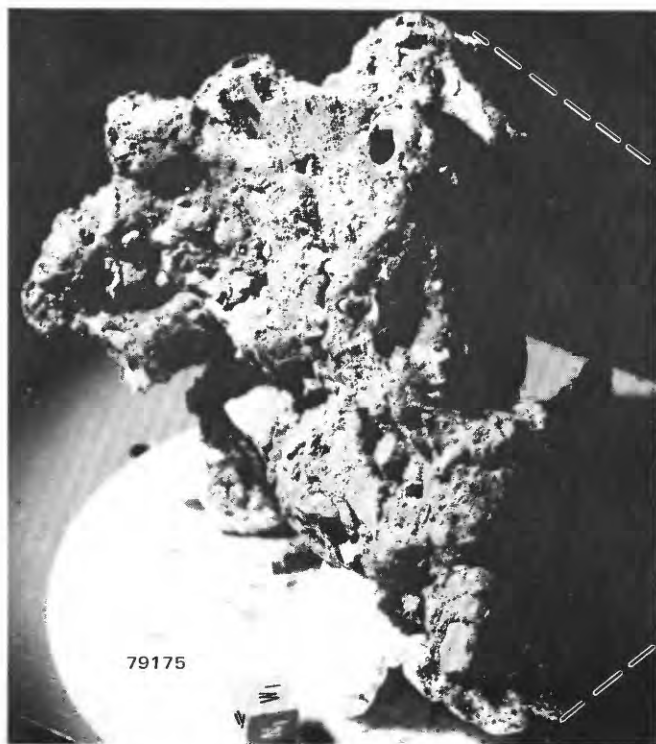


FIGURE 231.—Left, Sample 79175 with reconstructed lunar surface orientation and lighting. (View similar to NASA photograph S-73-19594.) Right, Sample 79175 before collection. (NASA photograph AS17-146-22430.)

*Major-element composition:**Chemical analyses of 79221*

	1	2	3
SiO <sub>2</sub> .....	41.67	41.63	41.65
Al <sub>2</sub> O <sub>3</sub> .....	13.57	13.48	13.52
FeO.....	15.37	15.43	15.40
MgO.....	10.22	10.30	10.26
CaO.....	11.18	11.19	11.18
Na <sub>2</sub> O.....	.34	.35	.34
K <sub>2</sub> O.....	.09	.11	.10
TiO <sub>2</sub> .....	6.52	6.48	6.50
P <sub>2</sub> O <sub>5</sub> .....	.06	.08	.07
MnO.....	.21	.20	.20
Cr <sub>2</sub> O <sub>3</sub> .....	.42	.44	.43
Total.....	99.65	99.69	99.65

1. 79221.2 (Apollo 17 PET, 1973).  
 2. 79221.30 (Rose and others, 1974).  
 3. Average of 1 and 2.

*Exposure age:*

<sup>22</sup>Na-<sup>26</sup>Al: minimum  $1.4 \pm 0.6$  m.y.; maximum  
 $1.7 \pm 0.8$  m.y. (Yokoyama and others, 1976).

Minimum track density: 11 m.y. for 2-cm layer at

surface in station 9 trench (Fleischer and Hart, 1974).

*Sample 79240-45*

*Type:* Sedimentary, unconsolidated (79240-44) and troctolite(?) breccia with an aphanitic matrix (79245).

*Size:* 79245, 3.2×2×1.5 cm.

*Weight:* 79240-44, 320.23 g; 79245, 10.11 g.

*Depth:* From 2 to 7 cm in trench.

*Location:* 65 m southeast of Van Serg crater rim crest.

*Illustrations:* Pans 28, 29; figure 224.

*Comments:* Sample, from the upper dark unit in the trench, is probably Van Serg ejecta. Sample 79245 is a fragment of highlands breccia that presumably was in the regolith in the Van Serg target.

*Petrographic descriptions:*

79240-44, dominantly fine-grained breccia and (or) metaclastic rock, basalt, some glass.

79245, metatroctolite(?). Plagioclase and olivine porphyroclasts in an aphanitic matrix.

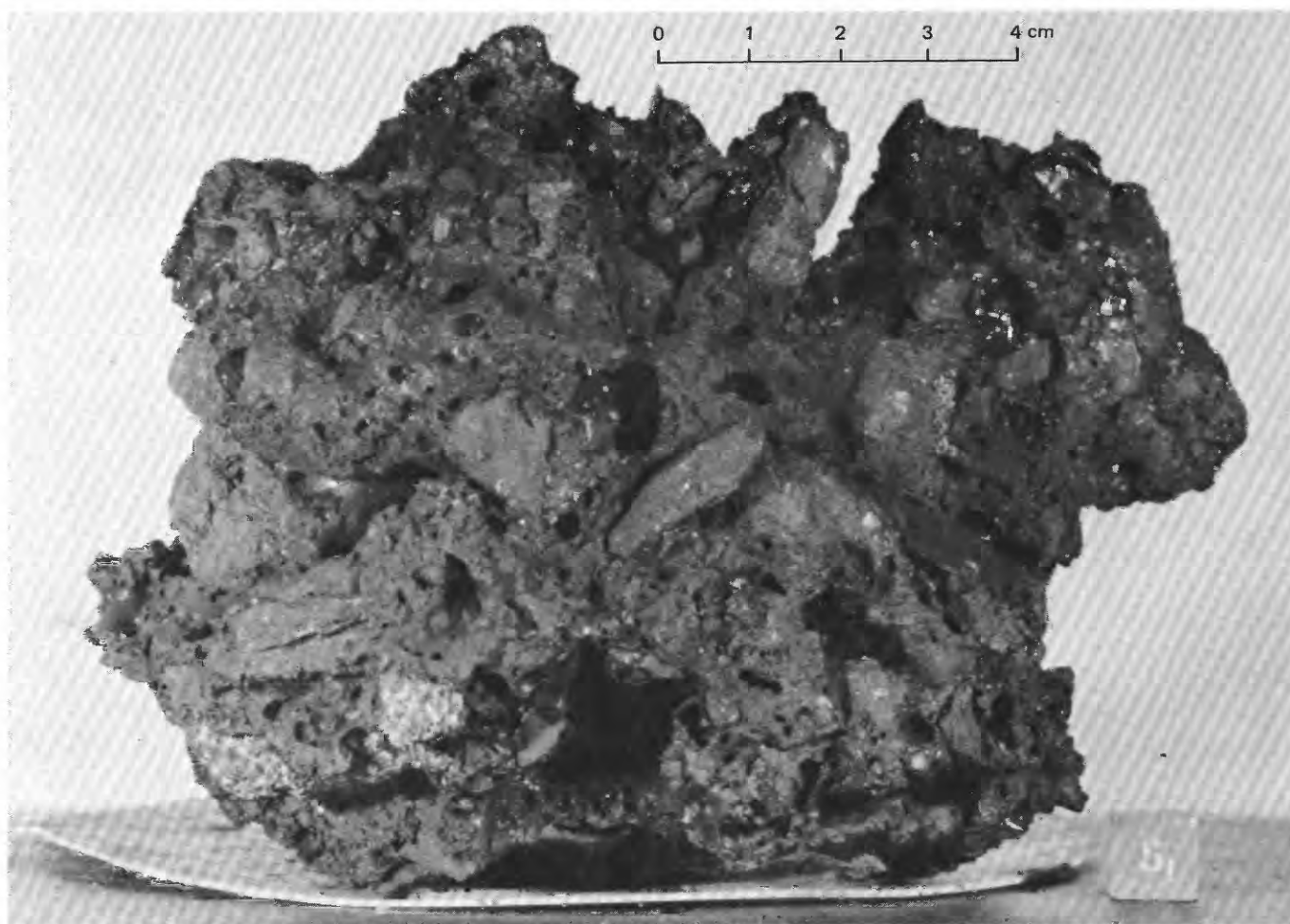


FIGURE 232.—Sample 79175. Polymict breccia with glassy matrix. (NASA photograph S-73-17782.)

*Major-element composition:**Chemical analysis of 79241*

SiO <sub>2</sub> .....	41.73
Al <sub>2</sub> O <sub>3</sub> .....	13.90
FeO .....	15.64
MgO .....	9.90
CaO .....	11.08
Na <sub>2</sub> O .....	.39
K <sub>2</sub> O .....	.09
TiO <sub>2</sub> .....	6.79
P <sub>2</sub> O <sub>5</sub> .....	.08
MnO .....	.20
Cr <sub>2</sub> O <sub>3</sub> .....	.46
Total .....	100.26

79241.28 (Rose and others, 1974).

*Exposure age:*

Minimum track density: Assuming that this sample represents a layer from 2 to 7 cm in depth that was deposited earlier than a layer from 0 to 2 cm (sample 79220-28), Fleischer and Hart (1974) calculated a surface exposure time of 8 m.y. and a total exposure time of 19 m.y. for 79241. However, there is no evidence to support the assumption that material from 2 to 7 cm in the trench was deposited at an earlier time than the material from 0 to 2 cm.

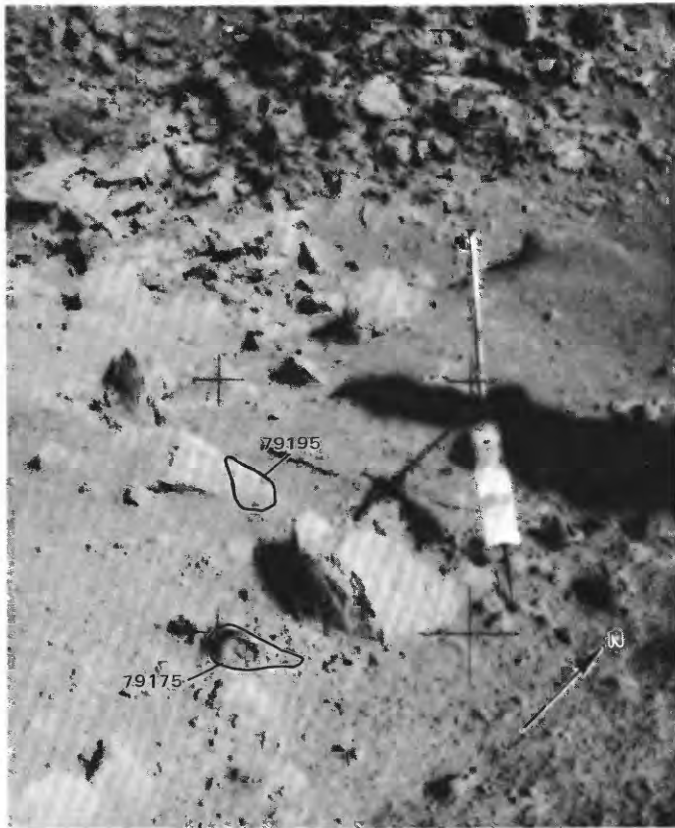


FIGURE 233.—Samples 79175 and 79195 before collection. (NASA photograph AS17-142-21795.)

*Sample 79260-65*

*Type:* Sedimentary, unconsolidated (79260-64) and basalt (79265).

*Size:* 79265, 1.3×1×1 cm.

*Weight:* 79260-64, 345.75 g; 79265, 2.6 g.

*Depth:* From 7 to 17 cm in trench.

*Location:* About 65 m southeast of Van Serg crater rim crest.

*Illustrations:* Pans 28, 29; figure 224.

*Comments:* Sample 79260-64, from lower light-gray unit exposed in trench, is probably ejecta from Van Serg crater. Sample 79265 is a subfloor basalt fragment that was in the regolith of the Van Serg target.

*Petrographic description:* 79260-64, dominantly basalt and fine-grained breccia and (or) metaclastic rock, some glass.

*Components of 90-150-μm fraction of 79261.1 (Heiken and McKay, 1974)*

Components	Volume percent
Agglutinate .....	22.3
Basalt, equigranular { .....	13.3
Basalt, variolitic { .....	
Breccia:	
Low grade <sup>1</sup> - brown .....	1.3
Low grade <sup>1</sup> - colorless .....	.3
Medium to high grade <sup>2</sup> .....	8.3
Anorthosite .....	.6
Cataclastic anorthosite <sup>1</sup> .....	.6
Norite .....	.3
Gabbro .....	..
Plagioclase .....	12.7
Clinopyroxene .....	16.6
Orthopyroxene .....	1.6
Olivine .....	..
Ilmenite .....	7.0
Glass:	
Orange .....	4.0
"Black" .....	2.6
Colorless .....	3.2
Brown .....	2.0
Gray, "ropy" .....	1.3
Other .....	1.6
Total number grains .....	300

<sup>1</sup>Metamorphic groups 1-3 of Warner (1972).<sup>2</sup>Metamorphic groups 4-8 of Warner (1972).<sup>3</sup>Includes crushed or shocked feldspar grains.*Major-element composition:**Chemical analyses of 79261*

	1	2	3
SiO <sub>2</sub> .....	42.26	42.58	42.42
Al <sub>2</sub> O <sub>3</sub> .....	14.43	14.51	14.47
FeO .....	14.60	14.69	14.64
MgO .....	9.82	9.67	9.74
CaO .....	11.48	11.35	11.42
Na <sub>2</sub> O .....	.35	.39	.37
K <sub>2</sub> O .....	.11	.10	.10
TiO <sub>2</sub> .....	6.09	6.28	6.18
P <sub>2</sub> O <sub>5</sub> .....	.07	.08	.08
MnO .....	.20	.19	.20
Cr <sub>2</sub> O <sub>3</sub> .....	.40	.41	.40
Total .....	99.81	100.25	100.02

1. 79261.2 (Apollo 17 PET, 1973).

2. 79261.29 (Rose and others, 1974).

3. Average of 1 and 2.

*Exposure age:*

$^{22}\text{Na}$ - $^{26}\text{Al}$ : maximum  $1.6 \pm 0.6$  m.y. (Yokoyama and others, 1976).

**Minimum track density:** Assuming that the three trench samples, from depths of 0 to 2 cm, 2 to 7 cm, and 7 to 17 cm, represent three distinct depositional events decreasing upward in age, Fleischer and Hart (1974) calculated a 5-m.y. exposure time for the lowest layer (79261) and a burial time of 19 m.y. to give a total age of 24 m.y. for 79261.

As noted for sample 79240-45, there is no evidence to support the assumption that the interval from 0 to 7 cm in the trench represents more than one depositional unit. The boundary at 7 cm could be, but is not necessarily, a contact between separate depositional units. Such units might be Van Serg ejecta (lower, light-gray unit) and overlying younger ejecta (upper, dark unit) from local impacts on the Van Serg ejecta blanket.

Sample 79510-19, 25-29, 35-37

*Type:* Sedimentary, unconsolidated (79510-14); olivine

basalt (79515-16); sedimentary, weakly lithified polymict breccia (79517-18); and nine small fragments of probable weakly lithified polymict breccia (79519, 25-29, 35-37).

*Size:* Largest fragment, 79515,  $4 \times 3.5 \times 3$  cm.

*Weight:* 79510-14, 320.3 g; 79515, 33 g; 79516-19, 25-29, 35-37, 60.23 g.

*Depth:* From upper few centimeters.

*Location:* From southeast rim of Van Serg crater.

*Illustrations:* Pan 28; figure 226.

*Comments:* Sample is Van Serg ejecta. Basalt samples 79515-16 are subfloor basalt fragments from the regolith in the Van Serg target. Weakly lithified polymict breccia fragments are samples of indurated regolith from the Van Serg target.

*Petrographic descriptions:*

79510-14, dominantly fine-grained breccia and (or) metaclastic rock, some glass, agglutinate.

79515, medium-grained vesicular olivine basalt.

79516, fine-grained olivine basalt.

79517, 18, polymict breccia with small clasts of basalt, metaclastic(?) rock, and mineral debris in a fine-grained friable matrix.



FIGURE 234.—Sample 79195. Weakly lithified polymict breccia. Large clast at left is mare basalt. (NASA photograph S-73-17788.)

*Major-element composition:**Chemical analysis of 79511*

SiO <sub>2</sub> .....	41.69
Al <sub>2</sub> O <sub>3</sub> .....	13.79
FeO.....	15.11
MgO.....	10.31
CaO.....	10.73
Na <sub>2</sub> O.....	.27
K <sub>2</sub> O.....	.18
TiO <sub>2</sub> .....	6.13
P <sub>2</sub> O <sub>5</sub> .....	.06
MnO.....	.27
Cr <sub>2</sub> O <sub>3</sub> .....	.43
Total.....	98.97

79511 (Mason and others, 1974).

**STATION LRV-12****LOCATION**

Station LRV-12 is located approximately 200 m north-northwest of the north rim of Sherlock crater (fig. 7E).

**OBJECTIVES**

The original plan called for a traverse station, 10B, at Sherlock Crater (fig. 5). Sampling stop LRV-12 was substituted on the return to the LM from station 9 when station 10B was cancelled due to the shortage of time.

**GENERAL OBSERVATIONS**

The surface in the station area is flat to gently rolling, blocky, and locally cratered (fig. 236). Rocks cover about 5 percent of the surface and reach 1 m in size. The larger boulders, most of which are partly buried, are smooth with subrounded to rounded shapes. Smaller fragments range from partially buried to perched

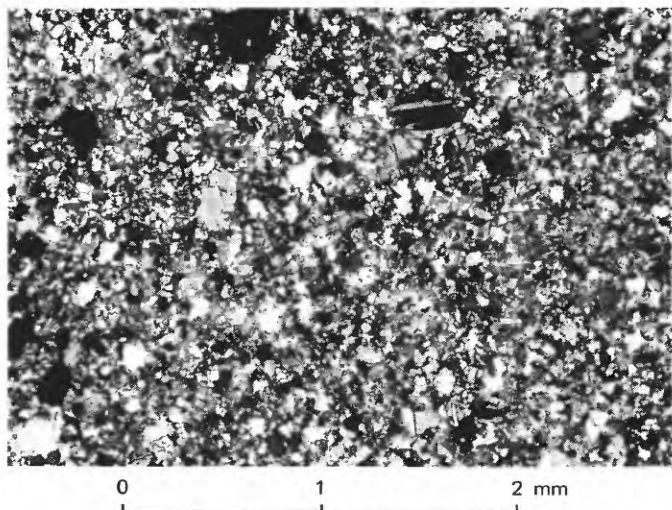


FIGURE 235.—Sample 79215. Photomicrograph showing metatrolite breccia consisting of moderately abundant plagioclase and olivine porphyroclasts in granoblastic matrix. Crossed polarizers.

on the surface. Most are rounded, but a few are subangular with planar sides.

Local craters are up to about 10 m in diameter. Some have excavated abundant rock fragments, presumably from the ejecta of Sherlock crater. Smaller craters, about 1 m in diameter, are rimmed with clods.

Two samples, sediment and a loose rock from the surface, were collected at station LRV-12.

**SUMMARY OF SAMPLING****Sample 70311-15**

*Type:* Sedimentary, unconsolidated (70311-14) and basalt (70315).

*Size:* 70315, 5×4.5×4.5 cm.

*Weight:* 70311-14, 119.16 g; 70315, 148.6 g.

*Depth:* From upper few centimeters.

*Location:* About 200 m north-northwest of Sherlock crater.

*Illustrations:* Figures 236, 237 (LRL).

*Comments:* Sample 70315, subfloor basalt, is probably part of the Sherlock crater ejecta. Sediment (70311-14) was scooped with the basalt sample.

*Petrographic descriptions:*

70311-14, dominantly basalt and breccia fragments, with some glass and agglutinates.

70315, medium-grained porphyritic vesicular basalt. Aggregates of clinopyroxene-ilmenite in a locally plumose groundmass of plagioclase, clinopyroxene, ilmenite, and accessory minerals.

**Sample 70320-24**

*Type:* Sedimentary, unconsolidated.

*Weight:* 233.36 g.

*Depth:* From upper few centimeters.

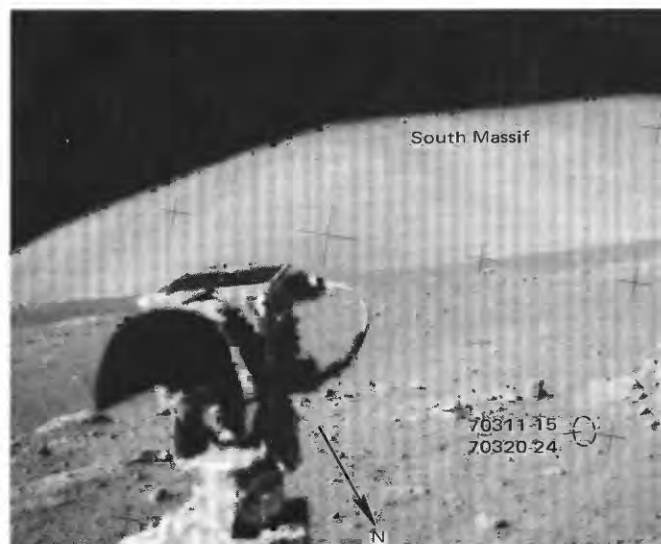


FIGURE 236.—Probable location of samples 70311-15 and 70320-24 at LRV-12. (NASA photograph AS17-143-21893.)

*Location:* About 200 m north-northwest of Sherlock crater.

*Illustrations:* Figure 236.

*Comments:* Sample is regolith material of the cluster ejecta.

*Petrographic descriptions:* 70320-24, dominantly basalt and breccia fragments with some glass and agglutinates.

## GEOLOGIC SYNTHESIS

### GENERAL SETTING AND HISTORICAL FRAMEWORK

The geologic setting and stratigraphic framework, interpreted after the Apollo 17 mission, have been discussed in several previous papers (Muehlberger and others, 1973; Apollo Field Geology Investigation Team, 1973; Reed and Wolfe, 1975; Wolfe and others, 1975; Wolfe and Reed, 1976). These are recapitulated and amplified in the following pages largely without further citation.

Briefly, we envision the massifs as the upper part of thick ejecta deposited on the rim of the transient cavity of the large southern Serenitatis basin, which was formed about 3.9 to 4.0 b.y. ago by the impact of a planetesimal. The ring structure and the approximately radial grabens that give the massif blocks definition were imposed on the ejecta blanket before deposition of the knobby-textured Sculptured Hills material. The mountainous terrain thus formed was partly flooded by the subfloor basalt, and the general region was mantled by a thin volcanic ash unit. After gentle warping

and tensional faulting in the Taurus-Littrow area, younger basalts were extruded to the west within Mare Serenitatis (pl. 1). During approximately the last 3.5 b.y., since deposition of the volcanic ash, continued bombardment by meteorites and secondary projectiles has produced a thick regolith. Relatively late in this interval, the Lee-Lincoln fault scarp resulted from structural adjustments. About 100 m.y. ago a swarm of secondary projectiles from Tycho formed the large cluster of craters east and south of the landing point (pl. 2); when the Tycho projectiles struck the north face of the South Massif, they mobilized fine-grained regolith material, which was redeposited on the valley floor as the light mantle. Small extensional faults cut the light mantle (pl. 2).

### SOUTHERN SERENITATIS BASIN STRUCTURE

On the basis of orbital gravity data (Sjogren and others, 1974a) and geologic interpretation, Scott (1974) suggested that two basins underlie Mare Serenitatis. The larger, more southerly basin is centered at approximately lat 24.5°N, long 18°E. Extending Scott's (1974) interpretation and modifying the ring structure previously shown by Wilhelms and McCauley (1971) for a single basin (fig. 3), Wolfe and Reed (1976) proposed a revised ring structure (fig. 238).

Ring 1 is represented by prominent wrinkle ridges whose distribution approximates a circle with a 200-km radius (Scott, 1974). Muehlberger (1974) suggested that a wrinkle ridge of this sort may be developed in the mare basalt where a drowned ring of the basin structure affects the compressional stress field that produced the ridges.

Ring 2 is represented by the arc of the Haemus Mountains. Extended to the northeast with the 290-km radius measured from the basin center to the Haemus Mountains, ring 2 underlies the basalt of easternmost Mare Serenitatis (fig. 238).

Fitting ring 3 to Scott's (1974) basin center, Wolfe and Reed (1976) connected segments of the second and third rings previously shown by Wilhelms and McCauley (1971) for a single Serenitatis basin (fig. 3). The connecting segment passes approximately through the Apollo 17 landing area (fig. 238).

Wilhelms and McCauley (1971) identified a fourth ring with a radius of about 670 km in the highlands southwest of Mare Serenitatis (figs. 3 and 238). Their third ring (fig. 3) lies about 530 km east of the southern Serenitatis basin center. It is difficult to say whether either of these segments represents a basin rim analogous to the fourth ring (Cordillera Mountains) of the Orientale basin or to the outer ring (Apennine Mountains) of the Imbrium basin. Such an outer ring may never have been well developed in the southern Serenitatis basin structure or may have been



FIGURE 237.—Sample 70315. Medium-grained vesicular basalt. (NASA photograph S-73-15453.)

largely obliterated by subsequent events.

The rings of the southern Serenitatis basin structure are correlated with those of the better preserved Orientale basin structure as shown in table 5. The correlation derives particular support from morphologic similarities suggesting that the outer Rook ring (ring 3 of the Orientale basin) and the Littrow ring (ring 3 of the southern Serenitatis basin) are analogous structures. The Rook Mountains in the southeastern part of the Orientale basin and the Apollo 17 landing area southeast of Mare Serenitatis are shown in orbital view at similar scale in figures 239 and 240. In each area, several massifs of similar shape and size are crudely aligned along trends radial to the basin centers, and linear grabenlike troughs approximately radial to the basin centers cut through the mountainous third rings. In the Apollo 17 area, mare basalt has flooded such troughs and buried the lower parts of the massifs.

The spatial relations in both basins of the massifs to the knobby terrain provides further support for the correlation of basin structures. The knobby-textured terrain of the Orientale basin (knobby basin material of Moore and others (1974); domical facies of Head (1974b); knobby facies of the Rook Formation of Scott and others (1977)) occurs in the grabenlike trough that transects the outer Rook ring (fig. 239) and extends over most of the surface between the Rook Mountains

TABLE 5.—Comparison of southern Serenitatis and Orientale basin structures

[Data for Orientale basin, except as indicated, from Moore and others (1974)]

	Southern Serenitatis basin— structure radii (kilometers)	Orientale basin— structure radii (kilometers)	Ratio of radii
Ring 1 .....	200	160 .....	1.25
Ring 2 .....	290 (Haemus ring)	240 (inner Rook ring) ..	1.21
Ring 3 .....	375 (Littrow ring)	300 (outer Rook ring) ..	1.25
Ring 4 .....	650?	450 (Cordillera ring) ...	1.44
Mascon (calculated surface disk) .....	<sup>1</sup> 221	<sup>2</sup> 150 .....	1.5

<sup>1</sup>Sjogren and others (1974b).

<sup>2</sup>Scott (1974).

and the scarp that forms the basinward face of the Cordillera Mountains (fig. 241). Comparable knobby-textured Sculptured Hills terrain forms a major part of the highlands adjacent to eastern Mare Serenitatis (fig. 240; pl. 1). It partly surrounds the Taurus-Littrow massifs much as its Orientale counterpart surrounds the Rook Mountain massifs, and it projects locally through the mare basalts that floor the grabenlike valleys. Head (1974a) made a similar correlation of the massifs and Sculptured Hills of the Apollo 17 region with the Alpes Mountains and Alpes Formation of the Imbrium basin.

Head (1974b) noted the predominance of knobby terrain at Orientale, between the Rook Mountains and the Cordillera scarp, and interpreted it as lineated ejecta on which the knobby or domical texture was imposed by seismic shaking during formation of the Cordillera scarp. In more recent mapping, Scott and others (1977) have interpreted the knobby-terrain material as an ejecta unit that is partly confined by the preexisting Cordillera scarp; where it overlaps the scarp, the knobby unit overlies the radially lineated Hevelius Formation, also interpreted as ejecta. Supporting evidence for the hypothesis that the knobby-terrain material is a discrete little-modified basin-ejecta unit comes from the Imbrium basin. Knobby-terrain material (Alpes Formation) occupies an extensive area within the Apennine ring in the northeast quadrant of the Imbrium basin. It also extends hundreds of kilometers, mainly east and south of the limits of the Imbrium ring structure (Wilhelms and McCauley, 1971). This distribution is a likely one for basin ejecta but is unlikely for a texture imposed on preexisting materials by seismic shaking associated with formation of the Apennine scarp. Distribution of the knobby-terrain material with respect to grabens, massifs, radially lineated ejecta, and basin-forming scarps, as outlined above, suggests that the knobby-terrain material is ejecta that was emplaced during basin formation but after development of the ring structure and the grabens.

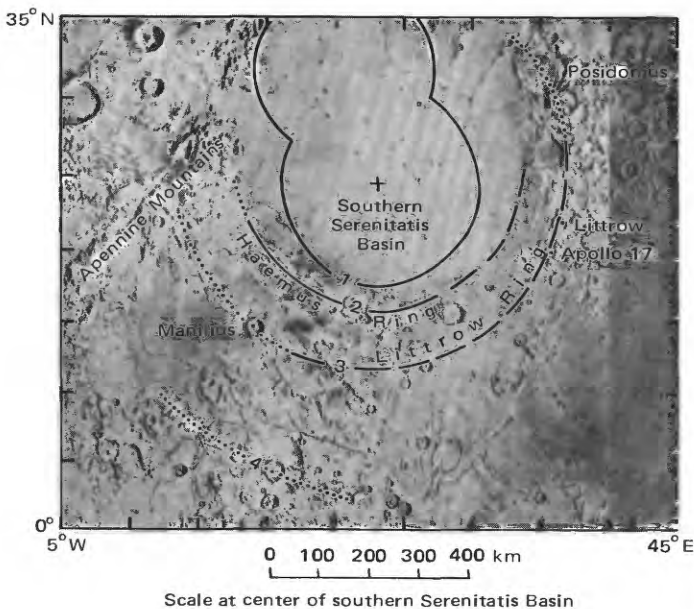


FIGURE 238.—Revised ring structure of Mare Serenitatis area. Solid-line segments from Scott (1974); dotted-line segments from Wilhelms and McCauley (1971); dashed-line segments from Wolfe and Reed (1976). Cross shows approximate center of southern Serenitatis basin. Numbers 1 through 4 identify basin rings discussed in text. Compare with figure 3. (From Wolfe and Reed, 1976.)

## SIGNIFICANCE OF THE THIRD RING

Assuming that the massifs and Sculptured Hills of the Taurus-Littrow area are genetic as well as morphologic analogs of the Rook Mountain massifs and knobby terrain of the Orientale basin, we can apply concepts to the Taurus-Littrow region that were developed from studies of the better preserved Orientale basin.

Several recent workers (Baldwin, 1972; McGetchin and others, 1973; Moore and others, 1974; Head, 1974b; McCauley, 1977) have suggested that the Rook Mountains are located approximately at the rim of the initial crater—the so-called transient cavity—that was excavated by basin-forming impact. Photogeologic support for this hypothesis has been developed by Head (1974b), who by analogy with the large crater Hausen (170 km in diameter) and the Schrödinger basin (320 km in diameter) suggested that the inner Rook ring (ring 2, table 5) is a central peak ring and that the outer Rook ring is the approximate rim of the transient cavity. Drawing on photogeologic interpretation of the Orientale basin and on data from terrestrial explosion craters, McCauley (1977) also concluded that the inner Rook ring is a central peak ring and that the Rook mountain massifs represent the crest of the transient

cavity rim.

We believe that the transient cavity in a multi-ring basin briefly approaches the bowl shape of a small lunar impact crater. However, the lunar crust and mantle lack the strength to maintain an open hole of such proportions; rapid modification occurs due to immediate isostatic adjustment and to centripetal movement of crust and mantle materials toward the transient cavity. McCauley (1977) has attributed formation of the Cordillera scarp (fig. 241) to such centripetal movement during the basin-forming event.

Moore and others (1974), in estimating thickness of ejecta from the calculated depths of buried craters, determined a thickness of 2-4 km of Orientale ejecta at the crest of the Cordillera ring. Plotting their empirical estimates of thickness against distance from the basin center, they selected the equation of McGetchin and others (1973) as a reasonable fit to their data for a transient cavity of 300-km radius. The equation is  $t = T(r/R)^{-3}$ , where  $T$  is the thickness of ejecta at the initial crater rim,  $R$  the radius of the initial crater, and  $t$  the thickness of ejecta at distance  $r$ , measured from the center of the crater. As fit to the empirical data by Moore and others, this equation predicts 12 km of

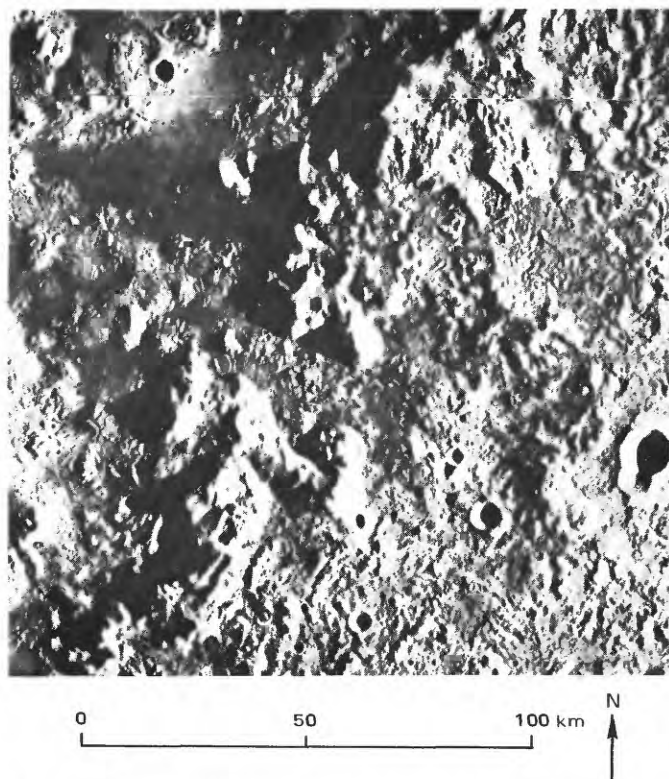


FIGURE 239.—Rook Mountains in the southeastern quadrant of the Orientale basin. Location of this area is shown in figure 241. (Lunar Orbiter IV high-resolution frame 181.) (From Wolfe and Reed, 1976.)

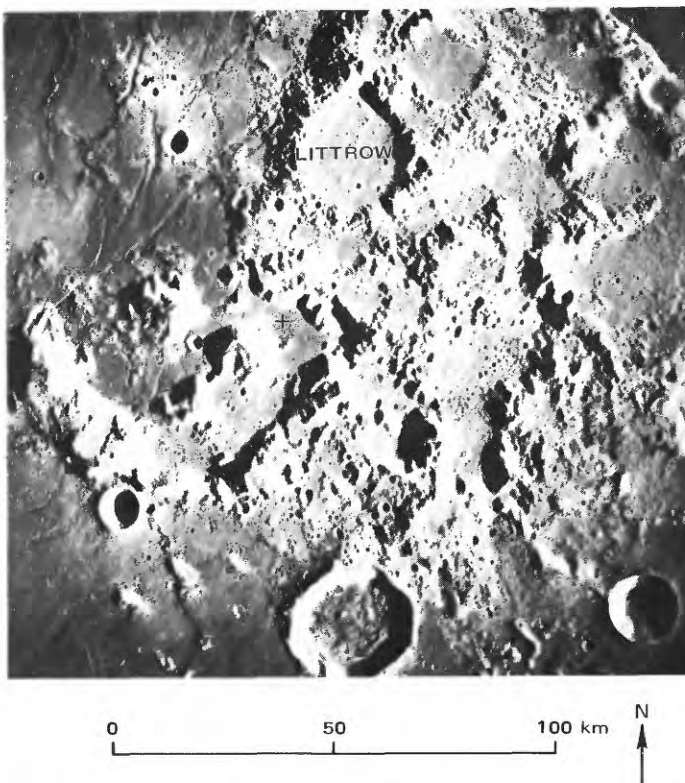


FIGURE 240.—Mountainous terrain southeast of Mare Serenitatis in the Apollo 17 region. Cross shows Apollo 17 landing point. (Mapping-camera photograph AS17-M-446.) (From Wolfe and Reed, 1976.)



FIGURE 241.—Eastern part of Orientale basin. Square shows location of figure 239. (Uncontrolled mosaic of Lunar Orbiter IV high-resolution images.) (From Wolfe and Reed, 1976.)

ejecta at the rim of the Orientale transient cavity and 3.6 km at a position equivalent to the Cordillera ring. Moore and others (1974) further pointed out that another equation of McGetchin and others (1973), for small experimental craters ( $T=0.04R$ , notation as above), predicts 12 km of ejecta at the rim of a transient crater 300 km in radius. Whether or not the calculated thicknesses are precisely correct, the ejecta at the outer Rook ring must be thicker than the 2-4 km determined empirically at the Cordillera crest.

The two equations (above) used by Moore and others (1974) are for craters with the shapes of small impact craters. Support for the assumption that the transient cavity approaches the shape of a small impact crater comes from comparison of ejecta volumes calculated from crater geometry and from interpretation of gravity data. Using the equation of McGetchin and others (1973) for cumulative volume ( $V$ ) at distances of  $r$  and greater ( $V=2\pi TR^2(R/r)$ , notation as above) and using  $R=300$  km,  $T=12$  km, Moore and others (1974) calculated the total volume of Orientale ejecta beyond the Cordillera rim to be about  $4.5 \times 10^6$  km<sup>3</sup>, a value in reasonable agreement with the  $5.3 \times 10^6$  km<sup>3</sup> estimated by Scott (1974) from interpretation of gravity data. These estimates of Orientale ejecta volume are significantly greater than the  $1.0$ - $2.0 \times 10^6$  km<sup>3</sup> that Head and others (1975) have suggested as a preferred estimate. In fact, when ejecta volume between the Rook Mountains and Cordillera scarp is included, the estimate of Moore and others is  $6.8 \times 10^6$  km<sup>3</sup>.

With respect to their much smaller estimates of volume, Head and others (1975) have suggested that the depth of excavation of Orientale was 6-14 km. Moore and others (1974), in contrast, applied Pike's equations for experimental craters ( $a = 0.225D^{0.96}$  and  $h = 0.043D^{0.91}$ , where  $a$  is the depth of the crater measured from the rim crest,  $h$  is the height of the rim above the local surroundings, and  $D$  is the diameter of the crater; all variables in kilometers) to estimate that the Orientale transient crater was about 85 km deep. It may have excavated a small amount of material from the lunar mantle (depth greater than 60 km).

Extrapolation to the slightly larger southern Serenitatis basin (table 5) suggests that the transient crater may have been more than 100 km deep and that many kilometers of ejecta was emplaced in the vicinity of the Apollo 17 landing site. The relation  $T=0.04R$ , which predicts 12 km of ejecta at the rim of the Orientale transient cavity, suggests a thickness of 15 km at the rim of the southern Serenitatis transient cavity. Even if this estimate is several times too large, the thickness of southern Serenitatis basin ejecta would exceed the height of the exposed faces of the massifs

from which samples were collected. Later, but still during the period of basin formation, the ring structure and radial faults that define the massifs were imposed on the ejecta.

#### STRATIGRAPHY OF THE TAURUS-LITTROW VALLEY

##### MASSIFS

The linearity of the Taurus-Littrow valley walls implies that the bounding faults, generated during formation of the southern Serenitatis basin, are steeply dipping. These faults are not now exposed. Perhaps the segment of the Lee-Lincoln scarp on the North Massif follows the zone of weakness along such a fault. Initially, high-angle fault surfaces formed oversteep massif slopes that must have been unstable and collapsed almost immediately to form wedges of colluvium along their lower parts (fig. 242). The bulk of the colluvium probably accumulated as the graben was forming. However, partial filling of Nansen crater shows that mass wasting has continued into recent time.

The massifs as mapped (pls. 1 and 2) include bedrock with a veneer of regolith on the upper slopes and, on the lower slopes, the upper parts of the colluvial wedges (fig. 242). Stations 2, 6, and 7 are on the colluvial wedges. The large boulders sampled at each of these stations rolled down over the wedges from the higher parts of the massifs. These intensively examined and sampled boulders are inferred to be representative of the outcrops and boulders that abound on the upper massif slopes. Boulder tracks and distributions of boulders on the massifs suggest that the station 2 boulders came from the upper third of the South Massif and the station 6 boulder from about one-third of the way up the North Massif. There is no strong suggestive evidence to indicate the source area on the North Massif for the station 7 boulder.

The boulder samples from all three stations as well as rock 73215 from the light mantle at station 3 have been studied intensively by teams of petrologists, geochemists, and geochronologists. Details are summarized in this report in the appropriate station and sample discussions. In general, the boulders are dominantly similar polymict breccia that consists of mineral and lithic clasts intimately mixed with a very fine coherent crystalline groundmass.

Directly observed and sampled lithic clasts range from metaclastic fragments smaller than 1 mm in size to the approximately  $0.5 \times 1.5$  m clast of norite cataclastite in the station 7 boulder. The larger clasts are derivatives of the plutonic dunite-anorthosite-norite-troctolite suite; all have undergone thermal metamorphism or cataclasis before or during incorporation

in the enclosing breccia; some have undergone later local cataclasis. Mineral clasts, generally with little if any evidence of shock metamorphism, are mainly plagioclase, pyroxene, and olivine.

There is general agreement that the breccia matrices are laden with fragments, but the petrography and origin of the crystalline groundmasses are controversial. The consortium for boulder 1 at station 2 concluded that the competent breccia of boulder 1 was thermally metamorphosed and partly melted (Ryder and others, 1975). In contrast, the consortia investigating boulders 2 and 3 at station 2, sample 73215 from station 3, and the station 6 and 7 boulders interpreted the breccia matrix to have formed from a mechanical mixture of relatively cold unshocked fragmental debris and impact-generated silicate melt. In their views the melt, charged with lithic and mineral clasts, crystallized to subophitic to poikilitic texture with no evidence of recrystallization due to thermal metamorphism (Dymek and others, 1976b; James and Blanchard, 1976; Simonds, 1975; Chao and others, 1974; Chao and others, 1975a). However, some isolated rocks (for example, 76055) that resemble elements in the matrix of the station 6 boulder are inferred to have been thermally metamorphosed and contain clasts with poikilitic texture also interpreted as products of thermal metamorphism (Chao, 1973).

As the process of impact pulverization, heating, and melting yields a continuum of products, and as these may be thoroughly intermixed in the depositional process, the extent to which the final lithic product represents crystallization of a melt or recrystallization of heated rock powder intermixed with melt seems more an academic question than a substantive distinction. For example, the extremes of thermally metamorphosed and crystallized melt components of the matrix yield the same age for the event that formed them.

Microprobe data indicate that the crystalline groundmass in boulders 2 and 3 from station 2 is lower in  $\text{Al}_2\text{O}_3$  and  $\text{MgO}$  (Dymek and others, 1976b) and that the groundmass in sample 73215 is lower in  $\text{Al}_2\text{O}_3$  and  $\text{CaO}$  (James and Blanchard, 1976) than is the bulk breccia. Those workers concluded that the crystalline matrix could not have originated solely by crushing or melting of parent material of the composition of the clast assemblage.

However, it should be noted that the process of cataclastic breakdown of the plutonic rocks commonly pulverized the mafic minerals more than the plagioclase and concentrated the mafic components in the breccia matrix, a process also observed in cataclastic products of terrestrial impact structures (Wilshire, 1971). On the other hand, the character of plutonic rocks in the returned samples indicates that before impact the crustal rocks were layered and had widely divergent bulk compositions over short vertical distances (Jackson and others, 1975); the chances of mixing compositionally distinct layers during impact would be good.

Dymek and others (1976b) found that the dominant clastic plagioclase is more calcic than the groundmass plagioclase and that clastic olivine and pyroxene tend to be more magnesian than their groundmass counterparts in boulders 2 and 3. These relations are compatible with the hypothesis that the more refractory materials of the target tend to remain as clasts; the less refractory materials contribute preferentially to the melt.

Simonds (1975) found in the station 6 boulder that with increasing grain size of the groundmass, clast abundance and the ratios of mafic to feldspathic clasts and of pyroxene to olivine clasts decrease, whereas groundmass pyroxene and plagioclase become, respectively, more magnesian and more calcic. He related these systematic variations to the effect on cooling of the melt of the initial ratio of clasts to melt. Where

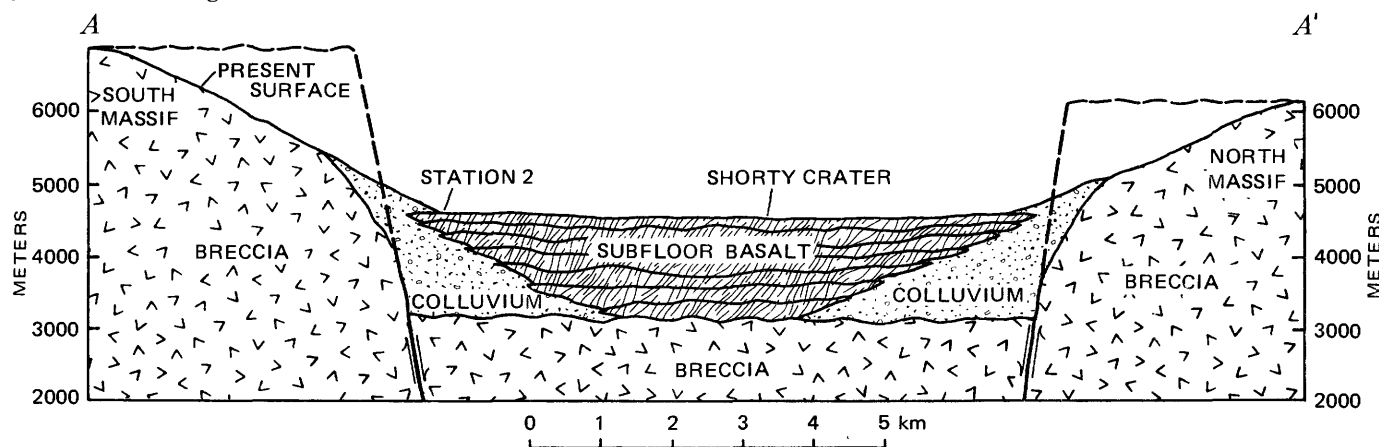


FIGURE 242.—Relations inferred among major subregolith units. Figure 6 shows line of section. Topographic profile derived from National Aeronautics and Space Administration 1:50,000-scale Lunar Topographic Map-Taurus-Littrow (1972). No vertical exaggeration. (From Wolfe and others, 1975.)

this ratio was high, the matrix was rapidly quenched; its grain size is extremely fine, and little or no digestion of clasts occurred. Where the ratio was lower, the melt was less rapidly quenched; hence, its grain size is coarser, and its composition was modified by digestion of the smaller and less refractory clasts.

In spite of these suggestions that the breccia formed by mixing of clasts and melt, the distinction between thermal metamorphic and melt origins for the crystalline groundmass is uncertain. The difficulty in petrologic interpretation is highlighted by the conclusion of James (1976b) that the sample 73215 aphanite, in her view an aggregate of clasts and impact melt, is equivalent in petrography and genesis to the competent breccia of boulder 1, which Ryder and others (1975) interpreted as high-grade metamorphic and partially melted. Chao and others (1975a) interpreted rims formed on xenocrysts in sample 77115 from the station 7 boulder as due to reaction during slow cooling of the enclosing melt. In the same paper, Huebner wrote a rebuttal arguing that the xenocryst rims resulted from subsolidus reaction with the matrix rather than from reaction with a melt (see discussion of sample 77115 for more detailed information). In addition, the compositional and textural relations reported by Simonds (1975) for the groundmass of the station 6 boulder samples could have resulted from progressing reaction between clasts and hot, fine-grained particulate matrix during thermal metamorphism.

In boulder 1 from station 2 and in samples 73215 and 73235 from station 3, the coherent crystalline breccia occurs as clasts in or is invaded by friable breccia or cataclasite. The Marble Cake clast in sample 72275 and the large clast in sample 72235 have cores of feldspathic cataclasite, partly fused in 72235, crudely interlayered and rimmed by crystalline polymict breccia. Polymict breccia and cataclasite are mutually interpenetrative; in the clast from sample 72235 the dark breccia coating is continuous with parts of the banded core. In these clasts both components, polymict breccia and feldspathic cataclasite, were undergoing cataclastic flow simultaneously (Ryder and others, 1975; Wilshire and Moore, 1974).

In sample 76255 from the station 6 boulder, fragments of coherent polymict breccia occur as clasts in norite cataclasite. Relations in the boulder and detailed petrographic study (Warner and others, 1976) show that the norite cataclasite is, in turn, a clast within coherent crystallized polymict breccia.

We infer that such intimate mixing of coherent crystalline breccia and friable breccia or cataclasite occurs not only at centimeter and meter scales, as seen in hand samples and boulders, but is characteristic in the

Taurus-Littrow massifs at scales of tens and hundreds of meters. A telephoto view shows that the upper part of the South Massif (fig. 243) consists of irregular and discontinuous light and dark patches. Boulders are more highly concentrated in the dark patches, which suggests that the dark patches are underlain by more coherent material than the light patches.

Schmitt (1973) reported seeing, high on the South Massif, a linear color boundary with an apparent dip of  $10^\circ$  to  $15^\circ$  W. He suggested that blue-gray material below the boundary and tan-gray material above the boundary may have been represented in separate boulders sampled at the base of the massif. Close examination of orbital and surface photographs shows that this color boundary (fig. 243) may result from fortuitous alinement of some of the light patches. We agree that lithologic differences exist in the massif but suggest that the lithologic units occur in discontinuous pods or lenses rather than as subhorizontal continuous strata. By extrapolation from the intimate intermixture of coherent crystalline breccia, friable breccia, and cataclasite in the sampled boulders, we suggest that the discontinuous lenses seen in the massifs represent the same three rock types. The boulders themselves represent a sample biased toward the more coherent crystalline breccia.

Major-element data, summarized in figure 244, show that the matrices of breccias from the massifs occupy a limited compositional range in which  $\text{Al}_2\text{O}_3$  values are approximately 16 to 23 percent. The major deviation from a well-defined narrow linear trend is shown in samples from rock 72275, which are deflected from the major trend toward the pigeonite basalt that occurs in the sample as clasts and as stringers of cataclasite (compare fig. 75). The matrices of the massif breccias, both competent and friable, are broadly noritic in composition. Rhodes and others (1974) recognized rocks in this compositional range as a major massif component, which they called noritic breccia.

A smaller group of analyzed samples is clustered at values of  $\text{Al}_2\text{O}_3$  of approximately 25 to 28 percent along the same linear trend (fig. 244). These are feldspathic plutonic or metaplutonic rocks—troctolite, gabbro, olivine norite, or their crushed or thermally metamorphosed equivalents—that occur as clasts in the breccia or were collected as loose rocks. Rhodes and others (1974) recognized this group as a second major massif component, which they called anorthositic gabbro on the basis of chemical composition.

An analyzed clast from sample 72255, boulder 1, station 2, extends the linear trend to the composition of anorthosite ( $\text{Al}_2\text{O}_3$  greater than 35 percent). Sample 77215, the large norite cataclasite from the station 7

boulder, and the Civet Cat norite clast from sample 72255, boulder 1, station 2, extend the linear trend in the opposite direction to  $\text{Al}_2\text{O}_3$  values of 14 to 16 percent (fig. 244). Norite samples (78235 and 78527) from the Sculptured Hills have intermediate compositions that are similar but not identical to the breccia matrices.

Major-element data for the regolith samples, summarized in figures 245 and 246, indicate that the highlands component of the regolith can be interpreted as a mixture of comminuted debris derived from breccia matrix material (approximately 16-23 percent  $\text{Al}_2\text{O}_3$ , fig. 244) and feldspathic plutonic and metaplutonic rock (approximately 25-28 percent  $\text{Al}_2\text{O}_3$ , fig. 244). The more feldspathic component occurs as clasts within the breccia; presumably it also occurs within the lenses and stringers of friable cataclasite that we believe are a significant part of the massif rocks.

Rhodes and others (1974) gave "prevalent" compositions, plotted in figures 245 and 246, for the two massif components that they called noritic breccia and anorthositic gabbro. The compositions fit the data of figure 244 well at  $\text{Al}_2\text{O}_3$  values of approximately 18.0 and 26.5 percent; hence the joint between them in figures 245 and 246 reasonably represents the linear trends of figure 244. The highlands-regolith and light-mantle compositions (figs. 245 and 246) show a broad linear trend due to admixture of basalt and ash debris with highlands material. Data points for samples from stations 2, 2a, and 3, where basalt and ash components are minimal or absent, lie on or near the noritic breccia-anorthositic gabbro join. Their positions along the join suggest that the breccia matrix component (noritic breccia of Rhodes and others) is significantly more abundant than the more feldspathic component (anorthositic gabbro of Rhodes and others). In contrast,

Rhodes and others (1974) interpreted chemical data from the sediment samples as indicating general predominance of their anorthositic gabbro component. In either case, the sediment composition may not truly represent the bulk massif composition. It suggests, however, that relatively feldspathic material ( $\text{Al}_2\text{O}_3$  greater than about 25 percent) is more voluminous than might be inferred from its frequency in the massif rock samples.

The massif samples represent rocks from different parts of the two massifs. Those from station 2 probably came from about 1,500 m above the valley floor. The massif breccia at station 3, in the light mantle, came from regolith material transported from an unknown area, perhaps the upper part, of the South Massif. The station 6 boulder apparently rolled from about 500 m above the valley floor on the North Massif, and the source of the station 7 boulder on the North Massif is unknown.

These samples are strikingly uniform in petrographic character and in chemical composition. The only significant deviation from the very narrow range in major-element compositions of the breccia matrix is probably due to local admixture of the pigeonite basalt debris of sample 72275 (figs. 75, 244). Winzer and others (1975a), summarizing large-ion lithophile element data for boulder 1 from station 2, sample 73215, and the stations 6 and 7 boulders, concluded that all are so closely similar as to be considered identical.

Morgan and others (1975) found that most of the Apollo 17 massif breccia shows a distinctive meteoritic trace-element distribution (their group 2) that they believe represents the trace-element signature of the projectile that impacted to form the Serenitatis basin (southern Serenitatis basin of this report). Samples from boulder 1 have a distinctively different trace-

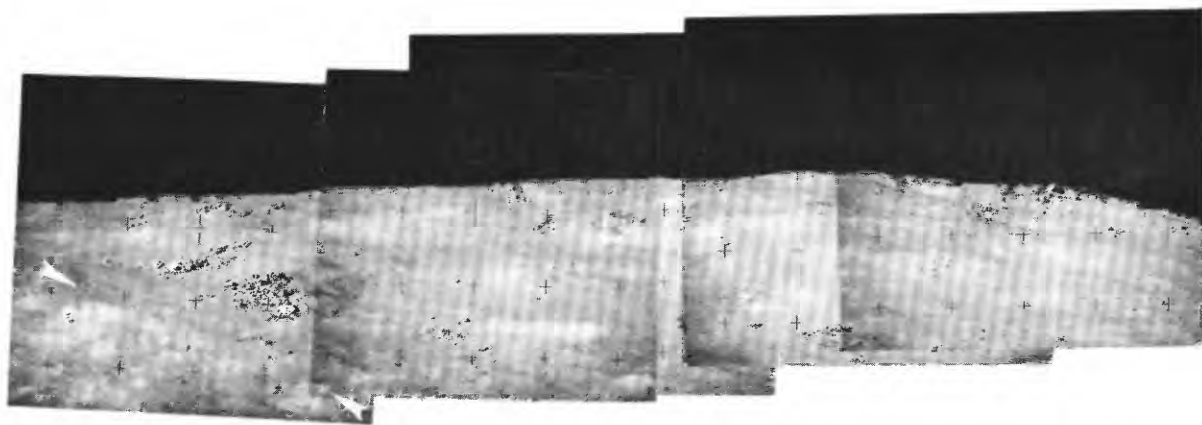


FIGURE 243.—Telephoto panorama showing light-colored and bouldery patches on South Massif. Large patch of boulders at left may be source of station 2 boulders. Arrows are approximately aligned with color boundary described by Schmitt (1973). Width of view is approximately 6 km. (NASA photographs AS17-144-22051-22057.) (From Reed and Wolfe, 1975.)

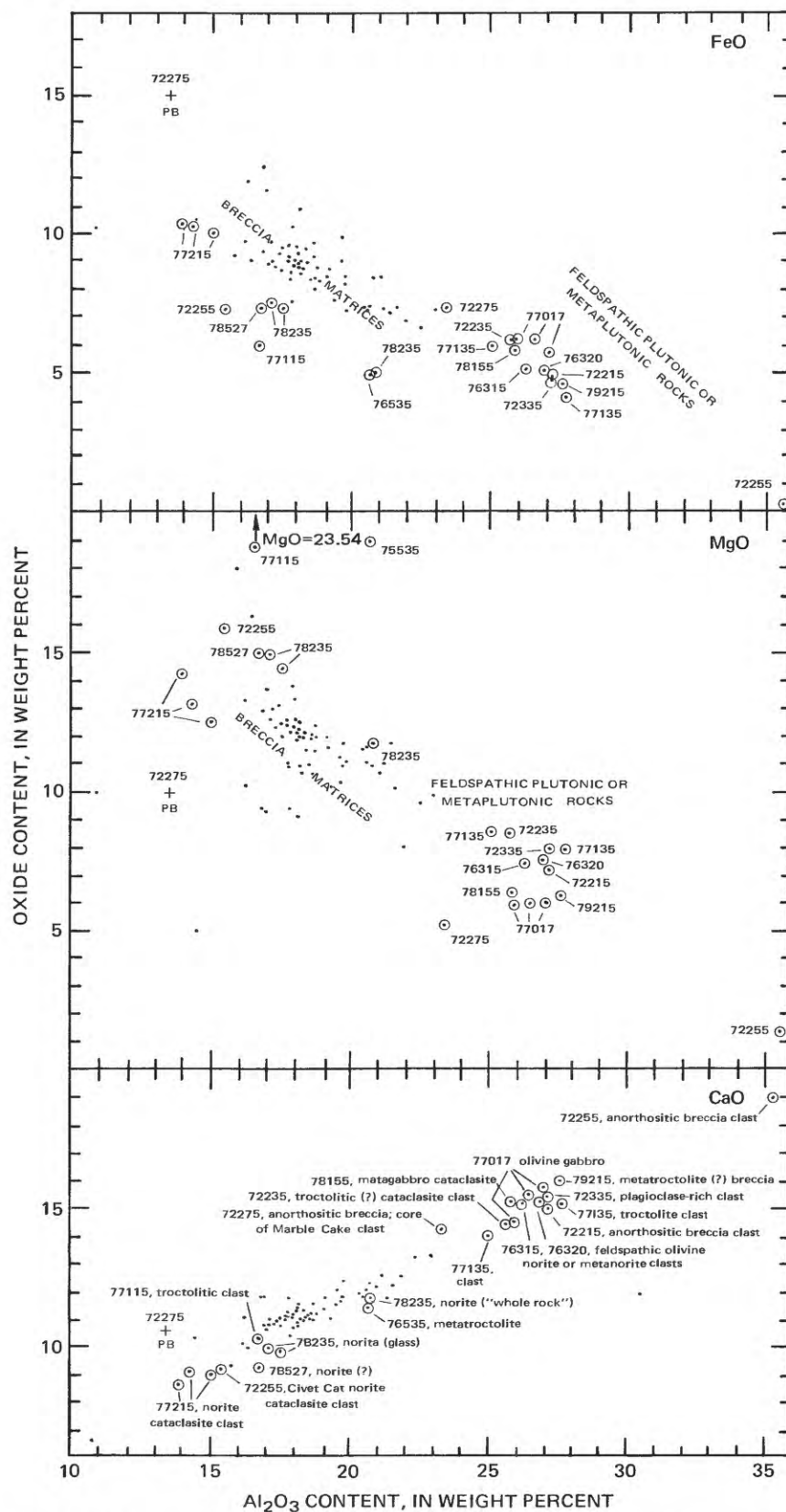


FIGURE 244.—Summary plots of FeO, MgO, and CaO contents in relation to  $\text{Al}_2\text{O}_3$  content for all analyzed Apollo 17 highlands rocks. See sample descriptions for analyses and sources of data. Dots, matrix or presumed matrix of massif breccia; circled dots, plutonic or metaplutonic rocks of the massifs and Sculptured Hills; +PB, pigeonite basalt of sample 72275.

element pattern (their group 3). However, trace-element patterns of groups 2 and 3 have been identified from about a centimeter apart within apparently identical matrix material in sample 73215 (James and others, 1975a). Hence, the two distinct trace-element distributions apparently occur within the same basin ejecta unit.

We conclude from the narrow range of rock types, textures, and major- and trace-element compositions that samples from widely differing parts of the two massifs are virtually identical rocks derived from a single grossly homogeneous ejecta unit represented by at least the exposed portions of the massifs. In detail, the ejecta unit is heterogeneous. It consists of complexly intermixed pods or lenses of coherent polymict breccia, friable polymict breccia, and cataclasite formed from crushed plutonic or metaplutonic rock.

During the southern Serenitatis impact, target material was fractured, sheared, crushed, or melted depending upon its location with respect to the wall of the

rapidly expanding transient cavity. Crushed rock and melt, mobilized and violently mixed, moved upward along the margins of the growing crater with the shearing motion of cataclastic flow (Wilshire and Moore, 1974). This shearing effect is recorded in such fabrics as the lamination of boulder 1 from station 2, the crude interlayering of feldspathic cataclasite and dark competent breccia in some of the clasts of boulder 1, lithologic banding and development of schlieren in sample 73215, and the occurrence in the station 7 boulder of vesicles in green-gray breccia that are both elongated and aligned in trains parallel to the contact with the enveloped blue-gray breccia.

Mobilization and cataclastic flow mixed relatively cold, unshocked mineral and lithic debris with hot, pulverized to molten rock. Extreme temperature gradients existed through short distances. At millimeter and submillimeter scales, thermal equilibrium between superheated melt and cold clasts was largely achieved within seconds (Simonds, 1975; Onorato and others,

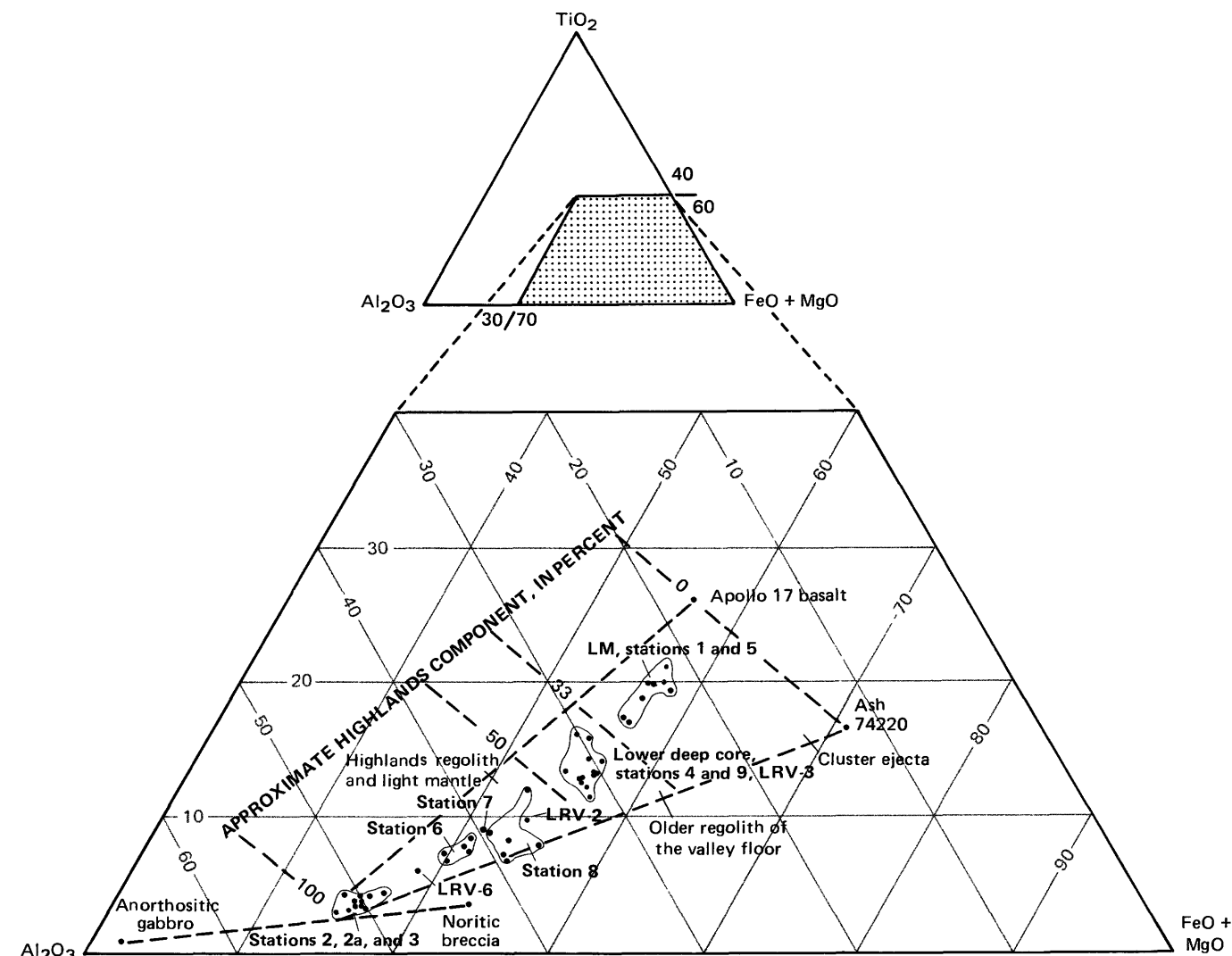


FIGURE 245.—Relative amounts of  $\text{TiO}_2$ ,  $\text{Al}_2\text{O}_3$ , and  $\text{FeO} + \text{MgO}$  in sediment samples grouped by station and stratigraphic unit. Compare with figure 246. Apollo 17 basalt, anorthositic gabbro, and noritic breccia values from Rhodes and others (1974). See sample descriptions for analyses and sources of data for sediment samples.

1976). Where quenching times were sufficiently long, small and less refractory clasts were preferentially digested by the melt; the surviving clasts tend to be biased toward the more refractory compositions (Simonds, 1975). In addition, finely particulate groundmass material may have been biased toward more mafic composition because of preferential concentration in the groundmass of the more easily crushed mafic minerals. These factors may account for the slight differences between crystalline groundmass compositions and bulk breccia matrix compositions reported by Dymek and others (1976b) and by James and Blanchard (1976). On a larger scale, quenched melt fractions were themselves disrupted and mixed with continuously disrupted solid debris during ejection. This produced rocks such as boulder 1, station 2, that contain clasts of the same dark microbreccia as forms the matrix of the coherent breccia.

Immediately after deposition, the ejecta deposit was thermally heterogeneous at scales from centimeters to tens or hundreds of meters. Hot fragmental to partly molten ejecta and relatively cool cataclasite and coherent lithic clasts were intermixed in a melange of lenses, pods, and veins. In this environment, crystallization of the breccia matrix may have resulted both from cooling of the partial melts and from thermal metamorphism of fine-grained materials. Because of the large thermal heterogeneities, the final matrix ranges over short distances from friable to granoblastic or poikilitic and impact fused.

The massif boulders show breccia-within-breccia. Clasts of breccia have been interpreted as recording impact events before the one that created the apparently youngest matrix, and they have led to the conclusion that the target material was largely preexisting breccia (for example, Ryder and others, 1975; Wolfe

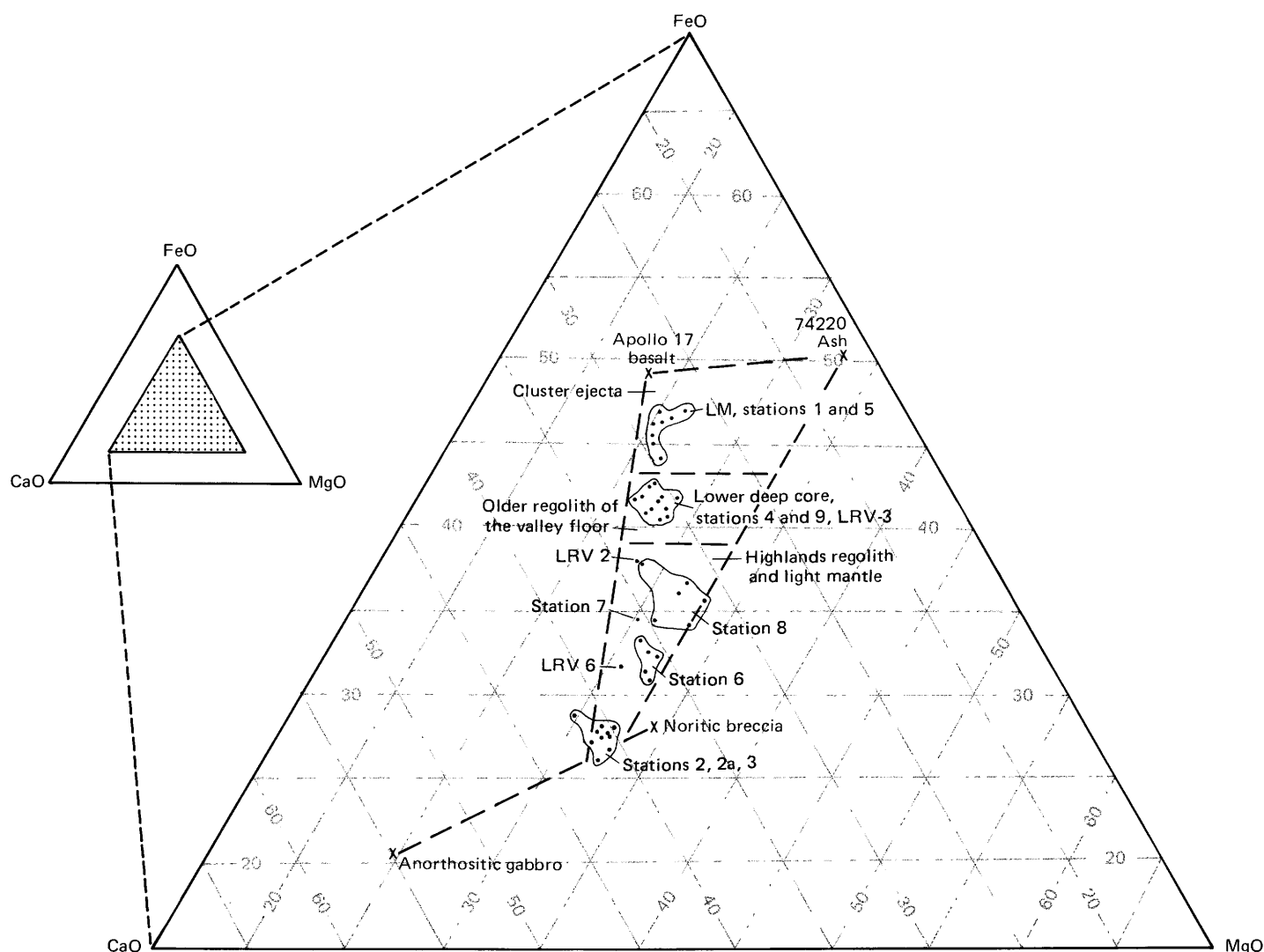


FIGURE 246.—Relative amounts of FeO, CaO, and MgO in sediment samples grouped by station and stratigraphic unit. Compare with figure 245. Apollo 17 basalt, anorthositic gabbro, and noritic breccia values from Rhodes and others (1974). See sample descriptions for analyses and sources of data for sediment samples.

and Reed, 1976). However, in the thermally heterogeneous ejecta deposit that we postulate, friable and competent crystalline breccia in juxtaposition can be interpreted as products of the same impact event rather than of multiple impacts. Hence, clasts of breccia and the matrix that encloses them are commonly similar in composition. For example, the competent-breccia rind of the Marble Cake clast in sample 72275 shows the same distinctive relative enrichment in FeO and CaO and relative depletion in MgO with respect to  $\text{Al}_2\text{O}_3$  (fig. 75) that characterizes the enclosing friable matrix.

The station 7 boulder provides evidence that clasts of aggregated ejecta may develop and maintain coherence during transport and deposition of the ejecta. Fractured blue-gray breccia is enclosed in a matrix of relatively unfractured vesicular greenish-gray breccia (figs. 180 and 185). Vesicles in the apparently younger greenish-gray breccia are flattened and aligned in trains parallel to the contact. The apparently older blue-gray breccia envelops and intrudes a large fragile clast of norite cataclasite (sample 77215). The matrices of the two breccias are nearly identical in composition (fig. 179) and have more or less similar finely crystalline texture. In agreement with Winzer and others (1977), we believe that their similar compositions and textures are unlikely to have resulted from separate impact events. In addition, the apparently older breccia, with its fragile clast, shows no evidence of the cataclasis that might be expected had it been target material that was crushed and melted to form the apparently younger breccia. Hence, we postulate that the blue-gray breccia aggregated and developed sufficient coherence during transport of the ejecta to develop and maintain fractures while being enclosed in still highly mobile cogenetic ejecta.

In accord with the postulate that breccia-within-breccia fabric may form in single impact events, we suggest that the material that was crushed and melted to create the massif breccia was largely excavated for the first time by the southern Serenitatis impact. The population of clasts of identifiable plutonic parentage indicates that the target was a plutonic complex that included dunite, norite, troctolite, gabbro, and anorthosite. Textural evidence from some of the samples (for example, metadunite 72415-18 and metatroctolite 76535) shows that some of the plutonic target rocks had undergone a prolonged deep-seated thermal metamorphism, the Apollonian metamorphism of Stewart (1975), before their excavation by the southern Serenitatis impact.

The linear compositional trends of the breccia matrix (fig. 244) may represent a mixing line. The dominant end members may have been (1) crushed or melted

norite broadly like the norite cataclasite of sample 77215 and the Civet Cat clast in sample 72255 and (2) crushed or melted rock derived from the more feldspathic plutonic rocks (approximately 25 to 28 percent  $\text{Al}_2\text{O}_3$ , fig. 244). Parent rocks of more extreme composition (for example, metadunite 72415-18, metatroctolite 76535, and anorthosite like the highly aluminous clast from sample 72255) were minor components. Winzer and others (1977) reached similar conclusions.

Plutonic rocks with a compositional range much like that of the southern Serenitatis target rocks occur together in relatively small plutonic bodies in the Earth's crust. Hence, no part of the suite is necessarily a sample of lunar mantle.

Chromian spinel-bronzite-diopside symplectites in metatroctolite 76535 may have formed during slow crystallization of a pluton at a 10-30-km depth (Gooley and others, 1974). Because of the uncertainties involved, Dymek and others (1975) objected to this specific depth calculation, but they agreed that the rock had crystallized at fairly great depth. Stewart (1975) inferred from the granular-polygonal texture that the sample had been annealed on the order of  $10^8$  years at a depth of 7 km or more.

Spinel cataclasites from samples collected at stations 2, 3, and 6 have the mineral assemblage anorthosite-aluminous enstatite-olivine-spinel. If this is an equilibrium assemblage, it may have crystallized at pressures of about 3 to 7.5 kb, equivalent to lunar depths of about 60 to 150 km. The small amount of iron in the assemblages may reduce the estimated pressure, but estimated depths are consistent with derivation from the lower crust (Bence and others, 1974; Bence and McGee, 1976).

Approximately 90 radiometric age determinations for Apollo 17 highlands rocks are summarized graphically in figure 247. If, as we believe, these rocks are samples of ejecta from the southern Serenitatis basin, their radiometric ages may date the impact. However, interpretation is complicated because the radiogenic clocks of the target materials were not uniformly reset. Many rocks contain relict grains of the original plutonic assemblage that retain to various degrees their crystallization ages. Others retain a preexcavation metamorphic overprint, and some may have been modified by smaller, more recent impacts.

Several samples clearly record events older than the southern Serenitatis impact. Partly metamorphosed dunite 72417, from boulder 3 at station 2, and troctolite 76535 have Rb-Sr isochron ages, respectively, of 4.55 and 4.61 b.y. These have been interpreted as primary crystallization ages (Papanastassiou and Wasserburg, 1975, 1976). Ages near 4.25 b.y. have also been

determined for metatroctolite 76535 by other techniques. Papanastassiou and Wasserburg (1976)

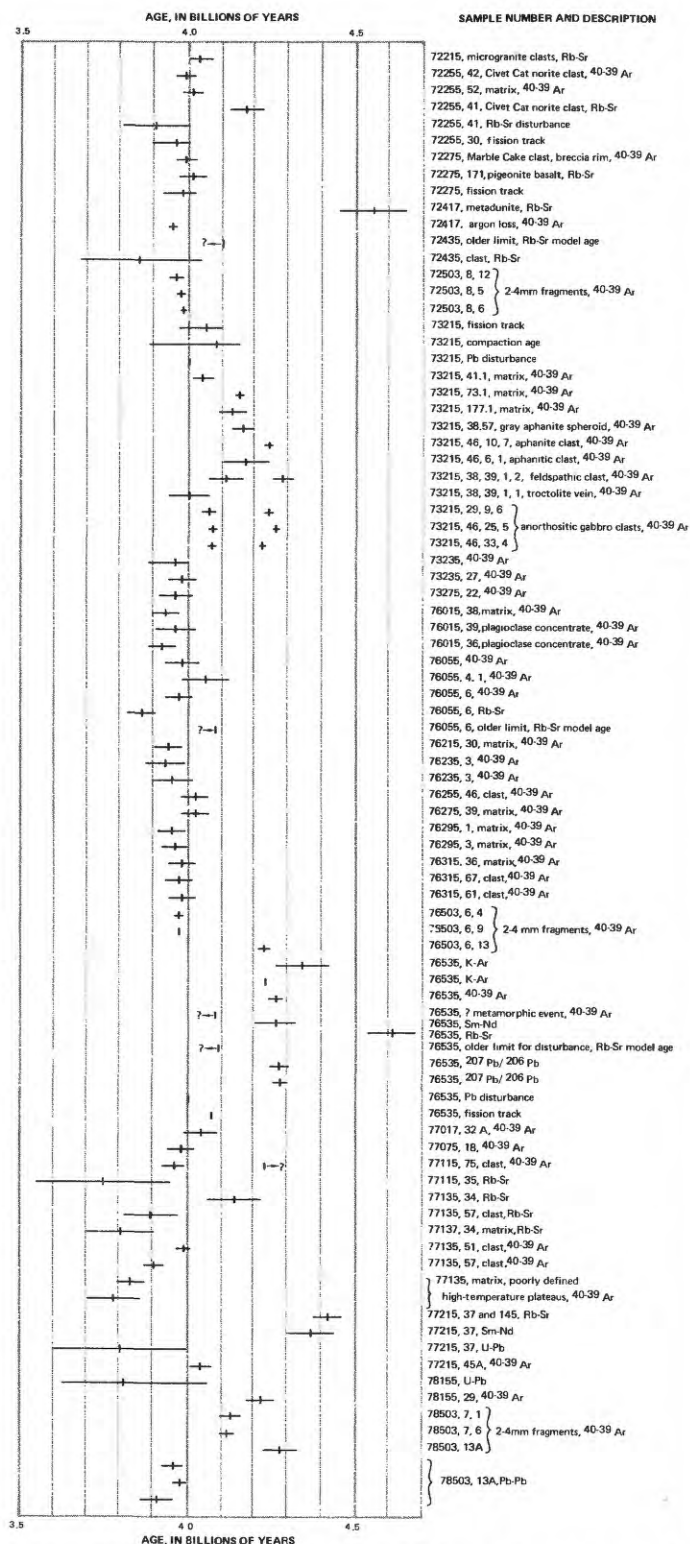


FIGURE 247.—Graphic summary of published radiometric ages for Apollo 17 highlands rock samples. See individual sample discussions for sources of data.

suggested that the temperature of the parent troctolite body remained sufficiently high until approximately 4.25 b.y. ago to permit degassing of Ar and chemical and isotopic exchange of Sm and Nd. Rb-Sr systems, equilibrated 4.61 b.y. ago when the rock initially crystallized, were protected from exchange by impervious enclosing olivine. The proposed episode of elevated temperature could have been responsible for the deep-seated thermal metamorphism that recrystallized both the troctolite and the dunite (Apollonian metamorphism of Stewart, 1975).

Other rocks whose radiometric ages record distinct presouthern Serenitatis events include the Civet Cat norite clast from boulder 1 at station 2, 4.17 b.y. (Compston and others, 1975); clasts in sample 73215 from station 3, approximately 4.25 b.y. (Jessberger and others, 1976b); norite cataclasite clast 77215 from the station 7 boulder, approximately 4.4 b.y. (Nakamura and others, 1976); and some 2-4-mm fragments, 4.13-4.28 b.y. (Schaeffer and others, 1976; Schaeffer and Husain, 1974; Kirsten and Horn, 1974). These ages are younger limits for primary crystallization or for older metamorphic events, because some isotopic equilibration or degassing of argon may have occurred in the southern Serenitatis impact.

Some plutonic or metaplutonic fragments in the ejecta apparently had their radiogenic clocks completely reset. For example, sample 76235, olivine metanorite cataclasite from a large clast in the station 6 boulder, gave  $^{40-39}\text{Ar}$  ages of 3.93 and 3.95 b.y. (Cadogan and Turner, 1976). These are equivalent to the ages determined for the enclosing breccia (fig. 247). Cadogan and Turner (1976) inferred that the clast was strongly heated, resulting in complete degassing of argon during the impact that assembled the materials of the station 6 boulder.

The majority of radiometric ages for massif breccia were determined by the  $^{40-39}\text{Ar}$  technique. Except for two dates for sample 77135 that were determined from short, poorly defined, high-temperature plateaus (Stettler and others, 1974), the  $^{40-39}\text{Ar}$  ages range from 3.90 to 4.24 b.y. and are strongly clustered between approximately 3.9 and 4.0 b.y. (fig. 247).

All of the  $^{40-39}\text{Ar}$  breccia ages greater than 4.05 b.y. are from sample 73215. Evaluating their results for 73215, Jessberger and others (1976b) considered an age of approximately 4.05 b.y. as an older limit for the event that formed the aphanitic breccia matrix, because the abundant small clasts were presumably incompletely outgassed.

If outgassing of argon ranged from partial to complete or nearly complete in the southern Serenitatis ejecta, the measured ages may approach or reach a lower limit that is equivalent to the age of the southern

Serenitatis impact. The concentration of  $^{40-39}\text{Ar}$  ages between 3.9 and 4.0 b.y. may represent that limit, which is in agreement with the conclusion of Cadogan and Turner (1976) that the materials of the station 6 boulder were assembled  $3.96 \pm 0.04$  b.y. ago. Rb-Sr ages for clasts of microgranite and pigeonite basalt, respectively 4.03 and 4.01 b.y. (Compston and others, 1975), impose older limits on the assembly of boulder 1 that are compatible with the overall  $^{40-39}\text{Ar}$  results.

Six Rb-Sr ages of breccia or of clasts within breccia and one U-Pb age (clast in 77215) are in the range from 3.75 to 3.90 b.y. Except for the  $3.86 \pm 0.04$ -b.y. age for breccia 76055 (Tera and others, 1974b), published analytical errors for these ages are sufficiently large to overlap the 3.9 to 4.0 b.y. concentration of  $^{40-39}\text{Ar}$  ages (fig. 247).

For three of these samples (77115,35; 77137,34; 77215,37) the mean ages, 3.75-3.80 b.y. (Nakamura and others, 1976; Nunes and others, 1976; Nunes and others, 1974), are within the range of mean ages determined by both Rb-Sr and  $^{40-39}\text{Ar}$  techniques for subfloor basalt samples. Photogeologic and field evidence indicate that the massif materials are older than the sampled part of the subfloor basalt. Hence, these younger ages ( $\leq 3.80$  b.y.) for massif materials do not date the age of breccia formation.

The other four young Rb-Sr ages are (1) an estimate of  $3.90 \pm 0.1$  b.y. for a Rb-Sr disturbance recorded in Civet Cat norite clast 72255,41 (Compston and others, 1974), (2) a Rb-Sr isochron age of  $3.85 \pm 0.18$  b.y. for a clast in sample 72435 (Papanastassiou and Wasserburg, 1975), (3) a two-point Rb-Sr isochron age of  $3.86 \pm 0.04$  b.y. for metamorphosed breccia 76055 (Tera and others, 1974b), and (4) a Rb-Sr isochron age of  $3.89 \pm 0.08$  b.y. (Nunes and others, 1974) for a clast, sample 77135,57, which also gave a  $^{40-39}\text{Ar}$  age of  $3.90 \pm 0.03$  b.y. (Stettler and others, 1975). At best, these data may suggest that the 3.9 to 4.0 b.y. cluster of  $^{40-39}\text{Ar}$  ages could be slightly older than the true age of the southern Serenitatis impact, perhaps because of argon entrapment.

#### SCULPTURED HILLS

As already described, material of the Sculptured Hills, by analogy to the knobby facies of the Montes Rook Formation of the Orientale basin (Scott and others, 1977), is interpreted as ejecta of the southern Serenitatis basin. The unit was deposited after deposition and faulting of the massif breccia. The Sculptured Hills differ markedly from the massifs because of their distinctive hummocky topographic form, undulating gentler slopes, absence of resistant ledges, and near-absence of boulders.

Orbital and lunar surface photographs show that station 8 is in an area of dark, relatively fine surficial

material. Regolith samples contain a large admixture of valley-floor material, probably dominantly ash (figs. 245 and 246). Rock fragments are mainly basalt and regolith breccia. Apparently the station 8 area is largely mantled by ejecta from the valley floor and by volcanic ash. Hence, we do not have a definitive sample of Sculptured Hills material.

No crystalline breccia was seen by the crew or included among the larger samples. Three fragments that might represent crystalline breccia matrix material were found among the 27 fragments of 2-4-mm size that were examined in sample 78503 (Bence and others, 1974). The other 24 fragments were identified as basalt (14), regolith breccia (5), glass (2), and anorthosite-norite-troctolite (3).

Three highland rocks weighing more than 5 g were sampled. These are metagabbro cataclasite (78155), norite boulder (78235-38, 78255), and a noritic rake-sample fragment (78527). Any or all of these could have been transported from outside the Sculptured Hills to the station 8 area by impacts younger than the southern Serenitatis basin event. However, if they are Sculptured Hills fragments and if competent massif-type breccia really is scarce or absent as suggested by its absence in the samples, by the scarcity of boulders and ledges, and by the hummocky subdued topographic form of the Sculptured Hills, we can tentatively suggest that the Sculptured Hills unit is predominantly friable cataclasite excavated from the plutonic and metaplutonic rocks of the southern Serenitatis target.

#### HIGHLANDS MATERIALS YOUNGER THAN THE SOUTHERN SERENITATIS BASIN

Basin ejecta younger than the southern Serenitatis basin may occur in the Taurus-Littrow highlands. Moore and others (1974) have suggested that the Apollo 17 site lies within the area that may have been blanketed by Imbrium ejecta. Crisium ejecta might also be present in the Apollo 17 area. Scott and Pohn (1972) have mapped lineated terrain north of the crater Littrow as well as still farther north in the vicinity of the Taurus Mountains. They suggested that in the latter area the lineated terrain, which is radial to the Imbrium basin and was mapped by Wilhelms and McCauley (1971) as the Fra Mauro Formation, may include Imbrium ejecta. The lineated terrain north of Littrow, which was regarded as pre-Imbrium by Wilhelms and McCauley (1971), is not radial to either Imbrium or Crisium; we assume that it represents basin or large-crater ejecta deposited before the Imbrium impact. Scott and Pohn (1972) did not recognize any lineated terrain south of Littrow. The preservation of pre-Imbrium lineated terrain north of Littrow and the

absence of sculpturing related to Imbrium or Crisium in the Taurus-Littrow area suggest that Imbrium and Crisium ejecta, if present, are thin or scattered in the Taurus-Littrow area.

Further evidence that ejecta from Imbrium or Crisium is thin, scattered, or absent in the Apollo 17 area is provided by the preservation of the Sculptured Hills topography. If our correlation of the Littrow ring and the outer Rook ring is valid, the Sculptured Hills terrain is related in origin to the southern Serenitatis impact. Its distinctive topography would not be visible through great thicknesses of Imbrium and Crisium ejecta.

In addition to the physiographic evidence, the chemical and petrographic similarities of the massif breccia samples, particularly the boulders from stations 2, 6, and 7 and breccia samples 73215, 73235, and 73275 from station 3, strongly suggest that they represent ejecta from a single impact. There is no compelling evidence from the samples that ejecta from basins younger than southern Serenitatis has been sampled.

#### SUBFLOOR BASALT

Basalt, estimated to be about 1,400 m thick in the landing site (Cooper and others, 1974), partially flooded the Taurus-Littrow graben. It rests on a surface that is presumably underlain by breccia near the axis of the valley and by the colluvial wedges near the valley margins (fig. 242). Because the informal name subfloor basalt has been used repeatedly for the basalt of the landing site since the time of the mission, we continue its use here. It is part of a regionally extensive unit designated Imb<sub>2</sub> in plate 1.

The upper surface of the subfloor basalt is overlain by volcanic ash and impact-generated regolith with an estimated average combined thickness of 14 m (fig. 248). All sampled basalt was collected from the regolith.

Basalt fragments a centimeter or more in size were collected at all stations except 2 and 2a and some of the LRV stops. Basalt boulders half a meter or more in size were sampled in the LM area and at stations 1, 4, and 5. Boulders at stations 1, 4, and 5 may have been excavated for the first time from the subfloor basalt by the impacts that formed, respectively, Steno, Shorty, and Camelot craters. Smaller fragments and the boulders of the LM area (for example Geophone rock) cannot be related to specific source craters. Most are probably from the upper part, perhaps the upper 100 m or so, of the subfloor basalt.

On the basis of direct field observations, Schmitt (1973) described the basalt blocks in the central valley floor as "mostly massive, tan to pinkish gray coarse-grained ilmenite basalt having a generally coarsely

ophitic and vesicular texture." Layering in the blocks at Camelot crater was recognized as due to differences in vesicle concentrations. Vugs and vesicles range from less than 1 percent to 30 percent by volume in the basalts, and their occurrence as layers is described in several of the station 1 rake samples (Butler, 1973).

The mineral proportions in the basalts vary widely. A compilation by Papike and others (1976) gives the following ranges (excluding one sample with 54 percent mesostasis): clinopyroxene 42-51 percent; olivine 0-10 percent; plagioclase 14-33 percent; opaque minerals (mainly ilmenite, armalcolite, spinel) 15-30 percent; silica (tridymite?) 0-5 percent. Textures range from very fine (grain size 0.25 mm or less) to coarse (grain size up to 2-3 mm).

The Apollo 17 basalt has been divided into two types on the basis of texture and mineralogy (Papike and others, 1974; Papike and others, 1976; Brown and others, 1975; Warner and others, 1975b). Most of the examined samples are in the very-high-titanium basalt group of Papike and others (1976). They include both fine- and coarse-grained olivine basalts that are broadly similar in major-element composition and that have been inferred to vary in grain size because of differences in cooling rates (Papike and others, 1974, 1976; Warner and others, 1975b).

The second type, Apollo 17 low-potassium basalt of Papike and others (1976), resembles the Apollo 11 low-potassium basalt in texture and mineralogy. This basalt, characterized by scarcity or absence of olivine, is represented by the large blocks on the rim of Camelot crater (samples 75015, 75035, 75055) and by 5 out of more than 100 basaltic rake-sample and 2-4-mm fragments (Papike and others, 1974; Warner and others, 1975b) from widely separated parts of the traverse area.

The early published major-element chemical data suggested that the basalts formed two narrowly ranging and mutually exclusive compositional groups that coincided with the two petrographic groups. The olivine-poor basalts (Apollo 17 low-potassium type) were quartz normative; the dominant olivine basalts (very-high-titanium basalt) were olivine normative. Papike and others (1974) suggested that the abundant fine- and coarse-grained basalt of the latter type might be from, respectively, the rapidly cooled top and the slowly cooled center of a single lava flow. Subsequently, Papike and others (1976) concluded that the absence of a systematic correlation between major-element composition and grain size may indicate that the very-high-titanium basalt samples came from multiple cooling units.

Considering the restricted occurrence of the quartz-normative basalt (Apollo 17 low-potassium type) on the

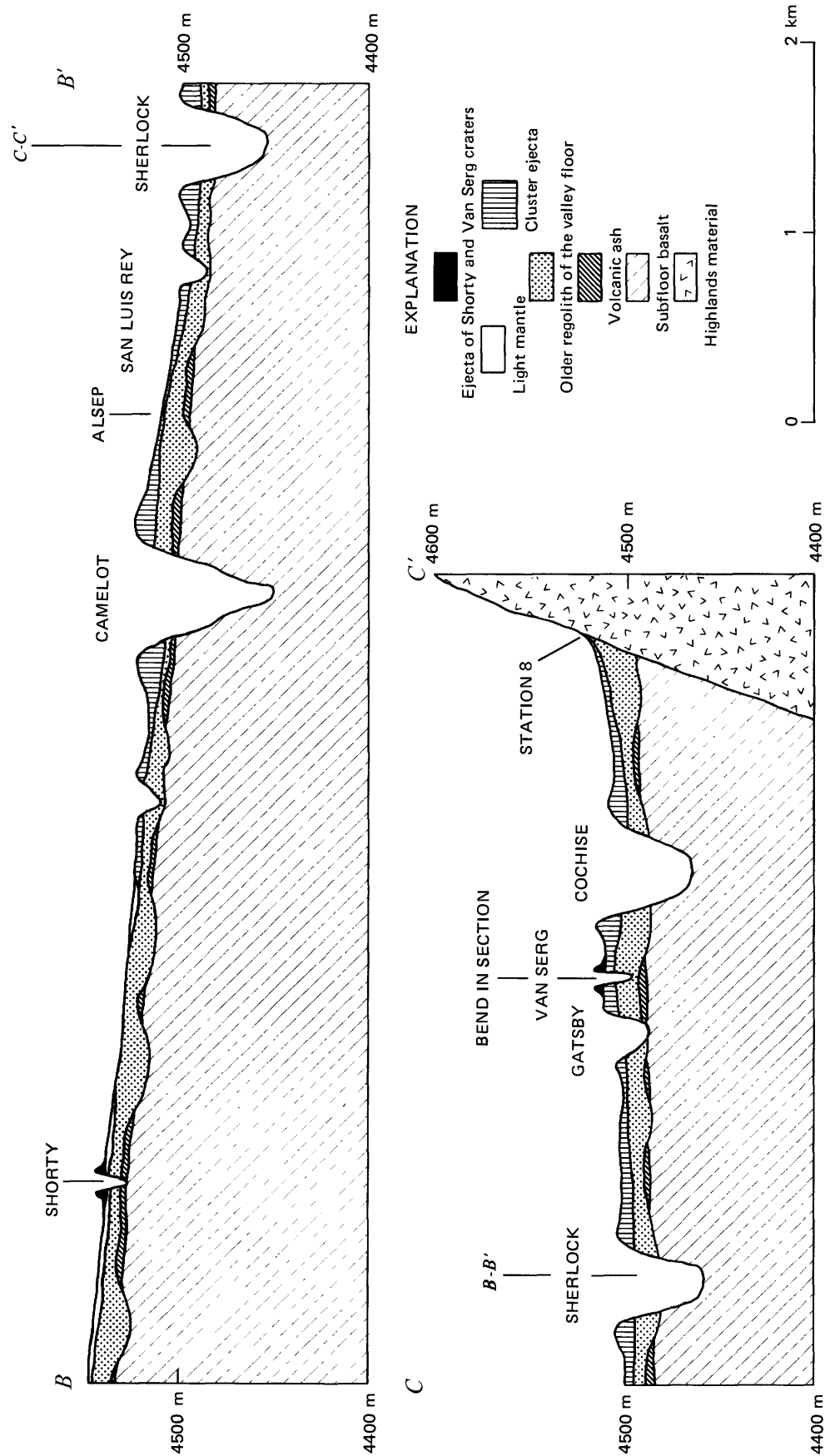


FIGURE 248.—Cross sections showing relations inferred among the subfloor basalt and the overlying volcanic ash and regolith units. Figure 6 shows locations of sections. Topographic profile derived from National Aeronautics and Space Administration 1:50 000-scale Lunar Topographic Map-Taurus-Littrow (1972). Vertical exaggeration is  $\times 10$ . (Modified from Wolfe and others, 1975.)



spect to Shorty, Steno, and Camelot craters. Type C basalt samples 74255 and 74275, came from, respectively, 5-m and 20-cm boulders on the rim of Shorty crater (fig. 120). Type C basalts have been identified at no other locality. Field and topographic evidence suggests that the Shorty impact excavated down to or just into the subfloor basalt. Hence, it is probable that the type C basalt represents the uppermost subfloor basalt in the vicinity of Shorty.

Type B basalt was collected at station 1 from two half-meter boulders on the rim of a fresh 10-m crater (figs. 35, 41) located 150 m from the rim crest of the 600-m Steno crater. It is likely that the impact that formed the 10-m crater reexcavated these boulders from the Steno crater ejecta, or at least repositioned them. Because the boulders are 150 m out on the Steno ejecta blanket, they probably came from an intermediate depth, perhaps some tens of meters, in the Steno target.

The highly fractionated type A basalt samples were collected from three large blocks on the rim of the 650-m crater Camelot (figs. 132, 135). Because they occur on the rim of the largest sampled crater, they may be from the deepest sampled part of the subfloor basalt. A depth of 100 m or more is possible.

The simplest interpretation of these relations is that at least three flow units, in ascending order, highly fractionated type A basalt, type B basalt, and type C basalt, are represented in the basalt samples. Whether types A, B, and C occur as single or multiple flow units and whether such multiple units are complexly inter-layered with each other as well as with basalt represented by samples of uncertain affiliation are presently unknown.

Radiometric ages for the subfloor basalt are almost entirely between 3.67 and 3.83 b.y. (fig. 250). The data are insufficient to strongly support or refute stratigraphic interpretations. However, all seven ages determined for samples 75035 and 75055, which are highly fractionated type A basalts from Camelot crater, have mean values of 3.76 to 3.83 b.y. This occurrence at the older end of the age range weakly supports the inference from field relations that the samples from Camelot may be among the stratigraphically lowest. No other type A basalts have been dated. The single age for a type B basalt (sample 70215) is even older, 3.84 b.y. Three ages determined for type C basalt (sample 74255 and 74275) range from 3.70 to 3.83 b.y., completely overlapping the range reported for the Camelot blocks.

Rhodes and others (1976) concluded that the well-defined basalt types A, B, and C are not related to each other by low-pressure crystal fractionation but are derived from separate parent magmas whose trace-ele-

ment distributions require derivation from chemically distinct parts of a heterogeneous source.

Models of possible source region characteristics have been reviewed by Papike and others (1976). Briefly, they are (1) the cumulate model, in which the basalt was generated by partial melting of cumulate rocks formed as complements to the feldspathic crust in the early melting and differentiation of the outer 1,000 km of the Moon; (2) the primitive source model, wherein the basalt was generated by partial melting of undifferentiated primitive lunar material equivalent in composition to the bulk composition of the Moon; and (3) the assimilative model, in which low-titanium melt was generated in primitive lunar material inferred, in this model, to exist below 400 km. High-titanium basalt is inferred to have been generated by assimilation when the low-titanium basaltic liquid passed through the cumulate zone below the feldspathic lunar crust.

#### VOLCANIC ASH

Weakly coherent material consisting of orange glass

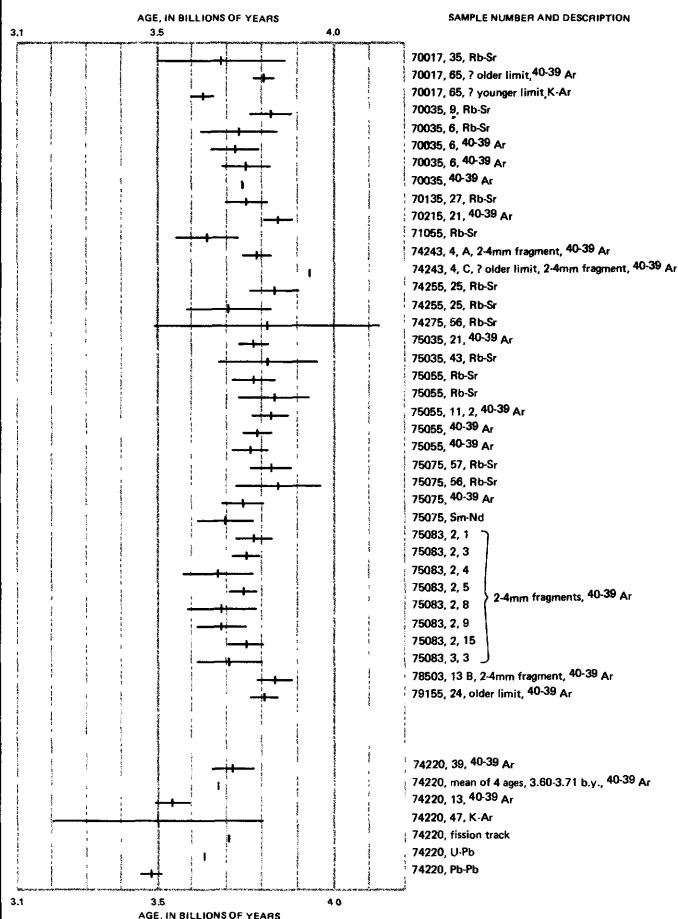


FIGURE 250.— Published radiometer ages for samples of subfloor basalt and volcanic ash. See individual sample discussions for sources of data.

beads was sampled in a trench on the rim of Shorty crater. Color photographs show that the sampled area is one of several patches of orange "soil" on the rim and walls of Shorty. The orange material exposed in the trench is 80 cm wide and may extend for several meters parallel to the axis of the rim crest. It is bounded laterally by gray sediment that represents valley-floor regolith material. A 70-cm drive tube placed in the axial part of the colored zone bottomed in a deposit of opaque black glass beads; the contact between the orange and black glass beads is apparently at about a 25-cm depth in the drive tube.

Heiken and others (1974) described the black and orange materials as well-sorted droplets ranging in size from less than 1  $\mu\text{m}$  to about 1 mm; mean grain size is about 40  $\mu\text{m}$ . The orange droplets consist of homogeneous orange glass. A few contain olivine phenocrysts, and nearly half are partly or completely crystallized to ilmenite or intergrown ilmenite and olivine. The black droplets are partly to completely crystallized equivalents of the orange glass droplets. No droplets contain lithic debris or shocked crystal fragments.

The orange and black droplets show striking chemical homogeneity. The bulk sample (74220) from the rim of Shorty crater is much more mafic than the subfloor basalt and is distinctly different in trace-element composition (Apollo 17 PET, 1973). Citing the chemical and petrographic homogeneity and the absence of lithic and shocked crystal fragments, Heiken and others (1974) concluded that the glass beads were introduced as a pyroclastic deposit produced by fire fountaining near the edge of Mare Serenitatis. The deposit represents a magma distinct from that which formed the underlying subfloor basalt.

We interpret the patches of orange material on the rim and walls of Shorty crater as clods of ejecta excavated from a unit of volcanic ash in the Shorty target area (fig. 242). The dimensions of the sampled patch suggest that the unit of ungardened ash in the target must once have been at least 70 cm thick. That the sampled clod represents a once-widespread sheet is suggested by the ubiquitous occurrence of orange and black droplets in all of the valley-floor regolith samples (Heiken and McKay, 1974).

Even greater regional extent of the ash is indicated by telescopic spectral mapping. The Apollo 17 landing site lies within an area that was previously mapped as dark-mantle material (Scott and Carr, 1972) near the southeastern edge of Mare Serenitatis. Adams and others (1974) showed that this area is characterized by abnormally high ultraviolet and near-infrared reflectance. They found that the black droplets from Shorty crater have a unique reflectance spectrum that is also characterized by high reflectance in the ultraviolet and

near-infrared and concluded that regolith in the spectrally distinct region contains a significant black droplet component. Albedo data of H. E. Holt (Muehlberger and others, 1973) also suggest that dark material, most probably the black droplets, has been added to impact-generated basaltic and highlands regolith in an extensive area, including the landing site, near the southeastern edge of Mare Serenitatis. Such regolith, darkened by admixed ash, is the so-called dark mantle. Its distribution is the basis for mapping the extent of the volcanic ash (pl. 1).

Heiken and others (1974), citing the occurrence of basalt fragments on the Shorty crater rim, suggested that the ash unit was rapidly buried after its deposition, either by later basalt flows or by a large ejecta blanket, protecting the materials sampled at Shorty crater from the solar wind and micrometeorites. It seems probable to us, however, that basalt flows do not overlie the ash. Shorty excavated clods of volcanic ash from within about 14 m of the precrater surface. A basalt flow that overlies the ash in the Shorty target area would occupy a significant part of that 14-m interval. The largest block seen on the Shorty crater rim is about 5 m across. Excavation of basalt from a 5-m-thick flow overlying the volcanic ash would most probably be recorded by an abundance of basalt blocks on the crater rim and walls. Although a few basalt blocks do occur, the wall, rim, and flank materials of Shorty are predominantly unconsolidated fine-grained material, which suggests that no such flow is present. Furthermore, in topographic profiles of Shorty and other craters, we have recognized no evidence to suggest that a coherent basalt overlies relatively incoherent ash in the interval between the surface and the crater floors.

Another line of reasoning also favors the occurrence of the volcanic ash above the youngest subfloor basalt. In 19 samples of dark regolith material from the valley floor (LM area, station 1, LRV-3, station 4 excluding the nearly pure ash of trench sample 74220 and drive tube 74001, station 5, LRV-7, LRV-8, and station 9), the ubiquitous orange and black droplets average 10.6 percent and reach nearly 20 percent of the 90-150- $\mu\text{m}$  fraction (Heiken and McKay, 1974). In addition, interpretation of spectral data indicates that they occur in the regolith over a much broader area than the landing site proper (Adams and others, 1974). Their significant abundance and widespread occurrence in the regolith, which imply that the ash was easily accessible to impact gardening over a wide area, are better explained by the occurrence of the glass-bead unit above, rather than below, the youngest subfloor basalt flows.

Many of the impact craters that formed since the volcanic ash was deposited extended downward into the

underlying subfloor basalt. Therefore, the ash now occurs only as discontinuous remnants (fig. 242).

The original thickness of the ash can be estimated only indirectly. It must be at least as great as the minimum dimension of the clods of ash on the Shorty crater rim (presumably greater than 70 cm), and it must be less than the combined thickness of ash and valley-floor regolith.

Craters with flat floors or central mounds have been formed experimentally in targets where unconsolidated material overlies coherent material; the difference in elevation between the precrater surface and the crater floor in such craters is approximately equivalent to the thickness of the unconsolidated layer (Oberbeck and Quaide, 1967; Quaide and Oberbeck, 1968). Profiles were made by analytical stereoplotter of all flat-floored or central-mound craters that we could identify on orbital panoramic camera photographs of the Taurus-Littrow valley floor. For 39 of the 40 craters profiled, the measured difference in elevation between the estimated precrater surface and the floor is between 5 and 28 m; approximately three-fourths are clustered at values from 8 to 17 m (fig. 251). The mean for the entire group is about 14 m.

Profiles show that the floors of Van Serg, Shorty, and Gatsby craters are respectively about 11, 14, and 17 m below their estimated target surfaces. Crew observations, lunar surface photographs, and returned samples suggest that the Van Serg impact did not excavate subfloor basalt at 11 m and that Shorty crater may have just reached the subfloor basalt at 14 m (Muehlberger and others, 1973; Apollo Field Geology Investigation Team, 1973; Schmitt, 1973). Enlarged panoramic camera photographs show nearly a dozen meter-size or larger blocks in and near Gatsby crater, which suggests that Gatsby excavated subfloor basalt at a depth of about 17 m. Abundant large blocks are visible in and around most of the craters larger than Gatsby.

The data from Van Serg, Shorty, and Gatsby as well as from the 40 crater profiles suggest that 14 m is a reasonable estimate for the average thickness of unconsolidated material above the subfloor basalt. The results of the active seismic experiment are permissive with respect to this estimated average. Cooper and others (1974) have offered two models based on the seismic data: (1) The top of the basalt is at a depth of 7-12 m, and (2) the top of the basalt is at a depth of 32 m.

If the average proportion of orange and black drop-lets measured by Heiken and McKay (1974) in dark regolith samples of the valley floor (10.6 percent) is representative of the proportion of ash in the 14-m average thickness of unconsolidated deposits, it implies that a minimum thickness of the original ash bed was

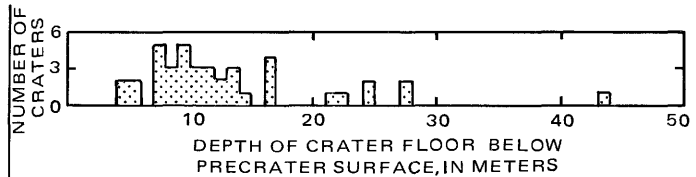


FIGURE 251.—Elevation differences between precrater surfaces and floors of flat-floored or central-mound craters. (From Wolfe and others, 1975.)

approximately 1.5 m. Two observations suggest that the original thickness was greater than 1.5 m: (1) The occurrence of clods of pure ash in the ejecta of Shorty crater shows that not all of the original ash deposit has been mixed into the regolith, and (2) the impacts that formed the many large fresh craters in the landing area (pl. 2) excavated deep into the subfloor basalt. The widespread ejecta of these craters is relatively enriched in basalt debris, hence relatively poor in volcanic ash. Therefore, the 10.6-percent average is probably a minimum value for the average proportion of volcanic ash in the unconsolidated deposits of the valley floor.

The regolith at the Apollo 11 site, developed on basalt similar in composition and age to the subfloor basalt, is 3 to 6 m thick (Shoemaker and others, 1970). An equivalent thickness probably would have formed on the subfloor basalt at Taurus-Littrow if there were no other contributing sources. However, the nearby highlands have provided a large amount of debris to the valley floor (figs. 245 and 246), perhaps enough to increase the regolith thickness 5 to 10 m. Given an average combined thickness of 14 m, we can speculate that the original ash thickness was 4-9 m. Much of that ash has been reworked by impact gardening so that it now occurs as a component of the regolith.

Radiometric age measurements (fig. 250) support the hypothesis that the ash overlies the youngest subfloor basalt. Mean ages determined for the ash range from 3.48 to 3.71 b.y. Hence they overlap a few of the younger ages determined for the subfloor basalt. Ages determined for large blocks of basalt (samples 74255 and 74275) on the rim of Shorty, which may represent the stratigraphically highest basalt included among the samples, range from 3.70 to 3.82 b.y., barely overlapping the range of ages for volcanic ash sample 74220.

Tera and Wasserburg (1976) determined a Pb-Pb age of  $3.48 \pm 0.03$  b.y. for carefully separated and cleaned glass spheres. They suggested that Ar entrapment and Pb contamination by components other than orange glass in sample 74220 were responsible for the greater ages determined by other investigators. All Apollo 17 basalt ages determined so far are distinctly older than this 3.48 b.y. age for the volcanic ash (fig. 250).

A dark mantle with local orange and red material has been described in the Sulpicius Gallus region at the

southwest edge of Mare Serenitatis (Lucchitta and Schmitt, 1974). It has low albedo and an unusually smooth surface like the smooth dark surface of the so-called dark mantle of the Taurus-Littrow region (Lucchitta, 1973). Presumably it also represents a deposit of volcanic ash (Head, 1974c; Lucchitta and Schmitt, 1974), and it could be correlative with the ash of the Apollo 17 area. As in the Taurus-Littrow region, the Sulpicius Gallus dark mantle occurs on older highly faulted mare basalts. Younger, lighter appearing basalt of Mare Serenitatis overlaps the faulted basalt and its mantling ash deposits in both regions (pl. 1; Howard and others, 1973). On the basis of crater morphology, Boyce (1976) has estimated the age of the younger lava in the southern part of Mare Serenitatis at  $3.4 \pm 0.1$  b.y.

The abnormal thickness of unconsolidated ash-bearing material overlying the subfloor basalt resulted in the formation of a relatively smooth dark surface, interpreted before the mission as the manifestation of a very youthful dark mantling deposit. Statistical crater studies (Lucchitta and Sanchez, 1975) showed that large craters (diameter greater than 175 m) are more abundant on the dark surface than on the lighter surface of Mare Serenitatis, a result in accord with the age differences interpreted on photogeologic grounds. However, there is a marked deficiency of craters in the 100-200-m size range on the dark-mantled surface; the density of craters in this size range is less than half that on the light mare surface. As an alternative to the now untenable hypothesis that the smaller craters were buried by a younger dark mantle deposit, we suggest that they have been degraded beyond recognition at an abnormally high rate because they formed in an abnormally thick layer of unconsolidated material. Their counterparts in age and size on Mare Serenitatis, where normally thin regolith overlies mare basalt, have been well preserved because the volumes of those craters are largely within basalt rather than within soft ash and regolith.

#### REGOLITH

Impact-generated regolith of the Taurus-Littrow valley is a mechanical mixture that consists largely of debris derived from the highlands, from the subfloor basalt, and from the volcanic ash. Chemical compositions of regolith material (figs. 245, 246) form a continuum from the nearly pure highlands material of station 2 and the light mantle to the basalt-rich regolith of the LM area and stations 1 and 5. Geologic relations in combination with compositions enable us to distinguish highlands regolith and three major valley-floor units: (1) older regolith of the valley floor, (2) cluster ejecta, and (3) light mantle (fig. 242). A plot showing relative amounts of  $\text{TiO}_2$ ,  $\text{Al}_2\text{O}_3$ , and  $\text{FeO} + \text{MgO}$  in sediment

samples (fig. 245) suggests that highlands material makes up more than 50 percent of sediment collected at highlands and light-mantle stations, approximately 33 to 50 percent of sediment in the older valley-floor regolith, and less than 33 percent in samples of cluster ejecta. A second plot (fig. 246), showing relative amounts of  $\text{CaO}$ ,  $\text{MgO}$ , and  $\text{FeO}$ , shows an almost identical distribution of data points, except that the apparent proportions of highlands component are slightly lower. Boundaries between the three groups of regolith samples have been drawn in figure 246 at positions equivalent to approximately 45 and 25 percent highlands material.

#### HIGHLANDS REGOLITH

Nearly pure highlands regolith is exemplified by the sediment samples from station 2 at the base of the South Massif and station 2a on the nearby surface of the light mantle. The compositions of these samples approximate a mixture of the two major components of the massif (fig. 244), breccia matrix material (noritic breccia of figures 245 and 246) and feldspathic plutonic or metaplutonic rocks (anorthositic gabbro of figures 245 and 246), and a small amount of basalt and ash debris from the valley floor. Heiken and McKay (1974) recognized a few percent of ash and basalt in the 90-150- $\mu\text{m}$  fraction in these particular samples. Rhodes and others (1974) suggested on chemical grounds that they contain, on the average, about 6 percent ash, 2 percent basalt, and approximately equal amounts of noritic breccia and anorthositic gabbro. The near absence of valley-floor material at station 2 and the chemical similarity between regolith samples from stations 2, 2a, and 3 (figs. 245 and 246) suggest that the light mantle may completely cover the surface in the station 2 area.

At stations 6, 7, and 8, at the bases of the North Massif and Sculptured Hills, the sediment compositions reflect the addition of a large valley-floor component. Such an admixture is to be expected close to the mare-highlands boundary and may be enhanced at these particular stations, which we interpret as down-range from the abundant clustered craters of the valley floor. Subfloor basalt fragments, included among the samples from stations 6, 7, and 8, are all presumably ejecta fragments from craters of the valley floor.

The data points for stations 6 and 8 are near or coincident with the join drawn between the volcanic ash and highlands compositions in the triangular diagrams (figs. 245, 246). Possibly volcanic ash reworked from the surfaces of the North Massif and Sculptured Hills is a major component at these stations. For station 8 in particular this would be in agreement with the photo-

geologic observation that the station is in an area of dark smooth surficial material. However, orange and black glass are relatively minor components of the 90-150- $\mu$ m sediment fractions at these stations (Heiken and McKay, 1974). Debris from magnesium-rich norite similar in composition to samples 78235 and 78527 from station 8 or, to a lesser extent, debris from the noritic massif matrix material would also tend to drive the sediment compositions toward, if not below, the highlands-volcanic ash join.

#### OLDER REGOLITH OF THE VALLEY FLOOR

The older regolith of the valley floor is debris generated by impact processes over the long period ( $\sim 3.5$  b.y.) between emplacement of the volcanic ash and the much more recent formation of the cluster ejecta and light mantle. Samples include sediment and regolith breccia from ejecta on the rim of Van Serg crater (station 9), gray ejecta from the trench on the rim of Shorty crater (station 4), sediment from the lower 2 m of the deep drill (70001-70009), and sediment collected at LRV-3. The unit is a mixture of basalt debris, ash, and highlands debris (figs. 245, 246; Heiken and McKay, 1974; Rhodes and others, 1974). Highlands component makes up approximately 30 to 50 percent; hence, the older regolith unit is intermediate within the compositional continuum from highlands and light-mantle sediment to basalt-rich cluster ejecta. Its thoroughly mixed character implies a long history of homogenization of ejecta derived largely from the local highlands, the subfloor basalt, and the volcanic ash.

#### CLUSTER EJECTA

The uppermost part of the regolith in the area of the LM and stations 1 and 5 consists of basalt-rich sediment with significant but subordinate admixtures of highlands debris and ash (figs. 245 and 246; Heiken and McKay, 1974; Rhodes and others, 1974). The base of this unit, denoted here as the cluster ejecta, occurs between 30 and 93 cm depths (approximate positions of the analyzed samples denoted 70008 and 70006, respectively, in fig. 10) in the deep drill stem. The petrography of samples from deep drill segment 70008 (Heiken and McKay, 1974) suggests that basalt-rich sediment may extend downward at least as far as the 59-cm depth (sample 70008,239). Curtis and Wasserburg (1975b) suggested from their evaluation of neutron fluence that a uniform and distinctive shallow interval is represented in approximately the upper 60-70 cm of the deep drill stem. The abundance of basalt debris suggests that this distinctive unit is dominated by ejecta from craters large enough to have excavated subfloor-basalt bedrock. Such craters form the large

cluster in the landing area (pl. 2). They are part of a system, including many smaller craters, that is also present on top of the South Massif and in the northern highlands. Figure 252 shows its extent in the Taurus-Littrow area and delineates the areas most heavily affected on the valley floor.

Camelot crater and the three craters Henry, Shakespeare, and Cochise near the north edge of the Taurus-Littrow valley appear more degraded and therefore were previously interpreted as older than the prominent clustered craters south and east of the LM (for example, Lucchitta, 1972; Wolfe and others, 1975). However, topographic profiles made by analytical stereoplotter show that the depth-to-diameter ratio of Camelot crater is similar to that of the larger craters south and east of the LM. Hence, we now regard Camelot as part of the large cluster outlined in figure 252.

Depth-to-diameter ratios for the three northern craters are less than those of large craters east and south of the LM. Perhaps the three craters formed where colluvium from the North Massif was relatively thick; that is, coherent subfloor basalt was more deeply buried in the targets for the Henry, Shakespeare, and Cochise impacts than it was for craters near the center of the valley. If so, their more subdued forms may reflect relatively greater thickness of incoherent target material rather than relatively greater age. We now tentatively also include the three northern craters in the extensive crater cluster (fig. 252).

The relatively youthful appearance of the craters south and east of the LM in comparison with Camelot, Henry, Shakespeare, and Cochise may be due to the abundance of smaller craters, also part of the cluster, that have sculptured the walls, rims, and ejecta blankets of the larger craters. Camelot and the three northern craters differ because of the absence of abundant smaller associated craters. Hence, they have smoother looking rims and ejecta blankets.

A large part of the traverse area is pitted by the clustered craters and covered by their ejecta. A theoretical ejecta distribution calculated by Lucchitta and Sanchez (1975) for the larger craters (fig. 253) suggests that cluster ejecta occurs widely on the valley floor. This distribution is based on the equation of McGetchin, Settle, and Head (1973):  $T=0.04 R$ , and  $t=T(r/R)^{-3.0}$ , where  $T$  is thickness of ejecta at the crater rim,  $R$  the radius of the crater, and  $t$  the thickness of ejecta at a distance  $r$ , measured from the center of the crater. The distribution shown in figure 253 should be construed only as a theoretical approximation. However, it predicts a thickness of cluster ejecta at the deep-drill site that is in reasonable agreement with the observed thickness of basalt-rich sediment in the upper part of

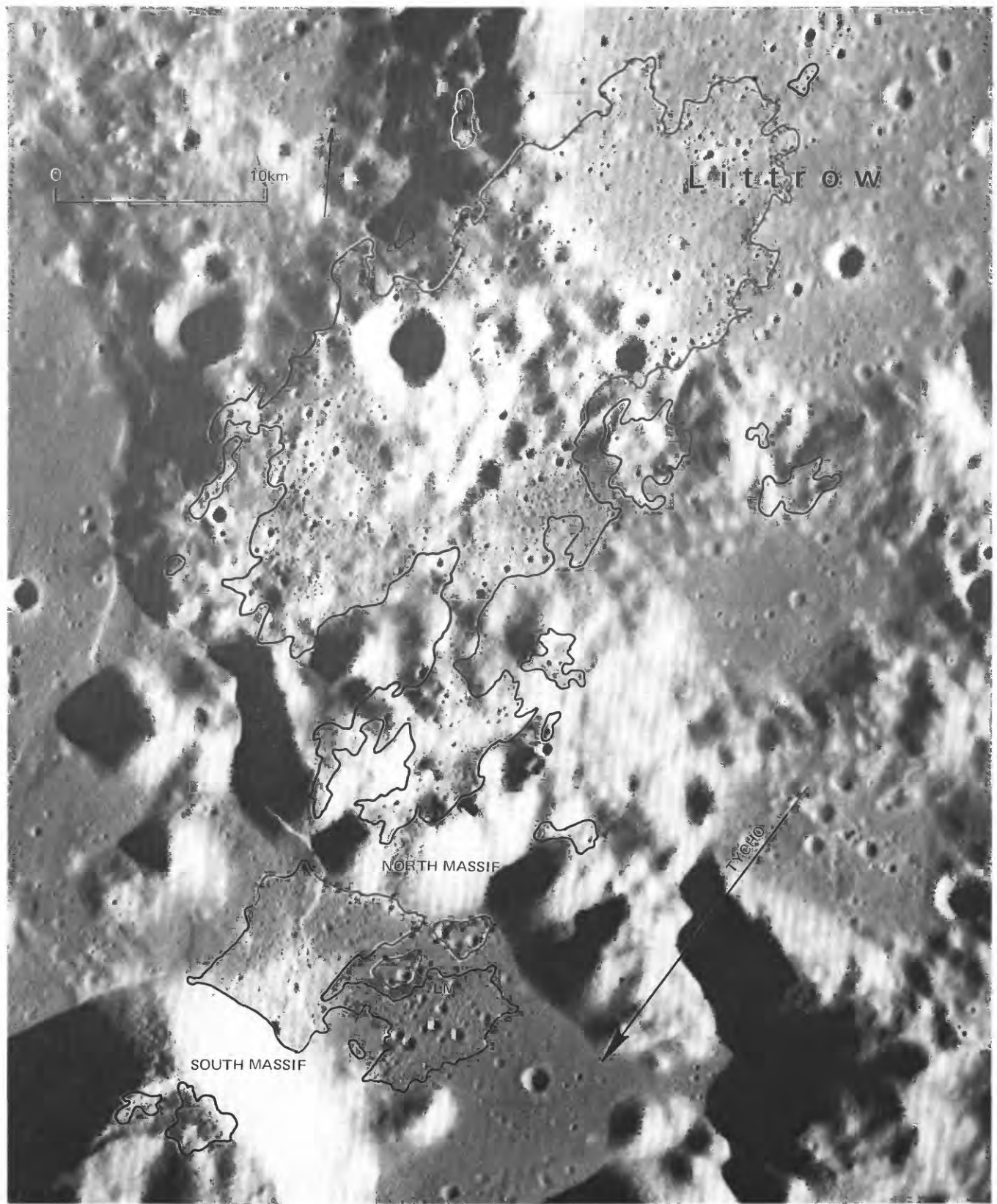


FIGURE 252.—Areal distribution of clustered craters in Taurus-Littrow area. Cluster is aligned toward Tycho, and craters are morphologically like Tycho secondary craters. (Modified from Lucchitta, 1977; NASA photograph M-17-447.)

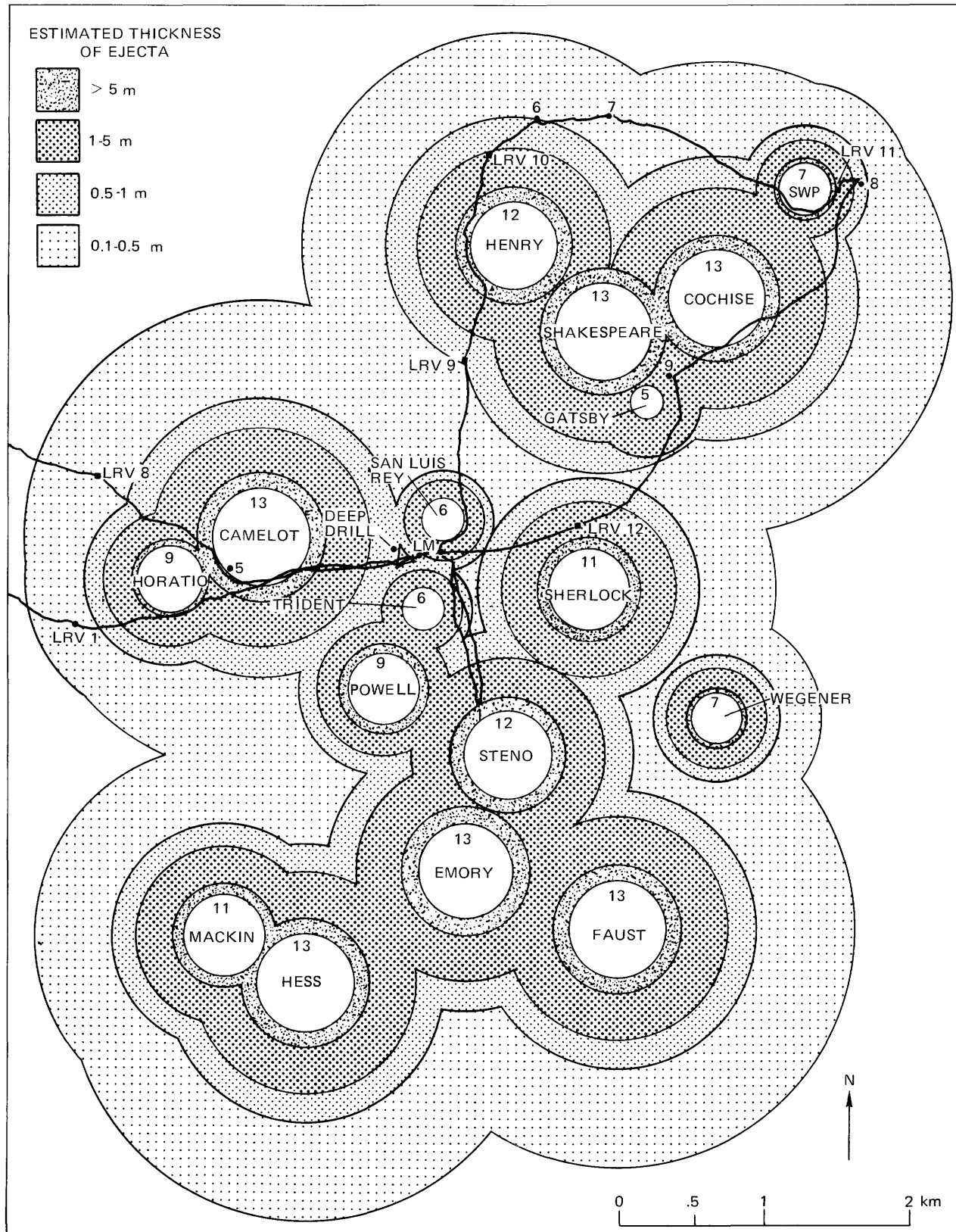


FIGURE 253.—Theoretical distribution of ejecta from larger craters in Apollo 17 landing area. Number within each crater shows theoretical thickness (in meters) of ejecta at crater rim. Aggregate thickness of overlapping ejecta blankets is not portrayed. (Adopted from Lucchitta and Sanchez, 1975.)

the drill core.

Exposure ages determined for samples from large basalt boulders in the LM area range from 95 to 106 m.y. The boulders are best interpreted as part of the cluster ejecta. Samples from the two half-meter boulders from the rim of a fresh 10-m crater at station 1 have exposure ages of 102 and 110 m.y. They are probably ejecta fragments from Steno crater that were excavated, or at least repositioned, by the impact that formed the 10-m crater. The approximate equivalence of the station 1 exposure ages to those of the LM-area boulders suggests that the station 1 boulders were not significantly shielded before the 10-m crater was formed. These data suggest that the cluster ejecta was deposited about 100 m.y. ago. Carefully selecting samples for which they interpreted simple exposure histories, Arvidson and others (1976b) calculated a mean age of  $96 \pm 5$  m.y. for the clustered craters.

Samples of the three large boulders of highly fractionated basalt from the rim of Camelot crater have exposure ages ranging from 70 to 95 m.y. The 70-m.y. date is a track age determined for sample 75055. Three argon ages for the same sample range from 85 to 95 m.y., in approximate agreement with the data from the LM area and station 1. Sample 75015 gave an exposure age of  $92 \pm 4$  m.y., and sample 75035 gave ages of 72 and 80 m.y. The boulders from which these were collected may have had complex histories, possibly including catastrophic rupture to form the two boulders from a single one. Hence, the exposure ages measured for samples 75015 and 75035 may be less than the age of Camelot crater (Arvidson and others, 1976b).

In a study of secondary crater clusters over a large part of the Moon, Lucchitta (1977) found that clusters formed by projectiles from Tycho have a distinctive, easily recognized morphologic pattern. She concluded that the Taurus-Littrow cluster (fig. 252) was formed by impacts of projectiles from Tycho. Evidence includes the following: (1) Clustered craters in the Taurus-Littrow area show close morphologic resemblance to Tycho secondary clusters elsewhere on the Moon; (2) grooved and braided surfaces in the Taurus-Littrow cluster, as in other Tycho secondary clusters, are characterized by V-shaped patterns that open directly away from Tycho; and (3) the Taurus-Littrow cluster is elongate in the approximate direction of a Tycho radial (fig. 252). As one would expect, no Tycho ejecta has been recognized among the Apollo 17 samples. Exposure age data summarized above suggest that the clustered craters and, presumably, Tycho were formed about 100 m.y. ago.

#### LIGHT MANTLE

The light mantle is a deposit of light-colored predom-

inantly fine-grained unconsolidated material with fingerlike projections that extend 6 km across the valley floor from the South Massif (pls. 1 and 2). The unit feathers out at its margins away from the South Massif. Near the distal end, Shorty crater and a smaller nearby crater penetrate the light mantle to the underlying darker regolith material. However, near the South Massif, craters as large as 75 m in diameter do not penetrate to darker underlying material.

Rock fragments collected from the light mantle are dominantly breccia like those from the massif stations. Sediment samples from stations 2, 2a, and 3 contain no more than a few percent of basalt and ash from the valley floor. However, samples from LRV-2 and LRV-6, from thin light mantle relatively far from the South Massif, contain a significantly larger valley-floor component (figs. 245 and 246). The highlands component of the light-mantle sediment samples is approximated by a mixture of the two major compositional groups, noritic breccia matrix material and feldspathic plutonic or metaplutonic rocks, that we recognize in the massif samples.

The composition of the light mantle, the lithologic similarity of its scattered rock fragments to samples collected at the massif stations, the general predominance of fine-grained material, and its geometric form as a raylike body extending outward from the South Massif, suggest that it consists of redeposited regolith material from the South Massif. The light mantle has been interpreted as the deposit of an avalanche triggered, perhaps, by the impact on the South Massif of secondary projectiles from Tycho (Scott and others, 1972; Howard, 1973; Muehlberger and others, 1973). Regional study of Tycho secondary crater clusters (Lucchitta, 1977) has shown that the light mantle is a local manifestation of the Taurus-Littrow crater cluster (fig. 252) and has confirmed the earlier hypothesis that South Massif regolith material was mobilized by impacting secondary projectiles from Tycho. Citing the morphologic similarity between the light mantle surface adjacent to the South Massif and the finely braided ejecta with V-shaped grooves and ridges seen downrange from Tycho secondary clusters, Lucchitta (1977) concluded that the light mantle was primarily ejecta launched from Tycho secondary craters on the crest and north face of the South Massif rather than regolith material jarred into avalanche motion. It seems most likely that the Tycho secondary impacts on the steep massif face mobilized unconsolidated regolith material in both ballistic and avalanche modes to produce the light mantle.

The light mantle is older than Shorty crater, estimated from exposure ages of crater rim materials to have formed between 10 and 30 m.y. ago. The boulders

at station 2 were probably emplaced after deposition of the relatively boulder-free light mantle. Leich and others (1975) concluded that boulder 1 has been in its present position at the base of the South Massif for about 42 m.y. If our view is correct that the light mantle and the clustered craters on the valley floor to the east were all produced by impacting projectiles from Tycho, then these features are temporally equivalent. Accordingly, Arvidson and others (1976a) included the 107-m.y. exposure age of station 2 rake-sample fragment 72535 in the group of selected exposure age data from which they calculated a  $96 \pm 5$ -m.y. estimate for the age of the light mantle and clustered craters. We concur that the light mantle, like the cluster ejecta, is approximately 100 m.y. old.

#### STRUCTURAL GEOLOGY

We recognize three major groups of deformational events. In order of decreasing age, they are (1) block faulting of the highlands, (2) deformation of the mare surfaces, and (3) development of the ridge-scarp system.

##### BLOCK FAULTING OF THE HIGHLANDS

Some boundaries of massif blocks are linear topographic breaks that resemble fault traces. They occur at contacts with adjacent blocks, with Sculptured Hills material, and with subfloor basalt (pl. 1). The most prominent ones, shown in figure 254, do not extend into the basalts. Some are found, however, within Sculptured Hills material.

The linear topographic breaks are presumably fault related but are not necessarily the actual fault traces, which we believe are either buried by thick wedges of colluvium (fig. 242) or mantled by Sculptured Hills material deposited after block faulting was initiated. Surfaces of the colluvial wedges or mantling Sculptured Hills deposits tend to parallel the buried fault surfaces. Some of the faulting, however, post-dates deposition of the Sculptured Hills material.

Previous workers (Scott and Carr, 1972; Head, 1974a) concluded that (1) the massifs now stand where steeply dipping faults, activated during basin formation, coincide with the systematic older fractures of the lunar grid (Strom, 1964) and (2) faults in the Taurus-Littrow area may have been reactivated by the later Imbrium event. A graphic summary (fig. 255) of the bearings and cumulative lengths of the fault-related topographic breaks (fig. 254) confirms their high degree of coincidence with the lunar grid maxima. The dominant Taurus-Littrow maximum, approximately N.  $60^\circ$  W., coincides with the well-defined northwest maximum of the lunar grid but differs by about  $10^\circ$ - $15^\circ$  from radials through the landing point

from the Imbrium and southern Serenitatis basin centers. Hence, the dominant strike of the block faults is approximately radial to the southern Serenitatis basin, but it is skewed slightly clockwise, presumably because of the control exerted by the older fractures. Whether or not the block faults were reactivated by the Imbrium impact cannot be determined.

##### DEFORMATION OF THE MARE SURFACES

A broad topographic low within mare basalt parallels the southeast margin of Mare Serenitatis (fig. 256). The deepest part of this broad trough is about 600 m lower than the central part of Mare Serenitatis, which is located near lat  $24.5^\circ$  N., long  $18^\circ$  E. It is also more than 1,800 m lower than the mare surface near the crater Vitruvius in the southeast corner of plate 1. Stratigraphic relations suggest that the two older Imbrian basalt units ( $Ib_1$  and  $Ib_2$ ) are successively overlapped downslope toward the trough axis by the two younger Imbrian units ( $Ib_3$  and  $Ib_4$ ) (fig. 256). The older basalts are characterized by relatively rough surfaces compared to the younger lavas and are marked by deep linear and sinuous rilles, faults, and collapse depressions having different sizes and shapes. The overlap relations are best shown in the wide reentrant extending southeast between the craters Dawes and Fabbioni, where all four units are exposed. Along the shelflike eastern margin of Mare Serenitatis west of the crater Clerke, the youngest basalt (unit  $Ib_4$ ) has presumably completely overlapped the second youngest ( $Ib_3$ ) and embays the third youngest unit ( $Ib_2$ ) (fig. 256).

The mare surfaces continue to rise southeast outside the map area into the Tranquillitatis basin; overall relief measured from the axis of the Serenitatis trough is nearly 3 km. If the oldest and topographically highest basalt unit ( $Ib_1$ ) originally had an approximately horizontal upper surface and if it is buried by the younger basalts beneath the axis of the synclinal trough, then a minimum of about 3 km of structural relief (more than 2 km within the map area) has been developed on it. This is a minimum figure and does not take into account the thickness of the overlying basalt flows within Mare Serenitatis. Gravity data indicate that an excess mass distribution of  $1,050 \text{ kg/cm}^2$  is present on the floor of Mare Serenitatis (Sjogren and others, 1974a). If the basin was isostatically compensated before extrusion of the mare basalts, the excess mass could represent a superisostatic load equivalent to an average thickness of between 3 and 4 km of basalt. If the basin cavity was not compensated, however, the density contrast between basalt and anorthositic terra material, probably about  $0.4 \text{ g/cm}^3$  (Kaula, 1975), should be used in calculating the basalt thickness. This would amount to a basalt fill of about 25 km. A smaller es-



FIGURE 254.—Major linear topographic breaks in Taurus-Littrow highlands. Although some may coincide with traces of faults, most are probably offset from faults that they parallel by colluvial deposits or by mantling Sculptured Hills material. (NASA photograph M-17-1219.)

timated density contrast would result in a proportionally greater hypothetical thickness. The actual thickness of fill probably lies somewhere between these two extremes. In any case, a total relative uplift of several kilometers must have occurred, provided the basalts had initially level upper surfaces.

Some of the older basalt units ( $Ib_1$ ,  $Ib_2$ ,  $Ib_3$ ) may have originated partly from within the Tranquillitatis basin and flowed downslope into Serenitatis. The upper contact between the second and third oldest ( $Ib_2$  and  $Ib_3$  respectively) units, for example, is very uncertain (pl. 1), and the younger unit ( $Ib_3$ ) may extend farther southeast or southwest. The long sinuous rilles of the third oldest ( $Ib_3$ ) unit, within the reentrant in the southeastern part of the map area, indicate that this basalt flowed down a sloping older mare surface. These rilles are interpreted to be collapsed lava tubes or lava channels requiring the fluid flow of basalt during their formation. As these rilles extend directly downslope nearly normal to the topographic contours, it seems reasonable that the basalt unit in which they occur had

an initial slope in the same direction, if not of the same magnitude as the present surface in this area.

The mare basalts and plains material in the vicinity of the Apollo 17 landing area (Muehlberger, 1974) have been warped into a broad flat-topped arch. The axis of this fold lies between the craters Clerke and Littrow and extends south toward Mons Argaeus near the crater Fabbioni (fig. 256). This arch is expressed neither in the younger basalts north of Clerke nor in the older flows south of Mons Argaeus. Its faulted west limb is overlapped by the younger basalt ( $Ib_4$ ) of Mare Serenitatis (pl. 1).

A sinuous depression north of Mons Argaeus (pl. 1) crosses the southern part of the arch. If the depression represents a lava channel or tube within the second-oldest unit ( $Ib_2$ ) it has been deformed by development of the arch so that lava flowing northward in its southern part would now have to flow uphill for the first 10 km before beginning its descent northwestward toward Mare Serenitatis.

Formation of the marginal trough in eastern Mare

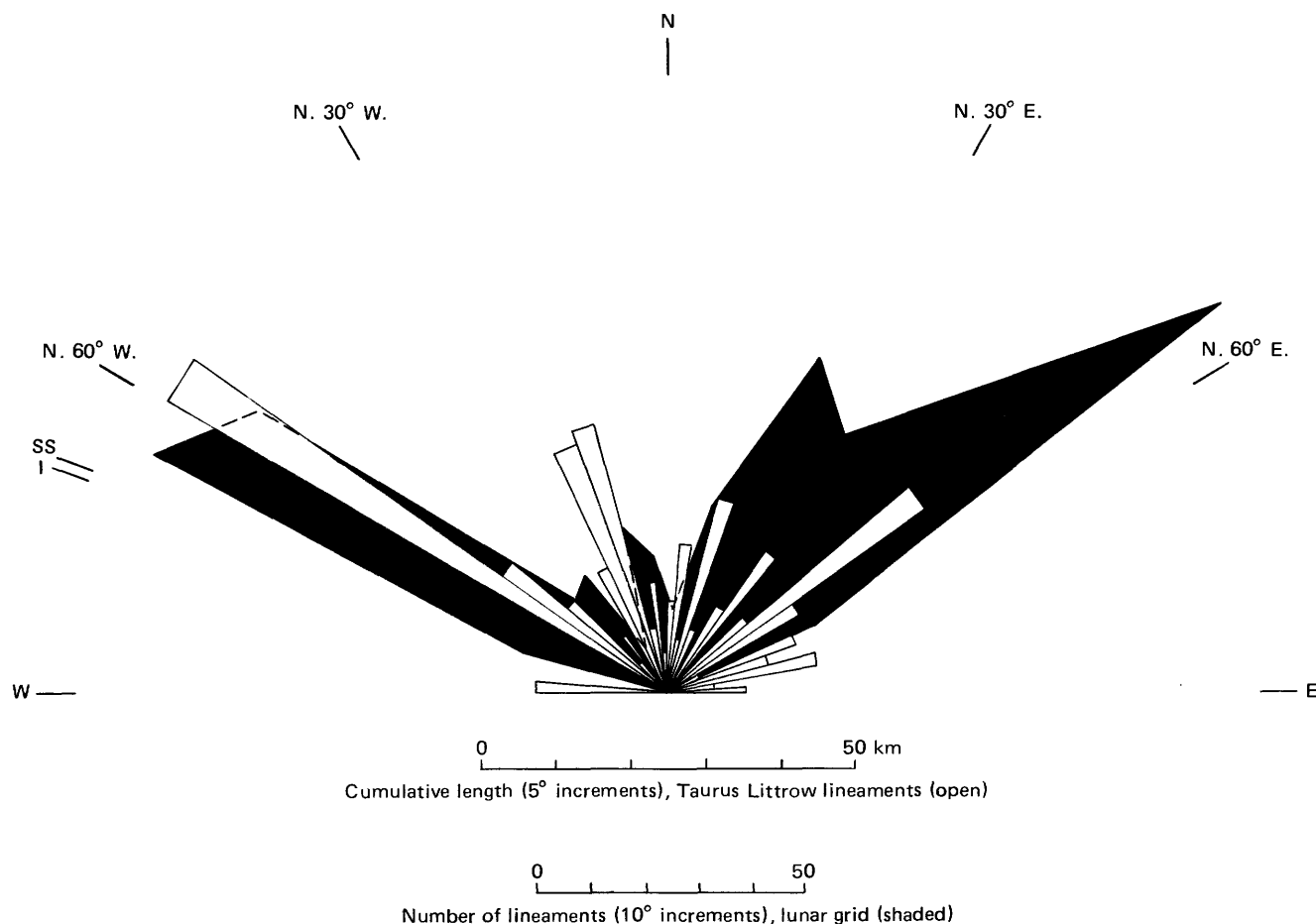


FIGURE 255.—Cumulative lengths in 5° increments of lineaments of figure 254 (open pattern). Shaded pattern is Strom's (1964) azimuth-frequency diagram of lineaments in part of the Moon's northern hemisphere. SS, I, azimuths of radials through Apollo 17 landing point from centers of southern Serenitatis and Imbrium basins, respectively. Southern Serenitatis basin center, 24.5° N., 18° E. (Scott, 1974); Imbrium basin center, 37° N. 19° W. (Stuart-Alexander and Howard, 1970).

Serenitatis (fig. 256) postdates the emplacement of all the mapped basalt units. The youngest basalt unit (Ib<sub>4</sub>) extends from the basin center outward (east) across the axis of the trough (fig. 256). Its contact with underlying flows does not follow the present topography within the low region, as would be expected if folding

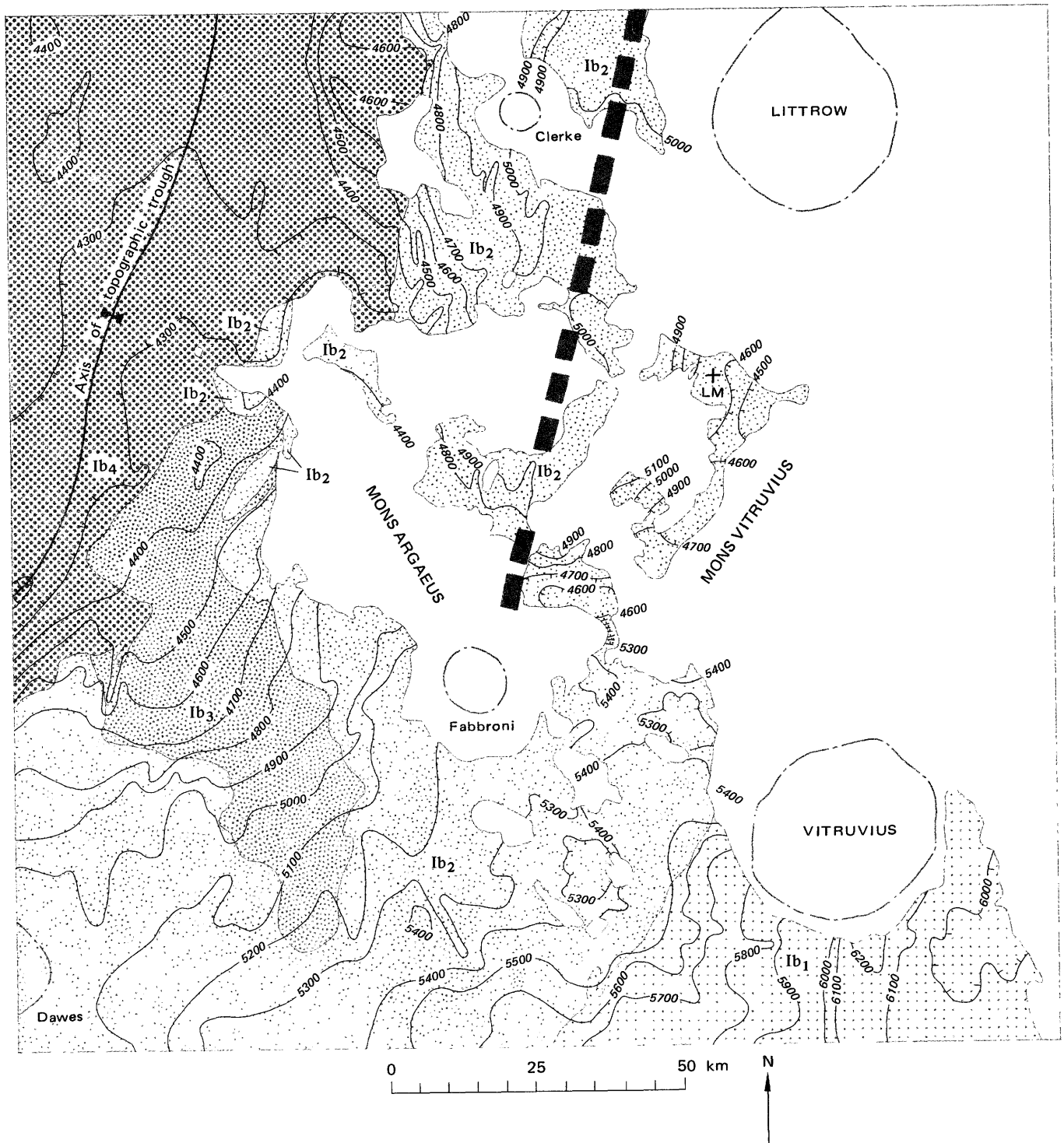


FIGURE 256.—Topographic contours on mare basalt units (Ib<sub>1</sub>–Ib<sub>4</sub>) of Taurus-Littrow region (Ib<sub>1</sub>, oldest; Ib<sub>4</sub>, youngest). Heavy broken line is approximate crest of broad flat-topped arch of Muehlberger (1974). Contours generalized from National Aeronautics and Space Administration Lunar Topographic Orthophotomaps LTO42C2.3; LTO43D1.4. Contour interval is 100 m.

had occurred before its extrusion.

#### DEVELOPMENT OF THE RIDGE-SCARP SYSTEM

The Lee-Lincoln scarp is the easternmost of a broad band of wrinkle ridges and scarps that transect mare and highlands in the Taurus-Littrow area. They extend south-southeast from Mare Serenitatis and the adjacent highlands near the crater Clerke almost to the crater Vitruvius (pl. 1).

North of the Taurus-Littrow valley, on the North Massif and in the Sculptured Hills unit between the North Massif and Clerke (pl. 1), the Lee-Lincoln system extends as well-defined single nearly linear east- to northeast-facing scarps arranged en echelon. They generally trend nearly north, but one segment parallels the south edge of the North Massif. This segment may follow the trace of the older massif-bounding fault, which may have been reactivated so as to break the coluvial wedge during formation of the Lee-Lincoln scarp (Head, 1974a; Wolfe and others, 1975).

On the valley floor the Lee-Lincoln scarp resembles an asymmetrical mare ridge. The east-facing scarp, up to about 80 m high, consists of irregular, imbricate, and overlapping lobes (pl. 2; figs. 6, 7A, B).

The scarp cuts the crater Lara and is overlain by the light mantle. Therefore the main movement took place between the formation of Lara and deposition of the light mantle. However, a few fresh-looking scarplets may cut the light mantle, which suggests that some movement may have occurred relatively recently (<100 m.y.). In addition, the light mantle is cut by a system of fresh high-angle faults and grabens located 2 to 3 km west of the Lee-Lincoln scarp and trending approximately parallel to it (pl. 2).

Hypotheses attributing the formation of mare ridges to volcanic processes, tectonic processes, and combinations of the two were reviewed by Lucchitta (1976). She concluded that the wrinkle ridges and related highland scarps, including specifically the Lee-Lincoln system, were formed by faulting for three reasons. (1) Mare ridges cross stratigraphic units of differing age (pl. 1), including the rims of craters that are much younger than the underlying mare units (for example, an unmapped 2.5-km crater near the south end of Dorsa Aldrovandi on pl. 1; Lara crater on pl. 2 and fig. 7A); hence, they are not primary constructional features of the units on which they occur. (2) The Lee-Lincoln system continues from mare materials of the valley floor into highlands material of the massifs and Sculptured Hills, where it resembles a simple system of faults, up on the west. (3) No fragments of volcanic rock sufficiently young to support a hypothesis of volcanic origin for any part of the Lee-Lincoln system have been found in the Apollo 17 samples.

In a detailed topographic analysis, Lucchitta (1976) found that a fault plane at the base of the Lee-Lincoln scarp would generally be nearly vertical and that more segments have dips that indicate reverse faulting than normal faulting. However, fresh small grabens and high-angle faults that parallel the scarp 2 to 3 km to the west (pl. 2) indicate that tensional stress may have been present locally. These relations are compatible with a model in which local extension and local shortening result from vertical tectonic movements (Sanford, 1959). Normal faults may develop over relatively raised areas and reverse faults over relatively depressed areas (fig. 257).

The cause of these vertical movements is not clear. Muehlberger (1974) interpreted the mare-ridge structures as wrinkles in the surface as a result of global compression. Other investigators have considered them to be the result of crumpling due to gravitational settling of the mare surface into a reduced space (Bryan, 1973; Maxwell and others, 1975). Another possibility is that the tectonic effects result from long-term isostatic adjustments related to basin formation or to the redistribution of lunar mantle material when the voluminous mare basalts were generated and extruded. Whatever the reason, such adjustments apparently have continued into relatively recent (post dating the light mantle) time as minor episodic faulting.

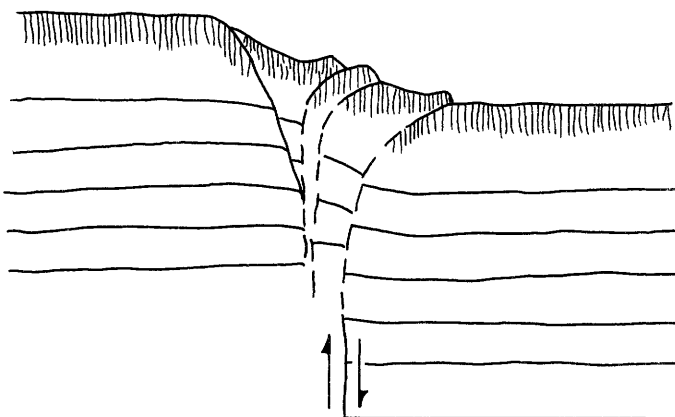


FIGURE 257.—Schematic cross section showing how morphology of Lee-Lincoln scarp on Taurus-Littrow valley floor might result from high-angle faulting of subfloor basalt. Sketch after drawings by Sanford (1959). Note normal faulting under tension over relatively raised block and reverse faulting on relatively lowered block (from Lucchitta, 1976).

#### REFERENCES CITED

- Adams, J. B., Pieters, C., and McCord, T. B., 1974. Orange glass—Evidence for regional deposits of pyroclastic origin on the Moon, *m* Proceedings Fifth Lunar Science Conference, v. 1: *Geochim. et Cosmochim. Acta*, Supp. 5, p. 171-186.
- Albee, A. L., Dymek, R. F., and DePaolo, D. J., 1975. Spinel symplectites—High-pressure solid-state reaction or late-stage magmatic crystallization?, *m* Lunar Science VII, Abstracts of papers

- submitted to the Seventh Lunar Science Conference: Houston, Lunar Sci. Inst., p. 1-3.
- Apollo Field Geology Investigation Team, 1973, Geologic exploration of Taurus-Littrow: Apollo 17 landing site: *Science*, v. 182, p. 672-680.
- 1975, Apollo 17 landing site geology: U.S. Geol. Survey Open-File Rept. 75-437, 435 p.
- Apollo 17 Preliminary Examination Team, 1973, Apollo 17 lunar samples—Chemical and petrographic description: *Science*, v. 182, no. 4113, p. 659-672.
- Arvidson, R., Crozaz, G., Drozd, R. J., Hohenberg, C. M., and Morgan, C. J., 1975, Cosmic ray exposure ages of features and events at the Apollo landing sites: *The Moon*, v. 13, p. 259-276.
- Arvidson, R., Drozd, R., Guinness, E., Hohenberg, C., Morgan, C., Morrison, R., and Oberbeck, V., 1976a, Cosmic ray exposure ages of Apollo 17 samples and implications for the age of Tycho, in *Lunar Science VII. Abstracts of papers submitted to the Seventh Lunar Science Conference*: Houston, Lunar Sci. Inst., p. 25-27.
- 1976b, Cosmic ray exposure ages of Apollo 17 samples and the age of Tycho, in *Proceedings Seventh Lunar Science Conf.*, v. 3: *Geochim. et Cosmochim. Acta*, Supp. 7, p. 2817-2832.
- Baldwin, R. B., 1972, The tsunami model of the origin of ring structures concentric with large lunar craters: *Physics Earth and Planetary Interiors*, v. 6, p. 327-339.
- Bansal, B., Wiesmann, H., and Nyquist, L., 1975, Rb-Sr ages and initial  $^{87}\text{Sr}/^{86}\text{Sr}$  ratios for Apollo 17 mare basalts, in *Origins of mare basalts and their implications for lunar evolution*: Houston, Lunar Sci. Inst., p. 1-5.
- Bence, A. E., Delano, J. W., and Papike, J. J., 1974, Petrology of the highlands massifs at Taurus-Littrow—An analysis of the 2-4 mm soil fraction, in *Proceedings Fifth Lunar Science Conference*, v. 1: *Geochim. et Cosmochim. Acta*, Supp. 5, p. 785-827.
- Bence, A. E., and McGee, J., 1976, Significance of the assemblage anorthite-aluminous enstatite/forsterite aluminous spinel in the lunar highlands: *Geol. Soc. America, Abs. with Programs*, v. 8, no. 6, p. 772.
- Bence, A. E., Papike, J. J., Sueno, S., and Delano, J. W., 1973, Pyroxene poikiloblastic rocks from the lunar highlands: in *Proceedings Fourth Lunar Science Conference*, v. 1: *Geochim. et Cosmochim. Acta*, Supp. 4, p. 597-611.
- Bhandari, N., Bhattacharya, S. K., and Padia, J. T., 1976, Solar flare records in lunar rocks, in *Lunar Science VII. Abstracts of papers submitted to the Seventh Lunar Science Conference*: Houston, Lunar Sci. Inst., p. 49-51.
- Bickel, C. E., Warner, J. L., and Phinney, W. C., 1976a, 79215—A unique, early lunar breccia, in *Lunar Science VII. Abstracts of papers submitted to the Seventh Lunar Science Conference*: Houston, Lunar Sci. Inst., p. 55-57.
- 1976b, Petrology of 79215—Brecciation of a lunar cumulate, in *Proceedings Seventh Lunar Science Conf.*, v. 2: *Geochim. et Cosmochim. Acta*, Supp. 7, p. 1793-1819.
- Blanchard, D. P., Haskin, L. A., Jacobs, J. W., Brannon, J. C., and Korotev, R. L., 1974, Major and trace elements in rocks 72215, 72235, 72255, and 72275 from boulder 1, station 2, Apollo 17, in *Interdisciplinary studies of samples from Boulder 1, Station 2, Apollo 17*, v. 2: *Consortium Indomitabile, Smithsonian Astrophys. Observatory*, p. IV-1 to IV-12.
- 1975, Major and trace element chemistry of boulder 1 at station 2, Apollo 17: *The Moon*, v. 14, p. 359-371.
- Bogard, D. D., Nyquist, L. E., and Hirsch, W. C., 1974, Noble gases in Apollo 17 boulders and soils, in *Lunar Science V. Abstracts of papers submitted to the Fifth Lunar Science Conference*: Houston, Lunar Sci. Inst., p. 73-75.
- Boyce, J. M., 1976, Ages of flow units in the lunar nearside maria based on Lunar Orbiter IV photographs, in *Proceedings Seventh Lunar Science Conference*, v. 3: *Geochim. et Cosmochim. Acta*, Supp. 7, p. 2717-2728.
- Braddy, D., Hutcheon, I. D., and Price, P. B., 1975, Crystal chemistry of Pu and U and concordant fission track ages of lunar zircons and whitlockites, in *Proceedings Sixth Lunar Science Conference*, v. 3: *Geochim. et Cosmochim. Acta*, Supp. 6, p. 3587-3600.
- Brown, G. M., Peckett, A., Emeleus, C. H., Phillips, R., and Pinsent, R. H., 1975, Petrology and mineralogy of Apollo 17 mare basalts, in *Proceedings Sixth Lunar Science Conference*, v. 1: *Geochim. et Cosmochim. Acta*, Supp. 6, p. 1-13.
- Bryan, W. B., 1973, Wrinkle ridges as deformed surface crust on ponded mare lava, in *Proceedings Fourth Lunar Science Conference*, v. 1: *Geochim. et Cosmochim. Acta*, Supp. 4, p. 93-106.
- Bull, R. K., and Durrani, S. A., 1976, The charged-particle track record of some lunar soils and its interpretation, in *Lunar Science VII. Abstracts of papers submitted to the Seventh Lunar Science Conference*: Houston, Lunar Sci. Inst., p. 102-104.
- Butler, Patrick, Jr., compiler, 1973, Lunar sample information catalog, Apollo 17: Houston, Lunar Receiving Lab., Lyndon B. Johnson Space Center, 447 p.
- Cadogan, P. H., and Turner, G., 1976, The chronology of the Apollo 17 station 6 boulder, in *Proceedings Seventh Lunar Science Conference*, v. 2: *Geochim. et Cosmochim. Acta*, Supp. 7, p. 2267-2285.
- Carr, M. H., 1966, Geologic map of the Mare Serenitatis region of the Moon: U.S. Geol. Survey Misc. Geol. Inv. Map I-489, scale 1:1,000,000.
- 1972, Sketch map of the region around candidate Littrow Apollo landing sites: Apollo 15 Prelim. Sci. Rept., NASA Spec. Pub. 289, p. 25-63 to 25-65.
- Carr, M. H., Howard, K. A., and El-Baz, Farouk, 1971, Geologic maps of the Apennine-Hadley region of the Moon: U.S. Geol. Survey Geologic Atlas of the Moon, Map I-723, 2 sheets, scales 1:250,000 and 1:50,000.
- Carter, J. L., Taylor, H. C. J., and Padovani, Elaine, 1973, Morphology and chemistry of particles from Apollo 17 soils 74220, 74241, and 75081: *EOS, Am. Geophys. Union Trans.*, v. 54, no. 6, p. 582-584.
- Chao, E. C. T., 1973, The petrology of 76055,10, a thermally metamorphosed fragment-laden olivine microrite hornfels, in *Proceedings Fourth Lunar Science Conference*, v. 1: *Geochim. et Cosmochim. Acta*, Supp. 4, p. 719-732.
- Chao, E. C. T., and Minkin, J. A., 1974, The petrogenesis of 77135, a fragment-laden pigeonite feldspathic basalt—A major highland rock type, in *Lunar Science V. Abstracts of papers submitted to the Fifth Lunar Science Conference*: Houston, Lunar Sci. Inst., p. 112-114.
- Chao, E. C. T., Minkin, J. A., and Thompson, C. L., 1974, Preliminary petrographic description and geologic implications of the Apollo 17 station 7 boulder consortium samples: *Earth and Planetary Sci. Letters*, v. 23, p. 413-428.
- 1975a, The petrogenesis of 77115 and its xenocrysts—description and preliminary interpretation, in *Lunar Science VI. Abstracts of papers submitted to the Sixth Lunar Science Conference*: Houston, Lunar Sci. Inst., p. 134-136.
- 1976a, The petrology of 77215, a noritic impact ejecta breccia, in *Lunar Science VII. Abstracts of papers submitted to the Seventh Lunar Science Conference*: Houston, Lunar Sci. Inst., p. 129-131.

- 1976b, The petrology of 77215, a noritic impact ejecta breccia, in *Proceedings Seventh Lunar Science Conference*, v. 2: *Geochim. et Cosmochim. Acta*, Supp. 7, p. 2287-2308.
- Chao, E. C. T., Minkin, J. A., Thompson, C. L., and Huebner, J. S., 1975b, The petrogenesis of 77115 and its xenocrysts—description and preliminary interpretation, in *Proceedings Sixth Lunar Science Conference*, v. 1: *Geochim. et Cosmochim. Acta*, Supp. 6, p. 493-515.
- Compston, W., Foster, J. J., and Gray, C. M., 1975, Rb-Sr ages of clasts from within boulder 1, station 2, Apollo 17: *The Moon*, v. 14, p. 445-462.
- Cooper, M. R., Kovach, R. L., and Watkins, J. S., 1974, Lunar near-surface structure: *Rev. Geophysics and Space Physics*, v. 12, p. 291-308.
- Crozaz, G., Drozd, R., Hohenberg, C., Morgan, C., Ralston, C., Walker, R., and Yugas, D., 1974, Lunar surface dynamics—Some general conclusions and new results from Apollo 16 and 17, in *Proceedings Fifth Lunar Science Conference*, v. 3: *Geochim. et Cosmochim. Acta*, Supp. 5, p. 2475-2499.
- Crozaz, G., and Plachy, A. L., 1976a, Origin of the Apollo 17 deep drill coarse-grained layer, in *Lunar Science VII*, Abstracts of papers submitted to the Seventh Lunar Science Conference: Houston, Lunar Sci. Inst., p. 178-180.
- 1976b, Origin of the Apollo 17 deep drill coarse-grained layer, in *Proceedings Seventh Lunar Science Conference*, v. 1: *Geochim. et Cosmochim. Acta*, Supp. 7, p. 123-131.
- Curtis, D. B., and Wasserburg, G. J., 1975a, Apollo 17 neutron stratigraphy—Sedimentation and mixing in the lunar regolith: *The Moon*, v. 13, p. 185-227.
- 1975b, Processes of sedimentation and mixing in the lunar regolith inferred from neutron fluence measurements, in *Lunar Science VI*, Abstracts of papers submitted to the Sixth Lunar Science Conference: Houston, Lunar Sci. Inst., p. 172-174.
- Dowty, E., Keil, K., and Prinz, M., 1974, Igneous rocks from Apollo 16 rake samples, in *Proceedings Fifth Lunar Science Conference*, v. 1: *Geochim. et Cosmochim. Acta*, Supp. 5, p. 431-445.
- Dragon, J. C., Johnson, N. L., Pepin, R. O., Bates, A., Coscio, M. R., Jr., and Murthy, V. R., 1975, The Apollo 17 deep drill core—A possible depositional model, in *Lunar Science VI*, Abstracts of papers submitted to the Sixth Lunar Science Conference: Houston, Lunar Sci. Inst., p. 196-198.
- Duncan, A. R., Erlank, A. J., Willis, J. P., Sher, M. K., and Ahrens, L. H., 1974, Trace element evidence for a two-stage origin of some titaniferous mare basalts, in *Proceedings Fifth Lunar Science Conference*, v. 2: *Geochim. et Cosmochim. Acta*, Supp. 5, p. 1147-1157.
- Duncan, A. R., Sher, M. K., Abraham, Y. C., Erlank, A. J., Willis, J. P., and Ahrens, L. H., 1976, Source region constraints for lunar basalt types inferred from trace element chemistry, in *Lunar Science VII*, Abstracts of papers submitted to the Seventh Lunar Science Conference: Houston, Lunar Sci. Inst., p. 218-220.
- Dymek, R. F., Albee, A. L., and Chodos, A. A., 1975, Comparative petrology of lunar cumulate rocks of possible primary origin—Dunite 72415, troctolite 76535, norite 78235, and anorthosite 62236, in *Proceedings Sixth Lunar Science Conference*, v. 1: *Geochim. et Cosmochim. Acta*, Supp. 6, p. 301-341.
- 1976a, Chemical and mineralogical homogeneity of boulder 2, in *Lunar Science VII*, Abstracts of papers submitted to the Seventh Lunar Science Conference: Houston, Lunar Sci. Inst., p. 230-232.
- 1976b, Petrology and origin of boulders 2 and 3, Apollo 17 station 2, in *Proceedings Seventh Lunar Science Conference*, v. 2: *Geochim. et Cosmochim. Acta*, Supp. 7, p. 2335-2378.
- Eberhardt, P., Eugster, O., Geiss, J., Graf, H., Grögler, N., Guggis-berg, S., Jungck, M., Maurer, P., Mörgeli, M., and Stettler, A., 1974, Solar wind and cosmic radiation history of Taurus-Littrow regolith, in *Lunar Science V*, Abstracts of papers submitted to the Fifth Lunar Science Conference: Houston, Lunar Sci. Inst., p. 197-199.
- Eberhardt, P., Eugster, O., Geiss, J., Graf, H., Grögler, N., Mörgeli, M., and Stettler, A., 1975,  $Kr^{81}$ -Kr exposure ages of some Apollo 14, Apollo 16, and Apollo 17 rocks, in *Lunar Science VI*, Abstracts of papers submitted to the Sixth Lunar Science Conference: Houston, Lunar Sci. Inst., p. 233-235.
- Eberhardt, P., Geiss, J., Grogler, N., Maurer, P., and Stettler, A., 1973,  $^{39}Ar$ - $^{40}Ar$  ages of lunar material: *Meteoritics*, v. 8, p. 360-361.
- El-Baz, Farouk, 1972, The cinder field of the Taurus-Littrow mountains: Apollo 15 Prelim. Sci. Rept., NASA Spec. Pub. 289, p. 25-66 to 25-71.
- El-Baz, Farouk, and Worden, A. M., 1972, Visual observations from lunar orbit: Apollo 15 Prelim. Sci. Rept., NASA Spec. Pub. 289, p. 25-1 to 25-27.
- Evensen, N. M., Murthy, V. R., and Coscio, M. R., Jr., 1973, Rb-Sr ages of some mare basalts and the isotopic and trace element systematics in lunar fines, in *Proceedings Fourth Lunar Science Conference*, v. 2: *Geochim. et Cosmochim. Acta*, Supp. 4, p. 1707-1724.
- Fleischer, R. L., and Hart, H. R., Jr., 1974, Surface history of some Apollo 17 lunar soils: *Geochim. et Cosmochim. Acta*, v. 38, p. 1615-1623.
- Fleischer, R. L., Hart, H. R., Jr., and Giard, W. R., 1974, Surface history of lunar soil and soil columns: *Geochim. et Cosmochim. Acta*, v. 38, p. 365-380.
- Glass, B. P., 1973, Major element analysis of glass particles from the Apollo 17 orange soil (sample 74220.89) [abs.]: *EOS, Am. Geophys. Union Trans.*, v. 54, no. 6, p. 590-591.
- Gooley, R., Brett, R., Warner, J., and Smyth, J. R., 1974, A lunar rock of deep crustal origin—Sample 76535: *Geochim. et Cosmochim. Acta*, v. 38, p. 1329-1340.
- Goswami, N. J., Braddy, D., and Price, P. B., 1976a, Microstratigraphy of the lunar regolith and compaction ages of lunar and meteoritic breccias, in *Lunar Science VII*, Abstracts of papers submitted to the Seventh Lunar Science Conference: Houston, Lunar Sci. Inst., p. 328-330.
- 1976b, Microstratigraphy of the lunar regolith and compaction ages of lunar breccias, in *Proceedings Seventh Lunar Science Conf.*, v. 1: *Geochim. et Cosmochim. Acta*, Supp. 7, p. 55-74.
- Goswami, N. J., and Hutcheon, I. D., 1975, Cosmic ray exposure history and compaction age of boulder 1 from station 2: *The Moon*, v. 14, nos. 3/4, p. 395-406.
- Hartmann, W. K., and Wood, C. A., 1971, Moon—Origin and evolution of multi-ring basins: *The Moon*, v. 3, p. 3-78.
- Head, J. W., 1974a, Morphology and structure of the Taurus-Littrow highlands (Apollo 17)—Evidence for origin and evolution: *The Moon*, v. 9, p. 355-395.
- 1974b, Orientale multi-ringed basin interior and implications for the petrogenesis of lunar highland samples: *The Moon*, v. 11, p. 327-356.
- 1974c, Lunar dark-mantle deposits—Possible clues to the distribution of early mare deposits, in *Proceedings Fifth Lunar Science Conference*, v. 2: *Geochim. et Cosmochim. Acta*, Supp. 5, p. 207-222.
- Head, J. W., Settle, Mark, and Stein, Ross, 1975, Volume of material ejected from major lunar basins—Implications for the depth of excavation of lunar samples, in *Lunar Science VI*, Abstracts of papers submitted to the Sixth Lunar Science Conference: Houston, Lunar Sci. Inst., p. 352-354.
- Heiken, Grant, compiler, 1974, A catalog of lunar soils: Houston,

- Natl. Aeronautics Space Admin., 221 p.
- Heiken, G. H., Butler, Patrick, Jr., Simonds, C. H., Phinney, W. C., Warner, Jeffrey, Schmitt, H. H., Bogard, D. D., and Pearce, W. G., 1973, Preliminary data on boulders at station 6, Apollo 17 landing site: NASA Tech. Memo. X-58116, JSC-08484, 56 p.
- Heiken, G. H., and McKay, D. S., 1974, Petrography of Apollo 17 soils, in *Proceedings Fifth Lunar Science Conference*, v. 1: *Geochim. et Cosmochim. Acta*, Supp. 5, p. 843-860.
- Heiken, G. H., McKay, D. S., and Brown, R. W., 1974, Lunar deposits of possible pyroclastic origin: *Geochim. et Cosmochim. Acta*, v. 38, p. 1703-1718.
- Helmke, P. A., Blanchard, D. P., Jacobs, J. W., Telander, K. M., and Haskin, L. A., 1973, Major and trace elements in materials from the Apollo 17 deep drill core [abs.]: *EOS, Am. Geophys. Union Trans.*, v. 54, no 6, p. 595.
- Helz, R. T., and Appleman, D. E., 1974, Poikilitic and cumulate textures in rock 77017, a crushed anorthositic gabbro, in *Lunar Science V, Abstracts of papers submitted to the Fifth Lunar Science conference*: Houston, Lunar Sci. Inst., p. 322-324.
- Hinners, N. W., 1973, Apollo 17 site selection: Apollo 17 Prelim. Sci. Rept., NASA Spec. Pub., 330, p. 1-1 to 1-5.
- Hintenberger, H., and Weber, H. W., 1973, Trapped rare gases in lunar fines and breccias, in *Proceedings Fourth Lunar Science Conference*, v. 2: *Geochim. et Cosmochim. Acta*, Supp. 4, p. 2003-2019.
- Hinthorne, J. R., and Conrad, R. L., 1976 Comparison of Pb-Pb with argon ages in highlands fragment 78503, 13, A, in *Lunar Science VII, Abstracts of papers submitted to the Seventh Lunar Science Conference*: Houston, Lunar Sci. Inst., p. 373-375.
- Hinthorne, J. R., Conrad, R., and Andersen, C. A., 1975, Lead-lead age and trace element abundances in lunar troctolite, 76535, in *Lunar Science VI, Abstracts of papers submitted to the Sixth Lunar Science Conference*: Houston, Lunar Sci. Inst., p. 373-375.
- Holmes, Arthur, 1928, The nomenclature of petrology, with references to selected literature [2d ed.]: London, Thomas Murby and Co., [repr., New York, Hafner Pub. Co., 1971], 284 p.
- Howard, K. A., 1973, Avalanche mode of motion—Implications from lunar examples: *Science*, v. 180, p. 1052-1055.
- Howard, K. A., Carr, M. H., and Muehlberger, W. R., 1973, Basalt stratigraphy of southern Mare Serenitatis: Apollo 17 Prelim. Sci. Rept., NASA SP-330, p. 29-1 to 29-12.
- Huneke, J. C., Jessberger, E. K., Podosek, F. A., and Wasserburg, G. J., 1973,  $^{40}\text{Ar}/^{39}\text{Ar}$  measurements in Apollo 16 and 17 samples and the chronology of metamorphic and volcanic activity in the Taurus-Littrow region, in *Proceedings Fourth Lunar Science Conference*, v. 2: *Geochim. et Cosmochim. Acta*, Supp. 4, p. 1725-1756.
- Huneke, J. C., and Wasserburg, G. J., 1975, Trapped  $^{40}\text{Ar}$  in troctolite 76535 and evidence for enhanced  $^{40}\text{Ar}/^{39}\text{Ar}$  age plateaus, in *Lunar Science VI, Abstracts of papers submitted to the Sixth Lunar Science Conference*: Houston, Lunar Sci. Inst., p. 417-419.
- Husain, Liaquat, and Schaeffer, O. A., 1973, Lunar volcanism—Age of the glass in the Apollo 17 orange soil: *Science*, v. 180, p. 1358-1360.
- 1975, Lunar evolution—The first 600 million years: *Geophys. Research Letters*, v. 2, p. 29-32.
- Hutcheon, I. D., Macdougall, D., Price, P. B., Hörz, F., Morrison, D., and Schneider, E., 1974a, Rock 72315—A new lunar standard for solar flare and micrometeorite exposure, in *Lunar Science V, Abstracts of papers submitted to the Fifth Lunar Science Conference*: Houston, Lunar Sci. Inst., p. 378-380.
- Hutcheon, I. D., Macdougall, D., and Stevenson, J., 1974b, Apollo 17 particle track studies—Surface residence times and fission track ages for orange glass and large boulders, in *Proceedings Fifth Lunar Science Conference*, v. 3: *Geochim. et Cosmochim. Acta*, Supp. 5, p. 2597-2608.
- Irving, A. J., 1975, Chemical, mineralogical, and textural systematics of non-mare melt rocks—Implications for lunar impact and volcanic processes: *Proceedings Sixth Lunar Science Conference*, v. 1: *Geochim. et Cosmochim. Acta*, Supp. 6, p. 363-394.
- Jackson, E. D., Sutton, R. L., and Wilshire, H. G., 1975, Structure and petrology of a cumulus norite boulder sampled by Apollo 17 in Taurus-Littrow valley, the Moon: *Geol. Soc. America Bull.*, v. 86, p. 433-442.
- James, O. B., 1975, Petrography of the matrix of light gray (consortium) breccia 73215, in *Lunar Science VI, Abstracts of papers submitted to the Sixth Lunar Conference*: Houston, Lunar Sci. Inst., p. 438-440.
- 1976a, Petrology of aphanitic lithologies in consortium breccia 73215, in *Lunar Science VII, Abstracts of papers submitted to the Seventh Lunar Science Conference*: Houston, Lunar Sci. Inst., p. 420-422.
- 1976b, Petrology of aphanitic lithologies in consortium breccia 73215, in *Proceedings Seventh Lunar Science Conf.*, v. 2: *Geochim. et Cosmochim. Acta*, Supp. 7, p. 2145-2178.
- 1977, Lunar highlands breccias generated by major impacts: Soviet-American Conf. on the Cosmochemistry of the Moon and Planets, NASA, Spec. Pub. 370, p. 637-658.
- James, O. B., and Blanchard, D. P., 1976, Consortium studies of light-gray breccia 73215—Introduction, subsample distribution data, and summary of results, in *Proceedings of the Seventh Lunar Science Conference*, v. 2: *Geochim. et Cosmochim. Acta*, Supp. 7, p. 2131-2143.
- James, O. B., Blanchard, D. P., Jacobs, J. W., Brannon, J. C., Haskin, L. A., Brecher, A., Compston, W., Marti, K., Lugmair, G. W., Gros, J., Takahashi, H., and Braddy, D., 1976, Consortium studies of aphanitic lithologies and two anorthositic gabbro clasts in breccia 73215, in *Lunar Science VII, Abstracts of papers submitted to the Seventh Lunar Science Conference*: Houston, Lunar Sci. Inst., p. 423-425.
- James, O. B., Brecher, A., Blanchard, D. P., Jacobs, J. W., Brannon, J. C., Korotev, R. L., Haskin, L. A., Higuchi, H., Morgan, J. W., Anders, E., Silver, L. T., Marti, K., Braddy, D., Hutcheon, I. D., Kirsten, T., Kerridge, J. F., Kaplan, I. R., Pillinger, C. T., and Gardiner, L. R., 1975a, Consortium studies of matrix of light gray breccia 73215, in *Proceedings Sixth Lunar Science Conference*, v. 1: *Geochim. et Cosmochim. Acta*, Supp. 6, p. 547-577.
- James, O. B., Marti, K., Braddy, D., Hutcheon, I. D., Brecher, A., Silver, L. T., Blanchard, D. P., Jacobs, J. W., Brannon, J. C., Korotev, R. L., and Haskin, L. A., 1975b, Consortium studies of matrix of light gray breccia 73215, in *Lunar Science VI, Abstracts of papers submitted to the Sixth Lunar Science Conference*: Houston, Lunar Sci. Inst., p. 435-437.
- Jessberger, E. K., Horn, P., and Kirsten, T., 1975,  $^{39}\text{Ar}/^{40}\text{Ar}$  dating of lunar rocks—A methodical investigation of mare basalt 75075, in *Lunar Science VI, Abstracts of papers submitted to the Sixth Lunar Science Conference*: Houston, Lunar Sci. Inst., p. 441-443.
- Jessberger, E. K., Kirsten, T., and Staudacher, T., 1976a, Ages of plutonic clasts in consortium breccia 73215, in *Lunar Science VII, Abstracts of papers submitted to the Seventh Lunar Science Conference*: Houston, Lunar Sci. Inst., p. 431-433.
- 1976b, Argon-argon ages of consortium breccia 73215, in *Proceedings Seventh Lunar Science Conference*, v. 2: *Geochim. et Cosmochim. Acta*, Supp. 7, p. 2201-2215.

- Kaula, W. M., 1975, The gravity and shape of the moon: EOS, Am. Geophys. Union Trans., v. 56, no. 6, p. 309-316.
- Kirsten, T., and Horn, P., 1974, Chronology of the Taurus-Littrow region III—Ages of mare basalts and highland breccias and some remarks about the interpretation of lunar highland rock ages, in *Proceedings Fifth Lunar Science Conference*, v. 2: Geochim. et Cosmochim. Acta, Supp. 5, p. 1451-1475.
- Kirsten, T., Horn, P., Heymann, D., Hubner, W., and Storzer, D., 1973, Apollo 17 crystalline rocks and soil—Rare gases, ion tracks, and ages [abs.]: EOS, Am. Geophys. Union Trans., v. 54, no. 6, p. 595-597.
- Laul, J. C., Hill, D. W., and Schmitt, R. A., 1974, Chemical studies of Apollo 16 and 17 samples, in *Proceedings Fifth Lunar Science Conference*, v. 2: Geochim. et Cosmochim. Acta, Supp. 5, p. 1047-1066.
- Laul, J. C., and Schmitt, R. A., 1974, Chemical composition of boulder 2 rocks and soils, Apollo 17, station 2: Earth and Planetary Sci. Letters, v. 23, p. 206-219.
- 1975a, Chemical composition of Apollo 17 samples—Boulder breccias (2), rake breccias (8) and others, in *Lunar Science VI, Abstracts of papers submitted to the Sixth Lunar Science Conference*: Houston, Lunar Sci. Inst., p. 489-491.
- 1975b, Dunite 72417—A chemical study and interpretation, in *Proceedings Sixth Lunar Science Conference*, v. 2: Geochim. et Cosmochim. Acta, Supp. 6, p. 1231-1254.
- Laul, J. C., Schmitt, R. A., Robyn, M., and Goles, G. G., 1975, Chemical composition of 18 Apollo 17 rake basalts and one basalt-breccia, in *Lunar Science VI, Abstracts of papers submitted to the Sixth Lunar Science Conference*: Houston, Lunar Sci. Inst., p. 492-494.
- Leich, D. A., Kahl, S. B., Kirschbaum, A. R., Niemeyer, S., and Phinney, D., 1975, Rare gas constraints on the history of boulder 1, station 2, Apollo 17: The Moon, v. 14, p. 407-444.
- Longhi, J., Walker, D., Grove, T. L., Stolper, E. M., and Hays, J. F., 1974, The petrology of the Apollo 17 mare basalts, in *Proceedings Fifth Lunar Science Conference*, v. 1: Geochim. et Cosmochim. Acta, Supp. 5, p. 447-469.
- Lucchitta, B. K., 1972, Geologic map of part of the Taurus-Littrow region of the Moon, in Scott, D. H., Lucchitta, B. K., and Carr, M. H., *Geologic maps of the Taurus-Littrow region of the Moon*: U.S. Geol. Survey Misc. Geol. Inv. Map I-800, sheet 2, scale 1:50,000.
- 1973, Photogeology of the dark material in the Taurus-Littrow region of the Moon, in *Proceedings Fourth Lunar Science Conference*, v. 1: Geochim. et Cosmochim. Acta, Supp. 4, p. 149-162.
- 1976, Mare ridges and related highland scarps—Result of vertical tectonism?, in *Proceedings Seventh Lunar Science Conf.*, v. 3: Geochim. et Cosmochim. Acta, Supp. 7, p. 2761-2782.
- 1977, Crater clusters and light mantle at the Apollo 17 site—A result of secondary impact from Tycho: Icarus, v. 30, p. 80-96.
- Lucchitta, B. K., and Sanchez, A. G., 1975, Crater studies in the Apollo 17 region, in *Proceedings Sixth Lunar Science Conference*, v. 3: Geochim. et Cosmochim. Acta, Supp. 6, p. 2427-2441.
- Lucchitta, B. K., and Schmitt, H. H., 1974, Orange material in the Sulpicius Gallus formation at the southwestern edge of Mare Serenitatis, in *Proceedings Fifth Lunar Science Conference*, v. 1: Geochim. et Cosmochim. Acta, Supp. 5, p. 223-234.
- Lugmair, G. W., Marti, K., Kurtz, J. P., and Scheinin, N. B., 1976, History and genesis of lunar troctolite 76535 or: How old is old?, in *Proceedings Seventh Lunar Science Conference*, v. 2: Geochim. et Cosmochim. Acta, Supp. 7, p. 2009-2033.
- Lugmair, G. W., Scheinin, N. B., and Marti, K., 1975a, Sm-Nd age of Apollo 17 basalt 75075—Two-stage igneous processes in mare basalt genesis, in *Lunar Science VI, Abstracts of papers submitted to the Sixth Lunar Science Conference*: Houston, Lunar Sci. Inst., p. 531-533.
- 1975b, Sm-Nd age and history of Apollo 17 basalt 75075—Evidence for early differentiation of the lunar exterior, in *Proceedings Sixth Lunar Science Conference*, v. 2: Geochim. et Cosmochim. Acta, Supp. 6, p. 1419-1429.
- McCallum, I. S., and Mathez, E. A., 1975, Petrology of noritic cumulates and a partial melting model for the genesis of Fra Mauro basalts, in *Proceedings Sixth Lunar Science Conference*, v. 1: Geochim. et Cosmochim. Acta, Supp. 6, p. 395-414.
- McCauley, J. F., 1977, Orientale and Caloris: Physics of the Earth and Planetary Interiors, v. 15, p. 220-250.
- McGetchin, T. R., and Head, J. W., 1973, Lunar cinder cones: Science, v. 180, p. 68-71.
- McGetchin, T. R., Settle, M., and Head, J. W., 1973, Radial thickness variation in impact crater ejecta: Implications for lunar basin deposits: Earth and Planetary Sci. Letters, v. 20, p. 226-236.
- Marvin, U. B., 1975, The boulder: The Moon, v. 14, p. 315-326.
- Mason, Brian, Jacobson, Sara, Nelen, J. A., Melson, W. G., Simkin, Tom, and Thompson, G., 1974, Regolith compositions from the Apollo 17 mission, in *Proceedings Fifth Lunar Science Conference*, v. 1: Geochim. et Cosmochim. Acta, Supp. 5, p. 879-885.
- Maxwell, T. A., El-Baz, Farouk, and Ward, S. H., 1975, Distribution, morphology, and origin of ridges and arches in Mare Serenitatis: Geol. Soc. America Bull., v. 86, p. 1273-1278.
- Miller, M. D., Pacer, R. A., Ma, M.-S., Hawke, B. R., Lookhart, G. L., and Ehmann, W. D., 1974, Compositional studies of the lunar regolith at the Apollo 17 site, in *Proceedings Fifth Lunar Science Conference*, v. 2: Geochim. et Cosmochim. Acta, Supp. 5, p. 1079-1086.
- Moore, H. J., 1969, Subsurface deformation resulting from missile impact, in *Geological Survey Research 1969*: U.S. Geol. Survey Prof. Paper 650-B, p. B107-B112.
- 1971, Craters produced by missile impacts: Jour. Geophys. Research, v. 76, p. 5750-5755.
- Moore, H. J., Hodges, C. A., and Scott, D. H., 1974, Multi-ringed basins—Illustrated by Orientale and associated features: *Proceedings Fifth Lunar Science Conference*: Geochim. et Cosmochim. Acta, Supp. 5, v. 1, p. 71-100.
- Morgan, J. W., Higuchi, H., and Anders, Edward, 1975, Meteoritic material in a boulder from the Apollo 17 site—Implications for its origin: The Moon, v. 14, p. 373-383.
- Muehlberger, W. R., 1974, Structural history of southeastern Mare Serenitatis and adjacent highlands, in *Proceedings Fifth Lunar Science Conference*, v. 1: Geochim. et Cosmochim. Acta, Supp. 5, p. 101-110.
- Muehlberger, W. R., Batson, R. M., Boudette, E. L., Duke, C. M., Eggleton, R. E., Elston, D. P., England, A. W., Freeman, V. L., Hait, M. H., Hall, T. A., Head, J. W., Hodges, C. A., Holt, H. E., Jackson, E. D., Jordan, J. A., Larson, K. B., Milton, D. J., Reed, V. S., Rennilson, J. J., Schaber, G. G., Schafer, J. P., Silver, L. T., Stuart-Alexander, D., Sutton, R. L., Swann, G. A., Tyner, R. L., Ulrich, G. E., Wilshire, H. G., Wolfe, E. W., and Young, J. W., 1972, Preliminary geologic investigation of the Apollo 16 landing site: Apollo 16 Preliminary Science Report, NASA Spec. Pub. 315, p. 6-1 to 6-81.
- Muehlberger, W. R., Batson, R. M., Cernan, E. A., Freeman, V. L., Hait, M. H., Holt, H. E., Howard, K. A., Jackson, E. D., Larson, K. B., Reed, V. S., Rennilson, J. J., Schmitt, H. H., Scott, D. H., Sutton, R. L., Stuart-Alexander, D., Swann, G. A., Trask, N. J., Ulrich, G. E., Wilshire, H. G., and Wolfe, E. W., 1973, Preliminary geologic investigation of the Apollo 17 landing site: Apollo 17 Preliminary Science Report, NASA Spec. Pub. 330, p. 6-1 to 6-91.

- Murthy, V. R., 1976, Rb-Sr studies of A-17 mare basalts and some general considerations [of] early terrestrial and lunar evolution, in *Lunar Science VII, Abstracts of papers submitted to the Seventh Lunar Science Conference*: Houston, Lunar Sci. Inst., p. 585-587.
- Nakamura, Noboru, Tatsumoto, Mitsunobu, Nunes, P. D., Unruh, D. M., Schwab, A. P., and Wildeman, T. R., 1976, 4.4 b.y.-old clast in Boulder 7, Apollo 17—A comprehensive chronological study by U-Pb, Rb-Sr, and Sm-Nd methods, in *Proceedings Seventh Lunar Science Conference*, v. 2: *Geochim. et Cosmochim. Acta*, Supp. 7, p. 2309-2333.
- Nava, D. F., 1974, Chemical compositions of some soils and rock types from the Apollo 15, 16, and 17 lunar sites, in *Proceedings Fifth Lunar Science Conference*, v. 2: *Geochim. et Cosmochim. Acta*, Supp. 5, p. 1087-1096.
- Nunes, P. D., Nakamura, N., and Tatsumoto, M., 1976, 4.4 b.y. old clast in boulder 7, Apollo 17, in *Lunar Science VII, Abstracts of papers submitted to the Seventh Lunar Science Conference*: Houston, Lunar Sci. Inst., p. 631-633.
- Nunes, P. D., and Tatsumoto, M., 1975, U-Th-Pb systematics of anorthositic gabbro 78155, in *Lunar Science VI, Abstracts of papers submitted to the Sixth Lunar Science Conference*: Houston, Lunar Sci. Inst., p. 607-609.
- Nunes, P. D., Tatsumoto, M., and Unruh, D. M., 1974, U-Th-Pb and Rb-Sr systematics of Apollo 17 boulder 7 from the North Massif of the Taurus-Littrow valley: *Earth and Planetary Sci. Letters*, v. 23, p. 445-452.
- Nyquist, L. E., Bansal, B. M., and Wiesmann, H., 1975, Rb-Sr ages and initial  $^{87}\text{Sr}/^{86}\text{Sr}$  for Apollo 17 basalts and KREEP basalt 15386, in *Proceedings Sixth Lunar Science Conference*, v. 2: *Geochim. et Cosmochim. Acta*, Supp. 6, p. 1445-1465.
- , 1976, Sr isotopic constraints on the petrogenesis of Apollo 17 mare basalts, in *Lunar Science VII, Abstracts of papers submitted to the Seventh Lunar Science Conference*: Houston, Lunar Sci. Inst., p. 636-638.
- Nyquist, L. E., Bansal, B. M., Wiesmann, H., and Jahn, B.-M., 1974, Taurus-Littrow chronology—Some constraints on early lunar crustal development, in *Proceedings Fifth Lunar Science Conference*, v. 2: *Geochim. et Cosmochim. Acta*, Supp. 5, p. 1515-1539.
- Oberbeck, V. R., and Quaide, W. L., 1967, Estimated thickness of a fragmental surface layer of Oceanus Procellarum: *Jour. Geophys. Research*, v. 72, no. 18, p. 4697-4704.
- Onorato, P. I. K., Uhlmann, D. R., and Simonds, C. H., 1976, Heat flow in impact melts—Apollo 17 station 6 boulder and some applications to other breccias and xenolith laden melts, in *Proceedings Seventh Lunar Science Conference*, v. 2: *Geochim. et Cosmochim. Acta*, Supp. 7, p. 2449-2467.
- Page, N. J., 1970, Geologic map of the Cassini quadrangle of the Moon: U.S. Geol. Survey Misc. Inv. Map I-666, Scale 1:1,000,000.
- Papanastassiou, D. A., and Wasserburg, G. J., 1975, Rb-Sr study of a lunar dunite and evidence for early lunar differentiates, in *Proceedings Sixth Lunar Science Conference*, v. 2: *Geochim. et Cosmochim. Acta*, Supp. 6, p. 1467-1489.
- , 1976, Rb-Sr age of troctolite 76535, in *Proceedings Seventh Lunar Science Conference*, v. 2: *Geochim. et Cosmochim. Acta*, Supp. 7, p. 2035-2054.
- Papike, J. J., Bence, A. E., and Lindsley, D. H., 1974, Mare basalts from the Taurus-Littrow region of the Moon, in *Proceedings of the Fifth Lunar Science Conference*, v. 1: *Geochim. et Cosmochim. Acta*, Supp. 5, p. 471-504.
- Papike, J. J., Hodges, F. N., Bence, A. E., Cameron, Maryellen, and Rhodes, J. M., 1976, Mare basalts—Crystal chemistry, mineralogy, and petrology: *Rev. Geophysics and Space Physics*, v. 14, no. 4, p. 475-540.
- Pepin, R. O., Dragon, J. C., Johnson, N. L., Bates, A., Coscio, M. R. Jr., and Murthy, V. R., 1975, Rare gases and Ca, Sr, and Ba in Apollo 17 drill-core fines, in *Proceedings Sixth Lunar Science Conference*, v. 2: *Geochim. et Cosmochim. Acta*, Supp. 6, p. 2027-2055.
- Phinney, D., Kahl, S. B., and Reynolds, J. H., 1975,  $^{40}\text{Ar}$ - $^{39}\text{Ar}$  dating of Apollo 16 and 17 rocks, in *Proceedings Sixth Lunar Science Conference*, v. 2: *Geochim. et Cosmochim. Acta*, Supp. 6, p. 1593-1608.
- Phinney, W. C., Anders, E., Bogard, D., Butler, P., Gibson, E., Gose, W., Heikien, G., Hohenberg, C., Nyquist, L., Pearce, W., Rhodes, M., Silver, L., Simonds, C., Strangway, D., Turner, G., Walker, R., Warner, J., and Yuhas, D., 1974, Progress report: Station 6 Boulder Consortium, in *Lunar Science V, supplement A, Special Session of Consortium Papers*: Houston, Lunar Sci. Inst., p. 7-13.
- Phinney, W. C., McKay, D. S., Simonds, C. H., and Warner, J. L., 1976, Lithification of vitric- and clastic-matrix breccias: SEM petrography, in *Proceedings Seventh Lunar Science Conference*, v. 2: *Geochim. et Cosmochim. Acta*, Supp. 7, p. 2469-2492.
- Pieters, Carle, McCord, T. B., Zisk, Stanley, and Adams, J. B., 1973, Lunar black spots and nature of the Apollo 17 landing area: *Jour. Geophys. Research*, v. 78, no. 26, p. 5867-5875.
- Quaide, W. L., and Oberbeck, V. R., 1968, Thickness determinations of the lunar surface layer from lunar impact craters: *Jour. Geophys. Research*, v. 73, no. 16, p. 5247-5270.
- Reed, V. S., and Wolfe, E. W., 1975, Origin of the Taurus-Littrow massifs, in *Proceedings Sixth Lunar Science Conference*: *Geochim. et Cosmochim. Acta*, Supp. 5, v. 3, p. 2443-2461.
- Reid, A. M., Lofgren, G. E., Heiken, G. H., Brown, R. W., and Moreland, G., 1973, Apollo 17 orange glass, Apollo 15 green glass and Hawaiian lava fountain glass [abs.]: *EOS, Am. Geophys. Union Trans.*, v. 54, no. 6, p. 606-607.
- Reynolds, D. L., 1954, Fluidization as a geological process and its bearing on the problem of intrusive granites: *Am Jour. Sci.*, v. 252, no. 10, p. 577-613.
- Rhodes, J. M., Hubbard, N. J., Wiesmann, H., Rodgers, K. V., Brannon, J. C., and Bansal, B. M., 1976, Chemistry, classification and petrogenesis of Apollo 17 mare basalts, in *Proceedings Seventh Lunar Science Conference*, v. 2: *Geochim. et Cosmochim. Acta*, Supp. 7, p. 1467-1489.
- Rhodes, J. M., Rodgers, K. V., Shih, C., Bansal, B. M., Nyquist, L. E., Wiesmann, H., and Hubbard, N. J., 1974, The relationships between geology and soil chemistry at the Apollo 17 landing site, in *Proceedings Fifth Lunar Science Conference*, v. 2: *Geochim. et Cosmochim. Acta*, Supp. 5, p. 1097-1117.
- Rose, H. J., Jr., Baedeker, P. A., Berman, Sol, Christian, R. P., Dwornik, E. J., Finkelman, R. B., and Schnepfe, M. M., 1975, Chemical composition of rocks and soils returned by the Apollo 15, 16, and 17 missions, in *Proceedings Sixth Lunar Science Conference*, v. 2: *Geochim. et Cosmochim. Acta*, Supp. 6, p. 1363-1373.
- Rose, H. J., Jr., Cuttitta, Frank, Berman, Sol, Brown, F. W., Carron, M. K., Christian, R. P., Dwornik, E. J., and Greenland, L. P., 1974, Chemical composition of rocks and soils at Taurus-Littrow, in *Proceedings Fifth Lunar Science Conference*, v. 2: *Geochim. et Cosmochim. Acta*, Supp. 5, p. 1119-1133.

- Ryder, Graham, Stoesser, D. B., Marvin, U. B., Bower, J. F., and Wood, J. A., 1975, Boulder 1, station 2, Apollo 17—Petrology and petrogenesis: *The Moon*, v. 14, p. 327-358.
- Sanford, A. R., 1959, Analytical and experimental study of simple geologic structures: *Geol. Soc. America Bull.*, v. 70, p. 19-52.
- Schaeffer, O. A., and Husain, Liaquat, 1974, Chronology of lunar basin formation and ages of lunar anorthositic rocks, *in* Lunar Science V, Abstracts of papers submitted to the Fifth Lunar Science Conference: Houston, Lunar Sci. Inst., p. 663-665.
- Schaeffer, O. A., Husain, Liaquat, and Schaeffer, G. A., 1976, Ages of highland rocks—The chronology of lunar basin formation revisited, *in* Proceedings Seventh Lunar Science Conference, v. 2: *Geochim. et Cosmochim. Acta*, Supp. 7, p. 2067-2092.
- Schmitt, H. H., 1973, Apollo 17 report on the valley of Taurus-Littrow: *Science*, v. 182, p. 681-690.
- Scoon, J. H., 1974, Chemical analysis of lunar samples from the Apollo 16 and 17 collections, *in* Lunar Science V, Abstracts of papers submitted to the Fifth Lunar Science Conference: Houston, Lunar Sci. Inst., p. 690-692.
- Scott, D. H., 1974, The geologic significance of some lunar gravity anomalies, *in* Proceedings Fifth Lunar Science Conference, v. 3: *Geochim. et Cosmochim. Acta*, Supp. 5, p. 3025-3036.
- Scott, D. H., and Carr, M. H., 1972, Geologic map of part of the Taurus-Littrow region of the Moon, *in* Scott, D. H., Lucchitta, B. K., and Carr, M. H., Geologic maps of the Taurus-Littrow region of the Moon: U.S. Geol. Survey Misc. Geol. Inv. Map I-800, sheet 1, scale 1:250,000.
- Scott, D. H., Lucchitta, B. K., and Carr, M. H., 1972, Geologic maps of the Taurus-Littrow region of the Moon: U.S. Geol. Survey Misc. Geol. Inv. Map I-800, two sheets, sheet 1, Scott and Carr, scale 1:250,000; sheet 2, Lucchitta, scale 1:50,000.
- Scott, D. H., McCauley, J. F., and West, M. N., 1977, Geologic map of the west side of the Moon: U.S. Geol. Survey Misc. Geol. Inv. Map I-1034, scale 1:5,000,000.
- Scott, D. H., and Pohn, H. A., 1972, Geologic map of the Macrobis quadrangle of the Moon: U.S. Geol. Survey Misc. Geol. Inv. Map I-799, scale 1:1,000,000.
- Sevier, J. R., 1972, Apollo 17 Traverse planning data [3d ed.]: Houston, Manned Spacecraft Center.
- Shih, Chi-Yu, Haskin, L. A., Wiesmann, Henry, Bansal, B. M., and Brannon, J. C., 1975, On the origin of high-Ti mare basalts, *in* Proceedings Sixth Lunar Science Conference, v. 2: *Geochim. et Cosmochim. Acta*, Supp. 6, p. 1255-1285.
- Shoemaker, E. M., 1960, Penetration mechanics of high velocity meteorites illustrated by Meteor Crater, Arizona: *Internat. Geol. Cong. XXI Sess., Pt. XVIII*, Copenhagen, Proc., p. 418-434.
- Shoemaker, E. M., Hait, M. H., Swann, G. A., Schleicher, D. L., Dahlem, D. H., Schaber, G. G., and Sutton, R. L., 1970, Lunar regolith at Tranquillity Base: *Science*, v. 167, p. 452-455.
- Shoemaker, E. M., Gault, D. E., Moore, H. J., and Lugn, R. V., 1973, Hypervelocity impact of steel into Coconino sandstone: *Am. Jour. Sci.*, v. 261, p. 668-682.
- Silver, L. T., 1974, Patterns of U-Th-Pb distributions and isotope relations in Apollo 17 soils, *in* Lunar Science V, Abstracts of papers submitted to the Fifth Lunar Science Conference: Houston, Lunar Sci. Inst., p. 706-708.
- Simonds, C. H., 1973, Sintering and hot pressing of Fra Mauro composition glass and the lithification of lunar breccias: *Am. Jour. Sci.*, v. 273, p. 428-439.
- , 1975, Thermal regimes in impact melts and the petrology of the Apollo 17 station 6 boulder, *in* Proceedings Sixth Lunar Science Conference, v. 1: *Geochim. et Cosmochim. Acta*, Supp. 6, p. 641-672.
- Simonds, C. H., Warner, J. L., and Phinney, W. C., 1973, Petrology of Apollo 16 poikilitic rocks, *in* Proceedings Fourth Lunar Science Conference, v. 1: *Geochim. et Cosmochim. Acta*, Supp. 4, p. 613-632.
- Sjogren, W. L., Wimberly, R. N., and Wollenhaupt, W. R., 1974a, Lunar gravity: Apollo 17: *The Moon*, v. 11, p. 41-52.
- , 1974b, Apollo 17 gravity results, *in* Lunar Science V, Abstracts of papers submitted to the Fifth Lunar Science Conference: Houston, Lunar Sci. Inst., p. 712-714.
- Snee, L. W., and Ahrens, T. J., 1975, Shock-induced deformation features in terrestrial peridotite and lunar dunite, *in* Proceedings Sixth Lunar Science Conference, v. 1: *Geochim. et Cosmochim. Acta*, Supp. 6, p. 833-842.
- Stettler, A., Eberhardt, P., Geiss, J., and Grögler, N., 1974,  $^{39}\text{Ar}$ - $^{40}\text{Ar}$  ages of samples from the Apollo 17 station 7 boulder and implications for its formation: *Earth and Planetary Sci. Letters*, v. 23, p. 453-461.
- Stettler, A., Eberhardt, P., Geiss, J., Grögler, N., and Guggisberg, S., 1975, Age sequence in the Apollo 17 station 7 boulder, *in* Lunar Science VI, Abstracts of papers submitted to the Sixth Lunar Science Conference: Houston, Lunar Sci. Inst., p. 771-773.
- Stettler, A., Eberhardt, P., Geiss, J., Grögler, N., and Maurer, P., 1973,  $\text{Ar}^{39}$ - $\text{Ar}^{40}$  ages and  $\text{Ar}^{37}$ - $\text{Ar}^{38}$  exposure ages of lunar rocks, *in* Proceedings Fourth Lunar Science Conference, v. 2: *Geochim. et Cosmochim. Acta*, Supp. 4, p. 1865-1888.
- Stewart, D. B., 1975, Apollonian metamorphic rocks—The products of prolonged subsolidus equilibration, *in* Lunar Science VI, Abstracts of papers submitted to the Sixth Lunar Science Conference: Houston, Lunar Sci. Inst., p. 774-776.
- Stoesser, D. B., Marvin, U. B., and Bower, J. F., 1974a, Petrology and petrogenesis of boulder 1, *in* Interdisciplinary studies of samples from boulder 1, station 2, Apollo 17, v. 2: Consortium Indomitabile, Smithsonian Astrophys. Observatory, p. III-1 to III-51.
- Stoesser, D. B., Wolfe, R. W., Wood, J. A., and Bower, J. F., 1974b, Petrology, *in* Interdisciplinary studies of samples from boulder 1, station 2, Apollo 17, v. 1, Sec. III: Consortium Indomitabile, Smithsonian Astrophys. Observatory, p. 35-110.
- Storzer, D., Poupeau, G., and Krätschmer, W., 1973, Track-exposure and formation ages of some lunar samples, *in* Proceedings Fourth Lunar Science Conference, v. 3: *Geochim. et Cosmochim. Acta*, Supp. 4, p. 2363-2377.
- Strom, R. G., 1964, Analysis of lunar lineaments. 1. Tectonic maps of the Moon: Tucson, Ariz. Univ. Lunar and Planetary Lab. Commun., v. 2, no. 39, p. 205-221.
- Stuart-Alexander, D. E., and Howard, K. A., 1970, Lunar maria and circular basins—A review: *Icarus*, v. 12, p. 440-456.
- Tatsumoto, M., Nunes, P. D., Knight, R. J., Hedge, C. E., and Unruh, D. M., 1973, U-Th-Pb, Rb-Sr, and K measurements of two Apollo 17 samples [abs.]: EOS, Am. Geophys. Union Trans., v. 54, no. 6, p. 614-615.
- Tatsumoto, M., Nunes, P. D., Knight, R. J., and Unruh, D. M., 1974, Rb-Sr and U-Th-Pb systematics of boulders 1 and 7, Apollo 17, *in* Lunar Science V, Abstracts of papers submitted to the Fifth Lunar Science Conference: Houston, Lunar Sci. Inst., p. 774-776.
- Tera, Fouad, Papanastassiou, D. A., and Wasserburg, G. J., 1974a, The lunar time scale and a summary of isotopic evidence for a terminal lunar cataclysm, *in* Lunar Science V, Abstracts of papers submitted to the Fifth Lunar Science Conference: Houston, Lunar Sci. Inst., p. 792-794.
- , 1974b, Isotopic evidence for a terminal lunar cataclysm: *Earth and Planetary Sci. Letters*, v. 22, p. 1-21.
- Tera, Fouad, and Wasserburg, G. J., 1976, Lunar ball games and other sports, *in* Lunar Science VII, Abstracts of papers submitted to the Seventh Lunar Science Conference: Houston, Lunar Sci. Inst., p. 858-860.

- Turner, Grenville, and Cadogan, P. H., 1975, The history of lunar bombardment inferred from  $^{40}\text{Ar}$ - $^{39}\text{Ar}$  dating of highland rocks, in *Proceedings Sixth Lunar Science Conference*, v. 2: *Geochim. et Cosmochim. Acta*, Supp. 6, p. 1509-1538.
- Turner, Grenville, Cadogan, P. H., and Yonge, C. J., 1973, Argon selenochronology, in *Proceedings Fourth Lunar Science Conference*, v. 2: *Geochim. et Cosmochim. Acta*, Supp. 4, p. 1889-1914.
- Waltz, S. R., and Nagle, J. S., 1976, Dissection description of the upper Apollo 17 drill string, in *Lunar Science VII, Abstracts of papers submitted to the Seventh Lunar Science Conference*: Houston, Lunar Sci. Inst., p. 910-911.
- Wänke, H., Baddenhausen, H., Dreibus, G., Jagoutz, E., Kruse, H., Palme, H., Spettel, B., and Teschke, F., 1973, Multielement analyses of Apollo 16 and 17 samples and the bulk composition of the moon, in *Proceedings Fourth Lunar Science Conference*, v. 2: *Geochim. et Cosmochim. Acta*, Supp. 4, p. 1461-1481.
- Wänke, H., Palme, H., Baddenhausen, H., Dreibus, G., Jagoutz, E., Kruse, H., Spettel, B., Teschke, F., and Thacker, R., 1974, Chemistry of Apollo 16 and 17 samples—Bulk composition, late stage accumulation and early differentiation of the Moon, in *Proceedings Fifth Lunar Science Conference*, v. 2: *Geochim. et Cosmochim. Acta*, Supp. 5, p. 1307-1335.
- 1975, New data on the chemistry of lunar samples—Primary matter in the lunar highlands and the bulk composition of the Moon, in *Proceedings Sixth Lunar Science Conference*, v. 2: *Geochim. et Cosmochim. Acta*, Supp. 6, p. 1313-1340.
- Warner, J. L., 1972, Metamorphism of Apollo 14 breccias, in *Proceedings Third Lunar Science Conference*, v. 1: *Geochim. et Cosmochim. Acta*, Supp. 3, p. 623-643.
- Warner, J. L., Simonds, C. H., and Phinney, W. C., 1976, Apollo 17, station 6 boulder sample 76255—Absolute petrology of breccia matrix and igneous clasts, in *Proceedings Seventh Lunar Science Conference*, v. 2: *Geochim. et Cosmochim. Acta*, Supp. 7, p. 2233-2250.
- Warner, R., Keil, K., Murali, A. V., and Schmitt, R. A., 1975a, Petrogenetic relationships among Apollo 17 basalts, in *Origin of mare basalts and their implications for lunar evolution*: Houston, Lunar Sci. Inst., p. 179-183.
- Warner, R., Prinz, M., and Keil, K., 1975b, Mineralogy and petrology of mare basalts from Apollo 17 rake sample in, *Lunar Science VI, Abstracts of papers submitted to the Sixth Lunar Science Conference*: Houston, Lunar Sci. Inst., p. 850-852.
- Wilhelms, D. E., and McCauley, J. F., 1971, Geologic map of the near side of the Moon: U.S. Geol. Survey, Geol. Atlas of the Moon, Map I-703, scale 1:5,000,000.
- Wilshire, H. G., 1971, Pseudotachylite from the Vredefort ring, South Africa: *Jour. Geology*, v. 79, p. 195-206.
- 1974, Provenance of terra breccias, in *Lunar Science V, Abstracts of papers submitted to the Fifth Lunar Science Conference*: Houston, Lunar Sci. Inst., p. 846-847.
- Wilshire, H. G., and Jackson, E. D., 1972, Petrology and stratigraphy of the Fra Mauro Formation at the Apollo 14 site: U.S. Geol. Survey Prof. Paper 785, 26 p.
- Wilshire, H. G., and Moore, H. J., 1974, Glass-coated lunar rock fragments: *Jour. Geology*, v. 82, p. 403-417.
- Wilshire, H. G., Stuart-Alexander, D. E., and Jackson, E. D., 1973, Apollo 16 rocks—Petrology and classification: *Jour. Geophys. Research*, v. 78, p. 2371-2372.
- Wilshire, H. G., Stuart-Alexander, D. E., and Schwarzman, E. C., 1981, Petrology and distribution of the returned samples, Apollo 16, in *Geology of the Apollo 16 area, central lunar highlands*: U.S. Geol. Survey Prof. Paper 1048, p. 127-146.
- Winzer, S. R., Nava, D. F., Schuhmann, S., Lum, R. K. L., and Philpotts, J. A., 1975a, Origin of the station 7 boulder—A note, in *Proceedings Sixth Lunar Science Conference*, v. 1: *Geochim. et Cosmochim. Acta*, Supp. 6, p. 707-710.
- Winzer, S. R., Nava, D. F., Lum, R. K. L., Schuhmann, S., Shuford, Schuhmann, P., and Philpotts, J. A., 1975b, Origin of 78235, a lunar norite cumulate, in *Proceedings Sixth Lunar Science Conference*, v. 2: *Geochim. et Cosmochim. Acta*, Supp. 6, p. 1219-1229.
- Winzer, S. R., Nava, C. R., Schuhmann, S., Shuford, Kouns, C. W., Lum, R. K. L., and Philpotts, J. A., 1974, Major, minor and trace element abundances in samples from the Apollo 17 station 7 boulder—Implications for the origin of early lunar crustal rocks: *Earth and Planetary Sci. Letters*, v. 23, p. 439-444.
- Winzer, S. R., Nava, D. F., Schuhmann, P. J., Lum, R. K. L., Schuhmann, S., Lindstrom, M. M., Lindstrom, D. J., and Philpotts, J. A., 1977, The Apollo 17 "melt sheet": Chemistry, age, and Rb/Sr systematics: *Earth and Planetary Sci. Letters*, v. 33, no. 3, p. 389-400.
- Winzer, S. R., Nava, D. F., Schuhmann, P. J., Schuhmann, S., Shuford, Lindstrom, M. M., Lum, R. K. L., Lindstrom, D. J., and Philpotts, J. A., 1976, Origin of melts, breccias and rocks from the Apollo 17 landing site, in *Lunar Science VII, Abstracts of papers submitted to the Seventh Lunar Science Conference*: Houston, Lunar Sci. Inst., p. 941-943.
- Wolfe, E. W., and Freeman, V. L., 1972, Detailed geologic map—Apollo 17 (Taurus-Littrow) landing area: U.S. Geol. Survey open-file map, 1:25,000.
- Wolfe, E. W., Freeman, V. L., Lucchitta, B. K., Scott, D. H., Head, J. W., and Schmitt, H. H., 1972a, Geologic setting of the Apollo 17 site [abs.]: *Geol. Soc. America Abs. with Programs*, v. 4, no. 7, p. 710.
- Wolfe, E. W., Freeman, V. L., Muehlberger, W. R., Head, J. W., Schmitt, H. H., and Sevier, J. R., 1972b, Apollo 17 exploration of Taurus-Littrow: *Geotimes*, v. 17, no. 11, p. 14-18.
- Wolfe, E. W., Lucchitta, B. K., Reed, V. S., Ulrich, G. E., and Sanchez, A. G., 1975, Geology of the Taurus-Littrow valley floor, in *Proceedings Sixth Lunar Science Conference*, v. 3: *Geochim. et Cosmochim. Acta*, Supp. 6, p. 2463-2482.
- Wolfe, E. W., and Reed, V. S., 1976, Geology of the massifs at the Apollo 17 landing site: U.S. Geol. Survey Jour. Research, v. 4, no. 2, p. 171-180.
- Yokoyama, Y., Guichard, F., Reyss, J. L., and Sato, J., 1976, Dating of fresh lunar craters by cosmogenic  $^{22}\text{Na}$ - $^{26}\text{Al}$  studies and a preliminary study on the  $^{26}\text{Al}$ - $^{53}\text{Mn}$  method, in *Lunar Science VII, Abstracts of papers submitted to the Seventh Lunar Science Conference*: Houston, Lunar Sci. Inst., p. 956-958.

# APOLLO 17 LUNAR SURFACE PHOTOGRAPHY

By RAYMOND M. BATSON, KATHLEEN B. LARSON, and RICHARD L. TYLER

## INTRODUCTION

Pictures taken on the surface of the Moon by the crew of Apollo 17 were used in four ways to support geologic investigation of the landing site: (1) documentation of sample collection and illustration of crew commentary; (2) determination of the precise locations of stations, samples, and traverse routes; (3) mensuration of features of geologic interest; and (4) measurement of surface reflectance (discussed in Muehlberger and others, 1973). A total of 2,218 frames was exposed on the lunar surface with Hasselblad electric data cameras. Unless otherwise specified, the pictures were taken on 70-mm film using 60-mm lenses (the camera is described by Kammerer, 1973). Most of these photographs were taken according to practiced procedures designed for geologic documentation.

## PHOTOGRAPHIC PROCEDURES

Sample documentation pictures were taken to show the in-place character of a returned sample or of a feature that could not be returned. Before sampling, a downsun photograph for photometric study and a cross-sun stereoscopic pair were taken of the chosen sample area. After sampling, a picture from about the same place as the stereoscopic pictures was taken of the sample area to establish the identity of the collected sample by its absence from the field seen in the pre-sampling pictures. An additional photograph, also from the cross-sun position, was taken of the Lunar Roving Vehicle (LRV) to establish the position of the sample within the station area. Where time was short or footing awkward, one or more of these pictures was omitted. Additional documentation of uncollectable rock features was done with closeup stereoscopic pairs taken from less than 1 meter away.

Panoramas (pls. 3-9) were taken at each station to permit precise location of the station by resection and to illustrate and supplement geologic descriptions by the crew. A complete panorama consists of 15 or more overlapping photographs covering a total of 360°. The overlap zones between pictures in panoramas can be viewed stereoscopically because the aiming direction of the camera was changed and the lens position was

shifted slightly each time a picture was taken. This provides a stereoscopic baseline a few centimeters long, which is useful for study of topography within 50 to 100 m of the camera.

Pictures were taken with a 500-mm focal length lens on a Hasselblad camera to permit study of features inaccessible to the crew.

The lunar module pilot (LMP) took pictures at approximately regular intervals while the LRV was in motion. These photographs were used to reconstruct the traverse and to examine surface characteristics over wide areas. During these "en route" sequences, particularly at points of deployment of explosive packages, the commander drove the LRV in a tight circle while the LMP took photographs, resulting in what has been termed an "LRV panorama."

The LMP was equipped with a special sampler for collecting samples while seated on the LRV. Before sample collection, the LRV was driven toward the sample area, and a picture was taken by each astronaut, providing a stereopair. After the sample was collected, the LMP took one or more pictures (toward distinctive features where possible) to aid in locating the sample area.

Additional pictures were taken to illustrate deployment of the ALSEP and other subjects not directly related to geologic observation and sampling.

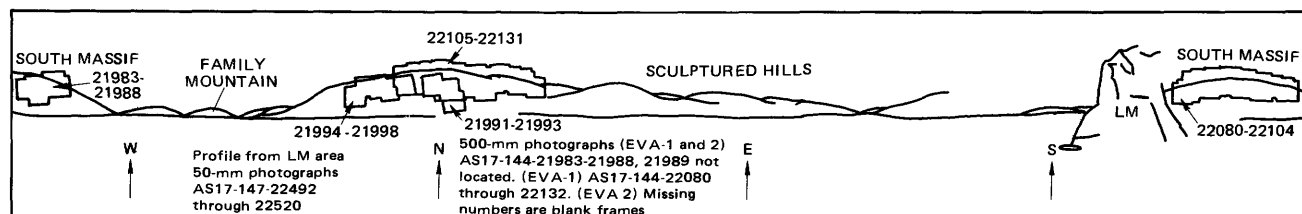
## THE PHOTOGRAPHIC DATA SET

The photographic data set is a catalog of all pictures taken on the lunar surface from both inside and outside the lunar module during the Apollo 17 mission using electric Hasselblad cameras with 60-mm and 500-mm lenses and 70-mm film. Pictures taken from lunar orbit are not listed in the tabulations. Information concerning coverage with the 500-mm camera is given in figure 258. Statistics about film usage are contained in table 6.

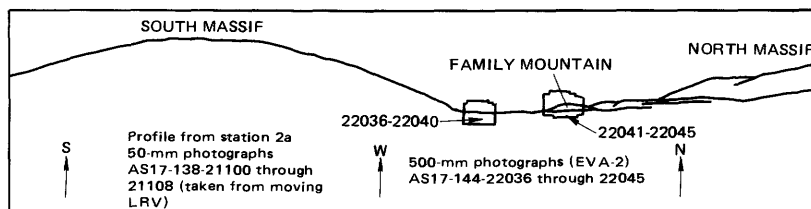
The tables are arranged for the following specific purposes:

1. To identify the pictures taken at a specific location or during a specific lunar surface activity (table 7).
2. To identify when and where a specific picture was taken and its subject matter (table 8).
3. To identify the camera with which a specific picture

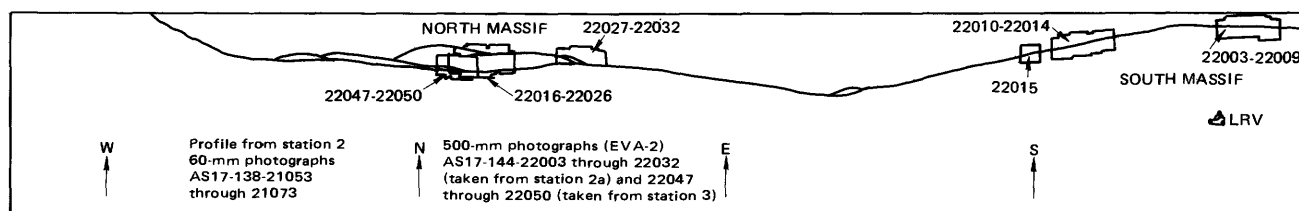
## 500-mm PHOTOGRAPHS FROM LM AREA



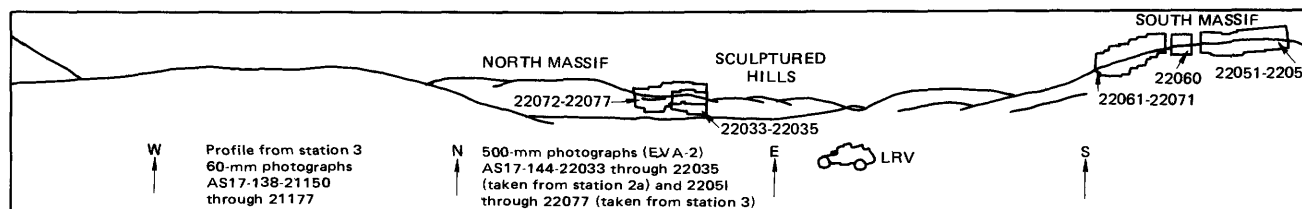
## 500-mm PHOTOGRAPHS FROM STATION 2a



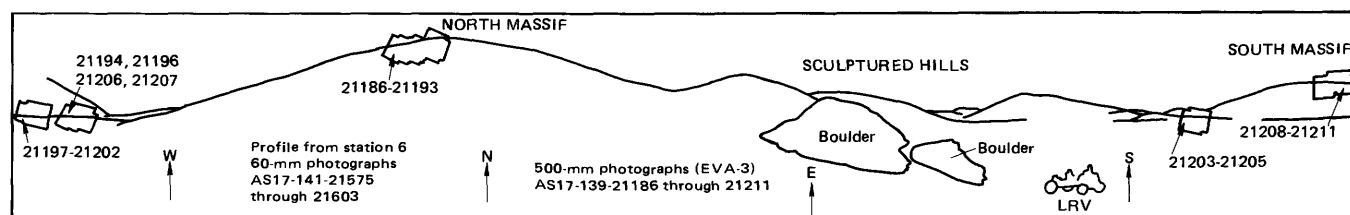
## 500-mm PHOTOGRAPHS FROM STATIONS 2a and 3



## 500-mm PHOTOGRAPHS FROM STATIONS 2a AND 3



## 500-mm PHOTOGRAPHS FROM STATION 6



## 500-mm PHOTOGRAPHS FROM STATION 9

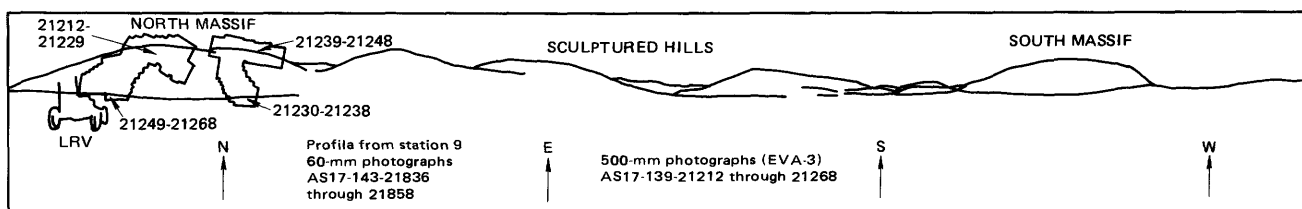


FIGURE 258.—Lunar surface areas photographed with the Apollo 17 500-mm camera.

TABLE 6.—Usage of film on the lunar surface during the Apollo 17 mission

EVA	Station	Film magazine	Focal length (mm)	Frames	Station total	EVA total
Pre	LM Window	A	60	23	23	23
1	LM	B	60	14		
1	LM	A	60	36		
1	LM	R	500	20	70	
1	ALSEP	H	60	41		
1	ALSEP	A	60	79	120	
1	SEP-1a	B	60	4		
1	SEP-1a	H	60	16	20	
1	1a	B	60	39		
1	1a	H	60	38	77	
1	1a-SEP	B	60	2		
1	1a-SEP	H	60	87	89	
1	SEP	B	60	12	12	
1	SEP-LM	B	60	5	5	
1	LM	C	60	29	29	422
2	SEP	G	60	17	17	
2	SEP-2	G	60	126		
2	SEP-2	C	60	5	131	
2	2	G	60	3		
2	2	C	60	80		
2	2	I	60	47	130	
2	2-2a	I	60	21	21	
2	2a	I	60	13		
2	2a	R	500	44	57	
2	2a-3	C	60	1		
2	2a-3	I	60	34	35	
2	3	I	60	39		
2	3	C	60	2		
2	3	R	500	33	74	
2	3-4	J	60	35		
2	3-4	C	60	1	36	
2	4	J	60	40		
2	4	C	60	44	84	
2	4-5	J	60	59	59	
2	5	J	60	34		
2	5	D	60	51	85	
2	5-LM	J	60	14		
2	5-LM	D	60	1	15	
2	ALSEP	D	60	7	7	
2	LM	R	500	53	53	804
2-3	LM-Window	E	60	8		
2-3	LM-Window	D	60	31	39	39
3	LM	E	60	33	33	
3	SEP	L	60	8	8	
3	SEP-6	E	60	8		
3	SEP-6	L	60	57	65	
3	6	E	60	110		
3	6	L	60	62		
3	6	F	60	9		
3	6	K	500	26	207	
3	6-7	L	60	9	9	
3	7	L	60	22		
3	7	M	60	2		
3	7	F	60	66	90	
3	7-8	M	60	27		
3	7-8	F	60	1	28	
3	8	M	60	48		
3	8	F	60	39	87	
3	8-9	M	60	45		
3	8-9	F	60	9	54	
3	9	B	60	3		
3	9	M	60	43		
3	9	N	60	25		
3	9	F	60	38		
3	9	K	500	57	166	
3	9-LM	B	60	6		
3	9-LM	N	60	68	74	
3	LM	B	60	28		
3	LM	N	60	4	32	
3	ALSEP	B	60	17	17	
3	LM	B	60	8	8	
3	RIP	N	60	4	4	
3	SEP	N	60	3	3	
3	LM	N	60	5	5	890
Post	LM Window	N	60	40	40	40
Total.....						2,218

was taken (table 9).

The sequence of lunar surface photographs and the Ground Elapsed Time (GET) at which the pictures were taken were determined by study of the detailed transcript of verbal communications between the astronauts and the control center and of the lunar-surface television videotapes. Times assigned to panorama photographs and to pictures taken while the LRV was in motion were largely based on interpolation between the best known times of start and finish. At several stations where the television showed a panorama being taken, the times of individual frames could be measured directly. When crew descriptions could be matched to specific pictures within an LRV driving photograph sequence, times could be precisely assigned to those frames, which served as control for interpolation.

#### CARTOGRAPHIC PROCEDURES

Methods of making measurements and planimetric maps used in this report included (1) estimation of fragment size and distance by the use of perspective grids (fig. 259), and (2) angular measurements on panoramas for resection of stations, and intersection of data points. Many of these methods are discussed by Batson (1969a, 1969b). A more general text in simple graphical photogrammetry was published by Williams (1969).

The use of a perspective grid assumes a flat surface and a known height of the camera above the surface. The accuracy of distance measurement varies directly with the accuracy with which camera height is known. A 5 percent error in camera height will introduce a 5 percent error in distance, and hence, size measurements. Deviation of the surface from the horizontal has the same effect as error in camera height measurements at specific points. For example, direct measurements of the shape of a rock cannot be accurately made except in the horizontal plane at known distance below the camera. The shape of the rock, as plotted with a perspective grid, will therefore be badly distorted.

While it may be possible to make reasonable corrections for rock shapes and sizes intuitively, undulations in the surface are less readily detectable. In spite of these difficulties, the perspective grid method can be used effectively by one skilled in interpreting Apollo surface pictures.

Approximate scales can be placed on near-field objects in pictures containing the gnomon by using an ellipse template. The Apollo 17 gnomon (for example, fig. 35) stands on three legs that, on a flat surface, define a circle 61.7 cm in diameter. The "fore and aft" scale, and the "side-to-side" scale of areas in the vicinity of the gnomon can be determined by fitting an el-

Table 7.--Chronological listing of 70mm Apollo 17 lunar surface pictures

MAG	PHOTO	SEQ	GET	EVA	STA	REMARKS
A	147-22469	1		PRE	LM	LM WINDOW PAN
A	147-22470	2		PRE	LM	LM WINDOW PAN
A	147-22471	3		PRE	LM	LM WINDOW PAN
A	147-22472	4		PRE	LM	LM WINDOW PAN
A	147-22473	5		PRE	LM	LM WINDOW PAN
A	147-22474	6		PRE	LM	LM WINDOW PAN
A	147-22475	7		PRE	LM	LM WINDOW PAN
A	147-22476	8		PRE	LM	LM WINDOW PAN
A	147-22477	9		PRE	LM	LM WINDOW PAN
A	147-22478	10		PRE	LM	LM WINDOW PAN
A	147-22479	11		PRE	LM	LM WINDOW PAN
A	147-22480	12		PRE	LM	LM WINDOW PAN
A	147-22481	13		PRE	LM	LM WINDOW PAN
A	147-22482	14		PRE	LM	LM WINDOW PAN
A	147-22483	15		PRE	LM	LM WINDOW PAN
A	147-22484	16		PRE	LM	LM WINDOW PAN
A	147-22485	17		PRE	LM	LM WINDOW PAN
A	147-22486	18		PRE	LM	LM WINDOW PAN
A	147-22487	19		PRE	LM	LM WINDOW PAN
A	147-22488	20		PRE	LM	LM WINDOW PAN
A	147-22489	21		PRE	LM	LM WINDOW PAN
A	147-22490	22		PRE	LM	LM WINDOW PAN
A	147-22491	23		PRE	LM	LM WINDOW PAN
A	147-22492	24	04 19 35	1	LM	PAN N OF LM
A	147-22493	25	04 19 35+	1	LM	PAN N OF LM
A	147-22494	26	04 19 35+	1	LM	PAN N OF LM
A	147-22495	27	04 19 35+	1	LM	PAN N OF LM
A	147-22496	28	04 19 35+	1	LM	PAN N OF LM
A	147-22497	29	04 19 35+	1	LM	PAN N OF LM
A	147-22498	30	04 19 35+	1	LM	PAN N OF LM
A	147-22499	31	04 19 35+	1	LM	PAN N OF LM
A	147-22500	32	04 19 35+	1	LM	PAN N OF LM
A	147-22501	33	04 19 35+	1	LM	PAN N OF LM
A	147-22502	34	04 19 35+	1	LM	PAN N OF LM
A	147-22503	35	04 19 35+	1	LM	PAN N OF LM
A	147-22504	36	04 19 35+	1	LM	PAN N OF LM
A	147-22505	37	04 19 35+	1	LM	PAN N OF LM
A	147-22506	38	04 19 35+	1	LM	PAN N OF LM
A	147-22507	39	04 19 35+	1	LM	PAN N OF LM
A	147-22508	40	04 19 35+	1	LM	PAN N OF LM
A	147-22509	41	04 19 35+	1	LM	PAN N OF LM
A	147-22510	42	04 19 35+	1	LM	PAN N OF LM
A	147-22511	43	04 19 35+	1	LM	PAN N OF LM
A	147-22512	44	04 19 35+	1	LM	PAN N OF LM
A	147-22513	45	04 19 35+	1	LM	PAN N OF LM
A	147-22514	46	04 19 35+	1	LM	PAN N OF LM
A	147-22515	47	04 19 35+	1	LM	PAN N OF LM
A	147-22516	48	04 19 35+	1	LM	PAN N OF LM
A	147-22517	49	04 19 35+	1	LM	PAN N OF LM
A	147-22518	50	04 19 35+	1	LM	PAN N OF LM
A	147-22519	51	04 19 35+	1	LM	PAN N OF LM
A	147-22520	52	04 19 35+	1	LM	PAN N OF LM
A	147-22521	53	04 19 35+	1	LM	CDR DRIVING LRV
A	147-22522	54	04 19 35+	1	LM	CDR DRIVING LRV
A	147-22523	55	04 19 35+	1	LM	CDR DRIVING LRV
A	147-22524	56	04 19 35+	1	LM	CDR DRIVING LRV
A	147-22525	57	04 19 35+	1	LM	CDR DRIVING LRV
A	147-22526	58	04 19 35+	1	LM	CDR DRIVING LRV
A	147-22527	59	04 19 35+	1	LM	CDR DRIVING LRV
B	134-20376	60	04 19 35+	1	LM	MISC
B	134-20377	61	04 19 42	1	LM	LM, FLAG
B	134-20378	62	04 19 42+	1	LM	LM, FLAG
B	134-20379	63	04 19 42+	1	LM	LM, FLAG
B	134-20380	64	04 19 42+	1	LM	LM, FLAG
B	134-20381	65	04 19 42+	1	LM	LM, FLAG
B	134-20382	66	04 19 42+	1	LM	LM, FLAG
B	134-20383	67	04 19 43	1	LM	FLAG
B	134-20384	68	04 19 43+	1	LM	FLAG
B	134-20385	69	04 19 43+	1	LM	FLAG
B	134-20386	70	04 19 43+	1	LM	FLAG
B	134-20387	71	04 19 44	1	LM	FLAG
B	134-20388	72	04 19 50	1	LM	FOOTPAD
B	134-20389	73	04 19 50+	1	LM	LRV
A	147-22528	74	04 21 56	1	ALSEP	PPAN OF GEOPHONE LOC
A	147-22529	75	04 21 56+	1	ALSEP	PPAN OF GEOPHONE LOC
A	147-22530	76	04 21 56+	1	ALSEP	PPAN OF GEOPHONE LOC
A	147-22531	77	04 21 56+	1	ALSEP	PPAN OF GEOPHONE LOC
A	147-22532	78	04 21 56+	1	ALSEP	PPAN OF GEOPHONE LOC
A	147-22533	79	04 21 56	1	ALSEP	CU GEOPHONE ROCK
A	147-22534	80	04 21 58+	1	ALSEP	CU GEOPHONE ROCK
A	147-22535	81	04 21 58+	1	ALSEP	GEOPHONE ROCK, STEREO
A	147-22536	82	04 21 58+	1	ALSEP	GEOPHONE ROCK, STEREO
A	147-22537	83	04 21 58+	1	ALSEP	GEOPHONE
A	147-22538	84	04 21 58+	1	ALSEP	DS
A	147-22539	85	04 21 58+	1	ALSEP	?
A	147-22540	86	04 21 58+	1	ALSEP	?
A	147-22541	87	04 21 58+	1	ALSEP	DS
A	147-22542	88	04 21 58+	1	ALSEP	PAN NEAR GEOPHONE ROCK
A	147-22543	89	04 21 42	1	ALSEP	PAN NEAR GEOPHONE ROCK
A	147-22544	90	04 21 53+	1	ALSEP	PAN NEAR GEOPHONE ROCK

Table 7.--Chronological listing of 70mm Apollo 17 lunar surface pictures--Continued

MAG	PHOTO	SEQ	GET	ZVA	STA	REMARKS
A	147-22545	91	04 21 58+	1	ALSEP	PAN NEAR GEOPHONE ROCK
A	147-22546	92	04 21 58+	1	ALSEP	PAN NEAR GEOPHONE ROCK
A	147-22547	93	04 21 58+	1	ALSEP	PAN NEAR GEOPHONE ROCK
A	147-22548	94	04 21 58+	1	ALSEP	PAN NEAR GEOPHONE ROCK
A	147-22549	95	04 21 58+	1	ALSEP	PAN NEAR GEOPHONE ROCK
A	147-22550	96	04 21 58+	1	ALSEP	PAN NEAR GEOPHONE ROCK
A	147-22551	97	04 21 58+	1	ALSEP	PAN NEAR GEOPHONE ROCK
A	147-22552	98	04 21 58+	1	ALSEP	PAN NEAR GEOPHONE ROCK
A	147-22553	99	04 21 58+	1	ALSEP	PAN NEAR GEOPHONE ROCK
A	147-22554	100	04 21 58+	1	ALSEP	PAN NEAR GEOPHONE ROCK
A	147-22555	101	04 21 58+	1	ALSEP	PAN NEAR GEOPHONE ROCK
A	147-22556	102	04 21 58+	1	ALSEP	PAN NEAR GEOPHONE ROCK
A	147-22557	103	04 21 58+	1	ALSEP	PAN NEAR GEOPHONE ROCK
A	147-22558	104	04 21 58+	1	ALSEP	PAN NEAR GEOPHONE ROCK
A	147-22559	105	04 21 58+	1	ALSEP	PAN NEAR GEOPHONE ROCK
A	147-22560	106	04 21 58+	1	ALSEP	PAN NEAR GEOPHONE ROCK
A	147-22561	107	04 21 58+	1	ALSEP	PAN NEAR GEOPHONE ROCK
A	147-22562	108	04 22 04	1	ALSEP	GEOPHONE
A	147-22563	109	04 22 04+	1	ALSEP	?
A	147-22564	110	04 22 04+	1	ALSEP	?
A	147-22565	111	04 22 07	1	ALSEP	PAN AT C/S
A	147-22566	112	04 22 07+	1	ALSEP	PAN AT C/S
A	147-22567	113	04 22 07+	1	ALSEP	PAN AT C/S
A	147-22568	114	04 22 07+	1	ALSEP	PAN AT C/S
A	147-22569	115	04 22 07+	1	ALSEP	PAN AT C/S
A	147-22570	116	04 22 07+	1	ALSEP	PAN AT C/S
A	147-22571	117	04 22 07+	1	ALSEP	PAN AT C/S
A	147-22572	118	04 22 07+	1	ALSEP	PAN AT C/S
A	147-22573	119	04 22 07+	1	ALSEP	PAN AT C/S
A	147-22574	120	04 22 07+	1	ALSEP	PAN AT C/S
A	147-22575	121	04 22 07+	1	ALSEP	PAN AT C/S
A	147-22576	122	04 22 07+	1	ALSEP	PAN AT C/S
A	147-22577	123	04 22 07+	1	ALSEP	PAN AT C/S
A	147-22578	124	04 22 07+	1	ALSEP	PAN AT C/S
A	147-22579	125	04 22 07+	1	ALSEP	PAN AT C/S
A	147-22580	126	04 22 07+	1	ALSEP	PAN AT C/S
A	147-22581	127	04 22 07+	1	ALSEP	PAN AT C/S
A	147-22582	128	04 22 07+	1	ALSEP	PAN AT C/S
A	147-22583	129	04 22 07+	1	ALSEP	PAN AT C/S
A	147-22584	130	04 22 07+	1	ALSEP	PAN AT C/S
A	147-22585	131	04 22 07+	1	ALSEP	PAN AT C/S
A	147-22586	132	04 22 07+	1	ALSEP	PAN AT C/S
A	147-22587	133	04 22 07+	1	ALSEP	PAN AT C/S
A	147-22588	134	04 22 07+	1	ALSEP	PAN AT C/S
A	147-22589	135	04 22 11	1	ALSEP	PPAN
A	147-22590	136	04 22 11+	1	ALSEP	PPAN
A	147-22591	137	04 22 11+	1	ALSEP	PPAN
A	147-22592	138	04 22 11+	1	ALSEP	PPAN
A	147-22593	139	04 22 11+	1	ALSEP	PPAN
A	147-22594	140	04 22 11+	1	ALSEP	PPAN
A	147-22595	141	04 22 11+	1	ALSEP	PPAN
A	147-22596	142	04 22 11+	1	ALSEP	PPAN
A	147-22597	143	04 22 11+	1	ALSEP	PPAN
A	147-22598	144	04 22 11+	1	ALSEP	PPAN, CDR DRILLING
A	147-22599	145	04 22 11+	1	ALSEP	PPAN, CDR DRILLING
A	147-22600	146	04 22 11+	1	ALSEP	PPAN
A	147-22601	147	04 22 11+	1	ALSEP	PPAN
A	147-22602	148	04 22 11+	1	ALSEP	PPAN
A	147-22603	149	04 22 11+	1	ALSEP	PPAN
A	147-22604	150	04 22 11+	1	ALSEP	PPAN
A	147-22605	151	04 22 11+	1	ALSEP	PPAN
A	147-22606	152	04 22 11+	1	ALSEP	PPAN
H	136-20682	153	04 22 18	1	ALSEP	MISC, FOGGED
H	136-20683	154	04 22 18+	1	ALSEP	PAN
H	136-20684	155	04 22 18+	1	ALSEP	PAN
H	136-20685	156	04 22 18+	1	ALSEP	PAN
H	136-20686	157	04 22 18+	1	ALSEP	PAN
H	136-20687	158	04 22 18+	1	ALSEP	PAN
H	136-20688	159	04 22 18+	1	ALSEP	PAN
H	136-20689	160	04 22 18+	1	ALSEP	PAN
H	136-20690	161	04 22 18+	1	ALSEP	PAN
H	136-20691	162	04 22 18+	1	ALSEP	PAN
H	136-20692	163	04 22 18+	1	ALSEP	PAN
H	136-20693	164	04 22 18+	1	ALSEP	PAN
H	136-20694	165	04 22 18+	1	ALSEP	PAN
H	136-20695	166	04 22 18+	1	ALSEP	PAN
H	136-20696	167	04 22 18+	1	ALSEP	PAN
H	136-20697	168	04 22 18+	1	ALSEP	PAN
H	136-20698	169	04 22 18+	1	ALSEP	PAN
H	136-20699	170	04 22 18+	1	ALSEP	PAN
H	136-20700	171	04 22 18+	1	ALSEP	PAN
H	136-20701	172	04 22 18+	1	ALSEP	PAN
H	136-20702	173	04 22 18+	1	ALSEP	PAN
H	136-20703	174	04 22 18+	1	ALSEP	PAN
H	136-20704	175	04 22 18+	1	ALSEP	PAN
H	136-20705	176	04 22 18+	1	ALSEP	PAN
H	136-20706	177	04 22 18+	1	ALSEP	PAN
H	136-20707	178	04 22 18+	1	ALSEP	PAN
H	136-20708	179	04 22 18+	1	ALSEP	PAN
H	136-20709	180	04 22 18+	1	ALSEP	PAN

Table 7.--Chronological listing of 70mm Apollo 17 lunar surface pictures--Continued

MAG	PHOTO	SEQ	GET	EVA	STA	REMARKS
H 136-20710		181	04 22 18+	1	ALSEP	PAN
H 136-20711		182	04 22 18+	1	ALSEP	C/S, HEAT FLOW PROBE 1
H 136-20712		183	04 22 18+	1	ALSEP	C/S, HEAT FLOW PROBE 1
H 136-20713		184	04 22 18+	1	ALSEP	C/S, HEAT FLOW PROBE 1
H 136-20714		185	04 22 25	1	ALSEP	PARTING ROCK XS
H 136-20715		186	04 22 25+	1	ALSEP	PARTING ROCK XS
H 136-20716		187	04 22 25+	1	ALSEP	PARTING ROCK CU
H 136-20717		188	04 22 25+	1	ALSEP	PARTING ROCK CU
H 136-20718		189	04 22 36	1	ALSEP	PARTING ROCK, SPL 70160-04, 35 DS
H 136-20719		190	04 22 36	1	ALSEP	PARTING ROCK, SPL 70160-04, 05 DS
H 136-20720		191	04 22 42	1	ALSEP	SPL 70180-84,85, DEEP CORE 70001-09, NEUTRON FLUX
H 136-20721		192	04 22 42+	1	ALSEP	SPL 70180-84,85, DEEP CORE 70001-09 XSB
H 136-20722		193	04 22 42+	1	ALSEP	SPL 70180-84,85, DEEP CORE 70001-09 XSA
H 136-20723		194	04 23 11	1	SEP-1	
H 136-20724		195	04 23 11+	1	SEP-1	
H 136-20725		196	04 23 11+	1	SEP-1	
H 136-20726		197	04 23 11+	1	SEP-1	
H 136-20727		198	04 23 11+	1	SEP-1	
B 134-20390		199	04 23 11+	1	SEP-1	
H 136-20728		200	04 23 11+	1	SEP-1	
B 134-20391		201	04 23 11+	1	SEP-1	
B 134-20392		202	04 23 11+	1	SEP-1	
H 136-20729		203	04 23 11+	1	SEP-1	
H 136-20730		204	04 23 11+	1	SEP-1	
H 136-20731		205	04 23 11+	1	SEP-1	
H 136-20732		206	04 23 11+	1	SEP-1	
H 136-20733		207	04 23 11+	1	SEP-1	
H 136-20734		208	04 23 11+	1	SEP-1	
H 136-20735		209	04 23 11+	1	SEP-1	
H 136-20736		210	04 23 11+	1	SEP-1	
H 136-20737		211	04 23 11+	1	SEP-1	
B 134-20393		212	04 23 11+	1	SEP-1	
H 136-20738		213	04 23 11+	1	SEP-1	
H 136-20739		214	04 23 29	1		SPL 71110, 35-37, 71040-44, 45-49, 71055, 71060-64, 65-69, 85-89, 95-97 DS
H 136-20740		215	04 23 32+	1		SPL 71110, 35-37, 71040-44, 45-49, 71055, 71060-64, 65-69, 85-89, 95-97 LOC
B 134-20394		216	04 23 32+	1		SPL 71110, 35-37, 71040-44, 45-49, 71055, 71060-64, 65-69, 85-89, 95-97 XSB
B 134-20395		217	04 23 32+	1		SPL 71110, 35-37, 71040-44, 45-49, 71055, 71060-64, 65-69, 85-89, 95-97 XSB
B 134-20396		218	04 23 32+	1		SPL 71110, 35-37, 71040-44, 45-49, 71055, 71060-64, 65-69, 85-89, 95-97 XSA
H 136-20741		219	04 23 42	1		SPL 71130, 35-36, 71150, 55-57, 71175 DS
B 134-20397		220	04 23 42+	1		SPL 71130, 35-36, 71150, 55-57, 71175 XSB
B 134-20398		221	04 23 42+	1		SPL 71130, 35-36, 71150, 55-57, 71175 XSB
B 134-20399		222	04 23 43	1		SPL 71130, 43-36, 71150, 55-57, 71175 XSA
B 134-20400		223	04 23 43+	1		SPL 71130, 35-36, 71150, 55-57, 71175 LOC
B 134-20401		224	04 23 43+	1		SPL 71130, 35-36, 71150, 55-57, 71175 CU
B 134-20402		225	04 23 43+	1		SPL 71130, 35-36, 71150, 55-57, 71175 CU
B 134-20403		226	04 23 43+	1		SPL 71130, 35-36, 71150, 55-57, 71175 CU
B 134-20404		227	04 23 43+	1		SPL 71130, 35-36, 71150, 55-57, 71175 CU
H 136-20742		228	04 23 43+	1		SPL 71500-04, 05-09, 15, 71525-29, 35-39, 45-49, 55-59, 65-69, 75-79, 85-89, 95-97 LOC
H 136-20743		229	04 23 43+	1		SPL 71500-04, 05-09, 15, 71525-29, 35-39, 45-49, 55-59, 65-69, 75-79, 85-89, 95-97 DS
B 134-20405		230	04 23 43+	1		SPL 71500-04, 05-09, 15, 71525-29, 35-39, 45-49, 55-59, 65-69, 75-79, 85-89, 95-97 XSB
B 134-20406		231	04 23 43+	1		SPL 71500-04, 05-09, 15, 71525-29, 35-39, 45-49, 55-59, 65-69, 75-79, 85-89, 95-97 XSB
B 134-20407		232	04 23 43+	1		SPL 71500-04, 05-09, 15, 71525-29, 35-39, 45-49, 55-59, 65-69, 75-79, 85-89, 95-97 XSB
B 134-20408		233	04 23 43	1		PAN
B 134-20409		234	04 23 46+	1		PAN
B 134-20410		235	04 23 46+	1		PAN
B 134-20411		236	04 23 46+	1		PAN
B 134-20412		237	04 23 46+	1		PAN
B 134-20413		238	04 23 46+	1		PAN
B 134-20414		239	04 23 46+	1		PAN
B 134-20415		240	04 23 46+	1		PAN
B 134-20416		241	04 23 46+	1		PAN
B 134-20417		242	04 23 46+	1		PAN
B 134-20418		243	04 23 46+	1		PAN
B 134-20419		244	04 23 46+	1		PAN
B 134-20420		245	04 23 46+	1		PAN
B 134-20421		246	04 23 46+	1		PAN
B 134-20422		247	04 23 46+	1		PAN, EP-6 LOC
B 134-20423		248	04 23 46+	1		PAN, EP-6 LOC
B 134-20424		249	04 23 46+	1		PAN, EP-6 LOC
B 134-20425		250	04 23 46+	1		PAN, SPL 71500-04, 05-09, 15, 71525-29, 35-39, 45-49, 55-59, 65-69, 75-79, 85-89, 95-97 LOC
B 134-20426		251	04 23 46+	1		PAN, SPL 71500-04, 05-09, 15, 71525-29, 35-39, 45-49, 55-59, 65-69, 75-79, 85-89, 95-97 LOC
B 134-20427		252	04 23 46+	1		PAN, SPL 71500-04, 05-09, 15, 71525-29, 35-39, 45-49, 55-59, 65-69, 75-79, 85-89, 95-97 LOC
B 134-20428		253	04 23 46+	1		PAN
B 134-20429		254	04 23 46+	1		PAN
B 134-20430		255	04 23 46+	1		PAN
B 134-20431		256	04 23 46+	1		PAN
B 134-20432		257	04 23 46	1		SPL 71500-04, 05-09, 15, 71525-29, 35-39, 45-49, 55-59, 65-69, 75-79, 85-89, 95-97 XSA
H 136-20744		258	04 23 51	1		PAN
H 136-20745		259	04 23 51+	1		PAN
H 136-20746		260	04 23 51+	1		PAN
H 136-20747		261	04 23 51+	1		PAN
H 136-20748		262	04 23 51+	1		PAN
H 136-20749		263	04 23 51+	1		PAN
H 136-20750		264	04 23 51+	1		PAN
H 136-20751		265	04 23 51+	1		PAN
H 136-20752		266	04 23 51+	1		PAN
H 136-20753		267	04 23 51+	1		PAN
H 136-20754		268	04 23 51+	1		PAN
H 136-20755		269	04 23 51+	1		PAN
H 136-20756		270	04 23 51+	1		PAN

Table 7.--Chronological listing of 70mm Apollo 17  
lunar surface pictures--Continued

MAG	PHOTO	SEQ	GET	EVA	STA	REMARKS
H 136-20757	271	04 23 51+	1	1	1	PAN
H 136-20758	272	04 23 51+	1	1	1	PAN
H 136-20759	273	04 23 51+	1	1	1	PAN
H 136-20760	274	04 23 51+	1	1	1	PAN
H 136-20761	275	04 23 51+	1	1	1	PAN
H 136-20762	276	04 23 51+	1	1	1	PAN
H 136-20763	277	04 23 51+	1	1	1	PAN
H 136-20764	278	04 23 51+	1	1	1	PAN
H 136-20765	279	04 23 51+	1	1	1	PAN
H 136-20766	280	04 23 51+	1	1	1	PAN
H 136-20767	281	04 23 51+	1	1	1	PAN
H 136-20768	282	04 23 51+	1	1	1	PAN
H 136-20769	283	04 23 51+	1	1	1	PAN
H 136-20770	284	04 23 51+	1	1	1	PAN
H 136-20771	285	04 23 51+	1	1	1	PAN
H 136-20772	286	04 23 51+	1	1	1	PAN
H 136-20773	287	04 23 51+	1	1	1	PAN
H 136-20774	288	04 23 51+	1	1	1	PAN
H 136-20775	289	04 23 51+	1	1	1	PAN
H 136-20776	290	04 23 51+	1	1	1	PAN
H 136-20777	291	04 23 55	1	1-SEP		
H 136-20778	292	04 23 55+	1	1-SEP		
H 136-20779	293	04 23 55+	1	1-SEP		
H 136-20780	294	04 23 55+	1	1-SEP		
H 136-20781	295	04 23 55+	1	1-SEP		
H 136-20782	296	04 23 55+	1	1-SEP		
H 136-20783	297	04 23 55+	1	1-SEP		
H 136-20784	298	04 23 55+	1	1-SEP		
H 136-20785	299	04 23 55+	1	1-SEP		
H 136-20786	300	04 23 55+	1	1-SEP		
H 136-20787	301	04 23 55+	1	1-SEP		
H 136-20788	302	04 23 55+	1	1-SEP		
H 136-20789	303	04 23 55+	1	1-SEP		
H 136-20790	304	04 23 55+	1	1-SEP		
H 136-20791	305	04 23 55+	1	1-SEP		
H 136-20792	306	04 23 55+	1	1-SEP		
H 136-20793	307	04 23 55+	1	1-SEP		
H 136-20794	308	04 23 55+	1	1-SEP		
H 136-20795	309	04 23 55+	1	1-SEP		
H 136-20796	310	04 23 55+	1	1-SEP		
H 136-20797	311	04 23 55+	1	1-SEP		
H 136-20798	312	04 23 55+	1	1-SEP		
H 136-20799	313	04 23 55+	1	1-SEP		
H 136-20800	314	04 23 55+	1	1-SEP		
H 136-20801	315	04 23 55+	1	1-SEP		
H 136-20802	316	04 23 55+	1	1-SEP		
H 136-20803	317	04 23 55+	1	1-SEP		
H 136-20804	318	04 23 55+	1	1-SEP		
H 136-20805	319	04 23 55+	1	1-SEP		
H 136-20806	320	04 23 55+	1	1-SEP		
H 136-20807	321	04 23 55+	1	1-SEP		
H 136-20808	322	04 23 55+	1	1-SEP		
H 136-20809	323	04 23 55+	1	1-SEP		
H 136-20810	324	04 23 55+	1	1-SEP		
H 136-20811	325	04 23 55+	1	1-SEP		
H 136-20812	326	04 23 58	1	1-SEP	EP-7 LOC, LRV PPAN	
H 136-20813	327	04 23 58+	1	1-SEP	EP-7 LOC, LRV PPAN	
H 136-20814	328	04 23 58+	1	1-SEP	EP-7 LOC, LRV PPAN	
H 136-20815	329	04 23 58+	1	1-SEP	EP-7 LOC, LRV PPAN	
H 136-20816	330	04 23 58+	1	1-SEP	EP-7 LOC	
H 136-20817	331	04 23 58+	1	1-SEP	EP-7 LOC	
H 136-20818	332	05 00 02	1	1-SEP	EP-7 LOC, LRV PPAN	
H 136-20819	333	05 00 02+	1	1-SEP	EP-7 LOC, LRV PPAN	
H 136-20820	334	05 00 02+	1	1-SEP	EP-7 LOC, LRV PPAN	
H 136-20821	335	05 00 02+	1	1-SEP	EP-7 LOC, LRV PPAN	
H 136-20822	336	05 00 02+	1	1-SEP	EP-7 LOC, LRV PPAN	
H 136-20823	337	05 00 02+	1	1-SEP	EP-7 LOC, LRV PPAN	
H 136-20824	338	05 00 02+	1	1-SEP	EP-7 LOC, LRV PPAN	
H 136-20825	339	05 00 02+	1	1-SEP	EP-7 LOC, LRV PPAN	
H 136-20826	340	05 00 02+	1	1-SEP	EP-7 LOC, LRV PPAN	
H 136-20827	341	05 00 02+	1	1-SEP	EP-7 LOC, LRV PPAN	
H 136-20828	342	05 00 02+	1	1-SEP	EP-7 LOC, LRV PPAN	
H 136-20829	343	05 00 02+	1	1-SEP	EP-7 LOC, LRV PPAN	
H 136-20830	344	05 00 02+	1	1-SEP	EP-7 LOC, LRV PPAN	
H 136-20831	345	05 00 02+	1	1-SEP		
H 136-20832	346	05 00 02+	1	1-SEP		
H 136-20833	347	05 00 02+	1	1-SEP		
H 136-20834	348	05 00 02+	1	1-SEP		
H 136-20835	349	05 00 02+	1	1-SEP		
H 136-20836	350	05 00 02+	1	1-SEP		
H 136-20837	351	05 00 02+	1	1-SEP		
H 136-20838	352	05 00 02+	1	1-SEP		
H 136-20839	353	05 00 02+	1	1-SEP		
H 136-20840	354	05 00 02+	1	1-SEP		
H 136-20841	355	05 00 02+	1	1-SEP		
H 136-20842	356	05 00 02+	1	1-SEP		
H 136-20843	357	05 00 02+	1	1-SEP		
H 136-20844	358	05 00 02+	1	1-SEP		
H 136-20845	359	05 00 02+	1	1-SEP		
H 136-20846	360	05 00 02+	1	1-SEP		

Table 7.--Chronological listing of 70mm Apollo 17 lunar surface pictures--Continued

MAG	PHOTO	SEQ	GET	EVA	STA	REMARKS
H	136-20845	361	05 00 02+	1	1-SEP	
H	136-20846	362	05 00 02+	1	1-SEP	
H	136-20847	363	05 00 02+	1	1-SEP	
H	136-20848	364	05 00 02+	1	1-SEP	
H	136-20849	365	05 00 02+	1	1-SEP	
H	136-20850	366	05 00 02+	1	1-SEP	
H	136-20851	367	05 00 02+	1	1-SEP	
H	136-20852	368	05 00 02+	1	1-SEP	
H	136-20853	369	05 00 02+	1	1-SEP	
H	136-20854	370	05 00 02+	1	1-SEP	
H	136-20855	371	05 00 02+	1	1-SEP	
H	136-20856	372	05 00 02+	1	1-SEP	
H	136-20857	373	05 00 02+	1	1-SEP	
H	136-20858	374	05 00 02+	1	1-SEP	
H	136-20859	375	05 00 02+	1	1-SEP	
H	136-20860	376	05 00 02+	1	1-SEP	
H	136-20861	377	05 00 02+	1	1-SEP	
H	136-20862	378	05 00 02+	1	1-SEP	
H	136-20863	379	05 00 02+	1	1-SEP	
B	134-20435	380	05 00 23	1	SEP	SEP ANTENNA DEPLOYMENT
B	134-20436	381	05 00 23+	1	SEP	SEP ANTENNA DEPLOYMENT
B	134-20437	382	05 00 26	1	SEP	PPAN
B	134-20438	383	05 00 26+	1	SEP	PPAN
B	134-20439	384	05 00 26+	1	SEP	PPAN
B	134-20440	385	05 00 26+	1	SEP	PPAN
B	134-20441	386	05 00 26+	1	SEP	PPAN
B	134-20442	387	05 00 26+	1	SEP	PPAN
B	134-20443	388	05 00 26+	1	SEP	PPAN
B	134-20444	389	05 00 26+	1	SEP	PPAN
B	134-20445	390	05 00 26+	1	SEP	PPAN
B	134-20446	391	05 00 26+	1	SEP	PPAN
B	134-20447	392	05 00 11	1	SEP-LM	
B	134-20448	393	05 00 11+	1	SEP-LM	
B	134-20449	394	05 00 11+	1	SEP-LM	BLANK
B	134-20450	395	05 00 11+	1	SEP-LM	BLANK
B	134-20451	396	05 00 11+	1	SEP-LM	BLANK
C	137-20866	397	05 18 21	2	LM	PAN S OF LM
C	137-20867	398	05 18 21+	2	LM	PAN S OF LM
C	137-20868	399	05 18 21+	2	LM	PAN S OF LM
C	137-20869	400	05 18 21+	2	LM	PAN S OF LM
C	137-20870	401	05 18 21+	2	LM	PAN S OF LM
C	137-20871	402	05 18 21+	2	LM	PAN S OF LM
C	137-20872	403	05 18 21+	2	LM	PAN S OF LM
C	137-20873	404	05 18 21+	2	LM	PAN S OF LM
C	137-20874	405	05 18 21+	2	LM	PAN S OF LM
C	137-20875	406	05 18 21+	2	LM	PAN S OF LM
C	137-20876	407	05 18 21+	2	LM	PAN S OF LM
C	137-20877	408	05 18 21+	2	LM	PAN S OF LM
C	137-20878	409	05 18 21+	2	LM	PAN S OF LM
C	137-20879	410	05 18 21+	2	LM	PAN S OF LM
C	137-20880	411	05 18 21+	2	LM	PAN S OF LM
C	137-20881	412	05 18 21+	2	LM	PAN S OF LM
C	137-20882	413	05 18 21+	2	LM	PAN S OF LM
C	137-20883	414	05 18 21+	2	LM	PAN S OF LM
C	137-20884	415	05 18 21+	2	LM	PAN S OF LM
C	137-20885	416	05 18 21+	2	LM	PAN S OF LM
C	137-20886	417	05 18 21+	2	LM	PAN S OF LM
C	137-20887	418	05 18 21+	2	LM	PAN S OF LM
C	137-20888	419	05 18 21+	2	LM	PAN S OF LM
C	137-20889	420	05 18 21+	2	LM	PAN S OF LM
C	137-20890	421	05 18 21+	2	LM	PAN S OF LM
C	137-20891	422	05 18 21+	2	LM	PAN S OF LM
C	137-20892	423	05 18 21+	2	LM	PAN S OF LM
C	137-20893	424	05 18 22	2	LM	PAN S OF LM
C	137-20894	425	05 18 22+	2	LM	LRV
G	135-20533	426	05 18 41	2	SEP	SPL 70255 XS
G	135-20534	427	05 18 41+	2	SEP	SPL 70255 XS
G	135-20535	428	05 18 41+	2	SEP	SPL 70255 XS
G	135-20536	429	05 18 41+	2	SEP	SPL 70255 XS
G	135-20537	430	05 18 41+	2	SEP	SPL 70255 XS
G	135-20538	431	05 18 41+	2	SEP	SPL 70255 LOC
G	135-20539	432	05 18 48	2	SEP	SPL 70270-74,75 XSB
G	135-20540	433	05 18 48	2	SEP	SPL 70270-74,75 XSB
G	135-20541	434	05 18 48	2	SEP	SPL 70270-74,75 LOC
G	135-20542	435	05 18 48+	2	SEP	LRV
G	135-20543	436	05 18 48+	2	SEP	LRV
G	135-20544	437	05 18 48+	2	SEP	LRV
G	135-20545	438	05 18 48+	2	SEP	LRV
G	135-20546	439	05 18 48+	2	SEP	LRV
G	135-20547	440	05 18 48+	2	SEP	LRV
G	135-20548	441	05 18 48+	2	SEP	LRV
G	135-20549	442	05 18 48+	2	SEP	LRV
G	135-20550	443	05 18 51	2	SEP-2	
G	135-20551	444	05 18 51+	2	SEP-2	
G	135-20552	445	05 18 51+	2	SEP-2	
G	135-20553	446	05 18 51+	2	SEP-2	
G	135-20554	447	05 18 51+	2	SEP-2	
G	135-20555	448	05 18 51+	2	SEP-2	
G	135-20556	449	05 18 51+	2	SEP-2	
G	135-20557	450	05 18 51+	2	SEP-2	

Table 7.--Chronological listing of 70mm Apollo 17  
lunar surface pictures--Continued

MAG	PHOTO	SEQ	GET	EVA	STA	REMARKS
G	135-20558	451	05 18 51+	2	SEP-2	
G	135-20559	452	05 18 51+	2	SEP-2	
G	135-20560	453	05 18 51+	2	SEP-2	
G	135-20561	454	05 18 51+	2	SEP-2	
G	135-20562	455	05 18 51+	2	SEP-2	
G	135-20563	456	05 18 55	2	SEP-2	LRV PPAN, EP-4
G	135-20564	457	05 18 55+	2	SEP-2	LRV PPAN, EP-4
G	135-20565	458	05 18 55+	2	SEP-2	LRV PPAN, EP-4
G	135-20566	459	05 18 55+	2	SEP-2	LRV PPAN, EP-4
G	135-20567	460	05 18 55+	2	SEP-2	LRV PPAN, EP-4
G	135-20568	461	05 18 55+	2	SEP-2	LRV PPAN, EP-4
G	135-20569	462	05 18 55+	2	SEP-2	LRV PPAN, EP-4
G	135-20570	463	05 18 55+	2	SEP-2	
G	135-20571	464	05 18 55+	2	SEP-2	
G	135-20572	465	05 18 55+	2	SEP-2	
G	135-20573	466	05 18 55+	2	SEP-2	
G	135-20574	467	05 18 55+	2	SEP-2	
G	135-20575	468	05 18 55+	2	SEP-2	
G	135-20576	469	05 18 55+	2	SEP-2	
G	135-20577	470	05 18 55+	2	SEP-2	
G	135-20578	471	05 18 55+	2	SEP-2	
G	135-20579	472	05 18 55+	2	SEP-2	
G	135-20580	473	05 18 55+	2	SEP-2	
G	135-20581	474	05 18 55+	2	SEP-2	
G	135-20582	475	05 18 55+	2	SEP-2	
G	135-20583	476	05 18 55+	2	SEP-2	
G	135-20584	477	05 18 55+	2	SEP-2	
G	135-20585	478	05 18 55+	2	SEP-2	
G	135-20586	479	05 18 55+	2	SEP-2	
G	135-20587	480	05 18 55+	2	SEP-2	
G	135-20588	481	05 18 55+	2	SEP-2	
G	135-20589	482	05 18 55+	2	SEP-2	
G	135-20590	483	05 18 55+	2	SEP-2	
G	135-20591	484	05 18 55+	2	SEP-2	
G	135-20592	485	05 18 55+	2	SEP-2	
G	135-20593	486	05 18 55+	2	SEP-2	
G	135-20594	487	05 18 55+	2	SEP-2	
G	135-20595	488	05 18 55+	2	SEP-2	
G	135-20596	489	05 18 55+	2	SEP-2	
G	135-20597	490	05 18 55+	2	SEP-2	
G	135-20598	491	05 18 55+	2	SEP-2	
G	135-20599	492	05 18 55+	2	SEP-2	
G	135-20600	493	05 18 55+	2	SEP-2	
G	135-20601	494	05 18 55+	2	SEP-2	
G	135-20602	495	05 18 55+	2	SEP-2	
G	135-20603	496	05 18 55+	2	SEP-2	
G	135-20604	497	05 18 55+	2	SEP-2	
G	135-20605	498	05 18 55+	2	SEP-2	
G	135-20606	499	05 18 55+	2	SEP-2	
G	135-20607	500	05 18 55+	2	SEP-2	
G	135-20608	501	05 18 55+	2	SEP-2	
G	135-20609	502	05 18 55+	2	SEP-2	
G	135-20610	503	05 18 55+	2	SEP-2	
G	135-20611	504	05 18 55+	2	SEP-2	
G	135-20612	505	05 18 55+	2	SEP-2	
G	135-20613	506	05 18 55+	2	SEP-2	
G	135-20614	507	05 18 55+	2	SEP-2	
G	135-20615	508	05 18 55+	2	SEP-2	
G	135-20616	509	05 18 55+	2	SEP-2	
G	135-20617	510	05 18 55+	2	SEP-2	
G	135-20618	511	05 18 55+	2	SEP-2	
G	135-20619	512	05 18 55+	2	SEP-2	
G	135-20620	513	05 18 55+	2	SEP-2	
G	135-20621	514	05 18 55+	2	SEP-2	
G	135-20622	515	05 18 55+	2	SEP-2	
G	135-20623	516	05 19 14	2	SEP-2	SPL 72130-34,35
G	135-20624	517	05 19 14+	2	SEP-2	SPL 72130-34,35
G	135-20625	518	05 19 14+	2	SEP-2	SPL 72130-34,35
G	135-20626	519	05 19 14+	2	SEP-2	SPL 72130-34,35
G	135-20627	520	05 19 14+	2	SEP-2	SPL 72130-34,35, STEREO OF 137-20893
C	137-20895	521	05 19 14+	2	SEP-2	SPL 72130-34,35
G	135-20628	522	05 19 14+	2	SEP-2	
G	135-20629	523	05 19 14+	2	SEP-2	
G	135-20630	524	05 19 14+	2	SEP-2	
G	135-20631	525	05 19 14+	2	SEP-2	
G	135-20632	526	05 19 14+	2	SEP-2	
G	135-20633	527	05 19 14+	2	SEP-2	
G	135-20634	528	05 19 14+	2	SEP-2	
G	135-20635	529	05 19 14+	2	SEP-2	
G	135-20636	530	05 19 14+	2	SEP-2	
G	135-20637	531	05 19 14+	2	SEP-2	
G	135-20638	532	05 19 14+	2	SEP-2	
G	135-20639	533	05 19 14+	2	SEP-2	
G	135-20640	534	05 19 14+	2	SEP-2	
G	135-20641	535	05 19 14+	2	SEP-2	SPL 72140-44,45
G	135-20642	536	05 19 24	2	SEP-2	SPL 72140-44,45
C	137-20896	537	05 19 24+	2	SEP-2	SPL 72140-44,45, STEREO OF 135-20643
G	135-20643	538	05 19 24+	2	SEP-2	SPL 72140-44,45, STEREO OF 137-20896
G	135-20644	539	05 19 24+	2	SEP-2	
G	135-20645	540	05 19 24+	2	SEP-2	

Table 7.--Chronological listing of 70mm Apollo 17  
lunar surface pictures--Continued

MAG	PHOTO	SEQ	GET	EVA	STA	REMARKS
G	135-20646	541	05 19 24+	2	SEP-2	
G	135-20647	542	05 19 24+	2	SEP-2	
G	135-20648	543	05 19 24+	2	SEP-2	
C	137-20897	544	05 19 30	2	SEP-2	SPL 72155, STEREO OF 135-20649
G	135-20649	545	05 19 30+	2	SEP-2	SPL 72155, 72160-64, STEREO OF 137-20897
C	137-20898	546	05 19 30+	2	SEP-2	
G	135-20650	547	05 19 30+	2	SEP-2	
G	135-20651	548	05 19 30+	2	SEP-2	
G	135-20652	549	05 19 30+	2	SEP-2	
G	135-20653	550	05 19 30+	2	SEP-2	
C	137-20899	551	05 19 30+	2	SEP-2	
G	135-20654	552	05 19 30+	2	SEP-2	
G	135-20655	553	05 19 30+	2	SEP-2	
G	135-20656	554	05 19 30+	2	SEP-2	
G	135-20657	555	05 19 30+	2	SEP-2	
G	135-20658	556	05 19 30+	2	SEP-2	
G	135-20659	557	05 19 30+	2	SEP-2	
G	135-20660	558	05 19 30+	2	SEP-2	
G	135-20661	559	05 19 30+	2	SEP-2	
G	135-20662	560	05 19 30+	2	SEP-2	
G	135-20663	561	05 19 30+	2	SEP-2	
G	135-20664	562	05 19 30+	2	SEP-2	
G	135-20665	563	05 19 30+	2	SEP-2	
G	135-20666	564	05 19 30+	2	SEP-2	
G	135-20667	565	05 19 30+	2	SEP-2	
G	135-20668	566	05 19 30+	2	SEP-2	
G	135-20669	567	05 19 30+	2	SEP-2	
G	135-20670	568	05 19 30+	2	SEP-2	
G	135-20671	569	05 19 30+	2	SEP-2	
G	135-20672	570	05 19 30+	2	SEP-2	
G	135-20673	571	05 19 30+	2	SEP-2	
G	135-20674	572	05 19 30+	2	SEP-2	
G	135-20675	573	05 19 30+	2	SEP-2	
G	135-20676	574	05 19 30+	2	2	MISC
G	135-20677	575	05 19 30+	2	2	MISC
G	135-20678	576	05 19 30+	2	2	MISC
I	138-21028	577		2	2	FOGGED
C	137-20900	578	05 20 22	2	2	SPL 72215, 72220-24, 72235, 72240-44, 72255, 72260-64, 72275 XSB
C	137-20901	579	05 20 22+	2	2	SPL 72215, 72220-24, 72235, 72240-44, 72255, 72260-64, 72275 XSB
C	137-20902	580	05 20 22+	2	2	SPL 72215, 72220-24, 72235, 72240-44, 72255, 72260-64, 72275 XSA
C	137-20903	581	05 20 22+	2	2	SPL 72215, 72220-24, 72235, 72240-44, 72255, 72260-64, 72275 XSA
C	137-20904	582	05 20 22+	2	2	SPL 72215, 72220-24, 72235, 72240-44, 72255, 72260-64, 72275 XSA
C	137-20905	583	05 20 22+	2	2	SPL 72215, 72220-24, 72235, 72240-44, 72255, 72260-64, 72275 XSA
C	137-20906	584	05 20 22+	2	2	SPL 72215, 72220-24, 72235, 72240-44, 72255, 72260-64, 72275 XSA
C	137-20907	585	05 20 22+	2	2	SPL 72215, 72220-24, 72235, 72240-44, 72255, 72260-64, 72275 XSA
C	137-20908	586	05 20 22+	2	2	SPL 72215, 72220-24, 72235, 72240-44, 72255, 72260-64, 72275 XSA
C	137-20909	587	05 20 22+	2	2	SPL 72215, 72220-24, 72235, 72240-44, 72255, 72260-64, 72275 XSA
I	138-21029	588	05 20 23	2	2	SPL 72215, 72220-24, 72235, 72240-44, 72255, 72260-64, 72275 XS F-L
I	138-21030	589	05 20 23+	2	2	SPL 72215, 72220-24, 72235, 72240-44, 72255, 72260-64, 72275 XS F-L
I	138-21031	590	05 20 23+	2	2	SPL 72215, 72220-24, 72235, 72240-44, 72255, 72260-64, 72275 XS F-L
I	138-21032	591	05 20 23+	2	2	SPL 72215, 72220-24, 72235, 72240-44, 72255, 72260-64, 72275 XS F-L
I	138-21033	592	05 20 23+	2	2	SPL 72215, 72220-24, 72235, 72240-44, 72255, 72260-64, 72275 XS F-L
I	138-21034	593	05 20 23+	2	2	SPL 72215, 72220-24, 72235, 72240-44, 72255, 72260-64, 72275 XS F-L
I	138-21035	594	05 20 23+	2	2	SPL 72215, 72220-24, 72235, 72240-44, 72255, 72260-64, 72275 XS F-L
I	138-21036	595	05 20 30	2	2	SPL 72215, 72220-24, 72235, 72240-44, 72255, 72260-64, 72275 DSA STEREO
I	138-21037	596	05 20 30+	2	2	SPL 72215, 72220-24, 72235, 72240-44, 72255, 72260-64, 72275 DSA STEREO
C	137-20910	597	05 20 31	2	2	SPL 72315 ROCK, EARTH
C	137-20911	598	05 20 31+	2	2	SPL 72315 ROCK, EARTH
C	137-20912	599	05 20 31+	2	2	SPL 72315, 72320-24, 72335, 72355, 72375, 72395 XSB
C	137-20913	600	05 20 31+	2	2	SPL 72315, 72320-24, 72335, 72355, 72375, 72395 XSB
C	137-20914	601	05 20 31+	2	2	SPL 72315, 72320-24, 72335, 72355, 72375, 72395 XSB
C	137-20915	602	05 20 31+	2	2	SPL 72315, 72320-24, 72335, 72355, 72375, 72395 XSB
C	137-20916	603	05 20 31+	2	2	SPL 72315, 72320-24, 72335, 72355, 72375, 72395 XSB
C	137-20917	604	05 20 31+	2	2	SPL 72315 ROCK
C	137-20918	605	05 20 31+	2	2	SPL 72315 ROCK
C	137-20919	606	05 20 31+	2	2	SPL 72315 ROCK
C	137-20920	607	05 20 31+	2	2	SPL 72315 ROCK
C	137-20921	608	05 20 31+	2	2	SPL 72315 ROCK
C	137-20922	609	05 20 31+	2	2	SPL 72315 ROCK
C	137-20923	610	05 20 31+	2	2	SPL 72315 ROCK
C	137-20924	611	05 20 31+	2	2	SPL 72315 ROCK
C	137-20925	612	05 20 31+	2	2	SPL 72315 ROCK
I	138-21038	613	05 20 40	2	2	SPL 72315, 72320-24, 72335, 72355, 72375, 72395 DS
I	138-21039	614	05 20 40+	2	2	SPL 72315, 72320-24, 72335, 72355, 72375, 72395 LJC
I	138-21040	615	05 20 40+	2	2	SPL 72315, 72320-24, 72335, 72355, 72375, 72395 XSA
I	138-21041	616	05 20 40+	2	2	SPL 72315, 72320-24, 72335, 72355, 72375, 72395 XSA
I	138-21042	617	05 20 40+	2	2	SPL 72315, 72320-24, 72335, 72355, 72375, 72395 XSA
C	137-20926	618	05 20 41	2	2	PAN
C	137-20927	619	05 20 41+	2	2	PAN
C	137-20928	620	05 20 41+	2	2	PAN
C	137-20929	621	05 20 41+	2	2	PAN
C	137-20930	622	05 20 41+	2	2	PAN
C	137-20931	623	05 20 41+	2	2	PAN
C	137-20932	624	05 20 41+	2	2	PAN
C	137-20933	625	05 20 41+	2	2	PAN
C	137-20934	626	05 20 41+	2	2	PAN
C	137-20935	627	05 20 41+	2	2	PAN
C	137-20936	628	05 20 41+	2	2	PAN
C	137-20937	629	05 20 41+	2	2	PAN
C	137-20938	630	05 20 41+	2	2	PAN

Table 7.--Chronological listing of 70mm Apollo 17  
lunar surface pictures--Continued

MAG	PHOTO	SEQ	GET	EVA	STA	REMARKS
C	137-20939	631	05 20 41+	2	2	PAN
C	137-20940	632	05 20 41+	2	2	PAN
C	137-20941	633	05 20 41+	2	2	PAN
C	137-20942	634	05 20 41+	2	2	PAN
C	137-20943	635	05 20 41+	2	2	PAN
C	137-20944	636	05 20 41+	2	2	PAN
C	137-20945	637	05 20 41+	2	2	PAN
C	137-20946	638	05 20 41+	2	2	PAN
C	137-20947	639	05 20 41+	2	2	PAN
C	137-20948	640	05 20 41+	2	2	PAN
C	137-20949	641	05 20 41+	2	2	PAN
C	137-20950	642	05 20 41+	2	2	PAN
C	137-20951	643	05 20 41+	2	2	PAN
C	137-20952	644	05 20 41+	2	2	PAN
C	137-20953	645	05 20 41+	2	2	PAN
C	137-20954	646	05 20 41+	2	2	PAN
C	137-20955	647	05 20 41+	2	2	PAN
C	137-20956	648	05 20 41+	2	2	PAN
C	137-20957	649	05 20 41+	2	2	EARTH
C	137-20958	650	05 20 41+	2	2	EARTH
C	137-20959	651	05 20 41+	2	2	EARTH
C	137-20960	652	05 20 41+	2	2	SPL 72315 ROCK, EARTH
C	137-20961	653	05 20 41+	2	2	SPL 72315 ROCK, EARTH
I	138-21043	654	05 20 41+	2	2	SPL 72500-04,05,72535-39,45-49,55-59 XSB
I	138-21044	655	05 20 41+	2	2	SPL 72500-04,05,72535-39,45-49,55-59 XSB
I	138-21045	656	05 20 41+	2	2	SPL 72500-04,05,72535-39,45-49,55-59 XSB
I	138-21046	657	05 20 41+	2	2	SPL 72500-04,05,72535-39,45-49,55-59 XSB
C	137-20962	658	05 20 47	2	2	SPL 72500-04,05,72535-39,45-49,55-59 XSA
I	138-21047	659	05 20 47+	2	2	SPL 72415-18,72430-34,35,72440-44,72460-64 DSB
I	138-21048	660	05 20 47+	2	2	SPL 72415-18,72430-34,35,72440-44,72460-64 LOC
I	138-21049	661	05 20 47+	2	2	SPL 72415-18,72430-34,35,72440-44,72460-64 DSB
C	137-20963	662	05 20 50	2	2	SPL 72415-18,72430-34,35,72440-44,72460-64 XSB
C	137-20964	663	05 20 50+	2	2	SPL 72415-18,72430-34,35,72440-44,72460-64 XSB
C	137-20965	664	05 20 50+	2	2	SPL 72415-18,72430-34,35,72440-44,72460-64 XSA
C	137-20966	665	05 20 50+	2	2	SPL 72415-18,72430-34,35,72440-44,72460-64 CU
C	137-20967	666	05 20 50+	2	2	SPL 72415-18,72430-34,35,72440-44,72460-64 CU
C	137-20968	667	05 20 50+	2	2	SPL 72415-18,72430-34,35,72440-44,72460-64 CU
C	137-20969	668	05 20 50+	2	2	SPL 72415-18,72430-34,35,72440-44,72460-64 CU
C	137-20970	669	05 20 50+	2	2	SPL 72415-18,72430-34,35,72440-44,72460-64 CU
C	137-20971	670	05 20 50+	2	2	SPL 72415-18,72430-34,35,72440-44,72460-64 CU
C	137-20972	671	05 20 52	2	2	SPL 72415-18,72430-34,35,72440-44,72460-64 CU
C	137-20973	672	05 20 52+	2	2	SPL 72415-18,72430-34,35,72440-44,72460-64 CU
I	138-21050	673	05 20 52	2	2	SMALL PIT CTR F-L
I	138-21051	674	05 20 52	2	2	SMALL PIT CTR F-L
I	138-21052	675	05 20 52	2	2	SMALL PIT CTR F-L
I	138-21053	676	05 20 58	2	2	PAN
I	138-21054	677	05 20 58+	2	2	PAN
I	138-21055	678	05 20 58+	2	2	PAN
I	138-21056	679	05 20 58+	2	2	PAN
I	138-21057	680	05 20 58+	2	2	PAN
I	138-21058	681	05 20 58+	2	2	PAN
I	138-21059	682	05 20 58+	2	2	PAN
I	138-21060	683	05 20 58+	2	2	PAN
I	138-21061	684	05 20 58+	2	2	PAN
I	138-21062	685	05 20 58+	2	2	PAN
I	138-21063	686	05 20 58+	2	2	PAN
I	138-21064	687	05 20 58+	2	2	PAN
I	138-21065	688	05 20 58+	2	2	PAN
I	138-21066	689	05 20 58+	2	2	PAN
I	138-21067	690	05 20 58+	2	2	PAN
I	138-21068	691	05 20 58+	2	2	PAN
I	138-21069	692	05 20 58+	2	2	PAN
I	138-21070	693	05 20 58+	2	2	PAN
I	138-21071	694	05 20 58+	2	2	PAN
I	138-21072	695	05 20 58+	2	2	PAN
I	138-21073	696	05 20 58+	2	2	PAN
C	137-20974	697	05 20 59	2	2	SPL 72700-04,05,72735-38 XSB
C	137-20975	698	05 20 59+	2	2	SPL 72700-04,05,72735-38 XSB
C	137-20976	699	05 20 59+	2	2	SPL 72700-04,05,72735-38 LOC
C	137-20977	700	05 20 59+	2	2	SPL 72700-04,05,72735-38 LOC
C	137-20978	701	05 21 00	2	2	SPL 72700-04,05,72735-38 XSA
I	138-21074	702	05 21 00+	2	2	SPL 72700-04,05,72735-38 DSA
C	137-20979	703	05 21 00+	2	2	LRV
I	138-21075	704	05 21 07	2	2-3	
I	138-21076	705	05 21 07+	2	2-3	
I	138-21077	706	05 21 10	2	2-3	LRV PAN
I	138-21078	707	05 21 10+	2	2-3	LRV PAN
I	138-21079	708	05 21 10+	2	2-3	LRV PAN
I	138-21080	709	05 21 10+	2	2-3	LRV PAN
I	138-21081	710	05 21 10+	2	2-3	LRV PAN
I	138-21082	711	05 21 10+	2	2-3	LRV PAN
I	138-21083	712	05 21 10+	2	2-3	LRV PAN
I	138-21084	713	05 21 10+	2	2-3	LRV PAN
I	138-21085	714	05 21 10+	2	2-3	LRV PAN
I	138-21086	715	05 21 10+	2	2-3	LRV PAN
I	138-21087	716	05 21 10+	2	2-3	LRV PAN
I	138-21088	717	05 21 10+	2	2-3	LRV PAN
I	138-21089	718	05 21 10+	2	2-3	LRV PAN
I	138-21090	719	05 21 10+	2	2-3	LRV PAN
I	138-21091	720	05 21 10+	2	2-3	LRV PAN

Table 7.--Chronological listing of 70mm Apollo 17  
lunar surface pictures--Continued

MAG	PHOTO	SEQ	GET	EVA	STA	REMARKS
I	138-21092	721	05 21 10+	2	2-3	LRV PAN
I	138-21093	722	05 21 10+	2	2-3	
I	138-21094	723	05 21 10+	2	2-3	
I	138-21095	724	05 21 10+	2	2-3	
I	138-21096	725	05 21 17	2	2-3	SPL 73130-34 XSB
I	138-21097	726	05 21 17+	2	2-3	SPL 73130-34 XSB
I	138-21098	727	05 21 17+	2	2-3	SPL 73140-44,45-46 OR 73150-54,55-56 XSB
I	138-21099	728	05 21 17+	2	2-3	SPL 73140-44,45-46 OR 73150-54,55-56 XSB
I	138-21100	729	05 21 25	2	2-3	LRV PPAN
I	138-21101	730	05 21 25+	2	2-3	LRV PPAN
I	138-21102	731	05 21 25+	2	2-3	LRV PPAN
I	138-21103	732	05 21 25+	2	2-3	LRV PPAN
I	138-21104	733	05 21 25+	2	2-3	LRV PPAN
I	138-21105	734	05 21 25+	2	2-3	LRV PPAN
I	138-21106	735	05 21 25+	2	2-3	LRV PPAN
I	138-21107	736	05 21 25+	2	2-3	LRV PPAN
I	138-21108	737	05 21 25+	2	2-3	LRV PPAN
C	137-20980	738	05 21 25+	2	2-3	
I	138-21109	739	05 21 25+	2	2-3	
I	138-21110	740	05 21 25+	2	2-3	
I	138-21111	741	05 21 25+	2	2-3	
I	138-21112	742	05 21 25+	2	2-3	
I	138-21113	743	05 21 25+	2	2-3	
I	138-21114	744	05 21 25+	2	2-3	
I	138-21115	745	05 21 25+	2	2-3	
I	138-21116	746	05 21 25+	2	2-3	
I	138-21117	747	05 21 25+	2	2-3	
I	138-21118	748	05 21 25+	2	2-3	
I	138-21119	749	05 21 25+	2	2-3	
I	138-21120	750	05 21 25+	2	2-3	
I	138-21121	751	05 21 25+	2	2-3	
I	138-21122	752	05 21 25+	2	2-3	
I	138-21123	753	05 21 25+	2	2-3	
I	138-21124	754	05 21 25+	2	2-3	
I	138-21125	755	05 21 25+	2	2-3	
I	138-21126	756	05 21 25+	2	2-3	
I	138-21127	757	05 21 25+	2	2-3	
I	138-21128	758	05 21 25+	2	2-3	
I	138-21129	759	05 21 25+	2	2-3	
I	138-21130	760	05 21 25+	2	2-3	
I	138-21131	761	05 21 25+	2	2-3	
I	138-21132	762	05 21 25+	2	2-3	
I	138-21133	763	05 21 25+	2	2-3	
I	138-21134	764	05 21 25+	2	2-3	
I	138-21135	765	05 21 25+	2	2-3	
I	138-21136	766	05 21 25+	2	2-3	
I	138-21137	767	05 21 25+	2	2-3	
I	138-21138	768	05 21 25+	2	2-3	
I	138-21139	769	05 21 25+	2	2-3	
I	138-21140	770	05 21 25+	2	2-3	
I	138-21141	771	05 21 25+	2	2-3	
I	138-21142	772	05 21 25+	2	2-3	
I	138-21143	773	05 21 51	2	3	TR SPL 73210-14, 15-19, 73220-24, 25, 73235, 73240-44, 45, 73255, 73250-64, 73275, 73280-84, 85 X
I	138-21144	774	05 21 51+	2	3	TR SPL 73210-14, 15-19, 73220-24, 25, 73235, 73240-44, 45, 73255, 73260-64, 73275, 73280-84, 85 X
I	138-21145	775	05 21 51+	2	3	TR SPL 73210-14, 15-19, 73220-24, 25, 73235, 73240-44, 45, 73255, 73250-64, 73275, 73280-84, 85 X
I	138-21146	776	05 21 51+	2	3	TR SPL 73210-14, 15-19, 73220-24, 25, 73235, 73240-44, 45, 73255, 73260-64, 73275, 73280-84, 85 D
I	138-21147	777	05 21 51+	2	3	TR SPL 73210-14, 15-19, 73220-24, 25, 73235, 73240-44, 45, 73255, 73260-64, 73275, 73280-84, 85 D
I	138-21148	778	05 21 51+	2	3	TR SPL 73210-14, 15-19, 73220-24, 25, 73235, 73240-44, 45, 73255, 73250-64, 73275, 73280-84, 85 X
I	138-21149	779	05 21 51+	2	3	TR SPL 73210-14, 15-19, 73220-24, 25, 73235, 73240-44, 45, 73255, 73250-64, 73275, 73280-84, 85 X
I	138-21150	780	05 22 13	2	3	PAN
I	138-21151	781	05 22 13+	2	3	PAN
I	138-21152	782	05 22 13+	2	3	PAN
I	138-21153	783	05 22 13+	2	3	PAN
I	138-21154	784	05 22 13+	2	3	PAN
I	138-21155	785	05 22 13+	2	3	PAN
I	138-21156	786	05 22 13+	2	3	PAN
I	138-21157	787	05 22 13+	2	3	PAN
I	138-21158	788	05 22 13+	2	3	PAN
I	138-21159	789	05 22 13+	2	3	PAN
I	138-21160	790	05 22 13+	2	3	PAN
I	138-21161	791	05 22 13+	2	3	PAN
I	138-21162	792	05 22 13+	2	3	PAN
I	138-21163	793	05 22 13+	2	3	PAN
I	138-21164	794	05 22 13+	2	3	PAN
I	138-21165	795	05 22 13+	2	3	PAN
I	138-21166	796	05 22 13+	2	3	PAN
I	138-21167	797	05 22 13+	2	3	PAN
I	138-21168	798	05 22 13+	2	3	PAN
I	138-21169	799	05 22 13+	2	3	PAN
I	138-21170	800	05 22 13+	2	3	PAN
I	138-21171	801	05 22 13+	2	3	PAN
I	138-21172	802	05 22 13+	2	3	PAN
I	138-21173	803	05 22 13+	2	3	PAN
I	138-21174	804	05 22 13+	2	3	PAN
I	138-21175	805	05 22 13+	2	3	PAN
I	138-21176	806	05 22 13+	2	3	PAN
I	138-21177	807	05 22 13+	2	3	PAN
I	138-21178	808	05 22 13+	2	3	TR SPL 73215-19, 73220-24, 25, 73235, 73240-44, 45, 73255, 73260-64, 73275, 73280-84, 85 XSA
I	138-21179	809	05 22 13+	2	3	TR SPL 73215-19, 73220-24, 25, 73235, 73240-44, 45, 73255, 73260-64, 73275, 73280-84, 85 XSA
I	138-21180	810	05 22 13+	2	3	TR SPL 73215-19, 73220-24, 25, 73235, 73240-44, 45, 73255, 73260-64, 73275, 73280-84, 85 XSA

Table 7.--Chronological listing of 70mm Apollo 17  
lunar surface pictures--Continued

MAG	PHOTO	SEQ	GET	RVA	STA	REMARKS
I	138-21181	811	05 22 13	2	3	NISC
C	137-20981	812	05 22 15	2	3	DT SPL 73002/73001 (CSVC)
C	137-20982	813	05 22 15+	2	3	DT SPL 73002/73001 (CSVC)
J	133-20194	814	05 22 26	2	3-4	
J	133-20195	815	05 22 26+	2	3-4	
J	133-20196	816	05 22 26+	2	3-4	
J	133-20197	817	05 22 26+	2	3-4	
J	133-20198	818	05 22 26+	2	3-4	
J	133-20199	819	05 22 26+	2	3-4	
J	133-20200	820	05 22 26+	2	3-4	
J	133-20201	821	05 22 26+	2	3-4	
J	133-20202	822	05 22 26+	2	3-4	
J	133-20203	823	05 22 26+	2	3-4	
J	133-20204	824	05 22 26+	2	3-4	
J	133-20205	825	05 22 26+	2	3-4	
J	133-20206	826	05 22 26+	2	3-4	
J	133-20207	827	05 22 26+	2	3-4	
J	133-20208	828	05 22 31	2	3-4	SPL 74110-14,15-19, STEREO OF 137-20983
C	137-20983	829	05 22 31+	2	3-4	SPL 74110-14,15-19, STEREO OF 133-20208
J	133-20209	830	05 22 31+	2	3-4	
J	133-20210	831	05 22 31+	2	3-4	
J	133-20211	832	05 22 31+	2	3-4	
J	133-20212	833	05 22 31+	2	3-4	
J	133-20213	834	05 22 31+	2	3-4	
J	133-20214	835	05 22 31+	2	3-4	
J	133-20215	836	05 22 31+	2	3-4	
J	133-20216	837	05 22 31+	2	3-4	
J	133-20217	838	05 22 31+	2	3-4	
J	133-20218	839	05 22 31+	2	3-4	
J	133-20219	840	05 22 31+	2	3-4	
J	133-20220	841	05 22 31+	2	3-4	
J	133-20221	842	05 22 31+	2	3-4	
J	133-20222	843	05 22 31+	2	3-4	
J	133-20223	844	05 22 31+	2	3-4	
J	133-20224	845	05 22 31+	2	3-4	
J	133-20225	846	05 22 31+	2	3-4	
J	133-20226	847	05 22 31+	2	3-4	
J	133-20227	848	05 22 31+	2	3-4	
J	133-20228	849	05 22 31+	2	3-4	
J	133-20229	850	05 22 46	2	4	PAN
J	133-20230	851	05 22 46+	2	4	PAN
J	133-20231	852	05 22 46+	2	4	PAN
J	133-20232	853	05 22 46+	2	4	PAN
J	133-20233	854	05 22 46+	2	4	PAN
J	133-20234	855	05 22 46+	2	4	PAN
J	133-20235	856	05 22 46+	2	4	PAN
J	133-20236	857	05 22 46+	2	4	PAN
J	133-20237	858	05 22 46+	2	4	PAN
J	133-20238	859	05 22 46+	2	4	PAN
J	133-20239	860	05 22 46+	2	4	PAN
J	133-20240	861	05 22 46+	2	4	PAN
J	133-20241	862	05 22 46+	2	4	PAN
J	133-20242	863	05 22 46+	2	4	PAN
J	133-20243	864	05 22 46+	2	4	PAN
J	133-20244	865	05 22 46+	2	4	PAN
J	133-20245	866	05 22 46+	2	4	PAN
J	133-20246	867	05 22 46+	2	4	PAN
J	133-20247	868	05 22 46+	2	4	PAN
J	133-20248	869	05 22 46+	2	4	PAN
J	133-20249	870	05 22 46+	2	4	PAN
J	133-20250	871	05 22 46+	2	4	PAN
J	133-20251	872	05 22 46+	2	4	PAN
J	133-20252	873	05 22 46+	2	4	PAN
J	133-20253	874	05 22 46+	2	4	PAN
J	133-20254	875	05 22 46+	2	4	PAN
J	133-20255	876	05 22 46+	2	4	PAN
J	133-20256	877	05 22 46+	2	4	PAN
C	137-20984	878	05 22 52	2	4	TR SPL 74220,74240-49,45-49,74260 XSA
C	137-20985	879	05 22 52+	2	4	TR SPL 74220,74240-49,45-49,74260 XSA
C	137-20986	880	05 22 52+	2	4	TR SPL 74220,74240-44,45-49,74260 XSA
C	137-20987	881	05 22 52+	2	4	TR SPL 74220,74240-44,45-49,74260 XSA
C	137-20988	882	05 22 52+	2	4	TR SPL 74220,74240-44,45-49,74260 XSA
C	137-20989	883	05 22 52+	2	4	TR SPL 74220,74240-44,45-49,74260 XSA
C	137-20990	884	05 22 52+	2	4	TR SPL 74220,74240-44,45-49,74260 DSA
J	133-20257	885	05 22 59	2	4	BLANK
J	133-20258	886	05 22 59+	2	4	BLANK
J	133-20259	887	05 22 59+	2	4	BLANK
J	133-20260	888	05 22 59+	2	4	BLANK
J	133-20261	889	05 22 59+	2	4	BLANK
J	133-20262	890	05 22 59+	2	4	BLANK
J	133-20263	891	05 22 59+	2	4	BLANK
J	133-20264	892	05 22 59+	2	4	BLANK
J	133-20265	893	05 22 59+	2	4	BLANK
J	133-20266	894	05 22 59+	2	4	BLANK
J	133-20267	895	05 22 59+	2	4	BLANK
J	133-20268	896	05 22 59+	2	4	BLANK
C	137-20991	897	05 23 08	2	4	PAN
C	137-20992	898	05 23 08+	2	4	PAN
C	137-20993	899	05 23 08+	2	4	PAN
C	137-20994	900	05 23 08+	2	4	PAN

Table 7.--Chronological listing of 70mm Apollo 17 lunar surface pictures--Continued

MAG	PHOTO	SEQ	GET	EVA	STA	REMARKS
C	137-20995	901	05 23 08+	2	4	PAN
C	137-20996	902	05 23 08+	2	4	PAN
C	137-20997	903	05 23 08+	2	4	PAN
C	137-20998	904	05 23 08+	2	4	PAN
C	137-20999	905	05 23 08+	2	4	PAN
C	137-21000	906	05 23 08+	2	4	PAN
C	137-21001	907	05 23 08+	2	4	PAN
C	137-21002	908	05 23 08+	2	4	PAN
C	137-21003	909	05 23 08+	2	4	PAN
C	137-21004	910	05 23 08+	2	4	PAN
C	137-21005	911	05 23 08+	2	4	PAN
C	137-21006	912	05 23 08+	2	4	PAN
C	137-21007	913	05 23 08+	2	4	PAN
C	137-21008	914	05 23 08+	2	4	PAN
C	137-21009	915	05 23 08+	2	4	PAN
C	137-21010	916	05 23 08+	2	4	PAN
C	137-21011	917	05 23 08+	2	4	PAN
C	137-21012	918	05 23 08+	2	4	PAN
C	137-21013	919	05 23 08+	2	4	PAN
C	137-21014	920	05 23 08+	2	4	PAN
C	137-21015	921	05 23 08+	2	4	PAN
C	137-21016	922	05 23 08+	2	4	PAN
C	137-21017	923	05 23 08+	2	4	PAN
C	137-21018	924	05 23 08+	2	4	PAN
C	137-21019	925	05 23 08+	2	4	PAN
C	137-21020	926	05 23 08+	2	4	PAN
C	137-21021	927	05 23 08+	2	4	PAN
C	137-21022	928	05 23 08+	2	4	PAN
C	137-21023	929	05 23 08+	2	4	PAN
C	137-21024	930	05 23 08+	2	4	PAN
C	137-21025	931	05 23 08+	2	4	PAN
C	137-21026	932	05 23 08+	2	4	PAN
C	137-21027	933	05 23 09	2	4	PAN
J	133-20269	934	05 23 16	2	4-5	
J	133-20270	935	05 23 16+	2	4-5	
J	133-20271	936	05 23 16+	2	4-5	
J	133-20272	937	05 23 16+	2	4-5	
J	133-20273	938	05 23 16+	2	4-5	
J	133-20274	939	05 23 16+	2	4-5	
J	133-20275	940	05 23 16+	2	4-5	
J	133-20276	941	05 23 16+	2	4-5	
J	133-20277	942	05 23 16+	2	4-5	
J	133-20278	943	05 23 16+	2	4-5	
J	133-20279	944	05 23 16+	2	4-5	
J	133-20280	945	05 23 27	2	4-5	SPL 75110-14, 15, RP-1
J	133-20281	946	05 23 27+	2	4-5	LRV PAN AT VICTORY
J	133-20282	947	05 23 27+	2	4-5	LRV PAN AT VICTORY
J	133-20283	948	05 23 27+	2	4-5	LRV PAN AT VICTORY
J	133-20284	949	05 23 27+	2	4-5	LRV PAN AT VICTORY
J	133-20285	950	05 23 27+	2	4-5	LRV PAN AT VICTORY
J	133-20286	951	05 23 27+	2	4-5	LRV PAN AT VICTORY
J	133-20287	952	05 23 27+	2	4-5	LRV PAN AT VICTORY
J	133-20288	953	05 23 27+	2	4-5	LRV PAN AT VICTORY
J	133-20289	954	05 23 27+	2	4-5	LRV PAN AT VICTORY
J	133-20290	955	05 23 27+	2	4-5	LRV PAN AT VICTORY
J	133-20291	956	05 23 27+	2	4-5	LRV PAN AT VICTORY
J	133-20292	957	05 23 27+	2	4-5	LRV PAN AT VICTORY
J	133-20293	958	05 23 27+	2	4-5	LRV PAN AT VICTORY
J	133-20294	959	05 23 27+	2	4-5	LRV PAN AT VICTORY
J	133-20295	960	05 23 27+	2	4-5	LRV PAN AT VICTORY
J	133-20296	961	05 23 27+	2	4-5	LRV PAN AT VICTORY
J	133-20297	962	05 23 27+	2	4-5	LRV PAN AT VICTORY
J	133-20298	963	05 23 27+	2	4-5	LRV PAN AT VICTORY
J	133-20299	964	05 23 27+	2	4-5	LRV PAN AT VICTORY
J	133-20300	965	05 23 27+	2	4-5	LRV PAN AT VICTORY
J	133-20301	966	05 23 27+	2	4-5	
J	133-20302	967	05 23 27+	2	4-5	
J	133-20303	968	05 23 27+	2	4-5	
J	133-20304	969	05 23 27+	2	4-5	
J	133-20305	970	05 23 27+	2	4-5	
J	133-20306	971	05 23 27+	2	4-5	
J	133-20307	972	05 23 27+	2	4-5	
J	133-20308	973	05 23 27+	2	4-5	
J	133-20309	974	05 23 27+	2	4-5	
J	133-20310	975	05 23 27+	2	4-5	
J	133-20311	976	05 23 27+	2	4-5	
J	133-20312	977	05 23 27+	2	4-5	
J	133-20313	978	05 23 27+	2	4-5	
J	133-20314	979	05 23 27+	2	4-5	
J	133-20315	980	05 23 27+	2	4-5	
J	133-20316	981	05 23 36	2	4-5	SPL 75120-24
J	133-20317	982	05 23 36+	2	4-5	SPL 75120-24
J	133-20318	983	05 23 36+	2	4-5	
J	133-20319	984	05 23 36+	2	4-5	
J	133-20320	985	05 23 36+	2	4-5	
J	133-20321	986	05 23 36+	2	4-5	
J	133-20322	987	05 23 36+	2	4-5	
J	133-20323	988	05 23 36+	2	4-5	
J	133-20324	989	05 23 36+	2	4-5	
J	133-20325	990	05 23 36+	2	4-5	

Table 7.--Chronological listing of 70mm Apollo 17  
lunar surface pictures--Continued

MAG	PHOTO	SEQ	GET	+ EVA	STA	REMARKS
J 133-20326	991	05 23 36+	2		4-5	
J 133-20327	992	05 23 36+	2		4-5	
D 145-22133	993		2		5	MISC
D 145-22134	994		2		5	MISC
D 145-22135	995		2		5	MISC
J 133-20328	996	05 23 56	2		5	SPL 75015,75035 DS
J 133-20329	997	05 23 56+	2		5	SPL 75015,75035 LOC
D 145-22136	998	05 23 56+	2		5	SPL 75015,75035 XSB
D 145-22137	999	05 23 56+	2		5	SPL 75015,75035 XSB
D 145-22138	1000	05 23 56+	2		5	SPL 75015,75035 XSB
D 145-22139	1001	05 23 58	2		5	SPL 75015,75035 XSA
D 145-22140	1002	05 23 58+	2		5	SPL 75015,75035 XSA
J 133-20330	1003	06 00 00	2		5	SPL 75055 F-L
J 133-20331	1004	06 00 00+	2		5	SPL 75055 F-L
J 133-20332	1005	06 00 00+	2		5	SPL 75055 F-L
J 133-20333	1006	06 00 00+	2		5	SPL 75055 F-L
J 133-20334	1007	06 00 00+	2		5	SPL 75055 F-L
J 133-20335	1008	06 00 00+	2		5	SPL 75055 DS
J 133-20336	1009	06 00 00+	2		5	SPL 75055 LOC
D 145-22141	1010	06 00 02	2		5	SPL 75055
D 145-22142	1011	06 00 02+	2		5	SPL 75055
D 145-22143	1012	06 00 02+	2		5	SPL 75055
D 145-22144	1013	06 00 02+	2		5	SPL 75055
D 145-22145	1014	06 00 02+	2		5	SPL 75055
D 145-22146	1015	06 00 02+	2		5	SPL 75055
D 145-22147	1016	06 00 02+	2		5	SPL 75055
D 145-22148	1017	06 00 02+	2		5	SPL 75055
D 145-22149	1018	06 00 02+	2		5	SPL 75055
D 145-22150	1019	06 00 02+	2		5	SPL 75055
D 145-22151	1020	06 00 02+	2		5	SPL 75055
D 145-22152	1021	06 00 02+	2		5	SPL 75055
D 145-22153	1022	06 00 03	2		5	SPL 75055
J 133-20337	1023	06 00 06	2		5	SPL 75060-64,65-66,75075 DS
J 133-20338	1024	06 00 06+	2		5	SPL 75060-64,65-66,75075 LOC
D 145-22154	1025	06 00 06+	2		5	SPL 75060-64,65-66,75075,75080-84,85-89 XS
D 145-22155	1026	06 00 06+	2		5	SPL 75060-64,65-66,75075,75080-84,85-89 XS
D 145-22156	1027	06 00 06+	2		5	SPL 75060-64,65-66,75075,75080-84,85-89 XS
D 145-22157	1028	06 00 06+	2		5	SPL 75060-64,65-66,75075,75080-84,85-89 XS
D 145-22158	1029	06 00 08	2		5	SPL 75060-64,65-66,75075,75080-84,85-89 XS
D 145-22159	1030	06 00 08+	2		5	PAN
D 145-22160	1031	06 00 08+	2		5	PAN
D 145-22161	1032	06 00 08+	2		5	PAN
D 145-22162	1033	06 00 08+	2		5	PAN
D 145-22163	1034	06 00 08+	2		5	PAN
D 145-22164	1035	06 00 08+	2		5	PAN
D 145-22165	1036	06 00 08+	2		5	PAN
D 145-22166	1037	06 00 08+	2		5	PAN
D 145-22167	1038	06 00 08+	2		5	PAN
D 145-22168	1039	06 00 08+	2		5	PAN
D 145-22169	1040	06 00 08+	2		5	PAN
D 145-22170	1041	06 00 08+	2		5	PAN
D 145-22171	1042	06 00 08+	2		5	PAN
D 145-22172	1043	06 00 08+	2		5	PAN
D 145-22173	1044	06 00 08+	2		5	PAN
D 145-22174	1045	06 00 08+	2		5	PAN
D 145-22175	1046	06 00 08+	2		5	PAN
D 145-22176	1047	06 00 08+	2		5	PAN
D 145-22177	1048	06 00 08+	2		5	PAN
D 145-22178	1049	06 00 08+	2		5	PAN
D 145-22179	1050	06 00 08+	2		5	PAN
D 145-22180	1051	06 00 08+	2		5	PAN
D 145-22181	1052	06 00 08+	2		5	PAN
D 145-22182	1053	06 00 08+	2		5	PAN
D 145-22183	1054	06 00 08+	2		5	PAN
J 133-20339	1055	06 00 10	2		5	PAN
J 133-20340	1056	06 00 10+	2		5	PAN
J 133-20341	1057	06 00 10+	2		5	PAN
J 133-20342	1058	06 00 10+	2		5	PAN
J 133-20343	1059	06 00 10+	2		5	PAN
J 133-20344	1060	06 00 10+	2		5	PAN
J 133-20345	1061	06 00 10+	2		5	PAN
J 133-20346	1062	06 00 10+	2		5	PAN
J 133-20347	1063	06 00 10+	2		5	PAN
J 133-20348	1064	06 00 10+	2		5	PAN
J 133-20349	1065	06 00 10+	2		5	PAN
J 133-20350	1066	06 00 10+	2		5	PAN
J 133-20351	1067	06 00 10+	2		5	PAN
J 133-20352	1068	06 00 10+	2		5	PAN
J 133-20353	1069	06 00 10+	2		5	PAN
J 133-20354	1070	06 00 10+	2		5	PAN
J 133-20355	1071	06 00 10+	2		5	PAN
J 133-20356	1072	06 00 10+	2		5	PAN
J 133-20357	1073	06 00 10+	2		5	PAN
J 133-20358	1074	06 00 10+	2		5	PAN
J 133-20359	1075	06 00 10+	2		5	PAN
J 133-20360	1076	06 00 10+	2		5	PAN
J 133-20361	1077	06 00 10+	2		5	PAN
J 133-20362	1078	06 00 15	2		5-LM	
J 133-20363	1079	06 00 15+	2		5-LM	
J 133-20364	1080	06 00 15+	2		5-LM	

Table 7.--Chronological listing of 70mm Apollo 17 lunar surface pictures--Continued

MAG	PHOTO	SEQ	GET	+ EVA	STA	REMARKS
J	133-20365	1081	06 00 15+	2	5-LM	
J	133-20366	1082	06 00 15+	2	5-LM	
J	133-20367	1083	06 00 15+	2	5-LM	
J	133-20368	1084	06 00 15+	2	5-LM	
J	133-20369	1085	06 00 15+	2	5-LM	
J	133-20370	1086	06 00 15+	2	5-LM	
J	133-20371	1087	06 00 15+	2	5-LM	
J	133-20372	1088	06 00 15+	2	5-LM	
J	133-20373	1089	06 00 15+	2	5-LM	
J	133-20374	1090	06 00 15+	2	5-LM	
J	133-20375	1091	06 00 15+	2	5-LM	
D	145-22184	1092	06 00 23	2	5-LM	EP-8 LOC
D	145-22185	1093	06 00 39+	2	ALSEP	SPL 70019 LOC
D	145-22186	1094	06 00 39+	2	ALSEP	SPL 70019 XSB
D	145-22187	1095	06 00 39+	2	ALSEP	SPL 70019 XSB
D	145-22188	1096	06 00 39+	2	ALSEP	SPL 70019 XSB
D	145-22189	1097	06 00 39+	2	ALSEP	SPL 70019 XSB
D	145-22190	1098	06 00 39+	2	ALSEP	SPL 70019 XSA
D	145-22191	1099	06 00 39+	2	ALSEP	SPL 70019 XSA
E	140-21351	1100		2-3	LM	BLANK
E	140-21352	1101		2-3	LM	LM WINDOW PAN
E	140-21353	1102		2-3	LM	LM WINDOW PAN
E	140-21354	1103		2-3	LM	LM WINDOW PAN
E	140-21355	1104		2-3	LM	LM WINDOW PAN
E	140-21356	1105		2-3	LM	LM WINDOW PAN
E	140-21357	1106		2-3	LM	LM WINDOW PAN
E	140-21358	1107		2-3	LM	LM WINDOW PAN
E	140-21359	1108	06 17 18	3	LM	PAN W OF LM
E	140-21360	1109	06 17 18+	3	LM	PAN W OF LM
E	140-21361	1110	06 17 18+	3	LM	PAN W OF LM
E	140-21362	1111	06 17 18+	3	LM	PAN W OF LM
E	140-21363	1112	06 17 18+	3	LM	PAN W OF LM
E	140-21364	1113	06 17 18+	3	LM	PAN W OF LM
E	140-21365	1114	06 17 18+	3	LM	PAN W OF LM
E	140-21366	1115	06 17 18+	3	LM	PAN W OF LM
E	140-21367	1116	06 17 18+	3	LM	PAN W OF LM
E	140-21368	1117	06 17 18+	3	LM	PAN W OF LM
E	140-21369	1118	06 17 18+	3	LM	PAN W OF LM
E	140-21370	1119	06 17 18+	3	LM	PAN W OF LM
E	140-21371	1120	06 17 18+	3	LM	PAN W OF LM
E	140-21372	1121	06 17 18+	3	LM	PAN W OF LM
E	140-21373	1122	06 17 18+	3	LM	PAN W OF LM
E	140-21374	1123	06 17 18+	3	LM	PAN W OF LM
E	140-21375	1124	06 17 18+	3	LM	PAN W OF LM
E	140-21376	1125	06 17 18+	3	LM	PAN W OF LM
E	140-21377	1126	06 17 18+	3	LM	PAN W OF LM
E	140-21378	1127	06 17 18+	3	LM	PAN W OF LM
E	140-21379	1128	06 17 18+	3	LM	PAN W OF LM
E	140-21380	1129	06 17 18+	3	LM	PAN W OF LM
E	140-21381	1130	06 17 20	3	LM	COSMIC RAY, SPL 70011 XSB
E	140-21382	1131	06 17 20+	3	LM	COSMIC RAY, SPL 70011 XSB
E	140-21383	1132	06 17 20+	3	LM	COSMIC RAY
E	140-21384	1133	06 17 20+	3	LM	COSMIC RAY
E	140-21385	1134	06 17 20+	3	LM	CDR, FLAG, LRV
E	140-21386	1135	06 17 20+	3	LM	CDR, FLAG, LRV
E	140-21387	1136	06 17 20+	3	LM	CDR, FLAG, LRV
E	140-21388	1137	06 17 20+	3	LM	CDR, FLAG, LRV
E	140-21389	1138	06 17 20+	3	LM	CDR, FLAG, LRV
E	140-21390	1139	06 17 20+	3	LM	CDR, FLAG, LRV
E	140-21391	1140	06 17 20+	3	LM	CDR, FLAG, LRV
L	141-21510	1141	06 17 36	3	SEP	SEP XS
L	141-21511	1142	06 17 36+	3	SEP	SEP XS
L	141-21512	1143	06 17 36+	3	SEP	PPAN OF SEP (RIGHT)
L	141-21513	1144	06 17 36+	3	SEP	PPAN OF SEP (RIGHT)
L	141-21514	1145	06 17 36+	3	SEP	PPAN OF SEP (RIGHT)
L	141-21515	1146	06 17 36+	3	SEP	PPAN OF SEP (LEFT)
L	141-21516	1147	06 17 36+	3	SEP	PPAN OF SEP (LEFT)
L	141-21517	1148	06 17 36+	3	SEP	PPAN OF SEP (LEFT)
L	141-21518	1149	06 17 40	3	SEP-6	
L	141-21519	1150	06 17 40+	3	SEP-6	
L	141-21520	1151	06 17 40+	3	SEP-6	
L	141-21521	1152	06 17 40+	3	SEP-6	
L	141-21522	1153	06 17 40+	3	SEP-6	
L	141-21523	1154	06 17 40+	3	SEP-6	
L	141-21524	1155	06 17 40+	3	SEP-6	
L	141-21525	1156	06 17 40+	3	SEP-6	
L	141-21526	1157	06 17 40+	3	SEP-6	
L	141-21527	1158	06 17 40+	3	SEP-6	
L	141-21528	1159	06 17 40+	3	SEP-6	
L	141-21529	1160	06 17 40+	3	SEP-6	
L	141-21530	1161	06 17 40+	3	SEP-6	
L	141-21531	1162	06 17 40+	3	SEP-6	
L	141-21532	1163	06 17 40+	3	SEP-6	
L	141-21533	1164	06 17 40+	3	SEP-6	
L	141-21534	1165	06 17 40+	3	SEP-6	
L	141-21535	1166	06 17 40+	3	SEP-6	
L	141-21536	1167	06 17 40+	3	SEP-6	
L	141-21537	1168	06 17 40+	3	SEP-6	
L	141-21538	1169	06 17 40+	3	SEP-6	
L	141-21539	1170	06 17 40+	3	SEP-6	

Table 7.--Chronological listing of 70mm Apollo 17  
lunar surface pictures--Continued

MAG	PHOTO	SEQ	GET	EVA	STA	REMARKS
L	141-21540	1171	06 17 40+	3	SEP-6	
L	141-21541	1172	06 17 40+	3	SEP-6	
L	141-21542	1173	06 17 52	3	SEP-6	SPL 76120-24
L	141-21543	1174	06 17 52+	3	SEP-6	SPL 76120-24
L	141-21544	1175	06 17 52+	3	SEP-6	SPL 76120-24, STEREO OF 140-21392
E	140-21392	1176	06 17 52+	3	SEP-6	SPL 76120-24, STEREO OF 141-21544
L	141-21545	1177	06 17 52+	3	SEP-6	
L	141-21546	1178	06 17 52+	3	SEP-6	
L	141-21547	1179	06 17 52+	3	SEP-6	
L	141-21548	1180	06 17 52+	3	SEP-6	
L	141-21549	1181	06 17 52+	3	SEP-6	
L	141-21550	1182	06 17 52+	3	SEP-6	
L	141-21551	1183	06 17 52+	3	SEP-6	
L	141-21552	1184	06 17 52+	3	SEP-6	
L	141-21553	1185	06 17 52+	3	SEP-6	
L	141-21554	1186	06 17 52+	3	SEP-6	
L	141-21555	1187	06 17 52+	3	SEP-6	
L	141-21556	1188	06 17 52+	3	SEP-6	
L	141-21557	1189	06 17 52+	3	SEP-6	
L	141-21558	1190	06 17 52+	3	SEP-6	
L	141-21559	1191	06 17 52+	3	SEP-6	
E	140-21393	1192	06 17 52+	3	SEP-6	
L	141-21560	1193	06 17 52+	3	SEP-6	
L	141-21561	1194	06 17 52+	3	SEP-6	
E	140-21394	1195	06 17 52+	3	SEP-6	
L	141-21562	1196	06 17 52+	3	SEP-6	
L	141-21563	1197	06 17 52+	3	SEP-6	
E	140-21395	1198	06 17 52+	3	SEP-6	
L	141-21564	1199	06 17 52+	3	SEP-6	
L	141-21565	1200	06 17 52+	3	SEP-6	
L	141-21566	1201	06 17 52+	3	SEP-6	SPL 76131-34,35-37, STEREO OF 140-21396
E	140-21396	1202	06 18 02	3	SEP-6	SPL 76131-34,35-37, STEREO OF 141-21566
E	140-21397	1203	06 18 02+	3	SEP-6	SPL 76131-34,35-37
E	140-21398	1204	06 18 02+	3	SEP-6	SPL 76131-34,35-37
E	140-21399	1205	06 18 02+	3	SEP-6	
L	141-21567	1206	06 18 02+	3	SEP-6	SPL 76131-34,35-37, TURNING PT ROCK, LM
L	141-21568	1207	06 18 02+	3	SEP-6	SPL 76131-34,35-37, TURNING PT ROCK, LM
L	141-21569	1208	06 18 02+	3	SEP-6	
L	141-21570	1209	06 18 02+	3	SEP-6	
L	141-21571	1210	06 18 02+	3	SEP-6	
L	141-21572	1211	06 18 02+	3	SEP-6	
L	141-21573	1212	06 18 02+	3	SEP-6	
L	141-21574	1213	06 18 02+	3	SEP-6	
E	140-21400	1214	06 18 11	3	6	MISC
L	141-21575	1215	06 19 18	3	6	PAN
L	141-21576	1216	06 19+18	3	6	PAN
L	141-21577	1217	06 19+18	3	6	PAN
L	141-21578	1218	06 19+18	3	6	PAN
L	141-21579	1219	06 19+18	3	6	PAN
L	141-21580	1220	06 19+18	3	6	PAN
L	141-21581	1221	06 19+18	3	6	PAN
L	141-21582	1222	06 19+18	3	6	PAN
L	141-21583	1223	06 19+18	3	6	PAN
L	141-21584	1224	06 19+18	3	6	PAN
L	141-21585	1225	06 19+18	3	6	PAN
L	141-21586	1226	06 19+18	3	6	PAN
L	141-21587	1227	06 19+18	3	6	PAN
L	141-21588	1228	06 19+18	3	6	PAN
L	141-21589	1229	06 19+18	3	6	PAN
L	141-21590	1230	06 19+18	3	6	PAN
L	141-21591	1231	06 19+18	3	6	PAN
L	141-21592	1232	06 19+18	3	6	PAN
L	141-21593	1233	06 19+18	3	6	PAN
L	141-21594	1234	06 19+18	3	6	PAN
L	141-21595	1235	06 19+18	3	6	PAN
L	141-21596	1236	06 19+18	3	6	PAN
L	141-21597	1237	06 19+18	3	6	PAN
L	141-21598	1238	06 19+18	3	6	PAN
L	141-21599	1239	06 19+18	3	6	PAN
L	141-21600	1240	06 19+18	3	6	PAN
L	141-21601	1241	06 19+18	3	6	PAN
L	141-21602	1242	06 19+18	3	6	PAN
L	141-21603	1243	06 20 18	3	6	PAN
L	141-21604	1244	06 18 21	3	6	SPL 76240-44,45-46,76260-64,65,76280-84,85-86 DSB, LOC
L	141-21605	1245	06 18 21	3	6	SPL 76240-44,45-46,76260-64,65,76280-84,85-86 DSB, LOC
E	140-21401	1246	06 18 25	3	6	SPL 76240-44,45-46,76260-64,65,76280-84,85-86 XS
E	140-21402	1247	06 18 25+	3	6	SPL 76240-44,45-46,76260-64,65,76280-84,85-86 XS
E	140-21403	1248	06 18 25+	3	6	SPL 76240-44,45-46,76260-64,65,76280-84,85-86 XS
E	140-21404	1249	06 18 25+	3	6	SPL 76240-44,45-46,76260-64,65,76280-84,85-86 XS
E	140-21405	1250	06 18 25+	3	6	SPL 76240-44,45-46,76260-64,65,76280-84,85-86 XS
E	140-21406	1251	06 18 25+	3	6	SPL 76240-44,45-46,76260-64,65,76280-84,85-86 XS
E	140-21407	1252	06 18 25+	3	6	SPL 76240-44,45-46,76260-64,65,76280-84,85-86 XS
E	140-21408	1253	06 18 25+	3	6	SPL 76240-44,45-46,76260-64,65,76280-84,85-86 XS
E	140-21409	1254	06 18 29	3	6	SPL 76240-44,45-46,76260-64,65,76280-84,85-86 LOC
L	141-21606	1255	06 18 29+	3	6	SPL 76240-44,45-46,76260-64,65,76280-84,85-86 DSA, LOC
L	141-21607	1256	06 18 26	3	6	SPL 76015,76215 DSB
E	140-21410	1257	06 18 26	3	6	SPL 76215 XSB
E	140-21411	1258	06 18 26	3	6	SPL 76015 XSB
E	140-21412	1259	06 18 26	3	6	SPL 76015,76215 LOC
E	140-21413	1260	06 18 26	3	6	SPL 76015 XSA

Table 7.--Chronological listing of 70mm Apollo 17 lunar surface pictures--Continued

MAG	PHOTO	SEQ	GET	EVA	STA	REMARKS
E 140-21414	1261	06 18 36	3	6	6	F-L OF BOULDER
E 140-21415	1262	06 18 36+	3	6	6	F-L OF BOULDER
E 140-21416	1263	06 18 36+	3	6	6	F-L OF BOULDER
E 140-21417	1264	06 18 36+	3	6	6	F-L OF BOULDER
E 140-21418	1265	06 18 36+	3	6	6	F-L OF BOULDER
E 140-21419	1266	06 18 36+	3	6	6	F-L OF BOULDER
E 140-21420	1267	06 18 36+	3	6	6	F-L OF BOULDER, SPL 76215 XSB
E 140-21421	1268	06 18 36+	3	6	6	F-L OF BOULDER, SPALLED AREA
E 140-21422	1269	06 18 36+	3	6	6	F-L OF BOULDER, SPL 76215 XSB
E 140-21423	1270	06 18 36+	3	6	6	F-L OF BOULDER, SPALLED AREA
E 140-21424	1271	06 18 36+	3	6	6	F-L OF BOULDER, SPL 76215 XSB
E 140-21425	1272	06 18 36+	3	6	6	F-L OF BOULDER
E 140-21426	1273	06 18 36+	3	6	6	F-L OF BOULDER
E 140-21427	1274	06 18 36+	3	6	6	F-L OF BOULDER
E 140-21428	1275	06 18 36+	3	6	6	F-L OF BOULDER
E 140-21429	1276	06 18 36+	3	6	6	F-L OF BOULDER
E 140-21430	1277	06 18 36+	3	6	6	F-L OF BOULDER
E 140-21431	1278	06 18 36+	3	6	6	F-L OF BOULDER
E 140-21432	1279	06 18 36+	3	6	6	F-L OF BOULDER
E 140-21433	1280	06 18 36+	3	6	6	F-L OF BOULDER
E 140-21434	1281	06 18 36+	3	6	6	F-L OF BOULDER
E 140-21435	1282	06 18 36+	3	6	6	F-L OF BOULDER, SPL 76315 XSB
E 140-21436	1283	06 18 36+	3	6	6	F-L OF BOULDER, SPL 76315 XSB
E 140-21437	1284	06 18 36+	3	6	6	F-L OF BOULDER, SPL 76315 XSB
E 140-21438	1285	06 18 36+	3	6	6	F-L OF BOULDER, SPL 76315 XSB
E 140-21439	1286	06 18 36+	3	6	6	F-L OF BOULDER, SPL 76315 XSB
E 140-21440	1287	06 18 36+	3	6	6	F-L OF BOULDER
L 141-21608	1288	06 18 38	3	6	6	SPL 76215,76235-39,76305-07 XSB
L 141-21609	1289	06 18 38+	3	6	6	SPL 76235-39,76255,76275,76295,76305-07 XSB
L 141-21610	1290	06 18 38+	3	6	6	SPL 76235-39,76255,76275,76295,76305-07,76320* LOC
E 140-21441	1291	06 18 38+	3	6	6	SPL 76235-39,76255,76275,76295,76305-07 XSB
L 141-21611	1292	06 18 38+	3	6	6	CU SPL 76235-39,76305-07 AREA
L 141-21612	1293	06 18 38+	3	6	6	CU SPL 76235-39,76305-07 AREA
L 141-21613	1294	06 18 38+	3	6	6	CU
L 141-21614	1295	06 18 38+	3	6	6	CU
L 141-21615	1296	06 18 48	3	6	6	SPL 76255,76275 XSB
L 141-21616	1297	06 18 48+	3	6	6	SPL 76315 XSA
L 141-21617	1298	06 18 48+	3	6	6	SPL 76315 XSA
L 141-21618	1299	06 18 48+	3	6	6	SPL 76315 XSA
L 141-21619	1300	06 18 48+	3	6	6	SPL 76315 XSA
L 141-21620	1301	06 18 48+	3	6	6	SPL 76315 XSA
E 140-21442	1302	06 18 49	3	6	6	CU 6 F-L OF SPL 76315,76320-24 BOULDER
E 140-21443	1303	06 18 49+	3	6	6	CU 6 F-L OF SPL 76315,76320-24 BOULDER
E 140-21444	1304	06 18 49+	3	6	6	CU 6 F-L OF SPL 76315,76320-24 BOULDER, SPL 76235-39,76305-07 XSB
E 140-21445	1305	06 18 49+	3	6	6	CU 6 F-L OF SPL 76315,76320-24 BOULDER, SPL 76235-39,76305-07 XSB
E 140-21446	1306	06 18 49+	3	6	6	CU 6 F-L OF SPL 76315,76320-24 BOULDER
E 140-21447	1307	06 18 49+	3	6	6	CU 6 F-L OF SPL 76315,76320-24 BOULDER, SPL 76255 XSB
E 140-21448	1308	06 18 49+	3	6	6	CU 6 F-L OF SPL 76315,76320-24 BOULDER, SPL 76255 XSB
E 140-21449	1309	06 18 49+	3	6	6	CU 6 F-L OF SPL 76315,76320-24 BOULDER, SPL 76255 XSB
E 140-21450	1310	06 18 49+	3	6	6	CU 6 F-L OF SPL 76315,76320-24 BOULDER
E 140-21451	1311	06 18 49+	3	6	6	CU 6 F-L OF SPL 76315,76320-24 BOULDER
E 140-21452	1312	06 18 49+	3	6	6	CU 6 F-L OF SPL 76315,76320-24 BOULDER, SPL 76295 XSA
E 140-21453	1313	06 18 49+	3	6	6	CU 6 F-L OF SPL 76315,76320-24 BOULDER, SPL 76235-39,76255,76305-07 XSA
E 140-21454	1314	06 18 49+	3	6	6	CU 6 F-L OF SPL 76315,76320-24 BOULDER, SPL 76235-39,76305-07 XSA
E 140-21455	1315	06 18 49+	3	6	6	CU 6 F-L OF SPL 76315,76320-24 BOULDER, SPL 76295 XSA
E 140-21456	1316	06 18 49+	3	6	6	CU 6 F-L OF SPL 76315,76320-24 BOULDER, SPL 75255,76275 XSA
E 140-21457	1317	06 18 49+	3	6	6	CU 6 F-L OF SPL 76315,76320-24 BOULDER, SPL 76295 XSA
E 140-21458	1318	06 18 49+	3	6	6	CU 6 F-L OF SPL 76315,76320-24 BOULDER, SPL 76255,76275 XSA
E 140-21459	1319	06 18 49+	3	6	6	CU 6 F-L OF SPL 76315,76320-24 BOULDER, SPL 76255,76275 DSA
E 140-21460	1320	06 18 49+	3	6	6	CU 6 F-L OF SPL 76315,76320-24 BOULDER
E 140-21461	1321	06 18 49+	3	6	6	CU 6 F-L OF SPL 76315,76320-24 BOULDER
E 140-21462	1322	06 18 49+	3	6	6	CU 6 F-L OF SPL 76315,76320-24 BOULDER
E 140-21463	1323	06 18 49+	3	6	6	CU 6 F-L OF SPL 76315,76320-24 BOULDER
E 140-21464	1324	06 18 49+	3	6	6	CU 6 F-L OF SPL 76315,76320-24 BOULDER
E 140-21465	1325	06 18 49+	3	6	6	CU 6 F-L OF SPL 76315,76320-24 BOULDER
E 140-21466	1326	06 18 49+	3	6	6	CU 6 F-L OF SPL 76315,76320-24 BOULDER
E 140-21467	1327	06 18 49+	3	6	6	CU 6 F-L OF SPL 76315,76320-24 BOULDER
E 140-21468	1328	06 18 49+	3	6	6	CU 6 F-L OF SPL 76315,76320-24 BOULDER
E 140-21469	1329	06 18 49+	3	6	6	CU 6 F-L OF SPL 76315,76320-24 BOULDER
E 140-21470	1330	06 18 49+	3	6	6	CU 6 F-L OF SPL 76315,76320-24 BOULDER
E 140-21471	1331	06 18 49+	3	6	6	CU 6 F-L OF SPL 76315,76320-24 BOULDER
E 140-21472	1332	06 18 49+	3	6	6	CU 6 F-L OF SPL 76315,76320-24 BOULDER
E 140-21473	1333	06 18 49+	3	6	6	CU 6 F-L OF SPL 76315,76320-24 BOULDER
E 140-21474	1334	06 18 49+	3	6	6	CU 6 F-L OF SPL 76315,76320-24 BOULDER, SPL 76320-24 XSB
E 140-21475	1335	06 18 49+	3	6	6	CU 6 F-L OF SPL 76315,76320-24 BOULDER
E 140-21476	1336	06 18 49+	3	6	6	CU 6 F-L OF SPL 76315,76320-24 BOULDER
E 140-21477	1337	06 18 49+	3	6	6	CU 6 F-L OF SPL 76315,76320-24 BOULDER
E 140-21478	1338	06 18 49+	3	6	6	CU 6 F-L OF SPL 76315,76320-24 BOULDER
E 140-21479	1339	06 18 49+	3	6	6	CU 6 F-L OF SPL 76315,76320-24 BOULDER
E 140-21480	1340	06 18 49+	3	6	6	CU 6 F-L OF SPL 76315,76320-24 BOULDER, SPL 76295 XSA
E 140-21481	1341	06 18 49+	3	6	6	CU 6 F-L OF SPL 76315,76320-24 BOULDER, SPL 76320-24 XSA
E 140-21482	1342	06 18 50	3	6	6	CU 6 F-L OF SPL 76315,76320-24 BOULDER, SPL 76320-24 XSA
E 140-21483	1343	06 18 54	3	6	6	PAN
E 140-21484	1344	06 18 54+	3	6	6	PAN
E 140-21485	1345	06 18 54+	3	6	6	PAN
E 140-21486	1346	06 18 54+	3	6	6	PAN
E 140-21487	1347	06 18 54+	3	6	6	PAN
E 140-21488	1348	06 18 54+	3	6	6	PAN
E 140-21489	1349	06 18 54+	3	6	6	PAN
E 140-21490	1350	06 18 54+	3	6	6	PAN

Table 7.--Chronological listing of 70mm Apollo 17  
lunar surface pictures--Continued

MAG	PHOTO	SEQ	GET	EVA	STA	REMARKS
E	140-21491	1351	06 18 54+	3	6	PAN
E	140-21492	1352	06 18 54+	3	6	PAN
E	140-21493	1353	06 18 54+	3	6	PAN
E	140-21494	1354	06 18 54+	3	6	PAN
E	140-21495	1355	06 18 54+	3	6	PAN
E	140-21496	1356	06 18 54+	3	6	PAN
E	140-21497	1357	06 18 54+	3	6	PAN
E	140-21498	1358	06 18 54+	3	6	PAN
E	140-21499	1359	06 18 54+	3	6	PAN
E	140-21500	1360	06 18 54+	3	6	PAN
E	140-21501	1361	06 18 54+	3	6	PAN
E	140-21502	1362	06 18 54+	3	6	PAN
E	140-21503	1363	06 18 54+	3	6	PAN
E	140-21504	1364	06 18 54+	3	6	PAN
E	140-21505	1365	06 18 54+	3	6	PAN
E	140-21506	1366	06 18 54+	3	6	PAN
E	140-21507	1367	06 18 54+	3	6	PAN
E	140-21508	1368	06 18 54+	3	6	PAN
E	140-21509	1369	06 18 55	3	6	PAN
L	141-21621	1370	06 18 55+	3	6	SPL 76500-05,06,76535-39,45-49,55-59,65-69,75-77 XSB
L	141-21622	1371	06 18 55+	3	6	SPL 76500-05,06,76535-39,45-49,55-59,65-69,75-77 XSB
L	141-21623	1372	06 18 55+	3	6	SPL 76500-05,06,76535-39,45-49,55-59,65-69,75-77 XSB
L	141-21624	1373	06 18 55+	3	6	SPL 76500-05,06,76535-39,45-49,55-59,65-69,75-77 XSB
L	141-21625	1374	06 19 01	3	6	SPL 76500-05,06,76535-39,45-49,55-59,65-69,75-77 XSA
L	141-21626	1375	06 19 01+	3	6	SPL 76500-05,06,76535-39,45-49,55-59,65-69,75-77 XSA
L	141-21627	1376	06 19 01+	3	6	SPL 76500-05,06,76535-39,45-49,55-59,65-69,75-77 XSA
F	146-22289	1377	06 19 05	3	6	MISC
F	146-22290	1378	06 19 05+	3	6	MISC
F	146-22291	1379	06 19 08	3	6	DT SPL 76001 XSD
F	146-22292	1380	06 19 08+	3	6	DT SPL 76001 XSD
F	146-22293	1381	06 19 08+	3	6	DT SPL 76001 LOC
F	146-22294	1382	06 19 08+	3	6	DT SPL 76001 LOC
F	146-22295	1383	06 19 08+	3	6	DT SPL 76001 XSA
F	146-22296	1384	06 19 08+	3	2	LRV
F	146-22297	1385	06 19 08+	3	2	LRV
L	141-21628	1386	06 19 08+	3	6	F-L OF BOULDER US
L	141-21629	1387	06 19 08+	3	6	F-L OF BOULDER US
L	141-21630	1388	06 19 08+	3	6	F-L OF BOULDER US
L	141-21631	1389	06 19 08+	3	6	F-L OF BOULDER XS
L	141-21632	1390	06 19 08+	3	6	F-L OF BOULDER XS
L	141-21633	1391	06 19 08+	3	6	F-L OF BOULDER XS
L	141-21634	1392	06 19 08+	3	6	F-L OF BOULDER XS
L	141-21635	1393	06 19 10	3	6	DS
L	141-21636	1394	06 19 10+	3	6	DS
L	141-21637	1395	06 19 25	3	6-7	
L	141-21638	1396	06 19 25+	3	6-7	
L	141-21639	1397	06 19 25+	3	6-7	
L	141-21640	1398	06 19 25+	3	6-7	
L	141-21641	1399	06 19 25+	3	6-7	
L	141-21642	1400	06 19 25+	3	6-7	
L	141-21643	1401	06 19 25+	3	6-7	
L	141-21644	1402	06 19 25+	3	6-7	
L	141-21645	1403	06 19 25+	3	6-7	
L	141-21646	1404	06 19 30	3	7	PAN, NEAR FIELD ONLY (11 FT FOCUS)
L	141-21647	1405	06 19 30+	3	7	PAN, NEAR FIELD ONLY (11 FT FOCUS)
L	141-21648	1406	06 19 30+	3	7	PAN, NEAR FIELD ONLY (11 FT FOCUS)
L	141-21649	1407	06 19 30+	3	7	PAN, NEAR FIELD ONLY (11 FT FOCUS)
L	141-21650	1408	06 19 30+	3	7	PAN, NEAR FIELD ONLY (11 FT FOCUS)
L	141-21651	1409	06 19 30+	3	7	PAN, NEAR FIELD ONLY (11 FT FOCUS)
L	141-21652	1410	06 19 30+	3	7	PAN, NEAR FIELD ONLY (11 FT FOCUS)
L	141-21653	1411	06 19 30+	3	7	PAN, NEAR FIELD ONLY (11 FT FOCUS)
L	141-21654	1412	06 19 30+	3	7	PAN, NEAR FIELD ONLY (11 FT FOCUS)
L	141-21655	1413	06 19 30+	3	7	PAN, NEAR FIELD ONLY (11 FT FOCUS)
L	141-21656	1414	06 19 30+	3	7	PAN, NEAR FIELD ONLY (11 FT FOCUS)
L	141-21657	1415	06 19 30+	3	7	PAN, NEAR FIELD ONLY (11 FT FOCUS)
L	141-21658	1416	06 19 30+	3	7	PAN, NEAR FIELD ONLY (11 FT FOCUS)
L	141-21659	1417	06 19 30+	3	7	PAN, NEAR FIELD ONLY (11 FT FOCUS)
L	141-21660	1418	06 19 30+	3	7	PAN, NEAR FIELD ONLY (11 FT FOCUS)
L	141-21661	1419	06 19 30+	3	7	PAN, NEAR FIELD ONLY (11 FT FOCUS)
L	141-21662	1420	06 19 30+	3	7	PAN, NEAR FIELD ONLY (11 FT FOCUS)
L	141-21663	1421	06 19 30+	3	7	PAN, NEAR FIELD ONLY (11 FT FOCUS)
L	141-21664	1422	06 19 30+	3	7	PAN, NEAR FIELD ONLY (11 FT FOCUS)
L	141-21665	1423	06 19 30+	3	7	PAN, NEAR FIELD ONLY (11 FT FOCUS)
L	141-21666	1424	06 19 30+	3	7	PAN, NEAR FIELD ONLY (11 FT FOCUS)
L	141-21667	1425	06 19 30+	3	7	PAN, NEAR FIELD ONLY (11 FT FOCUS)
F	146-22298	1426	06 19 35	3	7	BOULDER F-L, SPL 77115,77135 XSB
F	146-22299	1427	06 19 35+	3	7	BOULDER F-L, SPL 77115,77135 XSB
F	146-22300	1428	06 19 35+	3	7	BOULDER F-L, SPL 77075*,77095*,77115,77135 XSB
F	146-22301	1429	06 19 35+	3	7	BOULDER F-L
F	146-22302	1430	06 19 35+	3	7	BOULDER F-L
F	146-22303	1431	06 19 35+	3	7	BOULDER F-L
F	146-22304	1432	06 19 35+	3	7	BOULDER F-L
F	146-22305	1433	06 19 35+	3	7	BOULDER F-L, AREA OF SPL 77075-77,77215 XSB
F	146-22306	1434	06 19 35+	3	7	BOULDER F-L, AREA OF SPL 77075-77,77215 XSB
F	146-22307	1435	06 19 35+	3	7	BOULDER F-L, SPL 77075-77,77215 XSB
F	146-22308	1436	06 19 35+	3	7	BOULDER F-L, SPL 77075-77,77215 XSB
F	146-22309	1437	06 19 35+	3	7	BOULDER F-L, SPL 77075-77,77215 XSB
F	146-22310	1438	06 19 35+	3	7	BOULDER F-L, SPL 77075-77,77215 XSB
F	146-22311	1439	06 19 35+	3	7	BOULDER F-L, SPL 77075-77,77215 XSB
F	146-22312	1440	06 19 35+	3	7	BOULDER F-L, SPL 77075-77,77215 XSB

Table 7.--Chronological listing of 70mm Apollo 17 lunar surface pictures--Continued

SLAC	PHOTO	SEQ	GET	EVA	STA	REMARKS
F	146-22313	1441	06 19 35+	3	7	BOULDER F-L, SPL 77075-77,77215 XSB
F	146-22314	1442	06 19 35+	3	7	BOULDER F-L, SPL 77075-77,77215 XSB
F	146-22315	1443	06 19 35+	3	7	BOULDER F-L, SPL 77075-77,77215 XSB
F	146-22316	1444	06 19 35+	3	7	BOULDER CU
F	146-22317	1445	06 19 35+	3	7	BOULDER CU
F	146-22318	1446	06 19 35+	3	7	BOULDER CU
F	146-22319	1447	06 19 35+	3	7	BOULDER CU
F	146-22320	1448	06 19 35+	3	7	BOULDER CU
F	146-22321	1449	06 19 35+	3	7	BOULDER CU
F	146-22322	1450	06 19 35+	3	7	BOULDER CU
F	146-22323	1451	06 19 35+	3	7	BOULDER CU
F	146-22324	1452	06 19 35+	3	7	BOULDER CU
F	146-22325	1453	06 19 35+	3	7	BOULDER CU
F	146-22326	1454	06 19 35+	3	7	BOULDER CU
F	146-22327	1455	06 19 35+	3	7	BOULDER CU, SPL 77075-77,77215 XSB
F	146-22328	1456	06 19 35+	3	7	BOULDER CU, SPL 77075-77,77215 XSB
F	146-22329	1457	06 19 40	3	7	BOULDER CU, SPL 77075-77,77215 XSA
F	146-22330	1458	06 19 40+	3	7	BOULDER CU, SPL 77075-77,77215 XSA
F	146-22331	1459	06 19 40+	3	7	SPL 77135 XSD
F	146-22332	1460	06 19 40+	3	7	SPL 77135 XSD
F	146-22333	1461	06 19 40+	3	7	SPL 77135 XSD
F	146-22334	1462	06 19 40+	3	7	SPL 77135 XSD
F	146-22335	1463	06 19 40+	3	7	SPL 77135 XSD
F	146-22336	1464	06 19 40+	3	7	SPL 77115,77135 XSA
F	146-22337	1465	06 19 40+	3	7	SPL 77115,77135 XSA
F	146-22338	1466	06 19 40+	3	7	SPL 77115,77135 XSA
F	146-22339	1467	06 19 46	3	7	PAN
F	146-22340	1468	06 19 46+	3	7	PAN
F	146-22341	1469	06 19 46+	3	7	PAN
F	146-22342	1470	06 19 46+	3	7	PAN
F	146-22343	1471	06 19 46+	3	7	PAN
F	146-22344	1472	06 19 46+	3	7	PAN
F	146-22345	1473	06 19 46+	3	7	PAN
F	146-22346	1474	06 19 46+	3	7	PAN
F	146-22347	1475	06 19 46+	3	7	PAN
F	146-22348	1476	06 19 46+	3	7	PAN
F	146-22349	1477	06 19 46+	3	7	PAN
F	146-22350	1478	06 19 46+	3	7	PAN
F	146-22351	1479	06 19 46+	3	7	PAN
F	146-22352	1480	06 19 46+	3	7	PAN
F	146-22353	1481	06 19 46+	3	7	PAN
F	146-22354	1482	06 19 46+	3	7	PAN
F	146-22355	1483	06 19 46+	3	7	PAN
F	146-22356	1484	06 19 46+	3	7	PAN
F	146-22357	1485	06 19 46+	3	7	PAN
F	146-22358	1486	06 19 46+	3	7	PAN
F	146-22359	1487	06 19 46+	3	7	PAN
F	146-22360	1488	06 19 46+	3	7	PAN
F	146-22361	1489	06 19 46+	3	7	PAN
F	146-22362	1490	06 19 46+	3	7	PAN
F	146-22363	1491	06 19 47	3	7	PAN
M	142-21669	1492			7	FOGGED
M	142-21670	1493			7	MISC
M	142-21671	1494	06 19 52	3	7-8	
M	142-21672	1495	06 19 52+	3	7-8	
M	142-21673	1496	06 19 52+	3	7-8	
M	142-21674	1497	06 19 52+	3	7-8	
M	142-21675	1498	06 19 52+	3	7-8	
M	142-21676	1499	06 19 52+	3	7-8	
M	142-21677	1500	06 19 52+	3	7-8	
M	142-21678	1501	06 19 52+	3	7-8	
M	142-21679	1502	06 19 52+	3	7-8	
M	142-21680	1503	06 19 52+	3	7-8	
M	142-21681	1504	06 19 52+	3	7-8	
M	142-21682	1505	06 19 52+	3	7-8	
F	146-22364	1506	06 19 52+	3	7-8	
M	142-21683	1507	06 19 52+	3	7-8	
M	142-21684	1508	06 19 52+	3	7-8	
M	142-21685	1509	06 19 52+	3	7-8	
M	142-21686	1510	06 19 52+	3	7-8	
M	142-21687	1511	06 19 52+	3	7-8	
M	142-21688	1512	06 19 52+	3	7-8	
M	142-21689	1513	06 19 52+	3	7-8	
M	142-21690	1514	06 19 52+	3	7-8	
M	142-21691	1515	06 19 52+	3	7-8	
M	142-21692	1516	06 20 03	3	7-8	SPL 78120-24?
M	142-21693	1517	06 20 03+	3	7-8	SPL 78120-24?
M	142-21694	1518	06 20 03+	3	7-8	SPL 78120-24?
M	142-21695	1519	06 20 03+	3	7-8	SPL 78120-24?
M	142-21696	1520	06 20 03+	3	7-8	SPL 78120-24?
M	142-21697	1521	06 20 03+	3	7-8	
F	146-22365	1522	06 20 13+	3	8	SPL 78135 XSB
F	146-22366	1523	06 20 13+	3	8	SPL 78135 XSB
F	146-22367	1524	06 20 13+	3	8	SPL 78135 LOC
F	146-22368	1525	06 20 13+	3	8	SPL 78135 XSA
M	142-21698	1526	06 20 14	3	8	SPL 78230-34,35-36,38 XSB
M	142-21699	1527	06 20 14+	3	8	SPL 78230-34,35-36,38 XSB
M	142-21700	1528	06 20 14+	3	8	SPL 78230-34,35-36,38 XSB
M	142-21701	1529	06 20 14+	3	8	SPL 78230-34,35-36,38 DSB
M	142-21702	1530	06 20 14+	3	8	SPL 78230-34,35-36,38 LOC
M	142-21703	1531	06 20 16	3	8	SPL 78230-34,35-36,38 DSB

Table 7.--Chronological listing of 70mm Apollo 17  
lunar surface pictures--Continued

MAG	PHOTO	SEQ	GET	EVA	STA	REMARKS
M	142-21704	1532	06 20 17	3	8	SPL 78220-24 XS
M	142-21705	1533	06 20 17+	3	8	SPL 78220-24 XS
F	146-22369	1534	06 18 20	3	8	SPL 78235-36, 38 (AFTER ROLLING) XSB
F	146-22370	1535	06 18 20+	3	8	SPL 78235-36, 38 (AFTER ROLLING) XSB
F	146-22371	1536	06 20 24	3	8	SPL 78235-36, 38 (AFTER ROLLING) XSA
F	146-22372	1537	06 20 26	3	8	SPL 78250-55 XSB
F	146-22373	1538	06 20 26+	3	8	SPL 78250-55 XSB
F	146-22374	1539	06 20 26+	3	8	SPL 78250-55 XSA
F	146-22375	1540	06 20 27	3	8	PAN (BROKEN)
F	146-22376	1541	06 20 27+	3	8	PAN (BROKEN)
F	146-22377	1542	06 20 27+	3	8	PAN (BROKEN)
F	146-22378	1543	06 20 27+	3	8	PAN (BROKEN)
F	146-22379	1544	06 20 27+	3	8	PAN (BROKEN)
F	146-22380	1545	06 20 27+	3	8	PAN (BROKEN)
F	146-22381	1546	06 20 27+	3	8	PAN (BROKEN)
F	146-22382	1547	06 20 27+	3	8	PAN (BROKEN)
F	146-22383	1548	06 20 27+	3	8	PAN (BROKEN)
F	146-22384	1549	06 20 27+	3	8	PAN (BROKEN)
F	146-22385	1550	06 20 27+	3	8	PAN (BROKEN)
F	146-22386	1551	06 20 27+	3	8	PAN (BROKEN)
F	146-22387	1552	06 20 27+	3	8	PAN (BROKEN)
F	146-22388	1553	06 20 27+	3	8	PAN (BROKEN)
F	146-22389	1554	06 20 27+	3	8	PAN (BROKEN)
F	146-22390	1555	06 20 27+	3	8	PAN (BROKEN)
F	146-22391	1556	06 20 27+	3	8	PAN (BROKEN)
F	146-22392	1557	06 20 27+	3	8	PAN (BROKEN)
F	146-22393	1558	06 20 27+	3	8	PAN (BROKEN)
F	146-22394	1559	06 20 27+	3	8	PAN (BROKEN)
F	146-22395	1560	06 20 27+	3	8	PAN (BROKEN)
F	146-22396	1561	06 20 27+	3	8	PAN (BROKEN)
F	146-22397	1562	06 20 27+	3	8	PAN (BROKEN)
F	146-22398	1563	06 20 27+	3	8	SPL 78255 XSA
M	142-21706	1564	06 20 32	3	8	SPL 78155, 78500-04, 05-09, 15-18, 78535-39, 45-49, 55-59, 65-69, 75-79, 85-89, 95-99 XSB F-L
M	142-21707	1565	06 20 32+	3	8	SPL 78155, 78500-04, 05-09, 15-18, 78535-39, 45-49, 55-59, 65-69, 75-79, 85-89, 95-99 XSB F-L
M	142-21708	1566	06 20 32+	3	8	SPL 78155, 78500-04, 05-09, 15-18, 78535-39, 45-49, 55-59, 65-69, 75-79, 85-89, 95-99 XSB F-L
M	142-21709	1567	06 20 32+	3	8	SPL 78155, 78500-04, 05-09, 15-18, 78535-39, 45-49, 55-59, 65-69, 75-79, 85-89, 95-99 XSB F-L
M	142-21710	1568	06 20 32+	3	8	SPL 78155, 78500-04, 05-09, 15-18, 78535-39, 45-49, 55-59, 65-69, 75-79, 85-89, 95-99 XSB F-L
M	142-21711	1569	06 20 32+	3	8	SPL 78155, 78500-04, 05-09, 15-18, 78535-39, 45-49, 55-59, 65-69, 75-79, 85-89, 95-99 XSB F-L
M	142-21712	1570	06 20 32+	3	8	SPL 78155, 78500-04, 05-09, 15-18, 78535-39, 45-49, 55-59, 65-69, 75-79, 85-89, 95-99 XSB F-L
M	142-21713	1571	06 20 32+	3	8	SPL 78155, 78500-04, 05-09, 15-18, 78535-39, 45-49, 55-59, 65-69, 75-79, 85-89, 95-99 XSB F-L
M	142-21714	1572	06 20 32+	3	8	SPL 78155, 78500-04, 05-09, 15-18, 78535-39, 45-49, 55-59, 65-69, 75-79, 85-89, 95-99 XSB F-L
M	142-21715	1573	06 20 32+	3	8	SPL 78155, 78500-04, 05-09, 15-18, 78535-39, 45-49, 55-59, 65-69, 75-79, 85-89, 95-99 XSB F-L
M	142-21716	1574	06 20 34	3	8	SPL 78155, 78500-04, 05-09, 15-18, 78535-39, 45-49, 55-59, 65-69, 75-79, 85-89, 95-99 XSB F-L
F	146-22399	1575	06 20 35	3	8	SPL 78155, 78500-04, 05-09, 15-18, 78535-39, 45-49, 55-59, 65-69, 75-79, 85-89, 95-99 XSB
F	146-22400	1576	06 20 35+	3	8	SPL 78155, 78500-04, 05-09, 15-18, 78535-39, 45-49, 55-59, 65-69, 75-79, 85-89, 95-99 XSB
F	146-22401	1577	06 20 35+	3	8	SPL 78155, 78500-04, 05-09, 15-18, 78535-39, 45-49, 55-59, 65-69, 75-79, 85-89, 95-99 XSB
F	146-22402	1578	06 20 35+	3	8	SPL 78155, 78500-04, 05-09, 15-18, 78535-39, 45-49, 55-59, 65-69, 75-79, 85-89, 95-99 XSB
F	146-22403	1579	06 20 35+	3	8	SPL 78155, 78500-04, 05-09, 15-18, 78535-39, 45-49, 55-59, 65-69, 75-79, 85-89, 95-99 XSB
M	142-21717	1580	06 20 42	3	8	TR SPL 78420-24, 78440-44, 78460-64, 65, 78480-84 XSB
M	142-21718	1581	06 20 42+	3	8	TR SPL 78420-24, 78440-44, 78460-64, 65, 78480-84 XSB
M	142-21719	1582	06 20 42+	3	8	TR SPL 78420-24, 78440-44, 78460-64, 65, 78480-84 XSB, LJC
M	142-21720	1583	06 20 45	3	8	TR SPL 78420-24, 78440-44, 78460-64, 65, 78480-84 XSA
M	142-21721	1584	06 20 45+	3	8	TR SPL 78420-24, 78440-44, 78460-64, 65, 78480-84 XSA
M	142-21722	1585	06 20 45+	3	8	TR SPL 78420-24, 78440-44, 78460-64, 65, 78480-84 XSA
M	142-21723	1586	06 20 45+	3	8	TR SPL 78420-24, 78440-44, 78460-64, 65, 78480-84 XSA
M	142-21724	1587	06 20 45+	3	8	TR SPL 78420-24, 78440-44, 78460-64, 65, 78480-84 XSA
M	142-21725	1588	06 20 45+	3	8	TR SPL 78420-24, 78440-44, 78460-64, 65, 78480-84 XSA
M	142-21726	1589	06 20 46	3	8	PAN
M	142-21727	1590	06 20 46+	3	8	PAN
M	142-21728	1591	06 20 46+	3	8	PAN
M	142-21729	1592	06 20 46+	3	8	PAN
M	142-21730	1593	06 20 46+	3	8	PAN
M	142-21731	1594	06 20 46+	3	8	PAN
M	142-21732	1595	06 20 46+	3	8	PAN
M	142-21733	1596	06 20 46+	3	8	PAN
M	142-21734	1597	06 20 46+	3	8	PAN
M	142-21735	1598	06 20 46+	3	8	PAN
M	142-21736	1599	06 20 46+	3	8	PAN
M	142-21737	1600	06 20 46+	3	8	PAN
M	142-21738	1601	06 20 46+	3	8	PAN
M	142-21739	1602	06 20 46+	3	8	PAN
M	142-21740	1603	06 20 46+	3	8	PAN
M	142-21741	1604	06 20 46+	3	8	PAN
M	142-21742	1605	06 20 46+	3	8	PAN
M	142-21743	1606	06 20 46+	3	8	PAN
M	142-21744	1607	06 20 46+	3	8	PAN
M	142-21745	1608	06 20 47	3	8	PAN
M	142-21746	1609	06 20 55	3	8-9	
M	142-21747	1610	06 20 55+	3	8-9	
M	142-21748	1611	06 20 55+	3	8-9	
M	142-21749	1612	06 20 55+	3	8-9	
M	142-21750	1613	06 20 55+	3	8-9	
M	142-21751	1614	06 20 55+	3	8-9	
M	142-21752	1615	06 20 55+	3	8-9	
M	142-21753	1616	06 20 55+	3	8-9	
M	142-21754	1617	06 20 55+	3	8-9	
M	142-21755	1618	06 20 55+	3	8-9	
M	142-21756	1619	06 20 55+	3	8-9	
M	142-21757	1620	06 20 55+	3	8-9	
M	142-21758	1621	06 20 55+	3	8-9	
M	142-21759	1622	06 20 55+	3	8-9	

Table 7.--Chronological listing of 70mm Apollo 17  
lunar surface pictures--Continued

MAG	PHOTO	SEQ	GET	EVA	STA	REMARKS
M	142-21760	1623	06 20 55+	3	8-9	
M	142-21761	1624	06 20 55+	3	8-9	
M	142-21762	1625	06 20 55+	3	8-9	
M	142-21763	1626	06 20 55+	3	8-9	
M	142-21764	1627	06 20 55+	3	8-9	
M	142-21765	1628	06 20 55+	3	8-9	
M	142-21766	1629	06 20 55+	3	8-9	
M	142-21767	1630	06 20 55+	3	8-9	
F	146-22404	1631	06 20 55+	3	8-9	
F	146-22405	1632	06 20 55+	3	8-9	
F	146-22406	1633	06 20 55+	3	8-9	
F	146-22407	1634	06 20 55+	3	8-9	
F	146-22408	1635	06 20 55+	3	8-9	
M	142-21768	1636	06 20 55+	3	8-9	
M	142-21769	1637	06 20 55+	3	8-9	
M	142-21770	1638	06 20 55+	3	8-9	
M	142-21771	1639	06 20 55+	3	8-9	
M	142-21772	1640	06 20 55+	3	8-9	
M	142-21773	1641	06 20 55+	3	8-9	
M	142-21774	1642	06 20 55+	3	8-9	
M	142-21775	1643	06 20 55+	3	8-9	
F	146-22409	1644	06 20 55+	3	8-9	
M	142-21776	1645	06 20 55+	3	8-9	
M	142-21777	1646	06 20 55+	3	8-9	
M	142-21778	1647	06 20 55+	3	8-9	
M	142-21779	1648	06 20 55+	3	8-9	
M	142-21780	1649	06 20 55+	3	8-9	
F	146-22410	1650	06 20 55+	3	8-9	
M	142-21781	1651	06 20 55+	3	8-9	
F	146-22411	1652	06 20 55+	3	8-9	
M	142-21782	1653	06 20 55+	3	8-9	
F	146-22412	1654	06 20 55+	3	8-9	
M	142-21783	1655	06 20 55+	3	8-9	
M	142-21784	1656	06 20 55+	3	8-9	
M	142-21785	1657	06 20 55+	3	8-9	
M	142-21786	1658	06 20 55+	3	8-9	
M	142-21787	1659	06 20 55+	3	8-9	
M	142-21788	1660	06 20 55+	3	8-9	
M	142-21789	1661	06 20 55+	3	8-9	
M	142-21790	1662	06 20 55+	3	8-9	
M	142-21791	1663	06 21 25	3	9	SPL 79115,79120-24,79135,79510-14,15-19,25-29,35-37 DSB
M	142-21792	1664	06 21 25+	3	9	SPL 79115,79120-24,79135,79510-14,15-19,25-29,35-37 LOC
M	142-21793	1665	06 21 25+	3	9	SPL 79115,79120-24,79135,79510-14,15-19,25-29,35-37 LOC
M	142-21794	1666	06 21 25+	3	9	SPL 79115,79120-24,79135,79510-14,15-19,25-29,35-37 LOC
F	146-22413	1667	06 21 26	3	9	SPL 79115,79120-24,79135,79510-14,15-19,25-29,35-37 XSB
F	146-22414	1668	06 21 26+	3	9	SPL 79115,79120-24,79135,79510-14,15-19,25-29,35-37 XSB
F	146-22415	1669	06 21 29	3	9	SPL 79115,79120-24,79135,79510-14,15-19,25-29,35-37 XSA
F	146-22416	1670	06 21 29+	3	9	SPL 79115,79120-24,79135,79510-14,15-19,25-29,35-37 XSA
F	146-22417	1671	06 21 29+	3	9	SPL 79115,79120-24,79135,79510-14,15-19,25-29,35-37 XSA
F	146-22418	1672	06 21 29+	3	9	SPL 79115,79120-24,79135,79510-14,15-19,25-29,35-37 XSA
M	142-21795	1673	06 21 35	3	9	SPL 79175,79195 DSB
M	142-21796	1674	06 21 35+	3	9	SPL 79175,79195 LOC
M	142-21797	1675	06 21 35+	3	9	SPL 79175,79195 LOC
F	146-22419	1676	06 21 35+	3	9	SPL 79175,79195 XSB
F	146-22420	1677	06 21 35+	3	9	SPL 79175,79195 XSB
F	146-22421	1678	06 21 35+	3	9	SPL 79175,79195 XSB
F	146-22422	1679	06 21 39	3	9	SPL 79175,79195 XSA
F	146-22423	1680	06 21 41	3	9	PPAN
F	146-22424	1681	06 21 41+	3	9	PPAN
F	146-22425	1682	06 21 41+	3	9	PPAN
F	146-22426	1683	06 21 41+	3	9	PPAN
F	146-22427	1684	06 21 41+	3	9	PPAN
F	146-22428	1685	06 21 41+	3	9	PPAN
F	146-22429	1686	06 21 41+	3	9	PPAN
F	146-22430	1687	06 21 41+	3	9	PPAN
F	146-22431	1688	06 21 41+	3	9	PPAN
F	146-22432	1689	06 21 41+	3	9	PPAN
F	146-22433	1690	06 21 41+	3	9	PPAN
F	146-22434	1691	06 21 41+	3	9	PPAN
F	146-22435	1692	06 21 41+	3	9	PPAN
F	146-22436	1693	06 21 41+	3	9	PPAN
F	146-22437	1694	06 21 41+	3	9	PPAN
F	146-22438	1695	06 21 41+	3	9	PPAN
F	146-22439	1696	06 21 41+	3	9	PPAN
F	146-22440	1697	06 21 41+	3	9	PPAN
F	146-22441	1698	06 21 41+	3	9	PPAN
F	146-22442	1699	06 21 41+	3	9	PPAN
F	146-22443	1700	06 21 41+	3	9	PPAN
F	146-22444	1701	06 21 41+	3	9	PPAN
F	146-22445	1702	06 21 41+	3	9	PPAN
F	146-22446	1703	06 21 41+	3	9	PPAN
F	146-22447	1704	06 21 41+	3	9	PPAN
F	146-22448	1705	06 21 41+	3	9	PPAN
F	146-22449	1706	06 21 41+	3	9	PPAN
F	146-22450	1707	06 21 41+	3	9	PPAN
M	142-21798	1708	06 21 42	3	9	PAN
M	142-21799	1709	06 21 42+	3	9	PAN
M	142-21800	1710	06 21 42+	3	9	PAN
M	142-21801	1711	06 21 42+	3	9	PAN
M	142-21802	1712	06 21 42+	3	9	PAN
M	142-21803	1713	06 21 42+	3	9	PAN

Table 7.--Chronological listing of 70mm Apollo 17  
lunar surface pictures--Continued

MAG	PHOTO	SEQ	GET	EVA	STA	REMARKS
M	142-21804	1714	06 21 42+	3	9	PAN
M	142-21805	1715	06 21 42+	3	9	PAN
M	142-21806	1716	06 21 42+	3	9	PAN
M	142-21807	1717	06 21 42+	3	9	PAN
M	142-21808	1718	06 21 42+	3	9	PAN
M	142-21809	1719	06 21 42+	3	9	PAN
M	142-21810	1720	06 21 42+	3	9	PAN
M	142-21811	1721	06 21 42+	3	9	PAN
M	142-21812	1722	06 21 42+	3	9	PAN
M	142-21813	1723	06 21 42+	3	9	PAN
M	142-21814	1724	06 21 42+	3	9	PAN
M	142-21815	1725	06 21 42+	3	9	PAN
M	142-21816	1726	06 21 42+	3	9	PAN
M	142-21817	1727	06 21 42+	3	9	PAN
M	142-21818	1728	06 21 42+	3	9	PAN
M	142-21819	1729	06 21 42+	3	9	PAN
M	142-21820	1730	06 21 42+	3	9	PAN
M	142-21821	1731	06 21 42+	3	9	PAN
M	142-21822	1732	06 21 42+	3	9	PAN
M	142-21823	1733	06 21 42+	3	9	PAN
M	142-21824	1734	06 21 42+	3	9	PAN
M	142-21825	1735	06 21 50	3	9	SPL BAG 52Y XSB, LOC NOT RETURNED
M	142-21826	1736	06 21 50+	3	9	SPL BAG 52Y LOC NOT RETURNED
M	142-21827	1737	06 21 50+	3	9	TR SPL 79220-24,25-28,79240-44,45,79260-64,65 XSA
M	142-21828	1738	06 21 50+	3	9	TR SPL 79220-24,25-28,79240-44,45,79260-64,65 XSA
M	142-21829	1739	06 21 50+	3	9	TR SPL 79220-24,25-28,79240-44,45,79260-64,65 XSA
M	142-21830	1740	06 21 50+	3	9	MISC
M	142-21831	1741	06 21 50+	3	9	MISC
M	142-21832	1742	06 21 50+	3	9	
M	142-21833	1743	06 21 50+	3	9	
N	143-21834	1744	06 22 00	3	9	FOGGED
N	143-21835	1745	06 22 00+	3	9	MISC
N	143-21836	1746	06 22 00+	3	9	PAN, DT SPL 79002/79001 LOC
N	143-21837	1747	06 22 00+	3	9	PAN, DT SPL 79002/79001, EP-5 LOC
N	143-21838	1748	06 22 00+	3	9	PAN, DT SPL 79002/79001, EP-5 LOC
N	143-21839	1749	06 22 00+	3	9	PAN
N	143-21840	1750	06 22 00+	3	9	PAN
N	143-21841	1751	06 22 00+	3	9	PAN
N	143-21842	1752	06 22 00+	3	9	PAN
N	143-21843	1753	06 22 00+	3	9	PAN
N	143-21844	1754	06 22 00+	3	9	PAN
N	143-21845	1755	06 22 00+	3	9	PAN
N	143-21846	1756	06 22 00+	3	9	PAN
N	143-21847	1757	06 22 00+	3	9	PAN
N	143-21848	1758	06 22 00+	3	9	PAN
N	143-21849	1759	06 22 00+	3	9	PAN
N	143-21850	1760	06 22 00+	3	9	PAN
N	143-21851	1761	06 22 00+	3	9	PAN
N	143-21852	1762	06 22 00+	3	9	PAN
N	143-21853	1763	06 22 00+	3	9	PAN
N	143-21854	1764	06 22 00+	3	9	PAN
N	143-21855	1765	06 22 00+	3	9	PAN
N	143-21856	1766	06 22 00+	3	9	PAN
N	143-21857	1767	06 22 00+	3	9	PAN
N	143-21858	1768	06 22 01	3	9	PAN
B	134-20452	1769	06 22 01+	3	9	LRV, FOGGED
B	134-20453	1770	06 22 01+	3	9	LRV, FOGGED
B	134-20454	1771	06 22 01+	3	9	LRV, FOGGED
N	143-21859	1772	06 22 09	3	9-LM	
N	143-21860	1773	06 22 09+	3	9-LM	
N	143-21861	1774	06 22 09+	3	9-LM	
N	143-21862	1775	06 22 09+	3	9-LM	
N	143-21863	1776	06 22 09+	3	9-LM	
N	143-21864	1777	06 22 09+	3	9-LM	
N	143-21865	1778	06 22 09+	3	9-LM	
N	143-21866	1779	06 22 09+	3	9-LM	
N	143-21867	1780	06 22 09+	3	9-LM	
N	143-21868	1781	06 22 09+	3	9-LM	
N	143-21869	1782	06 22 09+	3	9-LM	
N	143-21870	1783	06 22 09+	3	9-LM	
N	143-21871	1784	06 22 09+	3	9-LM	
N	143-21872	1785	06 22 09+	3	9-LM	
N	143-21873	1786	06 22 09+	3	9-LM	
N	143-21874	1787	06 22 09+	3	9-LM	
N	143-21875	1788	06 22 09+	3	9-LM	
N	143-21876	1789	06 22 09+	3	9-LM	
N	143-21877	1790	06 22 09+	3	9-LM	
N	143-21878	1791	06 22 09+	3	9-LM	
N	143-21879	1792	06 22 09+	3	9-LM	
N	143-21880	1793	06 22 09+	3	9-LM	
N	143-21881	1794	06 22 09+	3	9-LM	
N	143-21882	1795	06 22 09+	3	9-LM	
N	143-21883	1796	06 22 09+	3	9-LM	
N	143-21884	1797	06 22 09+	3	9-LM	
N	143-21885	1798	06 22 09+	3	9-LM	
N	143-21886	1799	06 22 09+	3	9-LM	
N	143-21887	1800	06 22 09+	3	9-LM	
N	143-21888	1801	06 22 09+	3	9-LM	
N	143-21889	1802	06 22 09+	3	9-LM	
N	143-21890	1803	06 22 09+	3	9-LM	
N	143-21891	1804	06 22 09+	3	9-LM	

Table 7.--Chronological listing of 70mm Apollo 17 lunar surface pictures--Continued

MAG	PHOTO	SEQ	GET	EVA	STA	REMARKS
N	143-21892	1805	06 22 20	3	9-LM	SPL 70315,70320-24
N	143-21893	1806	06 22 20+	3	9-LM	SPL 70315,70320-24
N	143-21894	1807	06 22 20+	3	9-LM	SPL 70315,70320-24, STEREO OF 134-20455
B	134-20455	1808	06 22 20+	3	9-LM	SPL 70315,70320-24, STEREO OF 143-21894
M	143-21895	1809	06 22 20+	3	9-LM	
B	134-20456	1810	06 22 20+	3	9-LM	
N	143-21896	1811	06 22 20+	3	9-LM	
N	143-21897	1812	06 22 20+	3	9-LM	
N	143-21898	1813	06 22 20+	3	9-LM	
N	143-21899	1814	06 22 20+	3	9-LM	
N	143-21900	1815	06 22 20+	3	9-LM	
N	143-21901	1816	06 22 20+	3	9-LM	
N	143-21902	1817	06 22 20+	3	9-LM	
N	143-21903	1818	06 22 20+	3	9-LM	
N	143-21904	1819	06 22 20+	3	9-LM	
N	143-21905	1820	06 22 20+	3	9-LM	
N	143-21906	1821	06 22 20+	3	9-LM	
N	143-21907	1822	06 22 20+	3	9-LM	
N	143-21908	1823	06 22 20+	3	9-LM	
N	143-21909	1824	06 22 20+	3	9-LM	
N	143-21910	1825	06 22 20+	3	9-LM	
N	143-21911	1826	06 22 20+	3	9-LM	
N	143-21912	1827	06 22 20+	3	9-LM	
N	143-21913	1828	06 22 20+	3	9-LM	
N	143-21914	1829	06 22 20+	3	9-LM	
N	143-21915	1830	06 22 20+	3	9-LM	
N	143-21916	1831	06 22 20+	3	9-LM	
N	143-21917	1832	06 22 20+	3	9-LM	
N	143-21918	1833	06 22 20+	3	9-LM	
N	143-21919	1834	06 22 20+	3	9-LM	
N	143-21920	1835	06 22 20+	3	9-LM	
N	143-21921	1836	06 22 20+	3	9-LM	
N	143-21922	1837	06 22 20+	3	9-LM	
N	143-21923	1838	06 22 20+	3	9-LM	
N	143-21924	1839	06 22 32	3	9-LM	EP-2 LOC
B	134-20457	1840	06 22 32+	3	9-LM	LM
N	143-21925	1841	06 22 35	3	9-LM	SPL 70215
N	143-21926	1842	06 22 35+	3	9-LM	SPL 70215
B	134-20458	1843	06 22 35+	3	9-LM	LM
B	134-20459	1844	06 22 35+	3	9-LM	LM
B	134-20460	1845	06 22 35+	3	9-LM	LM
N	143-21927	1846	06 22 45	3	LM	SPL 70011 DSA
N	143-21928	1847	06 22 45+	3	LM	SPL 70011 DSA
N	143-21929	1848	06 22 45+	3	LM	SPL 70011 XSA
N	143-21930	1849	06 22 45+	3	LM	SPL 70011 XSA
B	134-20461	1850	06 22 58+	3	LM	LM, EARTH
B	134-20462	1851	06 22 58+	3	LM	LM, EARTH
B	134-20463	1852	06 22 58+	3	LM	LM, EARTH
B	134-20464	1853	06 22 58+	3	LM	LM, EARTH
B	134-20465	1854	06 22 58+	3	LM	FLAG
B	134-20466	1855	06 22 58+	3	LM	FLAG
B	134-20467	1856	06 22 58+	3	LM	FLAG
B	134-20468	1857	06 22 58+	3	LM	FLAG
B	134-20469	1858	06 22 58+	3	LM	LM
B	134-20470	1859	06 22 58+	3	LM	LM
B	134-20471	1860	06 22 58+	3	LM	LM, LRV
B	134-20472	1861	06 22 58+	3	LM	LM, LRV
B	134-20473	1862	06 22 59	3	LM	CDR, LRV
B	134-20474	1863	06 22 59+	3	LM	CDR, LRV
B	134-20475	1864	06 22 59+	3	LM	CDR, LRV
B	134-20476	1865	06 22 59+	3	LM	CDR, LRV
B	134-20477	1866	06 22 59+	3	LM	CDR, LRV
B	134-20478	1867	06 22 59+	3	LM	CDR, LRV
B	134-20479	1868	06 22 59+	3	LM	CDR, LRV
B	134-20480	1869	06 22 59+	3	LM	LM
B	134-20481	1870	06 22 59+	3	LM	LM
B	134-20482	1871	06 22 59+	3	LM	LM
B	134-20483	1872	06 22 59+	3	LM	LM
B	134-20484	1873	06 22 59+	3	LM	LM
B	134-20485	1874	06 22 59+	3	LM	LM
B	134-20486	1875	06 22 59+	3	LM	LM
B	134-20487	1876	06 22 59+	3	LM	LM
B	134-20488	1877	06 22 59+	3	LM	LM
B	134-20489	1878	06 23 29+	3	ALSEP	C/S
B	134-20490	1879	06 23 29+	3	ALSEP	C/S
B	134-20491	1880	06 23 29+	3	ALSEP	C/S
B	134-20492	1881	06 23 30	3	ALSEP	HEAT FLOW PROBE
B	134-20493	1882	06 23 30+	3	ALSEP	HEAT FLOW PROBE
B	134-20494	1883	06 23 30+	3	ALSEP	HEAT FLOW PROBE
B	134-20495	1884	06 23 30+	3	ALSEP	HEAT FLOW PROBE
B	134-20496	1885	06 23 30+	3	ALSEP	HEAT FLOW PROBE
B	134-20497	1886	06 23 30+	3	ALSEP	HEAT FLOW PROBE
B	134-20498	1887	06 23 32	3	ALSEP	LMS
B	134-20499	1888	06 23 32+	3	ALSEP	LMS
B	134-20500	1889	06 23 34	3	ALSEP	LEAM
B	134-20501	1890	06 23 34+	3	ALSEP	LSG
B	134-20502	1891	06 23 34+	3	ALSEP	LSG

Table 7.--Chronological listing of 70mm Apollo 17  
lunar surface pictures--Continued

MAG	PHOTO	SEQ	SET	EVA	STA	REMARKS
B	134-20503	1892	06 23 34+	3	ALSEP	LNPE, SPL 70175
B	134-20504	1893	06 23 34+	3	ALSEP	LNPE, SPL 70175
B	134-20505	1894	06 23 34+	3	ALSEP	LNPE, SPL 70175
N	143-21931	1895	06 23 39	3	RIP	LRV
N	143-21932	1896	06 23 39	3	RIP	LRV
N	143-21933	1897	06 23 39	3	RIP	LRV
N	143-21934	1898	06 23 39	3	RIP	LRV
B	134-20506	1899	06 23 49	3	LM	LM, FLAG
B	134-20507	1900	06 23 49	3	LM	LM, FLAG
B	134-20508	1901	06 23 49+	3	LM	LM, FLAG
B	134-20509	1902	06 23 49+	3	LM	LM, FLAG
B	134-20510	1903	06 23 49+	3	LM	LM, FLAG
B	134-20511	1904	06 23 49+	3	LM	LM, FLAG
B	134-20512	1905	06 23 49+	3	LM	LM, FLAG
B	134-20513	1906	06 23 49+	3	LM	LM, FLAG
N	143-21935	1907	06 23 49+	3	SEP	EP-3 LOC,70035
N	143-21936	1908	06 23 49+	3	SEP	EP-3 LOC,70035
N	143-21937	1909	06 23 49+	3	SEP	EP-3 LOC,70035
N	143-21938	1910	06 23 49+	3	LM	E OF LM
N	143-21939	1911	06 23 49+	3	LM	E OF LM
N	143-21940	1912	06 23 49+	3	LM	E OF LM
N	143-21941	1913	06 23 49+	3	LM	LMP, FLAG
N	143-21942	1914		POST	LM	BLANK
N	143-21943	1915		POST	LM	LM WINDOW PAN
N	143-21944	1916		POST	LM	LM WINDOW PAN
N	143-21945	1917		POST	LM	LM WINDOW PAN
N	143-21946	1918		POST	LM	LM WINDOW PAN
N	143-21947	1919		POST	LM	LM WINDOW PAN
N	143-21948	1920		POST	LM	LM WINDOW PAN
N	143-21949	1921		POST	LM	LM WINDOW PAN
N	143-21950	1922		POST	LM	LM WINDOW PAN
N	143-21951	1923		POST	LM	LM WINDOW PAN
N	143-21952	1924		POST	LM	LM WINDOW PAN
N	143-21953	1925		POST	LM	LM WINDOW PAN
N	143-21954	1926		POST	LM	LM WINDOW PAN
N	143-21955	1927		POST	LM	LM WINDOW PAN
N	143-21956	1928		POST	LM	LM WINDOW PAN
N	143-21957	1929		POST	LM	LM WINDOW PAN
N	143-21958	1930		POST	LM	LM WINDOW PAN
N	143-21959	1931		POST	LM	LM WINDOW PAN
N	143-21960	1932		POST	LM	LM WINDOW PAN
N	143-21961	1933		POST	LM	LM WINDOW PAN
N	143-21962	1934		POST	LM	LM WINDOW PAN
N	143-21963	1935		POST	LM	LM WINDOW PAN
N	143-21964	1936		POST	LM	LM WINDOW PAN
N	143-21965	1937		POST	LM	LM WINDOW PAN
N	143-21966	1938		POST	LM	LM WINDOW PAN
N	143-21967	1939		POST	LM	LM WINDOW PAN
N	143-21968	1940		POST	LM	LM WINDOW PAN
N	143-21969	1941		POST	LM	LM WINDOW PAN
N	143-21970	1942		POST	LM	LM WINDOW PAN
N	143-21971	1943		POST	LM	LM WINDOW PAN
N	143-21972	1944		POST	LM	LM WINDOW PAN
N	143-21973	1945		POST	LM	LM WINDOW PAN
N	143-21974	1946		POST	LM	LM WINDOW PAN
N	143-21975	1947		POST	LM	LM WINDOW PAN
N	143-21976	1948		POST	LM	LM WINDOW PAN
N	143-21977	1949		POST	LM	LM WINDOW PAN
N	143-21978	1950		POST	LM	LM WINDOW PAN
N	143-21979	1951		POST	LM	LM WINDOW PAN
N	143-21980	1952		POST	LM	LM WINDOW PAN
N	143-21981	1953		POST	LM	LM WINDOW PAN
N	143-21982	1954		POST	LM	LM WINDOW PAN
D	145-22192	1955		POST	LM	LM WINDOW PAN, FOGGED
D	145-22193	1956		POST	LM	LM WINDOW PAN
D	145-22194	1957		POST	LM	LM WINDOW PAN
D	145-22195	1958		POST	LM	LM WINDOW PAN
D	145-22196	1959		POST	LM	LM WINDOW PAN
D	145-22197	1960		POST	LM	LM WINDOW PAN
D	145-22198	1961		POST	LM	LM WINDOW PAN
D	145-22199	1962		POST	LM	LM WINDOW PAN
D	145-22200	1963		POST	LM	LM WINDOW PAN
D	145-22201	1964		POST	LM	LM WINDOW PAN
D	145-22202	1965		POST	LM	LM WINDOW PAN
D	145-22203	1966		POST	LM	LM WINDOW PAN
D	145-22204	1967		POST	LM	LM WINDOW PAN
D	145-22205	1968		POST	LM	LM WINDOW PAN
D	145-22206	1969		POST	LM	LM WINDOW PAN
D	145-22207	1970		POST	LM	LM WINDOW PAN
D	145-22208	1971		POST	LM	LM WINDOW PAN
D	145-22209	1972		POST	LM	LM WINDOW PAN
D	145-22210	1973		POST	LM	LM WINDOW PAN
D	145-22211	1974		POST	LM	LM WINDOW PAN
D	145-22212	1975		POST	LM	LM WINDOW PAN
D	145-22213	1976		POST	LM	LM WINDOW PAN
D	145-22214	1977		POST	LM	LM WINDOW PAN
D	145-22215	1978		POST	LM	LM WINDOW PAN
D	145-22216	1979		POST	LM	LM WINDOW PAN
D	145-22217	1980		POST	LM	LM WINDOW PAN
D	145-22218	1981		POST	LM	LM WINDOW PAN
D	145-22219	1982		POST	LM	LM WINDOW PAN
D	145-22220	1983		POST	LM	LM WINDOW PAN
D	145-22221	1984		POST	LM	LM WINDOW PAN
D	145-22222	1985		POST	LM	LM WINDOW PAN

Table 8.--*Sequential listing within each 70 mm magazine, Apollo 17 lunar surface pictures (magazine J, black and white, 60 mm focal length)*

MAG	PHOTO	SEQ	GET	EVA	STA	REMARKS
J 133-20194	814	05	22	26	2	3-4
J 133-20195	815	05	22	26+	2	3-4
J 133-20196	816	05	22	26+	2	3-4
J 133-20197	817	05	22	26+	2	3-4
J 133-20198	818	05	22	26+	2	3-4
J 133-20199	819	05	22	26+	2	3-4
J 133-20200	820	05	22	26+	2	3-4
J 133-20201	821	05	22	26+	2	3-4
J 133-20202	822	05	22	26+	2	3-4
J 133-20203	823	05	22	26+	2	3-4
J 133-20204	824	05	22	26+	2	3-4
J 133-20205	825	05	22	26+	2	3-4
J 133-20206	826	05	22	26+	2	3-4
J 133-20207	827	05	22	26+	2	3-4
J 133-20208	828	05	22	31	2	3-4
J 133-20209	830	05	22	31+	2	3-4
J 133-20210	831	05	22	31+	2	3-4
J 133-20211	832	05	22	31+	2	3-4
J 133-20212	833	05	22	31+	2	3-4
J 133-20213	834	05	22	31+	2	3-4
J 133-20214	835	05	22	31+	2	3-4
J 133-20215	836	05	22	31+	2	3-4
J 133-20216	837	05	22	31+	2	3-4
J 133-20217	838	05	22	31+	2	3-4
J 133-20218	839	05	22	31+	2	3-4
J 133-20219	840	05	22	31+	2	3-4
J 133-20220	841	05	22	31+	2	3-4
J 133-20221	842	05	22	31+	2	3-4
J 133-20222	843	05	22	31+	2	3-4
J 133-20223	844	05	22	31+	2	3-4
J 133-20224	845	05	22	31+	2	3-4
J 133-20225	846	05	22	31+	2	3-4
J 133-20226	847	05	22	31+	2	3-4
J 133-20227	848	05	22	31+	2	3-4
J 133-20228	849	05	22	31+	2	3-4
J 133-20229	850	05	22	46	2	4 PAN
J 133-20230	851	05	22	46+	2	4 PAN
J 133-20231	852	05	22	46+	2	4 PAN
J 133-20232	853	05	22	46+	2	4 PAN
J 133-20233	854	05	22	46+	2	4 PAN
J 133-20234	855	05	22	46+	2	4 PAN
J 133-20235	856	05	22	46+	2	4 PAN
J 133-20236	857	05	22	46+	2	4 PAN
J 133-20237	858	05	22	46+	2	4 PAN
J 133-20238	859	05	22	46+	2	4 PAN
J 133-20239	860	05	22	46+	2	4 PAN
J 133-20240	861	05	22	46+	2	4 PAN
J 133-20241	862	05	22	46+	2	4 PAN
J 133-20242	863	05	22	46+	2	4 PAN
J 133-20243	864	05	22	46+	2	4 PAN
J 133-20244	865	05	22	46+	2	4 PAN
J 133-20245	866	05	22	46+	2	4 PAN
J 133-20246	867	05	22	46+	2	4 PAN
J 133-20247	868	05	22	46+	2	4 PAN
J 133-20248	869	05	22	46+	2	4 PAN
J 133-20249	870	05	22	46+	2	4 PAN
J 133-20250	871	05	22	46+	2	4 PAN
J 133-20251	872	05	22	46+	2	4 PAN
J 133-20252	873	05	22	46+	2	4 PAN
J 133-20253	874	05	22	46+	2	4 PAN
J 133-20254	875	05	22	46+	2	4 PAN
J 133-20255	876	05	22	46+	2	4 PAN
J 133-20256	877	05	22	46+	2	4 PAN
J 133-20257	885	05	22	59	2	4 BLANK
J 133-20258	886	05	22	59+	2	4 BLANK
J 133-20259	887	05	22	59+	2	4 BLANK
J 133-20260	888	05	22	59+	2	4 BLANK
J 133-20261	889	05	22	59+	2	4 BLANK
J 133-20262	890	05	22	59+	2	4 BLANK
J 133-20263	891	05	22	59+	2	4 BLANK
J 133-20264	892	05	22	59+	2	4 BLANK
J 133-20265	893	05	22	59+	2	4 BLANK
J 133-20266	894	05	22	59+	2	4 BLANK
J 133-20267	895	05	22	59+	2	4 BLANK
J 133-20268	896	05	22	59+	2	4 BLANK
J 133-20269	934	05	23	16	2	4-5
J 133-20270	935	05	23	16+	2	4-5
J 133-20271	936	05	23	16+	2	4-5
J 133-20272	937	05	23	16+	2	4-5
J 133-20273	938	05	23	16+	2	4-5
J 133-20274	939	05	23	16+	2	4-5
J 133-20275	940	05	23	16+	2	4-5
J 133-20276	941	05	23	16+	2	4-5
J 133-20277	942	05	23	16+	2	4-5
J 133-20278	943	05	23	16+	2	4-5
J 133-20279	944	05	23	16+	2	4-5
J 133-20280	945	05	23	27	2	4-5
J 133-20281	946	05	23	27+	2	4-5
J 133-20282	947	05	23	27+	2	4-5
J 133-20283	948	05	23	27+	2	4-5

SPL 74110-14,15-19, STEREO OF 137-20983

SPL 75110-14,15, EP-1  
LRV PAN AT VICTORY  
LRV PAN AT VICTORY  
LRV PAN AT VICTORY

Table 8.--*Sequential listing within each 70 mm magazine, Apollo 17 lunar surface pictures (magazine J, black and white, 60 mm focal length)--Continued*

MAG	PHOTO	SEQ	GET	EVA	STA	REMARKS
J 133-20284		949	05 23 27+	2	4-5	LRV PAN AT VICTORY
J 133-20285		950	05 23 27+	2	4-5	LRV PAN AT VICTORY
J 133-20286		951	05 23 27+	2	4-5	LRV PAN AT VICTORY
J 133-20287		952	05 23 27+	2	4-5	LRV PAN AT VICTORY
J 133-20288		953	05 23 27+	2	4-5	LRV PAN AT VICTORY
J 133-20289		954	05 23 27+	2	4-5	LRV PAN AT VICTORY
J 133-20290		955	05 23 27+	2	4-5	LRV PAN AT VICTORY
J 133-20291		956	05 23 27+	2	4-5	LRV PAN AT VICTORY
J 133-20292		957	05 23 27+	2	4-5	LRV PAN AT VICTORY
J 133-20293		958	05 23 27+	2	4-5	LRV PAN AT VICTORY
J 133-20294		959	05 23 27+	2	4-5	LRV PAN AT VICTORY
J 133-20295		960	05 23 27+	2	4-5	LRV PAN AT VICTORY
J 133-20296		961	05 23 27+	2	4-5	LRV PAN AT VICTORY
J 133-20297		962	05 23 27+	2	4-5	LRV PAN AT VICTORY
J 133-20298		963	05 23 27+	2	4-5	LRV PAN AT VICTORY
J 133-20299		964	05 23 27+	2	4-5	LRV PAN AT VICTORY
J 133-20300		965	05 23 27+	2	4-5	LRV PAN AT VICTORY
J 133-20301		966	05 23 27+	2	4-5	
J 133-20302		967	05 23 27+	2	4-5	
J 133-20303		968	05 23 27+	2	4-5	
J 133-20304		969	05 23 27+	2	4-5	
J 133-20305		970	05 23 27+	2	4-5	
J 133-20306		971	05 23 27+	2	4-5	
J 133-20307		972	05 23 27+	2	4-5	
J 133-20308		973	05 23 27+	2	4-5	
J 133-20309		974	05 23 27+	2	4-5	
J 133-20310		975	05 23 27+	2	4-5	
J 133-20311		976	05 23 27+	2	4-5	
J 133-20312		977	05 23 27+	2	4-5	
J 133-20313		978	05 23 27+	2	4-5	
J 133-20314		979	05 23 27+	2	4-5	
J 133-20315		980	05 23 27+	2	4-5	
J 133-20316		981	05 23 36	2	4-5	SPL 75120-24
J 133-20317		982	05 23 36+	2	4-5	SPL 75120-24
J 133-20318		983	05 23 36+	2	4-5	
J 133-20319		984	05 23 36+	2	4-5	
J 133-20320		985	05 23 36+	2	4-5	
J 133-20321		986	05 23 36+	2	4-5	
J 133-20322		987	05 23 36+	2	4-5	
J 133-20323		988	05 23 36+	2	4-5	
J 133-20324		989	05 23 36+	2	4-5	
J 133-20325		990	05 23 36+	2	4-5	
J 133-20326		991	05 23 36+	2	4-5	
J 133-20327		992	05 23 36+	2	4-5	
J 133-20328		996	05 23 56	2	5	SPL 75015,75035 DS
J 133-20329		997	05 23 56+	2	5	SPL 75015,75035 LOC
J 133-20330		1003	06 00 00	2	5	SPL 75055 F-L
J 133-20331		1004	06 00 00+	2	5	SPL 75055 F-L
J 133-20332		1005	06 00 00+	2	5	SPL 75055 F-L
J 133-20333		1006	06 00 00+	2	5	SPL 75055 F-L
J 133-20334		1007	06 00 00+	2	5	SPL 75055 F-L
J 133-20335		1008	06 00 00+	2	5	SPL 75055 DS
J 133-20336		1009	06 00 00+	2	5	SPL 75055 LOC
J 133-20337		1023	06 00 06	2	5	SPL 75060-64,65-66,75075 DS
J 133-20338		1024	06 00 06+	2	5	SPL 75060-64,65-66,75075 LOC
J 133-20339		1055	06 00 10	2	5	PAN
J 133-20340		1056	06 00 10+	2	5	PAN
J 133-20341		1057	06 00 10+	2	5	PAN
J 133-20342		1058	06 00 10+	2	5	PAN
J 133-20343		1059	06 00 10+	2	5	PAN
J 133-20344		1060	06 00 10+	2	5	PAN
J 133-20345		1061	06 00 10+	2	5	PAN
J 133-20346		1062	06 00 10+	2	5	PAN
J 133-20347		1063	06 00 10+	2	5	PAN
J 133-20348		1064	06 00 10+	2	5	PAN
J 133-20349		1065	06 00 10+	2	5	PAN
J 133-20350		1066	06 00 10+	2	5	PAN
J 133-20351		1067	06 00 10+	2	5	PAN
J 133-20352		1068	06 00 10+	2	5	PAN
J 133-20353		1069	06 00 10+	2	5	PAN
J 133-20354		1070	06 00 10+	2	5	PAN
J 133-20355		1071	06 00 10+	2	5	PAN
J 133-20356		1072	06 00 10+	2	5	PAN
J 133-20357		1073	06 00 10+	2	5	PAN
J 133-20358		1074	06 00 10+	2	5	PAN
J 133-20359		1075	06 00 10+	2	5	PAN
J 133-20360		1076	06 00 10+	2	5	PAN
J 133-20361		1077	06 00 10+	2	5	PAN
J 133-20362		1078	06 00 15	2	5-LM	
J 133-20363		1079	06 00 15+	2	5-LM	
J 133-20364		1080	06 00 15+	2	5-LM	
J 133-20365		1081	06 00 15+	2	5-LM	
J 133-20366		1082	06 00 15+	2	5-LM	
J 133-20367		1083	06 00 15+	2	5-LM	
J 133-20368		1084	06 00 15+	2	5-LM	
J 133-20369		1085	06 00 15+	2	5-LM	
J 133-20370		1086	06 00 15+	2	5-LM	
J 133-20371		1087	06 00 15+	2	5-LM	
J 133-20372		1088	06 00 15+	2	5-LM	
J 133-20373		1089	06 00 15+	2	5-LM	
J 133-20374		1090	06 00 15+	2	5-LM	
J 133-20375		1091	06 00 15+	2	5-LM	

Table 8.--Sequential listing within each 70 mm magazine, Apollo 17 lunar surface pictures (magazine J, black and white, 60 mm focal length)--Continued

MAG	PHOTO	SEQ	GET	EVA	STA	REMARKS
B 134-20376	60	04 19 35+	1	LM	MISC	
B 134-20377	61	04 19 42	1	LM	LM, FLAG	
B 134-20378	62	04 19 42+	1	LM	LM, FLAG	
B 134-20379	63	04 19 42+	1	LM	LM, FLAG	
B 134-20380	64	04 19 42+	1	LM	LM, FLAG	
B 134-20381	65	04 19 42+	1	LM	LM, FLAG	
B 134-20382	66	04 19 42+	1	LM	LM, FLAG	
B 134-20383	67	04 19 43	1	LM	FLAG	
B 134-20384	68	04 19 43+	1	LM	FLAG	
B 134-20385	69	04 19 43+	1	LM	FLAG	
B 134-20386	70	04 19 43+	1	LM	FLAG	
B 134-20387	71	04 19 44	1	LM	FLAG	
B 134-20388	72	04 19 50	1	LM	FOOTPAD	
B 134-20389	73	04 19 50+	1	LM	LRV	
B 134-20390	199	04 23 11+	1	SEP-1		
B 134-20391	201	04 23 11+	1	SEP-1		
B 134-20392	202	04 23 11+	1	SEP-1		
B 134-20393	212	04 23 11+	1	SEP-1		
B 134-20394	216	04 23 32+	1	1	SPL 71710, 35-37, 71040-44, 45-49, 71055, 71060-54, 65-69, 85-89, 95-97 XSB	
B 134-20395	217	04 23 32+	1	1	SPL 71710, 35-37, 71040-44, 45-49, 71055, 71060-54, 65-69, 85-89, 95-97 XSB	
B 134-20396	218	04 23 32+	1	1	SPL 71710, 35-37, 71040-44, 45-49, 71055, 71060-54, 65-69, 85-89, 95-97 XSA	
B 134-20397	220	04 23 42+	1	1	SPL 71130, 35-36, 71150, 55-57, 71175 XSB	
B 134-20398	221	04 23 42+	1	1	SPL 71130, 35-36, 71150, 55-57, 71175 XSB	
B 134-20399	222	04 23 43	1	1	SPL 71130, 43-36, 71150, 55-57, 71175 XSA	
B 134-20400	223	04 23 43+	1	1	SPL 71130, 35-36, 71150, 55-57, 71175 LOC	
B 134-20401	224	04 23 43+	1	1	SPL 71130, 35-36, 71150, 55-57, 71175 CU	
B 134-20402	225	04 23 43+	1	1	SPL 71130, 35-36, 71150, 55-57, 71175 CU	
B 134-20403	226	04 23 43+	1	1	SPL 71130, 35-36, 71150, 55-57, 71175 CU	
B 134-20404	227	04 23 43+	1	1	SPL 71130, 35-36, 71150, 55-57, 71175 CU	
B 134-20405	230	04 23 43+	1	1	SPL 71500-04, 05-09, 15, 71525-29, 35-39, 45-49, 55-59, 65-69, 75-79, 85-89, 95-97 XSB	
B 134-20406	231	04 23 43+	1	1	SPL 71500-04, 05-09, 15, 71525-29, 35-39, 45-49, 55-59, 65-69, 75-79, 85-89, 95-97 XSB	
B 134-20407	232	04 23 43+	1	1	SPL 71500-04, 05-09, 15, 71525-29, 35-39, 45-49, 55-59, 65-69, 75-79, 85-89, 95-97 XSB	
B 134-20408	233	04 23 43	1	1	PAN	
B 134-20409	234	04 23 46+	1	1	PAN	
B 134-20410	235	04 23 46+	1	1	PAN	
B 134-20411	236	04 23 46+	1	1	PAN	
B 134-20412	237	04 23 46+	1	1	PAN	
B 134-20413	238	04 23 46+	1	1	PAN	
B 134-20414	239	04 23 46+	1	1	PAN	
B 134-20415	240	04 23 46+	1	1	PAN	
B 134-20416	241	04 23 46+	1	1	PAN	
B 134-20417	242	04 23 46+	1	1	PAN	
B 134-20418	243	04 23 46+	1	1	PAN	
B 134-20419	244	04 23 46+	1	1	PAN	
B 134-20420	245	04 23 46+	1	1	PAN	
B 134-20421	246	04 23 46+	1	1	PAN	
B 134-20422	247	04 23 46+	1	1	PAN, EP-6 LOC	
B 134-20423	248	04 23 46+	1	1	PAN, EP-6 LOC	
B 134-20424	249	04 23 46+	1	1	PAN, EP-6 LOC	
B 134-20425	250	04 23 46+	1	1	PAN, SPL 71500-04, 05-09, 15, 71525-29, 35-39, 45-49, 55-59, 65-69, 75-79, 85-89, 95-97 LOC	
B 134-20426	251	04 23 46+	1	1	PAN, SPL 71500-04, 05-09, 15, 71525-29, 35-39, 45-49, 55-59, 65-69, 75-79, 85-89, 95-97 LOC	
B 134-20427	252	04 23 46+	1	1	PAN, SPL 71500-04, 05-09, 15, 71525-29, 35-39, 45-49, 55-59, 65-69, 75-79, 85-89, 95-97 LOC	
B 134-20428	253	04 23 46+	1	1	PAN	
B 134-20429	254	04 23 46+	1	1	PAN	
B 134-20430	255	04 23 46+	1	1	PAN	
B 134-20431	256	04 23 46+	1	1	PAN	
B 134-20432	257	04 23 46+	1	1	SPL 71500-04, 05-09, 15, 71525-29, 35-39, 45-49, 55-59, 65-69, 75-79, 85-89, 95-97 XSA	
B 134-20433	330	04 23 58+	1	1-SEP	EP-7 LOC	
B 134-20434	331	04 23 58+	1	1-SEP	EP-7 LOC	
B 134-20435	380	05 00 23	1	SEP	SEP ANTENNA DEPLOYMENT	
B 134-20436	381	05 00 23+	1	SEP	SEP ANTENNA DEPLOYMENT	
B 134-20437	382	05 00 26	1	SEP	PPAN	
B 134-20438	383	05 00 26+	1	SEP	PPAN	
B 134-20439	384	05 00 26+	1	SEP	PPAN	
B 134-20440	385	05 00 26+	1	SEP	PPAN	
B 134-20441	386	05 00 26+	1	SEP	PPAN	
B 134-20442	387	05 00 26+	1	SEP	PPAN	
B 134-20443	388	05 00 26+	1	SEP	PPAN	
B 134-20444	389	05 00 26+	1	SEP	PPAN	
B 134-20445	390	05 00 26+	1	SEP	PPAN	
B 134-20446	391	05 00 26+	1	SEP	PPAN	
B 134-20447	392	05 00 11	1	SEP-LM		
B 134-20448	393	05 00 11+	1	SEP-LM		
B 134-20449	394	05 00 11+	1	SEP-LM	BLANK	
B 134-20450	395	05 00 11+	1	SEP-LM	BLANK	
B 134-20451	396	05 00 11+	1	SEP-LM	BLANK	
B 134-20452	1769	06 22 01+	3	9	LRV, FOGGED	
B 134-20453	1770	06 22 01+	3	9	LRV, FOGGED	
B 134-20454	1771	06 22 01+	3	9	LRV, FOGGED	
B 134-20455	1808	06 22 20+	3	9-LM	SPL 70315, 70320-24, STEREO OF 143-21894	
B 134-20456	1810	06 22 20+	3	9-LM		
B 134-20457	1840	06 22 32+	3	9-LM	LM	
B 134-20458	1843	06 22 35+	3	9-LM	LM	
B 134-20459	1844	06 22 35+	3	9-LM	LM	
B 134-20460	1845	06 22 35+	3	9-LM	LM	
B 134-20461	1850	06 22 58+	3	LM	LM, EARTH	
B 134-20462	1851	06 22 58+	3	LM	LM, EARTH	
B 134-20463	1852	06 22 58+	3	LM	LM, EARTH	
B 134-20464	1853	06 22 58+	3	LM	LM, EARTH	
B 134-20465	1854	06 22 58+	3	LM	FLAG	
B 134-20466	1855	06 22 58+	3	LM	FLAG	
B 134-20467	1856	06 22 58+	3	LM	FLAG	
B 134-20468	1857	06 22 58+	3	LM	FLAG	
B 134-20469	1858	06 22 58+	3	LM	LM	
B 134-20470	1859	06 22 58+	3	LM	LM	
B 134-20471	1860	06 22 58+	3	LM	LMP, LRV	
B 134-20472	1861	06 22 58+	3	LM	LMP, LRV	
B 134-20473	1862	06 22 59	3	LM	CDR, LRV	

Table 8.--Sequential listing within each 70 mm magazine, Apollo 17 lunar surface pictures (magazine J, black and white, 60 mm focal length)--Continued

MAG	PHOTO	SEQ	GET	EVA	STA	REMARKS
B 134-20474	1863	06 22 59+	3	LM	CDR, LRV	
B 134-20475	1864	06 22 59+	3	LM	CDR, LRV	
B 134-20476	1865	06 22 59+	3	LM	CDR, LRV	
B 134-20477	1866	06 22 59+	3	LM	CDR, LRV	
B 134-20478	1867	06 22 59+	3	LM	CDR, LRV	
B 134-20479	1868	06 22 59+	3	LM	CDR, LRV	
B 134-20480	1869	06 22 59+	3	LM	LM	
B 134-20481	1870	06 22 59+	3	LM	LM	
B 134-20482	1871	06 22 59+	3	LM	LM	
B 134-20483	1872	06 22 59+	3	LM	LM	
B 134-20484	1873	06 22 59+	3	LM	LM	
B 134-20485	1874	06 22 59+	3	LM	LM	
B 134-20486	1875	06 22 59+	3	LM	LM	
B 134-20487	1876	06 22 59+	3	LM	LM	
B 134-20488	1877	06 22 59+	3	LM	LM	
B 134-20489	1878	06 23 29+	3	ALSEP	C/S	
B 134-20490	1879	06 23 29+	3	ALSEP	C/S	
B 134-20491	1880	06 23 29+	3	ALSEP	C/S	
B 134-20492	1881	06 23 30	3	ALSEP	HEAT FLOW PROBE	
B 134-20493	1882	06 23 30+	3	ALSEP	HEAT FLOW PROBE	
B 134-20494	1883	06 23 30+	3	ALSEP	HEAT FLOW PROBE	
B 134-20495	1884	06 23 30+	3	ALSEP	HEAT FLOW PROBE	
B 134-20496	1885	06 23 30+	3	ALSEP	HEAT FLOW PROBE	
B 134-20497	1886	06 23 30+	3	ALSEP	HEAT FLOW PROBE	
B 134-20498	1887	06 23 32	3	ALSEP	LMS	
B 134-20499	1888	06 23 32+	3	ALSEP	LMS	
B 134-20500	1889	06 23 34	3	ALSEP	LEAM	
B 134-20501	1890	06 23 34+	3	ALSEP	LSG	
B 134-20502	1891	06 23 34+	3	ALSEP	LSG	
B 134-20503	1892	06 23 34+	3	ALSEP	LNPE, SPL 70175	
B 134-20504	1893	06 23 34+	3	ALSEP	LNPE, SPL 70175	
B 134-20505	1894	06 23 34+	3	ALSEP	LNPE, SPL 70175	
B 134-20506	1899	06 23 49	3	LM	LM, FLAG	
B 134-20507	1900	06 23 49	3	LM	LM, FLAG	
B 134-20508	1901	06 23 49+	3	LM	LM, FLAG	
B 134-20509	1902	06 23 49+	3	LM	LM, FLAG	
B 134-20510	1903	06 23 49+	3	LM	LM, FLAG	
B 134-20511	1904	06 23 49+	3	LM	LM, FLAG	
B 134-20512	1905	06 23 49+	3	LM	LM, FLAG	
B 134-20513	1906	06 23 49+	3	LM	LM, FLAG	

Table 8.--*Sequential listing within each 70 mm magazine, Apollo 17 lunar surface pictures (magazine J, black and white, 60 mm focal length)--Continued*

MAG	PHOTO	SEQ	GET	EVA	STA	REMARKS
G 135-20533	426	05 18 41	2	SEP	SPL 70255 XS	
G 135-20534	427	05 18 41+	2	SEP	SPL 70255 XS	
G 135-20535	428	05 18 41+	2	SEP	SPL 70255 XS	
G 135-20536	429	05 18 41+	2	SEP	SPL 70255 XS	
G 135-20537	430	05 18 41+	2	SEP	SPL 70255 XS	
G 135-20538	431	05 18 41+	2	SEP	SPL 70255 LOC	
G 135-20539	432	05 18 48	2	SEP	SPL 70270-74,75 XSB	
G 135-20540	433	05 18 48	2	SEP	SPL 70270-74,75 XSB	
G 135-20541	434	05 18 48	2	SEP	SPL 70270-74,75 LOC	
G 135-20542	435	05 18 48+	2	SEP	LRV	
G 135-20543	436	05 18 48+	2	SEP	LRV	
G 135-20544	437	05 18 48+	2	SEP	LRV	
G 135-20545	438	05 18 48+	2	SEP	LRV	
G 135-20546	439	05 18 48+	2	SEP	LRV	
G 135-20547	440	05 18 48+	2	SEP	LRV	
G 135-20548	441	05 18 48+	2	SEP	LRV	
G 135-20549	442	05 18 48+	2	SEP	LRV	
G 135-20550	443	05 18 51	2	SEP-2		
G 135-20551	444	05 18 51+	2	SEP-2		
G 135-20552	445	05 18 51+	2	SEP-2		
G 135-20553	446	05 18 51+	2	SEP-2		
G 135-20554	447	05 18 51+	2	SEP-2		
G 135-20555	448	05 18 51+	2	SEP-2		
G 135-20556	449	05 18 51+	2	SEP-2		
G 135-20557	450	05 18 51+	2	SEP-2		
G 135-20558	451	05 18 51+	2	SEP-2		
G 135-20559	452	05 18 51+	2	SEP-2		
G 135-20560	453	05 18 51+	2	SEP-2		
G 135-20561	454	05 18 51+	2	SEP-2		
G 135-20562	455	05 18 51+	2	SEP-2		
G 135-20563	456	05 18 55	2	SEP-2	LRV PPAN, EP-4	
G 135-20564	457	05 18 55+	2	SEP-2	LRV PPAN, EP-4	
G 135-20565	458	05 18 55+	2	SEP-2	LRV PPAN, EP-4	
G 135-20566	459	05 18 55+	2	SEP-2	LRV PPAN, EP-4	
G 135-20567	460	05 18 55+	2	SEP-2	LRV PPAN, EP-4	
G 135-20568	461	05 18 55+	2	SEP-2	LRV PPAN, EP-4	
G 135-20569	462	05 18 55+	2	SEP-2	LRV PPAN, EP-4	
G 135-20570	463	05 18 55+	2	SEP-2		
G 135-20571	464	05 18 55+	2	SEP-2		
G 135-20572	465	05 18 55+	2	SEP-2		
G 135-20573	466	05 18 55+	2	SEP-2		
G 135-20574	467	05 18 55+	2	SEP-2		
G 135-20575	468	05 18 55+	2	SEP-2		
G 135-20576	469	05 18 55+	2	SEP-2		
G 135-20577	470	05 18 55+	2	SEP-2		
G 135-20578	471	05 18 55+	2	SEP-2		
G 135-20579	472	05 18 55+	2	SEP-2		
G 135-20580	473	05 18 55+	2	SEP-2		
G 135-20581	474	05 18 55+	2	SEP-2		
G 135-20582	475	05 18 55+	2	SEP-2		
G 135-20583	476	05 18 55+	2	SEP-2		
G 135-20584	477	05 18 55+	2	SEP-2		
G 135-20585	478	05 18 55+	2	SEP-2		
G 135-20586	479	05 18 55+	2	SEP-2		
G 135-20587	480	05 18 55+	2	SEP-2		
G 135-20588	481	05 18 55+	2	SEP-2		
G 135-20589	482	05 18 55+	2	SEP-2		
G 135-20590	483	05 18 55+	2	SEP-2		
G 135-20591	484	05 18 55+	2	SEP-2		
G 135-20592	485	05 18 55+	2	SEP-2		
G 135-20593	486	05 18 55+	2	SEP-2		
G 135-20594	487	05 18 55+	2	SEP-2		
G 135-20595	488	05 18 55+	2	SEP-2		
G 135-20596	489	05 18 55+	2	SEP-2		
G 135-20597	490	05 18 55+	2	SEP-2		
G 135-20598	491	05 18 55+	2	SEP-2		
G 135-20599	492	05 18 55+	2	SEP-2		
G 135-20600	493	05 18 55+	2	SEP-2		
G 135-20601	494	05 18 55+	2	SEP-2		
G 135-20602	495	05 18 55+	2	SEP-2		
G 135-20603	496	05 18 55+	2	SEP-2		
G 135-20604	497	05 18 55+	2	SEP-2		
G 135-20605	498	05 18 55+	2	SEP-2		
G 135-20606	499	05 18 55+	2	SEP-2		
G 135-20607	500	05 18 55+	2	SEP-2		
G 135-20608	501	05 18 55+	2	SEP-2		
G 135-20609	502	05 18 55+	2	SEP-2		
G 135-20610	503	05 18 55+	2	SEP-2		
G 135-20611	504	05 18 55+	2	SEP-2		
G 135-20612	505	05 18 55+	2	SEP-2		
G 135-20613	506	05 18 55+	2	SEP-2		
G 135-20614	507	05 18 55+	2	SEP-2		
G 135-20615	508	05 18 55+	2	SEP-2		

Table 8.--*Sequential listing within each 70 mm magazine, Apollo 17 lunar surface pictures (magazine J, black and white, 60 mm focal length)--Continued*

MAG	PHOTO	SEQ	GET	EVA	STA	REMARKS
G 135-20616		509	05 18 55+	2	SEP-2	
G 135-20617		510	05 18 55+	2	SEP-2	
G 135-20618		511	05 18 55+	2	SEP-2	
G 135-20619		512	05 18 55+	2	SEP-2	
G 135-20620		513	05 18 55+	2	SEP-2	
G 135-20621		514	05 18 55+	2	SEP-2	
G 135-20622		515	05 18 55+	2	SEP-2	
G 135-20623		516	05 19 14	2	SEP-2	SPL 72130-34,35
G 135-20624		517	05 19 14+	2	SEP-2	SPL 72130-34,35
G 135-20625		518	05 19 14+	2	SEP-2	SPL 72130-34,35
G 135-20626		519	05 19 14+	2	SEP-2	SPL 72130-34,35
G 135-20627		520	05 19 14+	2	SEP-2	SPL 72130-34,35
G 135-20628		522	05 19 14+	2	SEP-2	SPL 72130-34,35, STEREO OF 137-20893
G 135-20629		523	05 19 14+	2	SEP-2	
G 135-20630		524	05 19 14+	2	SEP-2	
G 135-20631		525	05 19 14+	2	SEP-2	
G 135-20632		526	05 19 14+	2	SEP-2	
G 135-20633		527	05 19 14+	2	SEP-2	
G 135-20634		528	05 19 14+	2	SEP-2	
G 135-20635		529	05 19 14+	2	SEP-2	
G 135-20636		530	05 19 14+	2	SEP-2	
G 135-20637		531	05 19 14+	2	SEP-2	
G 135-20638		532	05 19 14+	2	SEP-2	
G 135-20639		533	05 19 14+	2	SEP-2	
G 135-20640		534	05 19 14+	2	SEP-2	
G 135-20641		535	05 19 14+	2	SEP-2	SPL 72140-44,45
G 135-20642		536	05 19 24	2	SEP-2	SPL 72140-44,45
G 135-20643		538	05 19 24+	2	SEP-2	SPL 72140-44,45, STEREO OF 137-20896
G 135-20644		539	05 19 24+	2	SEP-2	
G 135-20645		540	05 19 24+	2	SEP-2	
G 135-20646		541	05 19 24+	2	SEP-2	
G 135-20647		542	05 19 24+	2	SEP-2	
G 135-20648		543	05 19 24+	2	SEP-2	
G 135-20649		545	05 19 30+	2	SEP-2	SPL 72155,72160-64, STEREO OF 137-20897
G 135-20650		547	05 19 30+	2	SEP-2	
G 135-20651		548	05 19 30+	2	SEP-2	
G 135-20652		549	05 19 30+	2	SEP-2	
G 135-20653		550	05 19 30+	2	SEP-2	
G 135-20654		552	05 19 30+	2	SEP-2	
G 135-20655		553	05 19 30+	2	SEP-2	
G 135-20656		554	05 19 30+	2	SEP-2	
G 135-20657		555	05 19 30+	2	SEP-2	
G 135-20658		556	05 19 30+	2	SEP-2	
G 135-20659		557	05 19 30+	2	SEP-2	
G 135-20660		558	05 19 30+	2	SEP-2	
G 135-20661		559	05 19 30+	2	SEP-2	
G 135-20662		560	05 19 30+	2	SEP-2	
G 135-20663		561	05 19 30+	2	SEP-2	
G 135-20664		562	05 19 30+	2	SEP-2	
G 135-20665		563	05 19 30+	2	SEP-2	
G 135-20666		564	05 19 30+	2	SEP-2	
G 135-20667		565	05 19 30+	2	SEP-2	
G 135-20668		566	05 19 30+	2	SEP-2	
G 135-20669		567	05 19 30+	2	SEP-2	
G 135-20670		568	05 19 30+	2	SEP-2	
G 135-20671		569	05 19 30+	2	SEP-2	
G 135-20672		570	05 19 30+	2	SEP-2	
G 135-20673		571	05 19 30+	2	SEP-2	
G 135-20674		572	05 19 30+	2	SEP-2	
G 135-20675		573	05 19 30+	2	SEP-2	
G 135-20676		574	05 19 30+	2		MISC
G 135-20677		575	05 19 30+	2		MISC
G 135-20678		576	05 19 30+	2		MISC

Table 8.--*Sequential listing within each 70 mm magazine, Apollo 17 lunar surface pictures (magazine J, black and white, 60 mm focal length)--Continued*

MAG	PHOTO	SEQ	GET	EVA	STA	REMARKS
H 136-20682	153	04 22 18	1	ALSEP	MISC, FOGGED	
H 136-20683	154	04 22 18+	1	ALSEP	PAN	
H 136-20684	155	04 22 18+	1	ALSEP	PAN	
H 136-20685	156	04 22 18+	1	ALSEP	PAN	
H 136-20686	157	04 22 18+	1	ALSEP	PAN	
H 136-20687	158	04 22 18+	1	ALSEP	PAN	
H 136-20688	159	04 22 18+	1	ALSEP	PAN	
H 136-20689	160	04 22 18+	1	ALSEP	PAN	
H 136-20690	161	04 22 18+	1	ALSEP	PAN	
H 136-20691	162	04 22 18+	1	ALSEP	PAN	
H 136-20692	163	04 22 18+	1	ALSEP	PAN	
H 136-20693	164	04 22 18+	1	ALSEP	PAN	
H 136-20694	165	04 22 18+	1	ALSEP	PAN	
H 136-20695	166	04 22 18+	1	ALSEP	PAN	
H 136-20696	167	04 22 18+	1	ALSEP	PAN	
H 136-20697	168	04 22 18+	1	ALSEP	PAN	
H 136-20698	169	04 22 18+	1	ALSEP	PAN	
H 136-20699	170	04 22 18+	1	ALSEP	PAN	
H 136-20700	171	04 22 18+	1	ALSEP	PAN	
H 136-20701	172	04 22 18+	1	ALSEP	PAN	
H 136-20702	173	04 22 18+	1	ALSEP	PAN	
H 136-20703	174	04 22 18+	1	ALSEP	PAN	
H 136-20704	175	04 22 18+	1	ALSEP	PAN	
H 136-20705	176	04 22 18+	1	ALSEP	PAN	
H 136-20706	177	04 22 18+	1	ALSEP	PAN	
H 136-20707	178	04 22 18+	1	ALSEP	PAN	
H 136-20708	179	04 22 18+	1	ALSEP	PAN	
H 136-20709	180	04 22 18+	1	ALSEP	PAN	
H 136-20710	181	04 22 18+	1	ALSEP	PAN	
H 136-20711	182	04 22 18+	1	ALSEP	C/S, HEAT FLOW PROBE 1	
H 136-20712	183	04 22 18+	1	ALSEP	C/S, HEAT FLOW PROBE 1	
H 136-20713	184	04 22 18+	1	ALSEP	C/S, HEAT FLOW PROBE 1	
H 136-20714	185	04 22 25	1	ALSEP	PARTING ROCK XS	
H 136-20715	186	04 22 25+	1	ALSEP	PARTING ROCK XS	
H 136-20716	187	04 22 25+	1	ALSEP	PARTING ROCK CU	
H 136-20717	188	04 22 25+	1	ALSEP	PARTING ROCK CU	
H 136-20718	189	04 22 36	1	ALSEP	PARTING ROCK, SPL 70160-04, 05 DS	
H 136-20719	190	04 22 36	1	ALSEP	PARTING ROCK, SPL 70160-04, 05 DS	
H 136-20720	191	04 22 42	1	ALSEP	SPL 70180-84,85, DEEP CORE 70001-09, NEUTRON FLUX	
H 136-20721	192	04 22 42+	1	ALSEP	SPL 70180-84,85, DEEP CORE 70001-09 XSB	
H 136-20722	193	04 22 42+	1	ALSEP	SPL 70180-84,85, DEEP CORE 70001-09 XSA	
H 136-20723	194	04 23 11	1	SEP-1		
H 136-20724	195	04 23 11+	1	SEP-1		
H 136-20725	196	04 23 11+	1	SEP-1		
H 136-20726	197	04 23 11+	1	SEP-1		
H 136-20727	198	04 23 11+	1	SEP-1		
H 136-20728	200	04 23 11+	1	SEP-1		
H 136-20729	203	04 23 11+	1	SEP-1		
H 136-20730	204	04 23 11+	1	SEP-1		
H 136-20731	205	04 23 11+	1	SEP-1		
H 136-20732	206	04 23 11+	1	SEP-1		
H 136-20733	207	04 23 11+	1	SEP-1		
H 136-20734	208	04 23 11+	1	SEP-1		
H 136-20735	209	04 23 11+	1	SEP-1		
H 136-20736	210	04 23 11+	1	SEP-1		
H 136-20737	211	04 23 11+	1	SEP-1		
H 136-20738	213	04 23 11+	1	SEP-1		
H 136-20739	214	04 23 29	1	1	SPL 71710,35-37,71040-44,45-49,71055,71060-64,65-69,85-89,95-97 DS	
H 136-20740	215	04 23 32+	1	1	SPL 71710,35-37,71040-44,45-49,71055,71060-64,65-69,85-89,95-97 LOC	
H 136-20741	219	04 23 42	1	1	SPL 71130,35-36,71150,55-57,71175 DS	
H 136-20742	228	04 23 43+	1	1	SPL 71500-04,05-09,15,71525-29,35-39,45-49,55-59,65-69,75-79,85-89,95-97 LOC	
H 136-20743	229	04 23 43+	1	1	SPL 71500-04,05-09,15,71525-29,35-39,45-49,55-59,65-69,75-79,85-89,95-97 DS	
H 136-20744	258	04 23 51	1	1	PAN	
H 136-20745	259	04 23 51+	1	1	PAN	
H 136-20746	260	04 23 51+	1	1	PAN	
H 136-20747	261	04 23 51+	1	1	PAN	
H 136-20748	262	04 23 51+	1	1	PAN	
H 136-20749	263	04 23 51+	1	1	PAN	
H 136-20750	264	04 23 51+	1	1	PAN	
H 136-20751	265	04 23 51+	1	1	PAN	
H 136-20752	266	04 23 51+	1	1	PAN	
H 136-20753	267	04 23 51+	1	1	PAN	
H 136-20754	268	04 23 51+	1	1	PAN	
H 136-20755	269	04 23 51+	1	1	PAN	
H 136-20756	270	04 23 51+	1	1	PAN	
H 136-20757	271	04 23 51+	1	1	PAN	
H 136-20758	272	04 23 51+	1	1	PAN	
H 136-20759	273	04 23 51+	1	1	PAN	
H 136-20760	274	04 23 51+	1	1	PAN	
H 136-20761	275	04 23 51+	1	1	PAN	
H 136-20762	276	04 23 51+	1	1	PAN	
H 136-20763	277	04 23 51+	1	1	PAN	
H 136-20764	278	04 23 51+	1	1	PAN	
H 136-20765	279	04 23 51+	1	1	PAN	
H 136-20766	280	04 23 51+	1	1	PAN	
H 136-20767	281	04 23 51+	1	1	PAN	
H 136-20768	282	04 23 51+	1	1	PAN	
H 136-20769	283	04 23 51+	1	1	PAN	
H 136-20770	284	04 23 51+	1	1	PAN	
H 136-20771	285	04 23 51+	1	1	PAN	
H 136-20772	286	04 23 51+	1	1	PAN	

Table 8.--Sequential listing within each 70 mm magazine, Apollo 17 lunar surface pictures (magazine J, black and white, 60 mm focal length)--Continued

MAG	PHOTO	SEQ	GET	EVA	STA	REMARKS
H 136-20773	287	04	23 51+	1	1	PAN
H 136-20774	288	04	23 51+	1	1	PAN
H 136-20775	289	04	23 51+	1	1	PAN
H 136-20776	290	04	23 51+	1	1	PAN
H 136-20777	291	04	23 55	1	1-SEP	
H 136-20778	292	04	23 55+	1	1-SEP	
H 136-20779	293	04	23 55+	1	1-SEP	
H 136-20780	294	04	23 55+	1	1-SEP	
H 136-20781	295	04	23 55+	1	1-SEP	
H 136-20782	296	04	23 55+	1	1-SEP	
H 136-20783	297	04	23 55+	1	1-SEP	
H 136-20784	298	04	23 55+	1	1-SEP	
H 136-20785	299	04	23 55+	1	1-SEP	
H 136-20786	300	04	23 55+	1	1-SEP	
H 136-20787	301	04	23 55+	1	1-SEP	
H 136-20788	302	04	23 55+	1	1-SEP	
H 136-20789	303	04	23 55+	1	1-SEP	
H 136-20790	304	04	23 55+	1	1-SEP	
H 136-20791	305	04	23 55+	1	1-SEP	
H 136-20792	306	04	23 55+	1	1-SEP	
H 136-20793	307	04	23 55+	1	1-SEP	
H 136-20794	308	04	23 55+	1	1-SEP	
H 136-20795	309	04	23 55+	1	1-SEP	
H 136-20796	310	04	23 55+	1	1-SEP	
H 136-20797	311	04	23 55+	1	1-SEP	
H 136-20798	312	04	23 55+	1	1-SEP	
H 136-20799	313	04	23 55+	1	1-SEP	
H 136-20800	314	04	23 55+	1	1-SEP	
H 136-20801	315	04	23 55+	1	1-SEP	
H 136-20802	316	04	23 55+	1	1-SEP	
H 136-20803	317	04	23 55+	1	1-SEP	
H 136-20804	318	04	23 55+	1	1-SEP	
H 136-20805	319	04	23 55+	1	1-SEP	
H 136-20806	320	04	23 55+	1	1-SEP	
H 136-20807	321	04	23 55+	1	1-SEP	
H 136-20808	322	04	23 55+	1	1-SEP	
H 136-20809	323	04	23 55+	1	1-SEP	
H 136-20810	324	04	23 55+	1	1-SEP	
H 136-20811	325	04	23 55+	1	1-SEP	
H 136-20812	326	04	23 58	1	1-SEP	EP-7 LOC, LRV PPAN
H 136-20813	327	04	23 58+	1	1-SEP	EP-7 LOC, LRV PPAN
H 136-20814	328	04	23 58+	1	1-SEP	EP-7 LOC, LRV PPAN
H 136-20815	329	04	23 58+	1	1-SEP	EP-7 LOC, LRV PPAN
H 136-20816	332	05	00 02	1	1-SEP	EP-7 LOC, LRV PPAN
H 136-20817	333	05	00 02+	1	1-SEP	EP-7 LOC, LRV PPAN
H 136-20818	334	05	00 02+	1	1-SEP	EP-7 LOC, LRV PPAN
H 136-20819	335	05	00 02+	1	1-SEP	EP-7 LOC, LRV PPAN
H 136-20820	336	05	00 02+	1	1-SEP	EP-7 LOC, LRV PPAN
H 136-20821	337	05	00 02+	1	1-SEP	EP-7 LOC, LRV PPAN
H 136-20822	338	05	00 02+	1	1-SEP	EP-7 LOC, LRV PPAN
H 136-20823	339	05	00 02+	1	1-SEP	EP-7 LOC, LRV PPAN
H 136-20824	340	05	00 02+	1	1-SEP	EP-7 LOC, LRV PPAN
H 136-20825	341	05	00 02+	1	1-SEP	EP-7 LOC, LRV PPAN
H 136-20826	342	05	00 02+	1	1-SEP	EP-7 LOC, LRV PPAN
H 136-20827	343	05	00 02+	1	1-SEP	EP-7 LOC, LRV PPAN
H 136-20828	344	05	00 02+	1	1-SEP	EP-7 LOC, LRV PPAN
H 136-20829	345	05	00 02+	1	1-SEP	
H 136-20830	346	05	00 02+	1	1-SEP	
H 136-20831	347	05	00 02+	1	1-SEP	
H 136-20832	348	05	00 02+	1	1-SEP	
H 136-20833	349	05	00 02+	1	1-SEP	
H 136-20834	350	05	00 02+	1	1-SEP	
H 136-20835	351	05	00 02+	1	1-SEP	
H 136-20836	352	05	00 02+	1	1-SEP	
H 136-20837	353	05	00 02+	1	1-SEP	
H 136-20838	354	05	00 02+	1	1-SEP	
H 136-20839	355	05	00 02+	1	1-SEP	
H 136-20840	356	05	00 02+	1	1-SEP	
H 136-20841	357	05	00 02+	1	1-SEP	
H 136-20842	358	05	00 02+	1	1-SEP	
H 136-20843	359	05	00 02+	1	1-SEP	
H 136-20844	360	05	00 02+	1	1-SEP	
H 136-20845	361	05	00 02+	1	1-SEP	
H 136-20846	362	05	00 02+	1	1-SEP	
H 136-20847	363	05	00 02+	1	1-SEP	
H 136-20848	364	05	00 02+	1	1-SEP	
H 136-20849	365	05	00 02+	1	1-SEP	
H 136-20850	366	05	00 02+	1	1-SEP	
H 136-20851	367	05	00 02+	1	1-SEP	
H 136-20852	368	05	00 02+	1	1-SEP	
H 136-20853	369	05	00 02+	1	1-SEP	
H 136-20854	370	05	00 02+	1	1-SEP	
H 136-20855	371	05	00 02+	1	1-SEP	
H 136-20856	372	05	00 02+	1	1-SEP	
H 136-20857	373	05	00 02+	1	1-SEP	
H 136-20858	374	05	00 02+	1	1-SEP	
H 136-20859	375	05	00 02+	1	1-SEP	
H 136-20860	376	05	00 02+	1	1-SEP	
H 136-20861	377	05	00 02+	1	1-SEP	
H 136-20862	378	05	00 02+	1	1-SEP	
H 136-20863	379	05	00 02+	1	1-SEP	

Table 8.--*Sequential listing within each 70 mm magazine, Apollo 17 lunar surface pictures (magazine J, black and white, 60 mm focal length)--Continued*

MAG	PHOTO	SEQ	GET	EVA	STA	REMARKS
C 137-20866		397	05 18 21	2	LM	PAN S OF LM
C 137-20867		398	05 18 21+	2	LM	PAN S OF LM
C 137-20868		399	05 18 21+	2	LM	PAN S OF LM
C 137-20869		400	05 18 21+	2	LM	PAN S OF LM
C 137-20870		401	05 18 21+	2	LM	PAN S OF LM
C 137-20871		402	05 18 21+	2	LM	PAN S OF LM
C 137-20872		403	05 18 21+	2	LM	PAN S OF LM
C 137-20873		404	05 18 21+	2	LM	PAN S OF LM
C 137-20874		405	05 18 21+	2	LM	PAN S OF LM
C 137-20875		406	05 18 21+	2	LM	PAN S OF LM
C 137-20876		407	05 18 21+	2	LM	PAN S OF LM
C 137-20877		408	05 18 21+	2	LM	PAN S OF LM
C 137-20878		409	05 18 21+	2	LM	PAN S OF LM
C 137-20879		410	05 18 21+	2	LM	PAN S OF LM
C 137-20880		411	05 18 21+	2	LM	PAN S OF LM
C 137-20881		412	05 18 21+	2	LM	PAN S OF LM
C 137-20882		413	05 18 21+	2	LM	PAN S OF LM
C 137-20883		414	05 18 21+	2	LM	PAN S OF LM
C 137-20884		415	05 18 21+	2	LM	PAN S OF LM
C 137-20885		416	05 18 21+	2	LM	PAN S OF LM
C 137-20886		417	05 18 21+	2	LM	PAN S OF LM
C 137-20887		418	05 18 21+	2	LM	PAN S OF LM
C 137-20888		419	05 18 21+	2	LM	PAN S OF LM
C 137-20889		420	05 18 21+	2	LM	PAN S OF LM
C 137-20890		421	05 18 21+	2	LM	PAN S OF LM
C 137-20891		422	05 18 21+	2	LM	PAN S OF LM
C 137-20892		423	05 18 21+	2	LM	PAN S OF LM
C 137-20893		424	05 18 22	2	LM	PAN S OF LM
C 137-20894		425	05 18 22+	2	LM	LRV
C 137-20895		521	05 19 14+	2	SEP-2	SPL 72130-34,35
C 137-20896		537	05 19 24+	2	SEP-2	SPL 72140-44,45, STEREO OF 135-20643
C 137-20897		544	05 19 30	2	SEP-2	SPL 72155, STEREO OF 135-20649
C 137-20898		546	05 19 30+	2	SEP-2	
C 137-20899		551	05 19 30+	2	SEP-2	
C 137-20900		578	05 20 22	2	2	SPL 72215, 72220-24, 72235, 72240-44, 72255, 72250-64, 72275 XSB
C 137-20901		579	05 20 22+	2	2	SPL 72215, 72220-24, 72235, 72240-44, 72255, 72250-64, 72275 XSB
C 137-20902		580	05 20 22+	2	2	SPL 72215, 72220-24, 72235, 72240-44, 72255, 72250-64, 72275 XSA
C 137-20903		581	05 20 22+	2	2	SPL 72215, 72220-24, 72235, 72240-44, 72255, 72250-64, 72275 XSA
C 137-20904		582	05 20 22+	2	2	SPL 72215, 72220-24, 72235, 72240-44, 72255, 72250-64, 72275 XSA
C 137-20905		583	05 20 22+	2	2	SPL 72215, 72220-24, 72235, 72240-44, 72255, 72250-64, 72275 XSA
C 137-20906		584	05 20 22+	2	2	SPL 72215, 72220-24, 72235, 72240-44, 72255, 72250-64, 72275 XSA
C 137-20907		585	05 20 22+	2	2	SPL 72215, 72220-24, 72235, 72240-44, 72255, 72250-64, 72275 XSA
C 137-20908		586	05 20 22+	2	2	SPL 72215, 72220-24, 72235, 72240-44, 72255, 72250-64, 72275 XSA
C 137-20909		587	05 20 22+	2	2	SPL 72215, 72220-24, 72235, 72240-44, 72255, 72250-64, 72275 XSA
C 137-20910		597	05 20 31	2	2	SPL 72315 ROCK, EARTH
C 137-20911		598	05 20 31+	2	2	SPL 72315 ROCK, EARTH
C 137-20912		599	05 20 31+	2	2	SPL 72315, 72320-24, 72335, 72355, 72375, 72395 XSB
C 137-20913		600	05 20 31+	2	2	SPL 72315, 72320-24, 72335, 72355, 72375, 72395 XSB
C 137-20914		601	05 20 31+	2	2	SPL 72315, 72320-24, 72335, 72355, 72375, 72395 XSB
C 137-20915		602	05 20 31+	2	2	SPL 72315, 72320-24, 72335, 72355, 72375, 72395 XSB
C 137-20916		603	05 20 31+	2	2	SPL 72315, 72320-24, 72335, 72355, 72375, 72395 XSB
C 137-20917		604	05 20 31+	2	2	SPL 72315 ROCK
C 137-20918		605	05 20 31+	2	2	SPL 72315 ROCK
C 137-20919		606	05 20 31+	2	2	SPL 72315 ROCK
C 137-20920		607	05 20 31+	2	2	SPL 72315 ROCK
C 137-20921		608	05 20 31+	2	2	SPL 72315 ROCK
C 137-20922		609	05 20 31+	2	2	SPL 72315 ROCK
C 137-20923		610	05 20 31+	2	2	SPL 72315 ROCK
C 137-20924		611	05 20 31+	2	2	SPL 72315 ROCK
C 137-20925		612	05 20 31+	2	2	SPL 72315 ROCK
C 137-20926		618	05 20 41	2	2	PAN
C 137-20927		619	05 20 41+	2	2	PAN
C 137-20928		620	05 20 41+	2	2	PAN
C 137-20929		621	05 20 41+	2	2	PAN
C 137-20930		622	05 20 41+	2	2	PAN
C 137-20931		623	05 20 41+	2	2	PAN
C 137-20932		624	05 20 41+	2	2	PAN
C 137-20933		625	05 20 41+	2	2	PAN
C 137-20934		626	05 20 41+	2	2	PAN
C 137-20935		627	05 20 41+	2	2	PAN
C 137-20936		628	05 20 41+	2	2	PAN
C 137-20937		629	05 20 41+	2	2	PAN
C 137-20938		630	05 20 41+	2	2	PAN
C 137-20939		631	05 20 41+	2	2	PAN
C 137-20940		632	05 20 41+	2	2	PAN
C 137-20941		633	05 20 41+	2	2	PAN
C 137-20942		634	05 20 41+	2	2	PAN
C 137-20943		635	05 20 41+	2	2	PAN
C 137-20944		636	05 20 41+	2	2	PAN
C 137-20945		637	05 20 41+	2	2	PAN
C 137-20946		638	05 20 41+	2	2	PAN
C 137-20947		639	05 20 41+	2	2	PAN
C 137-20948		640	05 20 41+	2	2	PAN
C 137-20949		641	05 20 41+	2	2	PAN
C 137-20950		642	05 20 41+	2	2	PAN
C 137-20951		643	05 20 41+	2	2	PAN
C 137-20952		644	05 20 41+	2	2	PAN
C 137-20953		645	05 20 41+	2	2	PAN
C 137-20954		646	05 20 41+	2	2	PAN
C 137-20955		647	05 20 41+	2	2	PAN

Table 8.--*Sequential listing within each 70 mm magazine, Apollo 17 lunar surface pictures (magazine J, black and white, 60 mm focal length)--Continued*

MAG	PHOTO	S&Q	GET	EVA	STA	REMARKS
C 137-20956	648	05 20 41+	2	2	2	PAN
C 137-20957	649	05 20 41+	2	2	2	EARTH
C 137-20958	650	05 20 41+	2	2	2	EARTH
C 137-20959	651	05 20 41+	2	2	2	EARTH
C 137-20960	652	05 20 41+	2	2	2	SPL 72315 ROCK, EARTH
C 137-20961	653	05 20 41+	2	2	2	SPL 72315 ROCK, EARTH
C 137-20962	658	05 20 47	2	2	2	SPL 72500-04, 05, 72535-39, 45-49, 55-59 XSA
C 137-20963	662	05 20 50	2	2	2	SPL 72415-18, 72430-34, 35, 72440-44, 72460-64 XSB
C 137-20964	663	05 20 50+	2	2	2	SPL 72415-18, 72430-34, 35, 72440-44, 72460-64 XSB
C 137-20965	664	05 20 50+	2	2	2	SPL 72415-18, 72430-34, 35, 72440-44, 72460-64 XSA
C 137-20966	665	05 20 50+	2	2	2	SPL 72415-18, 72430-34, 35, 72440-44, 72460-64 CU
C 137-20967	666	05 20 50+	2	2	2	SPL 72415-18, 72430-34, 35, 72440-44, 72460-64 CU
C 137-20968	667	05 20 50+	2	2	2	SPL 72415-18, 72430-34, 35, 72440-44, 72460-64 CU
C 137-20969	668	05 20 50+	2	2	2	SPL 72415-18, 72430-34, 35, 72440-44, 72460-64 CU
C 137-20970	669	05 20 50+	2	2	2	SPL 72415-18, 72430-34, 35, 72440-44, 72460-64 CU
C 137-20971	670	05 20 50+	2	2	2	SPL 72415-18, 72430-34, 35, 72440-44, 72460-64 CU
C 137-20972	671	05 20 52	2	2	2	SPL 72415-18, 72430-34, 35, 72440-44, 72460-64 CU
C 137-20973	672	05 20 52+	2	2	2	SPL 72415-18, 72430-34, 35, 72440-44, 72460-64 CU
C 137-20974	697	05 20 59	2	2	2	SPL 72700-04, 05, 72735-38 XSB
C 137-20975	698	05 20 59+	2	2	2	SPL 72700-04, 05, 72735-38 XSB
C 137-20976	699	05 20 59+	2	2	2	SPL 72700-04, 05, 72735-38 LOC
C 137-20977	700	05 20 59+	2	2	2	SPL 72700-04, 05, 72735-38 LOC
C 137-20978	701	05 21 00	2	2	2	SPL 72700-04, 05, 72735-38 XSA
C 137-20979	703	05 21 00+	2	2	2	LRV
C 137-20980	738	05 21 25+	2	2-3	2	
C 137-20981	812	05 22 15	2	3	3	DT SPL 73002/73001 (CSVC)
C 137-20982	813	05 22 15+	2	3	3	DT SPL 73002/73001 (CSVC)
C 137-20983	829	05 22 31+	2	3-4	3	SPL 74110-14, 15-19, STEREO OF 133-20208
C 137-20984	878	05 22 52	2	4	4	TR SPL 74220, 74240-49, 45-49, 74260 XSA
C 137-20985	879	05 22 52+	2	4	4	TR SPL 74220, 74240-49, 45-49, 74260 XSA
C 137-20986	880	05 22 52+	2	4	4	TR SPL 74220, 74240-44, 45-49, 74260 XSA
C 137-20987	881	05 22 52+	2	4	4	TR SPL 74220, 74240-44, 45-49, 74260 XSA
C 137-20988	882	05 22 52+	2	4	4	TR SPL 74220, 74240-44, 45-49, 74260 XSA
C 137-20989	883	05 22 52+	2	4	4	TR SPL 74220, 74240-44, 45-49, 74260 XSA
C 137-20990	884	05 22 52+	2	4	4	TR SPL 74220, 74240-44, 45-49, 74260 DSA
C 137-20991	897	05 23 08	2	4	4	PAN
C 137-20992	898	05 23 08+	2	4	4	PAN
C 137-20993	899	05 23 08+	2	4	4	PAN
C 137-20994	900	05 23 08+	2	4	4	PAN
C 137-20995	901	05 23 08+	2	4	4	PAN
C 137-20996	902	05 23 08+	2	4	4	PAN
C 137-20997	903	05 23 08+	2	4	4	PAN
C 137-20998	904	05 23 08+	2	4	4	PAN
C 137-20999	905	05 23 08+	2	4	4	PAN
C 137-21000	906	05 23 08+	2	4	4	PAN
C 137-21001	907	05 23 08+	2	4	4	PAN
C 137-21002	908	05 23 08+	2	4	4	PAN
C 137-21003	909	05 23 08+	2	4	4	PAN
C 137-21004	910	05 23 08+	2	4	4	PAN
C 137-21005	911	05 23 08+	2	4	4	PAN
C 137-21006	912	05 23 08+	2	4	4	PAN
C 137-21007	913	05 23 08+	2	4	4	PAN
C 137-21008	914	05 23 08+	2	4	4	PAN
C 137-21009	915	05 23 08+	2	4	4	PAN
C 137-21010	916	05 23 08+	2	4	4	PAN
C 137-21011	917	05 23 08+	2	4	4	PAN
C 137-21012	918	05 23 08+	2	4	4	PAN
C 137-21013	919	05 23 08+	2	4	4	PAN
C 137-21014	920	05 23 08+	2	4	4	PAN
C 137-21015	921	05 23 08+	2	4	4	PAN
C 137-21016	922	05 23 08+	2	4	4	PAN
C 137-21017	923	05 23 08+	2	4	4	PAN
C 137-21018	924	05 23 08+	2	4	4	PAN
C 137-21019	925	05 23 08+	2	4	4	PAN
C 137-21020	926	05 23 08+	2	4	4	PAN
C 137-21021	927	05 23 08+	2	4	4	PAN
C 137-21022	928	05 23 08+	2	4	4	PAN
C 137-21023	929	05 23 08+	2	4	4	PAN
C 137-21024	930	05 23 08+	2	4	4	PAN
C 137-21025	931	05 23 08+	2	4	4	PAN
C 137-21026	932	05 23 08+	2	4	4	PAN
C 137-21027	933	05 23 09	2	4	4	PA'

Table 8.--*Sequential listing within each 70 mm magazine, Apollo 17 lunar surface pictures (magazine J, black and white, 60 mm focal length)--Continued*

MAG	PHOTO	SEQ	GET	EVA	STA	REMARKS
I 138-21028		577		2	2	FOGGED
I 138-21029		588	05 20 23	2	2	SPL 72215,72220-24,72235,72240-44,72255,72260-64,72275 XS F-L
I 138-21030		589	05 20 23+	2	2	SPL 72215,72220-24,72235,72240-44,72255,72260-64,72275 XS F-L
I 138-21031		590	05 20 23+	2	2	SPL 72215,72220-24,72235,72240-44,72255,72260-64,72275 XS F-L
I 138-21032		591	05 20 23+	2	2	SPL 72215,72220-24,72235,72240-44,72255,72260-64,72275 XS F-L
I 138-21033		592	05 20 23+	2	2	SPL 72215,72220-24,72235,72240-44,72255,72260-64,72275 XS F-L
I 138-21034		593	05 20 23+	2	2	SPL 72215,72220-24,72235,72240-44,72255,72260-64,72275 XS F-L
I 138-21035		594	05 20 23+	2	2	SPL 72215,72220-24,72235,72240-44,72255,72260-64,72275 XS F-L
I 138-21036		595	05 20 30	2	2	SPL 72215,72220-24,72235,72240-44,72255,72260-64,72275 DSA SPEREO
I 138-21037		596	05 20 30+	2	2	SPL 72215,72220-24,72235,72240-44,72255,72260-64,72275 DSA SPEREO
I 138-21038		613	05 20 40	2	2	SPL 72315,72320-24,72335,72355,72375,72395 DSA
I 138-21039		614	05 20 40+	2	2	SPL 72315,72320-24,72335,72355,72375,72395 LOC
I 138-21040		615	05 20 40+	2	2	SPL 72315,72320-24,72335,72355,72375,72395 XSA
I 138-21041		616	05 20 40+	2	2	SPL 72315,72320-24,72335,72355,72375,72395 XSA
I 138-21042		617	05 20 40+	2	2	SPL 72315,72320-24,72335,72355,72375,72395 XSA
I 138-21043		654	05 20 41+	2	2	SPL 72500-04,05,72535-39,45-49,55-59 XSB
I 138-21044		655	05 20 41+	2	2	SPL 72500-04,05,72535-39,45-49,55-59 XSB
I 138-21045		656	05 20 41+	2	2	SPL 72500-04,05,72535-39,45-49,55-59 XSB
I 138-21046		657	05 20 41+	2	2	SPL 72500-04,05,72535-39,45-49,55-59 XSB
I 138-21047		659	05 20 47+	2	2	SPL 72415-18,72430-34,35,72440-44,72460-64 DSB
I 138-21048		660	05 20 47+	2	2	SPL 72415-18,72430-34,35,72440-44,72460-64 LOC
I 138-21049		661	05 20 47+	2	2	SPL 72415-18,72430-34,35,72440-44,72460-64 DSB
I 138-21050		673	05 20 52	2	2	SMALL PIT CTR F-L
I 138-21051		674	05 20 52	2	2	SMALL PIT CTR F-L
I 138-21052		675	05 20 52	2	2	SMALL PIT CTR F-L
I 138-21053		676	05 20 58	2	2	PAN
I 138-21054		677	05 20 58+	2	2	PAN
I 138-21055		678	05 20 58+	2	2	PAN
I 138-21056		679	05 20 58+	2	2	PAN
I 138-21057		680	05 20 58+	2	2	PAN
I 138-21058		681	05 20 58+	2	2	PAN
I 138-21059		682	05 20 58+	2	2	PAN
I 138-21060		683	05 20 58+	2	2	PAN
I 138-21061		684	05 20 58+	2	2	PAN
I 138-21062		685	05 20 58+	2	2	PAN
I 138-21063		686	05 20 58+	2	2	PAN
I 138-21064		687	05 20 58+	2	2	PAN
I 138-21065		688	05 20 58+	2	2	PAN
I 138-21066		689	05 20 58+	2	2	PAN
I 138-21067		690	05 20 58+	2	2	PAN
I 138-21068		691	05 20 58+	2	2	PAN
I 138-21069		692	05 20 58+	2	2	PAN
I 138-21070		693	05 20 58+	2	2	PAN
I 138-21071		694	05 20 58+	2	2	PAN
I 138-21072		695	05 20 58+	2	2	PAN
I 138-21073		696	05 20 58+	2	2	PAN
I 138-21074		702	05 21 00+	2	2	SPL 72700-04,05,72735-38 DSA
I 138-21075		704	05 21 07	2	2-3	
I 138-21076		705	05 21 07+	2	2-3	
I 138-21077		706	05 21 10	2	2-3	LRV PAN
I 138-21078		707	05 21 10+	2	2-3	LRV PAN
I 138-21079		708	05 21 10+	2	2-3	LRV PAN
I 138-21080		709	05 21 10+	2	2-3	LRV PAN
I 138-21081		710	05 21 10+	2	2-3	LRV PAN
I 138-21082		711	05 21 10+	2	2-3	LRV PAN
I 138-21083		712	05 21 10+	2	2-3	LRV PAN
I 138-21084		713	05 21 10+	2	2-3	LRV PAN
I 138-21085		714	05 21 10+	2	2-3	LRV PAN
I 138-21086		715	05 21 10+	2	2-3	LRV PAN
I 138-21087		716	05 21 10+	2	2-3	LRV PAN
I 138-21088		717	05 21 10+	2	2-3	LRV PAN
I 138-21089		718	05 21 10+	2	2-3	LRV PAN
I 138-21090		719	05 21 10+	2	2-3	LRV PAN
I 138-21091		720	05 21 10+	2	2-3	LRV PAN
I 138-21092		721	05 21 10+	2	2-3	LRV PAN
I 138-21093		722	05 21 10+	2	2-3	
I 138-21094		723	05 21 10+	2	2-3	
I 138-21095		724	05 21 10+	2	2-3	
I 138-21096		725	05 21 17	2	2-3	SPL 73130-34 XSB
I 138-21097		726	05 21 17+	2	2-3	SPL 73130-34 XSB
I 138-21098		727	05 21 17+	2	2-3	SPL 73140-44,45-46 OR 73150-54,55-56 XSB
I 138-21099		728	05 21 17+	2	2-3	SPL 73140-44,45-46 OR 73150-54,55-56 XSB
I 138-21100		729	05 21 25	2	2-3	LRV PPAN
I 138-21101		730	05 21 25+	2	2-3	LRV PPAN
I 138-21102		731	05 21 25+	2	2-3	LRV PPAN
I 138-21103		732	05 21 25+	2	2-3	LRV PPAN
I 138-21104		733	05 21 25+	2	2-3	LRV PPAN
I 138-21105		734	05 21 25+	2	2-3	LRV PPAN
I 138-21106		735	05 21 25+	2	2-3	LRV PPAN
I 138-21107		736	05 21 25+	2	2-3	LRV PPAN
I 138-21108		737	05 21 25+	2	2-3	LRV PPAN
I 138-21109		739	05 21 25+	2	2-3	
I 138-21110		740	05 21 25+	2	2-3	
I 138-21111		741	05 21 25+	2	2-3	
I 138-21112		742	05 21 25+	2	2-3	
I 138-21113		743	05 21 25+	2	2-3	
I 138-21114		744	05 21 25+	2	2-3	
I 138-21115		745	05 21 25+	2	2-3	
I 138-21116		746	05 21 25+	2	2-3	
I 138-21117		747	05 21 25+	2	2-3	

Table 8.--Sequential listing within each 70 mm magazine, Apollo 17 lunar surface pictures (magazine J, black and white, 60 mm focal length)--Continued

MAG	PHOTO	SEQ	GET	EVA	STA	REMARKS
I 138-21118	748	05	21 25+	2	2-3	
I 138-21119	749	05	21 25+	2	2-3	
I 138-21120	750	05	21 25+	2	2-3	
I 138-21121	751	05	21 25+	2	2-3	
I 138-21122	752	05	21 25+	2	2-3	
I 138-21123	753	05	21 25+	2	2-3	
I 138-21124	754	05	21 25+	2	2-3	
I 138-21125	755	05	21 25+	2	2-3	
I 138-21126	756	05	21 25+	2	2-3	
I 138-21127	757	05	21 25+	2	2-3	
I 138-21128	758	05	21 25+	2	2-3	
I 138-21129	759	05	21 25+	2	2-3	
I 138-21130	760	05	21 25+	2	2-3	
I 138-21131	761	05	21 25+	2	2-3	
I 138-21132	762	05	21 25+	2	2-3	
I 138-21133	763	05	21 25+	2	2-3	
I 138-21134	764	05	21 25+	2	2-3	
I 138-21135	765	05	21 25+	2	2-3	
I 138-21136	766	05	21 25+	2	2-3	
I 138-21137	767	05	21 25+	2	2-3	
I 138-21138	768	05	21 25+	2	2-3	
I 138-21139	769	05	21 25+	2	2-3	
I 138-21140	770	05	21 25+	2	2-3	
I 138-21141	771	05	21 25+	2	2-3	
I 138-21142	772	05	21 25+	2	2-3	
I 138-21143	773	05	21 51	2	3	TR SPL 73210-14,15-19,73220-24,25,73235,73240-44,45,73255,73260-64,73275,73280-84,85 X
I 138-21144	774	05	21 51+	2	3	TR SPL 73210-14,15-19,73220-24,25,73235,73240-44,45,73255,73260-64,73275,73280-84,85 X
I 138-21145	775	05	21 51+	2	3	TR SPL 73210-14,15-19,73220-24,25,73235,73240-44,45,73255,73260-64,73275,73280-84,85 X
I 138-21146	776	05	21 51+	2	3	TR SPL 73210-14,15-19,73220-24,25,73235,73240-44,45,73255,73260-64,73275,73280-84,85 X
I 138-21147	777	05	21 51+	2	3	TR SPL 73210-14,15-19,73220-24,25,73235,73240-44,45,73255,73260-64,73275,73280-84,85 D
I 138-21148	778	05	21 51+	2	3	TR SPL 73210-14,15-19,73220-24,25,73235,73240-44,45,73255,73260-64,73275,73280-84,85 D
I 138-21149	779	05	21 51+	2	3	TR SPL 73210-14,15-19,73220-24,25,73235,73240-44,45,73255,73260-64,73275,73280-84,85 X
I 138-21150	780	05	22 13	2	3	PAN
I 138-21151	781	05	22 13+	2	3	PAN
I 138-21152	782	05	22 13+	2	3	PAN
I 138-21153	783	05	22 13+	2	3	PAN
I 138-21154	784	05	22 13+	2	3	PAN
I 138-21155	785	05	22 13+	2	3	PAN
I 138-21156	786	05	22 13+	2	3	PAN
I 138-21157	787	05	22 13+	2	3	PAN
I 138-21158	788	05	22 13+	2	3	PAN
I 138-21159	789	05	22 13+	2	3	PAN
I 138-21160	790	05	22 13+	2	3	PAN
I 138-21161	791	05	22 13+	2	3	PAN
I 138-21162	792	05	22 13+	2	3	PAN
I 138-21163	793	05	22 13+	2	3	PAN
I 138-21164	794	05	22 13+	2	3	PAN
I 138-21165	795	05	22 13+	2	3	PAN
I 138-21166	796	05	22 13+	2	3	PAN
I 138-21167	797	05	22 13+	2	3	PAN
I 138-21168	798	05	22 13+	2	3	PAN
I 138-21169	799	05	22 13+	2	3	PAN
I 138-21170	800	05	22 13+	2	3	PAN
I 138-21171	801	05	22 13+	2	3	PAN
I 138-21172	802	05	22 13+	2	3	PAN
I 138-21173	803	05	22 13+	2	3	PAN
I 138-21174	804	05	22 13+	2	3	PAN
I 138-21175	805	05	22 13+	2	3	PAN
I 138-21176	806	05	22 13+	2	3	PAN
I 138-21177	807	05	22 13+	2	3	PAN
I 138-21178	808	05	22 13+	2	3	TR SPL 73215-19,73220-24,25,73235,73240-44,45,73255,73260-64,73275,73280-84,85 XSA
I 138-21179	809	05	22 13+	2	3	TR SPL 73215-19,73220-24,25,73235,73240-44,45,73255,73260-64,73275,73280-84,85 XSA
I 138-21180	810	05	22 13+	2	3	TR SPL 73215-19,73220-24,25,73235,73240-44,45,73255,73260-64,73275,73280-84,85 XSA
I 138-21181	811	05	22 13	2	3	MISC

Table 8.--Sequential listing within each 70 mm magazine, Apollo 17 lunar surface pictures (magazine J, black and white, 60 mm focal length)--Continued

MAG	PHOTO	SEQ	GET	EVA	STA	REMARKS
K 139-21186			06 19 05	3	6	N MASSIF
K 139-21187			06 19 05+	3	6	N MASSIF, FOGGED
K 139-21188			06 19 05+	3	6	N MASSIF
K 139-21189			06 19 05+	3	6	N MASSIF
K 139-21190			06 19 05+	3	6	N MASSIF
K 139-21191			06 19 05+	3	6	N MASSIF
K 139-21192			06 19 05+	3	6	N MASSIF
K 139-21193			06 19 05+	3	6	N MASSIF
K 139-21194			06 19 05+	3	6	TOWARD STA 3
K 139-21195			06 19 05+	3	6	BLANK
K 139-21196			06 19 05+	3	6	TOWARD STA 3
K 139-21197			06 19 05+	3	6	TOWARD STA 2
K 139-21198			06 19 05+	3	6	TOWARD STA 2
K 139-21199			06 19 05+	3	6	TOWARD STA 2
K 139-21200			06 19 05+	3	6	TOWARD STA 2
K 139-21201			06 19 05+	3	6	TOWARD STA 2
K 139-21202			06 19 05+	3	6	TOWARD STA 2
K 139-21203			06 19 05+	3	6	LM
K 139-21204			06 19 05+	3	6	LM
K 139-21205			06 19 05+	3	6	LM
K 139-21206			06 19 05+	3	6	TOWARD STA 3
K 139-21207			06 19 05+	3	6	TOWARD STA 3
K 139-21208			06 19 05+	3	6	S MASSIF
K 139-21209			06 19 05+	3	6	S MASSIF
K 139-21210			06 19 05+	3	6	S MASSIF
K 139-21211			06 19 05+	3	6	S MASSIF
K 139-21212			06 21 42+	3	9	N MASSIF
K 139-21213			06 21 42+	3	9	N MASSIF
K 139-21214			06 21 42+	3	9	N MASSIF
K 139-21215			06 21 42+	3	9	N MASSIF
K 139-21216			06 21 42+	3	9	N MASSIF
K 139-21217			06 21 42+	3	9	N MASSIF
K 139-21218			06 21 42+	3	9	N MASSIF
K 139-21219			06 21 42+	3	9	N MASSIF
K 139-21220			06 21 42+	3	9	N MASSIF
K 139-21221			06 21 42+	3	9	N MASSIF
K 139-21222			06 21 42+	3	9	N MASSIF
K 139-21223			06 21 42+	3	9	N MASSIF
K 139-21224			06 21 42+	3	9	N MASSIF
K 139-21225			06 21 42+	3	9	N MASSIF
K 139-21226			06 21 42+	3	9	N MASSIF
K 139-21227			06 21 42+	3	9	N MASSIF
K 139-21228			06 21 42+	3	9	N MASSIF
K 139-21229			06 21 42+	3	9	N MASSIF
K 139-21230			06 21 42+	3	9	BASE OF N MASSIF
K 139-21231			06 21 42+	3	9	BASE OF N MASSIF
K 139-21232			06 21 42+	3	9	BASE OF N MASSIF
K 139-21233			06 21 42+	3	9	BASE OF N MASSIF
K 139-21234			06 21 42+	3	9	BASE OF N MASSIF
K 139-21235			06 21 42+	3	9	BASE OF N MASSIF
K 139-21236			06 21 42+	3	9	BASE OF N MASSIF
K 139-21237			06 21 42+	3	9	BASE OF N MASSIF
K 139-21238			06 21 42+	3	9	BASE OF N MASSIF
K 139-21239			06 21 42+	3	9	E OF N MASSIF
K 139-21240			06 21 42+	3	9	E OF N MASSIF
K 139-21241			06 21 42+	3	9	E OF N MASSIF
K 139-21242			06 21 42+	3	9	E OF N MASSIF
K 139-21243			06 21 42+	3	9	E OF N MASSIF
K 139-21244			06 21 42+	3	9	E OF N MASSIF
K 139-21245			06 21 42+	3	9	E OF N MASSIF
K 139-21246			06 21 42+	3	9	E OF N MASSIF
K 139-21247			06 21 42+	3	9	E OF N MASSIF
K 139-21248			06 21 42+	3	9	E OF N MASSIF
K 139-21249			06 21 42+	3	9	BOULDER TRACKS ON N MASSIF
K 139-21250			06 21 42+	3	9	BOULDER TRACKS ON N MASSIF
K 139-21251			06 21 42+	3	9	BOULDER TRACKS ON N MASSIF
K 139-21252			06 21 42+	3	9	BOULDER TRACKS ON N MASSIF
K 139-21253			06 21 42+	3	9	BOULDER TRACKS ON N MASSIF
K 139-21254			06 21 42+	3	9	BOULDER TRACKS ON N MASSIF
K 139-21255			06 21 42+	3	9	BOULDER TRACKS ON N MASSIF
K 139-21256			06 21 42+	3	9	BOULDER TRACKS ON N MASSIF
K 139-21257			06 21 42+	3	9	BOULDER TRACKS ON N MASSIF
K 139-21258			06 21 42+	3	9	BOULDER TRACKS ON N MASSIF
K 139-21259			06 21 42+	3	9	BOULDER TRACKS ON N MASSIF
K 139-21260			06 21 42+	3	9	BOULDER TRACKS ON N MASSIF
K 139-21261			06 21 42+	3	9	BOULDER TRACKS ON N MASSIF
K 139-21262			06 21 42+	3	9	BOULDER TRACKS ON N MASSIF
K 139-21263			06 21 42+	3	9	BOULDER TRACKS ON N MASSIF
K 139-21264			06 21 42+	3	9	BOULDER TRACKS ON N MASSIF
K 139-21265			06 21 42+	3	9	BOULDER TRACKS ON N MASSIF
K 139-21266			06 21 42+	3	9	BOULDER TRACKS ON N MASSIF
K 139-21267			06 21 42+	3	9	BOULDER TRACKS ON N MASSIF
K 139-21268			06 21 42+	3	9	BOULDER TRACKS ON N MASSIF
K 139-21269			06 21 42+	3	9	BLANK
K 139-21270			06 21 42+	3	9	BLANK
K 139-21271			06 21 42+	3	9	BLANK
K 139-21272			06 21 42+	3	9	BLANK
K 139-21273			06 21 42+	3	9	BLANK
K 139-21274			06 21 42+	3	9	BLANK
K 139-21275			06 21 42+	3	9	BLANK
K 139-21276			06 21 42+	3	9	BLANK
K 139-21277 -			21350	+		ORBIT

Table 8.--*Sequential listing within each 70 mm magazine, Apollo 17 lunar surface pictures (magazine J, black and white, 60 mm focal length)--Continued*

MAG	PHOTO	SEQ	GET	EVA	STA	REMARKS
E 140-21351		1100		2-3	LM	BLANK
E 140-21352		1101		2-3	LM	LM WINDOW PAN
E 140-21353		1102		2-3	LM	LM WINDOW PAN
E 140-21354		1103		2-3	LM	LM WINDOW PAN
E 140-21355		1104		2-3	LM	LM WINDOW PAN
E 140-21356		1105		2-3	LM	LM WINDOW PAN
E 140-21357		1106		2-3	LM	LM WINDOW PAN
E 140-21358		1107		2-3	LM	LM WINDOW PAN
E 140-21359		1108	06 17 18	3	LM	PAN W OF LM
E 140-21360		1109	06 17 18+	3	LM	PAN W OF LM
E 140-21361		1110	06 17 18+	3	LM	PAN W OF LM
E 140-21362		1111	06 17 18+	3	LM	PAN W OF LM
E 140-21363		1112	06 17 18+	3	LM	PAN W OF LM
E 140-21364		1113	06 17 18+	3	LM	PAN W OF LM
E 140-21365		1114	06 17 18+	3	LM	PAN W OF LM
E 140-21366		1115	06 17 18+	3	LM	PAN W OF LM
E 140-21367		1116	06 17 18+	3	LM	PAN W OF LM
E 140-21368		1117	06 17 18+	3	LM	PAN W OF LM
E 140-21369		1118	06 17 18+	3	LM	PAN W OF LM
E 140-21370		1119	06 17 18+	3	LM	PAN W OF LM
E 140-21371		1120	06 17 18+	3	LM	PAN W OF LM
E 140-21372		1121	06 17 18+	3	LM	PAN W OF LM
E 140-21373		1122	06 17 18+	3	LM	PAN W OF LM
E 140-21374		1123	06 17 18+	3	LM	PAN W OF LM
E 140-21375		1124	06 17 18+	3	LM	PAN W OF LM
E 140-21376		1125	06 17 18+	3	LM	PAN W OF LM
E 140-21377		1126	06 17 18+	3	LM	PAN W OF LM
E 140-21378		1127	06 17 18+	3	LM	PAN W OF LM
E 140-21379		1128	06 17 18+	3	LM	PAN W OF LM
E 140-21380		1129	06 17 18+	3	LM	PAN W OF LM
E 140-21381		1130	06 17 20	3	LM	COSMIC RAY, SPL 70011 XSB
E 140-21382		1131	06 17 20+	3	LM	COSMIC RAY, SPL 70011 XSB
E 140-21383		1132	06 17 20+	3	LM	COSMIC RAY
E 140-21384		1133	06 17 20+	3	LM	COSMIC RAY
E 140-21385		1134	06 17 20+	3	LM	CDR, FLAG, LRV
E 140-21386		1135	06 17 20+	3	LM	CDR, FLAG, LRV
E 140-21387		1136	06 17 20+	3	LM	CDR, FLAG, LRV
E 140-21388		1137	06 17 20+	3	LM	CDR, FLAG, LRV
E 140-21389		1138	06 17 20+	3	LM	CDR, FLAG, LRV
E 140-21390		1139	06 17 20+	3	LM	CDR, FLAG, LRV
E 140-21391		1140	06 17 20+	3	LM	CDR, FLAG, LRV
E 140-21392		1176	06 17 52+	3	SEP-6	SPL 76120-24, STEREO OF 141-21544
E 140-21393		1192	06 17 52+	3	SEP-6	
E 140-21394		1195	06 17 52+	3	SEP-6	
E 140-21395		1198	06 17 52+	3	SEP-6	
E 140-21396		1202	06 18 02	3	SEP-6	SPL 76131-34,35-37, STEREO OF 141-21566
E 140-21397		1203	06 18 02+	3	SEP-6	SPL 76131-34,35-37
E 140-21398		1204	06 18 02+	3	SEP-6	SPL 76131-34,35-37
E 140-21399		1205	06 18 02+	3	SEP-6	
E 140-21400		1214	06 18 11	3	6	MISC
E 140-21401		1246	06 18 25	3	6	SPL 76240-44,45-46,76260-64,65,76280-84,85-86 XS
E 140-21402		1247	06 18 25+	3	6	SPL 76240-44,45-46,76260-64,65,76280-84,85-86 XS
E 140-21403		1248	06 18 25+	3	6	SPL 76240-44,45-46,76260-64,65,76280-84,85-86 XS
E 140-21404		1249	06 18 25+	3	6	SPL 76240-44,45-46,76260-64,65,76280-84,85-86 XS
E 140-21405		1250	06 18 25+	3	6	SPL 76240-44,45-46,76260-64,65,76280-84,85-86 XS
E 140-21406		1251	06 18 25+	3	6	SPL 76240-44,45-46,76260-64,65,76280-84,85-86 XS
E 140-21407		1252	06 18 25+	3	6	SPL 76240-44,45-46,76260-64,65,76280-84,85-86 XS
E 140-21408		1253	06 18 25+	3	6	SPL 76240-44,45-46,76260-64,65,76280-84,85-86 XS
E 140-21409		1254	06 18 29	3	6	SPL 76240-44,45-46,76260-64,65,76280-84,85-86 LOC
E 140-21410		1257	06 18 26	3	6	SPL 76215 XSB
E 140-21411		1258	06 18 26	3	6	SPL 76015 XSB
E 140-21412		1259	06 18 26	3	6	SPL 76015,76215 LOC
E 140-21413		1260	06 18 26	3	6	SPL 76015 XSA
E 140-21414		1261	06 18 36	3	6	F-L OF BOULDER
E 140-21415		1262	06 18 36+	3	6	F-L OF BOULDER
E 140-21416		1263	06 18 36+	3	6	F-L OF BOULDER
E 140-21417		1264	06 18 36+	3	6	F-L OF BOULDER
E 140-21418		1265	06 18 36+	3	6	F-L OF BOULDER
E 140-21419		1266	06 18 36+	3	6	F-L OF BOULDER
E 140-21420		1267	06 18 36+	3	6	F-L OF BOULDER, SPL 76215 XSB
E 140-21421		1268	06 18 36+	3	6	F-L OF BOULDER, SPALLED AREA
E 140-21422		1269	06 18 36+	3	6	F-L OF BOULDER, SPL 76215 XSB
E 140-21423		1270	06 18 36+	3	6	F-L OF BOULDER, SPALLED AREA
E 140-21424		1271	06 18 36+	3	6	F-L OF BOULDER, SPL 76215 XSB
E 140-21425		1272	06 18 36+	3	6	F-L OF BOULDER
E 140-21426		1273	06 18 36+	3	6	F-L OF BOULDER
E 140-21427		1274	06 18 36+	3	6	F-L OF BOULDER
E 140-21428		1275	06 18 36+	3	6	F-L OF BOULDER
E 140-21429		1276	06 18 36+	3	6	F-L OF BOULDER
E 140-21430		1277	06 18 36+	3	6	F-L OF BOULDER
E 140-21431		1278	06 18 36+	3	6	F-L OF BOULDER
E 140-21432		1279	06 18 36+	3	6	F-L OF BOULDER
E 140-21433		1280	06 18 36+	3	6	F-L OF BOULDER
E 140-21434		1281	06 18 36+	3	6	F-L OF BOULDER
E 140-21435		1282	06 18 36+	3	6	F-L OF BOULDER, SPL 76315 XSB
E 140-21436		1283	06 18 36+	3	6	F-L OF BOULDER, SPL 76315 XSB
E 140-21437		1284	06 18 36+	3	6	F-L OF BOULDER, SPL 76315 XSB
E 140-21438		1285	06 18 36+	3	6	F-L OF BOULDER, SPL 76315 XSB
E 140-21439		1286	06 18 36+	3	6	F-L OF BOULDER, SPL 76315 XSB
E 140-21440		1287	06 18 36+	3	6	F-L OF BOULDER

Table 8.--Sequential listing within each 70 mm magazine, Apollo 17 lunar surface pictures (magazine J, black and white, 60 mm focal length)--Continued

MAG	PHOTO	SEQ	GET	EVA	STA	REMARKS
E 140-21441	1291	06 18 38+	3	6	SPL 76235-39,76255,76275,76295,76305-07 XSB	
E 140-21442	1302	06 18 49	3	6	CU 6 F-L OF SPL 76315,76320-24 BOULDER	
E 140-21443	1303	06 18 49+	3	6	CU 6 F-L OF SPL 76315,76320-24 BOULDER	
E 140-21444	1304	06 18 49+	3	6	CU 6 F-L OF SPL 76315,76320-24 BOULDER, SPL 75235-39,76305-07 XSB	
E 140-21445	1305	06 18 49+	3	6	CU 6 F-L OF SPL 76315,76320-24 BOULDER, SPL 75235-39,76305-07 XSB	
E 140-21446	1306	06 18 49+	3	6	CU 6 F-L OF SPL 76315,76320-24 BOULDER	
E 140-21447	1307	06 18 49+	3	6	CU 6 F-L OF SPL 76315,76320-24 BOULDER, SPL 76255 XSB	
E 140-21448	1308	06 18 49+	3	6	CU 6 F-L OF SPL 76315,76320-24 BOULDER, SPL 76255 XSB	
E 140-21449	1309	06 18 49+	3	6	CU 6 F-L OF SPL 76315,76320-24 BOULDER, SPL 76255 XSB	
E 140-21450	1310	06 18 49+	3	6	CU 6 F-L OF SPL 76315,76320-24 BOULDER	
E 140-21451	1311	06 18 49+	3	6	CU 6 F-L OF SPL 76315,76320-24 BOULDER	
E 140-21452	1312	06 18 49+	3	6	CU 6 F-L OF SPL 76315,76320-24 BOULDER, SPL 75295 XSA	
E 140-21453	1313	06 18 49+	3	6	CU 6 F-L OF SPL 76315,76320-24 BOULDER, SPL 75235-39,76255,76305-07 XSA	
E 140-21454	1314	06 18 49+	3	6	CU 6 F-L OF SPL 76315,76320-24 BOULDER, SPL 75235-39,76305-07 XSA	
E 140-21455	1315	06 18 49+	3	6	CU 6 F-L OF SPL 76315,76320-24 BOULDER, SPL 75295 XSA	
E 140-21456	1316	06 18 49+	3	6	CU 6 F-L OF SPL 76315,76320-24 BOULDER, SPL 76255,76275 XSA	
E 140-21457	1317	06 18 49+	3	6	CU 6 F-L OF SPL 76315,76320-24 BOULDER, SPL 75295 XSA	
E 140-21458	1318	06 18 49+	3	6	CU 6 F-L OF SPL 76315,76320-24 BOULDER, SPL 76255,76275 XSA	
E 140-21459	1319	06 18 49+	3	6	CU 6 F-L OF SPL 76315,76320-24 BOULDER, SPL 75255,76275 XSA	
E 140-21460	1320	06 18 49+	3	6	CU 6 F-L OF SPL 76315,76320-24 BOULDER	
E 140-21461	1321	06 18 49+	3	6	CU 6 F-L OF SPL 76315,76320-24 BOULDER	
E 140-21462	1322	06 18 49+	3	6	CU 6 F-L OF SPL 76315,76320-24 BOULDER	
E 140-21463	1323	06 18 49+	3	6	CU 6 F-L OF SPL 76315,76320-24 BOULDER	
E 140-21464	1324	06 18 49+	3	6	CU 6 F-L OF SPL 76315,76320-24 BOULDER	
E 140-21465	1325	06 18 49+	3	6	CU 6 F-L OF SPL 76315,76320-24 BOULDER	
E 140-21466	1326	06 18 49+	3	6	CU 6 F-L OF SPL 76315,76320-24 BOULDER	
E 140-21467	1327	06 18 49+	3	6	CU 6 F-L OF SPL 76315,76320-24 BOULDER	
E 140-21468	1328	06 18 49+	3	6	CU 6 F-L OF SPL 76315,76320-24 BOULDER	
E 140-21469	1329	06 18 49+	3	6	CU 6 F-L OF SPL 76315,76320-24 BOULDER	
E 140-21470	1330	06 18 49+	3	6	CU 6 F-L OF SPL 76315,76320-24 BOULDER	
E 140-21471	1331	06 18 49+	3	6	CU 6 F-L OF SPL 76315,76320-24 BOULDER	
E 140-21472	1332	06 18 49+	3	6	CU 6 F-L OF SPL 76315,76320-24 BOULDER	
E 140-21473	1333	06 18 49+	3	6	CU 6 F-L OF SPL 76315,76320-24 BOULDER	
E 140-21474	1334	06 18 49+	3	6	CU 6 F-L OF SPL 76315,76320-24 BOULDER, SPL 75320-24 XSB	
E 140-21475	1335	06 18 49+	3	6	CU 6 F-L OF SPL 76315,76320-24 BOULDER	
E 140-21476	1336	06 18 49+	3	6	CU 6 F-L OF SPL 76315,76320-24 BOULDER	
E 140-21477	1337	06 18 49+	3	6	CU 6 F-L OF SPL 76315,76320-24 BOULDER	
E 140-21478	1338	06 18 49+	3	6	CU 6 F-L OF SPL 76315,76320-24 BOULDER	
E 140-21479	1339	06 18 49+	3	6	CU 6 F-L OF SPL 76315,76320-24 BOULDER	
E 140-21480	1340	06 18 49+	3	6	CU 6 F-L OF SPL 76315,76320-24 BOULDER, SPL 75295 XSA	
E 140-21481	1341	06 18 49+	3	6	CU 6 F-L OF SPL 76315,76320-24 BOULDER	
E 140-21482	1342	06 18 50	3	6	CU 6 F-L OF SPL 76315,76320-24 BOULDER, SPL 76320-24 XSA	
E 140-21483	1343	06 18 54	3	6	PAN	
E 140-21484	1344	06 18 54+	3	6	PAN	
E 140-21485	1345	06 18 54+	3	6	PAN	
E 140-21486	1346	06 18 54+	3	6	PAN	
E 140-21487	1347	06 18 54+	3	6	PAN	
E 140-21488	1348	06 18 54+	3	6	PAN	
E 140-21489	1349	06 18 54+	3	6	PAN	
E 140-21490	1350	06 18 54+	3	6	PAN	
E 140-21491	1351	06 18 54+	3	6	PAN	
E 140-21492	1352	06 18 54+	3	6	PAN	
E 140-21493	1353	06 18 54+	3	6	PAN	
E 140-21494	1354	06 18 54+	3	6	PAN	
E 140-21495	1355	06 18 54+	3	6	PAN	
E 140-21496	1356	06 18 54+	3	6	PAN	
E 140-21497	1357	06 18 54+	3	6	PAN	
E 140-21498	1358	06 18 54+	3	6	PAN	
E 140-21499	1359	06 18 54+	3	6	PAN	
E 140-21500	1360	06 18 54+	3	6	PAN	
E 140-21501	1361	06 18 54+	3	6	PAN	
E 140-21502	1362	06 18 54+	3	6	PAN	
E 140-21503	1363	06 18 54+	3	6	PAN	
E 140-21504	1364	06 18 54+	3	6	PAN	
E 140-21505	1365	06 18 54+	3	6	PAN	
E 140-21506	1366	06 18 54+	3	6	PAN	
E 140-21507	1367	06 18 54+	3	6	PAN	
E 140-21508	1368	06 18 54+	3	6	PAN	
E 140-21509	1369	06 18 55	3	6	PAN	

Table 8.--Sequential listing within each 70 mm magazine, Apollo 17 lunar surface pictures (magazine J, black and white, 60 mm focal length)--Continued

MAG	PHOTO	SEQ	GET	EVA	STA	REMARKS
L 141-21510	1141	06 17 36	3	SEP	SEP XS	
L 141-21511	1142	06 17 36+	3	SEP	SEP XS	
L 141-21512	1143	06 17 36+	3	SEP	PPAN OF SEP (RIGHT)	
L 141-21513	1144	06 17 36+	3	SEP	PPAN OF SEP (RIGHT)	
L 141-21514	1145	06 17 36+	3	SEP	PPAN OF SEP (RIGHT)	
L 141-21515	1146	06 17 36+	3	SEP	PPAN OF SEP (LEFT)	
L 141-21516	1147	06 17 36+	3	SEP	PPAN OF SEP (LEFT)	
L 141-21517	1148	06 17 36+	3	SEP	PPAN OF SEP (LEFT)	
L 141-21518	1149	06 17 40	3	SEP-6		
L 141-21519	1150	06 17 40+	3	SEP-6		
L 141-21520	1151	06 17 40+	3	SEP-6		
L 141-21521	1152	06 17 40+	3	SEP-6		
L 141-21522	1153	06 17 40+	3	SEP-6		
L 141-21523	1154	06 17 40+	3	SEP-6		
L 141-21524	1155	06 17 40+	3	SEP-6		
L 141-21525	1156	06 17 40+	3	SEP-6		
L 141-21526	1157	06 17 40+	3	SEP-6		
L 141-21527	1158	06 17 40+	3	SEP-6		
L 141-21528	1159	06 17 40+	3	SEP-6		
L 141-21529	1160	06 17 40+	3	SEP-6		
L 141-21530	1161	06 17 40+	3	SEP-6		
L 141-21531	1162	06 17 40+	3	SEP-6		
L 141-21532	1163	06 17 40+	3	SEP-6		
L 141-21533	1164	06 17 40+	3	SEP-6		
L 141-21534	1165	06 17 40+	3	SEP-6		
L 141-21535	1166	06 17 40+	3	SEP-6		
L 141-21536	1167	06 17 40+	3	SEP-6		
L 141-21537	1168	06 17 40+	3	SEP-6		
L 141-21538	1169	06 17 40+	3	SEP-6		
L 141-21539	1170	06 17 40+	3	SEP-6		
L 141-21540	1171	06 17 40+	3	SEP-6		
L 141-21541	1172	06 17 40+	3	SEP-6		
L 141-21542	1173	06 17 52	3	SEP-6	SPL 76120-28	
L 141-21543	1174	06 17 52+	3	SEP-6	SPL 76120-28	
L 141-21544	1175	06 17 52+	3	SEP-6	SPL 76120-24, STEREO OF 140-21392	
L 141-21545	1177	06 17 52+	3	SEP-6		
L 141-21546	1178	06 17 52+	3	SEP-6		
L 141-21547	1179	06 17 52+	3	SEP-6		
L 141-21548	1180	06 17 52+	3	SEP-6		
L 141-21549	1181	06 17 52+	3	SEP-6		
L 141-21550	1182	06 17 52+	3	SEP-6		
L 141-21551	1183	06 17 52+	3	SEP-6		
L 141-21552	1184	06 17 52+	3	SEP-6		
L 141-21553	1185	06 17 52+	3	SEP-6		
L 141-21554	1186	06 17 52+	3	SEP-6		
L 141-21555	1187	06 17 52+	3	SEP-6		
L 141-21556	1188	06 17 52+	3	SEP-6		
L 141-21557	1189	06 17 52+	3	SEP-6		
L 141-21558	1190	06 17 52+	3	SEP-6		
L 141-21559	1191	06 17 52+	3	SEP-6		
L 141-21560	1193	06 17 52+	3	SEP-6		
L 141-21561	1194	06 17 52+	3	SEP-6		
L 141-21562	1196	06 17 52+	3	SEP-6		
L 141-21563	1197	06 17 52+	3	SEP-6		
L 141-21564	1199	06 17 52+	3	SEP-6		
L 141-21565	1200	06 17 52+	3	SEP-6		
L 141-21566	1201	06 17 52+	3	SEP-6	SPL 76131-34,35-37, STEREO OF 140-21396	
L 141-21567	1206	06 18 02+	3	SEP-6	SPL 76131-34,35-37, TURNING PT ROCK, LM	
L 141-21568	1207	06 18 02+	3	SEP-6	SPL 76131-34,35-37, TURNING PT ROCK, LM	
L 141-21569	1208	06 18 02+	3	SEP-6		
L 141-21570	1209	06 18 02+	3	SEP-6		
L 141-21571	1210	06 18 02+	3	SEP-6		
L 141-21572	1211	06 18 02+	3	SEP-6		
L 141-21573	1212	06 18 02+	3	SEP-6		
L 141-21574	1213	06 18 02+	3	SEP-6		
L 141-21575	1215	06 19 18	3	6	PAN	
L 141-21576	1216	06 19+18	3	6	PAN	
L 141-21577	1217	06 19+18	3	6	PAN	
L 141-21578	1218	06 19+18	3	6	PAN	
L 141-21579	1219	06 19+18	3	6	PAN	
L 141-21580	1220	06 19+18	3	6	PAN	
L 141-21581	1221	06 19+18	3	6	PAN	
L 141-21582	1222	06 19+18	3	6	PAN	
L 141-21583	1223	06 19+18	3	6	PAN	
L 141-21584	1224	06 19+18	3	6	PAN	
L 141-21585	1225	06 19+18	3	6	PAN	
L 141-21586	1226	06 19+18	3	6	PAN	
L 141-21587	1227	06 19+18	3	6	PAN	
L 141-21588	1228	06 19+18	3	6	PAN	
L 141-21589	1229	06 19+18	3	6	PAN	
L 141-21590	1230	06 19+18	3	6	PAN	
L 141-21591	1231	06 19+18	3	6	PAN	
L 141-21592	1232	06 19+18	3	6	PAN	
L 141-21593	1233	06 19+18	3	6	PAN	
L 141-21594	1234	06 19+18	3	6	PAN	
L 141-21595	1235	06 19+18	3	6	PAN	
L 141-21596	1236	06 19+18	3	6	PAN	
L 141-21597	1237	06 19+18	3	6	PAN	
L 141-21598	1238	06 19+18	3	6	PAN	
L 141-21599	1239	06 19+18	3	6	PAN	

Table 8.--*Sequential listing within each 70 mm magazine, Apollo 17 lunar surface pictures (magazine J, black and white, 60 mm focal length)--Continued*

MAG	PHOTO	SEQ	GET	EVA	STA	REMARKS
L 141-21600	1240	06 19+18	3	6		PAN
L 141-21601	1241	06 19+18	3	6		PAN
L 141-21602	1242	06 19+18	3	6		PAN
L 141-21603	1243	06 20 18	3	6		PAN
L 141-21604	1244	06 18 21	3	6		SPL 76240-44,45-46,76260-64,65,76280-84,85-85 DSB, LJC
L 141-21605	1245	06 18 21	3	6		SPL 76240-44,45-46,76260-64,65,76280-84,85-85 DSB, LJC
L 141-21606	1255	06 18 29+	3	6		SPL 76240-44,45-46,76260-64,65,76280-84,85-85 DSA, LJC
L 141-21607	1256	06 18 26	3	6		SPL 76015,76215 DSB
L 141-21608	1288	06 18 38	3	6		SPL 76215,76235-39,76305-07 XSB
L 141-21609	1289	06 18 38+	3	6		SPL 76235-39,76255,76275,76295,76305-07 XSB
L 141-21610	1299	06 18 38+	3	6		SPL 76235-39,76255,76275,76295,76305-07,76320* LJC
L 141-21611	1292	06 18 38+	3	6		CU SPL 76235-39,76305-07 AREA
L 141-21612	1293	06 18 38+	3	6		CU SPL 76235-39,76305-07 AREA
L 141-21613	1294	06 18 38+	3	6		CU
L 141-21614	1295	06 18 38+	3	6		CU
L 141-21615	1296	06 18 48	3	6		SPL 76255,76275 XSB
L 141-21616	1297	06 18 48+	3	6		SPL 76315 XSA
L 141-21617	1298	06 18 48+	3	6		SPL 76315 XSA
L 141-21618	1299	06 18 48+	3	6		SPL 76315 XSA
L 141-21619	1300	06 18 48+	3	6		SPL 76315 XSA
L 141-21620	1301	06 18 48+	3	6		SPL 76315 XSA
L 141-21621	1370	06 18 55+	3	6		SPL 76500-05,06,76535-39,45-49,55-59,65-69,75-77 XSB
L 141-21622	1371	06 18 55+	3	6		SPL 76500-05,06,76535-39,45-49,55-59,65-69,75-77 XSB
L 141-21623	1372	06 18 55+	3	6		SPL 76500-05,06,76535-39,45-49,55-59,65-69,75-77 XSB
L 141-21624	1373	06 18 55+	3	6		SPL 76500-05,06,76535-39,45-49,55-59,65-69,75-77 DSB
L 141-21625	1374	06 19 01	3	6		SPL 76500-05,06,76535-39,45-49,55-59,65-69,75-77 XSA
L 141-21626	1375	06 19 01+	3	6		SPL 76500-05,06,76535-39,45-49,55-59,65-69,75-77 XSA
L 141-21627	1376	06 19 01+	3	6		SPL 76500-05,06,76535-39,45-49,55-59,65-69,75-77 XSA
L 141-21628	1386	06 19 08+	3	6		F-L OF BOULDER US
L 141-21629	1387	06 19 08+	3	6		F-L OF BOULDER US
L 141-21630	1388	06 19 08+	3	6		F-L OF BOULDER US
L 141-21631	1389	06 19 08+	3	6		F-L OF BOULDER XS
L 141-21632	1390	06 19 08+	3	6		F-L OF BOULDER XS
L 141-21633	1391	06 19 08+	3	6		F-L OF BOULDER XS
L 141-21634	1392	06 19 08+	3	6		F-L OF BOULDER XS
L 141-21635	1393	06 19 10	3	6		DS
L 141-21636	1394	06 19 10+	3	6		DS
L 141-21637	1395	06 19 25	3	6-7		
L 141-21638	1396	06 19 25+	3	6-7		
L 141-21639	1397	06 19 25+	3	6-7		
L 141-21640	1398	06 19 25+	3	6-7		
L 141-21641	1399	06 19 25+	3	6-7		
L 141-21642	1400	06 19 25+	3	6-7		
L 141-21643	1401	06 19 25+	3	6-7		
L 141-21644	1402	06 19 25+	3	6-7		
L 141-21645	1403	06 19 25+	3	6-7		
L 141-21646	1404	06 19 30	3	7		PAN, NEAR FIELD ONLY (11 FT FOCUS)
L 141-21647	1405	06 19 30+	3	7		PAN, NEAR FIELD ONLY (11 FT FOCUS)
L 141-21648	1406	06 19 30+	3	7		PAN, NEAR FIELD ONLY (11 FT FOCUS)
L 141-21649	1407	06 19 30+	3	7		PAN, NEAR FIELD ONLY (11 FT FOCUS)
L 141-21650	1408	06 19 30+	3	7		PAN, NEAR FIELD ONLY (11 FT FOCUS)
L 141-21651	1409	06 19 30+	3	7		PAN, NEAR FIELD ONLY (11 FT FOCUS)
L 141-21652	1410	06 19 30+	3	7		PAN, NEAR FIELD ONLY (11 FT FOCUS)
L 141-21653	1411	06 19 30+	3	7		PAN, NEAR FIELD ONLY (11 FT FOCUS)
L 141-21654	1412	06 19 30+	3	7		PAN, NEAR FIELD ONLY (11 FT FOCUS)
L 141-21655	1413	06 19 30+	3	7		PAN, NEAR FIELD ONLY (11 FT FOCUS)
L 141-21656	1414	06 19 30+	3	7		PAN, NEAR FIELD ONLY (11 FT FOCUS)
L 141-21657	1415	06 19 30+	3	7		PAN, NEAR FIELD ONLY (11 FT FOCUS)
L 141-21658	1416	06 19 30+	3	7		PAN, NEAR FIELD ONLY (11 FT FOCUS)
L 141-21659	1417	06 19 30+	3	7		PAN, NEAR FIELD ONLY (11 FT FOCUS)
L 141-21660	1418	06 19 30+	3	7		PAN, NEAR FIELD ONLY (11 FT FOCUS)
L 141-21661	1419	06 19 30+	3	7		PAN, NEAR FIELD ONLY (11 FT FOCUS)
L 141-21662	1420	06 19 30+	3	7		PAN, NEAR FIELD ONLY (11 FT FOCUS)
L 141-21663	1421	06 19 30+	3	7		PAN, NEAR FIELD ONLY (11 FT FOCUS)
L 141-21664	1422	06 19 30+	3	7		PAN, NEAR FIELD ONLY (11 FT FOCUS)
L 141-21665	1423	06 19 30+	3	7		PAN, NEAR FIELD ONLY (11 FT FOCUS)
L 141-21666	1424	06 19 30+	3	7		PAN, NEAR FIELD ONLY (11 FT FOCUS)
L 141-21667	1425	06 19 30+	3	7		PAN, NEAR FIELD ONLY (11 FT FOCUS)

Table 8.--Sequential listing within each 70 mm magazine, Apollo 17 lunar surface pictures (magazine J, black and white, 60 mm focal length)--Continued

MAG	PHOTO	SEQ	GET	EVA	STA	REMARKS
M 142-21669	1492			3		FOGGBD
M 142-21670	1493			3		NISC
M 142-21671	1494	06 19 52	3		7-8	
M 142-21672	1495	06 19 52+	3		7-8	
M 142-21673	1496	06 19 52+	3		7-8	
M 142-21674	1497	06 19 52+	3		7-8	
M 142-21675	1498	06 19 52+	3		7-8	
M 142-21676	1499	06 19 52+	3		7-8	
M 142-21677	1500	06 19 52+	3		7-8	
M 142-21678	1501	06 19 52+	3		7-8	
M 142-21679	1502	06 19 52+	3		7-8	
M 142-21680	1503	06 19 52+	3		7-8	
M 142-21681	1504	06 19 52+	3		7-8	
M 142-21682	1505	06 19 52+	3		7-8	
M 142-21683	1507	06 19 52+	3		7-8	
M 142-21684	1508	06 19 52+	3		7-8	
M 142-21685	1509	06 19 52+	3		7-8	
M 142-21686	1510	06 19 52+	3		7-8	
M 142-21687	1511	06 19 52+	3		7-8	
M 142-21688	1512	06 19 52+	3		7-8	
M 142-21689	1513	06 19 52+	3		7-8	
M 142-21690	1514	06 19 52+	3		7-8	
M 142-21691	1515	06 19 52+	3		7-8	
M 142-21692	1516	06 20 03	3		7-8	SPL 78120-247
M 142-21693	1517	06 20 03+	3		7-8	SPL 78120-247
M 142-21694	1518	06 20 03+	3		7-8	SPL 78120-247
M 142-21695	1519	06 20 03+	3		7-8	SPL 78120-247
M 142-21696	1520	06 20 03+	3		7-8	SPL 78120-247
M 142-21697	1521	06 20 03+	3		7-8	
M 142-21698	1526	06 20 14	3		8	SPL 78230-34, 35-36, 38 XSB
M 142-21699	1527	06 20 14+	3		8	SPL 78230-34, 35-36, 38 XSB
M 142-21700	1528	06 20 14+	3		8	SPL 78230-34, 35-36, 38 XSB
M 142-21701	1529	06 20 14+	3		8	SPL 78230-34, 35-36, 38 DSB
M 142-21702	1530	06 20 14+	3		8	SPL 78230-34, 35-36, 38 LOC
M 142-21703	1531	06 20 16	3		8	SPL 78230-34, 35-36, 38 DSB
M 142-21704	1532	06 20 17	3		8	SPL 78220-24 XS
M 142-21705	1533	06 20 17+	3		8	SPL 78220-24 XS
M 142-21706	1564	06 20 32	3		8	SPL 78155, 78500-04, 05-09, 15-18, 78535-39, 45-49, 55-59, 65-69, 75-79, 85-89, 95-99 XSB F-L
M 142-21707	1565	06 20 32+	3		8	SPL 78155, 78500-04, 05-09, 15-18, 78535-39, 45-49, 55-59, 65-69, 75-79, 85-89, 95-99 XSB F-L
M 142-21708	1566	06 20 32+	3		8	SPL 78155, 78500-04, 05-09, 15-18, 78535-39, 45-49, 55-59, 65-69, 75-79, 85-89, 95-99 XSB F-L
M 142-21709	1567	06 20 32+	3		8	SPL 78155, 78500-04, 05-09, 15-18, 78535-39, 45-49, 55-59, 65-69, 75-79, 85-89, 95-99 DSB F-L
M 142-21710	1568	06 20 32+	3		8	SPL 78155, 78500-04, 05-09, 15-18, 78535-39, 45-49, 55-59, 65-69, 75-79, 85-89, 95-99 DSB F-L
M 142-21711	1569	06 20 32+	3		8	SPL 78155, 78500-04, 05-09, 15-18, 78535-39, 45-49, 55-59, 65-69, 75-79, 85-89, 95-99 DSB F-L
M 142-21712	1570	06 20 32+	3		8	SPL 78155, 78500-04, 05-09, 15-18, 78535-39, 45-49, 55-59, 65-69, 75-79, 85-89, 95-99 XSB F-L
M 142-21713	1571	06 20 32+	3		8	SPL 78155, 78500-04, 05-09, 15-18, 78535-39, 45-49, 55-59, 65-69, 75-79, 85-89, 95-99 XSB F-L
M 142-21714	1572	06 20 32+	3		8	SPL 78155, 78500-04, 05-09, 15-18, 78535-39, 45-49, 55-59, 65-69, 75-79, 85-89, 95-99 XSB F-L
M 142-21715	1573	06 20 32+	3		8	SPL 78155, 78500-04, 05-09, 15-18, 78535-39, 45-49, 55-59, 65-69, 75-79, 85-89, 95-99 XSB F-L
M 142-21716	1574	06 20 34	3		8	SPL 78155, 78500-04, 05-09, 15-18, 78535-39, 45-49, 55-59, 65-69, 75-79, 85-89, 95-99 XSB F-L
M 142-21717	1580	06 20 42	3		8	TR SPL 78420-24, 78440-44, 78460-64, 65, 78480-84 XSB
M 142-21718	1581	06 20 42+	3		8	TR SPL 78420-24, 78440-44, 78460-64, 65, 78480-84 XSB
M 142-21719	1582	06 20 42+	3		8	TR SPL 78420-24, 78440-44, 78460-64, 65, 78480-84 DSB, LOC
M 142-21720	1583	06 20 45	3		8	TR SPL 78420-24, 78440-44, 78460-64, 65, 78480-84 XSA
M 142-21721	1584	06 20 45+	3		8	TR SPL 78420-24, 78440-44, 78460-64, 65, 78480-84 XSA
M 142-21722	1585	06 20 45+	3		8	TR SPL 78420-24, 78440-44, 78460-64, 65, 78480-84 XSA
M 142-21723	1586	06 20 45+	3		8	TR SPL 78420-24, 78440-44, 78460-64, 65, 78480-84 XSA
M 142-21724	1587	06 20 45+	3		8	TR SPL 78420-24, 78440-44, 78460-64, 65, 78480-84 XSA
M 142-21725	1588	06 20 45+	3		8	TR SPL 78420-24, 78440-44, 78460-64, 65, 78480-84 XSA
M 142-21726	1589	06 20 46	3		8	PAN
M 142-21727	1590	06 20 46+	3		8	PAN
M 142-21728	1591	06 20 46+	3		8	PAN
M 142-21729	1592	06 20 46+	3		8	PAN
M 142-21730	1593	06 20 46+	3		8	PAN
M 142-21731	1594	06 20 46+	3		8	PAN
M 142-21732	1595	06 20 46+	3		8	PAN
M 142-21733	1596	06 20 46+	3		8	PAN
M 142-21734	1597	06 20 46+	3		8	PAN
M 142-21735	1598	06 20 46+	3		8	PAN
M 142-21736	1599	06 20 46+	3		8	PAN
M 142-21737	1600	06 20 46+	3		8	PAN
M 142-21738	1601	06 20 46+	3		8	PAN
M 142-21739	1602	06 20 46+	3		8	PAN
M 142-21740	1603	06 20 46+	3		8	PAN
M 142-21741	1604	06 20 46+	3		8	PAN
M 142-21742	1605	06 20 46+	3		8	PAN
M 142-21743	1606	06 20 46+	3		8	PAN
M 142-21744	1607	06 20 46+	3		8	PAN
M 142-21745	1608	06 20 47	3		8	PAN
M 142-21746	1609	06 20 55	3		8-9	
M 142-21747	1610	06 20 55+	3		8-9	
M 142-21748	1611	06 20 55+	3		8-9	
M 142-21749	1612	06 20 55+	3		8-9	
M 142-21750	1613	06 20 55+	3		8-9	
M 142-21751	1614	06 20 55+	3		8-9	
M 142-21752	1615	06 20 55+	3		8-9	
M 142-21753	1616	06 20 55+	3		8-9	
M 142-21754	1617	06 20 55+	3		8-9	
M 142-21755	1618	06 20 55+	3		8-9	
M 142-21756	1619	06 20 55+	3		8-9	
M 142-21757	1620	06 20 55+	3		8-9	
M 142-21758	1621	06 20 55+	3		8-9	

Table 8.--*Sequential listing within each 70 mm magazine, Apollo 17 lunar surface pictures (magazine J, black and white, 60 mm focal length)--Continued*

MAG	PHOTO	SEQ	GET	EVA	STA
M 142-21759	1622	06 20 55+	3	8-9	
M 142-21760	1623	06 20 55+	3	8-9	
M 142-21761	1624	06 20 55+	3	8-9	
M 142-21762	1625	06 20 55+	3	8-9	
M 142-21763	1626	06 20 55+	3	8-9	
M 142-21764	1627	06 20 55+	3	8-9	
M 142-21765	1628	06 20 55+	3	8-9	
M 142-21766	1629	06 20 55+	3	8-9	
M 142-21767	1630	06 20 55+	3	8-9	
M 142-21768	1636	06 20 55+	3	8-9	
M 142-21769	1637	06 20 55+	3	8-9	
M 142-21770	1638	06 20 55+	3	8-9	
M 142-21771	1639	06 20 55+	3	8-9	
M 142-21772	1640	06 20 55+	3	8-9	
M 142-21773	1641	06 20 55+	3	8-9	
M 142-21774	1642	06 20 55+	3	8-9	
M 142-21775	1643	06 20 55+	3	8-9	
M 142-21776	1645	06 20 55+	3	8-9	
M 142-21777	1646	06 20 55+	3	8-9	
M 142-21778	1647	06 20 55+	3	8-9	
M 142-21779	1648	06 20 55+	3	8-9	
M 142-21780	1649	06 20 55+	3	8-9	
M 142-21781	1651	06 20 55+	3	8-9	
M 142-21782	1653	06 20 55+	3	8-9	
M 142-21783	1655	06 20 55+	3	8-9	
M 142-21784	1656	06 20 55+	3	8-9	
M 142-21785	1657	06 20 55+	3	8-9	
M 142-21786	1658	06 20 55+	3	8-9	
M 142-21787	1659	06 20 55+	3	8-9	
M 142-21788	1660	06 20 55+	3	8-9	
M 142-21789	1661	06 20 55+	3	8-9	
M 142-21790	1662	06 20 55+	3	8-9	
M 142-21791	1663	06 21 25	3	9	SPL 79115,79120-24,79135,79510-14,15-19,25-29,35-37 DSB
M 142-21792	1664	06 21 25+	3	9	SPL 79115,79120-24,79135,79510-14,15-19,25-29,35-37 LOC
M 142-21793	1665	06 21 25+	3	9	SPL 79115,79120-24,79135,79510-14,15-19,25-29,35-37 LOC
M 142-21794	1666	06 21 25+	3	9	SPL 79115,79120-24,79135,79510-14,15-19,25-29,35-37 LOC
M 142-21795	1673	06 21 35	3	9	SPL 79175,79195 DSB
M 142-21796	1674	06 21 35+	3	9	SPL 79175,79195 LOC
M 142-21797	1675	06 21 35+	3	9	SPL 79175,79195 LOC
M 142-21798	1708	06 21 42	3	9	PAN
M 142-21799	1709	06 21 42+	3	9	PAN
M 142-21800	1710	06 21 42+	3	9	PAN
M 142-21801	1711	06 21 42+	3	9	PAN
M 142-21802	1712	06 21 42+	3	9	PAN
M 142-21803	1713	06 21 42+	3	9	PAN
M 142-21804	1714	06 21 42+	3	9	PAN
M 142-21805	1715	06 21 42+	3	9	PAN
M 142-21806	1716	06 21 42+	3	9	PAN
M 142-21807	1717	06 21 42+	3	9	PAN
M 142-21808	1718	06 21 42+	3	9	PAN
M 142-21809	1719	06 21 42+	3	9	PAN
M 142-21810	1720	06 21 42+	3	9	PAN
M 142-21811	1721	06 21 42+	3	9	PAN
M 142-21812	1722	06 21 42+	3	9	PAN
M 142-21813	1723	06 21 42+	3	9	PAN
M 142-21814	1724	06 21 42+	3	9	PAN
M 142-21815	1725	06 21 42+	3	9	PAN
M 142-21816	1726	06 21 42+	3	9	PAN
M 142-21817	1727	06 21 42+	3	9	PAN
M 142-21818	1728	06 21 42+	3	9	PAN
M 142-21819	1729	06 21 42+	3	9	PAN
M 142-21820	1730	06 21 42+	3	9	PAN
M 142-21821	1731	06 21 42+	3	9	PAN
M 142-21822	1732	06 21 42+	3	9	PAN
M 142-21823	1733	06 21 42+	3	9	PAN
M 142-21824	1734	06 21 42+	3	9	PAN
M 142-21825	1735	06 21 50	3	9	SPL BAG 52Y XSB, LOC NOT RETURNED
M 142-21826	1736	06 21 50+	3	9	SPL BAG 52Y LOC NOT RETURNED
M 142-21827	1737	06 21 50+	3	9	TR SPL 79220-24,25-28,79240-44,45,79260-64,55 XSA
M 142-21828	1738	06 21 50+	3	9	TR SPL 79220-24,25-28,79240-44,45,79260-64,55 XSA
M 142-21829	1739	06 21 50+	3	9	TR SPL 79220-24,25-28,79240-44,45,79260-64,55 XSA
M 142-21830	1740	06 21 50+	3	9	MISC
M 142-21831	1741	06 21 50+	3	9	MISC
M 142-21832	1742	06 21 50+	3	9	
M 142-21833	1743	06 21 50+	3	9	

Table 8.--*Sequential listing within each 70 mm magazine, Apollo 17 lunar surface pictures (magazine J, black and white, 60 mm focal length)--Continued*

MAG	PHOTO	SEQ	GET	EVA	STA	REMARKS
N 143-21834	1744	06 22 00	3	9		FOGGED
N 143-21835	1745	06 22 00+	3	9		MISC
N 143-21836	1746	06 22 00+	3	9		PAN, DT SPL 79002/79001 LOC
N 143-21837	1747	06 22 00+	3	9		PAN, DT SPL 79002/79001, EP-5 LOC
N 143-21838	1748	06 22 00+	3	9		PAN, DT SPL 79002/79001, EP-5 LOC
N 143-21839	1749	06 22 00+	3	9		PAN
N 143-21840	1750	06 22 00+	3	9		PAN
N 143-21841	1751	06 22 00+	3	9		PAN
N 143-21842	1752	06 22 00+	3	9		PAN
N 143-21843	1753	06 22 00+	3	9		PAN
N 143-21844	1754	06 22 00+	3	9		PAN
N 143-21845	1755	06 22 00+	3	9		PAN
N 143-21846	1756	06 22 00+	3	9		PAN
N 143-21847	1757	06 22 00+	3	9		PAN
N 143-21848	1758	06 22 00+	3	9		PAN
N 143-21849	1759	06 22 00+	3	9		PAN
N 143-21850	1760	06 22 00+	3	9		PAN
N 143-21851	1761	06 22 00+	3	9		PAN
N 143-21852	1762	06 22 00+	3	9		PAN
N 143-21853	1763	06 22 00+	3	9		PAN
N 143-21854	1764	06 22 00+	3	9		PAN
N 143-21855	1765	06 22 00+	3	9		PAN
N 143-21856	1766	06 22 00+	3	9		PAN
N 143-21857	1767	06 22 00+	3	9		PAN
N 143-21858	1768	06 22 01	3	9		PAN
N 143-21859	1772	06 22 09	3	9-LM		
N 143-21860	1773	06 22 09+	3	9-LM		
N 143-21861	1774	06 22 09+	3	9-LM		
N 143-21862	1775	06 22 09+	3	9-LM		
N 143-21863	1776	06 22 09+	3	9-LM		
N 143-21864	1777	06 22 09+	3	9-LM		
N 143-21865	1778	06 22 09+	3	9-LM		
N 143-21866	1779	06 22 09+	3	9-LM		
N 143-21867	1780	06 22 09+	3	9-LM		
N 143-21868	1781	06 22 09+	3	9-LM		
N 143-21869	1782	06 22 09+	3	9-LM		
N 143-21870	1783	06 22 09+	3	9-LM		
N 143-21871	1784	06 22 09+	3	9-LM		
N 143-21872	1785	06 22 09+	3	9-LM		
N 143-21873	1786	06 22 09+	3	9-LM		
N 143-21874	1787	06 22 09+	3	9-LM		
N 143-21875	1788	06 22 09+	3	9-LM		
N 143-21876	1789	06 22 09+	3	9-LM		
N 143-21877	1790	06 22 09+	3	9-LM		
N 143-21878	1791	06 22 09+	3	9-LM		
N 143-21879	1792	06 22 09+	3	9-LM		
N 143-21880	1793	06 22 09+	3	9-LM		
N 143-21881	1794	06 22 09+	3	9-LM		
N 143-21882	1795	06 22 09+	3	9-LM		
N 143-21883	1796	06 22 09+	3	9-LM		
N 143-21884	1797	06 22 09+	3	9-LM		
N 143-21885	1798	06 22 09+	3	9-LM		
N 143-21886	1799	06 22 09+	3	9-LM		
N 143-21887	1800	06 22 09+	3	9-LM		
N 143-21888	1801	06 22 09+	3	9-LM		
N 143-21889	1802	06 22 09+	3	9-LM		
N 143-21890	1803	06 22 09+	3	9-LM		
N 143-21891	1804	06 22 09+	3	9-LM		
N 143-21892	1805	06 22 20	3	9-LM		SPL 70315,70320-24
N 143-21893	1806	06 22 20+	3	9-LM		SPL 70315,70320-24
N 143-21894	1807	06 22 20+	3	9-LM		SPL 70315,70320-24, STEREO OF 134-20455
N 143-21895	1809	06 22 20+	3	9-LM		
N 143-21896	1811	06 22 20+	3	9-LM		
N 143-21897	1812	06 22 20+	3	9-LM		
N 143-21898	1813	06 22 20+	3	9-LM		
N 143-21899	1814	06 22 20+	3	9-LM		
N 143-21900	1815	06 22 20+	3	9-LM		
N 143-21901	1816	06 22 20+	3	9-LM		
N 143-21902	1817	06 22 20+	3	9-LM		
N 143-21903	1818	06 22 20+	3	9-LM		
N 143-21904	1819	06 22 20+	3	9-LM		
N 143-21905	1820	06 22 20+	3	9-LM		
N 143-21906	1821	06 22 20+	3	9-LM		
N 143-21907	1822	06 22 20+	3	9-LM		
N 143-21908	1823	06 22 20+	3	9-LM		
N 143-21909	1824	06 22 20+	3	9-LM		
N 143-21910	1825	06 22 20+	3	9-LM		
N 143-21911	1826	06 22 20+	3	9-LM		
N 143-21912	1827	06 22 20+	3	9-LM		
N 143-21913	1828	06 22 20+	3	9-LM		
N 143-21914	1829	06 22 20+	3	9-LM		
N 143-21915	1830	06 22 20+	3	9-LM		
N 143-21916	1831	06 22 20+	3	9-LM		
N 143-21917	1832	06 22 20+	3	9-LM		
N 143-21918	1833	06 22 20+	3	9-LM		
N 143-21919	1834	06 22 20+	3	9-LM		
N 143-21920	1835	06 22 20+	3	9-LM		
N 143-21921	1836	06 22 20+	3	9-LM		
N 143-21922	1837	06 22 20+	3	9-LM		
N 143-21923	1838	06 22 20+	3	9-LM		

Table 8.--*Sequential listing within each 70 mm magazine, Apollo 17 lunar surface pictures (magazine J, black and white, 60 mm focal length)--Continued*

MAG	PHOTO	SEQ	GET	EVA	STA	REMARKS
N 143-21924	1839	06 22 32	3		9-LM	EP-2 LOC
N 143-21925	1841	06 22 35	3		9-LM	SPL 70215
N 143-21926	1842	06 22 35+	3		9-LM	SPL 70215
N 143-21927	1846	06 22 45	3		LM	SPL 70011 DSA
N 143-21928	1847	06 22 45+	3		LM	SPL 70011 DSA
N 143-21929	1848	06 22 45+	3		LM	SPL 70011 XSA
N 143-21930	1849	06 22 45+	3		LM	SPL 70011 XSA
N 143-21931	1895	06 23 39	3		RIP	LRV
N 143-21932	1896	06 23 39	3		RIP	LRV
N 143-21933	1897	06 23 39	3		RIP	LRV
N 143-21934	1898	06 23 39	3		RIP	LRV
N 143-21935	1907	06 23 49+	3		SEP	EP-3 LOC, 70035
N 143-21936	1908	06 23 49+	3		SEP	EP-3 LOC, 70035
N 143-21937	1909	06 23 49+	3		SEP	EP-3 LOC, 70035
N 143-21938	1910	06 23 49+	3		LM	E OF LM
N 143-21939	1911	06 23 49+	3		LM	E OF LM
N 143-21940	1912	06 23 49+	3		LM	E OF LM
N 143-21941	1913	06 23 49+	3		LM	LMP, FLAG
N 143-21942	1914			POST	LM	BLANK
N 143-21943	1915			POST	LM	LM WINDOW PAN
N 143-21944	1916			POST	LM	LM WINDOW PAN
N 143-21945	1917			POST	LM	LM WINDOW PAN
N 143-21946	1918			POST	LM	LM WINDOW PAN
N 143-21947	1919			POST	LM	LM WINDOW PAN
N 143-21948	1920			POST	LM	LM WINDOW PAN
N 143-21949	1921			POST	LM	LM WINDOW PAN
N 143-21950	1922			POST	LM	LM WINDOW PAN
N 143-21951	1923			POST	LM	LM WINDOW PAN
N 143-21952	1924			POST	LM	LM WINDOW PAN
N 143-21953	1925			POST	LM	LM WINDOW PAN
N 143-21954	1926			POST	LM	LM WINDOW PAN
N 143-21955	1927			POST	LM	LM WINDOW PAN
N 143-21956	1928			POST	LM	LM WINDOW PAN
N 143-21957	1929			POST	LM	LM WINDOW PAN
N 143-21958	1930			POST	LM	LM WINDOW PAN
N 143-21959	1931			POST	LM	LM WINDOW PAN
N 143-21960	1932			POST	LM	LM WINDOW PAN
N 143-21961	1933			POST	LM	LM WINDOW PAN
N 143-21962	1934			POST	LM	LM WINDOW PAN
N 143-21963	1935			POST	LM	LM WINDOW PAN
N 143-21964	1936			POST	LM	LM WINDOW PAN
N 143-21965	1937			POST	LM	LM WINDOW PAN
N 143-21966	1938			POST	LM	LM WINDOW PAN
N 143-21967	1939			POST	LM	LM WINDOW PAN
N 143-21968	1940			POST	LM	LM WINDOW PAN
N 143-21969	1941			POST	LM	LM WINDOW PAN
N 143-21970	1942			POST	LM	LM WINDOW PAN
N 143-21971	1943			POST	LM	LM WINDOW PAN
N 143-21972	1944			POST	LM	LM WINDOW PAN
N 143-21973	1945			POST	LM	LM WINDOW PAN
N 143-21974	1946			POST	LM	LM WINDOW PAN
N 143-21975	1947			POST	LM	LM WINDOW PAN
N 143-21976	1948			POST	LM	LM WINDOW PAN
N 143-21977	1949			POST	LM	LM WINDOW PAN
N 143-21978	1950			POST	LM	LM WINDOW PAN
N 143-21979	1951			POST	LM	LM WINDOW PAN
N 143-21980	1952			POST	LM	LM WINDOW PAN
N 143-21981	1953			POST	LM	LM WINDOW PAN
N 143-21982	1954			POST	LM	LM WINDOW PAN

Table 8.--Sequential listing within each 70 mm magazine, Apollo 17 lunar surface pictures (magazine J, black and white, 60 mm focal length)--Continued

MAG	PHOTO	SEQ	GET	EVA	STA	REMARKS
R 144-21983				1	LM	S MASSIF
R 144-21984				1	LM	S MASSIF
R 144-21985				1	LM	S MASSIF
R 144-21986				1	LM	S MASSIF
R 144-21987				1	LM	S MASSIF
R 144-21988				1	LM	S MASSIF
R 144-21989				1	LM	S MASSIF
R 144-21990				1	LM	BLANK
R 144-21991				1	LM	BOULDER TRACKS ON N MASSIF
R 144-21992				1	LM	BOULDER TRACKS ON N MASSIF
R 144-21993				1	LM	BOULDER TRACKS ON N MASSIF
R 144-21994				1	LM	N MASSIF
R 144-21995				1	LM	N MASSIF
R 144-21996				1	LM	N MASSIF
R 144-21997				1	LM	N MASSIF
R 144-21998				1	LM	N MASSIF
R 144-21999				1	LM	BLANK
R 144-22000				1	LM	BLANK
R 144-22001				1	LM	BLANK
R 144-22002				1	LM	BLANK
R 144-22003		05 21 17		2	2A	S MASSIF
R 144-22004		05 21 17+		2	2A	S MASSIF, FOGGED
R 144-22005		05 21 17+		2	2A	S MASSIF
R 144-22006		05 21 17+		2	2A	S MASSIF
R 144-22007		05 21 17+		2	2A	S MASSIF
R 144-22008		05 21 17+		2	2A	S MASSIF
R 144-22009		05 21 17+		2	2A	S MASSIF
R 144-22010		05 21 17+		2	2A	S MASSIF
R 144-22011		05 21 17+		2	2A	S MASSIF
R 144-22012		05 21 17+		2	2A	S MASSIF
R 144-22013		05 21 17+		2	2A	S MASSIF
R 144-22014		05 21 17+		2	2A	S MASSIF
R 144-22015		05 21 17+		2	2A	S MASSIF
R 144-22016		05 21 17+		2	2A	N MASSIF
R 144-22017		05 21 17+		2	2A	N MASSIF
R 144-22018		05 21 17+		2	2A	N MASSIF
R 144-22019		05 21 17+		2	2A	N MASSIF
R 144-22020		05 21 17+		2	2A	N MASSIF
R 144-22021		05 21 17+		2	2A	N MASSIF
R 144-22022		05 21 17+		2	2A	N MASSIF
R 144-22023		05 21 17+		2	2A	N MASSIF
R 144-22024		05 21 17+		2	2A	N MASSIF
R 144-22025		05 21 17+		2	2A	N MASSIF
R 144-22026		05 21 17+		2	2A	N MASSIF
R 144-22027		05 21 17+		2	2A	N MASSIF
R 144-22028		05 21 17+		2	2A	N MASSIF
R 144-22029		05 21 17+		2	2A	N MASSIF
R 144-22030		05 21 17+		2	2A	N MASSIF
R 144-22031		05 21 17+		2	2A	N MASSIF
R 144-22032		05 21 17+		2	2A	N MASSIF
R 144-22033		05 21 17+		2	2A	SCULPTURED HILLS
R 144-22034		05 21 17+		2	2A	SCULPTURED HILLS
R 144-22035		05 21 17+		2	2A	SCULPTURED HILLS
R 144-22036		05 21 17+		2	2A	FAMILY MTN
R 144-22037		05 21 17+		2	2A	FAMILY MTN
R 144-22038		05 21 17+		2	2A	FAMILY MTN
R 144-22039		05 21 17+		2	2A	FAMILY MTN
R 144-22040		05 21 17+		2	2A	FAMILY MTN
R 144-22041		05 21 17+		2	2A	FAMILY MTN
R 144-22042		05 21 17+		2	2A	FAMILY MTN
R 144-22043		05 21 17+		2	2A	FAMILY MTN
R 144-22044		05 21 17+		2	2A	FAMILY MTN
R 144-22045		05 21 17+		2	2A	FAMILY MTN
R 144-22046		05 21 17+		2	2A	BLANK
R 144-22047		05 22 19+		2	3	BASE OF N MASSIF
R 144-22048		05 22 19+		2	3	BASE OF N MASSIF
R 144-22049		05 22 19+		2	3	BASE OF N MASSIF
R 144-22050		05 22 19+		2	3	BASE OF N MASSIF
R 144-22051		05 22 19+		2	3	S MASSIF
R 144-22052		05 22 19+		2	3	S MASSIF
R 144-22053		05 22 19+		2	3	S MASSIF
R 144-22054		05 22 19+		2	3	S MASSIF
R 144-22055		05 22 19+		2	3	S MASSIF
R 144-22056		05 22 19+		2	3	S MASSIF
R 144-22057		05 22 19+		2	3	S MASSIF
R 144-22058		05 22 19+		2	3	S MASSIF
R 144-22059		05 22 19+		2	3	S MASSIF
R 144-22060		05 22 19+		2	3	S MASSIF
R 144-22061		05 22 19+		2	3	S MASSIF
R 144-22062		05 22 19+		2	3	S MASSIF
R 144-22063		05 22 19+		2	3	S MASSIF
R 144-22064		05 22 19+		2	3	S MASSIF
R 144-22065		05 22 19+		2	3	S MASSIF
R 144-22066		05 22 19+		2	3	S MASSIF
R 144-22067		05 22 19+		2	3	S MASSIF
R 144-22068		05 22 19+		2	3	S MASSIF
R 144-22069		05 22 19+		2	3	S MASSIF
R 144-22070		05 22 19+		2	3	S MASSIF
R 144-22071		05 22 19+		2	3	S MASSIF
R 144-22072		05 22 19+		2	3	SCULPTURED HILLS

Table 8.--*Sequential listing within each 70 mm magazine, Apollo 17 lunar surface pictures (magazine J, black and white, 60 mm focal length)--Continued*

MAG	PHOTO	SEQ	G+T	EVA	STA	REMARKS
R 144-22073		05 22 19+	2	3		SCULPTURED HILLS
R 144-22074		05 22 19+	2	3		SCULPTURED HILLS
R 144-22075		05 22 19+	2	3		SCULPTURED HILLS
R 144-22076		05 22 19+	2	3		SCULPTURED HILLS
R 144-22077		05 22 19+	2	3		SCULPTURED HILLS
P 144-22078		05 22 19+	2	3		BLURRED
R 144-22079		05 22 19+	2	3		BLANK
P 144-22080		06 00 55+	2	LM	S	MASSIF
R 144-22081		06 00 55+	2	LM	S	MASSIF
R 144-22082		06 00 55+	2	LM	S	MASSIF
R 144-22083		06 00 55+	2	LM	S	MASSIF
R 144-22084		06 00 55+	2	LM	S	MASSIF
R 144-22085		06 00 55+	2	LM	S	MASSIF
R 144-22086		06 00 55+	2	LM	S	MASSIF
R 144-22087		06 00 55+	2	LM	S	MASSIF
R 144-22088		06 00 55+	2	LM	S	MASSIF
R 144-22089		06 00 55+	2	LM	S	MASSIF
P 144-22090		06 00 55+	2	LM	S	MASSIF
R 144-22091		06 00 55+	2	LM	S	MASSIF
R 144-22092		06 00 55+	2	LM	S	MASSIF
P 144-22093		06 00 55+	2	LM	S	MASSIF
R 144-22094		06 00 55+	2	LM	S	MASSIF
R 144-22095		06 00 55+	2	LM	S	MASSIF
P 144-22096		06 00 55+	2	LM	S	MASSIF
P 144-22097		06 00 55+	2	LM	S	MASSIF
R 144-22098		06 00 55+	2	LM	S	MASSIF
R 144-22099		06 00 55+	2	LM	S	MASSIF
R 144-22100		06 00 55+	2	LM	S	MASSIF
P 144-22101		06 00 55+	2	LM	S	MASSIF
R 144-22102		06 00 55+	2	LM	S	MASSIF
R 144-22103		06 00 55+	2	LM	S	MASSIF
R 144-22104		06 00 55+	2	LM	S	MASSIF
R 144-22105		06 00 55+	2	LM	N	MASSIF
R 144-22106		06 00 55+	2	LM	N	MASSIF
R 144-22107		06 00 55+	2	LM	N	MASSIF
R 144-22108		06 00 55+	2	LM	N	MASSIF
P 144-22109		06 00 55+	2	LM	N	MASSIF
P 144-22110		06 00 55+	2	LM	N	MASSIF
P 144-22111		06 00 55+	2	LM	N	MASSIF
R 144-22112		06 00 55+	2	LM	N	MASSIF
R 144-22113		06 00 55+	2	LM	N	MASSIF
R 144-22114		06 00 55+	2	LM	N	MASSIF
R 144-22115		06 00 55+	2	LM	N	MASSIF
P 144-22116		06 00 55+	2	LM	N	MASSIF
R 144-22117		06 00 55+	2	LM	N	MASSIF
R 144-22118		06 00 55+	2	LM	N	MASSIF
R 144-22119		06 00 55+	2	LM	N	MASSIF
R 144-22120		06 00 55+	2	LM	N	MASSIF
R 144-22121		06 00 55+	2	LM	N	MASSIF
R 144-22122		06 00 55+	2	LM	N	MASSIF
P 144-22123		06 00 55+	2	LM	N	MASSIF
P 144-22124		06 00 55+	2	LM	N	MASSIF
R 144-22125		06 00 55+	2	LM	N	MASSIF
R 144-22126		06 00 55+	2	LM	N	MASSIF
R 144-22127		06 00 55+	2	LM	N	MASSIF
R 144-22128		06 00 55+	2	LM	N	MASSIF
R 144-22129		06 00 55+	2	LM	N	MASSIF
R 144-22130		06 00 55+	2	LM	N	MASSIF
R 144-22131		06 00 55+	2	LM	N	MASSIF
R 144-22132		06 00 55+	2	LM	N	MASSIF

Table 8.--*Sequential listing within each 70 mm magazine, Apollo 17 lunar surface pictures (magazine J, black and white, 60 mm focal length)--Continued*

MAG	PHOTO	SEQ	GET	EVA	STA	REMARKS
D 145-22133	993			2	5	MISC
D 145-22134	994			2	5	MISC
D 145-22135	995			2	5	MISC
D 145-22136	998	05 23 56+	2	5		SPL 75015,75035 XSB
D 145-22137	999	05 23 56+	2	5		SPL 75015,75035 XSB
D 145-22138	1000	05 23 56+	2	5		SPL 75015,75035 XSB
D 145-22139	1001	05 23 58	2	5		SPL 75015,75035 XSA
D 145-22140	1002	05 23 58+	2	5		SPL 75015,75035 XSA
D 145-22141	1010	06 00 02	2	5		SPL 75055
D 145-22142	1011	06 00 02+	2	5		SPL 75055
D 145-22143	1012	06 00 02+	2	5		SPL 75055
D 145-22144	1013	06 00 02+	2	5		SPL 75055
D 145-22145	1014	06 00 02+	2	5		SPL 75055
D 145-22146	1015	06 00 02+	2	5		SPL 75055
D 145-22147	1016	06 00 02+	2	5		SPL 75055
D 145-22148	1017	06 00 02+	2	5		SPL 75055
D 145-22149	1018	06 00 02+	2	5		SPL 75055
D 145-22150	1019	06 00 02+	2	5		SPL 75055
D 145-22151	1020	06 00 02+	2	5		SPL 75055
D 145-22152	1021	06 00 02+	2	5		SPL 75055
D 145-22153	1022	06 00 03	2	5		SPL 75055
D 145-22154	1025	06 00 06+	2	5		SPL 75060-64,65-66,75075,75080-84,85-89 XS
D 145-22155	1026	06 00 06+	2	5		SPL 75060-64,65-66,75075,75080-84,85-89 XS
D 145-22156	1027	06 00 06+	2	5		SPL 75060-64,65-66,75075,75080-84,85-89 XS
D 145-22157	1028	06 00 06+	2	5		SPL 75060-64,65-66,75075,75080-84,85-89 XS
D 145-22158	1029	06 00 08	2	5		SPL 75060-64,65-66,75075,75080-84,85-89 XS
D 145-22159	1030	06 00 08+	2	5		PAN
D 145-22160	1031	06 00 08+	2	5		PAN
D 145-22161	1032	06 00 08+	2	5		PAN
D 145-22162	1033	06 00 08+	2	5		PAN
D 145-22163	1034	06 00 08+	2	5		PAN
D 145-22164	1035	06 00 08+	2	5		PAN
D 145-22165	1036	06 00 08+	2	5		PAN
D 145-22166	1037	06 00 08+	2	5		PAN
D 145-22167	1038	06 00 08+	2	5		PAN
D 145-22168	1039	06 00 08+	2	5		PAN
D 145-22169	1040	06 00 08+	2	5		PAN
D 145-22170	1041	06 00 08+	2	5		PAN
D 145-22171	1042	06 00 08+	2	5		PAN
D 145-22172	1043	06 00 08+	2	5		PAN
D 145-22173	1044	06 00 08+	2	5		PAN
D 145-22174	1045	06 00 08+	2	5		PAN
D 145-22175	1046	06 00 08+	2	5		PAN
D 145-22176	1047	06 00 08+	2	5		PAN
D 145-22177	1048	06 00 08+	2	5		PAN
D 145-22178	1049	06 00 08+	2	5		PAN
D 145-22179	1050	06 00 08+	2	5		PAN
D 145-22180	1051	06 00 08+	2	5		PAN
D 145-22181	1052	06 00 08+	2	5		PAN
D 145-22182	1053	06 00 08+	2	5		PAN
D 145-22183	1054	06 00 08+	2	5		PAN
D 145-22184	1092	06 00 23	2	5-LM		EP-8 LOC
D 145-22185	1093	06 00 39+	2	ALSEP		SPL 70019 LOC
D 145-22186	1094	06 00 39+	2	ALSEP		SPL 70019 XSB
D 145-22187	1095	06 00 39+	2	ALSEP		SPL 70019 XSB
D 145-22188	1096	06 00 39+	2	ALSEP		SPL 70019 XSB
D 145-22189	1097	06 00 39+	2	ALSEP		SPL 70019 XSB
D 145-22190	1098	06 00 39+	2	ALSEP		SPL 70019 XSA
D 145-22191	1099	06 00 39+	2	ALSEP		SPL 70019 XSA
D 145-22192	1955		POST	LM		LM WINDOW PAN, FOGGED
D 145-22193	1956		POST	LM		LM WINDOW PAN
D 145-22194	1957		POST	LM		LM WINDOW PAN
D 145-22195	1958		POST	LM		LM WINDOW PAN
D 145-22196	1959		POST	LM		LM WINDOW PAN
D 145-22197	1960		POST	LM		LM WINDOW PAN
D 145-22198	1961		POST	LM		LM WINDOW PAN
D 145-22199	1962		POST	LM		LM WINDOW PAN
D 145-22200	1963		POST	LM		LM WINDOW PAN
D 145-22201	1964		POST	LM		LM WINDOW PAN
D 145-22202	1965		POST	LM		LM WINDOW PAN
D 145-22203	1966		POST	LM		LM WINDOW PAN
D 145-22204	1967		POST	LM		LM WINDOW PAN
D 145-22205	1968		POST	LM		LM WINDOW PAN
D 145-22206	1969		POST	LM		LM WINDOW PAN
D 145-22207	1970		POST	LM		LM WINDOW PAN
D 145-22208	1971		POST	LM		LM WINDOW PAN
D 145-22209	1972		POST	LM		LM WINDOW PAN
D 145-22210	1973		POST	LM		LM WINDOW PAN
D 145-22211	1974		POST	LM		LM WINDOW PAN
D 145-22212	1975		POST	LM		LM WINDOW PAN
D 145-22213	1976		POST	LM		LM WINDOW PAN
D 145-22214	1977		POST	LM		LM WINDOW PAN
D 145-22215	1978		POST	LM		LM WINDOW PAN
D 145-22216	1979		POST	LM		LM WINDOW PAN
D 145-22217	1980		POST	LM		LM WINDOW PAN
D 145-22218	1981		POST	LM		LM WINDOW PAN
D 145-22219	1982		POST	LM		LM WINDOW PAN
D 145-22220	1983		POST	LM		LM WINDOW PAN
D 145-22221	1984		POST	LM		LM WINDOW PAN
D 145-22222	1985		POST	LM		LM WINDOW PAN
D 145-22223-22228						INSIDE LM
D 145-22229-22234						BLANK
D 145-22235-22288						COMMAND MODULE

Table 8.--*Sequential listing within each 70 mm magazine, Apollo 17 lunar surface pictures (magazine J, black and white, 60 mm focal length)--Continued*

MAG	PHOTO	SEQ	BT	EVA	STA	REMARKS
F 146-22289	1377	06 19 05	3	6	MISC	
F 146-22290	1378	06 19 05+	3	6	MISC	
F 146-22291	1379	06 19 08	3	6	DT SPL 76001 XSD	
F 146-22292	1380	06 19 08+	3	6	DT SPL 76001 XSD	
F 146-22293	1381	06 19 08+	3	6	DT SPL 76001 LOC	
F 146-22294	1382	06 19 08+	3	6	DT SPL 76001 LOC	
F 146-22295	1383	06 19 08+	3	6	DT SPL 76001 XSA	
F 146-22296	1384	06 19 08+	3	7	LRV	
F 146-22297	1385	06 19 08+	3	7	LRV	
F 146-22298	1426	06 19 35	3	7	BOULDER F-L, SPL 77115,77135 XSB	
F 146-22299	1427	06 19 35+	3	7	BOULDER F-L, SPL 77115,77135 XSB	
F 146-22300	1428	06 19 35+	3	7	BOULDER F-L, SPL 77075*,77095*,77115,77135 XSB	
F 146-22301	1429	06 19 35+	3	7	BOULDER F-L	
F 146-22302	1430	06 19 35+	3	7	BOULDER F-L	
F 146-22303	1431	06 19 35+	3	7	BOULDER F-L	
F 146-22304	1432	06 19 35+	3	7	BOULDER F-L	
F 146-22305	1433	06 19 35+	3	7	BOULDER F-L, AREA OF SPL 77075-77,77215 XSB	
F 146-22306	1434	06 19 35+	3	7	BOULDER F-L, AREA OF SPL 77075-77,77215 XSB	
F 146-22307	1435	06 19 35+	3	7	BOULDER F-L, SPL 77075-77,77215 XSB	
F 146-22308	1436	06 19 35+	3	7	BOULDER F-L, SPL 77075-77,77215 XSB	
F 146-22309	1437	06 19 35+	3	7	BOULDER F-L, SPL 77075-77,77215 XSB	
F 146-22310	1438	06 19 35+	3	7	BOULDER F-L, SPL 77075-77,77215 XSB	
F 146-22311	1439	06 19 35+	3	7	BOULDER F-L, SPL 77075-77,77215 XSB	
F 146-22312	1440	06 19 35+	3	7	BOULDER F-L, SPL 77075-77,77215 XSB	
F 146-22313	1441	06 19 35+	3	7	BOULDER F-L, SPL 77075-77,77215 XSB	
F 146-22314	1442	06 19 35+	3	7	BOULDER F-L, SPL 77075-77,77215 XSB	
F 146-22315	1443	06 19 35+	3	7	BOULDER F-L, SPL 77075-77,77215 XSB	
F 146-22316	1444	06 19 35+	3	7	BOULDER CU	
F 146-22317	1445	06 19 35+	3	7	BOULDER CU	
F 146-22318	1446	06 19 35+	3	7	BOULDER CU	
F 146-22319	1447	06 19 35+	3	7	BOULDER CU	
F 146-22320	1448	06 19 35+	3	7	BOULDER CU	
F 146-22321	1449	06 19 35+	3	7	BOULDER CU	
F 146-22322	1450	06 19 35+	3	7	BOULDER CU	
F 146-22323	1451	06 19 35+	3	7	BOULDER CU	
F 146-22324	1452	06 19 35+	3	7	BOULDER CU	
F 146-22325	1453	06 19 35+	3	7	BOULDER CU	
F 146-22326	1454	06 19 35+	3	7	BOULDER CU	
F 146-22327	1455	06 19 35+	3	7	BOULDER CU, SPL 77075-77,77215 XSB	
F 146-22328	1456	06 19 35+	3	7	BOULDER CU, SPL 77075-77,77215 XSB	
F 146-22329	1457	06 19 40	3	7	BOULDER CU, SPL 77075-77,77215 XSA	
F 146-22330	1458	06 19 40+	3	7	BOULDER CU, SPL 77075-77,77215 XSA	
F 146-22331	1459	06 19 40+	3	7	SPL 77135 XSD	
F 146-22332	1460	06 19 40+	3	7	SPL 77135 XSD	
F 146-22333	1461	06 19 40+	3	7	SPL 77135 XSD	
F 146-22334	1462	06 19 40+	3	7	SPL 77135 XSD	
F 146-22335	1463	06 19 40+	3	7	SPL 77135 XSD	
F 146-22336	1464	06 19 40+	3	7	SPL 77115,77135 XSA	
F 146-22337	1465	06 19 40+	3	7	SPL 77115,77135 XSA	
F 146-22338	1466	06 19 40+	3	7	SPL 77115,77135 XSA	
F 146-22339	1467	06 19 46	3	7	PAN	
F 146-22340	1468	06 19 46+	3	7	PAN	
F 146-22341	1469	06 19 46+	3	7	PAN	
F 146-22342	1470	06 19 46+	3	7	PAN	
F 146-22343	1471	06 19 46+	3	7	PAN	
F 146-22344	1472	06 19 46+	3	7	PAN	
F 146-22345	1473	06 19 46+	3	7	PAN	
F 146-22346	1474	06 19 46+	3	7	PAN	
F 146-22347	1475	06 19 46+	3	7	PAN	
F 146-22348	1476	06 19 46+	3	7	PAN	
F 146-22349	1477	06 19 46+	3	7	PAN	
F 146-22350	1478	06 19 46+	3	7	PAN	
F 146-22351	1479	06 19 46+	3	7	PAN	
F 146-22352	1480	06 19 46+	3	7	PAN	
F 146-22353	1481	06 19 46+	3	7	PAN	
F 146-22354	1482	06 19 46+	3	7	PAN	
F 146-22355	1483	06 19 46+	3	7	PAN	
F 146-22356	1484	06 19 46+	3	7	PAN	
F 146-22357	1485	06 19 46+	3	7	PAN	
F 146-22358	1486	06 19 46+	3	7	PAN	
F 146-22359	1487	06 19 46+	3	7	PAN	
F 146-22360	1488	06 19 46+	3	7	PAN	
F 146-22361	1489	06 19 46+	3	7	PAN	
F 146-22362	1490	06 19 46+	3	7	PAN	
F 146-22363	1491	06 19 47	3	7	PAN	
F 146-22364	1506	06 19 52+	3	7-8		
F 146-22365	1522	06 20 13+	3	8	SPL 78135 XSB	
F 146-22366	1523	06 20 13+	3	8	SPL 78135 XSB	
F 146-22367	1524	06 20 13+	3	8	SPL 78135 LOC	
F 146-22368	1525	06 20 13+	3	8	SPL 78135 XSA	
F 146-22369	1534	06 18 20	3	8	SPL 78235-36,38 (AFTER ROLLING) XSB	
F 146-22370	1535	06 18 20+	3	8	SPL 78235-36,38 (AFTER ROLLING) XSB	
F 146-22371	1536	06 20 24	3	8	SPL 78235-36,38 (AFTER ROLLING) XSA	
F 146-22372	1537	06 20 26	3	8	SPL 78250-55 XSB	
F 146-22373	1538	06 20 26+	3	8	SPL 78250-55 XSB	
F 146-22374	1539	06 20 26+	3	8	SPL 78250-55 XSA	
F 146-22375	1540	06 20 27	3	8	PAN (BROKEN)	
F 146-22376	1541	06 20 27+	3	8	PAN (BROKEN)	
F 146-22377	1542	06 20 27+	3	8	PAN (BROKEN)	
F 146-22378	1543	06 20 27+	3	8	PAN (BROKEN)	

Table 8.--Sequential listing within each 70 mm magazine, Apollo 17 lunar surface pictures (magazine J, black and white, 60 mm focal length)--Continued

MAG	PHOTO	SEQ	GST	EVA	STA	REMARKS
F 146-22379	1544	06 20 27+	3	8	PAN (BROKEN)	
F 146-22380	1545	06 20 27+	3	8	PAN (BROKEN)	
F 146-22381	1546	06 20 27+	3	8	PAN (BROKEN)	
F 146-22382	1547	06 20 27+	3	8	PAN (BROKEN)	
F 146-22383	1548	06 20 27+	3	8	PAN (BROKEN)	
F 146-22384	1549	06 20 27+	3	8	PAN (BROKEN)	
F 146-22385	1550	06 20 27+	3	8	PAN (BROKEN)	
F 146-22386	1551	06 20 27+	3	8	PAN (BROKEN)	
F 146-22387	1552	06 20 27+	3	8	PAN (BROKEN)	
F 146-22388	1553	06 20 27+	3	8	PAN (BROKEN)	
F 146-22389	1554	06 20 27+	3	8	PAN (BROKEN)	
F 146-22390	1555	06 20 27+	3	8	PAN (BROKEN)	
F 146-22391	1556	06 20 27+	3	8	PAN (BROKEN)	
F 146-22392	1557	06 20 27+	3	8	PAN (BROKEN)	
F 146-22393	1558	06 20 27+	3	8	PAN (BROKEN)	
F 146-22394	1559	06 20 27+	3	8	PAN (BROKEN)	
F 146-22395	1560	06 20 27+	3	8	PAN (BROKEN)	
F 146-22396	1561	06 20 27+	3	8	PAN (BROKEN)	
F 146-22397	1562	06 20 27+	3	8	PAN (BROKEN)	
F 146-22398	1563	06 20 27+	3	8	SPL 78255 XSA	
F 146-22399	1575	06 20 35+	3	8	SPL 78155,78500-04,05-09,15-18,78535-39,45-49,55-59,65-69,75-79,85-89,95-99 XSB	
F 146-22400	1576	06 20 35+	3	8	SPL 78155,78500-04,05-09,15-18,78535-39,45-49,55-59,65-69,75-79,85-89,95-99 XSB	
F 146-22401	1577	06 20 35+	3	8	SPL 78155,78500-04,05-09,15-18,78535-39,45-49,55-59,65-69,75-79,85-89,95-99 XSB	
F 146-22402	1578	06 20 35+	3	8	SPL 78155,78500-04,05-09,15-18,78535-39,45-49,55-59,65-69,75-79,85-89,95-99 LOC	
F 146-22403	1579	06 20 35+	3	8	SPL 78155,78500-04,05-09,15-18,78535-39,45-49,55-59,65-69,75-79,85-89,95-99 XSA	
F 146-22404	1631	06 20 55+	3	8-9		
F 146-22405	1632	06 20 55+	3	8-9		
F 146-22406	1633	06 20 55+	3	8-9		
F 146-22407	1634	06 20 55+	3	8-9		
F 146-22408	1635	06 20 55+	3	8-9		
F 146-22409	1644	06 20 55+	3	8-9		
F 146-22410	1650	06 20 55+	3	8-9		
F 146-22411	1652	06 20 55+	3	8-9		
F 146-22412	1654	06 20 55+	3	8-9		
F 146-22413	1667	05 21 26+	3	9	SPL 79115,79120-24,79135,79510-14,15-19,25-29,35-37 XSB	
F 146-22414	1668	06 21 26+	3	9	SPL 79115,79120-24,79135,79510-14,15-19,25-29,35-37 XSB	
F 146-22415	1669	06 21 29+	3	9	SPL 79115,79120-24,79135,79510-14,15-19,25-29,35-37 XSA	
F 146-22416	1670	06 21 29+	3	9	SPL 79115,79120-24,79135,79510-14,15-19,25-29,35-37 XSA	
F 146-22417	1671	06 21 29+	3	9	SPL 79115,79120-24,79135,79510-14,15-19,25-29,35-37 XSA	
F 146-22418	1672	06 21 29+	3	9	SPL 79115,79120-24,79135,79510-14,15-19,25-29,35-37 XSA	
F 146-22419	1676	06 21 35+	3	9	SPL 79175,79195 XSB	
F 146-22420	1677	06 21 35+	3	9	SPL 79175,79195 XSB	
F 146-22421	1678	06 21 35+	3	9	SPL 79175,79195 XSB	
F 146-22422	1679	06 21 39+	3	9	SPL 79175,79195 XSA	
F 146-22423	1680	06 21 41+	3	9	PPAN	
F 146-22424	1681	06 21 41+	3	9	PPAN	
F 146-22425	1682	06 21 41+	3	9	PPAN	
F 146-22426	1683	06 21 41+	3	9	PPAN	
F 146-22427	1684	06 21 41+	3	9	PPAN	
F 146-22428	1685	06 21 41+	3	9	PPAN	
F 146-22429	1686	06 21 41+	3	9	PPAN	
F 146-22430	1687	06 21 41+	3	9	PPAN	
F 146-22431	1688	06 21 41+	3	9	PPAN	
F 146-22432	1689	06 21 41+	3	9	PPAN	
F 146-22433	1690	06 21 41+	3	9	PPAN	
F 146-22434	1691	06 21 41+	3	9	PPAN	
F 146-22435	1692	06 21 41+	3	9	PPAN	
F 146-22436	1693	06 21 41+	3	9	PPAN	
F 146-22437	1694	06 21 41+	3	9	PPAN	
F 146-22438	1695	06 21 41+	3	9	PPAN	
F 146-22439	1696	06 21 41+	3	9	PPAN	
F 146-22440	1697	06 21 41+	3	9	PPAN	
F 146-22441	1698	06 21 41+	3	9	PPAN	
F 146-22442	1699	06 21 41+	3	9	PPAN	
F 146-22443	1700	06 21 41+	3	9	PPAN	
F 146-22444	1701	06 21 41+	3	9	PPAN	
F 146-22445	1702	06 21 41+	3	9	PPAN	
F 146-22446	1703	06 21 41+	3	9	PPAN	
F 146-22447	1704	06 21 41+	3	9	PPAN	
F 146-22448	1705	06 21 41+	3	9	PPAN	
F 146-22449	1706	06 21 41+	3	9	PPAN	
F 146-22450	1707	06 21 41+	3	9	PPAN	

Table 8.--Sequential listing within each 70 mm magazine, Apollo 17 lunar surface pictures (magazine J, black and white, 60 mm focal length)--Continued

MAG	PHOTO	SEQ	GET	EVA	STA	REMARKS
A 147-22469	1			PRE	LM	LM WINDOW PAN
A 147-22470	2			PRE	LM	LM WINDOW PAN
A 147-22471	3			PRE	LM	LM WINDOW PAN
A 147-22472	4			PRE	LM	LM WINDOW PAN
A 147-22473	5			PRE	LM	LM WINDOW PAN
A 147-22474	6			PRE	LM	LM WINDOW PAN
A 147-22475	7			PRE	LM	LM WINDOW PAN
A 147-22476	8			PRE	LM	LM WINDOW PAN
A 147-22477	9			PRE	LM	LM WINDOW PAN
A 147-22478	10			PRE	LM	LM WINDOW PAN
A 147-22479	11			PRE	LM	LM WINDOW PAN
A 147-22480	12			PRE	LM	LM WINDOW PAN
A 147-22481	13			PRE	LM	LM WINDOW PAN
A 147-22482	14			PRE	LM	LM WINDOW PAN
A 147-22483	15			PRE	LM	LM WINDOW PAN
A 147-22484	16			PRE	LM	LM WINDOW PAN
A 147-22485	17			PRE	LM	LM WINDOW PAN
A 147-22486	18			PRE	LM	LM WINDOW PAN
A 147-22487	19			PRE	LM	LM WINDOW PAN
A 147-22488	20			PRE	LM	LM WINDOW PAN
A 147-22489	21			PRE	LM	LM WINDOW PAN
A 147-22490	22			PRE	LM	LM WINDOW PAN
A 147-22491	23			PRE	LM	LM WINDOW PAN
A 147-22492	24	04 19 35	1	LM		PAN N OF LM
A 147-22493	25	04 19 35+	1	LM		PAN N OF LM
A 147-22494	26	04 19 35+	1	LM		PAN N OF LM
A 147-22495	27	04 19 35+	1	LM		PAN N OF LM
A 147-22496	28	04 19 35+	1	LM		PAN N OF LM
A 147-22497	29	04 19 35+	1	LM		PAN N OF LM
A 147-22498	30	04 19 35+	1	LM		PAN N OF LM
A 147-22499	31	04 19 35+	1	LM		PAN N OF LM
A 147-22500	32	04 19 35+	1	LM		PAN N OF LM
A 147-22501	33	04 19 35+	1	LM		PAN N OF LM
A 147-22502	34	04 19 35+	1	LM		PAN N OF LM
A 147-22503	35	04 19 35+	1	LM		PAN N OF LM
A 147-22504	36	04 19 35+	1	LM		PAN N OF LM
A 147-22505	37	04 19 35+	1	LM		PAN N OF LM
A 147-22506	38	04 19 35+	1	LM		PAN N OF LM
A 147-22507	39	04 19 35+	1	LM		PAN N OF LM
A 147-22508	40	04 19 35+	1	LM		PAN N OF LM
A 147-22509	41	04 19 35+	1	LM		PAN N OF LM
A 147-22510	42	04 19 35+	1	LM		PAN N OF LM
A 147-22511	43	04 19 35+	1	LM		PAN N OF LM
A 147-22512	44	04 19 35+	1	LM		PAN N OF LM
A 147-22513	45	04 19 35+	1	LM		PAN N OF LM
A 147-22514	46	04 19 35+	1	LM		PAN N OF LM
A 147-22515	47	04 19 35+	1	LM		PAN N OF LM
A 147-22516	48	04 19 35+	1	LM		PAN N OF LM
A 147-22517	49	04 19 35+	1	LM		PAN N OF LM
A 147-22518	50	04 19 35+	1	LM		PAN N OF LM
A 147-22519	51	04 19 35+	1	LM		PAN N OF LM
A 147-22520	52	04 19 35+	1	LM		PAN N OF LM
A 147-22521	53	04 19 35+	1	LM		CDR DRIVING LRV
A 147-22522	54	04 19 35+	1	LM		CDR DRIVING LRV
A 147-22523	55	04 19 35+	1	LM		CDR DRIVING LRV
A 147-22524	56	04 19 35+	1	LM		CDR DRIVING LRV
A 147-22525	57	04 19 35+	1	LM		CDR DRIVING LRV
A 147-22526	58	04 19 35+	1	LM		CDR DRIVING LRV
A 147-22527	59	04 19 35+	1	LM		CDR DRIVING LRV
A 147-22528	74	04 21 56	1	ALSEP		PPAN OF GEOPHONE LOC
A 147-22529	75	04 21 56+	1	ALSEP		PPAN OF GEOPHONE LOC
A 147-22530	76	04 21 56+	1	ALSEP		PPAN OF GEOPHONE LOC
A 147-22531	77	04 21 56+	1	ALSEP		PPAN OF GEOPHONE LOC
A 147-22532	78	04 21 56+	1	ALSEP		PPAN OF GEOPHONE LOC
A 147-22533	79	04 21 58	1	ALSEP		CU GEOPHONE ROCK
A 147-22534	80	04 21 58+	1	ALSEP		CU GEOPHONE ROCK
A 147-22535	81	04 21 58+	1	ALSEP		GEOPHONE ROCK, STEREO
A 147-22536	82	04 21 58+	1	ALSEP		GEOPHONE ROCK, STEREO
A 147-22537	83	04 21 58+	1	ALSEP		GEOPHONE
A 147-22538	84	04 21 58+	1	ALSEP		DS
A 147-22539	85	04 21 58+	1	ALSEP		?
A 147-22540	86	04 21 58+	1	ALSEP		?
A 147-22541	87	04 21 58+	1	ALSEP		DS
A 147-22542	88	04 21 58+	1	ALSEP		PAN NEAR GEOPHONE ROCK
A 147-22543	89	04 21-42	1	ALSEP		PAN NEAR GEOPHONE ROCK
A 147-22544	90	04 21 58+	1	ALSEP		PAN NEAR GEOPHONE ROCK
A 147-22545	91	04 21 58+	1	ALSEP		PAN NEAR GEOPHONE ROCK
A 147-22546	92	04 21 58+	1	ALSEP		PAN NEAR GEOPHONE ROCK
A 147-22547	93	04 21 58+	1	ALSEP		PAN NEAR GEOPHONE ROCK
A 147-22548	94	04 21 58+	1	ALSEP		PAN NEAR GEOPHONE ROCK
A 147-22549	95	04 21 58+	1	ALSEP		PAN NEAR GEOPHONE ROCK
A 147-22550	96	04 21 58+	1	ALSEP		PAN NEAR GEOPHONE ROCK
A 147-22551	97	04 21 58+	1	ALSEP		PAN NEAR GEOPHONE ROCK
A 147-22552	98	04 21 58+	1	ALSEP		PAN NEAR GEOPHONE ROCK
A 147-22553	99	04 21 58+	1	ALSEP		PAN NEAR GEOPHONE ROCK
A 147-22554	100	04 21 58+	1	ALSEP		PAN NEAR GEOPHONE ROCK
A 147-22555	101	04 21 58+	1	ALSEP		PAN NEAR GEOPHONE ROCK

Table 8.--Sequential listing within each 70 mm magazine, Apollo 17 lunar surface pictures (magazine J, black and white, 60 mm focal length)--Continued

MAG	PHOTO	SEQ	GET	EVA	STA	REMARKS
A 147-22556	102	04 21 58+	1	ALSEP	PAN NEAR GEOPHONE ROCK	
A 147-22557	103	04 21 58+	1	ALSEP	PAN NEAR GEOPHONE ROCK	
A 147-22558	104	04 21 58+	1	ALSEP	PAN NEAR GEOPHONE ROCK	
A 147-22559	105	04 21 58+	1	ALSEP	PAN NEAR GEOPHONE ROCK	
A 147-22560	106	04 21 58+	1	ALSEP	PAN NEAR GEOPHONE ROCK	
A 147-22561	107	04 21 58+	1	ALSEP	PAN NEAR GEOPHONE ROCK	
A 147-22562	108	04 22 04	1	ALSEP	GEOPHONE	
A 147-22563	109	04 22 04+	1	ALSEP	?	
A 147-22564	110	04 22 04+	1	ALSEP	?	
A 147-22565	111	04 22 07	1	ALSEP	PAN AT C/S	
A 147-22566	112	04 22 07+	1	ALSEP	PAN AT C/S	
A 147-22567	113	04 22 07+	1	ALSEP	PAN AT C/S	
A 147-22568	114	04 22 07+	1	ALSEP	PAN AT C/S	
A 147-22569	115	04 22 07+	1	ALSEP	PAN AT C/S	
A 147-22570	116	04 22 07+	1	ALSEP	PAN AT C/S	
A 147-22571	117	04 22 07+	1	ALSEP	PAN AT C/S	
A 147-22572	118	04 22 07+	1	ALSEP	PAN AT C/S	
A 147-22573	119	04 22 07+	1	ALSEP	PAN AT C/S	
A 147-22574	120	04 22 07+	1	ALSEP	PAN AT C/S	
A 147-22575	121	04 22 07+	1	ALSEP	PAN AT C/S	
A 147-22576	122	04 22 07+	1	ALSEP	PAN AT C/S	
A 147-22577	123	04 22 07+	1	ALSEP	PAN AT C/S	
A 147-22578	124	04 22 07+	1	ALSEP	PAN AT C/S	
A 147-22579	125	04 22 07+	1	ALSEP	PAN AT C/S	
A 147-22580	126	04 22 07+	1	ALSEP	PAN AT C/S	
A 147-22581	127	04 22 07+	1	ALSEP	PAN AT C/S	
A 147-22582	128	04 22 07+	1	ALSEP	PAN AT C/S	
A 147-22583	129	04 22 07+	1	ALSEP	PAN AT C/S	
A 147-22584	130	04 22 07+	1	ALSEP	PAN AT C/S	
A 147-22585	131	04 22 07+	1	ALSEP	PAN AT C/S	
A 147-22586	132	04 22 07+	1	ALSEP	PAN AT C/S	
A 147-22587	133	04 22 07+	1	ALSEP	PAN AT C/S	
A 147-22588	134	04 22 07+	1	ALSEP	PAN AT C/S	
A 147-22589	135	04 22 11	1	ALSEP	PPAN	
A 147-22590	136	04 22 11+	1	ALSEP	PPAN	
A 147-22591	137	04 22 11+	1	ALSEP	PPAN	
A 147-22592	138	04 22 11+	1	ALSEP	PPAN	
A 147-22593	139	04 22 11+	1	ALSEP	PPAN	
A 147-22594	140	04 22 11+	1	ALSEP	PPAN	
A 147-22595	141	04 22 11+	1	ALSEP	PPAN	
A 147-22596	142	04 22 11+	1	ALSEP	PPAN	
A 147-22597	143	04 22 11+	1	ALSEP	PPAN	
A 147-22598	144	04 22 11+	1	ALSEP	PPAN, CDR DRILLING	
A 147-22599	145	04 22 11+	1	ALSEP	PPAN, CDR DRILLING	
A 147-22600	146	04 22 11+	1	ALSEP	PPAN	
A 147-22601	147	04 22 11+	1	ALSEP	PPAN	
A 147-22602	148	04 22 11+	1	ALSEP	PPAN	
A 147-22603	149	04 22 11+	1	ALSEP	PPAN	
A 147-22604	150	04 22 11+	1	ALSEP	PPAN	
A 147-22605	151	04 22 11+	1	ALSEP	PPAN	
A 147-22606	152	04 22 11+	1	ALSEP	PPAN	

lipse to the feet of the gnomon image. If correctly placed, the ellipse corresponds to a circle of known dimensions on the ground where it stands. The fitting must be done by a skilled photointerpreter so that the long axis of the ellipse is placed as nearly as possible on the image at the intersection of the ground plane with a plane perpendicular to the line of sight of the camera. For measurements of small features near the gnomon, it is also helpful to know that the gray scale color bands on the wand and on the gnomon leg chart are 2 cm wide.

Photogrammetric measurement by stereoscopic pairs is the most accurate mapping method used on Apollo 17. In theory, absolute orientation can be controlled by the gimbaled wand on the gnomon, which is oriented to lunar vertical, and the trace on the surface of the wand

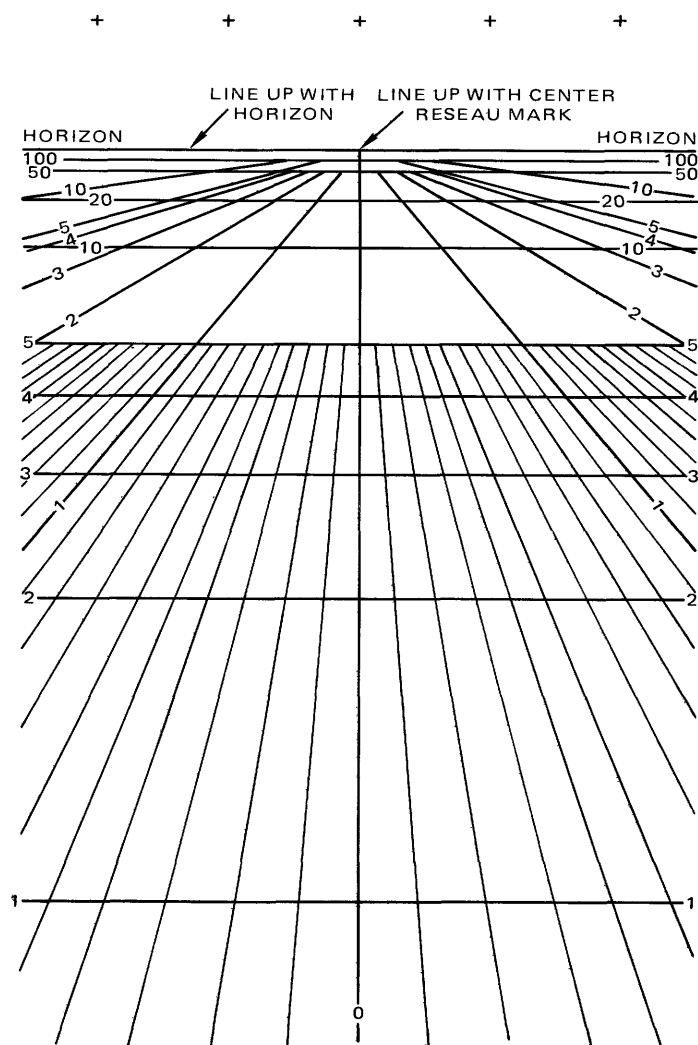


FIGURE 259.—Perspective grid used for estimating size and distance. Width of grid should equal width of lunar surface photograph on which measurements are to be made. Horizontal lines indicate distance, in meters, from camera. Converging lines show width of an object photographed in plane of flat lunar surface (notation in meters, measured from centerline).

TABLE 9.—Apollo 17 lunar surface film usage by camera number

S/N 1032 (60 mm focal length)		
147-22451	through 22606	(Mag A)
135-20533	through 20678	(Mag G)
136-20682	through 20863	(Mag H)
138-21028	through 21181	(Mag I)
133-20194	through 20375	(Mag J)
141-21510	through 21667	(Mag L)
142-21169	through 21833	(Mag M)
143-21834	through 21982	(Mag N)
S/N 1023 (60 mm focal length)		
134-20376	through 20513	(Mag B)
137-20866	through 21027	(Mag C)
145-22133	through 22222	(Mag D)
140-21351	through 21509	(Mag E)
146-22289	through 22450	(Mag F)
500-mm camera		
139-21186	through 21276	(Mag K)
144-21983	through 22132	(Mag R)

shadow, whose angle from lunar north is known for any given time during the lunar day. Difficulty was encountered with this procedure, however, because swinging of the wand was not effectively damped on the Apollo 17 gnomon. The orientations could be determined accurately only if pictures were taken several seconds after the gnomon was deployed. Maps made with the analytical plotter have less than 1 percent variation in scale throughout. Those that contain the gnomon are correctly oriented within 2° with respect to the lunar surface (if the wand had stopped swinging when pictures were taken).

Stations on traverse maps (figs. 6 and 7) were located, and planimetric station maps (for example, fig. 8) were made primarily from the panoramas. An assembled panorama mosaic can be used in much the same way as a theodolite for measurements of both horizontal and vertical angles. The locations of the sun and of the astronaut's shadow serve to orient the panorama with respect to lunar east and west. Intermediate directions are located by interpolation.

The traditional surveying method of three-point resection (Davis, 1959) was used to locate the panorama station on maps of the traverse area. In this method, the images of three or more features were identified on the panorama as well as on a vertical photograph taken of the same area from lunar orbit. Azimuths to these points were measured on the panorama and plotted on tracing paper as lines radiating from a point. The trac-

ing paper was placed over the vertical photograph and oriented so that each ray intersected the image of the appropriate feature. The point from which the lines radiated was then marked and identified as the panorama station. On most stations where feature identification was undisputed, resection rays identified the camera's location within 1 or 2 meters. In general, the nearer the points are to the camera and the more points there are, the more accurately the station can be located.

Station maps (for example, fig. 8) were prepared with perspective grid measurements on film camera panoramas and photographic copies of pictures in television panoramas. Where possible, perspective grid measurements were verified by intersecting rays from different panorama stations to known points on the maps. In addition, backsight photos toward the LRV, taken as part of the sample photographic procedure, were used to determine the distance (as a function of the known size of the vehicle) and, in some cases the azimuth, of sample collection areas from the LRV. The latter could be determined only when objects (in addition to the LRV) identifiable on the traverse map appeared in the backsight picture.

The detailed traverse path (figs. 6 and 7) was located in part from earth using a technique called Very Long Base Interferometry developed by Salzberg (1973).



This technique is capable of tracking the rate of change in the motion of the LRV with high precision. Data provided by Salzberg were thus used to draw the LRV tracks, which were then shifted so that they started and ended at the locations determined by resection with photographic panoramas.

#### REFERENCES CITED

- Batson, R. M., 1969a, Topographic mapping methods, Surveyor Program Results: Natl. Aeronautics Space Admin., Spec. Pub. 184, p. 42-45.
- 1969b, Photogrammetry with surface-based images: Appl. Optics, v. 8, no. 7, p. 1315-1322.
- Davis, R. E., 1959, Surveying, in Urquhart, L. F., Civil Engineering Handbook: New York, McGraw-Hill, p. 49-57.
- Kammerer, Joachim, 1973, The moon camera and its lenses: Photogram. Eng., v. 39, no. 1, p. 59-63.
- Muehlberger, W. R., Batson, R. M., Cernan, E. A., Freeman, V. L., Hait, M. H., Holt, H. E., Howard, K. A., Jackson, E. D., Larson, K. B., Reed, V. S., Rennilson, J. J., Schmitt, H. H., Scott, D. H., Sutton, R. L., Stuart-Alexander, D., Swann, G. A., Trask, N. J., Ulrich, G. E., Wilshire, H. G., and Wolfe, E. W., 1973, Preliminary geologic investigation of the Apollo 17 landing site: Apollo 17 Prelim. Sci. Rept., Natl. Aeronautics and Space Admin. Spec. Pub. 330, p. 6-1 to 6-91.
- Salzberg, I. M., 1973, Tracking of the Apollo lunar rover with interferometry techniques: Proc. Inst. of Elec. and Electronics Engineers, v. 61, no. 9, p. 1233-1236.
- Williams, J. C. C., 1969, Simple photogrammetry: New York, Academic Press, 211 pages.

## GLOSSARY

[This glossary is a list of definitions of special terms, acronyms, abbreviations, and symbols used in the photograph catalog, and on the panoramas and planimetric station maps. No attempt is made to give detailed descriptions of the functions of the devices defined. Such descriptions are available in NASA documents and in scientific literature]

ALSEP	Apollo Lunar Surface Experiments Package.	LSP	Lunar Seismic Profiling Experiment.
B & W, BW	Black and white film used in camera.	MAG	Film magazine.
Boulder ●	Letters refer to large blocks on maps and pans.	N	North.
BSLSS	Buddy Secondary Life Support System.	PAN Δ	Panorama. A series of pictures that provides a 360° view from a single point.
CDR	Commander.	POST	Designates pictures taken through the LM windows after EVA.
C/S	Central Station (ALSEP).	PPAN Δ	Partial panorama. A series of panoramic pictures taken over less than 360°.
CSVC	Core Sample Vacuum Container.	PRE	Designates pictures taken through the LM windows before EVA.
CTR ☉	Crater.	PROBE-1	Probe (number 1) for Heat Flow Experiment.
CU	A stereoscopic pair of pictures taken at closer range, generally less than 1 m, than the 2 or 3 m normally used to document geologic samples.	RTG	Radioisotope Thermoelectric Generator (ALSEP power supply).
DPS	Descent Propulsion System.	S	South.
DS	A picture taken with the camera aimed downsun.	SCB	Sample Collection Bag.
DSA	A picture taken downsun of a geologic sample area after the sample has been collected.	SEP	Surface Electrical Properties Experiment.
DSB	A picture taken downsun before collecting a geologic sample.	SEQ	A number assigned each picture to show its sequence within the lunar surface activity.
DT 73002/73001	Drive tube, upper/lower tube number.	SESC	Special Environmental Sample Container.
E	East.	SPL	Sample.
EP-6	Explosive Package (number 6) detonated after lunar liftoff as part of the LSP experiment.	SRC	Sample Return Container.
EVA	Extravehicular activity.	STA	Station area stop made during EVA, designated by a number.
F-L 	"Flight-line" stereoscopic pictures. An evenly spaced series of overlapping pictures taken with the camera approximately perpendicular to and always the same distance from a feature of geologic interest (for example, a boulder face).	TR SPL	Trench Sample.
GEO-2	Geophone Number 2.	US	Picture taken upsun (toward the sun).
GET	Ground Elapsed Time (time since launch).	W	West.
G/M	Geophone Module.	X	Sample location; "?" after sample number indicates that location is uncertain.
HFE	Heat Flow Experiment.	XS	Picture taken with the camera aimed cross-sun.
LEAM	Lunar Ejecta and Meteorite Experiment.	XSA	Cross-sun picture taken after sample collection.
LM	Lunar Module.	XSB	Cross-sun picture taken before sample collection.
LMP	Lunar Module Pilot.	XSD	A picture taken cross-sun during sample collection.
LMS	Lunar Mass Spectrometer.	3-4	Station designation indicating that a picture was taken en route between stations.
LNPE	Lunar Neutron Probe Experiment (also called NFE for Neutron Flux Experiment).	500 mm	Nominal focal length of the electric Hasselblad cameras with a telephoto lens that was used on the lunar surface.
LOC	Locator. A picture taken (usually toward the LRV) during geologic sample documentation that may be used to determine the location of the sample area.	60 mm	Nominal focal length of the electric Hasselblad cameras with normal-angle lenses that were used on the lunar surface.
LRL	Lunar Receiving Laboratory.	□	Rake sample location.
LRV 	Lunar Roving Vehicle, dot shows front of vehicle and location of TV camera.	70275	Rock sample number (final digits 5 through 9 assigned to rock fragments >1 cm in size).
LRV PAN	Panorama taken by the LMP from the LRV while it was being driven in a circle.	70320-24	Sediment sample number; sample includes no fragments ≥1 cm in size (only first five digits are normally shown on illustrations).
LSG	Lunar Surface Gravimeter.	70160-65	Sediment sample number; includes rock fragment ≥1 cm in size (70165).